THE AUTOPHAGY PATHWAY: BACTERIAL PATHOGEN IMMUNITY AND EVASION

EDITED BY: Chinnaswamy Jagannath, Jere W. McBride and Isabelle Vergne
PUBLISHED IN: Frontiers in Immunology and Frontiers in Microbiology

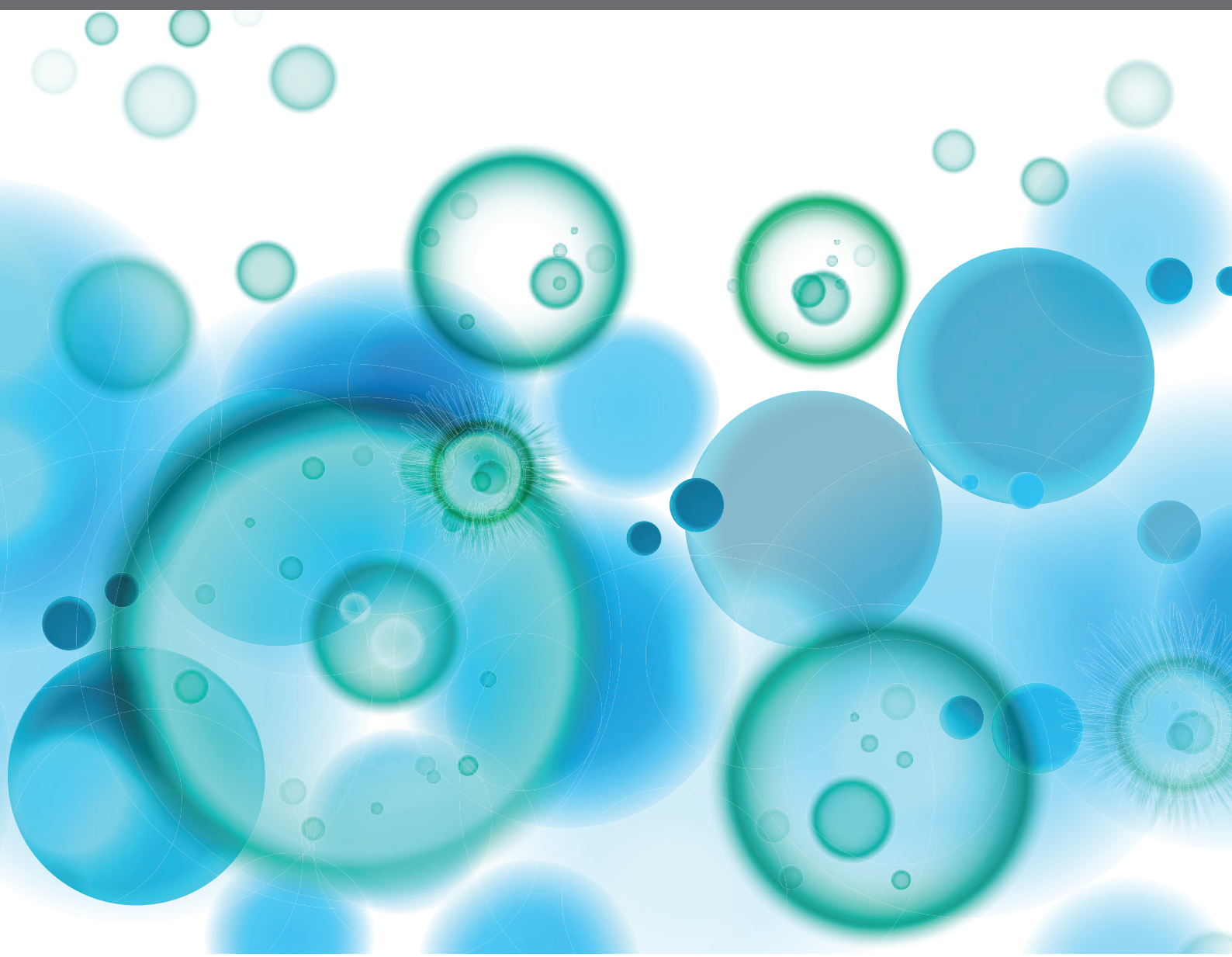

frontiers Research Topics

frontiers

ISSN 1664-8714
ISBN 978-2-88971-685-2
DOI 10.3389/978-2-88971-685-2

About Frontiers

Frontiers is more than just an open-access publisher of scholarly articles: it is a pioneering approach to the world of academia, radically improving the way scholarly research is managed. The grand vision of Frontiers is a world where all people have an equal opportunity to seek, share and generate knowledge. Frontiers provides immediate and permanent online open access to all its publications, but this alone is not enough to realize our grand goals.

Frontiers Journal Series

The Frontiers Journal Series is a multi-tier and interdisciplinary set of open-access, online journals, promising a paradigm shift from the current review, selection and dissemination processes in academic publishing. All Frontiers journals are driven by researchers for researchers; therefore, they constitute a service to the scholarly community. At the same time, the Frontiers Journal Series operates on a revolutionary invention, the tiered publishing system, initially addressing specific communities of scholars, and gradually climbing up to broader public understanding, thus serving the interests of the lay society, too.

Dedication to Quality

Each Frontiers article is a landmark of the highest quality, thanks to genuinely collaborative interactions between authors and review editors, who include some of the world's best academicians. Research must be certified by peers before entering a stream of knowledge that may eventually reach the public - and shape society; therefore, Frontiers only applies the most rigorous and unbiased reviews.
Frontiers revolutionizes research publishing by freely delivering the most outstanding research, evaluated with no bias from both the academic and social point of view. By applying the most advanced information technologies, Frontiers is catapulting scholarly publishing into a new generation.

What are Frontiers Research Topics?

Frontiers Research Topics are very popular trademarks of the Frontiers Journals Series: they are collections of at least ten articles, all centered on a particular subject. With their unique mix of varied contributions from Original Research to Review Articles, Frontiers Research Topics unify the most influential researchers, the latest key findings and historical advances in a hot research area! Find out more on how to host your own Frontiers Research Topic or contribute to one as an author by contacting the Frontiers Editorial Office: frontiersin.org/about/contact

THE AUTOPHAGY PATHWAY: BACTERIAL PATHOGEN IMMUNITY AND EVASION

Topic Editors:
Chinnaswamy Jagannath, Weill Cornell Medical College of Cornell University, United States
Jere W. McBride, University of Texas Medical Branch at Galveston, United States
Isabelle Vergne, UMR5089 Institut de Pharmacologie et de Biologie Structurale (IPBS), France

Citation: Jagannath, C., McBride, J. W., Vergne, I., eds. (2021). The Autophagy Pathway: Bacterial Pathogen Immunity and Evasion. Lausanne: Frontiers Media SA. doi: 10.3389/978-2-88971-685-2

Table of Contents

frontiers in Immunology

EDITORIAL
published: 28 September 2021
doi: 10.3389/fimmu.2021.768935

Editorial: The Autophagy Pathway: Bacterial Pathogen Immunity and Evasion

Chinnaswamy Jagannath[1], *Jere W. McBride*[2] *and Isabelle Vergne*[3]*

[1] Houston Methodist Research Institute, Weill Cornell Medical College of Cornell University, Houston, TX, United States, [2] Department of Pathology and Institute for Human Infections and Immunity, University of Texas Medical Branch, Galveston, TX, United States, [3] Institut de Pharmacologie et de Biologie Structurale, UMR 5089 CNRS - Université de Toulouse, Toulouse, France

Keywords: autophagy, immunometabolism, *Mycobacterium tuberculosis*, *Staphylococcus aureus*, *Salmonella typhimurium*, *Listeria monocytogenes*, *Anaplasmataceae*, host-directed therapies

Editorial on the Research Topic:

The Autophagy Pathway: Bacterial Pathogen Immunity and Evasion

OVERVIEW

Autophagy is a lysosomal degradative pathway which plays important roles in innate immunity against bacterial pathogens (1). Autophagy enables autophagosomes to engulf and deliver intracellular pathogens to the lysosomes for degradation. In addition, autophagy is implicated in the regulation of inflammation by modulating cytokine production. Not surprisingly, bacterial pathogens have developed multiple strategies to manipulate autophagy in order to survive inside the host (2). Although our knowledge of the interplay between bacterial pathogens and autophagy has considerably improved in the past fifteen years, many questions remain. In this Research Topic, we have assembled several research articles and reviews that respond to some of those questions in regard to the host and bacterial factors involved in autophagy regulation, the crosstalk between autophagy and other host defense mechanisms, and the manipulation of autophagy for host-directed therapies.

AUTOPHAGY AS A HOST DEFENSE MECHANISM

The role of autophagy in innate immunity is well conserved across eukaryotic kingdoms. Several vertebrate models such as mice and zebrafish have been essential for our understanding of the role of autophagy, *in vivo*, in bacterial infection (3, 4). Recently, the yellow mealworm beetle (*Tenebrio molitor*) model has also been developed to study *Listeria monocytogenes* infection (Jo et al.). In this model, authors have found a possible dialogue between autophagy and the NF-κB pathway as observed by others in mammalian cells. Autophagy is well known to extensively crosstalk with other innate immune responses including the inflammasome and type I interferon-mediated responses (1). In this Research Topic Paik et al. review the relationship between autophagy and immunometabolism in defense against mycobacterial infection. Both processes appear to be connected by two key kinases, mTOR and AMPK, which regulate TFEB, a central transcriptional

OPEN ACCESS

Edited and reviewed by:
Ian Marriott,
University of North Carolina at Charlotte, United States

***Correspondence:**
Isabelle Vergne
isabelle.vergne@ipbs.fr

Specialty section:
This article was submitted to Microbial Immunology, a section of the journal Frontiers in Immunology

Received: *01 September 2021*
Accepted: *13 September 2021*
Published: *28 September 2021*

Citation:
Jagannath C, McBride JW and Vergne I (2021) Editorial: The Autophagy Pathway: Bacterial Pathogen Immunity and Evasion. Front. Immunol. 12:768935. doi: 10.3389/fimmu.2021.768935

factor of autophagy and lysosome machinery. A central role of mTOR in immune responses was further highlighted by Etna et al. who found that rapamycin, an mTOR inhibitor and autophagy activator, modulates expression of regulatory cytokines in *Mycobacterium tuberculosis*-infected dendritic cells. Lastly, Gauron et al. unveiled an important function of another kinase PKCα which inhibits autophagy in the context of *Staphylococcus aureus*. Besides kinases, microRNAs extensively regulate bacterial autophagy (5). Liu et al. found that microRNA-106a dampens autophagy by repressing ULK1, ATG7 and ATG16L1 during mycobacterial infection. Taken together, these articles underscore the multiple roles of host kinases and microRNAs in autophagy regulation and their dialogue with other host defense mechanisms.

AUTOPHAGY MANIPULATION BY BACTERIAL PATHOGENS

Several intracellular bacterial pathogens can evade autophagy including *M. tuberculosis*, *L. monocytogenes and Salmonella* typhimurium (2). However, the underlying molecular mechanisms are not fully characterized. Zhou et al. found that *Salmonella* SpvC blocks autophagosome formation through its phosphothreonine lyase activity. Interestingly, Rao et al. observed a reduction of TFEB and lysosomal expression during *Salmonella* infection of macrophages, possibly through caspase-1 activation. Whether SpvC is implicated in that process remains to be investigated. In contrast to Salmonella, other bacterial pathogens exploit autophagy to persist and proliferate in host cells. Patterson et al. review our current knowledge of the interplay between autophagy and *Anaplasmataceae*. Members of this family exploit autophagy to acquire nutrients while avoiding lysosomal degradation. Interestingly, Bechelli et al. report that *Rickettsia australis* triggers Atg5-dependent autophagy to suppress inflammatory cytokines at both transcriptional and post-transcriptional levels, which favors pathogen survival. In non-phagocytic cells, autophagy is essential for intracellular survival of *Staphylococcus aureus* (Gauron et al.). Mulcahy et al. found that *S. aureus* intracellular survival also requires autophagy in primary human neutrophils, although, the specific role of autophagy in such cells was not elucidated. Importantly, the last stage of autophagy is blocked in both phagocytes and non-phagocytes. Overall, these findings bring novel molecular insights on how diverse bacterial pathogens can avoid or, in contrast, use autophagy to persist and flourish in their host.

AUTOPHAGY AS A TARGET FOR HOST-DIRECTED THERAPIES

With the continuous rise of bacterial multidrug resistance, alternative approaches to combat such pathogens has become a top priority. One promising avenue is to boost host immune responses including autophagy. This approach is particularly relevant for pathogens that are susceptible to autophagy such as *M. tuberculosis* (6). Strong et al. discuss in depth the opportunities and limitations of autophagy-based therapies against mycobacterial infections. The authors have compiled a list of autophagy-inducing compounds that have been tested on cellular and animal models of mycobacterial infection. Notably, some, if not all of these compounds may also modulate other immune responses as Paik et al. and Etna et al. have pointed out. Thus, a comprehensive analysis of the immune responses to infection after treatment with autophagy-inducing molecules may be extremely informative. Importantly, the involvement of autophagy in the control of bacterial infections should be evaluated in detail using *in vivo* models. In conclusion, autophagy appears to be a promising target for treating mycobacterial infections and, thus, it would be worth examining its potential in the context of other bacterial infections.

PERSPECTIVE AND FUTURE DIRECTIONS

Overall, this Research Topic highlights the intricate interplay between autophagy and various bacterial pathogens. A better understanding of the role and regulation of autophagy in various cellular niches and relevant animal models, as well as its crosstalk with other host defense mechanisms is essential if one wants to harness autophagy for therapeutic purposes.

AUTHOR CONTRIBUTIONS

IV conceived and wrote the first draft of this Editorial. CJ and JM reviewed and edited the manuscript. All authors contributed to the article and approved the submitted version.

FUNDING

CJ was supported by NIH RO1 AI-122070 (PI) and seed funds from HMRI, WCM. JM was supported by NIH AI123610, AI126144, and AI149136. IV was supported by Fondation pour la Recherche Médicale (Equipes FRM DEQ20180339208) and the Fondation MSDAvenir (Fight-TB project).

REFERENCES

1. Deretic V, Saitoh T, Akira S. Autophagy in Infection, Inflammation and Immunity. *Nat Rev Immunol* (2013) 13:722–37. doi: 10.1038/nri3532
2. Bah A, Vergne I. Macrophage Autophagy and Bacterial Infections. *Front Immunol* (2017) 8:1483. doi: 10.3389/fimmu.2017.01483
3. Levine B, Mizushima N, Virgin HW. Autophagy in Immunity and Inflammation. *Nature* (2011) 469:323–35. doi: 10.1038/nature09782
4. Munoz-Sanchez S, van der Vaart M, Meijer AH. Autophagy and Lc3-Associated Phagocytosis in Zebrafish Models of Bacterial Infections. *Cells* (2020) 9:2372. doi: 10.3390/cells9112372
5. Silwal P, Kim YS, Basu J, Jo EK. The Roles of microRNAs in Regulation of Autophagy During Bacterial Infection. *Semin Cell Dev Biol* (2020) 101:51–8. doi: 10.1016/j.semcdb.2019.07.011

6. Kilinc G, Saris A, Ottenhoff THM, Haks MC. Host-Directed Therapy to Combat Mycobacterial Infections. *Immunol Rev* (2021) 301:62–83. doi: 10.1111/imr.12951

Conflict of Interest: The authors declare that the research was conducted in the absence of any commercial or financial relationships that could be construed as a potential conflict of interest.

Publisher's Note: All claims expressed in this article are solely those of the authors and do not necessarily represent those of their affiliated organizations, or those of the publisher, the editors and the reviewers. Any product that may be evaluated in this article, or claim that may be made by its manufacturer, is not guaranteed or endorsed by the publisher.

frontiers in Immunology

ORIGINAL RESEARCH
published: 11 November 2020
doi: 10.3389/fimmu.2020.565545

Manipulation of Autophagy and Apoptosis Facilitates Intracellular Survival of *Staphylococcus aureus* in Human Neutrophils

Michelle E. Mulcahy[1], *Eóin C. O'Brien*[1], *Kate M. O'Keeffe*[1], *Emilio G. Vozza*[1], *Neal Leddy*[2] *and Rachel M. McLoughlin*[1]*

[1] Host-Pathogen Interactions Group, School of Biochemistry and Immunology, Trinity Biomedical Sciences Institute, Trinity College Dublin, Dublin, Ireland, [2] bioTEM, School of Biochemistry and Immunology, Trinity Biomedical Sciences Institute, Trinity College Dublin, Dublin, Ireland

OPEN ACCESS

Edited by:
Isabelle Vergne,
UMR5089 Institut de Pharmacologie et de Biologie Structurale (IPBS), France

Reviewed by:
Yongxia Liu,
Shandong Agricultural University, China
Michal Letek,
Universidad de León, Spain
Ingo Schmitz,
Ruhr University Bochum, Germany

***Correspondence:**
Rachel M. McLoughlin
rachel.mcloughlin@tcd.ie

Specialty section:
This article was submitted to Microbial Immunology, a section of the journal Frontiers in Immunology

Received: 25 May 2020
Accepted: 15 October 2020
Published: 11 November 2020

Citation:
Mulcahy ME, O'Brien EC, O'Keeffe KM, Vozza EG, Leddy N and McLoughlin RM (2020) Manipulation of Autophagy and Apoptosis Facilitates Intracellular Survival of Staphylococcus aureus in Human Neutrophils. Front. Immunol. 11:565545. doi: 10.3389/fimmu.2020.565545

Polymorphonuclear neutrophils (PMN) are critical for first line innate immune defence against *Staphylococcus aureus*. Mature circulating PMN maintain a short half-life ending in constitutive apoptotic cell death. This makes them unlikely candidates as a bacterial intracellular niche. However, there is significant evidence to suggest that *S. aureus* can survive intracellularly within PMN and this contributes to persistence and dissemination during infection. The precise mechanism by which *S. aureus* parasitizes these cells remains to be established. Herein we propose a novel mechanism by which *S. aureus* subverts both autophagy and apoptosis in PMN in order to maintain an intracellular survival niche during infection. Intracellular survival of *S. aureus* within primary human PMN was associated with an accumulation of the autophagic flux markers LC3-II and p62, while inhibition of the autophagy pathway led to a significant reduction in intracellular survival of bacteria. This intracellular survival of *S. aureus* was coupled with a delay in neutrophil apoptosis as well as increased expression of several anti-apoptotic factors. Importantly, blocking autophagy in infected PMN partially restored levels of apoptosis to that of uninfected PMN, suggesting a connection between the autophagic and apoptotic pathways during intracellular survival. These results provide a novel mechanism for *S. aureus* intracellular survival and suggest that *S. aureus* may be subverting crosstalk between the autophagic and apoptosis pathways in order to maintain an intracellular niche within human PMN.

Keywords: apoptosis, autophagy, neutrophils, p53, *S. aureus*

INTRODUCTION

Staphylococcus aureus is a leading global cause of bloodstream infection and is associated with a higher mortality rate than other bacteraemia, typically 25% (1, 2). Treatment of *S. aureus* bloodstream infection is becoming increasingly difficult due to antibiotic resistance. Bacteraemia can lead to metastatic infection in a subset of patients (3) and *S. aureus* persistent bacteraemia and

relapse of infection has been linked to survival within an intracellular reservoir (4). This 'Trojan Horse' theory has been implicated as a contributing factor in recurrent disease, with the indication that *S. aureus* may be particularly adept at surviving within polymorphonuclear neutrophils (PMN) (5).

PMN are critical in the innate immune response against *S. aureus* infection. Optimal PMN function is beneficial for the host during *S. aureus* infection; individuals with deficiencies in PMN activity such as those with chronic granulomatous disease suffer from recurrent *S. aureus* infections (6, 7). However, in murine models of *S. aureus* infection, high levels of PMN recruitment can contribute to dissemination and pathogenesis (8, 9) allowing *S. aureus* to survive intracellularly in a neutrophil-rich environment (10). *S. aureus* is considered a non-classical facultative intracellular pathogen (11, 12) and can survive within several cell types including keratinocytes, osteoblasts and leukocytes, including neutrophils (8, 13–15). Recently, we reported that during murine peritoneal infection, *S. aureus* was found predominantly within PMN disseminated from the peritoneal cavity to the bloodstream (16). These studies support the notion of intracellular survival in PMN as a possible bacterial virulence mechanism. This mechanism, however, is still unclear.

S. aureus survival in non-professional phagocytes has been linked to subversion of a cellular process called macroautophagy (hereafter called autophagy) (17, 18). Autophagy is a conserved eukaryotic process in which damaged organelles are recycled in order to create a supply of nutrients (19). Autophagy involves the *de novo* formation of a phagophore that eventually elongates to form a double-membraned phagosome, or autophagosome (20). Phagophore nucleation is initiated by an activation complex comprising of a class III PI3-kinase called vacuolar protein-sorting 34 (VPS34), Beclin-1, and ATG14 (21). Autophagosome formation is driven by the lipidation of the autophagy marker LC3-I to LC3-II (22). Targeted organelles are engulfed by the phagophore during autophagosome formation and subsequent fusion of the autophagosome with a lysosome degrades the autophagic cargo.

Previous studies have described divergent mechanisms for *S. aureus* intracellular survival and replication using the autophagic pathway in non-professional phagocytes. *S. aureus* was reported to survive and replicate in LC3-decorated autophagosomes in HeLa cells, followed by eventual escape into the cytoplasm (17). In murine fibroblasts, ubiquitinated *S. aureus* was trafficked to autophagosomes by selective autophagic chaperone proteins such as p62 but prevented autophagosome-lysosome fusion (18). Taken together, these data propose a role for autophagy during *S. aureus* invasion of non-professional phagocytes; however, a role of autophagy for *S. aureus* survival within primary human phagocytes after phagocytosis remains to be established.

PMN have a short half-life in humans (23). PMN turnover is controlled by constitutive apoptosis, making it a seemingly inadequate niche for bacterial intracellular survival. However, the normal course of apoptosis in human PMN can be modulated by *S. aureus* (24). During methicillin-resistant *S. aureus* (MRSA) infection, primary human PMN display an aberrant apoptosis phenotype (25). It is not known whether alterations in the apoptotic pathway in PMN after exposure to *S. aureus* are associated with intracellular survival.

This study explores the effect of *S. aureus* intracellular survival on the autophagic and apoptotic pathways in primary human PMN. We demonstrate that *S. aureus* intracellular survival depends on a functioning autophagic pathway and is associated with a delay in PMN apoptosis. Importantly, we have uncovered evidence that *S. aureus* may be manipulating both pathways in order to preserve an intracellular niche during bloodstream infection.

MATERIALS AND METHODS

Bacterial Strains and Growth Conditions

S. aureus strains PS80, PS80Δagr, USA300 LAC and USA300 LACΔagrC have been described previously (16, 26, 27). *S. aureus* strains were streaked from frozen stocks onto TSA plates and grown at 37°C for 24 h. Bacterial suspensions were prepared in sterile PBS and the OD at 600 nm adjusted to the desired equivalent CFU/ml consistent with previous studies (9, 16, 28).

Isolation of Primary Human Neutrophils

Neutrophils were isolated from the peripheral blood of healthy volunteers following informed consent and according to institutional ethical guidelines. Briefly, neutrophils were isolated by dextran sedimentation and gradient separation using Ficoll-Hypaque centrifugation (Lymphoprep, Axis-Shield). After erythrocyte lysis using ACK buffer (Gibco), PMN were resuspended in Dulbecco's Modified Eagles Medium (Sigma) supplemented with 10% fetal bovine serum (Sigma) and 1% L-glutamine (Sigma). PMN were adjusted to a final concentration of $2x10^6$ cells per replicate. Following isolation, PMN purity was >95% and viability >99% as determined by flow cytometry.

Staphylococcus aureus Intracellular Survival Assay

Bacteria were incubated with human IVIG (5 mg/ml, Kiovig) and Low-Tox Guinea Pig Complement (Cedarlane) for 20 min at 37°C in order to opsonise them for efficient uptake by PMN. Bacteria were then added to PMN at a MoI of 1:10. In some cases PMN were pre-treated with VPS34-IN1 (10 μM, Millipore), Bafilomycin A1 (100 nM, Sigma), Pifithrin-α (30μM, Merck) or a corresponding DMSO vehicle control for 30 min prior to inoculation with *S. aureus*. PMN were incubated with bacteria for 1 h with rotation at 37°C before addition of gentamicin (Sigma) at a final concentration of 200 μg/ml. PMN and bacteria were incubated for a further 1, 3, or 6 h with rotation before centrifugation. Gentamicin treatment was continued for the duration of the time-course to ensure no survival of extracellular bacteria. Media was plated onto TSA at 1, 3, and 6 h post gentamicin treatment to ensure that no bacteria survived extracellularly. PMN were lysed in 0.1% (v/v) Triton-X 100

(Sigma). Lysates were diluted in PBS and plated onto TSA for CFU enumeration. Under all conditions PMN viability began to decline 12 hours after blood was drawn from donors as has previously been reported (29–31).

Alternatively, to assess phagocytosis, cells were pre-treated and infected as above with GFP-expressing PS80 followed by gentamicin treatment for 30 min to eliminate extracellular bacteria. PMN were then fixed with Fix & Perm Medium A (Life Technologies) and analysed on BD FACSCanto II. The percentage of GFP-positive cells was used as an indicator of intracellular bacteria.

RNA Extraction, cDNA Synthesis, and Quantitative PCR

Total RNA was extracted using the Qiagen RNA extraction kit according to the manufacturers' instructions. RNA yield and quality were measured on a Spectrostar Nano spectrophotometer using an LVIS plate. RNA (250ng) was reverse-transcribed using a High-Capacity cDNA reverse transcription kit (Applied Biosystems) according to manufacturers' instructions. mRNA was quantified using quantitative PCR on a CFX96 Touch Real-Time PCR Detection System (Bio-Rad) using iTaq Sybr Green Supermix (Bio-Rad) according to manufacturers' recommendations. The following KiCqStart SYBR Green primer pairs (Sigma) were used: human *tp53* (Gene ID: 7157), *dram1* (Gene ID: 55332), *mcl1* (Gene ID:4170), *bcl2* (Gene ID: 596), *bcl2a1* (Gene ID:597), *bax* (Gene ID: 581), and *rn18s1* (Gene ID: 100008588). Expression was normalized to 18s RNA by the change-in-cycle-threshold (ΔΔCT) method.

Protein Expression

PMN were lysed in lysis buffer (1% (v/v) Triton-X-100 (Sigma), 5% (v/v) protease inhibitor cocktail (Sigma) and 5% (v/v) phosphatase inhibitor cocktail 3 (Sigma)). Lysate protein concentration was determined using a Pierce BCA assay kit (Thermo Fisher Scientific). A total of 5μg of protein was separated on 4–20% precast TGX polyacrylamide gels (Bio-Rad) and transferred onto polyvinylidene difluoride membranes. Membranes were incubated in AdvanBlock (Cell Signalling Technologies) before probing with rabbit anti-human LC3 IgG (D3U4C, Cell Signalling Technologies), rabbit anti-SQSTM1/p62 IgG (5114, Cell Signalling Technologies), rabbit anti-human caspase-3 IgG (9662, Cell Signalling Technology), rabbit anti-human Mcl-1 IgG (D2W9E, Cell Signalling Technology), rabbit anti-human A1/Bfl-1 IgG (D1A1C, Cell Signalling Technology), rabbit anti-human Bax IgG (D2E11, Cell Signalling Technology), rabbit anti-human p53 IgG (7F5, Cell Signalling Technology), rabbit anti-human phospho-p53 (Ser15) IgG (9284, Cell Signalling Technology), and rabbit anti-DRAM1 (ARP47432_P050, Aviva Systems Biology). Incubation with primary antibodies was followed by HRP-conjugated goat anti-rabbit IgG (7074, Cell Signalling Technology). Reactive bands were visualized using ECL detection and densitometry was performed using ImageLab developing system (Bio-Rad).

Flow Cytometry

To assess apoptosis, cells were stained using the Terminal deoxynucleotidyl transferase (TdT)-mediated dUTP nick end labelling (TUNEL) kit (Roche). PMN were fixed with Fix & Perm Medium A (Life Technologies) and permeabilized with nuclear permeabilization buffer before incubation with TUNEL reaction mixture according to manufacturer's instructions. To assess mitochondrial membrane potential, cells were stained using 5,5',6,6'-tetrachloro-1,1',3,3'-tetraethylbenzimidazolcarbocyanine iodide (JC-1) (BD Biosciences). Membrane depolarisation is characterized by a fluorescence emission shift from green (~529 nm, FL2) to red (~590, FL1). PMN (1 X 10^6 cells) were incubated with JC-1 for 15 min at 37°C and 5% CO_2 according to manufacturer's instructions. To determine intracellular p53 levels, PMN were fixed with Fix & Perm Medium A (Life Technologies) and permeabilized with nuclear permeabilization buffer before incubation with anti-p53 APC (MiltenyiBiotec) for 15 min at room temperature. All flow cytometric analysis was performed immediately with a BD FACSCanto II using FACS DIVA and FlowJo software.

Transmission Electron Microscopy

Infected PMN samples were fixed in glutaraldehyde (1.5%) overnight at 4°C. Samples were washed and then embedded in agarose (2%). Samples were then secondary fixed with osmium tetroxide (2% in 0.05M potassium phosphate buffer) before dehydration through increasing concentrations of ethanol. Samples were transitioned with propylene oxide into epoxy resin embedding medium then cured at 60°C for 24 h. Ultrathin sections were obtained using a Leica EM UC7 ultramicrotome and transferred on to 300 mesh copper TEM grids. Sample grids were stained with 0.5% aqueous uranyl acetate and Reynold's lead citrate. Sections were examined on a Jeol JEM1400 transmission electron microscope at 100 kV and imaged with AMT XR80 digital camera.

Statistical Analyses

Statistical analysis was performed using Prism Graphpad 8 software using ANOVA or repeated measures ANOVA. Comparisons between groups were made using Bonferroni post-tests or Tukey post-tests where appropriate.

RESULTS

Staphylococcus aureus Intracellular Survival Within Primary Human Neutrophils Requires the Agr Virulence Regulator and the Autophagy Pathway

In order to determine the ability of *S. aureus* to survive intracellularly within primary human PMN, PMN isolated from the peripheral blood of healthy volunteers were incubated with *S. aureus* strain PS80 for 1 h before gentamicin treatment to kill any non-phagocytosed extracellular bacteria. Intracellular CFU were assessed at 1, 3, and 6 h post-gentamicin treatment.

Survival of WT PS80 within PMN was significantly higher than that of PS80Δagr at 3 and 6 h post-gentamicin treatment (**Figure 1A**) highlighting the requirement for an agr-specific factor for intracellular survival.

To evaluate the role of the autophagy pathway during intracellular survival, PMN were treated with the VPS34-PI3K inhibitor VPS34-IN1 before exposure to PS80. Intracellular survival of PS80 in inhibitor-treated PMN was significantly reduced at 3 and 6 h post-gentamicin treatment compared to untreated, infected PMN (**Figure 1A**). The rate of phagocytosis of *S. aureus* by PMN was not affected by VPS34-IN1 treatment (**Figure S1**). These results indicate that inhibition of the autophagy pathway impairs the ability of *S. aureus* to survive intracellularly within human PMN. There was no further decrease in survival in PS80Δagr-infected, VPS34-IN1-treated PMN (**Figure 1A**), suggesting that an agr-specific factor is involved in manipulation of the autophagy pathway.

The assay was repeated with the USA300 strain LAC and an agrC-deficient isogenic mutant (USA300ΔagrC). Similar to PS80, intracellular survival of WT USA300 in inhibitor-treated PMN was significantly lower at each timepoint compared to untreated, infected PMN (**Figure 1B**). Intracellular CFU levels of USA300ΔagrC differed significantly from WT USA300 CFU at 1 h. Taken together, these results indicate that a functioning autophagy pathway facilitates *S. aureus* intracellular survival in PMN and that this mechanism of intracellular survival involves an agr-specific factor.

Autophagic Flux Is Disrupted in PMN Harboring *Staphylococcus aureus*

To assess autophagic flux in PMN harboring *S. aureus*, protein levels of autophagic markers LC3-II and p62 were determined in *S. aureus*-infected PMN compared to untreated controls at 1 and 3 h post-gentamicin treatment using Western immunoblotting. After 3 h, LC3-II levels were significantly higher in *S. aureus*-infected PMN compared to control cells (**Figures 1C, D**). These data indicate that the autophagy pathway is activated in infected PMN compared to untreated cells. Levels of p62 were also significantly increased in infected PMN after 3 h gentamicin treatment compared to untreated PMN (**Figures 1C, D**) which suggests that autophagic flux has been disrupted in *S. aureus*-infected cells and that autophagosomes may be accumulating during intracellular survival.

In order to further assess the effect of *S. aureus* on autophagic flux in PMN, PMN were pre-treated with the autophagy inhibitor Bafilomycin A1. Bafilomycin A1 treatment prevents autophagosome-lysosome fusion, therefore halting autophagic flux (32, 33). Intracellular survival of PS80 in Bafilomycin A1-treated PMN was significantly reduced at 3 and 6 h post-gentamicin treatment compared to untreated, infected PMN (**Figure 2A**), again indicating that a functioning autophagic pathway is required for intracellular survival. LC3 and p62 accumulation was determined in infected PMN compared to Bafilomycin A1 treated cells using Western immunoblotting. Increased levels of LC3 were observed in infected cells and

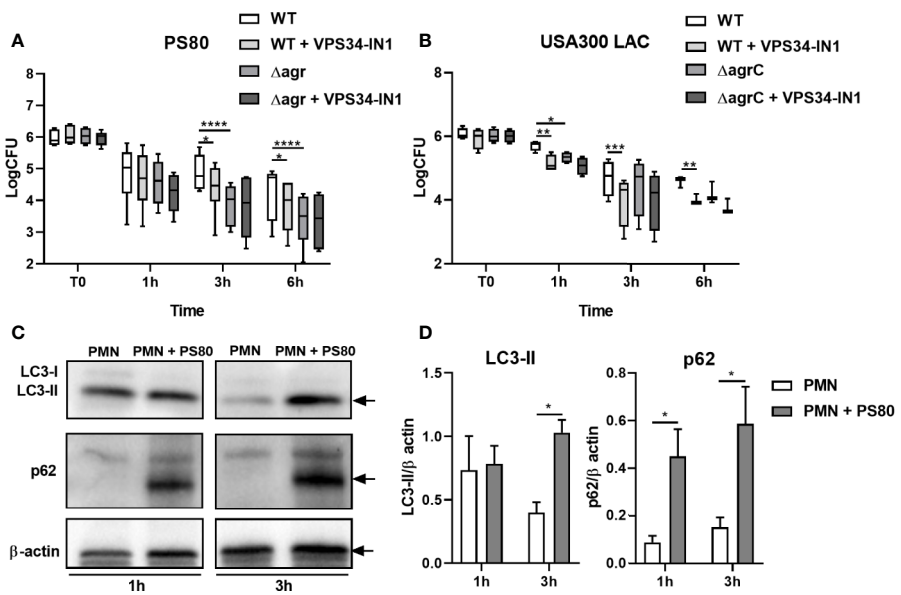

FIGURE 1 | *Staphylococcus aureus* intracellular survival within human neutrophils. Primary human neutrophils were treated with VPS34-IN1 (10 μM) or were left untreated and were then infected with pre-opsonized *S. aureus* PS80 WT or Δagr **(A)** or USA300 LAC WT or ΔagrC **(B)** (MoI 10) for 1 h. Following infection, PMN were treated with gentamicin (200 μg/ml) for the times indicated. At each timepoint, PMN lysates were plated onto TSA and CFU enumerated. Data are expressed as Log CFU (n = 6 donors for A, n = 3–4 donors for B). Statistical analyses were performed using two-way ANOVA with Bonferroni post-tests. **P* < 0.05; ***P* < 0.01; ****P* < 0.001; *****P* < 0.001.PMN protein lysates were probed for LC3 processing and p62 expression using Western immunoblotting **(C)** and analysed using densitometric analysis **(D)**. Data are expressed as protein expression normalized to β-actin control values for each sample ± SEM (n = 3 donors). Black arrows indicate the area of the blot used for densitometry. Statistical analyses were performed using two-way ANOVA with Bonferroni post-tests. **P* < 0.05.

Bafilomycin A1-treated cells compared to control PMN at 3 h post-gentamicin treatment (**Figures 2B, C**). No further increase in LC3 accumulation was evident in Bafilomycin A1-treated, infected cells compared to non-treated infected cells, suggesting that autophagosome-lysosome fusion has been blocked during intracellular survival. Accumulation of p62 was also increased in infected cells, Bafilomycin A1-treated cells and Bafilomycin A1-treated, infected cells at 3 h post-gentamicin treatment (**Figures 2B, C**), further indicating that normal autophagic flux has been altered. Taken together, these results indicate that *S. aureus* intracellular survival alters normal autophagic flux within PMN.

Although increased LC3-II levels are a strong indicator for an increase or block in autophagic flux, it can also be involved in non-canonical pathways that use autophagy machinery, such as LC3-associated phagocytosis (LAP). In order to confirm that *S. aureus* is using double-membraned autophagosomes as a niche, *S. aureus*-infected PMN were imaged using transmission electron microscopy at 3 h post-gentamicin treatment. Evidence of phagophore formation was observed (**Figures 2D,** i) and *S. aureus* dividing within double-membraned vesicles which are typically identified as autophagosomes (**Figures 2D,** ii, iii). Taken together, these data confirm that *S. aureus* uses the autophagy pathway in order to survive within human PMN during infection.

Staphylococcus aureus Intracellular Survival Delays Apoptosis in Human PMN

Our data indicate that *S. aureus* is using autophagosomes as a survival niche during infection in primary human PMN. We next assessed whether *S. aureus* could modulate PMN apoptosis in order to preserve its niche. Levels of early-stage apoptosis were determined by examining mitochondrial depolarization using JC-

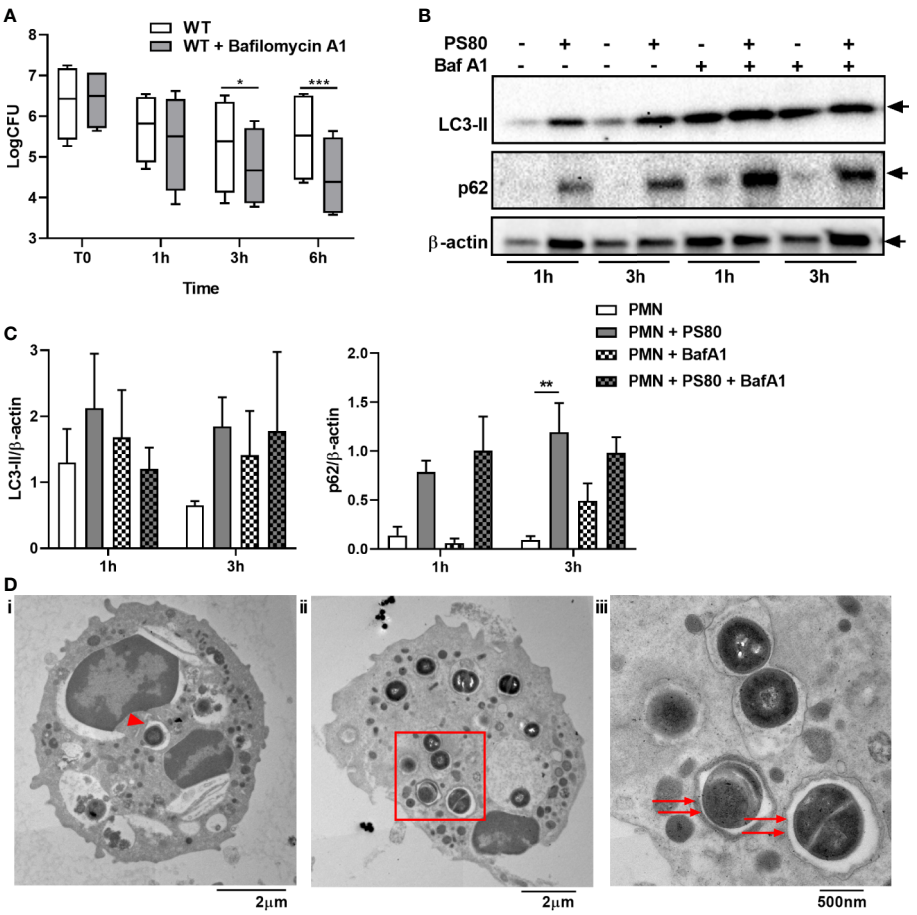

FIGURE 2 | *Staphylococcus aureus* intracellular survival within PMN is associated with a disruption in autophagic flux. Primary human neutrophils were treated with Bafilomycin A1 (100 nM) or were left untreated and were then infected with pre-opsonized *S. aureus* PS80 (Mol 10) for 1 h. Following infection, PMN were treated with gentamicin (200 μg/ml) for the times indicated. **(A)** At each timepoint, PMN lysates were plated onto TSA and CFU enumerated. Data are expressed as Log CFU (n = 4 donors). Statistical analyses were performed using two-way ANOVA with Bonferroni post-tests. $^{*}P < 0.05$; $^{***}P < 0.001$. At each timepoint, PMN protein lysates were probed for LC3 processing and p62 expression using Western immunoblotting **(B)** and analysed using densitometric analysis **(C)**. Data are expressed as protein expression normalized to β-actin control values for each sample ± SEM (n = 3–4 donors). Black arrows indicate the area of the blot used for densitometry. Statistical analyses were performed using two-way ANOVA with Bonferroni post-tests. $^{**}P < 0.01$. At 3 h, infected PMN were imaged using transmission electron microscopy **(D)**. Whole, PS80-infected PMN showing phagophore formation indicated by red arrowhead (i) and double-membraned autophagosomes indicated by red arrows (ii) and inset (iii). Original magnification for Ci: 3000x, Cii: 2500x, Ciii: 8000x.

1 staining and caspase-3 cleavage by Western immunoblotting in *S. aureus*-infected PMN. At 3 h post-gentamicin treatment, infected PMN displayed significantly less mitochondrial depolarization (**Figure 3A**) and significantly lower levels of caspase-3 cleavage (**Figure 3B**) compared to uninfected controls, indicating a delay in caspase-mediated apoptosis during intracellular survival. The effects of intracellular survival on late-stage apoptosis were then determined using TUNEL staining. At 6 h post-gentamicin treatment, a mean of 73.9% of untreated PMN were TUNEL-positive whereas infected PMN were significantly less apoptotic (**Figure 3C**, mean value: 49.4%), confirming that apoptosis is delayed during intracellular survival.

In order to determine if the observed changes in apoptosis were associated with the presence of intracellular *S. aureus* as a result of subverting the autophagy pathway, apoptosis levels were determined in infected PMN following pre-treatment with

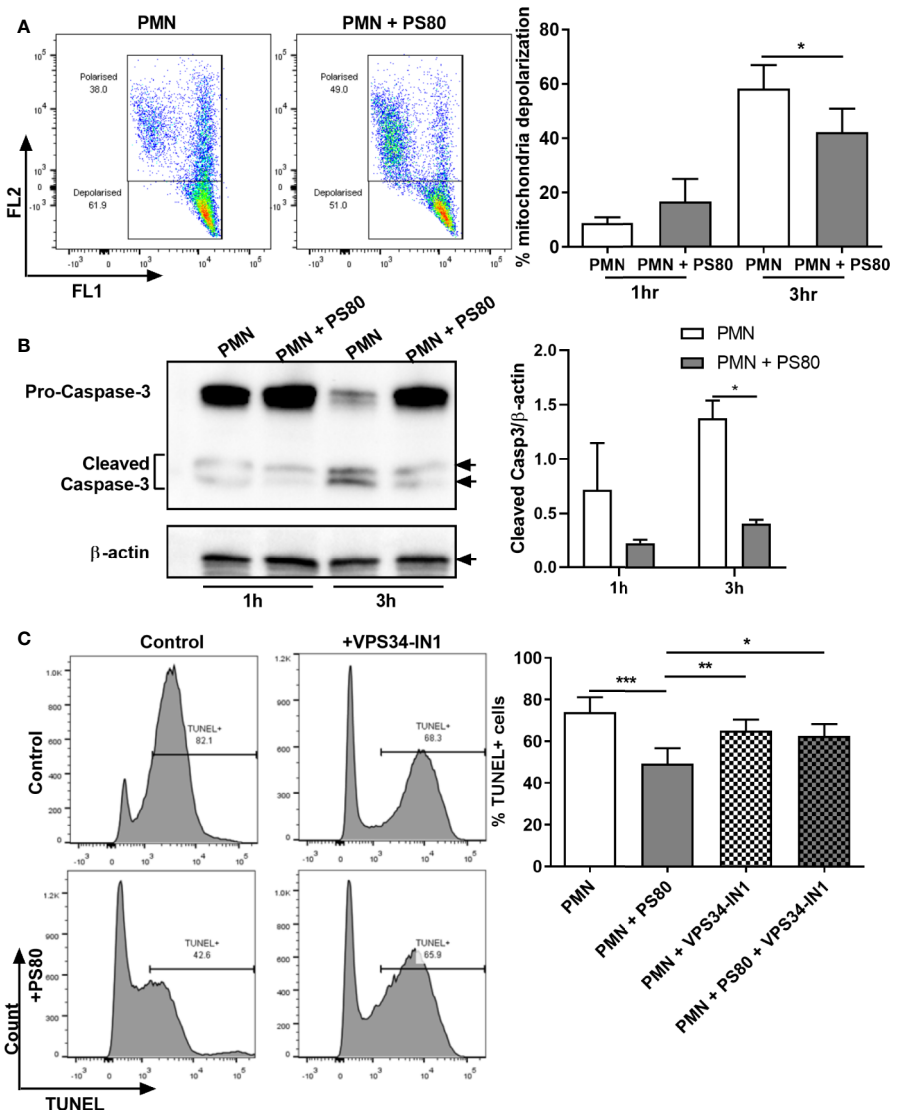

FIGURE 3 | Hallmarks of apoptosis are delayed during *Staphylococcus aureus* intracellular survival. Primary human neutrophils were left untreated or were pre-treated with VPS34-IN1 (10 μM) and infected with pre-opsonized *S. aureus* PS80 (MoI 10) for 1 h. Following infection, PMN were treated with gentamicin (200 μg/ml) for the times indicated. **(A)** At each timepoint, PMN were stained with JC-1 dye to measure mitochondrial membrane depolarization and analyzed by flow cytometry (n = 3 donors). Representative FACS plots for JC-1 staining at 3 h are shown. Membrane depolarisation is characterized by a reduction of fluorescence in Fluorescent channel (FL) 2 and corresponding increase in FL1 fluorescence. Statistical analysis was performed using a paired t test. **(B)** PMN protein lysates were probed for caspase-3 expression and analysed using densitometric analysis. Data are expressed as protein expression normalized by β-actin control values for each sample ± SEM (n = 3 donors). Black arrows indicate the area of the blot used for densitometry. Statistical analysis was performed using two-way ANOVA with Bonferroni post-tests. $^{*}P < 0.05$. **(C)** At 6 h, PMN were stained for DNA degradation using TUNEL staining and analysed by flow cytometry. Representative histograms for TUNEL-stained PMN for each treatment group are shown. Data are expressed as % TUNEL-positive cells ± SEM (n = 6 donors). Statistical analysis was performed using one-way ANOVA with Tukey post-tests. $^{*}P < 0.05$; $^{**}P < 0.01$; $^{***}P < 0.001$.

VPS34-IN1. After 6 h, VPS34-IN1-treated *S. aureus*-infected PMN had significantly more TUNEL-positive staining than infected, untreated PMN (**Figure 3C**, mean value: 62.7%). PMN treated with VPS34-IN1 alone displayed similar levels of TUNEL staining as VPS34-IN1-treated *S. aureus*-infected PMN and PMN alone (mean value: 65.2%). This indicates that the reduction in apoptosis observed in infected PMN was reversed by inhibiting autophagy-mediated intracellular survival. Although not statistically significant, a similar trend was evident for an increase in caspase-3 cleavage (**Figure S2A**) but less so for mitochondrial depolarization (**Figure S2B**) in infected, VPS34-IN1-treated PMN at 3 h post-gentamicin treatment. Taken together, these results indicate that apoptosis is delayed during *S. aureus* intracellular survival. Furthermore, blocking autophagy may partially relieve the inhibitory effect caused by *S. aureus* on the apoptosis pathway.

Staphylococcus aureus Intracellular Survival Is Associated With an Anti-Apoptotic Phenotype and Activation of the p53/DRAM Pathway

The delay in apoptosis observed in infected PMN coupled with the incomplete restoration of apoptosis in inhibitor-treated, infected PMN suggests a complex apoptotic phenotype is occurring during *S. aureus* intracellular survival. In order to further characterize this phenotype, expression of apoptotic genes involved in the intrinsic apoptotic pathway was determined using RT-PCR and corresponding protein

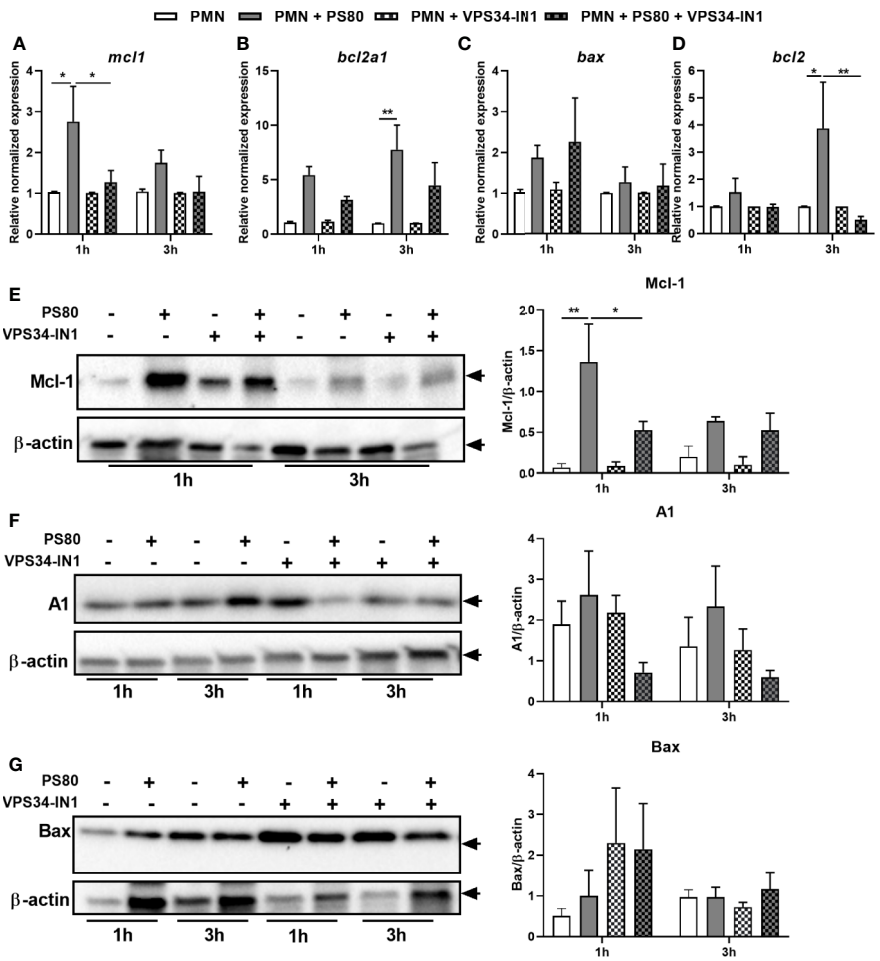

FIGURE 4 | *Staphylococcus aureus* intracellular survival is associated with changes in expression of apoptotic factors and an anti-apoptotic phenotype. Primary human neutrophils were left untreated or were pre-treated with VPS34-IN1 (10 μM) and were then infected with pre-opsonized *S. aureus* PS80 (MoI 10) for 1 h. Following infection, PMN were treated with gentamicin (200 μg/ml) for the times indicated. RNA was extracted and gene expression levels of *mcl1* **(A)**, *bcl2a1* **(B)**, *bax* **(C)**, and *bcl2* **(D)** assessed using quantitative RT-PCR at 1 and 3 h post-gentamicin treatment. Gene expression is plotted relative to gene expression in control PMN after normalization to 18s RNA ± SEM (n = 3–4 donors). Statistical analysis was performed using two-way ANOVA with Tukey post-tests. $^{*}P < 0.05$; $^{**}P < 0.01$. PMN protein lysates were probed for Mcl-1 **(E)**, A1/Bfl-1 **(F)**, and Bax **(G)** expression and analysed using densitometric analysis. Data are expressed as protein expression normalized by β-actin control values for each sample ± SEM (n = 3–4 donors). Black arrows indicate the area of the blot used for densitometry. Statistical analysis was performed using two-way ANOVA with Bonferroni post-tests. $^{*}P < 0.05$; $^{**}P < 0.01$.

expression was determined using Western immunoblotting. Expression of the anti-apoptotic factor *mcl1* was significantly increased at 1 h post-gentamicin treatment (**Figure 4A**) with a similar significant increase in protein expression evident at 1 h (**Figure 4E**). Gene expression of anti-apoptotic factors *bcl2a1* and *bcl2* were significantly increased after 3 h (**Figures 4B, D**). A similar trend towards higher protein level of A1/Bfl-1 was observed (**Figure 4F**); however, protein levels of Bcl-2 could not be detected in PMN under any conditions. Neither gene expression nor protein expression of pro-apoptotic factor *bax* was significantly increased in infected PMN at either timepoint (**Figures 4C, G**), confirming that intracellular survival elicits an anti-apoptotic phenotype in PMN.

These results indicate that the intrinsic apoptotic pathway is delayed during intracellular survival due to the upregulation of anti-apoptotic factors. Therefore, we next looked at transcriptional regulation of these factors by determining intracellular levels of the cell-cycle transcription factor p53. p53 is a well-defined positive regulator of the intrinsic apoptotic pathway; however, when localized to the nucleus, p53 can positively regulate autophagy in response to cellular stress (34, 35). Intracellular levels of p53 were determined in infected PMN using flow cytometry and expression of *tp53* was confirmed using RT-PCR and Western immunoblotting. At 3 h post-gentamicin treatment, intracellular levels of p53 were significantly higher in infected PMN compared to controls (**Figure 5A**). Gene and protein expression of p53 (**Figures 5B, C**) was significantly increased at 3 h post-gentamicin treatment. In order to confirm the intracellular location of p53, expression levels of p53 phosphorylated at Serine 15 (p53ser15) were determined. Phosphorylation of p53 at serine 15 has been previously shown to inhibit a nuclear export signal at the amino terminal of p53 (36); therefore, high levels of p53ser15 may indicate retention of p53 in the nucleus. Protein levels of p53ser15 were determined by Western immunoblotting (**Figure 5C**). High levels of p53ser15 were detected at 1 and 3 h post-gentamicin treatment compared to control PMN, suggesting that p53 is being retained in the nucleus during intracellular survival.

Nuclear p53 induces transcription of the pro-autophagic membrane protein Damage-Regulated Autophagy Monitor (DRAM). At 3 h post-gentamicin treatment, gene expression of *dram* (**Figure 6A**) was significantly increased in *S. aureus*-infected PMN. Although detection of DRAM at the protein level proved challenging, there was also evidence of increased DRAM protein expression at 3 h post-gentamicin treatment (**Figure S3**). This confirms that p53-activated gene transcription is occurring during intracellular survival, and suggests that autophagy-mediated intracellular survival is activating the p53/DRAM stress response pathway.

To determine whether the changes in apoptotic gene expression are directly influenced by autophagy-induced intracellular survival, gene and protein expression of Mcl-1, Bcl-2, A1/Bfl-1, and Bax was assessed in infected PMN pre-treated with VPS34-IN1. Autophagy inhibition resulted in

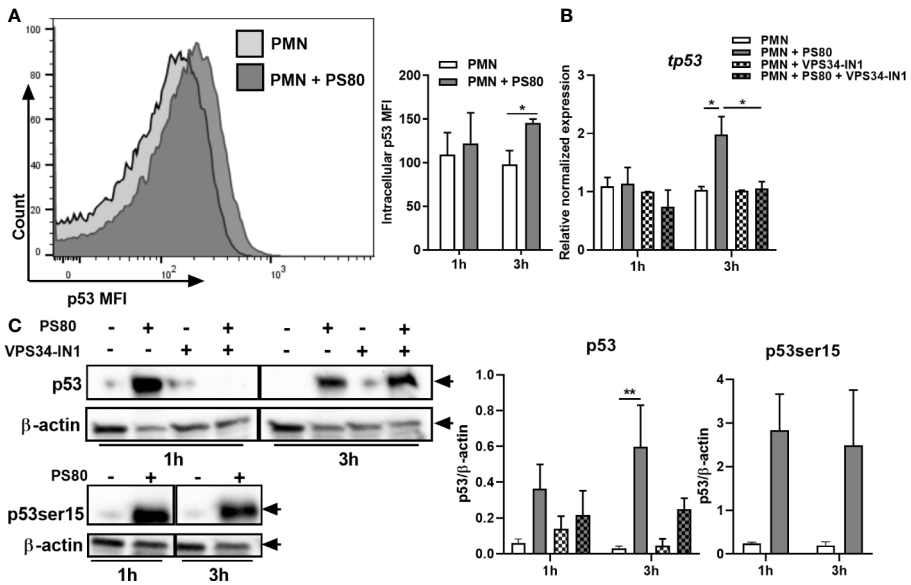

FIGURE 5 | The p53/DRAM pathway is activated during *Staphylococcus aureus* intracellular survival. Primary human neutrophils were left untreated or were pre-treated with VPS34-IN1 (10 μM) and were then infected with pre-opsonized *S. aureus* PS80 (MoI 10) for 1 h. Following infection, PMN were treated with gentamicin (200 μg/ml) for the times indicated. At each timepoint, intracellular staining for p53 was carried out and analysed by flow cytometry. **(A)** Representative FACS plot showing p53 intracellular staining at 3 h and MFI values of nuclear p53. RNA was extracted and gene expression levels of **(B)** *tp53* was assessed using quantitative RT-PCR. Gene expression is plotted relative to gene expression in control PMN after normalization to 18s RNA ± SEM (n = 3–4 donors). Statistical analysis was performed using two-way ANOVA. $^{*}P < 0.05$. **(C)** PMN protein lysates were probed for total p53 and p53ser15 expression and analysed using densitometric analysis. Data are expressed as protein expression normalized by β-actin control values for each sample ± SEM (n = 3–4 donors). Black arrows indicate the area of the blot used for densitometry. Statistical analysis was performed using two-way ANOVA with Bonferroni post-tests. $^{**}P < 0.01$.

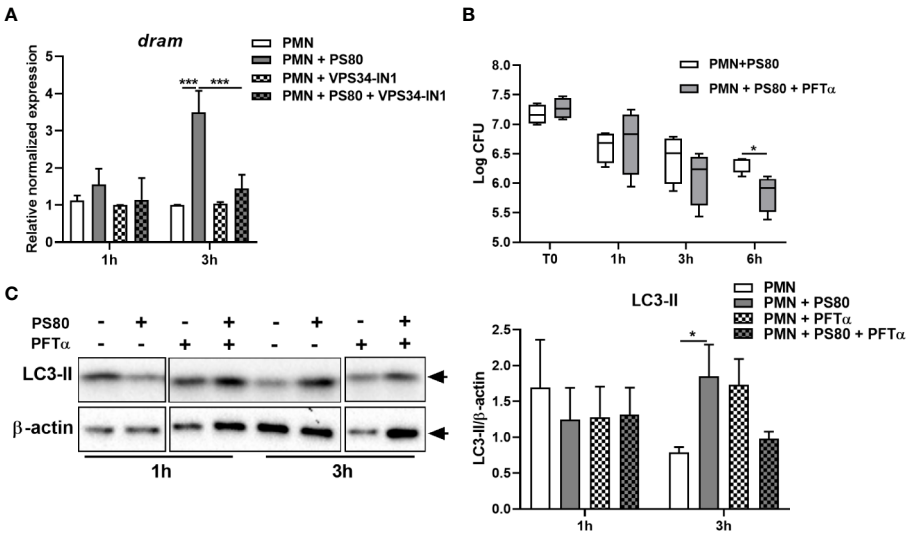

FIGURE 6 | Inhibition of p53 reduces *Staphylococcus aureus* intracellular survival in neutrophils. **(A)** Primary human neutrophils were left untreated or were pre-treated with VPS34-IN1 (10 μM) and were then infected with pre-opsonized *S. aureus* PS80 (MoI 10) for 1 h. Following infection, PMN were treated with gentamicin (200 μg/ml) for the times indicated. RNA was extracted and gene expression levels of *dram* assessed using quantitative RT-PCR. Gene expression is plotted relative to gene expression in control PMN after normalization to 18s RNA ± SEM (n = 3–4 donors). Statistical analysis was performed using two-way ANOVA. ***$P < 0.001$. **(B)** Primary human neutrophils were treated with Pifithrin-α (30μM) or were left untreated and were then infected with pre-opsonized *S. aureus* PS80 (MoI 10) for 1 h. Following infection, PMN were treated with gentamicin (200 μg/ml) for the times indicated. At each timepoint, PMN lysates were plated onto TSA and CFU enumerated. Data are expressed as Log CFU (n = 4 donors). Statistical analyses were performed using two-way ANOVA with Bonferroni post-tests. *$P < 0.05$. **(C)** PMN protein lysates were probed for LC3 processing using Western immunoblotting and analysed using densitometric analysis. Data are expressed as protein expression normalized to β-actin control values for each sample ± SEM (n = 3 donors). Black arrows indicate the area of the blot used for densitometry. Statistical analyses were performed using two-way ANOVA with Bonferroni post-tests. *$P < 0.05$.

significantly reduced expression of *mcl1* and *bcl2* at 1 and 3 h post-gentamicin treatment, respectively compared to untreated infected controls (**Figures 4A, D**). Mcl-1 protein expression in infected PMN was also reduced significantly after VPS34-IN1 treatment 1 h post-gentamicin treatment (**Figure 4E**). Gene expression of *bcl2a1* and *bax* were not significantly affected (**Figures 4C, E**) although when compared to infected PMN, A1/Bfl-1 protein expression appeared to decrease in infected PMN after VPS34-IN1 treatment, albeit not significantly (**Figure 4F**). Similarly, Bax protein expression appeared to increase after VPS34-IN1 treatment 1 h post-gentamicin treatment, but not significantly (**Figure 4G**). These results indicate that autophagy inhibition elicits a partial restoration of the apoptotic state in PMN during intracellular survival.

The effect of autophagy inhibition on the expression of *tp53* and *dram* was also assessed. Expression of *tp53* and *dram* were both significantly decreased in the presence of VPS34-IN1 at 3 h post-gentamicin treatment (**Figures 5B** and **6A**) and protein expression of p53 appeared decreased at 3 h post-gentamicin treatment compared to untreated, infected PMN (**Figure 5C**), indicating that the p53/DRAM pathway is also directly influenced by autophagy-mediated intracellular survival. In order to further assess the effect of the p53 pathway on intracellular survival, PMN were pre-treated with a p53 inhibitor, Pifithrin-α (PFTα) and intracellular survival was assessed. Intracellular survival of *S. aureus* in PFTα-treated PMN was significantly reduced at 6 h post-gentamicin treatment (**Figure 6B**). Gene expression of *tp53* and *dram* were assessed at 1 and 3 h post-gentamicin treatment and were confirmed to be lower in PFTα-treated cells (**Figure S4**). Autophagic flux was assessed in the presence of PFTα by determining the levels of LC3-II in infected PMN at 1 and 3 h post-gentamicin treatment. After 1 h gentamicin treatment, both untreated and PFTα-treated, infected PMN had similar protein levels of LC3-II (**Figure 6C**). After 3 h gentamicin-treatment, LC3-II protein levels were higher in infected PMN compared to uninfected PMN, whereas in PFTα-treated, infected PMN, LC3-II levels were lower compared to the corresponding uninfected control (**Figure 6C**) suggesting that autophagic flux has been restored. Together, these data indicate that the p53 pathway plays an important role in autophagy-mediated intracellular survival of *S. aureus*.

Overall, these data indicate that autophagy-mediated intracellular survival activates the p53/DRAM stress response while simultaneously promoting the expression of several anti-apoptotic factors which may counteract a pro-apoptotic role for p53. This promotes an anti-apoptotic, pro-autophagic phenotype in human PMN, prolonging the intracellular niche for *S. aureus*.

DISCUSSION

Staphylococcus aureus bloodstream infection is a significant cause of morbidity and mortality worldwide (1, 2, 37).

Persistence of bacteraemia and metastatic infection is associated with failure to eradicate the source of infection, suggesting that an intracellular reservoir for *S. aureus* exists (4). Due to the prevalence of *S. aureus* antibiotic resistance, new host-directed therapies are required where antibiotics are no longer effective. A detailed knowledge of how *S. aureus* manipulates the innate immune response and survives during bacteraemia is needed in order to develop these therapies. In this study, we show that *S. aureus* survives intracellularly within primary human PMN by manipulating the autophagy pathway to establish an intracellular niche, while simultaneously inhibiting the normal apoptotic pathway.

Previous studies have identified the autophagy pathway as a mechanism of intracellular survival for *S. aureus* during infection in several cell types *in vitro* (17, 18, 38), while subversion of autophagy within PMN for bacterial survival has previously been reported for *E. coli* (39). Interestingly, a recent study reported that *S. aureus* can survive within LC3-decorated phagosomes in PMN in larval zebrafish using the non-canonical form of autophagy, LAP (40). Using primary human PMN we observed *S. aureus* present in double-membraned autophagosomes using TEM which is a characteristic of canonical selective autophagy rather than LAP. However, a role for LAP in human PMN requires further investigation. Our study identifies a novel role for autophagy in *S. aureus* survival within a primary human professional phagocyte. A disruption in autophagic flux was evident in infected PMN and intracellular survival decreased significantly when autophagy was inhibited. These results provide strong evidence of manipulation of the autophagic pathway in *S. aureus* in order to survive intracellularly.

The changes in autophagy reported here are accompanied by a decrease in apoptosis in human PMN harboring *S. aureus*. These results reflect changes to the intrinsic apoptotic pathway that may prolong the PMN life cycle and therefore the intracellular niche for *S. aureus*. In previous studies examining changes in the PMN life cycle during *S. aureus* infection *in vitro*, PMN were reported to display regular markers of apoptosis but also exhibited signs of a dysregulated apoptosis phenotype (25). Other studies illustrated a delay in PMN apoptosis during *S. aureus* infection (24), and the apoptotic fate of PMN during *S. aureus* infection was shown to depend on multiplicity of infection (41). These conflicting accounts of the changes to PMN lifespan during *S. aureus* infection, coupled with our data, confirm that the apoptotic fate of PMN is context-dependent. Several *in vivo* studies have demonstrated rapid dissemination of *S. aureus* to secondary infection sites within hours of initial infection, and PMN have been implicated as potential mediators (16, 42). Furthermore, PMN isolated from *S. aureus* infection sites have been shown to contain viable bacteria capable of re-infecting a naïve host (8). Therefore, any delay, even briefly, in PMN apoptosis would give *S. aureus* a survival advantage for long enough to potentially proliferate and disseminate, supporting the "Trojan horse" theory of *S. aureus* immune evasion.

S. aureus survival in PMN is significantly reduced using an agr-deficient mutant. Furthermore, there was no further decrease in survival in Δagr-infected, VPS34-IN1-treated PMN, indicating that an agr-specific factor is important for autophagy-mediated intracellular survival. Previously, autophagy-dependent intracellular survival in HeLa cells was shown to depend on a factor controlled by the Agr operon (17). Subsequent work on *S. aureus* subversion of the autophagic pathway, has highlighted the role of the agr-regulated secreted toxin α-haemolysin (Hla) in driving the production of autophagosomes which facilitated bacterial replication in non-professional phagocytes (38). Furthermore, Hla expression is also essential for *S. aureus* phagosomal escape from cystic fibrosis epithelial cells (43). However, one study analysing the role of autophagy in *S. aureus* infection *in vivo* demonstrated that the autophagic pathway conferred protection against Hla-mediated toxic effects in a murine model of *S. aureus* systemic infection (44). While autophagy-deficient mice were more susceptible to lethality during *S. aureus* infection, challenge with a Hla-deficient strain led to increased survival. This suggests that the role of Hla in autophagy-mediated intracellular survival is not a straightforward one. Moreover, several studies have reported that Hla can induce cell death in the form of apoptosis and necrosis (45–48). The mechanism of Hla-induced cell death is unclear; some studies report that Hla induces caspase-independent cell death (47) while others report the involvement of Caspase-2, 3 and 8 (45, 46). Our data further implicates the involvement of an agr-specific factor in manipulating the autophagy network in human PMN but whether it is Hla has yet to be determined.

The transcription factor p53 plays a regulatory role in apoptosis and is activated as part of the host response to cellular stress, causing cell cycle arrest and initiating programmed cell death (49, 50). Our results indicate that p53 is activated following autophagy-mediated intracellular survival. This is in contrast to other studies that indicate that p53 is an autophagy inducer (34, 50, 51). However, a recent study has shown that the VPS34/Beclin-1 complex can act as a regulator of p53 due to its regulatory effect on the ubiquitin-specific protease, USP10, which mediates p53 deubiquitination (52). By regulating USP10 activity, the VPS34 autophagy activation complex can control p53 degradation, highlighting a regulatory relationship between the VPS34 complex and p53. In our model, p53 is transcriptionally active as evidenced by an increased expression of *dram*. However, the pro-apoptotic effects of p53 are not evident in our model as we see no significant change in the gene or protein expression of *bax* which is also transcriptionally activated by p53. As well as *dram*, nuclear p53 can drive the transcriptional activation of several autophagy related genes such as *ulk1* and *atg7* (51), and DRAM can directly mediate p53-induced autophagy (34). Expression of *dram* may be re-enforcing the pro-autophagic state in our model. Importantly, we demonstrate that p53 expression can promote autophagy-dependent intracellular survival since p53 inhibition using PFTα resulted in lower intracellular CFU coupled with increased autophagic flux. Decreased *tp53*/*dram* expression was observed after autophagy inhibition, confirming that the pro-autophagic effects of the p53/DRAM pathway are a direct result of *S. aureus*-induced autophagy.

Although DRAM can also drive p53-mediated apoptosis (34), it does not appear to be involved in promoting apoptosis during

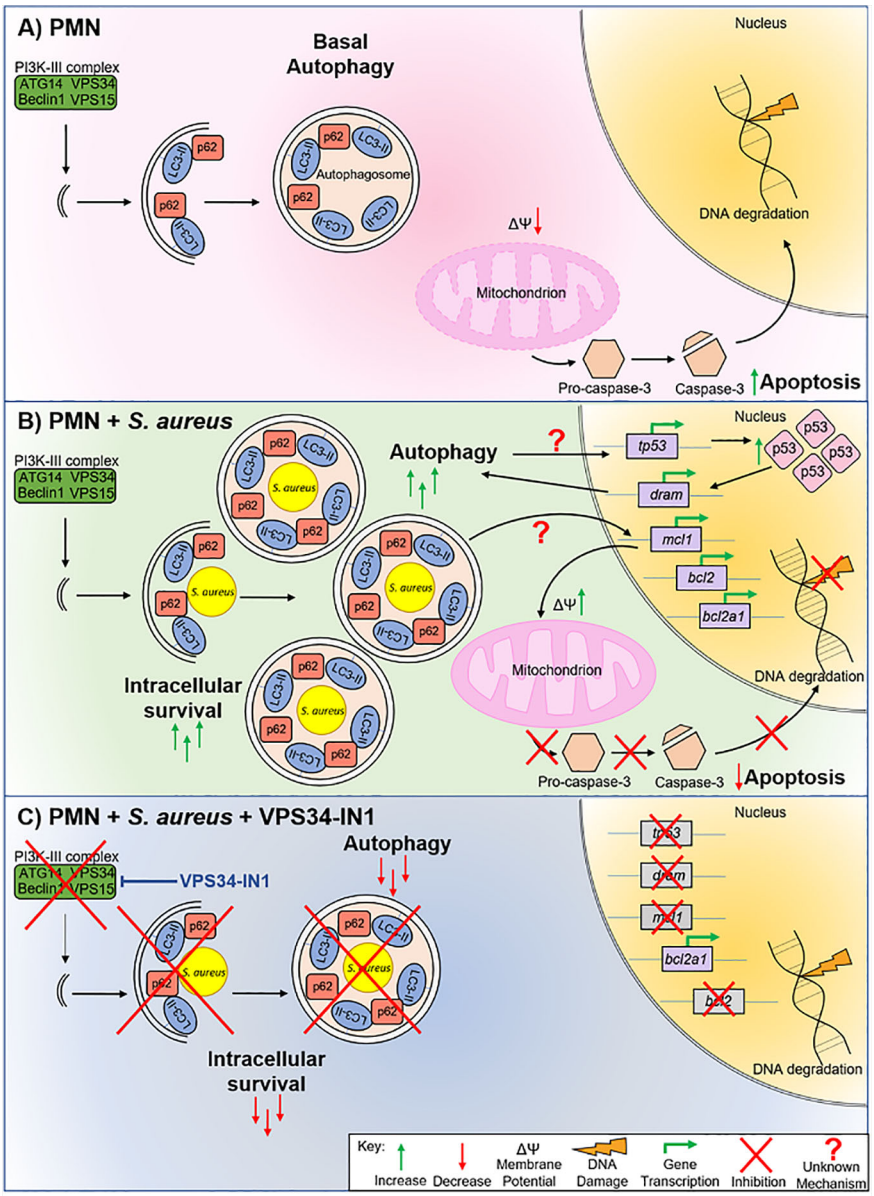

FIGURE 7 | Model of *S. aureus* intracellular survival in human PMN. Uninfected PMN **(A)** undergo basal autophagy. Programmed cell death also occurs *via* mitochondrial depolarization, caspase-3 cleavage and eventual DNA degradation. PMN harboring *S. aureus* **(B)** undergo a higher rate of autophagy. *S. aureus* is encapsulated in autophagosomes which facilitates intracellular survival. Autophagy-mediated intracellular survival triggers *tp53* transcription and p53 protein levels increase in the nucleus. Transcription of pro-autophagic factor *dram*, as well as anti-apoptotic factors *mcl1*, *bcl2* and *bcl2a1*, is increased. As a result of the expression of these anti-apoptotic factors, mitochondrial membrane depolarization is reduced, caspase-3 cleavage is inhibited, and DNA degradation is reduced, indicating a lower rate of apoptosis during intracellular survival. Blocking autophagy using VPS34-IN1 **(C)** decreases intracellular survival of *S. aureus* by removing the availability of an intracellular niche. Blocking autophagy also reduces transcription of *tp53*, *dram*, *mcl1*, and *bcl2* suggesting that crosstalk between the autophagy and apoptotic pathways occurs at this level. DNA degradation is returned to basal levels suggesting that blocking autophagy-mediated intracellular survival partially restores apoptosis in PMN.

S. aureus intracellular survival. Instead, we observed a striking induction of anti-apoptotic factors. Our results suggest that gene expression of Mcl-1 and Bcl-2 are activated as a direct result of autophagy-mediated intracellular survival since blocking autophagy in PMN inhibited the gene expression and lead to a reduction in protein expression of both. Mcl-1 and Bcl-2 can prevent Fas-mediated PMN apoptosis (53) and both are upregulated in PMN from patients with sepsis (54, 55). Furthermore, Mcl-1 and Bcl-2 transcription could protect macrophages from staurosporine-induced apoptosis during *S. aureus* infection (56). Although we saw an increase in Bcl2 gene expression, we could not confirm Bcl-2 protein expression using

Western immunoblotting. The absence of Bcl-2 protein expression in mature neutrophils has been reported previously (57). Expression of *bcl2a1*, which encodes A1/Bfl-1, was significantly upregulated during intracellular survival with a similar increase in protein expression. However, *bcl2a1* expression was not significantly affected by autophagy inhibition and therefore, A1/Bfl-1 may still be exerting some anti-apoptotic effects. This consistent expression of *bcl2a1* may account for why levels of mitochondrial depolarization and caspase-3 cleavage are not completely restored in infected, VPS34-IN1-treated PMN. A1/Bfl-1 has previously been implicated in delaying PMN apoptosis during *Anaplasma phagocytophilum* infection by maintaining high mitochondrial membrane potential and inhibiting caspase-3 activity (58). A1/Bfl-1 has been found to actually bind pro-caspase-3 and prevents its activation in immortalized motor neurons (59) and A1/Bfl-1 has been shown to overcome p53-mediated apoptosis (60). In our study, it seems that any pro-apoptotic effect of p53 is overwhelmed by a potent anti-apoptotic phenotype both linked to autophagy-mediated intracellular survival through Mcl-1 expression, and an autophagy-independent mechanism through A1/Bfl-1 expression. This may be enough to transiently maintain an anti-apoptotic status that is beneficial for intracellular survival. Further study may determine whether this is specifically mediated by a bacterial factor.

Based on our findings, we propose the following model: Under basal conditions, homeostatic autophagy occurs in PMN and PMN undergo spontaneous apoptosis as part of their normal lifespan (**Figure 7A**). After *S. aureus* exposure (**Figure 7B**), PMN harboring *S. aureus* accumulate autophagosomes which act as an intracellular niche. The p53 pathway is activated and p53 accumulates in the nucleus. Nuclear p53 drives transcription of *dram*, reinforcing a pro-autophagic phenotype. Transcription of anti-apoptotic factors *bcl2, mcl1* and *bcl2a1* is activated by autophagy-mediated intracellular survival *via* an unknown mechanism. The expression of these factors appears to be enough to overcome any pro-apoptotic effects of p53, leading to a slower rate of apoptosis as evidenced by inhibition of mitochondrial depolarization, a delay in caspase-3 cleavage and lower levels of DNA degradation. When autophagy is blocked using VPS34-IN1, autophagy-mediated intracellular survival is inhibited (**Figure 7C**). The transcription of *tp53, dram, mcl1* and *bcl2*, but not *bcl2a1* and *bax*, is inhibited following autophagy inhibition, leading to a partially restored apoptotic pathway in PMN.

The findings in this study illustrate that *S. aureus* infection in phagocytes represents a complex host-pathogen interaction. The changes identified in host pathways during intracellular survival present possible therapeutic targets as an additive treatment for *S. aureus* infection. Blanket autophagy inhibition should, however, be pursued with caution as this may lead to undesirable downstream effects for the host. However, inhibitors of anti-apoptotic factors such as Mcl-1, already in development in cancer therapy (61), may restore an appropriate apoptotic pathway in PMN and disrupt the intracellular niche for *S. aureus*. An intricate knowledge of the mechanism of manipulation of both pathways during *S. aureus* infection is crucial prior to providing more targeted treatment.

DATA AVAILABILITY STATEMENT

The raw data supporting the conclusions of this article will be made available by the authors, without undue reservation.

ETHICS STATEMENT

The studies involving human participants were reviewed and approved by School of Biochemistry and Immunology Research Ethics Committee, Trinity College Dublin. The patients/participants provided their written informed consent to participate in this study.

AUTHOR CONTRIBUTIONS

MM, KO'K, and RM conceived and designed experiments. MM, KO'K, EO'B, and NL performed experiments and collected data. MM, EO'B, and EV analyzed the data. MM and RM wrote the manuscript. All authors contributed to the article and approved the submitted version.

FUNDING

This work was supported by a Science Foundation Ireland Investigator Award (15/IA/3041) and a Wellcome Investigator Award (202846/Z/16/Z) to RM.

ACKNOWLEDGMENTS

We thank Andrew Edwards from Imperial College London for the gift of USA300 LAC ΔagrC and its parental strain. We also thank James Murray for his input on the autophagy studies.

SUPPLEMENTARY MATERIAL

The Supplementary Material for this article can be found online at: https://www.frontiersin.org/articles/10.3389/fimmu.2020.565545/full#supplementary-material

SUPPLEMENTARY FIGURE 1 | VPS34-IN1 has no effect on phagocytic uptake of *Staphylococcus aureus* in human neutrophils. Primary human neutrophils were pre-treated with VPS34-IN1 (10 μM) or DMSO for 30 min prior to infection with pre-opsonized *S. aureus* PS80-GFP (MoI 10) for 1 h. Following infection, PMN were treated with gentamicin (200 μg/ml) for 30 min. Cells were fixed and analyzed by flow cytometry. Data are expressed as mean %GFP-positive cells ± SEM (n = 2 donors).

SUPPLEMENTARY FIGURE 2 | VPS34-IN1 treatment may partially restore early apoptosis in PMN harboring *S. aureus*. Primary human neutrophils were left untreated or were pre-treated with VPS34-IN1 (10 μM) and were then infected with pre-opsonized *S. aureus* PS80 (MoI 10) for 1 h. Following infection, PMN were treated with gentamicin (200 μg/ml) for the times indicated. (A) PMN protein lysates were probed for caspase-3 cleavage and analysed using densitometric analysis. Data are expressed as protein expression normalized by β-actin control values for each sample ± SEM (n = 3 donors). (B) PMN were stained with JC-1 dye to measure mitochondrial membrane depolarization and analyzed by flow cytometry (n = 3 donors). Representative FACS plots for JC-1 staining at 3 h. Membrane depolarisation is characterized by a reduction of fluorescence in Fluorescent channel (FL) 2 and corresponding increase in FL1 fluorescence.

SUPPLEMENTARY FIGURE 3 | DRAM protein expression during *Staphylococcus aureus* intracellular survival in neutrophils. Primary human neutrophils were infected with pre-opsonized *S. aureus* PS80 (MoI 10) for 1 h. Following infection, PMN were treated with gentamicin (200 μg/ml) for 3 h. PMN protein lysates were probed for DRAM expression and analysed using densitometric analysis. Data are expressed as protein expression normalized by β-actin control values for each sample ± SEM (n = 2 donors). Two representative blots are shown. Black arrows indicate the area of the blot used for densitometry.

SUPPLEMENTARY FIGURE 4 | *tp53* and *dram* expression after Pifithrin-α treatment during *Staphylococcus aureus* intracellular survival in neutrophils. Primary human neutrophils were treated with Pifithrin-α (30μM) or were left untreated and were then infected with pre-opsonized *S. aureus* PS80 (MoI 10) for 1 h. Following infection, PMN were treated with gentamicin (200 μg/ml) for the times indicated. RNA was extracted and gene expression levels of (A) *tp53* and (B) *dram* were assessed using quantitative RT-PCR. Gene expression is plotted relative to gene expression in control PMN after normalization to 18s RNA ± SEM (n = 2 donors).

REFERENCES

1. van Hal SJ, Jensen SO, Vaska VL, Espedido BA, Paterson DL, Gosbell IB. Predictors of mortality in *Staphylococcus aureus* Bacteremia. *Clin Microbiol Rev* (2012) 25:362–86. doi: 10.1128/CMR.05022-11
2. Shorr AF, Tabak YP, Killian AD, Gupta V, Liu LZ, Kollef MH. Healthcare-associated bloodstream infection: A distinct entity? Insights from a large U.S. database. *Crit Care Med* (2006) 34:2588–95. doi: 10.1097/01.CCM.0000239121.09533.09
3. Vos FJ, Kullberg BJ, Sturm PD, Krabbe PF, van Dijk AP, Wanten GJ, et al. Metastatic infectious disease and clinical outcome in *Staphylococcus aureus* and *Streptococcus* species bacteremia. *Med (Baltimore)* (2012) 91:86–94. doi: 10.1097/MD.0b013e31824d7ed2
4. Khatib R, Johnson LB, Fakih MG, Riederer K, Khosrovaneh A, Shamse Tabriz M, et al. Persistence in *Staphylococcus aureus* bacteremia: incidence, characteristics of patients and outcome. *Scand J Infect Dis* (2006) 38:7–14. doi: 10.1080/00365540500372846
5. Thwaites GE, Gant V. Are bloodstream leukocytes Trojan Horses for the metastasis of *Staphylococcus aureus*? *Nat Rev Microbiol* (2011) 9:215–22. doi: 10.1038/nrmicro2508
6. Holland SM. Chronic granulomatous disease. *Hematol Oncol Clin North Am* (2013) 27:89–99, viii. doi: 10.1016/j.hoc.2012.11.002
7. van den Berg JM, van Koppen E, Ahlin A, Belohradsky BH, Bernatowska E, Corbeel L, et al. Chronic granulomatous disease: the European experience. *PloS One* (2009) 4:e5234. doi: 10.1371/journal.pone.0005234
8. Gresham HD, Lowrance JH, Caver TE, Wilson BS, Cheung AL, Lindberg FP. Survival of *Staphylococcus aureus* inside neutrophils contributes to infection. *J Immunol* (2000) 164:3713–22. doi: 10.4049/jimmunol.164.7.3713
9. McLoughlin RM, Solinga RM, Rich J, Zaleski KJ, Cocchiaro JL, Risley A, et al. CD4+ T cells and CXC chemokines modulate the pathogenesis of *Staphylococcus aureus* wound infections. *Proc Natl Acad Sci U S A* (2006) 103:10408–13. doi: 10.1073/pnas.0508961103
10. McLoughlin RM, Lee JC, Kasper DL, Tzianabos AO. IFN-gamma regulated chemokine production determines the outcome of *Staphylococcus aureus* infection. *J Immunol* (2008) 181:1323–32. doi: 10.4049/jimmunol.181.2.1323
11. Sendi P, Proctor RA. Staphylococcus aureus as an intracellular pathogen: the role of small colony variants. *Trends Microbiol* (2009) 17:54–8. doi: 10.1016/j.tim.2008.11.004
12. Fraunholz M, Sinha B. Intracellular Staphylococcus aureus: live-in and let die. *Front Cell Infect Microbiol* (2012) 2:43. doi: 10.3389/fcimb.2012.00043
13. Strobel M, Pfortner H, Tuchscherr L, Volker U, Schmidt F, Kramko N, et al. Post-invasion events after infection with Staphylococcus aureus are strongly dependent on both the host cell type and the infecting S. aureus strain. *Clin Microbiol Infect* (2016) 22:799–809. doi: 10.1016/j.cmi.2016.06.020
14. Kubica M, Guzik K, Koziel J, Zarebski M, Richter W, Gajkowska B, et al. A potential new pathway for Staphylococcus aureus dissemination: the silent survival of S. aureus phagocytosed by human monocyte-derived macrophages. *PloS One* (2008) 3:e1409. doi: 10.1371/journal.pone.0001409
15. Jorch SK, Surewaard BG, Hossain M, Peiseler M, Deppermann C, Deng J, et al. Peritoneal GATA6+ macrophages function as a portal for Staphylococcus aureus dissemination. *J Clin Invest* (2019) 129:4643–56. doi: 10.1172/JCI127286
16. O'Keeffe KM, Wilk MM, Leech JM, Murphy AG, Laabei M, Monk IR, et al. Manipulation of Autophagy in Phagocytes Facilitates *Staphylococcus aureus* Bloodstream Infection. *Infect Immun* (2015) 83:3445–57. doi: 10.1128/IAI.00358-15
17. Schnaith A, Kashkar H, Leggio SA, Addicks K, Kronke M, Krut O. *Staphylococcus aureus* subvert autophagy for induction of caspase-independent host cell death. *J Biol Chem* (2007) 282:2695–706. doi: 10.1074/jbc.M609784200
18. Neumann Y, Bruns SA, Rohde M, Prajsnar TK, Foster SJ, Schmitz I. Intracellular *Staphylococcus aureus* eludes selective autophagy by activating a host cell kinase. *Autophagy* (2016) 12:2069–84. doi: 10.1080/15548627.2016.1226732
19. Xie Z, Klionsky DJ. Autophagosome formation: core machinery and adaptations. *Nat Cell Biol* (2007) 9:1102–9. doi: 10.1038/ncb1007-1102
20. He C, Klionsky DJ. Regulation mechanisms and signaling pathways of autophagy. *Annu Rev Genet* (2009) 43:67–93. doi: 10.1146/annurev-genet-102808-114910
21. Itakura E, Kishi C, Inoue K, Mizushima N. Beclin 1 forms two distinct phosphatidylinositol 3-kinase complexes with mammalian Atg14 and UVRAG. *Mol Biol Cell* (2008) 19:5360–72. doi: 10.1091/mbc.e08-01-0080
22. Kabeya Y, Mizushima N, Ueno T, Yamamoto A, Kirisako T, Noda T, et al. LC3, a mammalian homologue of yeast Apg8p, is localized in autophagosome membranes after processing. *EMBO J* (2000) 19:5720–8. doi: 10.1093/emboj/19.21.5720
23. Pillay J, den Braber I, Vrisekoop N, Kwast LM, de Boer RJ, Borghans JA, et al. In vivo labeling with 2H2O reveals a human neutrophil lifespan of 5.4 days. *Blood* (2010) 116:625–7. doi: 10.1182/blood-2010-01-259028
24. Lotz S, Aga E, Wilde I, van Zandbergen G, Hartung T, Solbach W, et al. Highly purified lipoteichoic acid activates neutrophil granulocytes and delays their spontaneous apoptosis via CD14 and TLR2. *J Leukoc Biol* (2004) 75:467–77. doi: 10.1189/jlb.0803360
25. Greenlee-Wacker MC, Rigby KM, Kobayashi SD, Porter AR, DeLeo FR, Nauseef WM. Phagocytosis of *Staphylococcus aureus* by human neutrophils prevents macrophage efferocytosis and induces programmed necrosis. *J Immunol* (2014) 192:4709–17. doi: 10.4049/jimmunol.1302692
26. Pader V, Hakim S, Painter KL, Wigneshweraraj S, Clarke TB, Edwards AM. *Staphylococcus aureus* inactivates daptomycin by releasing membrane phospholipids. *Nat Microbiol* (2016) 2:16194. doi: 10.1038/nmicrobiol.2016.194
27. Painter KL, Hall A, Ha KP, Edwards AM. The Electron Transport Chain Sensitizes *Staphylococcus aureus* and *Enterococcus faecalis* to the Oxidative Burst. *Infect Immun* (2017) 85(12):e00659–17. doi: 10.1128/IAI.00659-17
28. Musilova J, Mulcahy ME, Kuijk MM, McLoughlin RM, Bowie AG. Toll-like receptor 2-dependent endosomal signaling by Staphylococcus aureus in monocytes induces type I interferon and promotes intracellular survival. *J Biol Chem* (2019) 294:17031–42. doi: 10.1074/jbc.RA119.009302
29. Schwartz JT, Barker JH, Kaufman J, Fayram DC, McCracken JM, Allen L-AH. *Francisella tularensis* Inhibits the Intrinsic and Extrinsic Pathways To Delay

Constitutive Apoptosis and Prolong Human Neutrophil Lifespan. *J Immunol* (2012) 188:3351. doi: 10.4049/jimmunol.1102863
30. Witko-Sarsat V, Mocek J, Bouayad D, Tamassia N, Ribeil J-A, Candalh C, et al. Proliferating cell nuclear antigen acts as a cytoplasmic platform controlling human neutrophil survival. *J Exp Med* (2010) 207:2631–45. doi: 10.1084/jem.20092241
31. Xu Y, Loison F, Luo HR. Neutrophil spontaneous death is mediated by down-regulation of autocrine signaling through GPCR, PI3Kγ, ROS, and actin. *Proc Natl Acad Sci* (2010) 107:2950–5. doi: 10.1073/pnas.0912717107
32. Yamamoto A, Tagawa Y, Yoshimori T, Moriyama Y, Masaki R, Tashiro Y. Bafilomycin A1 prevents maturation of autophagic vacuoles by inhibiting fusion between autophagosomes and lysosomes in rat hepatoma cell line, H-4-II-E cells. *Cell Struct Funct* (1998) 23:33–42. doi: 10.1247/csf.23.33
33. Klionsky DJ, Elazar Z, Seglen PO, Rubinsztein DC. Does bafilomycin A1 block the fusion of autophagosomes with lysosomes? *Autophagy* (2008) 4:849–50. doi: 10.4161/auto.6845
34. Crighton D, Wilkinson S, O'Prey J, Syed N, Smith P, Harrison PR, et al. DRAM, a p53-induced modulator of autophagy, is critical for apoptosis. *Cell* (2006) 126:121–34. doi: 10.1016/j.cell.2006.05.034
35. Budanov AV, Shoshani T, Faerman A, Zelin E, Kamer I, Kalinski H, et al. Identification of a novel stress-responsive gene Hi95 involved in regulation of cell viability. *Oncogene* (2002) 21:6017–31. doi: 10.1038/sj.onc.1205877
36. Zhang Y, Xiong Y. A p53 amino-terminal nuclear export signal inhibited by DNA damage-induced phosphorylation. *Science* (2001) 292:1910–5. doi: 10.1126/science.1058637
37. Fowler VGJr., Olsen MK, Corey GR, Woods CW, Cabell CH, Reller LB, et al. Clinical identifiers of complicated Staphylococcus aureus bacteremia. *Arch Intern Med* (2003) 163:2066–72. doi: 10.1001/archinte.163.17.2066
38. Mestre MB, Fader CM, Sola C, Colombo MI. Alpha-hemolysin is required for the activation of the autophagic pathway in *Staphylococcus aureus*-infected cells. *Autophagy* (2010) 6:110–25. doi: 10.4161/auto.6.1.10698
39. Chargui A, Cesaro A, Mimouna S, Fareh M, Brest P, Naquet P, et al. Subversion of autophagy in adherent invasive *Escherichia coli*-infected neutrophils induces inflammation and cell death. *PloS One* (2012) 7:e51727. doi: 10.1371/journal.pone.0051727
40. Prajsnar TK, Serba JJ, Dekker BM, Gibson JF, Masud S, Fleming A, et al. The autophagic response to Staphylococcus aureus provides an intracellular niche in neutrophils. *Autophagy* (2020) 15:1–15. doi: 10.1080/15548627.2020.1739443:1-15
41. Ocana MG, Asensi V, Montes AH, Meana A, Celada A, Valle-Garay E. Autoregulation mechanism of human neutrophil apoptosis during bacterial infection. *Mol Immunol* (2008) 45:2087–96. doi: 10.1016/j.molimm.2007.10.013
42. Pollitt EJG, Szkuta PT, Burns N, Foster SJ. Staphylococcus aureus infection dynamics. *PloS Pathog* (2018) 14:e1007112. doi: 10.1371/journal.ppat.1007112
43. Jarry TM, Memmi G, Cheung AL. The expression of alpha-haemolysin is required for Staphylococcus aureus phagosomal escape after internalization in CFT-1 cells. *Cell Microbiol* (2008) 10:1801–14. doi: 10.1111/j.1462-5822.2008.01166.x
44. Maurer K, Reyes-Robles T, Alonzo F,3, Durbin J, Torres VJ, Cadwell K. Autophagy mediates tolerance to Staphylococcus aureus alpha-toxin. *Cell Host Microbe* (2015) 17:429–40. doi: 10.1016/j.chom.2015.03.001
45. Bantel H, Sinha B, Domschke W, Peters G, Schulze-Osthoff K, Janicke RU. alpha-Toxin is a mediator of Staphylococcus aureus-induced cell death and activates caspases via the intrinsic death pathway independently of death receptor signaling. *J Cell Biol* (2001) 155:637–48. doi: 10.1083/jcb.200105081
46. Imre G, Heering J, Takeda AN, Husmann M, Thiede B, zu Heringdorf DM, et al. Caspase-2 is an initiator caspase responsible for pore-forming toxin-mediated apoptosis. *EMBO J* (2012) 31:2615–28. doi: 10.1038/emboj.2012.93
47. Haslinger-Loffler B, Wagner B, Bruck M, Strangfeld K, Grundmeier M, Fischer U, et al. Staphylococcus aureus induces caspase-independent cell death in human peritoneal mesothelial cells. *Kidney Int* (2006) 70:1089–98. doi: 10.1038/sj.ki.5001710
48. Essmann F, Bantel H, Totzke G, Engels IH, Sinha B, Schulze-Osthoff K, et al. Staphylococcus aureus alpha-toxin-induced cell death: predominant necrosis despite apoptotic caspase activation. *Cell Death Differ* (2003) 10:1260–72. doi: 10.1038/sj.cdd.4401301
49. Haupt S, Berger M, Goldberg Z, Haupt Y. Apoptosis - the p53 network. *J Cell Sci* (2003) 116:4077–85. doi: 10.1242/jcs.00739
50. Maiuri MC, Galluzzi L, Morselli E, Kepp O, Malik SA, Kroemer G. Autophagy regulation by p53. *Curr Opin Cell Biol* (2010) 22:181–5. doi: 10.1016/j.ceb.2009.12.001
51. Kenzelmann Broz D, Spano Mello S, Bieging KT, Jiang D, Dusek RL, Brady CA, et al. Global genomic profiling reveals an extensive p53-regulated autophagy program contributing to key p53 responses. *Genes Dev* (2013) 27:1016–31. doi: 10.1101/gad.212282.112
52. Liu J, Xia H, Kim M, Xu L, Li Y, Zhang L, et al. Beclin1 controls the levels of p53 by regulating the deubiquitination activity of USP10 and USP13. *Cell* (2011) 147:223–34. doi: 10.1016/j.cell.2011.08.037
53. Croker BA, O'Donnell JA, Nowell CJ, Metcalf D, Dewson G, Campbell KJ, et al. Fas-mediated neutrophil apoptosis is accelerated by Bid, Bak, and Bax and inhibited by Bcl-2 and Mcl-1. *Proc Natl Acad Sci U S A* (2011) 108:13135–40. doi: 10.1073/pnas.1110358108
54. Harter L, Mica L, Stocker R, Trentz O, Keel M. Mcl-1 correlates with reduced apoptosis in neutrophils from patients with sepsis. *J Am Coll Surg* (2003) 197:964–73. doi: 10.1016/j.jamcollsurg.2003.07.008
55. Andina N, Conus S, Schneider EM, Fey MF, Simon HU. Induction of Bim limits cytokine-mediated prolonged survival of neutrophils. *Cell Death Differ* (2009) 16:1248–55. doi: 10.1038/cdd.2009.50
56. Koziel J, Maciag-Gudowska A, Mikolajczyk T, Bzowska M, Sturdevant DE, Whitney AR, et al. Phagocytosis of *Staphylococcus aureus* by macrophages exerts cytoprotective effects manifested by the upregulation of antiapoptotic factors. *PloS One* (2009) 4:e5210. doi: 10.1371/journal.pone.0005210
57. Moulding DA, Akgul C, Derouet M, White MR, Edwards SW. BCL-2 family expression in human neutrophils during delayed and accelerated apoptosis. *J Leukoc Biol* (2001) 70:783–92. doi: 10.1189/jlb.70.5.783
58. Ge Y, Yoshiie K, Kuribayashi F, Lin M, Rikihisa Y. Anaplasma phagocytophilum inhibits human neutrophil apoptosis via upregulation of bfl-1, maintenance of mitochondrial membrane potential and prevention of caspase 3 activation. *Cell Microbiol* (2005) 7:29–38. doi: 10.1111/j.1462-5822.2004.00427.x
59. Iaccarino C, Mura ME, Esposito S, Carta F, Sanna G, Turrini F, et al. Bcl2-A1 interacts with pro-caspase-3: Implications for amyotrophic lateral sclerosis. *Neurobiol Dis* (2011) 43:642–50. doi: 10.1016/j.nbd.2011.05.013
60. D'Sa-Eipper C, Subramanian T, Chinnadurai G. bfl-1, a bcl-2 homologue, suppresses p53-induced apoptosis and exhibits potent cooperative transforming activity. *Cancer Res* (1996) 56:3879–82. doi: 10.1101/gad.252603
61. Xiang W, Yang CY, Bai L. MCL-1 inhibition in cancer treatment. *Onco Targets Ther* (2018) 11:7301–14. doi: 10.2147/OTT.S146228

Conflict of Interest: The authors declare that the research was conducted in the absence of any commercial or financial relationships that could be construed as a potential conflict of interest.

frontiers in Immunology

MINI REVIEW
published: 12 November 2020
doi: 10.3389/fimmu.2020.603951

An Interplay Between Autophagy and Immunometabolism for Host Defense Against Mycobacterial Infection

Seungwha Paik[1,2] *and Eun-Kyeong Jo*[1,2]*

[1] Department of Microbiology, Chungnam National University School of Medicine, Daejeon, South Korea, [2] Infection Control Convergence Research Center, Chungnam National University School of Medicine, Daejeon, South Korea

Autophagy, an intracellular catabolic pathway featuring lysosomal degradation, is a central component of the host immune defense against various infections including *Mycobacterium tuberculosis* (Mtb), the pathogen that causes tuberculosis. Mtb can evade the autophagic defense and drive immunometabolic remodeling of host phagocytes. Co-regulation of the autophagic and metabolic pathways may play a pivotal role in shaping the innate immune defense and inflammation during Mtb infection. Two principal metabolic sensors, AMP-activated protein kinase (AMPK) and mammalian target of rapamycin (mTOR) kinase, function together to control the autophagy and immunometabolism that coordinate the anti-mycobacterial immune defense. Here, we discuss our current understanding of the interplay between autophagy and immunometabolism in terms of combating intracellular Mtb, and how AMPK-mTOR signaling regulates antibacterial autophagy in terms of Mtb infection. We describe several autophagy-targeting agents that promote host antimicrobial defenses by regulating the AMPK-mTOR axis. A better understanding of the crosstalk between immunometabolism and autophagy, both of which are involved in host defense, is crucial for the development of innovative targeted therapies for tuberculosis.

Keywords: autophagy, immunometabolism, host defense, mycobacterial infection, AMP-activated protein kinase, mammalian target of rapamycin

OPEN ACCESS

Edited by:
Jere W. McBride, University of Texas Medical Branch at Galveston, United States

Reviewed by:
Annemarie H. Meijer, Leiden University, Netherlands
Chul-Su Yang, Hanyang University, South Korea

***Correspondence:**
Eun-Kyeong Jo
hayoungj@cnu.ac.kr

Specialty section:
This article was submitted to Microbial Immunology, a section of the journal Frontiers in Immunology

Received: *08 September 2020*
Accepted: *16 October 2020*
Published: *12 November 2020*

Citation:
Paik S and Jo E-K (2020) An Interplay Between Autophagy and Immunometabolism for Host Defense Against Mycobacterial Infection. Front. Immunol. 11:603951. doi: 10.3389/fimmu.2020.603951

INTRODUCTION

Mycobacterium tuberculosis (Mtb) causes human tuberculosis (TB), which remains a serious infectious disease worldwide (1). Mtb can counter host defenses by escaping phagolysosomal fusion, indeed residing within phagosomal structures (2, 3). Autophagy, a lysosomal degradation system that ensures homeostasis, is particularly sensitive to metabolic stress (4, 5). Autophagy is also a principal means of autonomous cellular defense, countering the Mtb-induced arrest of phagosomal maturation (6). Accumulating evidence suggests that immunometabolism is linked to regulation of the immune defense against pathogenic insults (7–12). Indeed, autophagy and immunometabolism interact extensively to control infection and inflammation (13, 14). Such crosstalk may determine the outcome of the innate effector pathways against a variety of infectious diseases, including TB.

Two serine/threonine kinases, adenosine 5′-monophosphate (AMP)-activated protein kinase (AMPK) and mammalian target of rapamycin (mTOR) kinase, play crucial roles in the integration of metabolic adaptation, autophagy, and immunometabolism in immune cells (15–17). The kinases sense intracellular metabolic status and serve as important upstream signaling regulators of immune responses, lysosomal activities, and host defenses during infections (15–17). Recent studies have highlighted the fact that transcription factor EB (TFEB) is a key mediator of the AMPK-mTOR axis (18), activating both autophagy and lysosomal biogenesis to promote innate immunity (19–21).

In this review, we discuss our current understanding of how autophagy and immunometabolism have a relationship when mounting a defense against Mtb infection. We describe recent advances in our understanding of AMPK-mTOR kinase signaling and pharmacological modulation of either or both autophagy and immunometabolism.

ROLE PLAYED BY AUTOPHAGY IN MYCOBACTERIAL INFECTION

Recent studies have highlighted the fact that a combination of metabolic, autophagic, and immune cell activities determine the outcome of Mtb infection (22, 23). Autophagy is a crucial host defense pathway targeting invasive intracellular pathogens including Mtb (24–26). In 2004, Deretic et al. found that interferon (IFN)-γ, a cytokine essential for induction of protective immunity against TB, activated macrophage autophagy to promote eradication of intracellular Mtb (27). Since that time, accumulating evidence has shown that many autophagy-activating pharmacological agents and/or small molecules trigger autophagy, leading to acidification of mycobacterial phagosomes by fusion with autophagosomes/lysosomes to restrict intracellular survival of Mtb (25, 26, 28–30).

During natural infection, Mtb translocation into the cytosol *via* ESX-1 triggers xenophagy pathway through p62-, NDP-52 (a selective autophagic receptor)–, and TBK-1–dependent pathways (31–33). In addition, the autophagy-related process LC3-associated phagocytosis (LAP) plays a role in phagosomal maturation and antimicrobial host defense (34, 35); however, Mtb CpsA, a LytR-CpsA-Psr (LCP) domain-containing protein, works to evade LAP during Mtb infection (36). The detailed mechanisms of several types of autophagy pathways in the context of mycobacterial infection have been extensively described elsewhere (25, 26, 28–30). In addition, a discussion of the Mtb effectors that induce, or allow evasion of, host xenophagy/LAP is beyond the scope of this review.

OVERVIEW OF IMMUNOMETABOLISM DURING MYCOBACTERIAL INFECTION

Metabolic reprogramming of innate immune cells is closely related to various cellular functions, including the production of pro-inflammatory cytokines/chemokines, autophagy activation, and mounting of antimicrobial responses to Mtb infection (22, 23, 37). It is generally thought that, upon Mtb infection, macrophages (the principal phagocytes active during infection) undergo metabolic reprogramming into M1-type macrophages in response to Mtb components or *via* Mtb phagocytosis. In these cells, pro-inflammatory molecules are upregulated and glycolysis is predominantly utilized to meet their bioenergetic and metabolic requirements, while M2-type macrophages and the non-infected/naïve cells exhibit anti-inflammatory characteristic and derive their energy from oxidative phosphorylation and fatty acid β-oxidation (FAO) (23). However, Mtb is able to perturb the metabolic switch of phagocytes that reminisce Warburg effect, a bioenergetic shift utilizing aerobic glycolysis, to facilitate bacterial pathogenesis *via* enhancement of intracellular bacterial survival and persistence (38). To support this, a recent study showed that Mtb infection restricts glycolysis and interleukin (IL)-1β production by upregulating miR-21, thereby favoring intracellular Mtb growth (39). Given the previous reports on how miR-21 inhibits autophagy in a variety of scenarios (40–42), it would be interesting to explore whether miR-21 suppresses autophagy to potentiate immunopathogenesis during Mtb infection. During chronic Mtb infection, the mitochondrial metabolism of CD8+ T cells becomes defective; mitochondrial dysfunction increases (37). It remains to be determined whether aerobic glycolysis is up- or down-regulated during chronic Mtb infection. Importantly, metformin, an activator of AMPK and autophagy, improved Mtb-specific CD8+ T cell immunity by rescuing T cell bioenergetics (37), although autophagy was not investigated in the context of such metformin-induced reinvigoration. It would be useful to clarify the function and mechanism of autophagy in the regulation of immunometabolic remodeling, and how this impacts host defenses during the various stages of Mtb infection.

It is also intriguing that Mtb-infected host cells exhibit different aspects of metabolic shift depending on the virulence of Mtb strains. A previous study revealed that genes associated with inflammation and metabolism were downregulated in virulent H37Rv strain when compared to attenuated H37Ra strain infection in human alveolar macrophages (43). In other studies, Mtb infection compromised metabolic reprogramming, while infection with the BCG or dead Mtb upregulated glycolytic flux in human monocyte-derived macrophages (44). Multidrug-resistant Mtb strains preferentially induce IFN-β that limits IL-1β induction, resulting reduced aerobic glycolysis when compared to drug susceptible Mtb strains (45). Since infections with live, virulent Mtb decelerate the metabolic switch shifting to glycolytic pathway of host cells, the future studies unveiling the molecular mechanisms controlled by mTOR and/or AMPK, which are master regulators of immunometabolism, in terms of virulence of Mtb strains will accelerate the development of anti-mycobacterial therapeutics.

Mtb modulates (interferes with) host cell lipid metabolism during infection. Mtb induces numerous proteins involved in

FAO; the lipids yield energy and act as building blocks for membrane synthesis (46). It remains to be determined whether FAO may suppress the host defense against Mtb infection. Either FAO blockade or a deficiency of the mitochondrial fatty acid transporter carnitine palmitoyltransferase 2 reduces the burden of Mtb both *in vitro* and *in vivo*. Mechanistically, FAO inhibition enhances mitochondrial reactive oxygen species (mitoROS) production, promoting NADPH oxidase activity and xenophagy in macrophages infected with Mtb (47). The activation of the peroxisome proliferator-activated receptor (PPAR)-α enhances an anti-mycobacterial immune defense by promoting lipid catabolism, and autophagy *via* TFEB (48). Although PPAR-α activation promotes the transcriptional activation of genes involved in FAO in macrophages (48), it should be clarified whether PPAR-α–mediated FAO drives anti-mycobacterial effects. Given the findings that blockade of FAO contributes to the antimicrobial host defense (47), future studies are needed to elucidate how the lipid metabolic reprogramming is linked to host autophagy/lipophagy to further regulate host defense against Mtb infection.

Recent studies showed that *de novo* fatty acid synthesis (FAS) is crucial in terms of the T cell immune defense during Mtb infection, whereas FAS does not affect the innate immune responses (49). An elevated level of oxidized low-density lipoprotein (oxLDL) promotes macrophage (lysosomal) cholesterol accumulation, which leads to lysosomal dysfunction, thus impairing the control of intracellular Mtb (50). These data may explain the link between diabetes mellitus (DM) and TB through oxLDL (50). DM patients usually exhibit elevated oxLDL levels and are susceptible to TB, presumably and partly due to lysosomal dysfunction (50). In accordance with these findings, simvastatin, which reduces plasma cholesterol levels, shows protective functions against Mtb infection in several different ways (51). It inhibits intracellular Mtb growth in human peripheral blood mononuclear cells, increases the proportion of natural killer T cells, promotes production of IL-1β and IL-12p70, and activates monocyte autophagy (51). In addition, statin, the cholesterol-lowering drug, inhibits intracellular Mtb growth in human macrophages through activation of autophagy and phagosomal maturation (52). Although the precise mechanisms that induce autophagy by statins have not been fully elucidated, these findings strongly suggest that inhibitors of cholesterol synthesis and/or oxLDLs may have potential therapeutic value for TB and

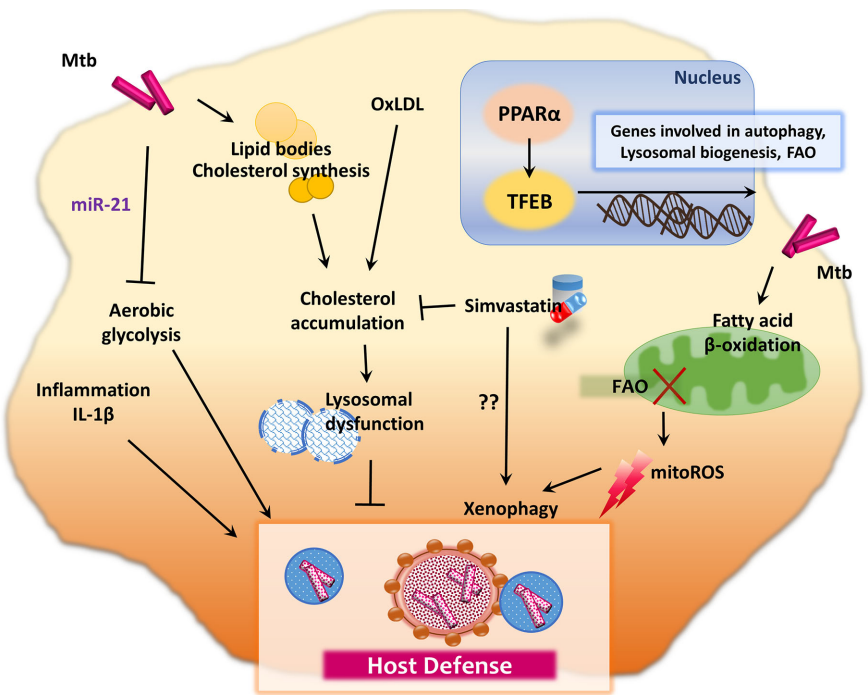

FIGURE 1 | Immunometabolic pathway during mycobacterial infection. Mtb intervene in host cell lipid metabolism for its own intracellular survival. During the metabolic reprogramming process, innate immune responses are induced to regulate the host defense system. For example, Mtb infection in macrophages restricts aerobic glycolysis and IL-1β production through upregulation of miR-21. Moreover, Mtb utilizes lipid synthesis and FAO process to obtain energy and building blocks for membrane synthesis. Inhibition of FAO leads to the enhancement of mitoROS, which promote xenophagy in macrophages infected with Mtb. However, there are also controversial results that FAO is promoted by PPAR-α, which mediates anti-mycobacterial immune defense through lysosomal biogenesis and autophagy activation, *via* TFEB. The elevation of oxLDL promotes the macrophage lysosomal dysfunction, which contributes to impaired control of intracellular Mtb and host defense. Simvastatin, an oral HMG-CoA reductase inhibitor, decreases plasma cholesterol levels and exhibits host protection against Mtb through autophagy induction in monocytes.

DM comorbidity. **Figure 1** summarizes immunometabolic regulation in macrophages during infection with Mtb, which further modulate host immunometabolism.

AMPK-MTOR AXIS CO-REGULATES AUTOPHAGY AND IMMUNOMETABOLISM

Both the AMPK and mTOR kinases are key metabolic and autophagic sensors. AMPK regulates energy metabolism and mitochondrial function (53, 54) as well as numerous biological pathways including autophagy, inflammation, and the host defense (17, 55–57). The AMPK pathway primarily activates mitochondrial metabolism, oxidative phosphorylation, and lipolysis and attenuates FAS and cholesterol biosynthesis (58, 59). AMPK enhances autophagy *via* ULK1 complex activation and mTOR complex 1 (mTORC1) inhibition (60, 61). By contrast, mTOR kinases (mTORC1 and mTORC2) suppress autophagy when energy levels are high (60). Both mTORC1 and AMPK function to integrate metabolic and autophagic signaling (60, 62), and are thus primary therapeutic targets for pulmonary TB (63, 64). The schematic overview of AMPK-mTOR axis regulating autophagy and immunometabolism is summarized in **Figure 2**.

AMPK REGULATES AUTOPHAGY AND METABOLISM OF THE INNATE HOST DEFENSE SYSTEM

AMPK: A Linker of Autophagy and Immunometabolism

AMPK activation by 5-aminoimidazole-4-carboxamide ribonucleotide (AICAR) or metformin counters Mtb infection (65–67). However, our understanding of the immunometabolic regulation of AMPK-mediated autophagic activators is incomplete in the context with host defense against Mtb infection. Recent studies have shown that certain metabolites stimulate the innate host defense *via* AMPK activation. In Mtb-infected Kupffer cells, both ornithine and imidazole inhibited intracellular Mtb growth; ornithine, but not imidazole, enhanced autophagy *via* AMPK activation (68). Future studies will identify how AMPK-activating metabolites restrict Mtb

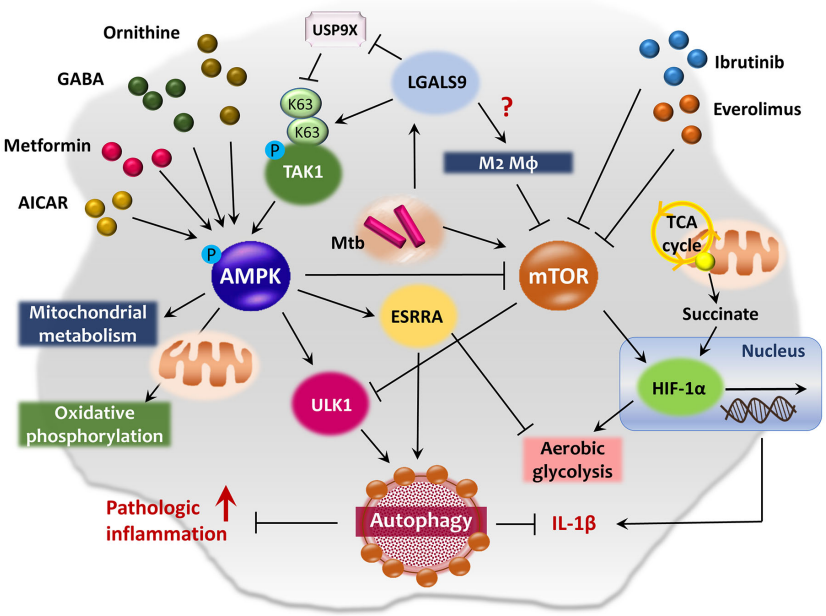

FIGURE 2 | AMPK-mTOR axis in the co-regulation of autophagy and immunometabolism. AMPK pathway primarily activates mitochondrial metabolism and oxidative phosphorylation, and induces autophagy through the activation of ULK1 and inhibition of mTOR pathway. AMPK activation by AICAR, metformin, ornithine or GABA exhibits antimicrobial effects against Mtb infection in macrophages. ESRRA is one of the AMPK-downstream signaling molecule which functions as an important transcription factor of ATGs and energy metabolism. Upon lysosomal damage, cytosolic lectin LGALS9 dissociates deubiquitinase USP9X from TAK1 and promotes K63-mediated ubiquitination of TAK1, thus leading to the activation of AMPK pathway. Whereas, the mTOR pathway activation promotes aerobic glycolysis and contributes Mtb to escape from autophagic degradation in host cells by blocking ULK1 complex formation. Meanwhile, mTOR signaling is closely related to HIF-1α expression in the regulation of immunometabolism during infection and aerobic glycolysis in both normal and cancer cells. Several anticancer drugs, such as ibrutinib and everolimus, induce autophagy and repress Mtb growth *via* inhibition of mTOR pathway in macrophages. In addition, succinate, an intermediate of TCA cycle, stimulates IL-1β production *via* HIF-1α activation in LPS-exposed macrophages.

growth. The metabolite and neurotransmitter gamma-aminobutyric acid (GABA) also activates AMPK, contributing to peripheral GABAergic host defenses by enhancing autophagy and phagosomal maturation during Mtb infection (69). GABA-mediated antibacterial autophagy requires the intracellular calcium influx that triggers AMPK signaling and transcriptional activation of autophagy-related genes (ATGs) including GABA type A receptor-associated protein-like 1 (GABARAPL1; an Atg8 homolog) (69).

AMPK and hypoxia-inducible factor (HIF)-1α are master regulators in the context of cancer-related aerobic glycolysis and oxidative phosphorylation. While AMPK negatively regulates both aerobic glycolysis and cellular biosynthesis, HIF-1α favors the growth advantage of cancer cells with reduced AMPK signaling (70). During Mtb infection, HIF-1α induces metabolic shift to aerobic glycolysis that amplifies macrophage activation and essentially mediates IFN-γ–dependent control of intracellular Mtb growth (71, 72). Future studies are recommended how the balance of AMPK signaling and HIF-1α pathway interplay to regulate host defense, and coordinates immunometabolism and autophagy in the context of Mtb infection.

Downstream Signals of the AMPK Pathway

Although the cited studies strongly suggest that AMPK pathway contributes to antimicrobial host defenses by activating autophagy, we do not yet fully understand how AMPK connects with downstream signaling molecules when co-regulating autophagy and immunometabolism. Recent studies found that estrogen-related receptor α (ESRRA) served as an AMPK-downstream signaling molecule, regulating transcriptional and post-translational modification of autophagy proteins (73). The transcription factor ESRRA affects mitochondrial biogenesis, energy metabolism (74), and immunometabolic remodeling (toward oxidative phosphorylation) during the development of innate immune responses (75). It would be interesting to explore whether ESRRA regulation of immunometabolism is linked to xenophagy during Mtb infection. Moreover, glucocorticoid signaling can also activate AMPK downstream pathways, which result in the induction of autophagy/mitophagy in skeletal muscle cells (76). Given the findings that GLP-1-directed glucocorticoid action reverses metabolic inflammation and obesity in obese mice (77), it would be interesting to investigate whether glucocorticoid signaling links host autophagy to metabolic reprogramming and how it regulates host defense against Mtb infection. Future mechanistic studies will close the gaps in our understanding of the mechanisms underlying AMPK-mediated orchestration of autophagy, immunometabolism, and host defense. These efforts will facilitate the development of novel therapeutics for TB through targeting AMPK pathway.

Upstream Signals of the AMPK Pathway

How is AMPK activated by Mtb infection? Recent studies have provided some answers. Several stimuli (including Mtb infection) trigger lysosomal membrane breaches detected by the cytosolic lectin LGALS9/galectin-9 (78). Lysosomal damage signals transduced by LGALS9 trigger dissociation of USP9X from the TAK1 complex, thus promoting K63-mediated ubiquitination of TAK1 (78). TAK1 (an upstream kinase) activates AMPK, autophagy, and antimicrobial responses to Mtb infection (79). Thus, the galectin and ubiquitin systems co-operate to activate AMPK-induced autophagy after lysosomal damage (79, 80). The cited studies did not explore the effects of LGALS9 on immunometabolism during lysosomal damage, but recent works on tumor-associated macrophages found that LGALS9 interacts with CD206 on M2 macrophages, driving angiogenesis and the production of chemokines including monocyte chemoattractant protein (MCP)-1 (81). It will be interesting to investigate immunometabolic regulation of LGALS9-AMPK pathways in the context of Mtb infection.

THE MTOR PATHWAY LINKS AUTOPHAGY AND IMMUNOMETABOLISM

Earlier studies found that Mtb and components thereof activate mTOR and Akt pathway signaling by host phagocytes (65, 82, 83). The Akt/mTOR pathway triggers gene expression and enzyme activity, promoting aerobic glycolysis in both normal and cancer cells (84, 85). Akt/mTOR signaling is closely linked to HIF-1α expression in the context of immunometabolic regulation during infection (86), and cancer-related aerobic glycolysis and tumor progression (87). In activated CD4+ T cells, pro-inflammatory tumor necrosis factor (TNF)-α production is mediated through glycolytic activity *via* the mTOR and HIF-1α pathways (88). In lipopolysaccharide (LPS)-exposed macrophages, the tricarboxylic acid (TCA) cycle intermediate succinate stimulates IL-1β production *via* HIF-1α activation (89). Recent studies highlight that HIF-1α is required for canonical and noncanonical autophagy to impact antifungal immunity (90, 91). However, it remains elucidated whether Akt/mTOR/HIF-1α signaling coordinates aerobic glycolysis and autophagy pathway to regulate host defense against Mtb infection.

The ability of Mtb to activate the Akt/mTOR pathway blocks ULK1 complex formation by phosphorylating it, which is one of the main components required for the autophagosome generation, allowing the bacterium to escape autophagic degradation by host cells (64). Several drugs/agents inhibit mTOR pathway activation, thereby promoting antimicrobial effects during Mtb infection. For example, the anti-chronic lymphocytic leukemia drug ibrutinib inhibited Mtb growth both *in vitro* and *in vivo*, activating autophagy *via* inhibition of the BTK/Akt/mTOR pathway (92). The effects of ibrutinib on M2 polarization and immunosuppression of nurse-like cells have been described; these cells are a subset of tumor-associated macrophages found in patients with chronic lymphocytic leukemia (93). However, it is not known whether ibrutinib-mediated autophagy activation changes the energy metabolism of host macrophages. The anticancer drug everolimus inhibits mTOR, activates autophagy, and exhibits antimicrobial effects during Mtb infection (64, 94). It is well known that everolimus shifts macrophage polarization toward the M2 phenotype and

downregulates the production of pro-inflammatory cytokines, thus improving the experimental outcomes of autoimmune neuritis (95). These data strongly suggest that mTOR inhibition activates antibacterial autophagy and anti-inflammatory M2-type macrophages. Indeed, mitochondrial oxidative phosphorylation and FAO are closely related to the shift to M2-like macrophages (96, 97). Thus, the mTOR-HIF-1α-mediated interplay between autophagy and immunometabolism is highly complex and require extensive molecular dissection to delineate host defensive mechanisms. An open question is whether mTOR/HIF-1α axis is a common defensive pathway through promoting glycolysis, or plays a unique protective or detrimental function directed at distinct stages of Mtb infection.

TFEB: A POTENTIAL COORDINATOR OF AUTOPHAGY AND METABOLISM DURING INFECTION

TFEB is a member of the MiT-TFE family of basic helix-loop-helix leucine-zipper transcription factors and a key regulator of lysosome biogenesis and autophagy (21, 98). Nuclear translocation of TFEB is required for the transcriptional activation of genes encoding autophagosomes and lysosomes; such translocation is regulated by mTOR-dependent phosphorylation of TFEB on Ser(211) (99). Emerging evidence suggests that TFEB is involved in mitochondrial quality control, maintaining metabolic homeostasis and mitochondrial biogenesis (100, 101). TFEB is also required for the expression of genes of mitochondrial biogenesis, FAO, and oxidative phosphorylation (102).

Several studies have suggested that the TFEB signaling axis is a promising target for autophagy-based host-directed therapeutics against Mtb. Activation of the adopted orphan nuclear receptor subfamily 1, group D, member 1 (NR1D1) by the agonist GSK4112 enhanced the autophagosomal and antimycobacterial functions of macrophages *via* TFEB activation (103). Recent studies have shown that SIRT3 is essential for development of anti-mycobacterial responses; SIRT3 activates PPAR-α–mediated TFEB nuclear translocation (104). Indeed, TFEB transcriptional activity is directly regulated by PPAR-α, a nuclear receptor involved in the regulation of metabolism, inflammation, and host defenses (48, 105, 106). However, the cited studies did not directly examine the role of TFEB in the regulation of immunometabolism in the context of mycobacterial infection. NR1D1 is a key integrator of metabolism with the circadian clock and inhibits pro-inflammatory M1 macrophages and NLRP3 inflammasome activation (107). SIRT3 and PPAR-α play crucial roles in mitochondrial quality control, oxidative phosphorylation, and FAO in various cell types (108, 109). Thus, TFEB, and its upstream signaling molecules, may orchestrate immunometabolism, autophagy, and the inflammatory response during Mtb infection.

A recent study found that immunity-related GTPase M (IRGM) and GABARAP interacted with TFEB to affect the mTOR pathway, further activating lysosomal biogenesis (110). Thus, a complicated upstream signaling network involving ATG8 proteins, IRGM, and tripartite motif family (TRIM) may perturb mTOR signaling to enhance TFEB nuclear translocation, activate lysosomal biogenesis, and trigger autophagic maturation during Mtb infection. Indeed, AMPK-mediated, lysosomal catabolic activity is mediated by MCOLN1/mucolipin 1, the lysosomal calcium channel (111), and TFEB (18, 112). Notably, the MCOLN1-TFEB pathway is essential for the host defense mediated by the disaccharide trehalose during co-infection with TB and human immunodeficiency virus (HIV) (113). Trehalose eliminates the HIV-induced impairment of xenophagic flux by enhancing nuclear translocation and activation of TFEB and MCOLN1/mucolipin 1 (113). As trehalose-mediated TFEB activation usefully inhibits atherogenic lipid accumulation by enhancing lysosomal autophagy (114, 115), it is possible that TFEB-mediated regulation of lipid metabolism is associated with the trehalose-induced antimicrobial activities in macrophages against Mtb (either alone or during co-infection with HIV). Future studies should address the immunometabolic regulation of TFEB in terms of activation of lysosomal biogenesis during Mtb infection. The pharamacological agents that facilitate host defense against Mtb infection discussed in the paper are summarized in **Table 1**.

TABLE 1 | Pharmacological agents that facilitate host defense against Mtb infection by regulating autophagy and immunometabolism.

Drugs/agents	Mechanisms	Effects	References
Simvastatin	HMG-CoA reductase inhibition	Inhibits plasma cholesterol levels and intracellular Mtb growth; Increases natural killer T cells, production of IL-1β and IL-12p70, and monocyte autophagy	(51)
AICAR	AMPK activation	Induces autophagy, phagosomal maturation, and antimicrobial responses against Mtb infection	(65)
Metformin	AMPK activation	Inhibits intracellular Mtb growth and TB immunopathology; Enhances efficacy of conventional anti-TB drugs	(66, 67)
Ornithine	AMPK activation	Inhibits intracellular Mtb growth through AMPK-mediated autophagy	(68)
GABA	AMPK activation	Enhances autophagy and phagosomal maturation during Mtb infection	(69)
Ibrutinib	BTK/Akt/mTOR pathway inhibition	Activates autophagy *via* inhibition of the BTK/Akt/mTOR pathway; Inhibits Mtb growth both *in vitro* and *in vivo*	(92)
Everolimus	mTOR inhibition	Inhibits mTOR pathway; Activates autophagy and antimicrobial effects during Mtb infection	(64, 94)
GSK4112	TFEB activation *via* NR1D1 stimulation	Enhances autophagosomal and antimycobacterial functions *via* TFEB activation	(103)
Trehalose	MCOLN1-TFEB pathway activation	Kills intracellular Mtb or NTMs by activating TFEB nuclear translocation *via* MCOLN1	(113)

AICAR 5-aminoimidazole-4-carboxamide ribonucleotide; AMPK, adenosine 5′-monophosphate-activated protein kinase; Mtb, mycobacterium tuberculosis; TB, tuberculosis; GABA, gamma-aminobutyric acid; BTK, Bruton's tyrosine kinase; mTOR, mammalian target of rapamycin; TFEB, transcription factor EB; MCOLN1, mucolipin 1.

CONCLUSION

Mtb infection triggers immunometabolic remodeling of host cells. Activation of autophagy in response to metabolic and infectious stresses further shapes immunometabolism; this determines the outcome of the host defense. We have begun to understand how autophagy and immunometabolism interact within various cell types during Mtb infection. During Mtb infection, macrophage metabolic shift to aerobic glycolysis appears to contribute antimicrobial host defense through activation of M1 macrophage-mediated inflammation. However, Mtb has evolved several strategies to evade from host glycolytic flux. Modulation of lipid metabolism may activate or inhibit host antimicrobial defense in different contexts, *via* connections with autophagy. Coordination of autophagy and immunometabolic remodeling may play important roles in terms of both the effector mechanisms in play and minimization of pathological inflammation during TB infection. However, the regulators of, and mechanisms whereby, autophagy and immunometabolism combine to mount an efficient defense during Mtb infection remain poorly known. In addition, the *in vivo* relationships between autophagy and immunometabolism are difficult to predict from *in vitro* data on individual cell types.

AMPK activation and mTOR inhibition may be of therapeutic utility against human TB. The AMPK signaling is well-known for its activity to enhance antibacterial autophagy against Mtb infection. However, it also promotes mitochondrial function and oxidative phosphorylation, but not aerobic glycolysis, and shifts macrophages toward the M2 type, potentially supporting microbial growth within host cells. In addition, mTOR-HIF-α pathway activation promotes aerobic glycolysis and inflammation, inducing granuloma formation and the host innate defense early during infection. However, uncontrolled activation of inflammation may trigger extensive immunopathology and neutrophil-mediated inflammation, negatively influencing the TB-infected host. Thus, the balanced activation of AMPK-mTOR axis may contribute to the control and/or clearance of intracellular Mtb and promotes host protective immune responses during infection.

Activation of TFEB, a key transcriptional factor of autophagy/lysosomal biogenesis, is regulated by the AMPK-mTOR axis. Future studies are warranted to elucidate whether and how TFEB-mediated lipid metabolism and autophagy activation are interconnected together in the context of host defense against Mtb infection. Although much remains to be learned about the interplay between autophagy and immunometabolism by which TFEB mediates its antimicrobial effects, its potential as a therapeutic target against TB will fuel further investigations into its coordination mechanisms. Our extensive knowledge of linking autophagy with immunometabolism that drive protective anti-TB immunity will help further development of novel host-directed therapeutics against Mtb infection.

AUTHOR CONTRIBUTIONS

All authors contributed to the article and approved the submitted version.

FUNDING

This work was supported by the National Research Foundation of Korea (NRF), grant funded by the Korea government (MSIT) (No. 2017R1A5A2015385) and by the framework of international cooperation program managed by National Research Foundation of Korea (2015K2A2A6002008).

ACKNOWLEDGMENTS

We are indebted to current and past members of our Medical Research Center (*i*-MRC) for discussions and investigations that contributed to this article. We apologize to colleagues whose work and publications could not be referenced owing to space constraints.

REFERENCES

1. World Health Organization. *Global Tuberculosis Report 2019* (2020). Available at: https://www.who.int/tb/global-report-2019 (Accessed September 8, 2020).
2. Queval CJ, Brosch R, Simeone R. The Macrophage: A Disputed Fortress in the Battle against *Mycobacterium tuberculosis*. *Front Microbiol* (2017) 8:2284:2284. doi: 10.3389/fmicb.2017.02284
3. Steinberg BE, Grinstein S. Pathogen destruction versus intracellular survival: the role of lipids as phagosomal fate determinants. *J Clin Invest* (2008) 118 (6):2002–11. doi: 10.1172/JCI35433
4. Ren J, Sowers JR, Zhang Y. Metabolic Stress, Autophagy, and Cardiovascular Aging: from Pathophysiology to Therapeutics. *Trends Endocrinol Metab* (2018) 29(10):699–711. doi: 10.1016/j.tem.2018.08.001
5. Sanchez-Martin P, Komatsu M. Physiological Stress Response by Selective Autophagy. *J Mol Biol* (2020) 432(1):53–62. doi: 10.1016/j.jmb.2019.06.013
6. Deretic V. Autophagy, an immunologic magic bullet: *Mycobacterium tuberculosis* phagosome maturation block and how to bypass it. *Future Microbiol* (2008) 3(5):517–24. doi: 10.2217/17460913.3.5.517
7. Pearce EJ, Pearce EL. Immunometabolism in 2017: Driving immunity: all roads lead to metabolism. *Nat Rev Immunol* (2018) 18(2):81–2. doi: 10.1038/nri.2017.139
8. Russell DG, Huang L, VanderVen BC. Immunometabolism at the interface between macrophages and pathogens. *Nat Rev Immunol* (2019) 19(5):291–304. doi: 10.1038/s41577-019-0124-9
9. Shi L, Jiang Q, Bushkin Y, Subbian S, Tyagi S. Biphasic Dynamics of Macrophage Immunometabolism during *Mycobacterium tuberculosis* Infection. *mBio* (2019) 10(2):e02550-18. doi: 10.1128/mBio.02550-18
10. Benmoussa K, Garaude J, Acin-Perez R. How Mitochondrial Metabolism Contributes to Macrophage Phenotype and Functions. *J Mol Biol* (2018) 430 (21):3906–21. doi: 10.1016/j.jmb.2018.07.003
11. Zhang S, Carriere J, Lin X, Xie N, Feng P. Interplay between Cellular Metabolism and Cytokine Responses during Viral Infection. *Viruses* (2018) 10(10):521. doi: 10.3390/v10100521
12. Van den Bossche J, Saraber DL. Metabolic regulation of macrophages in tissues. *Cell Immunol* (2018) 330:54–9. doi: 10.1016/j.cellimm.2018.01.009
13. Ramond E, Jamet A, Coureuil M, Charbit A. Pivotal Role of Mitochondria in Macrophage Response to Bacterial Pathogens. *Front Immunol* (2019) 10:2461. doi: 10.3389/fimmu.2019.02461
14. Gabande-Rodriguez E, Gomez de Las Heras MM, Mittelbrunn M. Control of Inflammation by Calorie Restriction Mimetics: On the Crossroad of Autophagy and Mitochondria. *Cells* (2019) 9(1):82. doi: 10.3390/cells9010082

15. Saravia J, Raynor JL, Chapman NM, Lim SA, Chi H. Signaling networks in immunometabolism. *Cell Res* (2020) 30(4):328–42. doi: 10.1038/s41422-020-0301-1
16. Savini M, Zhao Q, Wang MC. Lysosomes: Signaling Hubs for Metabolic Sensing and Longevity. *Trends Cell Biol* (2019) 29(11):876–87. doi: 10.1016/j.tcb.2019.08.008
17. Jo EK, Silwal P, Yuk JM. AMPK-Targeted Effector Networks in Mycobacterial Infection. *Front Microbiol* (2019) 10:520. doi: 10.3389/fmicb.2019.00520
18. Collodet C, Foretz M, Deak M, Bultot L, Metairon S, Viollet B, et al. AMPK promotes induction of the tumor suppressor FLCN through activation of TFEB independently of mTOR. *FASEB J* (2019) 33(11):12374–91. doi: 10.1096/fj.201900841R
19. El-Houjeiri L, Possik E, Vijayaraghavan T, Paquette M, Martina JA, Kazan JM, et al. The Transcription Factors TFEB and TFE3 Link the FLCN-AMPK Signaling Axis to Innate Immune Response and Pathogen Resistance. *Cell Rep* (2019) 26(13):3613–28.e6. doi: 10.1016/j.celrep.2019.02.102
20. Sardiello M. Transcription factor EB: from master coordinator of lysosomal pathways to candidate therapeutic target in degenerative storage diseases. *Ann N Y Acad Sci* (2016) 1371(1):3–14. doi: 10.1111/nyas.13131
21. Napolitano G, Ballabio A. TFEB at a glance. *J Cell Sci* (2016) 129(13):2475–81. doi: 10.1242/jcs.146365
22. Howard NC, Khader SA. Immunometabolism during *Mycobacterium tuberculosis* Infection. *Trends Microbiol* (2020) 28(10):832–50. doi: 10.1016/j.tim.2020.04.010
23. Kumar R, Singh P, Kolloli A, Shi L, Bushkin Y, Tyagi S, et al. Immunometabolism of Phagocytes During *Mycobacterium tuberculosis* Infection. *Front Mol Biosci* (2019) 6:105. doi: 10.3389/fmolb.2019.00105
24. Mendes AC, Ciccone M, Gazolla B, Bahia D. Epithelial Haven and Autophagy Breakout in Gonococci Infection. *Front Cell Dev Biol* (2020) 8:439. doi: 10.3389/fcell.2020.00439
25. Bergman P, Raqib R, Rekha RS, Agerberth B, Gudmundsson GH. Host Directed Therapy Against Infection by Boosting Innate Immunity. *Front Immunol* (2020) 11:1209. doi: 10.3389/fimmu.2020.01209
26. Chai Q, Wang L, Liu CH, Ge B. New insights into the evasion of host innate immunity by *Mycobacterium tuberculosis*. *Cell Mol Immunol* (2020) 17(9):901–13. doi: 10.1038/s41423-020-0502-z
27. Gutierrez MG, Master SS, Singh SB, Taylor GA, Colombo MI, Deretic V. Autophagy is a defense mechanism inhibiting BCG and *Mycobacterium tuberculosis* survival in infected macrophages. *Cell* (2004) 119(6):753–66. doi: 10.1016/j.cell.2004.11.038
28. Dara Y, Volcani D, Shah K, Shin K, Venketaraman V. Potentials of Host-Directed Therapies in Tuberculosis Management. *J Clin Med* (2019) 8(8):1166. doi: 10.3390/jcm8081166
29. Kim YS, Silwal P, Kim SY, Yoshimori T, Jo EK. Autophagy-activating strategies to promote innate defense against mycobacteria. *Exp Mol Med* (2019) 51(12):1–10. doi: 10.1038/s12276-019-0290-7
30. .Ferluga J, Yasmin H, Al-Ahdal MN, Bhakta S, Kishore U. Natural and trained innate immunity against *Mycobacterium tuberculosis*. *Immunobiology* (2020) 225(3):151951. doi: 10.1016/j.imbio.2020.151951
31. Munz C. Selective macroautophagy for immunity. *Immunity* (2010) 32(3):298–9. doi: 10.1016/j.immuni.2010.03.002
32. Manzanillo PS, Ayres JS, Watson RO, Collins AC, Souza G, Rae CS, et al. The ubiquitin ligase parkin mediates resistance to intracellular pathogens. *Nature* (2013) 501(7468):512–6. doi: 10.1038/nature12566
33. Watson RO, Manzanillo PS, Cox JS. Extracellular *M. tuberculosis* DNA targets bacteria for autophagy by activating the host DNA-sensing pathway. *Cell* (2012) 150(4):803–15. doi: 10.1016/j.cell.2012.06.040
34. Abnave P, Mottola G, Gimenez G, Boucherit N, Trouplin V, Torre C, et al. Screening in planarians identifies MORN2 as a key component in LC3-associated phagocytosis and resistance to bacterial infection. *Cell Host Microbe* (2014) 16(3):338–50. doi: 10.1016/j.chom.2014.08.002
35. Cheng Y, Schorey JS. Extracellular vesicles deliver *Mycobacterium* RNA to promote host immunity and bacterial killing. *EMBO Rep* (2019) 20(3):e46613. doi: 10.15252/embr.201846613
36. Koster S, Upadhyay S, Chandra P, Papavinasasundaram K, Yang G, Hassan A, et al. *Mycobacterium tuberculosis* is protected from NADPH oxidase and LC3-associated phagocytosis by the LCP protein CpsA. *Proc Natl Acad Sci USA* (2017) 114(41):E8711–E20. doi: 10.1073/pnas.1707792114
37. Russell SL, Lamprecht DA, Mandizvo T, Jones TT, Naidoo V, Addicott KW, et al. Compromised Metabolic Reprogramming Is an Early Indicator of CD8(+) T Cell Dysfunction during Chronic *Mycobacterium tuberculosis* Infection. *Cell Rep* (2019) 29(11):3564–79.e5. doi: 10.1016/j.celrep.2019.11.034
38. Shi L, Eugenin EA, Subbian S. Immunometabolism in Tuberculosis. *Front Immunol* (2016) 7:150. doi: 10.3389/fimmu.2016.00150
39. Hackett EE, Charles-Messance H, O'Leary SM, Gleeson LE, Munoz-Wolf N, Case S, et al. *Mycobacterium tuberculosis* Limits Host Glycolysis and IL-1beta by Restriction of PFK-M via MicroRNA-21. *Cell Rep* (2020) 30(1):124–36.e4. doi: 10.1016/j.celrep.2019.12.015
40. Gu Y, Fei Z, Zhu R. miR-21 modulates cisplatin resistance of gastric cancer cells by inhibiting autophagy via the PI3K/Akt/mTOR pathway. *Anticancer Drugs* (2020) 31(4):385–93. doi: 10.1097/CAD.0000000000000886
41. Huang S, Lin Y, Liang Z, Wu Z, Chen Y, Chen C. Erythropoietin helix B surface peptide modulates miR-21/Atg12 axis to alleviates cardiomyocyte hypoxia-reoxygenation injury. *Am J Transl Res* (2019) 11(4):2422–30.
42. Wang WJ, Yang W, Ouyang ZH, Xue JB, Li XL, Zhang J, et al. MiR-21 promotes ECM degradation through inhibiting autophagy via the PTEN/akt/mTOR signaling pathway in human degenerated NP cells. *BioMed Pharmacother* (2018) 99:725–34. doi: 10.1016/j.biopha.2018.01.154
43. Silver RF, Walrath J, Lee H, Jacobson BA, Horton H, Bowman MR, et al. Human alveolar macrophage gene responses to *Mycobacterium tuberculosis* strains H37Ra and H37Rv. *Am J Respir Cell Mol Biol* (2009) 40(4):491–504. doi: 10.1165/rcmb.2008-0219OC
44. Cumming BM, Addicott KW, Adamson JH, Steyn AJ. *Mycobacterium tuberculosis* induces decelerated bioenergetic metabolism in human macrophages. *Elife* (2018) 7:e39169. doi: 10.7554/eLife.39169
45. Howard NC, Marin ND, Ahmed M, Rosa BA, Martin J, Bambouskova M, et al. *Mycobacterium tuberculosis* carrying a rifampicin drug resistance mutation reprograms macrophage metabolism through cell wall lipid changes. *Nat Microbiol* (2018) 3(10):1099–108. doi: 10.1038/s41564-018-0245-0
46. Barisch C, Soldati T. Breaking fat! How mycobacteria and other intracellular pathogens manipulate host lipid droplets. *Biochimie* (2017) 141:54–61. doi: 10.1016/j.biochi.2017.06.001
47. Chandra P, He L, Zimmerman M, Yang G, Koster S, Ouimet M, et al. Inhibition of Fatty Acid Oxidation Promotes Macrophage Control of *Mycobacterium tuberculosis*. *mBio* (2020) 11(4):e01139-20. doi: 10.1128/mBio.01139-20
48. Kim YS, Lee HM, Kim JK, Yang CS, Kim TS, Jung M, et al. PPAR-alpha Activation Mediates Innate Host Defense through Induction of TFEB and Lipid Catabolism. *J Immunol* (2017) 198(8):3283–95. doi: 10.4049/jimmunol.1601920
49. Stuve P, Minarrieta L, Erdmann H, Arnold-Schrauf C, Swallow M, Guderian M, et al. De Novo Fatty Acid Synthesis During Mycobacterial Infection Is a Prerequisite for the Function of Highly Proliferative T Cells, But Not for Dendritic Cells or Macrophages. *Front Immunol* (2018) 9:495. doi: 10.3389/fimmu.2018.00495
50. Vrieling F, Wilson L, Rensen PCN, Walzl G, Ottenhoff THM, Joosten SA. Oxidized low-density lipoprotein (oxLDL) supports *Mycobacterium tuberculosis* survival in macrophages by inducing lysosomal dysfunction. *PloS Pathog* (2019) 15(4):e1007724. doi: 10.1371/journal.ppat.1007724
51. Guerra-De-Blas PDC, Bobadilla-Del-Valle M, Sada-Ovalle I, Estrada-Garcia I, Torres-Gonzalez P, Lopez-Saavedra A, et al. Simvastatin Enhances the Immune Response Against *Mycobacterium tuberculosis*. *Front Microbiol* (2019) 10:2097. doi: 10.3389/fmicb.2019.02097
52. Parihar SP, Guler R, Khutlang R, Lang DM, Hurdayal R, Mhlanga MM, et al. Statin therapy reduces the *mycobacterium tuberculosis* burden in human macrophages and in mice by enhancing autophagy and phagosome maturation. *J Infect Dis* (2014) 209(5):754–63. doi: 10.1093/infdis/jit550
53. Lin SC, Hardie DG. AMPK: Sensing Glucose as well as Cellular Energy Status. *Cell Metab* (2018) 27(2):299–313. doi: 10.1016/j.cmet.2017.10.009
54. Hardie DG, Lin SC. AMP-activated protein kinase - not just an energy sensor. *F1000Res* (2017) 6:1724. doi: 10.12688/f1000research.11960.1
55. Jansen T, Kvandova M, Daiber A, Stamm P, Frenis K, Schulz E, et al. The AMP-Activated Protein Kinase Plays a Role in Antioxidant Defense and

Regulation of Vascular Inflammation. *Antioxid (Basel)* (2020) 9(6):525. doi: 10.3390/antiox9060525
56. Tong X, Ganta RR, Liu Z. AMP-activated protein kinase (AMPK) regulates autophagy, inflammation and immunity and contributes to osteoclast differentiation and functionabs. *Biol Cell* (2020) 112(9):251–64. doi: 10.1111/boc.202000008
57. Li Y, Chen Y. AMPK and Autophagy. *Adv Exp Med Biol* (2019) 1206:85–108. doi: 10.1007/978-981-15-0602-4_4
58. Lyons CL, Roche HM. Nutritional Modulation of AMPK-Impact upon Metabolic-Inflammation. *Int J Mol Sci* (2018) 19(10):3092. doi: 10.3390/ijms19103092
59. Fullerton MD, Steinberg GR, Schertzer JD. Immunometabolism of AMPK in insulin resistance and atherosclerosis. *Mol Cell Endocrinol* (2013) 366 (2):224–34. doi: 10.1016/j.mce.2012.02.004
60. Inoki K, Kim J, Guan KL. AMPK and mTOR in cellular energy homeostasis and drug targets. *Annu Rev Pharmacol Toxicol* (2012) 52:381–400. doi: 10.1146/annurev-pharmtox-010611-134537
61. Kim J, Kundu M, Viollet B, Guan KL. AMPK and mTOR regulate autophagy through direct phosphorylation of Ulk1. *Nat Cell Biol* (2011) 13(2):132–41. doi: 10.1038/ncb2152
62. Wang H, Liu Y, Wang D, Xu Y, Dong R, Yang Y, et al. The Upstream Pathway of mTOR-Mediated Autophagy in Liver Diseases. *Cells* (2019) 8 (12):1597. doi: 10.3390/cells8121597
63. Sachan M, Srivastava A, Ranjan R, Gupta A, Pandya S, Misra A. Opportunities and Challenges for Host-Directed Therapies in Tuberculosis. *Curr Pharm Des* (2016) 22(17):2599–604. doi: 10.2174/1381612822666160128150636
64. Singh P, Subbian S. Harnessing the mTOR Pathway for Tuberculosis Treatment. *Front Microbiol* (2018) 9:70. doi: 10.3389/fmicb.2018.00070
65. Yang CS, Kim JJ, Lee HM, Jin HS, Lee SH, Park JH, et al. The AMPK-PPARGC1A pathway is required for antimicrobial host defense through activation of autophagy. *Autophagy* (2014) 10(5):785–802. doi: 10.4161/auto.28072
66. Yew WW, Chang KC, Chan DP, Zhang Y. Metformin as a host-directed therapeutic in tuberculosis: Is there a promise? *Tuberculosis (Edinb)* (2019) 115:76–80. doi: 10.1016/j.tube.2019.02.004
67. Singhal A, Jie L, Kumar P, Hong GS, Leow MK, Paleja B, et al. Metformin as adjunct antituberculosis therapy. *Sci Transl Med* (2014) 6(263):263ra159. doi: 10.1126/scitranslmed.3009885
68. Sivangala Thandi R, Radhakrishnan RK, Tripathi D, Paidipally P, Azad AK, Schlesinger LS, et al. Ornithine-A urea cycle metabolite enhances autophagy and controls *Mycobacterium tuberculosis* infection. *Nat Commun* (2020) 11 (1):3535. doi: 10.1038/s41467-020-17310-5
69. Kim JK, Kim YS, Lee HM, Jin HS, Neupane C, Kim S, et al. GABAergic signaling linked to autophagy enhances host protection against intracellular bacterial infections. *Nat Commun* (2018) 9(1):4184. doi: 10.1038/s41467-018-06487-5
70. Faubert B, Boily G, Izreig S, Griss T, Samborska B, Dong Z, et al. AMPK is a negative regulator of the Warburg effect and suppresses tumor growth in vivo. *Cell Metab* (2013) 17(1):113–24. doi: 10.1016/j.cmet.2012.12.001
71. Braverman J, Sogi KM, Benjamin D, Nomura DK, Stanley SA. HIF-1alpha Is an Essential Mediator of IFN-gamma-Dependent Immunity to *Mycobacterium tuberculosis*. *J Immunol* (2016) 197(4):1287–97. doi: 10.4049/jimmunol.1600266
72. Knight M, Stanley S. HIF-1alpha as a central mediator of cellular resistance to intracellular pathogens. *Curr Opin Immunol* (2019) 60:111–6. doi: 10.1016/j.coi.2019.05.005
73. Kim SY, Yang CS, Lee HM, Kim JK, Kim YS, Kim YR, et al. ESRRA (estrogen-related receptor alpha) is a key coordinator of transcriptional and post-translational activation of autophagy to promote innate host defense. *Autophagy* (2018) 14(1):152–68. doi: 10.1080/15548627.2017.1339001
74. Giguere V. Transcriptional control of energy homeostasis by the estrogen-related receptors. *Endocr Rev* (2008) 29(6):677–96. doi: 10.1210/er.2008-0017
75. Yuk JM, Kim TS, Kim SY, Lee HM, Han J, Dufour CR, et al. Orphan Nuclear Receptor ERRalpha Controls Macrophage Metabolic Signaling and A20 Expression to Negatively Regulate TLR-Induced Inflammation. *Immunity* (2015) 43(1):80–91. doi: 10.1016/j.immuni.2015.07.003
76. Troncoso R, Paredes F, Parra V, Gatica D, Vasquez-Trincado C, Quiroga C, et al. Dexamethasone-induced autophagy mediates muscle atrophy through mitochondrial clearance. *Cell Cycle* (2014) 13(14):2281–95. doi: 10.4161/cc.29272
77. Quarta C, Clemmensen C, Zhu Z, Yang B, Joseph SS, Lutter D, et al. Molecular Integration of Incretin and Glucocorticoid Action Reverses Immunometabolic Dysfunction and Obesity. *Cell Metab* (2017) 26(4):620–32 e6. doi: 10.1016/j.cmet.2017.08.023
78. Jia J, Bissa B, Brecht L, Allers L, Choi SW, Gu Y, et al. AMPK is activated during lysosomal damage via a galectin-ubiquitin signal transduction system. *Autophagy* (2020) 16(8):1550–2. doi: 10.1080/15548627.2020.1788890
79. Jia J, Bissa B, Brecht L, Allers L, Choi SW, Gu Y, et al. AMPK, a Regulator of Metabolism and Autophagy, Is Activated by Lysosomal Damage via a Novel Galectin-Directed Ubiquitin Signal Transduction System. *Mol Cell* (2020) 77 (5):951–69.e9. doi: 10.1016/j.molcel.2019.12.028
80. Jia J, Claude-Taupin A, Gu Y, Choi SW, Peters R, Bissa B, et al. MERIT, a cellular system coordinating lysosomal repair, removal and replacement. *Autophagy* (2020) 16(8):1539–41. doi: 10.1080/15548627.2020.1779451
81. Enninga EAL, Chatzopoulos K, Butterfield JT, Sutor SL, Leontovich AA, Nevala WK, et al. CD206-positive myeloid cells bind galectin-9 and promote a tumor-supportive microenvironment. *J Pathol* (2018) 245(4):468–77. doi: 10.1002/path.5093
82. Maiti D, Bhattacharyya A, Basu J. Lipoarabinomannan from *Mycobacterium tuberculosis* promotes macrophage survival by phosphorylating Bad through a phosphatidylinositol 3-kinase/Akt pathway. *J Biol Chem* (2001) 276 (1):329–33. doi: 10.1074/jbc.M002650200
83. Pathak SK, Basu S, Basu KK, Banerjee A, Pathak S, Bhattacharyya A, et al. Direct extracellular interaction between the early secreted antigen ESAT-6 of *Mycobacterium tuberculosis* and TLR2 inhibits TLR signaling in macrophages. *Nat Immunol* (2007) 8(6):610–8. doi: 10.1038/ni1468
84. Conciatori F, Bazzichetto C, Falcone I, Pilotto S, Bria E, Cognetti F, et al. Role of mTOR Signaling in Tumor Microenvironment: An Overview. *Int J Mol Sci* (2018) 19(8):2453. doi: 10.3390/ijms19082453
85. Robey RB, Hay N. Is Akt the "Warburg kinase"?-Akt-energy metabolism interactions and oncogenesis. *Semin Cancer Biol* (2009) 19(1):25–31. doi: 10.1016/j.semcancer.2008.11.010
86. Goncalves SM, Duarte-Oliveira C, Campos CF, Aimanianda V, Ter Horst R, Leite L, et al. Phagosomal removal of fungal melanin reprograms macrophage metabolism to promote antifungal immunity. *Nat Commun* (2020) 11(1):2282. doi: 10.1038/s41467-020-16120-z
87. Weng ML, Chen WK, Chen XY, Lu H, Sun ZR, Yu Q, et al. Fasting inhibits aerobic glycolysis and proliferation in colorectal cancer via the Fdft1-mediated AKT/mTOR/HIF1alpha pathway suppression. *Nat Commun* (2020) 11(1):1869. doi: 10.1038/s41467-020-15795-8
88. Endo K, Matsui R, Sugiyama M, Asami T, Inaba C, Kobayashi S, et al. Procyanidin B2 gallate regulates TNF-alpha production from T cells through inhibiting glycolytic activity via mTOR-HIF-1 pathway. *Biochem Pharmacol* (2020) 177:113952. doi: 10.1016/j.bcp.2020.113952
89. Tannahill GM, Curtis AM, Adamik J, Palsson-McDermott EM, McGettrick AF, Goel G, et al. Succinate is an inflammatory signal that induces IL-1beta through HIF-1alpha. *Nature* (2013) 496(7444):238–42. doi: 10.1038/nature11986
90. Friedrich D, Zapf D, Lohse B, Fecher RA, Deepe GSJr., Rupp J. The HIF-1alpha/LC3-II Axis Impacts Fungal Immunity in Human Macrophages. *Infect Immun* (2019) 87(7):e00125-19. doi: 10.1128/IAI.00125-19
91. Quaschling T, Friedrich D, Deepe GSJr., Rupp J. Crosstalk Between Autophagy and Hypoxia-Inducible Factor-1alpha in Antifungal Immunity. *Cells* (2020) 9(10):2150. doi: 10.3390/cells9102150
92. Hu Y, Wen Z, Liu S, Cai Y, Guo J, Xu Y, et al. Ibrutinib suppresses intracellular *mycobacterium tuberculosis* growth by inducing macrophage autophagy. *J Infect* (2020) 80(6):e19–26. doi: 10.1016/j.jinf.2020.03.003
93. Fiorcari S, Maffei R, Audrito V, Martinelli S, Ten Hacken E, Zucchini P, et al. Ibrutinib modifies the function of monocyte/macrophage population in chronic lymphocytic leukemia. *Oncotarget* (2016) 7(40):65968–81. doi: 10.18632/oncotarget.11782
94. Cerni S, Shafer D, To K, Venketaraman V. Investigating the Role of Everolimus in mTOR Inhibition and Autophagy Promotion as a Potential

Host-Directed Therapeutic Target in *Mycobacterium tuberculosis* Infection. *J Clin Med* (2019) 8(2):232. doi: 10.3390/jcm8020232
95. Han R, Gao J, Zhai H, Xiao J, Ding Y, Hao J. RAD001 (everolimus) attenuates experimental autoimmune neuritis by inhibiting the mTOR pathway, elevating Akt activity and polarizing M2 macrophages. *Exp Neurol* (2016) 280:106–14. doi: 10.1016/j.expneurol.2016.04.005
96. Angajala A, Lim S, Phillips JB, Kim JH, Yates C, You Z, et al. Diverse Roles of Mitochondria in Immune Responses: Novel Insights Into Immuno-Metabolism. *Front Immunol* (2018) 9:1605. doi: 10.3389/fimmu.2018.01605
97. Mills EL, O'Neill LA. Reprogramming mitochondrial metabolism in macrophages as an anti-inflammatory signal. *Eur J Immunol* (2016) 46 (1):13–21. doi: 10.1002/eji.201445427
98. Puertollano R, Ferguson SM, Brugarolas J, Ballabio A. The complex relationship between TFEB transcription factor phosphorylation and subcellular localization. *EMBO J* (2018) 37(11):e98804. doi: 10.15252/embj.201798804
99. Roczniak-Ferguson A, Petit CS, Froehlich F, Qian S, Ky J, Angarola B, et al. The transcription factor TFEB links mTORC1 signaling to transcriptional control of lysosome homeostasis. *Sci Signal* (2012) 5(228):ra42. doi: 10.1126/scisignal.2002790
100. Wang S, Chen Y, Li X, Zhang W, Liu Z, Wu M, et al. Emerging role of transcription factor EB in mitochondrial quality control. *BioMed Pharmacother* (2020) 128:110272. doi: 10.1016/j.biopha.2020.110272
101. Kim HJ, Joe Y, Rah SY, Kim SK, Park SU, Park J, et al. Carbon monoxide-induced TFEB nuclear translocation enhances mitophagy/mitochondrial biogenesis in hepatocytes and ameliorates inflammatory liver injury. *Cell Death Dis* (2018) 9(11):1060. doi: 10.1038/s41419-018-1112-x
102. Mansueto G, Armani A, Viscomi C, D'Orsi L, De Cegli R, Polishchuk EV, et al. Transcription Factor EB Controls Metabolic Flexibility during Exercise. *Cell Metab* (2017) 25(1):182–96. doi: 10.1016/j.cmet.2016.11.003
103. Chandra V, Bhagyaraj E, Nanduri R, Ahuja N, Gupta P. NR1D1 ameliorates *Mycobacterium tuberculosis* clearance through regulation of autophagy. *Autophagy* (2015) 11(11):1987–97. doi: 10.1080/15548627.2015.1091140
104. Kim TS, Jin YB, Kim YS, Kim S, Kim JK, Lee HM, et al. SIRT3 promotes antimycobacterial defenses by coordinating mitochondrial and autophagic functions. *Autophagy* (2019) 15(8):1356–75. doi: 10.1080/15548627.2019.1582743
105. Ghosh A, Jana M, Modi K, Gonzalez FJ, Sims KB, Berry-Kravis E, et al. Activation of peroxisome proliferator-activated receptor alpha induces lysosomal biogenesis in brain cells: implications for lysosomal storage disorders. *J Biol Chem* (2015) 290(16):10309–24. doi: 10.1074/jbc.M114.610659
106. Ghosh A, Pahan K. PPARalpha in lysosomal biogenesis: A perspective. *Pharmacol Res* (2016) 103:144–8. doi: 10.1016/j.phrs.2015.11.011
107. Wang S, Li F, Lin Y, Wu B. Targeting REV-ERBalpha for therapeutic purposes: promises and challenges. *Theranostics* (2020) 10(9):4168–82. doi: 10.7150/thno.43834
108. Zhang J, Xiang H, Liu J, Chen Y, He RR, Liu B. Mitochondrial Sirtuin 3: New emerging biological function and therapeutic target. *Theranostics* (2020) 10 (18):8315–42. doi: 10.7150/thno.45922
109. Chamouton J, Latruffe N. PPARalpha/HNF4alpha interplay on diversified responsive elements. Relevance in the regulation of liver peroxisomal fatty acid catabolism. *Curr Drug Metab* (2012) 13(10):1436–53. doi: 10.2174/138920012803762738
110. Kumar S, Jain A, Choi SW, da Silva GPD, Allers L, Mudd MH, et al. Mammalian Atg8 proteins and the autophagy factor IRGM control mTOR and TFEB at a regulatory node critical for responses to pathogens. *Nat Cell Biol* (2020) 22(8):973–85. doi: 10.1038/s41556-020-0549-1
111. Fernandez-Mosquera L, Yambire KF, Couto R, Pereyra L, Pabis K, Ponsford AH, et al. Mitochondrial respiratory chain deficiency inhibits lysosomal hydrolysis. *Autophagy* (2019) 15(9):1572–91. doi: 10.1080/15548627.2019.1586256
112. Xiang H, Zhang J, Lin C, Zhang L, Liu B, Ouyang L. Targeting autophagy-related protein kinases for potential therapeutic purpose. *Acta Pharm Sin B* (2020) 10(4):569–81. doi: 10.1016/j.apsb.2019.10.003
113. Sharma V, Makhdoomi M, Singh L, Kumar P, Khan N, Singh S, et al. Trehalose limits opportunistic mycobacterial survival during HIV co-infection by reversing HIV-mediated autophagy block. *Autophagy* (2020), 1–20. doi: 10.1080/15548627.2020.1725374
114. Sergin I, Evans TD, Zhang X, Bhattacharya S, Stokes CJ, Song E, et al. Exploiting macrophage autophagy-lysosomal biogenesis as a therapy for atherosclerosis. *Nat Commun* (2017) 8:15750. doi: 10.1038/ncomms15750
115. Emanuel R, Sergin I, Bhattacharya S, Turner J, Epelman S, Settembre C, et al. Induction of lysosomal biogenesis in atherosclerotic macrophages can rescue lipid-induced lysosomal dysfunction and downstream sequelae. *Arterioscler Thromb Vasc Biol* (2014) 34(9):1942–52. doi: 10.1161/ATVBAHA.114.303342

Conflict of Interest: The authors declare that the research was conducted in the absence of any commercial or financial relationships that could be construed as a potential conflict of interest.

frontiers in Microbiology

ORIGINAL RESEARCH
published: 26 November 2020
doi: 10.3389/fmicb.2020.573844

Salmonella and *S. aureus* Escape From the Clearance of Macrophages via Controlling TFEB

Shanshan Rao[1], *Tao Xu*[2], *Yu Xia*[2]* *and Hongfeng Zhang*[1]*

[1] Department of Pathology, Wuhan Central Hospital, Huazhong University of Science and Technology, Wuhan, China,
[2] Cancer Biology Research Center, Tongji Hospital, Huazhong University of Science and Technology, Wuhan, China

Phagosome- and xenophagosome-lysosome systems play a critical role in the defense of pathogenic bacteria, such as *Salmonella* and *S. aureus*, in macrophages. A great part of the bacteria escapes from the digestion and can survive through some mechanisms that are still poorly understood and which require further exploration. Here we identified that *Salmonella* inhibited the expression and activation of TFEB to blunt the functions of lysosomes and defense of clearance by activating caspase-1. The expression and activation of TFEB were enhanced early under the infection of *S. aureus*, which was followed by shrinkage to weaken lysosomal functions due to the delayed activation of ERK, mTOR, and STAT3. Thus, we have identified novel escape mechanisms for *Salmonella* and *S. aureus* to deepen and strengthen our strategies fighting with pathogens.

Keywords: *Salmonella*, *S. aureus*, lysosome, TFEB, escape

OPEN ACCESS

Edited by:
Maria Isabel Colombo, Universidad Nacional de Cuyo, Argentina

Reviewed by:
Roberto Botelho, Ryerson University, Canada
Gang Pei, Friedrich-Loeffler-Institute, Germany

***Correspondence:**
Yu Xia
xiayu_hb@sina.com
Hongfeng Zhang
zhf152@163.com

Specialty section:
This article was submitted to Microbial Immunology, a section of the journal Frontiers in Microbiology

Received: *19 June 2020*
Accepted: *20 October 2020*
Published: *26 November 2020*

Citation:
Rao S, Xu T, Xia Y and Zhang H (2020) Salmonella and S. aureus Escape From the Clearance of Macrophages via Controlling TFEB. Front. Microbiol. 11:573844. doi: 10.3389/fmicb.2020.573844

INTRODUCTION

Microbes have been alive in the world for thousands of years along with human beings, but the interplay between microbes and humans is still ongoing. When malignant bacteria infect the human body, the human immune system will work as a fighter against the invasion. The macrophage, as one of the innate immune cells, lends itself to protect us from bacterial infection first and foremost. In macrophages, phagosomes could act as a defense against a huge group of intracellular bacteria by fusing with lysosomes, but also a large group of invaders still survive through their processes of escape (Huang and Brumell, 2014). Meanwhile, the selective macro-autophagosome, known as xenophagosome, will capture the invaders or survivors to transport into lysosomes for clearance (Bauckman et al., 2015; Upadhyay and Philips, 2019; Xu et al., 2019). Obviously, lysosomes act as the terminator to suppress the survival of bacteria in macrophages.

The lysosome, known as "recycling center" of a cell, contains about 60 kinds of hydrolases within its single-membrane vesicles. Those hydrolases, such as cathepsins, collagenase, DNase, esterases, and so on work in an acidic pH (4.5–5.5) environment to degrade macromolecules, including lipid acids, DNA, and proteins (Perera and Zoncu, 2016; Ballabio and Bonifacino, 2020). Because of its powerful ability of digestion, disorders of lysosomal degradation result in a series of diseases, such as cancer, neurodegenerative diseases, metabolic disorders and so on, which are viewed as lysosomal storage disease (LSD) (Platt et al., 2018; Ballabio and Bonifacino, 2020). Specifically, inflammation and microbes infection are closely associated with lysosomes (Bauckman et al., 2015; Upadhyay and Philips, 2019; Xia et al., 2019; Xu et al., 2019).

TFEB, working as a critical regulator of autophagic and lysosomal functions, regulates the transcription of lysosomal membrane proteins and hydrolases, such as LAMP1/2, V-ATPase, cathepsin A/B/F, and so on (Settembre et al., 2011; Napolitano and Ballabio, 2016). The nuclear

TFEB could bind to the 10-base E-box-like palindromic sequence (CLEAR) which is shared by the promoter sequence of lysosomal genes (Palmieri et al., 2011). While a group of protein kinases such as mTORC1, ERK2, and AKT could phosphorylate TFEB at ser142 or ser211, and the phosphorylated TFEB can be assembled to a 14-3-3 complex in cytoplasm (Settembre et al., 2011; Martina et al., 2012; Palmieri et al., 2017). When TFEB is dephosphorylated by calcineurin and released from the 14-3-3 complex, it will enter into nucleus for its transcriptional functions (Medina et al., 2015). Meanwhile, the expression level of TFEB also greatly contributes to its activities and functions.

Although it is well-studied that phagocytosis and xenophagy play a great role in the defense of bacteria, it is true that a lot of intracellular invaders survive and replicate (Huang and Brumell, 2014). Do *Salmonella* and *Staphylococcus aureus* (*S. aureus*), as two of common pathogenic bacteria, cross-talk with lysosomes? As reported, the process of phagocytosis could promote the activities of lysosomes, because pathogens bind to the Fcγ receptors and fuel the TFEB (Gray et al., 2016). *S. aureus* could activate TFEB to up-regulate the expression of inflammatory cytokines in RAW264.7 cells (Visvikis et al., 2014). Enhancing the activities of TFEB to restore the process of xenophagy to restrict the survival of *Salmonella* (Ammanathan et al., 2019). Yet, the detailed and critical mechanisms of how *Salmonella* and *S. aureus* regulate the functions of lysosomes and TFEB expression remain to be explored.

Here, we focused on how *Salmonella* and *S. aureus* regulated the activities of lysosomes and expression of TFEB through directly infecting bone marrow derived macrophages (BMDMs). We identified different regulating phenotypes that *Salmonella* down-regulated the critical genes of lysosomes and *Tfeb* striking as the activation of caspase1, while *S. aureus* enhanced the expression of TFEB early, and was reined in later because of the activation of ERK, mTOR, and STAT3 signals. If we inhibited the activation of caspase1 or ERK, mTOR, and STAT3 signals, BMDMs restored the full expression of *tfeb* and restrained the replication of *Salmonella* and *S. aureus*. Thus, we found two novel survival mechanisms of *Salmonella* and *S. aureus*.

RESULTS

Salmonella Restricts the Expression of TFEB and Lysosomal Proteins, While *S. aureus* Boosts TFEB Early and Is Reined in Later

To explore how bacteria regulate the processes of lysosomal degradation, we infected BMDMs with *Salmonella* and *S. aureus* directly at a time gradient, and tested the lysosomal hydrolase genes, membrane genes and autophagic genes. Showing with histograms, we found that *Salmonella* remarkably restrained *Tfeb*, *Lamp1*, *V-Atpase*, hydrolase genes and autophagic genes, while *S. aureus* enhanced the transcription of those genes lightly (**Figures 1A,B**). Furthermore, under the infection of *S. aureus*, the level of *Tfeb* was up-regulated at 1 h, but gradually shrunk at 3 and 5 h (**Figure 1B**). As mentioned, *Tfeb* is an important transcription factor of lysosomal and autophagic genes, and thus we supposed that *Salmonella* and *S. aureus* controlled the transcription of *Tfeb*, which resulted in regulation of lysosomal and autophagic genes.

To confirm this, we tested the protein level of lysosomes and LC3 upon the infection of the two bacteria. The TFEB, LAMP1, ATP6V1A, ATP6V0D2, cathepsin B and LC3 were strongly inhibited by *Salmonella*. It was same with this gene that the protein level of TFEB was first enhanced, when BMDMs were cocultured with *S. aureus*, and then reined back (**Figure 2A** and **Supplementary Figures S1A–F**). We also verified with Immunofluorescence, and found similar phenotypes (**Figures 2B,C**). Meanwhile, nuclear localization rates of TFEB were notably increased at 1, 3 h and declined at 5 h with the infection of *S. aureus*, but not obviously in *Salmonella* group (**Figures 2B,D**). This means a discrepant regulation of TFEB activity by the two bacteria. Furthermore, we used LysoTracker red to stain acid vacuoles, and the mean fluorescence intensities (MFI) might relatively represent the lysosomal acidic strength. After infection for 5 h, we found that *Salmonella* could weaken the lysosomal acidity, while *S. aureus* could not (**Figures 2E–H**). Within vivo, C57/B6 mice were infected with *S. aureus* or *Salmonella* via intraperitoneal injection, and then we collected the peritoneal macrophages for testing with western-blot. We found TFEB, ATP6V1A, ATP6V0D2, and LC3 were increased under the treatment of *S. aureus* and inhibited by *Salmonella* (**Figure 2I** and **Supplementary Figure S1G**).

S. aureus Strikingly Activates ERK, mTOR, NFκB, and STAT3 Signaling Pathways, While *Salmonella* Activates Caspase-1

To figure out the detailed mechanisms, we infected BMDMs with *S. aureus* or *Salmonella* for 0, 1, 3, 5 h, and checked several signaling pathways that might regulate the expression and activity of TFEB. We found that ERK, mTOR, NFκB, and STAT3 could be activated obviously with treatment of *S. aureus*, but only slightly activated by *Salmonella* (**Figures 3A,C–G**). Meanwhile, as reported, The bacterium such as *Salmonella* or *Listeria* could activate inflammasomes (Wu et al., 2010; Zhao et al., 2011; Qu et al., 2016), and we tested the mature-caspase 1 level that was released to the supernatant. The results were that *S. aureus* could not activate caspase-1 but *Salmonella* could (**Figures 3B,H**).

VX-765 Restores the Expression of TFEB and Lysosomal Proteins With Administration of *Salmonella*, While ERKi, Rapamycin and S31-201 Accelerate the Expression of TFEB and Lysosomal Proteins With Administration of *S. aureus*

To verify which signal could regulate the expression of TFEB and lysosomal proteins, BMDMs were pre-treated with caspase-1 inhibitor, ERKi, rapamycin, S31-201 or IKK16 upon the infection of *Salmonella*. Because LAMP1 is a key marker of

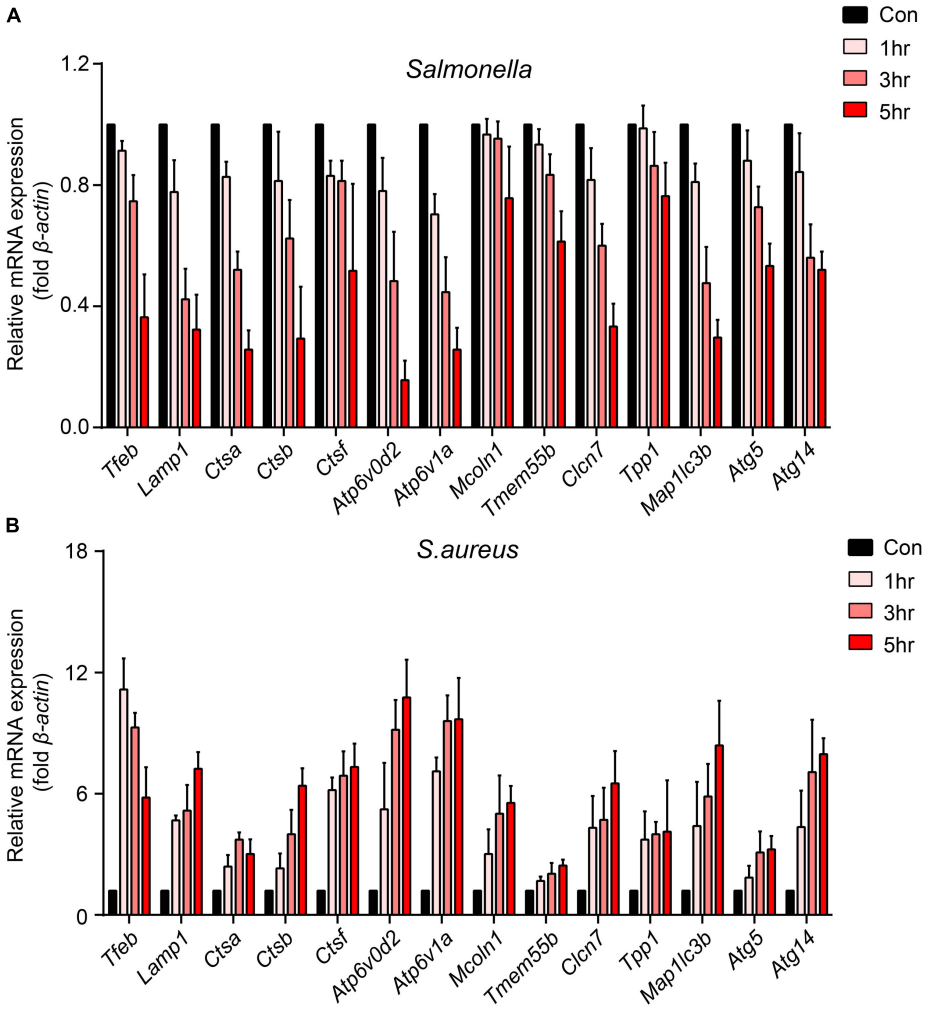

FIGURE 1 | *Salmonella* inhibits the transcription of *Tfeb* and autophagosome-lysosome relative genes, while *S. aureus* enhances the transcription of *Tfeb* early and reins in later. **(A,B)** BMDMs were infected with *Salmonella* **(A)** or *S. aureus* **(B)** at a MOI of 5 for 0, 1, 3, 5 h and measured the level of genes with real-time PCR. The presented mean values (± SEM) were from at least three independent experiments **(A,B)**.

lysosome and ATP6V0D2 has a great role in the autophagy-lysosome degradation process (Xia et al., 2019), we tested the protein and gene level of the two and TFEB. We found that TFEB, LAMP1, and ATP6V0D2 did not decrease anymore with treatment of VX-765 (**Figures 4A,B** and **Supplementary Figure S2A**), while there were no significant changes under the administration of ERK, mTOR, STAT3, or NFκB inhibitor (**Supplementary Figures S2B,C**). When BMDMs were infected with *S. aureus*, the LAMP1 and ATP6V0D2 were much more obviously increased and TFEB was continuously up-regulated in a time-dependent manner after treatments with ERK, mTOR and STAT3 inhibitor (**Figures 4C–E** and **Supplementary Figure S3A**). Meanwhile, BMDMs were treated with those inhibitors alone that could induce non-significant responses (**Supplementary Figures S4A–D**). Together, we suggested that *Salmonella* could inhibit the expression of TFEB through the activation of caspase-1, and the detailed mechanisms need further follow-up investigations. While *S. aureus* could block the sufficient expression of TFEB and lysosomal genes by activating ERK, mTOR, STAT3.

VX-765 Restores the Activity of TFEB With Administration of *Salmonella*, While ERKi, Rapamycin and S31-201 Promote the Activity of TFEB Under Infection of *S. aureus*

The expression level of TFEB was positive-regulated by the inhibitors upon the infection of *Salmonella* and *S. aureus*. To explore the activity of TFEB under bacterial infection with the treatment of inhibitors, we isolated the cytoplasm and nucleus of BMDMs to check the level of TFEB. The results showed that VX-765 could promote the TFEB to transfer into the nucleus under infection of *Salmonella* (**Figures 5A,C**), while S31-201, rapamycin and ERKi could dramatically increase the nuclear TFEB upon infection of *S. aureus* (**Figures 5B,D**).

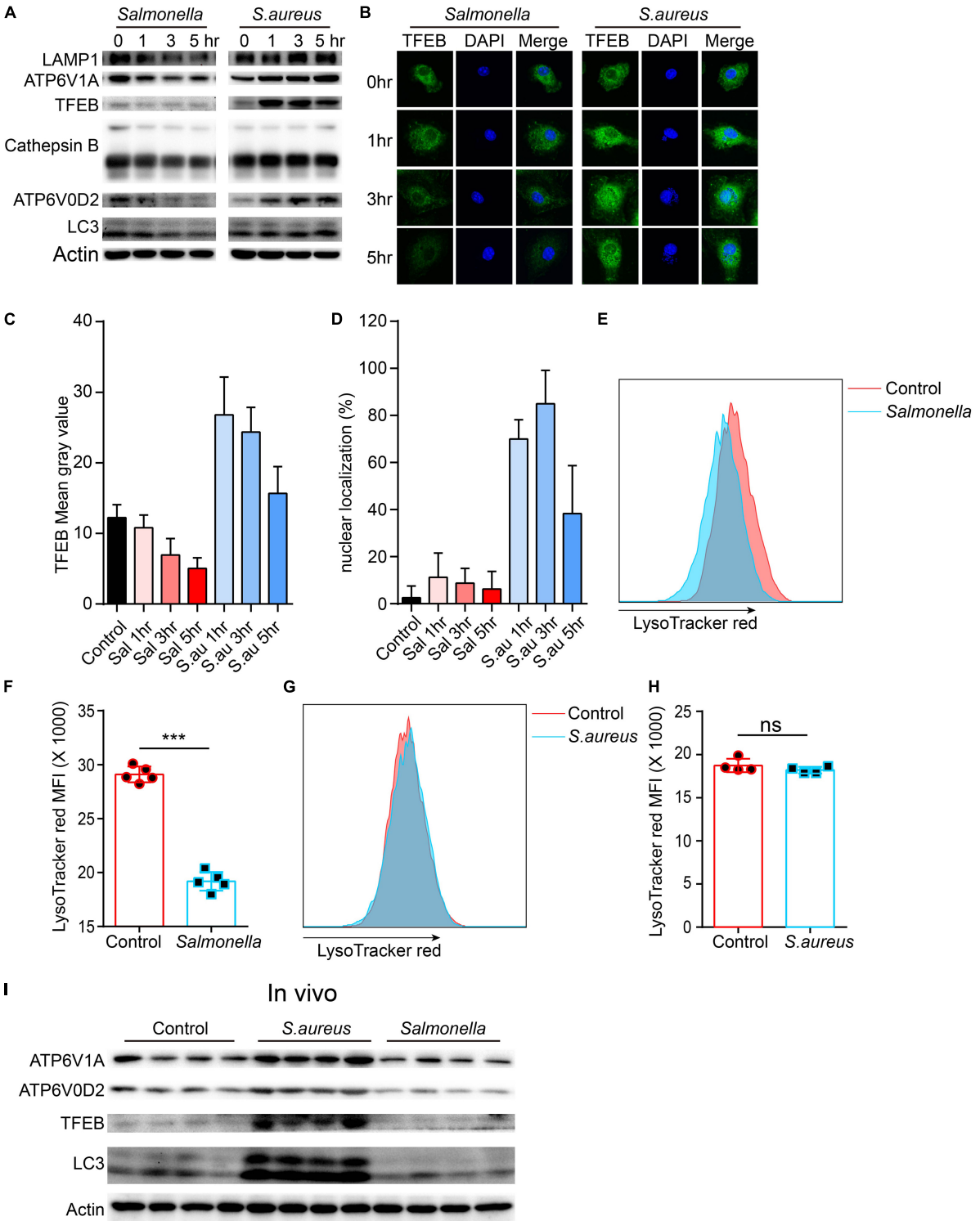

FIGURE 2 | *Salmonella* restrains the expression of TFEB and lysosomal proteins, while *S. aureus* boosts the expression of TFEB early and reins back later. **(A,B)** BMDMs were infected with *Salmonella* or *S. aureus* at a MOI of 5 for 0, 1, 3, 5 h. To measure the level of proteins with western-blot **(A)** and stain TFEB or nucleus with anti-TFEB antibody or DAPI **(B)**. **(C,D)** Quantification of the level of TFEB in cells at least five views **(C)** and the percentage of nuclear TFEB per cell (6 cells) in each group with Image J **(D)**. **(E–H)** BMDMs were infected with *Salmonella* or *S. aureus* for 5 h, and stained with LysoTracker red for 10 min, the representative images of MFI are shown **(E,G)**, and the quantitative data are shown **(F,H)**. Histograms depict mean values (± SEM). ***$p < 0.001$. **(I)** Mice were infected with *Salmonella* or *S. aureus* for 8 h and the level of TFEB in peritoneal macrophages was measured with western-blot ($n = 4$ in each group). Representative bands and pictures were from three independent experiments **(A,B,E,G)**.

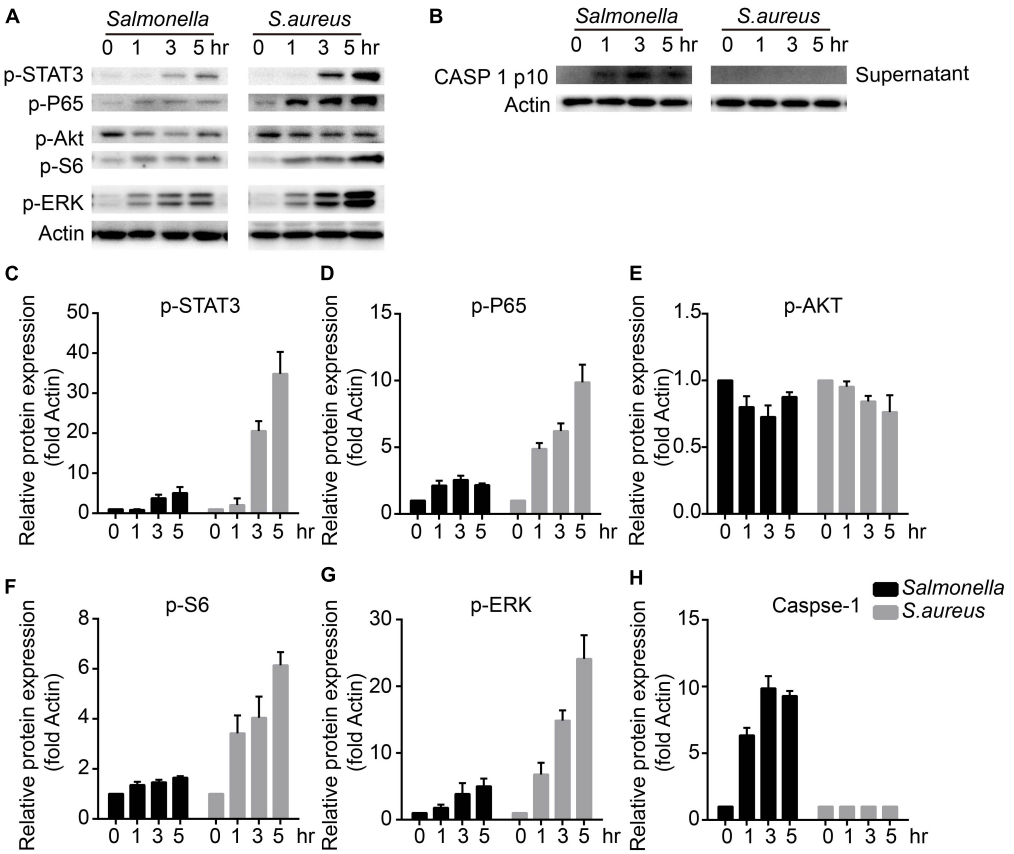

FIGURE 3 | *S. aureus* activates ERK, mTORC, NFκB and STAT3 signaling pathways, while *Salmonella* activates caspase-1. **(A–H)** BMDMs were infected with *Salmonella* or *S. aureus* at a MOI of 5 for 0, 1, 3, 5 h. To measure the activation of STAT3, P65, AKT, S6, ERK and caspase-1 released in the culture medium with western-blot **(A,B)**, and histograms show the quantitative statistics of those enzymes and caspase p10 level **(B–H)**. Representative bands were from three independent experiments **(A,B)**.

Meanwhile, to further verify the role of TFEB in the regulation of lysosomal proteins under bacterial infection, we constructed lentivirus to knock down *Tfeb* in BMDMs, and then infected with *Salmonella* and *S. aureus*. We found that if TFEB was knocked down, the ATP6V0D2 was obviously down-regulated on infection of bacteria alone or combined with inhibitors (**Figures 5E–J**).

VX-765 Reconstitutes the Defense of *Salmonella*, While ERKi, Rapamycin and S31-201 Enhance the Defense of *S. aureus*

Next, to confirm if the defense of bacteria could be reconstituted or enhanced after administration with inhibitors, inhibitors-primed BMDMs were cocultured with *Salmonella* or *S. aureus*, and measured the number of survivors in BMDMs with a gentamicin protection assay. The results announced that with treatment of caspase-1 inhibitor, less *Salmonella* survived than in the control group (**Figure 6A**), and less *S. aureus* were alive after administration of ERK, mTOR and STAT3 inhibitor (**Figure 6B**). To exclude the different endocytosis treatment with inhibitors, inhibitor-primed BMDMs were cocultured with FITC-Dextrain, and the results showed that there were non-significant changes among those inhibitor treatments (**Figures 6C,D**). Thus, with reconstituting or promoting the expression of TFEB by caspase-1 inhibitor or ERK, mTOR and STAT3 inhibitors, BMDMs strengthened the defense against the invasion of *Salmonella* and *S. aureus*.

DISCUSSION

Phagosome-lysosome and autophagosome-lysosome, as two critical mechanisms of digestion defense against the invasion of pathogens, could clear most intruders. But there are a large group of bacteria that continue to survive under excessive infection. Meanwhile, these pathogens have evolved some escape approaches to resist the clearance of immune cells (Huang and Brumell, 2014). In this study, we examined novel escape mechanisms for *Salmonella* and *S. aureus* with controlling the expression and activity of TFEB, and then regulating the degradation function of lysosomes. We also verified the detailed signaling pathways that participated in the regulation of the

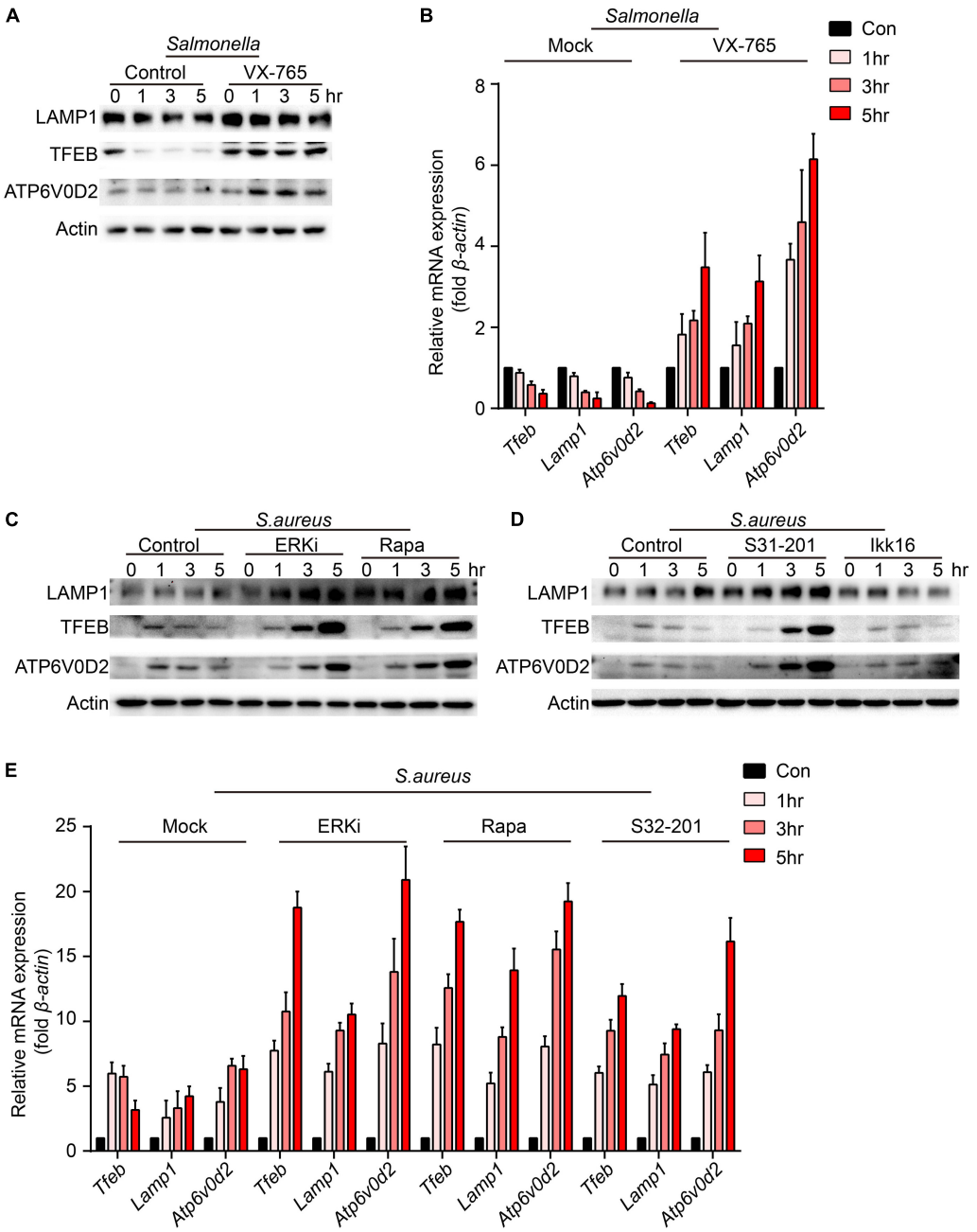

FIGURE 4 | VX-765 restores the level of TFEB and lysosomal proteins with infection of *Salmonella*, while ERKi, rapamycin and S31-201 accelerate the expression of TFEB and lysosomal proteins with infection of *S. aureus*. **(A,B)** BMDMs were pre-treated with 5 μM VX-765 for 1 h and then infected with *Salmonella* at an MOI of 5 for 0, 1, 3, 5 h. Testing the protein level **(A)** and gene level **(B)** of TFEB, LAMP1 and ATP6V0D2. **(C–E)** BMDMs were pre-treated with 500 nM SCH772984, 100 nM rapamycin, 10 μm S31-201, 200 nM IKK 16 or DMSO for 1 h and then infected with *S. aureus* at a MOI of 5 for 0, 1, 3, 5 h. Testing the protein level **(C,D)** and gene level **(E)** of TFEB, LAMP1 and ATP6V0D2. Representative bands were from three independent experiments **(A,C,D)** and the presented values of means (± SEM) were from three independent experiments **(B,E)**.

expression and function of TFEB and lysosomes, and through blocking those pathways restored or enhanced the function of lysosomes and defense of bacteria.

Salmonella is a classical intracellular pathogenic germ which induces colitis and poses a huge health burden (Hartz et al., 1950; Herp et al., 2019). Several escape mechanisms have been found that are used by *Salmonella* in order to survive. For example, when they infect epithelial cells or macrophages, those intracellular bacteria are wrapped up in vacuoles, termed as *Salmonella*-containing vacuoles (SCVs), through its T3SSs (SPI-1 and SPI-2) for better replication and ability to survive (Birmingham et al., 2006). Meanwhile, at the early invasion,

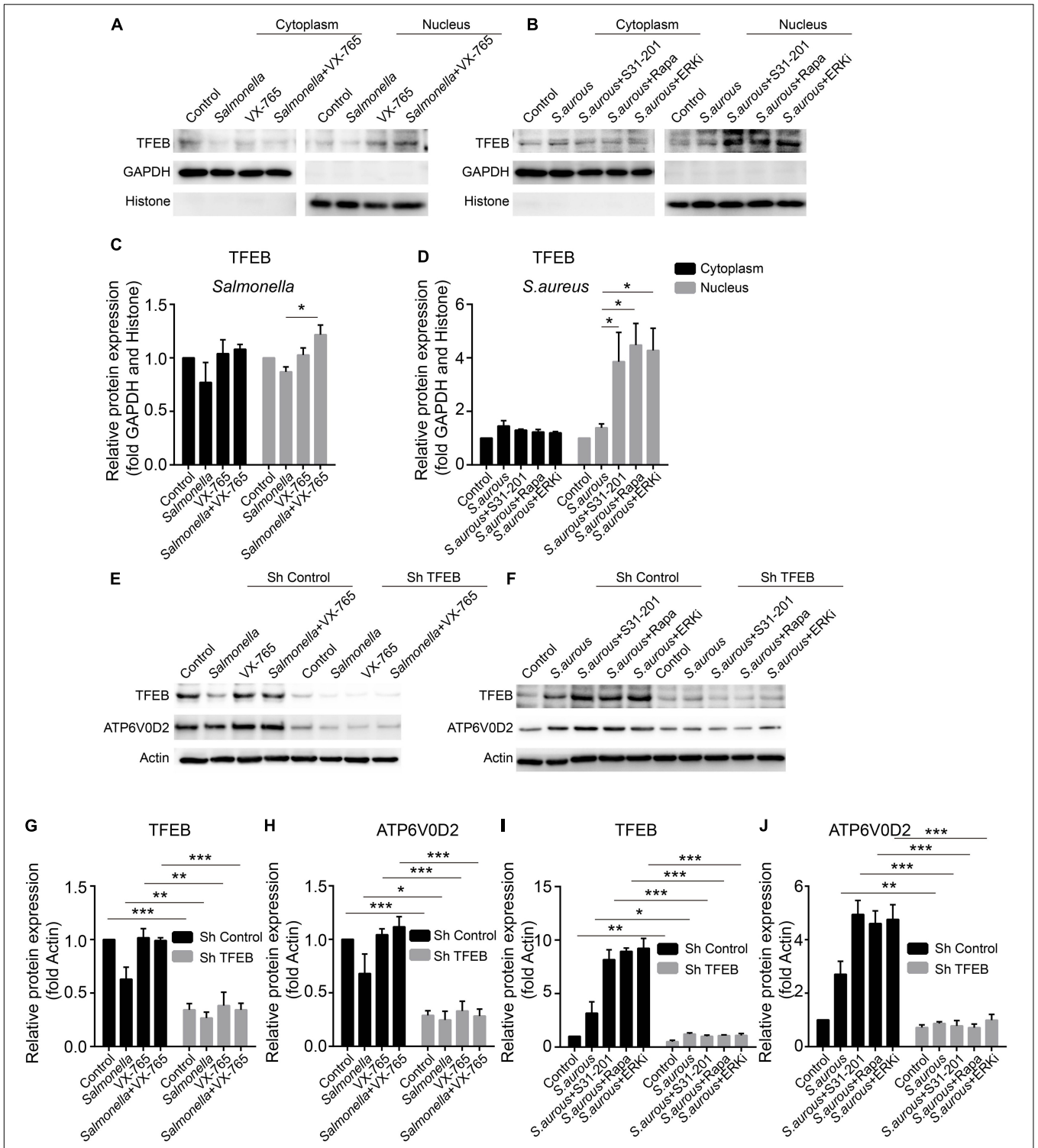

FIGURE 5 | VX-765 restores the activity of TFEB with infection of *Salmonella*, while ERKi, rapamycin and S31-201 promote the activity of TFEB under infection of *S. aureus*. **(A,B)** Mature BMDMs were plated into 6-well plates, and infected with *Salmonella* and *S. aureus* alone or combined with inhibitors for 3 h, and then, the cytoplasmic and nuclear TFEB were tested with western-blot. **(C,D)** The histograms show the statistics of distribution of TFEB in cytoplasm and nucleus. **(E–J)** Using lentivirus to knock down TFEB in BMDMs, and those cells were treated with bacteria alone or combined with inhibitors for 3 h. TFEB and ATP6V0D2 were tested with western-blot **(E,H)** and the quantitative data were displayed by histograms **(G–J)**. Histograms depict mean values (± SEM). $^{*}p < 0.05$; $^{**}p < 0.01$; $^{***}p < 0.001$. Representative bands were from three independent experiments **(A,B,E,F)**.

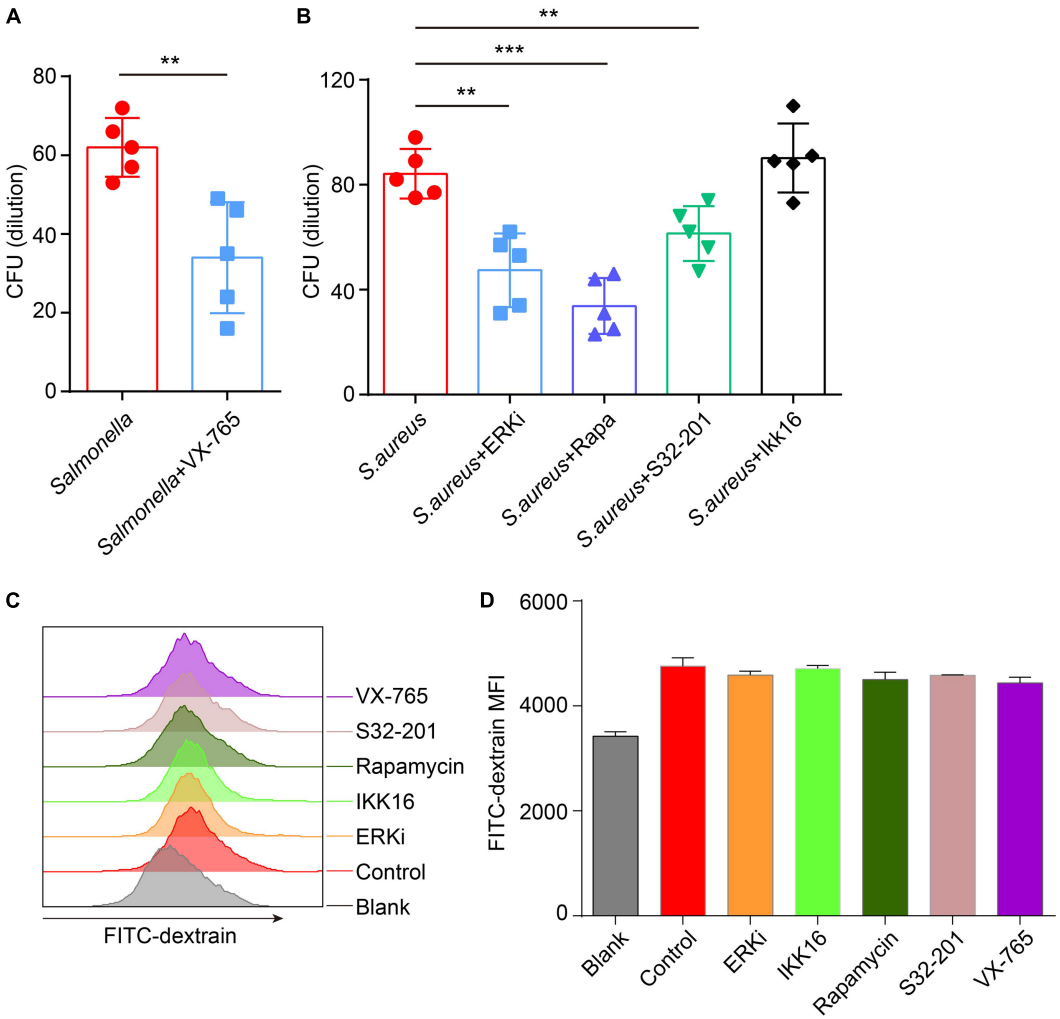

FIGURE 6 | VX-765 reconstitutes the defense of *Salmonella*, while SCH772984, rapamycin and S31-201 enhance the defense of *S. aureus*. **(A,B)** 5 μM VX-765-primed BMDMs were infected with *Salmonella* at a MOI of 2 **(A)**, and 500 nM SCH772984-, 100 nM rapamycin-, 10 μm S31-201- or 200 nM IKK 16-primed BMDMs were infected with *S. aureus* at a MOI of 2 **(B)**. Checking the survived bacteria per cell with gentamicin protection assay. **(C,D)** Inhibitor-primed BMDMs were incubated with FITC-Dextrain for 1 h and the MFI of FITC was measured with Flow cytometer **(C)**, and the MFI quantified **(D)**. Histograms depict mean values (± SEM). $^{**}p < 0.01$; $^{***}p < 0.001$. The presented values of means were from at least three independent experiments.

Salmonella could also trigger xenophagy as consuming energy and amino acid, but the process would quickly be suppressed via degrading Sirt1/LKB1/AMPK complexes (Ganesan et al., 2017). However, the detailed processes for escape should be further explored.

Under the infection of *Salmonella*, NLRC4 and NLRP3 inflammasomes could be activated within 1 h, cut the pro-caspase-1 into active caspase-1 in macrophages and induce pyroptosis (Monack et al., 2000; Lara-Tejero et al., 2006; Zhao et al., 2011; Qu et al., 2016). As reported, the totally knock-out *Caspase1* in mice, *Caspase1*$^{-/-}$ mice, even increased the susceptibility to *Salmonella* infection *in vivo* via other mechanisms, such as deficiency of cytokines or involvement of neutrophils (Lara-Tejero et al., 2006; Raupach et al., 2006; Miao et al., 2010). Although Denise M. Monack's group had published that intracellular living bacteria were equal between WT and *Caspase1*$^{-/-}$ macrophages through gentamicin protection assay (Monack et al., 2000), the caspase1-depdent cell death was robustly decreased in the caspase1$^{-/-}$ group (Lara-Tejero et al., 2006). Thus, whether or not caspase1 is involved in the defense of *Salmonella* in macrophages also needs to be investigated. In our present study, we had identified a critical role of caspase1 in regulating the expression of TFEB, and TFEB contributed to the resistance of pathogens involving *Salmonella* (Huang and Brumell, 2014; Ammanathan et al., 2019). In our gentamicin protection assay, we measured the living bacteria in each well by folding β-actin, and inhibition of caspase-1 activity obviously stunted the replication of *Salmonella*. Therefore, we introduced a new surviving pathway, "*Salmonella*-caspase1-TFEB-lysosome digestion-*Salmonella* survive," for *Salmonella*.

S. aureus is a common pathogenic bacteria to induce systemic infections or abscesses for humans and animals, although it is

commensal most of the time. Not only do neutrophils act as the first responders under the infection of *S. aureus*, but also macrophages have a critical role in clearance of the bacteria (Koziel et al., 2009; Flannagan et al., 2016; Moldovan and Fraunholz, 2019). The professional phagocytes, macrophages, uptake *S. aureus* within minutes to capture the bacteria with Rab-5 positive phagosomes, and those phagosomes need further maturation. Mature phagosomes can be fused with lysosomes to form phagolysosomes for killing bacteria (Moldovan and Fraunholz, 2019). But, a great part of those phagolysosomes could not completely digest *S. aureus* as they are lacking some necessary hydrolases (Jubrail et al., 2016). Those survivors could replicate in the acidic vacuoles and finally cause macrophage death (Jubrail et al., 2016; Tranchemontagne et al., 2016). Hence, we focused on the critical mechanisms for the escape of *S. aureus* in macrophages. Here, we found that *S. aureus* could activate some key protein kinases, such as ERK, mTOR, STAT3 and so on. ERK and mTOR had been well-studied to control the activity and expression of TFEB, while STAT3 was first verified to blunt the function of TFEB in macrophages under *S. aureus* infection (Li et al., 2018). Insufficient TFEB led to the disabling lysosomes and more bacteria survived.

In summary, in the battle of bacteria and macrophages, bacteria have generated some escape pathways for better survival. We have verified the great role of TFEB in the defense of bacteria, and explored critical mechanisms to regulate the expression and activity of TFEB during the infection of *Salmonella* and *S. aureus*. Those discoveries contribute to the strategies for the cure of infection dramatically.

MATERIALS AND METHODS

Reagents

Anti-LAMP1 (sc-20011), anti-caspase1 p10 (sc-514) antibodies were purchased from Santa Cruz Biotechnology. Anti-TFEB (ab2636), anti-ATP6V1A (ab 137574), donkey anti-goat IgG H&L (FITC; ab6881) antibodies were from Abcam. Anti-ATP6V0D2 (SAB2103221) antibody, DAPI (d9542) came from Sigma Aldrich. Anti-cathepsin B (#31718), anti-LC3B (#3868), anti-actin (#3700), phospho-STAT3 (Tyr705; #9145), phospho-NF-κB P65 (Ser536; #3033), phospho-AKT (Ser473; #4060), phospho-P44/42 MAPK (ERK1/2; Thr202/Tyr204; #4370), and-GAPDH (5174S) antibodies were purchased from Cell Signaling Technology. Anti-Histone H3 (ab1791) antibody was purchased from Abcam. SCH772984 (ERKi; S7101), rapamycin (mTORCi; S1039), S3I-201 (STAT3i; S1155), IKK-16 (IKK Inhibitor VII; S2882), VX-765 (caspase1i; S2228) were from Selleck. Gentamicin sulfate (1289003) and FITC-Dextran (FD4) were from Sigma Aldrich. LysoTracker red NDN-99 (L7528) was purchased from Thermo Fisher Scientific.

Cell Culture and Stimulation

All experiments were performed *in vitro* with mouse primary macrophages that were derived from bone marrow cells (BMDMs). Those cells were cultured with DMEM (Thermo Fisher Scientific, 11965092) medium containing 10% FBS, penicillin, streptomycin and 50ng/ml M-CSF (PeproTech, 315-02) for 7 days. BMDMs were cocultured with *Salmonella* and *S. aureus* at a desired MOI (2:1) in the gentamicin protection assay, while MOI (5:1) in direct infection or inhibitor-primed infection experiments.

mRNA Isolation and Real-Time PCR

Total mRNA was extracted from infected BMDMs with TRI Reagent (Sigma Aldrich; 93289) and reverse transcription using a kit from Thermo Fisher Scientific (4374966). Real-time PCR was performed with SYBR^{TM} Green mix (Thermo Fisher Scientific, A25742). All real-time PCR primers were listed as follows,

Tfeb-F: TTCTGCCCGGACTCAGTTTC;
Tfeb-R: TCTCGGGGTTGGAGCTGATA;
Lamp1-F: GCCTCAGCACTCTTTGAGGT;
Lamp1-R: GTTGGGGAAGGTCCATCCTG;
Atp6v0d2-F: TGCGGCAGGCTCTATCCAGAGG;
Atp6v0d2-R: CCACTGCCACCGACAGCGTC;
Ctsb-F: GGCCCAGTGGAGGGTGCCTT;
Ctsb-R: TGCGTGGGATTCCAGCCACAA;
Ctsf-F: CCACCTTGCAATGATCCCCT;
Ctsf-R: TTCACTGGGCTACAGTCCCT;
Ctsa-F: GGAGAGCAAGGACGCAAGG;
Ctsa-R: TGGCAATCAGGTTCCAAGCA;
Mcoln1-F: TTGCTCTCTGCCAGCGGTACTA;
Mcoln1-R: GCAGTCAGTAACCACCATCGGA;
Tmem55b-F: GTTCGATGCCCCTGTAACTGTC;
Tmem55b-R: CCCAGGTTGATGATTCTTTTGC;
Clcn7-F: GAGGAGGGACCTCAGTCTCA;
Clcn7-R: GGAGCTTCTCGTTGTGTGGA;
Tpp1-F: ATCTGGAACCTCGGCCTCTA;
Tpp1-R: CCTGTCCCATGCTGCTGATA;
Map1lc3a-F: TTGGTCAAGATCATCCGGCG;
Map1lc3a-R: TCTTGGGAGGCGTAGACCAT;
Atg5-F: TGCATCAAGTTCAGCTCTTCCT;
Atg5-R: CTGGGTAGCTCAGATGCTCG;
Atg14-F: GCTTCGAAGGTCACACATCC;
Atg14-R: CTTGAGGTCATGGCACTGTC;

Scrambled shRNA Lentiviral Plasmid Construction and Lentiviral Particles Generation

A short hairpin RNAs pair which targets *Tfeb* was cloned into pLVX-shRNA2 plasmid (Clontech Laboratories, Inc. 632179) with BamH I and EcoR I according to the protocol of ClonExpress® Ultra One Step Cloning Kit (C115) purchased from Vazyme, and the shRNA sequence as follow, forward: 5′-GATC CGGCAGTACTATGACTATGATTTCAAGAGAATCATAGTCA TAGTACTGCCGTTTTTG-3′, reverse: 5′-AATTCAAAAACGG CAGTACTATGACTATGATTCTCTTGAAATCATAGTCATAG TACTGCCG-3′. For producing lentiviral particles, the vector and packaging plasmids were transfected into 293T cells about 36 h and harvested the supernatant which contained lentivirus. Using these virus particles to transfect BMDMs to knock down *Tfeb*.

Western-Blot

Cellular proteins were extracted with RIPA buffer containing proteases and phosphatase inhibitor cocktail (Thermo Fisher Scientific, 78440) and quantified with a BCA kit (Thermo Fisher Scientific, A53226). Then, protein lysis was mixed with loading buffer and boiled at 100°C for 5–10 min. The well-prepared lysis was loaded into 10% SDS-PAGE gel for electrophoresis and transferred on to a PVDF membrane. Before being incubated with antibodies against TFEB, LAMP1, ATP6V0D2, ATP6V1A, cathepsin B, LC3, p-STAT3, p-P65, p-PS6, p-ERK, p-AKT, caspase1 p10, and actin, the membranes should be blocked with 5% BSA, and followed by incubating with HRP-secondary antibodies (Cell Signaling Technology, 7074; Abcam, ab6885). Finally, the membranes were exposed under X ray and the bands were quantified with Image J.

Immunofluorescence Staining and Confocal Microscopy

The cells were seeded on glass slides and fixed with 4% formaldehyde for 30 min, permeabilized by 0.05% Triton X-100 about 20 min, blocked with 5% BSA for 1 h and incubated with anti-TFEB antibody overnight at 4°C. The cells were incubated with FITC-anti-goat secondary antibody for 1 h and DAPI for 10 min in darkness. After fully washing, the slides were placed onto confocal microscopy (Zeiss, Germany) for taking fluorescent photos.

FITC-Dextran and LysoTracker Red Staining

The mature BMDMs were cultured in 48-well plates, and treated with 5 μM VX-765, 500 nM SCH772984, 100 nM rapamycin, 10 μm S31-201, 200 nM IKK 16 or DMSO for 1 h, and incubated with FITC-Dextran for 1 h, then the MFI was measured with a Flow cytometer (CytoFLEX, Beckman Coulter). For staining LysoTracker red, BMDMs were plated in 12-well plates, and cultured with *Salmonella* and *S. aureus* at 5 MOI for 5 h, and then, stained with LysoTracker red for 10 min. Lastly, the MFI was measured with a Flow cytometer (CytoFLEX, Beckman Coulter).

Infection Model *in vivo* and Bacteria Culture

The C57/B6 mice were purchased from *shanghai model organisms*. And our animal model was constructed according to the guidelines of the Institutional Animal Care. *Salmonella* (SL1344) and *S. aureus* (NCTC8325) were a gift from Xiang-ping Yang Lab. In the infection model, the single colonies of *Salmonella* and *S. aureus* were shaken in 2–4 ml LB medium for 5 h at 37°C and the concentration of bacteria was quantified to reach an OD_{600} of 0.5 with a spectrophotometer (Thermo Fisher Scientific™). Those sex-and age-matched mice were divided into three groups, including control group, *Salmonella* infection group, and *S. aureus* infection group. The experimental groups were administrated with 1×10^8 bacteria suspended in 0.5 ml DMEM medium through intraperitoneal injection for 8 h, and then the mice were sacrificed. Five milliliter germ-free PBS was injected into the peritoneum of the mice and kneaded gently. The macrophages were harvested from the ascites, and the cells lysed with RIPA buffer for western-blot.

Gentamicin Protection Assay

Salmonella and *S. aureus* were generated from single colonies as before. Mature BMDMs were cocultured with bacteria at an MOI of 2 for 1 h. After three rounds of washing with PBS, the infected BMDMs were incubated with 300 μg/ml gentamicin and 100 μg/ml gentamicin diluted in DMDM medium in turn for 1 h. After three rounds of washing with PBS, the BMDMs were lysed with 0.02% Triton x-100. Then one half of the lysis was diluted with LB into appropriate concentrations and seeded on LB plates for measuring the preliminary CFU. Another half of the protein lysis was quantified with a BCA kit and the final CFU per cell in each group was generated by the preliminary CFU folding protein concentration in each well.

Statistics

All of our data were quantified and drawn with GraphPad Prism 5 and presented as means (± SEM). The measurement of those data through a two tailed Student's *t*-test and *p*-values, considered as significant, should be less than 0.05.

DATA AVAILABILITY STATEMENT

The original contributions presented in the study are included in the article/**Supplementary Material**, further inquiries can be directed to the corresponding authors.

ETHICS STATEMENT

The animal study was reviewed and approved by the Wuhan Central Hospital, Huazhong University of Science and Technology, Wuhan. Written informed consent was obtained from the owners for the participation of their animals in this study.

AUTHOR CONTRIBUTIONS

SR and YX conceived and performed the experiments and analyzed the data. SR, TX, YX, and HZ wrote the manuscript. YX and HZ supervised the project. All authors contributed to the article and approved the submitted version.

ACKNOWLEDGMENTS

We thank Drs. Xiang-ping Yang and Qinlei Gao for the gifts of bacteria and technical guidance.

SUPPLEMENTARY MATERIAL

The Supplementary Material for this article can be found online at: https://www.frontiersin.org/articles/10.3389/fmicb.2020.573844/full#supplementary-material

REFERENCES

Ammanathan, V., Mishra, P., Chavalmane, A. K., Muthusamy, S., Jadhav, V., Siddamadappa, C., et al. (2019). Restriction of intracellular *Salmonella* replication by restoring TFEB-mediated xenophagy. *Autophagy* 16, 1584–1597. doi: 10.1080/15548627.2019.1689770

Ballabio, A., and Bonifacino, J. S. (2020). Lysosomes as dynamic regulators of cell and organismal homeostasis. *Nat. Rev. Mol. Cell Biol.* 21, 101–118. doi: 10.1038/s41580-019-0185-4

Bauckman, K. A., Owusu-Boaitey, N., and Mysorekar, I. U. (2015). Selective autophagy: xenophagy. *Methods* 75, 120–127. doi: 10.1016/j.ymeth.2014.12.005

Birmingham, C. L., Smith, A. C., Bakowski, M. A., Yoshimori, T., and Brumell, J. H. (2006). Autophagy controls *Salmonella* infection in response to damage to the *Salmonella*-containing vacuole. *J. Biol. Chem.* 281, 11374–11383. doi: 10.1074/jbc.M509157200

Flannagan, R. S., Heit, B., and Heinrichs, D. E. (2016). Intracellular replication of *Staphylococcus aureus* in mature phagolysosomes in macrophages precedes host cell death, and bacterial escape and dissemination. *Cell. Microbiol.* 18, 514–535. doi: 10.1111/cmi.12527

Ganesan, R., Hos, N. J., Gutierrez, S., Fischer, J., Stepek, J. M., Daglidu, E., et al. (2017). *Salmonella* Typhimurium disrupts Sirt1/AMPK checkpoint control of mTOR to impair autophagy. *PLoS Pathog.* 13:e1006227. doi: 10.1371/journal.ppat.1006227

Gray, M. A., Choy, C. H., Dayam, R. M., Ospina-Escobar, E., Somerville, A., Xiao, X., et al. (2016). Phagocytosis enhances lysosomal and bactericidal properties by activating the transcription factor TFEB. *Curr. Biol.* 26, 1955–1964. doi: 10.1016/j.cub.2016.05.070

Hartz, P. H., Pot, A. W., and Felsenfeld, O. (1950). Fatal fulminant colitis due to *Salmonella* Saint Paul. *Am. J. Clin. Pathol.* 20, 184–187. doi: 10.1093/ajcp/20.2.184

Herp, S., Brugiroux, S., Garzetti, D., Ring, D., Jochum, L. M., Beutler, M., et al. (2019). *Mucispirillum schaedleri* antagonizes *Salmonella* virulence to protect mice against colitis. *Cell Host Microbe* 25, 681–694.e8. doi: 10.1016/j.chom.2019.03.004

Huang, J., and Brumell, J. H. (2014). Bacteria-autophagy interplay: a battle for survival. *Nat. Rev. Microbiol.* 12, 101–114. doi: 10.1038/nrmicro3160

Jubrail, J., Morris, P., Bewley, M. A., Stoneham, S., Johnston, S. A., Foster, S. J., et al. (2016). Inability to sustain intraphagolysosomal killing of *Staphylococcus aureus* predisposes to bacterial persistence in macrophages. *Cell. Microbiol.* 18, 80–96. doi: 10.1111/cmi.12485

Koziel, J., Maciag-Gudowska, A., Mikolajczyk, T., Bzowska, M., Sturdevant, D. E., Whitney, A. R., et al. (2009). Phagocytosis of *Staphylococcus aureus* by macrophages exerts cytoprotective effects manifested by the upregulation of antiapoptotic factors. *PLoS One* 4:e5210. doi: 10.1371/journal.pone.0005210

Lara-Tejero, M., Sutterwala, F. S., Ogura, Y., Grant, E. P., Bertin, J., Coyle, A. J., et al. (2006). Role of the caspase-1 inflammasome in *Salmonella* Typhimurium pathogenesis. *J. Exp. Med.* 203, 1407–1412. doi: 10.1084/jem.20060206

Li, L., Sun, B., Gao, Y., Niu, H., Yuan, H., and Lou, H. (2018). STAT3 contributes to lysosomal-mediated cell death in a novel derivative of riccardin D-treated breast cancer cells in association with TFEB. *Biochem. Pharmacol.* 150, 267–279. doi: 10.1016/j.bcp.2018.02.026

Martina, J. A., Chen, Y., Gucek, M., and Puertollano, R. (2012). MTORC1 functions as a transcriptional regulator of autophagy by preventing nuclear transport of TFEB. *Autophagy* 8, 903–914. doi: 10.4161/auto.19653

Medina, D. L., Di Paola, S., Peluso, I., Armani, A., De Stefani, D., Venditti, R., et al. (2015). Lysosomal calcium signalling regulates autophagy through calcineurin and TFEB. *Nat. Cell Biol.* 17, 288–299. doi: 10.1038/ncb3114

Miao, E. A., Leaf, I. A., Treuting, P. M., Mao, D. P., Dors, M., Sarkar, A., et al. (2010). Caspase-1-induced pyroptosis is an innate immune effector mechanism against intracellular bacteria. *Nat. Immunol.* 11, 1136–1142. doi: 10.1038/ni.1960

Moldovan, A., and Fraunholz, M. J. (2019). In or out: phagosomal escape of *Staphylococcus aureus*. *Cell. Microbiol.* 21:e12997. doi: 10.1111/cmi.12997

Monack, D. M., Hersh, D., Ghori, N., Bouley, D., Zychlinsky, A., and Falkow, S. (2000). *Salmonella* exploits caspase-1 to colonize peyer's patches in a murine typhoid model. *J. Exp. Med.* 192, 249–258. doi: 10.1084/jem.192.2.249

Napolitano, G., and Ballabio, A. (2016). TFEB at a glance. *J. Cell Sci.* 129, 2475–2481. doi: 10.1242/jcs.146365

Palmieri, M., Impey, S., Kang, H., di Ronza, A., Pelz, C., Sardiello, M., et al. (2011). Characterization of the CLEAR network reveals an integrated control of cellular clearance pathways. *Hum. Mol. Genet.* 20, 3852–3866. doi: 10.1093/hmg/ddr306

Palmieri, M., Pal, R., Nelvagal, H. R., Lotfi, P., Stinnett, G. R., Seymour, M. L., et al. (2017). mTORC1-independent TFEB activation via Akt inhibition promotes cellular clearance in neurodegenerative storage diseases. *Nat. Commun.* 8:14338. doi: 10.1038/ncomms14338

Perera, R. M., and Zoncu, R. (2016). The lysosome as a regulatory hub. *Annu. Rev. Cell Dev. Biol.* 32, 223–253. doi: 10.1146/annurev-cellbio-111315-125125

Platt, F. M., d'Azzo, A., Davidson, B. L., Neufeld, E. F., and Tifft, C. J. (2018). Lysosomal storage diseases. *Nat. Rev. Dis. Primers* 4:27.

Qu, Y., Misaghi, S., Newton, K., Maltzman, A., Izrael-Tomasevic, A., Arnott, D., et al. (2016). NLRP3 recruitment by NLRC4 during *Salmonella* infection. *J. Exp. Med.* 213, 877–885. doi: 10.1084/jem.20132234

Raupach, B., Peuschel, S. K., Monack, D. M., and Zychlinsky, A. (2006). Caspase-1-mediated activation of interleukin-1beta (IL-1beta) and IL-18 contributes to innate immune defenses against *Salmonella enterica* serovar Typhimurium infection. *Infect. Immun.* 74, 4922–4926. doi: 10.1128/iai.00417-06

Settembre, C., Di Malta, C., Polito, V. A., Garcia Arencibia, M., Vetrini, F., Erdin, S., et al. (2011). TFEB links autophagy to lysosomal biogenesis. *Science* 332, 1429–1433. doi: 10.1126/science.1204592

Tranchemontagne, Z. R., Camire, R. B., O'Donnell, V. J., Baugh, J., and Burkholder, K. M. (2016). *Staphylococcus aureus* strain USA300 perturbs acquisition of lysosomal enzymes and requires phagosomal acidification for survival inside macrophages. *Infect. Immun.* 84, 241–253. doi: 10.1128/iai.00704-15

Upadhyay, S., and Philips, J. A. (2019). LC3-associated phagocytosis: host defense and microbial response. *Curr. Opin. Immunol.* 60, 81–90. doi: 10.1016/j.coi.2019.04.012

Visvikis, O., Ihuegbu, N., Labed, S. A., Luhachack, L. G., Alves, A. F., Wollenberg, A. C., et al. (2014). Innate host defense requires TFEB-mediated transcription of cytoprotective and antimicrobial genes. *Immunity* 40, 896–909. doi: 10.1016/j.immuni.2014.05.002

Wu, J., Fernandes-Alnemri, T., Fau-Alnemri, E. S., and Alnemri, E. S. (2010). Involvement of the AIM2, NLRC4, and NLRP3 inflammasomes in caspase-1 activation by *Listeria monocytogenes*. *J. Clin. Immunol.* 30, 693–702. doi: 10.1007/s10875-010-9425-2

Xia, Y., Liu, N., Xie, X., Bi, G., Ba, H., Li, L., et al. (2019). The macrophage-specific V-ATPase subunit ATP6V0D2 restricts inflammasome activation and bacterial infection by facilitating autophagosome-lysosome fusion. *Autophagy* 15, 960–975. doi: 10.1080/15548627.2019.1569916

Xu, Y., Zhou, P., Cheng, S., Lu, Q., Nowak, K., Hopp, A. K., et al. (2019). A bacterial effector reveals the V-ATPase-ATG16L1 axis that initiates xenophagy. *Cell* 178, 552–566.e20. doi: 10.1016/j.cell.2019.06.007

Zhao, Y., Yang, J., Shi, J., Gong, Y. N., Lu, Q., Xu, H., et al. (2011). The NLRC4 inflammasome receptors for bacterial flagellin and type III secretion apparatus. *Nature* 477, 596–600. doi: 10.1038/nature10510

Conflict of Interest: The authors declare that the research was conducted in the absence of any commercial or financial relationships that could be construed as a potential conflict of interest.

frontiers in Immunology

ORIGINAL RESEARCH
published: 05 January 2021
doi: 10.3389/fimmu.2020.610021

MicroRNA-106a Inhibits Autophagy Process and Antimicrobial Responses by Targeting ULK1, ATG7, and ATG16L1 During Mycobacterial Infection

Kunmei Liu[1,2†], Dantong Hong[3†], Fan Zhang[3†], Xin Li[3†], Meng He[3], Xuebo Han[3], Guolin Zhang[5], Guangxian Xu[1,3], Nicola J. Stonehouse[6], Zhongjia Jiang[3*], Weijun An[1,4*] and Le Guo[1,2,3*]*

[1] Ningxia Key Laboratory of Clinical and Pathogenic Microbiology, General Hospital of Ningxia Medical University, Yinchuan, China, [2] Ningxia Key Laboratory of Cerebrocranial Diseases, Ningxia Medical University, Yinchuan, China, [3] Department of Medical Laboratory, School of Clinical Medicine, Ningxia Medical University, Yinchuan, China, [4] Department of Orthopaedics, General Hospital of Ningxia Medical University, Yinchuan, China, [5] Suzhou Institute for Drug Control, Suzhou, China, [6] School of Molecular and Cellular Biology, Faculty of Biological Sciences, University of Leeds, Leeds, United Kingdom

Autophagy is a key element of innate immune response against invading pathogens including *Mycobacterium tuberculosis* (*M. tuberculosis*). The emerging roles of microRNAs in regulating host antimicrobial responses against *M. tuberculosis* have gained widespread attention. However, the process by which miRNAs specifically influence antibacterial autophagy during mycobacterial infection is largely uncharacterized. In this study, we demonstrate a novel role of miR-106a in regulating macrophage autophagy against *M. tuberculosis.* H37Ra infection leads to downregulation of miR-106a in a time- and dose-dependent manner and concomitant upregulation of its three targets (ULK1, ATG7, and ATG16L1) in THP-1 macrophages. MiR-106a could inhibit autophagy activation and antimicrobial responses to *M. tuberculosis* by targeting ULK1, ATG7, and ATG16L1. Overexpression of miR-106a dramatically inhibited H37Ra-induced activation of autophagy in human THP-1 macrophages, whereas inhibitors of miR-106a remarkably promoted H37Ra-induced autophagy. The inhibitory effect of miR-106a on autophagy process during mycobacterial infection was also confirmed by Transmission Electron Microscope (TEM) observation. More importantly, forced expression of miR-106a increased mycobacterial survival, while transfection with miR-106a inhibitors attenuated the survival of intracellular mycobacteria. Taken together, these data demonstrated that miR-106a functioned as a negative regulator in autophagy and antimicrobial effects by targeting ULK1, ATG7, and ATG16L1 during *M. tuberculosis* infection, which may provide a potential target for developing diagnostic reagents or antibacterials against tuberculosis.

Keywords: ***Mycobacterium tuberculosis*, autophagy, miR-106a, ULK1, ATG7, ATG16L1**

OPEN ACCESS

Edited by:
Jere W. McBride, University of Texas Medical Branch at Galveston, United States

Reviewed by:
Chul-Su Yang, Hanyang University, South Korea
Isabelle Vergne, UMR5089 Institut de Pharmacologie et de Biologie Structurale (IPBS), France

***Correspondence:**
Le Guo
guole@nxmu.edu.cn
Kunmei Liu
lkm198507@126.com
Weijun An
anweijun939@163.com
Zhongjia Jiang
jiangzhongjia1988@163.com

†These authors have contributed equally to this work

Specialty section:
This article was submitted to Microbial Immunology, a section of the journal Frontiers in Immunology

Received: *24 September 2020*
Accepted: *23 November 2020*
Published: *05 January 2021*

Citation:
Liu K, Hong D, Zhang F, Li X, He M, Han X, Zhang G, Xu G, Stonehouse NJ, Jiang Z, An W and Guo L (2021) MicroRNA-106a Inhibits Autophagy Process and Antimicrobial Responses by Targeting ULK1, ATG7, and ATG16L1 During Mycobacterial Infection. Front. Immunol. 11:610021. doi: 10.3389/fimmu.2020.610021

INTRODUCTION

Tuberculosis (TB) is a communicable disease that is one of the top 10 causes of death worldwide and the leading cause of death from a single infectious agent (1). *Mycobacterium tuberculosis* (*M. tuberculosis*) infects approximately one third of the global population, making *M. tuberculosis* the leading bacterial cause of death in humans worldwide (2). However, only about 10% of individuals infected with *M. tuberculosis* develop active TB, while the majority of cases, about 90%, exhibit latent infection, suggesting a crucial role for host innate immunity in controlling *M. tuberculosis* infection (3). As the first line of immune defense against *M. tuberculosis*, macrophages not only recognize *M. tuberculosis* by pattern recognition receptors (PRRs), but also present bacterial peptide from *M. tuberculosis* to T lymphocytes, thus resulting in the activation of adaptive immune responses against *M. tuberculosis* (4). Moreover, the activation of antibacterial autophagy through ubiquitination of *M. tuberculosis* promotes the innate immune response against *M. tuberculosis* infection (5). Upon infection by *M. tuberculosis*, macrophages can launch a variety of innate immune defenses against *M. tuberculosis* (6, 7). In contrast, *M. tuberculosis* utilizes many strategies to evade host defense response for surviving and persisting within human macrophages (8). For instance, *M. tuberculosis* can arrest normal phagosome maturation, and avoid fusion with lysosomes to escape degradation by lysosomal hydrolases (9, 10).

Autophagy is widely recognized as a cellular process that can encapsulate macromolecules, organelles, or intracellular pathogens in double membrane-layered vesicles and deliver them to lysosomes for degradation (11). A number of autophagy-related genes (ATGs) orchestrate signaling events that regulate autophagy flux including formation of phagophore, autophagosome formation and phagolysosomal maturation during microbial invasion (12, 13). Among the ATGs, ULK1, ATG7, and ATG16L1 are essential for autophagy. ULK1 is a key component in the ULK1 complex which is crucial for initiation and formation of autophagosome (14). ATG7 has dual functions in autophagy regulation. First, ATG7 is essential for formation of a functional autophagosome by conjugating ATG5 to ATG12 as an E1-like enzyme. Second, ATG7 conjugates LC3-I to phosphatidylethanolamine, forming a mature autophagosomal membrane protein, LC3-II (15). Moreover, ATG16L1 is a component of the ATG12–ATG5–ATG16L1 complex, which localizes to phagophore membranes and stimulates the transfer of LC3 from ATG3 to PE (16).

MicroRNAs (miRNAs) are a growing family of small non-coding RNAs that function as post-transcriptional regulators of gene expression by targeting mRNAs for translational repression or cleavage (17). Additionally, miRNAs have been proven to be involved in a variety of biological pathways, including development, homeostasis and diseases (18, 19). A growing body of evidence suggests that miRNAs also play important roles in regulating autophagy, especially in tumors (20, 21). However, the potential roles of miRNAs in regulating autophagy process during *M. tuberculosis* infection need to be further explored. In this study, we characterized the potential role of miR-106a in modulating autophagy process and affecting bacterial clearance in macrophages. Our study demonstrated that miR-106a expression was significantly decreased after mycobacterial infection in human THP-1 macrophages. Downexpression of miR-106a increased the expression levels of ULK1, ATG7, and ATG16L1 and promoted formation of autophagosomes in human THP-1 macrophages, thus attenuating bacterial survival. However, forced expression of miR-106a had the opposite effect. These findings provide a better understanding of miRNAs on regulating innate immunity and host defense against *M. tuberculosis*.

MATERIALS AND METHODS

Selection of Microarray Datasets and Analysis

The miRNA microarray dataset (GSE119494) was selected for analysis. GSE119494 contains miRNA expression data from PBMCs of three healthy donors and three active pulmonary tuberculosis (TB) patients. The miRNA expression profiling file was obtained, and the expression data of miR-17 family (miR-17, miR-20a, miR-20b, miR-106a, miR-106b, and miR-93) was selected for analysis. The data of miR-17 family were mean centered and represented by a heat map using Multi Experiment Viewer software (MeV).

Cells and Bacterial Culture

The human monocyte/macrophage cell line THP-1, human embryonic kidney 293T cells (HEK 293T), *Mycobacterium bovis* BCG and *M. tuberculosis* H37Ra were obtained from the American Type Culture Collection (ATCC). The THP-1 cells were cultured in suspension using RPMI1640 (GIBCO) supplemented with 10% fetal bovine serum and gentamycin. THP-1 cells were differentiated into adherent, well-spread macrophages with 100 nM phorbol 12-myristate 13-acetate (PMA, Sigma) to the well and maintenance for 3 days. BCG or H37Ra was grown in Middlebrook 7H9 broth medium (Goybio, China) supplemented with albumin dextrose catalase supplement.

Cell *T*ransfections and Chemical Reagent Treatment

The miR-106a mimics, miR-106a inhibitor, ATG7 siRNA, ATG16L1 siRNA, and ULK1 siRNA were purchased from GenePharma biotechnology company. To assay luciferase activity, HEK 293T cells were cotransfected with the pmirGLO luciferase constructs (WT or Mut) and miR-106a mimics or miR-106a inhibitor using Lipofectamine 2000 according to the manufacturer's instruction. For autophagy analysis, THP-1 macrophages were transfected with 50 nM mimic negative control (mimic nc) or miR-106a mimics; inhibitor negative control (inhibitor nc) or miR-106a inhibitor; 50 pmol ATG7 siRNA, ATG16L1 siRNA, or ULK1 siRNA according to the manufacturer's instructions. Several chemical reagents were

also used to treat THP-1 macrophages: a lysosome inhibitor, bafilomycin A1 (100 nM; Baf A1, Selleck); An autophagy inducer, rapamycin (50 μg/ml; Rapa, Solarbio Science & Technology Co.).

RNA Preparation, Real-Time PCR, and Western Blotting

For quantitative real-time PCR (RT-PCR) analysis, total RNA from cells was isolated using RNA simple Total RNA Kit (Tiangen Biotech), and miRNAs were performed using the miRcute miRNA isolation kit (Tiangen Biotech) according to the manufacturer's instructions. RT-PCR was performed using Hairpin-it^{TM} miRNAs RT-PCR Quantitation Kit (GenePharma, China) and samples were amplified for 40 cycles as follows: 95°C for 12 s, 62°C for 40 s, and 72°C for 30 s. The miR-106a expression was calculated relative to U6 snRNA. For Western blotting, proteins were loaded onto 12 or 15% SDS-PAGE gels and transferred to a polyvinylidene difluoride membrane (PVDF). Membranes were blocked in 5% non-fat milk in PBST for 1 h, and incubated with anti-ULK1(Abcam, ab167139), anti-ATG16L1 (Abcam, ab188642), anti-ATG7 (Abcam, ab52472), anti-LC3 (Abcam, ab51520), and anti-GAPDH (Abcam, ab245355). Immunoreactive band was performed using ECL reagent (Amersham Pharmacia) and quantified by using Image J software (NIH).

Bioinformatics Analysis, Plasmid Constructs, and Luciferase Assay

To perform miRNA profiling assays, we downloaded a miRNA expression dataset (GSE119494). The raw data are available on the Gene Expression Omnibus website (http://www.ncbi.nlm.nih.gov/geo/). The heatmap was analyzed by using Multiple Experiment Viewer version 4.9.0. miRNA targets were performed using miRanda (http://www.microrna.org) and TargetScan (http://www.targetscan.org). About 500 bp 3′-UTR fragments from ULK1, ATG16L1, or ATG7, containing the miR-106a-binding elements, were produced by PCR and were inserted into the pmirGLO dual-luciferase reporter vector (Promega). Mutant derivatives of the construct were also inserted into the pmirGLO dual-luciferase reporter vector (Promega). The HEK 293T cells were cultured into a 12-well plate and cotransfected with the luciferase constructs (WT or Mut) together with the miR-106a mimics or miR-106a inhibitors, respectively. Luciferase assays were performed at 24 h after transfection using the Dual-Luciferase Reporter Assay Kit (TransGen Biotech, Beijing).

Immunofluorescence Staining and Confocal Microscopy Analysis

The THP-1 macrophages were fixed with 4% paraformaldehyde (Sigma) followed by permeabilization with 0.2% Triton X-100 (Thermo Fisher Scientific). Cells were blocked with 3% BSA and labelled with Rabbit polyclonal to LC3 antibody (Abcam, ab51520) and visualized by Alexa Fluor 488-conjugated Affinipure Goat Anti-Rabbit IgG (Proteintech). Nuclei were stained with DAPI. The fluorescence images of cells were acquired and examined using a confocal microscope (Olympus, Japan). To quantify autophagy, the number of LC3 punctate dots was calculated by ImageJ Software (Version 1.49). At least 10 cells per experimental group were counted and each condition was assayed in triplicate.

Transmission Electron Microscopy

The THP-1 macrophages were collected and fixed in 2% glutaraldehyde, and then postfixed with 1% OsO4 for 2 h. After dehydration in a graded series of ethanol, the samples were transferred to propylene oxide and embedded in Epon. Ultrathin sections, about 80 nm thick, were cut and stained with uranyl acetate and lead citrate. Imaging was performed by a transmission electron microscopy (TEM, Hitachi H-7650). For each sample, group, 15 cellular cross-sections were counted.

Colony-Forming Unit Assay

To assess bacterial viability within human THP-1 macrophages, Colony-Forming Unit (CFU) assay was performed. Briefly, the THP-1 macrophages were transfected with miR-106a mimic, miR-106a inhibitor, mimic nc or inhibitor nc for 24 h, or treated with rapamycin plus miR-106a for 24 h. Moreover, the THP-1 macrophages were also transfected with miR-106a mimic in the presence of rapamycin (50 μg/ml) for 24 h. The cells were infected with H37Ra at a MOI of 10 for 3 h, and then washed with PBS to remove extracellular H37Ra. After that, the infected cells were cultured for an additional 24 h. Quantitative culturing was performed using 10-fold serial dilutions on Middlebrook 7H10 agar plates. Plates were incubated for 2 weeks, and colonies on plates were counted.

Statistical Analysis

The results are represented as mean ± SD of independent experiments. Statistical analyses were performed using two-tailed Student's *t*-test. Significant differences were assigned to p values <0.05, <0.01 and <0.001, denoted by *, **, and ***, respectively.

RESULTS

miR-106a Expression in Human Macrophages After Mycobacterial Infection

To evaluate the expression profiles of miR-17 family miRNAs in peripheral blood mononuclear cells (PBMCs) from patients with active pulmonary tuberculosis (TB), we analyzed miRNA microarray datasets (GSE119494) from the Gene Expression Omnibus (GEO) public database. The heatmap revealed that miR-106a and miR-17 showed the great magnitude of downregulation among the miR-17 family miRNAs (**Figure 1A**). In addition, we compared the expression of miR-106a and mir-17 in PBMCs from active pulmonary tuberculosis (TB) patients and healthy controls (HCs). The expression levels of miR-106a and miR-17 were significantly lower in PBMCs from active pulmonary TB patients than in HCs (**Figure 1B**). Previous

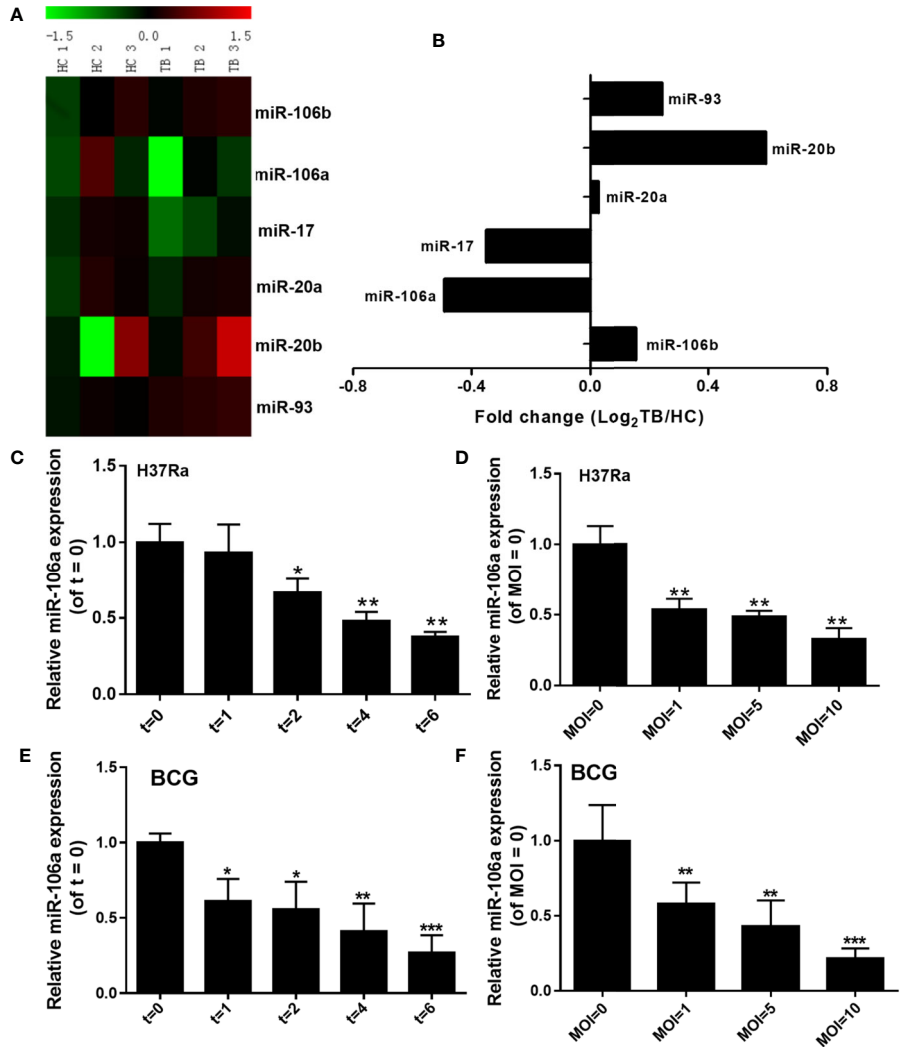

FIGURE 1 | miR-106a is reduced after mycobacterial infection *in vitro*. **(A)** Heatmap analysis shows downregulated (green) and upregulated (red) miRNAs in miR-17 family from tuberculosis (TB) patients and healthy controls (HCs) in the GEO public databases (GSE119494). **(B)** Expression levels of miR-17 family miRNAs in TB patients and HCs from the GEO public databases (GSE119494). Fold change was calculated by dividing the average signal intensity of TB patients by that of HCs. **(C)** The differentiated THP-1 macrophages were infected with H37Ra at a MOI of 10 for the indicated time points, and miR-106a expression was subsequently determined using qRT-PCR. The miR-106a expression levels are indicated relative to expression at 0 h. **(D)** The differentiated THP-1 macrophages were infected with H37Ra at indicated MOIs for 24 h. The miR-106a expression levels are indicated relative to expression without H37Ra infection. **(E)** The differentiated THP-1 macrophages were infected with BCG (MOI of 10) for the indicated time points, and miR-106a expression was subsequently determined using qRT-PCR. The miR-106a expression levels are indicated relative to expression at 0 h. **(F)** The differentiated THP-1 macrophages were infected with BCG at indicated MOIs for 24 h. The miR-106a expression levels are indicated relative to expression without BCG infection. All data above represent the means ± SD from at least three independent experiments. *$p < 0.05$, **$p < 0.01$, ***$p < 0.001$.

studies have showed that miR-17 was downregulated in macrophages and regulated autophagy by targeting Mcl-1 and STAT3 during mycobacterial infection (22). As miR-106a's functional role in regulation of *M. tuberculosis* infection remains uncharacterized, we choose miR-106a for our further study. We used *M. tuberculosis* H37Ra or *Mycobacterium bovis* BCG to infect the differentiated THP-1 macrophages, and found that both H37Ra (**Figures 1C, D**) and BCG (**Figures 1E, F**) strains could significantly reduce miR-106a expression in a time- and dose-dependent manner.

miR-106a Directly Targets ULK1, ATG7, and ATG16L1

To establish a direct molecular link, we next examined the ability of miR-106a to regulate ULK1, ATG7, and ATG16L1. As shown in **Figure 2A**, ULK1 holds a single 9mer seed match to miR-106a within the 3′-UTR while ATG16L1 and ATG7 contain a 7mer site and an 8mer site respectively. Moreover, more than three point mutations were introduced into the predicted miR-106a binding motifs. Overexpression of miR-106a significantly inhibited luciferase activity driven by the 3′-UTR constructs

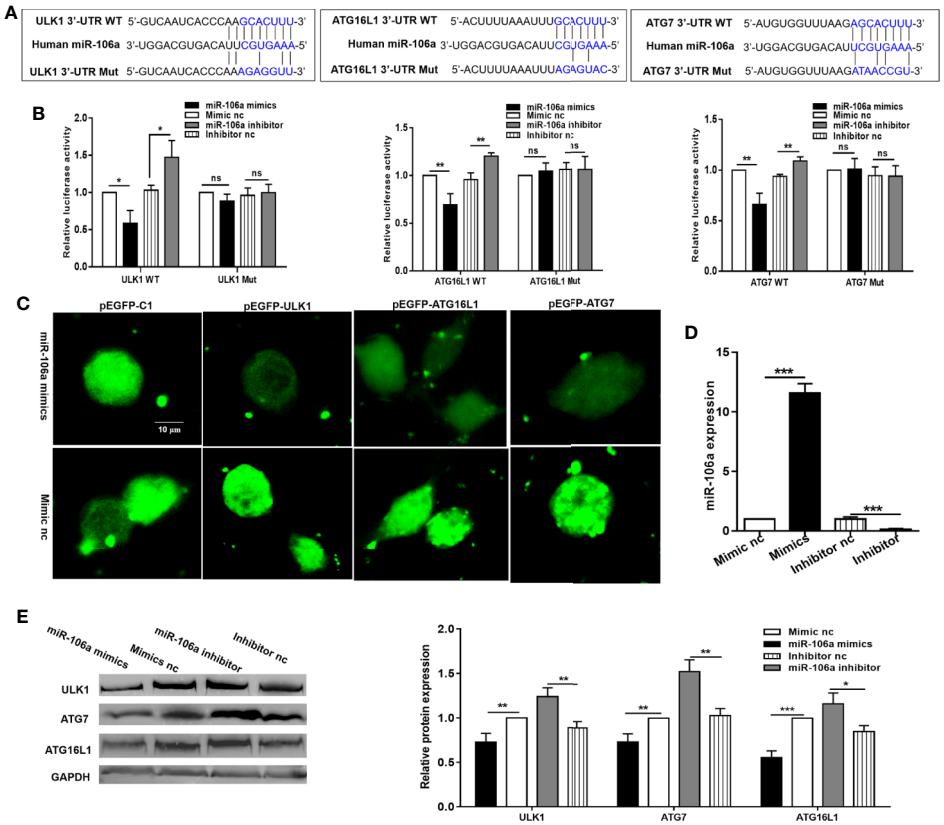

FIGURE 2 | miR-106a directly targets ULK1, ATG7, and ATG16L1. **(A)** Predicted binding between miR-106a and the seed matches in ULK1, ATG7 and ATG16L1 3′-UTRs. The sequence of the ULK1, ATG7, and ATG16L1 3′-UTR seed mutants used for the reporter assays. **(B)** miR-106a regulates ULK1, ATG7, and ATG16L1 3′-UTR reporters. Luciferase reporter assays 24 h after transfection with indicated pmirGLO dual-luciferase reporter vector, co-transfected with miR-106a mimics, miR-106a inhibitor or relevant negative controls (nc). **(C)** Representative fluorescent microscopic image confirm that GFP expression of the pEGFP-ULK1, pEGFP-ATG16L1 and pEGFP-ATG7 reporters was inhibited by miR-106a. HEK-293 cells were co-transfected with the GFP reporter vectors and compared with cells transfected with a mimic or control of miR-106a. Scale bars: 10 μm. **(D)** The THP-1 macrophages were transfected with miR-106a mimics, mimic nc, miR-106a inhibitor or inhibitor nc. The expression levels of miR-106a were measured by qRT-PCR. **(E)** miR-106a decreases ULK1, ATG7 and ATG16L1 protein levels. Western blot analysis 24 h after transfection with miR-106a mimics, mimic nc, miR-106a inhibitor or inhibitor nc. The ULK1, ATG7 and ATG16L1 bands were quantified relative to glyceraldehyde 3-phosphate dehydrogenase (GAPDH). Data represent the means ± SD from at least three independent experiments. *$p < 0.05$, **$p < 0.01$, ***$p < 0.001$.

(WT), while the mutant 3′-UTR constructs (Mut) either abolished or significantly reduced this effect. Additionally, miR-106a inhibitor significantly strengthened luciferase activity in HEK 293T cells expressing the 3′-UTR reporters, whereas mutation of the miR-106a-binding site abrogated this promotion of luciferase activity (**Figure 2B**), confirming that ULK1, ATG7, and ATG16L1 are putative targets of miR-106a. In order to directly address whether miR-106a binds to the 3′-UTR of target mRNAs, we generated three GFP reporter vectors containing the putative miR-106a binding sites within the 3′-UTRs of ULK1, ATG16L1 and ATG7. GFP fluorescence decreased significantly in cells co-transfected with miR-106a mimics and binding site-containing GFP reporter vectors. However, GFP fluorescence did not decrease significantly in cells transfected with mimic nc or with GFP reporters lacking binding sites (**Figure 2C**). Finally, we examined the effect of miR-106a on the endogenous ULK1, ATG7, and ATG16L1 proteins in THP-1 macrophages. High levels of miR-106a were detected in THP-1 macrophages after transfection with the miR-106a mimics. However, transfection with miR-106a inhibitor significantly reduced the expression levels of miR-106a (**Figure 2D**). As evident from **Figure 2E**, overexpression of miR-106a results in a significant decrease in the expression levels of ULK1, ATG7, and ATG16L1. However, miR-106a inhibitor results in an obvious upregulation of these proteins.

miR-106a Inhibits Induction of Autophagy in *Mycobacterium tuberculosis*-Infected Macrophages by Targeting ULK1, ATG7, and ATG16L1

To identify whether autophagy could be induced during *M. tuberculosis* infection, the LC3-II expression was investigated, which is considered to be an accurate indicator for autophagosome formation (23, 24). The result showed that there was a marked increase in LC3-II expression with H37Ra

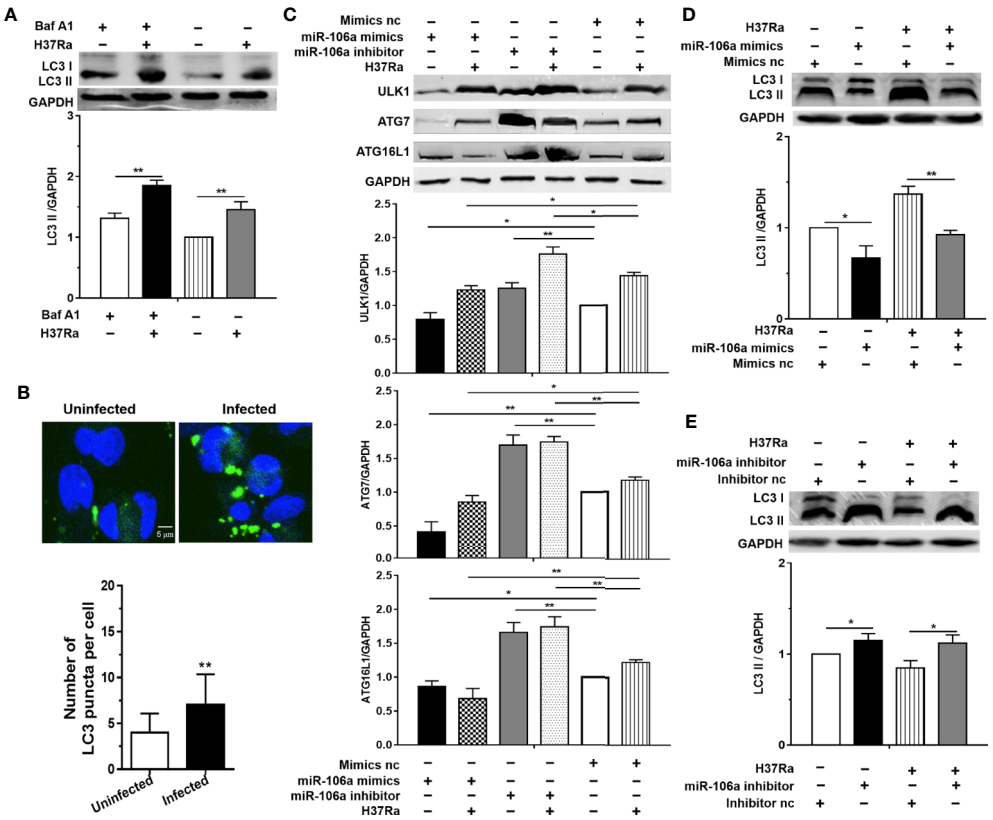

FIGURE 3 | miR-106a inhibits autophagy induction in macrophages by targeting ULK1, ATG7 and ATG16L1. **(A)** THP-1 macrophages were treated with Baf A1 (100 nM) for 2 h, and then were uninfected or infected with H37Ra. LC3-II expression was determined by Western blot, normalized to GAPDH expression. **(B)** THP-1 macrophages were uninfected or infected with H37Ra for 24 h. The cells were fixed and incubated with rabbit anti-LC3 antibody, and stained with goat anti-rabbit IgG (Alexa Fluor 488; green) to detect LC3 puncta by confocal microscopy. Scale bars: 5 μm. The number of LC3 puncta in each cell was also counted. (Uninfected, n = 20; Infected, n = 20). Experiments performed in triplicate. $^{**}p < 0.01$. **(C)** THP-1 macrophages were transfected with an miR-106a mimic or mimic nc; miR-106a inhibitor or inhibitor nc, and then infected with H37Ra for 24 h. ULK1, ATG7 and ATG16L1 protein levels were determined by Western blot, normalized to GAPDH expression. **(D, E)** The ratio of LC3-II to LC3-I were also determined by Western blot, normalized to GAPDH expression. Data represent the means ± SD from at least three independent experiments. $^{*}p < 0.05$, $^{**}p < 0.01$.

infection compared with an uninfected control (**Figure 3A**). In addition, bafilomycin A1 (Baf-A1) challenge led to further accumulation of LC3-II in THP-1 macrophages after H37Ra infection (**Figure 3A**), indicating that H37Ra infection promote autophagic processes. To further confirm that *M. tuberculosis* induce autophagy in THP-1 macrophages, the LC3-II puncta formation was detected by confocal microscopy. H37Ra-infected THP-1 macrophages displayed a significant increase in the number of LC3 puncta compared with uninfected THP-1 macrophages (**Figure 1B**). These results suggest that a complete autophagic response is induced after THP-1 macrophages were infected with H37Ra. To further explore whether miR-106a decreases endogenous ULK1, ATG7, and ATG16L1 during mycobacterial infection, H37Ra-infected THP-1 macrophages were transfected with miR-106a mimic or inhibitor, and protein levels of ULK1, ATG7, and ATG16L1 were measured by Western blot. As shown in **Figure 3C**, miR-106a overexpression decreased the protein levels of ULK1, ATG7, and ATG16L1 in uninfected and H37Ra-infected THP-1 macrophages. In contrast, these protein levels were significantly increased in uninfected and H37Ra-infected THP-1 macrophages, after endogenous miR-106a was blocked by the transfection of a miR-106a inhibitor. To test the hypothesis that miR-106a regulated autophagy in macrophages during *M. tuberculosis* infection, we tested the expression of LC3 by Western blot and counted LC3 puncta by fluorescence microscopy. Western blot results showed that transfection with miR-106a mimics decreased, whereas transfection with miR-106a inhibitor increased, the LC3-II expression in THP-1 macrophages before and after H37Ra infection (**Figures 3D, E**).

The results of confocal microscopy indicated that miR-106a mimics significantly decreased the number of LC3 puncta in THP-1 macrophages (**Figures 4A–C**). Conversely, the number of LC3 puncta was significantly increased in uninfected and H37Ra-infected THP-1 macrophages after transfection with miR-106a inhibitor, compared with the control condition (**Figures 4A–C**). Transfection with miR-106a mimics, ATG7 siRNA, ATG16L1 siRNA or ULK1 siRNA significantly reduced

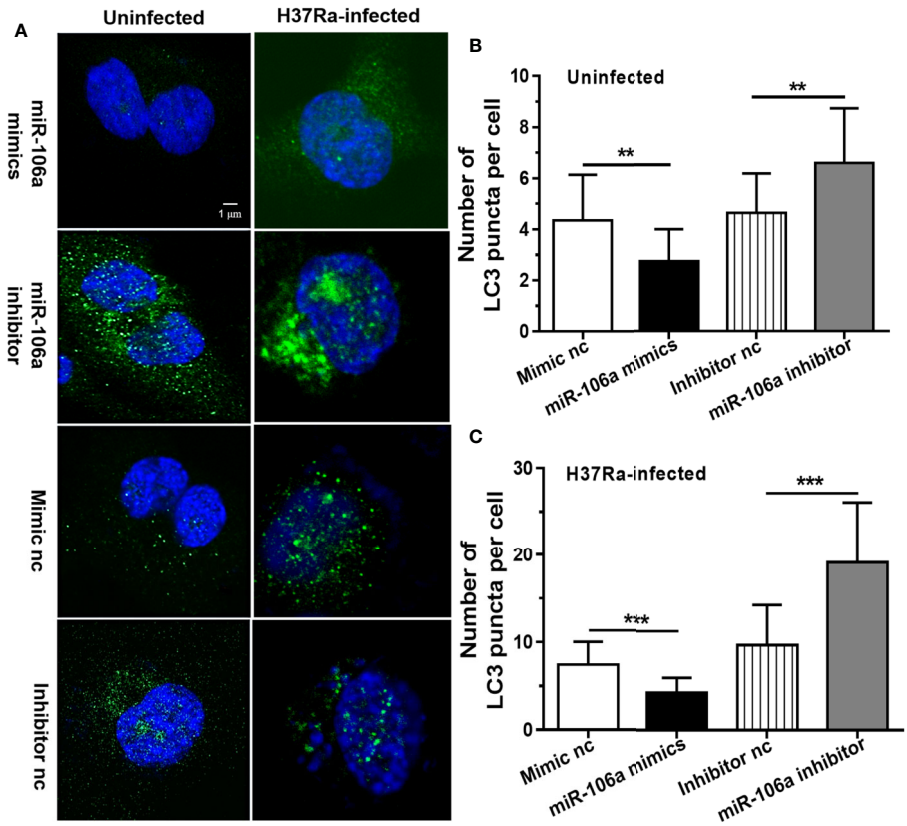

FIGURE 4 | miR-106a mimics significantly decreased the number of LC3 puncta in macrophages. **(A)** THP-1 macrophages were transfected with miR-106a mimic or inhibitor, and then treated with H37Ra for 24 h. The THP-1 macrophages were fixed and incubated with rabbit anti-LC3 antibody, and stained with goat anti-rabbit IgG (Alexa Fluor 488; green) to detect LC3 puncta by confocal microscopy (left, uninfected; right, infected). Scale bars: 1 μm. **(B, C)** Quantitative data of LC3 puncta analysis. (Mimic nc, n = 20; Inhibitor nc, n = 20; Mimic, n = 20; Inhibitor, n = 20). Data represent the means ± SD from three independent experiments. **p < 0.01, ***p < 0.001.

the protein expression levels of ATG7, ATG16L1, and ULK1 (**Figures 5A–C**), the LC3-II expression (**Figures 5D, E**) and the number of LC3 puncta (**Figures 6A, B**), in THP-1 macrophages with rapamycin, indicating that the siRNAs of ATG7, ATG16L1, and ULK1, and miR-106a mimics can inhibit autophagy. Collectively, these results indicate that miR-106a inhibit autophagy in macrophages.

TEM Confirms Repression of Autophagy by miR-106a

In order to gain insight into the regulation effect of miR-106a on autophagy during mycobacterial infection, we perform Transmission Electron Microscopy (TEM) to detected and quantified autophagosomes and autolysosomes. Notably, TEM images revealed an accumulation of numerous autophagosomes and autolysosomes in the cytoplasm of H37Ra-infected THP-1 macrophages transfected with miR-106a inhibitor. However, miR-106a mimics decreased the number of autophagosomes and autolysosomes, confirming our TEM analysis (**Figures 7A, C**). Moreover, transfection with miR-106a mimics could decrease the number of autophagosomes and autolysosomes per cellular cross-section in rapamycin-treated cells (**Figures 7B, D**).

miR-106a Promotes H37Ra Survival in Macrophages by Inhibiting Autophagy

The effects of miR-106a on intracellular survival of *M. tuberculosis* in human THP-1 macrophages were analyzed by colony-forming unit (CFU) assay. Importantly, miR-106a mimics promoted (**Figure 8A**), whereas miR-106a inhibitor decreased (**Figure 8B**), intracellular H37Ra growth, compared with the corresponding control conditions. These results support the hypothesis that miR-106a facilitates intracellular survival of H37Ra in macrophages. Moreover, transfection with miR-106a mimics plus rapamycin could promote H37Ra survival compared to treatment with rapamycin in H37Ra-infected THP-1 macrophages (**Figure 8A**), indicating that miR-106a can inhibit rapamycin-induced autophagy. In addition, transfection with mixed siRNA plus miR-106a inhibitor could not inhibit H37Ra survival compared to treatment with mixed siRNA (**Figure 8B**), indicating that miR-106a inhibitor can decrease *M. tuberculosis* CFU *via* autophagy.

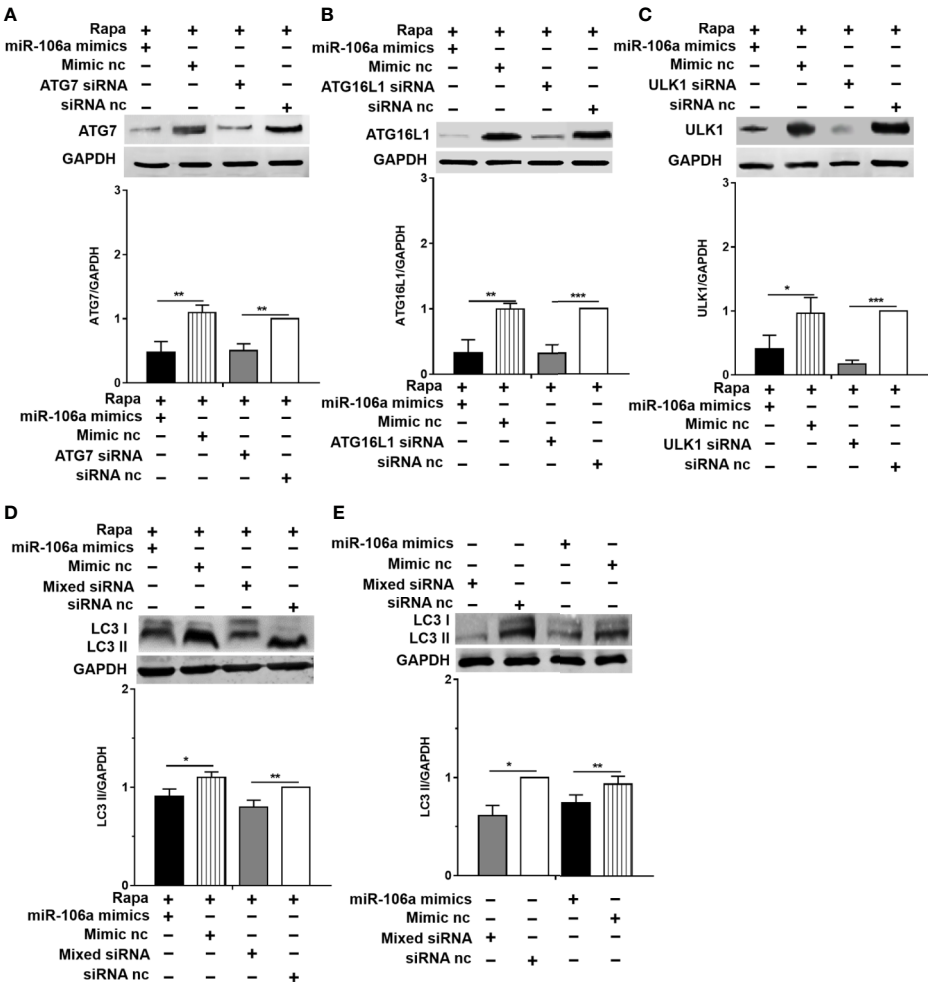

FIGURE 5 | miR-106a and the siRNAs of ATG7, ATG16L1 and ULK1 can inhibit the expression of LC3-II. **(A–C)** The THP-1 macrophages were treated with 50 μg/ml rapamycin for 2 h, and then transfected with miR-106a mimics, ATG7 siRNA, ATG16L1 siRNA or ULK1 siRNA for 24 h. After that, the protein levels of ATG16L1, ATG7 and ULK1 was determined by Western blot. **(D)** The THP-1 macrophages were treated with 50 μg/ml rapamycin for 2 h, and then transfected with miR-106a mimics, or mixture of ATG7 siRNA, ATG16L1 siRNA and ULK1 siRNA for 24 h. After that, LC3-II expression was determined by Western blot. **(E)** The THP-1 macrophages were transfected with miR-106a mimics, or mixture of ATG7 siRNA, ATG16L1 siRNA and ULK1 siRNA for 24 h. After that, LC3-II expression was determined by Western blot. Data represent the means ± SD from three independent experiments. *$p < 0.05$, **$p < 0.01$, ***$p < 0.001$.

DISCUSSION

Increasing evidence has demonstrated that autophagy plays an essential role in the host innate immune responses against mycobacterial infection (25, 26). However, the molecular mechanism of autophagy-mediated mycobacterial clearance remains unclear. There is growing evidence that miRNAs are regulators of genes involved in many aspects of immune system function, including differentiation of immune cells (27) and regulation of the host immune defense mechanisms against microbial infection (28). However, the immune regulatory functions of miRNAs in autophagy-mediated mycobacterial clearance, especially miR-17 family miRNAs, need to be further explored. In this study, we describe a novel role of miR-106a in modulating autophagy process and mycobacterial elimination in human macrophages by targeting ULK1, ATG7, and ATG16L1, which may provide a better understanding of the host innate immune responses against *M. tuberculosis*.

miR-106a is a member of miR-17 family miRNAs, which are broadly conserved and involved in a variety of biological pathways (29, 30). Evidence is mounting that miR-106a plays key regulatory roles in autophagy, especially in cancer. For instance, miR-106a inhibits tumor cell death in colorectal cancer by targeting ATG7 (31). miR-106a suppresses ULK1 expression and thereby sensitizes lung cancer cells to Src-TKI treatment (32). Moreover, miR-106a targets the important autophagy gene ULK1 in acute myeloid leukemia cells (33). Most importantly, a research has shown that miR-106a regulates macrophage inflammatory responses by targeting SIRPa, indicating a potential role of miR-106a in the host immune

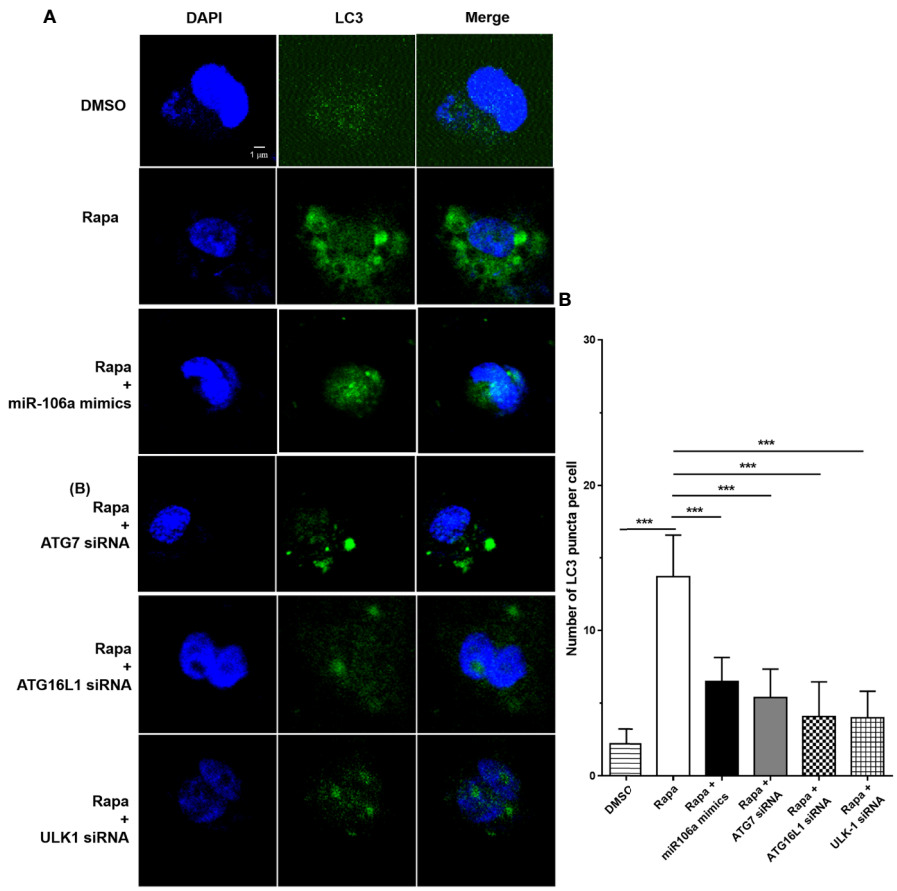

FIGURE 6 | The siRNAs of ATG7, ATG16L1 and ULK1 inhibited autophagosome formation. **(A)** The THP-1 macrophages were treated with 50 μg/ml rapamycin for 2 h, and then transfected with ATG7 siRNA, ATG16L1 siRNA, ULK1 siRNA or miR-106a mimics for 24 h. After that, the THP-1 macrophages were fixed and incubated with Rabbit Anti-LC3 antibody, followed by Alexa Fluor 488-conjugated goat anti-rabbit IgG. LC3 puncta formation was then detected by confocal microscopy. **(B)** Quantitative data of LC3 puncta analysis. (Rapa, n = 10; Rapa plus miR-106a mimics, n = 10; Rapa plus ATG7 siRNA, n = 10; Rapa plus ATG16L1 siRNA, n = 10; Rapa plus ULK1 siRNA, n = 10). Data represent the means ± SD from three independent experiments. ***$p < 0.001$.

response (34). However, the exact role of miR-106a in human macrophages during *M. tuberculosis* infection remains largely unclear. Indeed, our study showed that miR-106a functioned as a negative regulator in autophagy responses during *M. tuberculosis* infection, and inhibition of miR-106a expression promoted autophagy process to facilitate mycobacterial clearance.

Furthermore, we investigated the molecular mechanism by which miR-106a regulates autophagy responses in mycobacterial infected macrophages. We identified that ULK1, ATG16L1 and ATG7 are targets for miR-106a. ULK1, ATG7, and ATG16L1 are essential for autophagy. ULK1 can function in a complex with at least three protein partners: FIP200, ATG13 and ATG101. The formation of the autophagosome is mediated by the ULK1 complex (14). ULK1-deficient cells increased *M. tuberculosis* replication, and decreased selective autophagy (35). ATG7 is a master regulators of autophagy process, which is involved in autophagosome formation and vesicle progression (15). ATG7 knockout mice displayed increased susceptibility to *Klebsiella pneumoniae* infection, with decreased survival rates, increased bacterial burdens, and intensified lung injury (36). Moreover, ATG7-deficient macrophages exhibited enhanced mycobacterial uptake and growth by modulating the expression of scavenger receptors, and ATG7 knockout mice exhibited increased susceptibility to mycobacterial infection (37). ATG16L1 takes part in the elongation of the autophagosomal membrane (16). It has been reported that ATG16L1 conditional knockout mice exhibit defective autophagy and are more susceptible to *Salmonella* infection (38). Our study indicates that miR-106a downregulates ULK1, ATG7, and ATG16L1 proteins, thus inhibiting autophagy process in human macrophages.

Autophagy is a crucial defense immune response after the encounter of intracellular bacterial infection, including *M. tuberculosis* (39). Major steps in the process of autophagy contain initiation, nucleation, elongation, and autophagosome maturation as well as fusion of autophagosomes with lysosomes (40). Recent studies provide evidence that several miRNAs

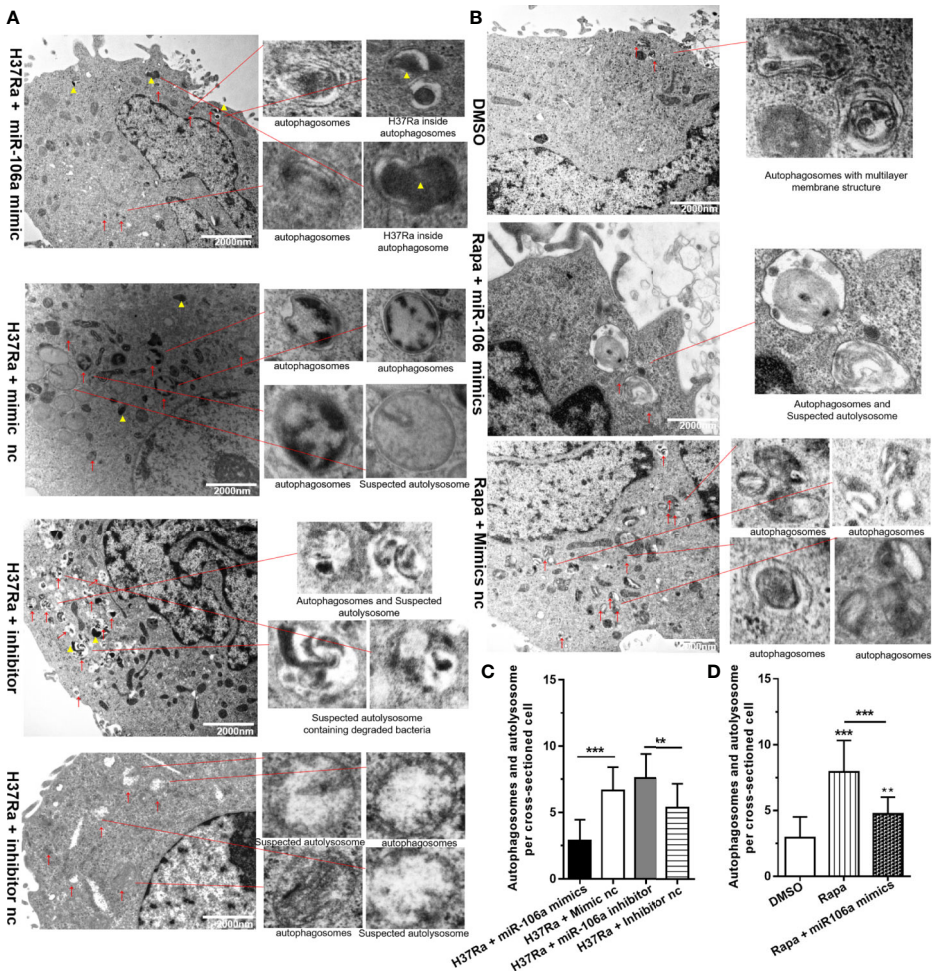

FIGURE 7 | The inhibitory effect on autophagy by miR-106a was confirmed by TEM detection. **(A)** The THP-1 macrophages were transfected with miR-106a mimic or miR-106a inhibitor, and then infected with H37Ra for 24 h. Representative images of TEM. Scale bars represent 2 μm. Autophagosomes or suspected autolysosomes denoted by red arrow heads. H37Ra indicated by yellow triangle. **(B)** The THP-1 macrophages were treated with 50 μg/ml rapamycin for 2 h, and then transfected with miR-106a mimics for 24 h. Representative images of TEM. Scale bars represent 2 μm. Autophagosomes or suspected autolysosomes denoted by red arrow heads. **(C, D)** The number of autophagosomes per cross-sectioned cell was counted (n = 15). Data represent the means ± SD from three independent experiments. **p < 0.01, ***p < 0.001.

modulate autophagy process during mycobacterial infection (41). For example, miR-125a inhibits autophagy process and antimicrobial responses through targeting UVRAG during mycobacterial infection (42). miR-155 accelerated the autophagic response to eliminate intracellular Mycobacteria by targeting Rheb in macrophages (43). However, miR-155 subverts autophagy by targeting ATG3 in human dendritic cells (44). It is reported that miR-17-5p regulates autophagy in *M. tuberculosis*-infected macrophages by targeting Mcl-1 and STAT3 (22). miR-27a promotes the intracellular survival of *M. tuberculosis* by regulating Ca^{2+}-associated autophagy (45). miR-144-5p inhibits antibacterial autophagy and the innate host immune response against *M. tuberculosis* in human monocytes and macrophages by targeting DRAM2 (46). *M. tuberculosis* can inhibit integrated pathways involved in autophagy to support bacterial intracellular survival and persistence by inducing miR-33 and miR-33* (47). Another study showed that miR-20a inhibits autophagic response and favors BCG survival in murine macrophages by targeting ATG7 and ATG16L1 (48). In the present study, miR-106a decreased in differentiated THP-1 macrophages after H37Ra infection. Functional assays demonstrated that inhibition of miR-106a promoted the processing of LC3 and the accumulation of LC3 puncta in uninfected and H37Ra-infected THP-1 macrophages, which indicates that functioned as a negative regulator of autophagy during mycobacterial infection. The inhibitory effect of miR-106a on autophagy during mycobacterial infection was also confirmed by TEM observation. In addition, we found that inhibited expression of miR-106a decreased the intracellular survival of H37Ra, whereas mimics of miR-106a increased mycobacterial survival, indicating

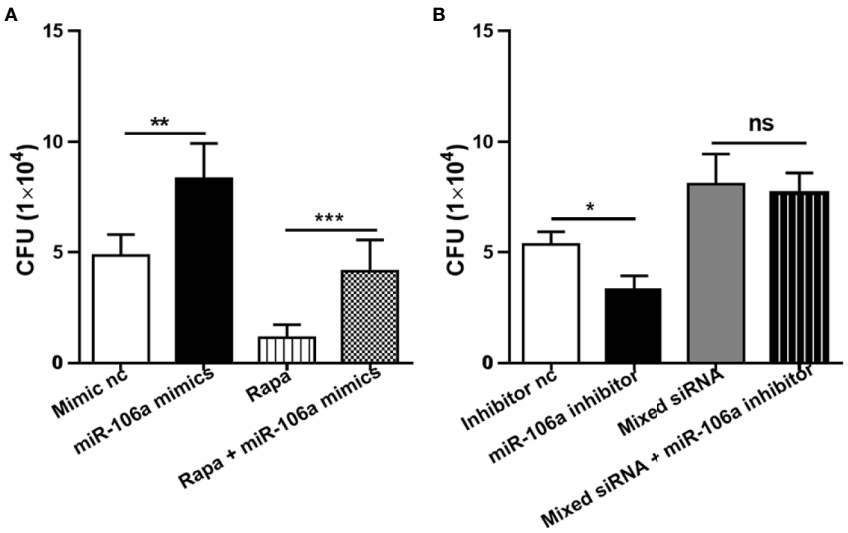

FIGURE 8 | Intracellular survival of H37Ra analyzed by counting CFU. **(A)** The THP-1 macrophages were treated with mimic nc, miR-106a mimics, rapamycin (50 μg/ml) or rapamycin plus miR-106a mimics for 24 h. After infection with H37Ra at a MOI of 10 for 3h, the cells were washed to remove extracellular bacteria, and cultured for an additional 24 h. The cells were lysed and mycobacterial viability (CFU) determined. $^{**}p < 0.01$, $^{***}p < 0.001$. **(B)** The THP-1 macrophages were treated with inhibitor nc, miR-106a inhibitor, mixed siRNA or mixed siRNA plus miR-106a inhibitor for 24 h. After infection with H37Ra at a MOI of 10 for 3h, the cells were washed to remove extracellular bacteria, and cultured for an additional 24 h. The cells were lysed and mycobacterial viability (CFU) determined. $^{*}p < 0.05$.

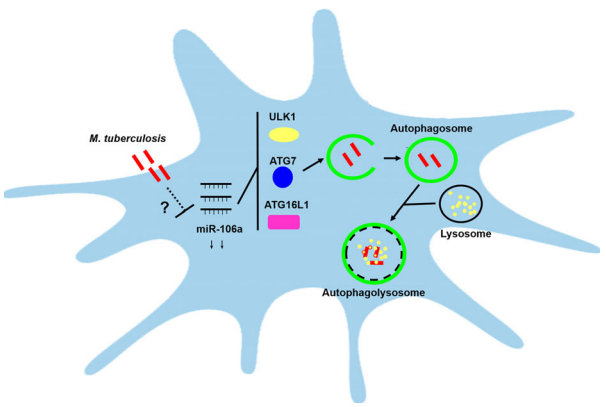

FIGURE 9 | Schematic diagram of miR-106a regulating autophagy by targeting ULK1, ATG7 and ATG16L1. miR-106a expression was downregulated in human macrophages after mycobacterial infection, however it remains unclear about the mechanisms by which miR-106a is reduced. miR-106a can perform the regulation of autophagy and antimicrobial responses by targeting ULK1, ATG7 and ATG16L1.

that downregulation of miR-106a promoted autophagy process as a novel mechanism for host defense against *M. tuberculosis* infection.

Overall, our study reveals a novel pathway through which host can promote autophagic response to facilitate mycobacterial clearance by reducing miR-106a. Furthermore, miR-106a performs the regulation of autophagy by targeting ULK1, ATG16L1 and ATG7 after mycobacterial infection (**Figure 9**). This study reveals a previously unrecognized role of miR-106a in autophagy regulation during mycobacterial infection, which may provide a potential target for diagnosis and treatments of tuberculosis.

DATA AVAILABILITY STATEMENT

The datasets presented in this study can be found in online repositories. The names of the repository/repositories and accession number(s) can be found in the article/supplementary material.

AUTHOR CONTRIBUTIONS

LG and KL conceived and designed the experiments. DH, FZ, XL, and MH performed the experiments. DH, FZ, and ZJ analyzed the data. XH, GZ, XH, WA, and GX contributed the reagents/materials/analysis tools. LG, KL, and NS wrote the manuscript. All authors contributed to the article and approved the submitted version.

FUNDING

This work was supported by the National Natural Science Foundation of China (81760359, 32070930, and 31660267), Key R & D Plan Project of Ningxia Autonomous Region (2020BFG02012), Natural Science Foundation of Ningxia (2020AAC03152, 2019AAC03079, 2018AAC02018 and 2018AAC03074), Science Research Project of Ningxia's

Colleges (NGY2020043 and NGY2018-75), Preponderant Discipline Construction Project of Ningxia Medical University (NGY2020043 and NGY2018-75), Science and Technology Project of Jiangsu Market Supervision Administration (KJ207561), First-Class Discipline Construction Founded Project of Ningxia Medical University and the School of Clinical Medicine (NXYLXK2017A05), Young Scientific and Technological Talents of Ningxia (TJGC2018079), Ningxia Youth Top Talent training Project and "Light of the West" Talent Training Programme of the Chinese Academy of Sciences.

REFERENCES

1. World Health Organization. *Global tuberculosis report 2020. World Health Organization* (2020). Available at: https://apps.who.int/iris/handle/10665/336069. License: CC BY-NC-SA 3.0 IGO.
2. Banuls AL, Sanou A, Anh NT, Godreuil S. *Mycobacterium tuberculosis*: ecology and evolution of a human bacterium. *J Med Microbiol* (2015) 64 (11):1261–9. doi: 10.1099/jmm.0.000171
3. Getahun H, Matteelli A, Chaisson RE, Raviglione M. Latent *Mycobacterium tuberculosis* infection. *N Engl J Med* (2015) 372(22):2127–35. doi: 10.1056/NEJMra1405427
4. Philips JA, Ernst JD. Tuberculosis pathogenesis and immunity. *Annu Rev Pathol* (2012) 7:353–84. doi: 10.1146/annurev-pathol-011811-132458
5. Franco LH, Nair VR, Scharn CR, Xavier RJ, Torrealba JR, Shiloh MU, et al. The Ubiquitin Ligase Smurf1 Functions in Selective Autophagy of *Mycobacterium tuberculosis* and Anti-tuberculous Host Defense. *Cell Host Microbe* (2017) 21(1):59–72. doi: 10.1016/j.chom.2016.11.002
6. Saiga H, Shimada Y, Takeda K. Innate immune effectors in mycobacterial infection. *Clin Dev Immunol* (2011) 2011:347594. doi: 10.1155/2011/347594
7. Sia JK, Georgieva M, Rengarajan J. Innate Immune Defenses in Human Tuberculosis: An Overview of the Interactions between *Mycobacterium tuberculosis* and Innate Immune Cells. *J Immunol Res* (2015) 2015:747543. doi: 10.1155/2015/747543
8. Liu CH, Liu H, Ge B. Innate immunity in tuberculosis: host defense vs pathogen evasion. *Cell Mol Immunol* (2017) 14(12):963–75. doi: 10.1038/cmi.2017.88
9. Baena A, Porcelli SA. Evasion and subversion of antigen presentation by *Mycobacterium tuberculosis*. *Tissue Antigens* (2009) 74(3):189–204. doi: 10.1111/j.1399-0039.2009.01301.x
10. Stanley SA, Cox JS. Host-pathogen interactions during *Mycobacterium tuberculosis* infections. *Curr Top Microbiol Immunol* (2013) 374:211–41. doi: 10.1007/82_2013_332
11. Deretic V, Saitoh T, Akira S. Autophagy in infection, inflammation and immunity. *Nat Rev Immunol* (2013) 13(10):722–37. doi: 10.1038/nri3532
12. Xie Y, Kang R, Sun X, Zhong M, Huang J, Klionsky DJ, et al. Posttranslational modification of autophagy-related proteins in macroautophagy. *Autophagy* (2015) 11(1):28–45. doi: 10.4161/15548627.2014.984267
13. Singh R, Cuervo AM. Autophagy in the cellular energetic balance. *Cell Metab* (2011) 13(5):495–504. doi: 10.1016/j.cmet.2011.04.004
14. Zachari M, Ganley IG. The mammalian ULK1 complex and autophagy initiation. *Essays Biochem* (2017) 61(6):585–96. doi: 10.1042/EBC20170021
15. Pattison JS, Osinska H, Robbins J. Atg7 induces basal autophagy and rescues autophagic deficiency in CryABR120G cardiomyocytes. *Circ Res* (2011) 109 (2):151–60. doi: 10.1161/CIRCRESAHA.110.237339
16. Archna A, Scrima A. Identification, biochemical characterization and crystallization of the central region of human ATG16L1. *Acta Crystallogr F Struct Biol Commun* (2017) 73(Pt 10):560–7. doi: 10.1107/S2053230X17013280
17. Hammond SM. An overview of microRNAs. *Adv Drug Delivery Rev* (2015) 87:3–14. doi: 10.1016/j.addr.2015.05.001
18. Shukla GC, Singh J, Barik S. MicroRNAs: Processing, Maturation, Target Recognition and Regulatory Functions. *Mol Cell Pharmacol* (2011) 3(3):83–92.
19. Staedel C, Darfeuille F. MicroRNAs and bacterial infection. *Cell Microbiol* (2013) 15(9):1496–507. doi: 10.1111/cmi.12159
20. Long J, He Q, Yin Y, Lei X, Li Z, Zhu W. The effect of miRNA and autophagy on colorectal cancer. *Cell Prolif* (2020) 53(10):e12900. doi: 10.1111/cpr.12900
21. Gozuacik D, Akkoc Y, Ozturk DG, Kocak M. Autophagy-Regulating microRNAs and Cancer. *Front Oncol* (2017) 7:65. doi: 10.3389/fonc.2017.00065
22. Kumar R, Sahu SK, Kumar M, Jana K, Gupta P, Gupta UD, et al. MicroRNA 17-5p regulates autophagy in *Mycobacterium tuberculosis*-infected macrophages by targeting Mcl-1 and STAT3. *Cell Microbiol* (2016) 18 (5):679–91. doi: 10.1111/cmi.12540
23. Klionsky DJ, Cuervo AM, Seglen PO. Methods for monitoring autophagy from yeast to human. *Autophagy* (2007) 3(3):181–206. doi: 10.4161/auto.3678
24. Yoshii SR, Mizushima N. Monitoring and Measuring Autophagy. *Int J Mol Sci* (2017) 18(9):1865. doi: 10.3390/ijms18091865
25. Wang J, Wang R, Wang H, Yang X, Yang J, Xiong W, et al. Glucocorticoids Suppress Antimicrobial Autophagy and Nitric Oxide Production and Facilitate Mycobacterial Survival in Macrophages. *Sci Rep* (2017) 7(1):982. doi: 10.1038/s41598-017-01174-9
26. Bah A, Lacarriere C, Vergne I. Autophagy-Related Proteins Target Ubiquitin-Free Mycobacterial Compartment to Promote Killing in Macrophages. *Front Cell Infect Microbiol* (2016) 6:53. doi: 10.3389/fcimb.2016.00053
27. Jeker LT, Bluestone JA. MicroRNA regulation of T-cell differentiation and function. *Immunol Rev* (2013) 253(1):65–81. doi: 10.1111/imr.12061
28. Tang B, Li N, Gu J, Zhuang Y, Li Q, Wang HG, et al. Compromised autophagy by MIR30B benefits the intracellular survival of Helicobacter pylori. *Autophagy* (2012) 8(7):1045–57. doi: 10.4161/auto.20159
29. Fuziwara CS, Kimura ET. Insights into Regulation of the miR-17-92 Cluster of miRNAs in Cancer. *Front Med (Lausanne)* (2015) 2:64. doi: 10.3389/fmed.2015.00064
30. Gruszka R, Zakrzewska M. The Oncogenic Relevance of miR-17-92 Cluster and Its Paralogous miR-106b-25 and miR-106a-363 Clusters in Brain Tumors. *Int J Mol Sci* (2018) 19(3):879. doi: 10.3390/ijms19030879
31. Hao H, Xia G, Wang C, Zhong F, Liu L, Zhang D. miR-106a suppresses tumor cells death in colorectal cancer through targeting ATG7. *Med Mol Morphol* (2017) 50(2):76–85. doi: 10.1007/s00795-016-0150-7
32. Rothschild SII, Gautschi O, Batliner J, Gugger M, Fey MF, Tschan MP. MicroRNA-106a targets autophagy and enhances sensitivity of lung cancer cells to Src inhibitors. *Lung Cancer* (2017) 107:73–83. doi: 10.1016/j.lungcan.2016.06.004
33. Jin J, Britschgi A, Schlafli AM, Humbert M, Shan-Krauer D, Batliner J, et al. Low Autophagy (ATG) Gene Expression Is Associated with an Immature AML Blast Cell Phenotype and Can Be Restored during AML Differentiation Therapy. *Oxid Med Cell Longev* (2018) 2018:1482795. doi: 10.1155/2018/1482795
34. Zhu D, Pan C, Li L, Bian Z, Lv Z, Shi L, et al. MicroRNA-17/20a/106a modulate macrophage inflammatory responses through targeting signal-regulatory protein alpha. *J Allergy Clin Immunol* (2013) 132(2):426–36 e8. doi: 10.1016/j.jaci.2013.02.005
35. Horne DJ, Graustein AD, Shah JA, Peterson G, Savlov M, Steele S, et al. Human ULK1 Variation and Susceptibility to *Mycobacterium tuberculosis* Infection. *J Infect Dis* (2016) 214(8):1260–7. doi: 10.1093/infdis/jiw347
36. Ye Y, Li X, Wang W, Ouedraogo KC, Li Y, Gan C, et al. Atg7 deficiency impairs host defense against Klebsiella pneumoniae by impacting bacterial clearance, survival and inflammatory responses in mice. *Am J Physiol Lung Cell Mol Physiol* (2014) 307(5):L355–63. doi: 10.1152/ajplung.00046.2014
37. Bonilla DL, Bhattacharya A, Sha Y, Xu Y, Xiang Q, Kan A, et al. Autophagy regulates phagocytosis by modulating the expression of scavenger receptors. *Immunity* (2013) 39(3):537–47. doi: 10.1016/j.immuni.2013.08.026
38. Conway KL, Kuballa P, Song JH, Patel KK, Castoreno AB, Yilmaz OH, et al. Atg16l1 is required for autophagy in intestinal epithelial cells and protection of mice from Salmonella infection. *Gastroenterology* (2013) 145(6):1347–57. doi: 10.1053/j.gastro.2013.08.035

39. Winchell CG, Steele S, Kawula T, Voth DE. Dining in: intracellular bacterial pathogen interplay with autophagy. *Curr Opin Microbiol* (2016) 29:9–14. doi: 10.1016/j.mib.2015.09.004
40. Nakamura S, Yoshimori T. New insights into autophagosome-lysosome fusion. *J Cell Sci* (2017) 130(7):1209–16. doi: 10.1242/jcs.196352
41. Kim JK, Kim TS, Basu J, Jo EK. MicroRNA in innate immunity and autophagy during mycobacterial infection. *Cell Microbiol* (2017) 19(1):e12678. doi: 10.1111/cmi.12687
42. Kim JK, Yuk JM, Kim SY, Kim TS, Jin HS, Yang CS, et al. MicroRNA-125a Inhibits Autophagy Activation and Antimicrobial Responses during Mycobacterial Infection. *J Immunol* (2015) 194(11):5355–65. doi: 10.4049/jimmunol.1402557
43. Wang J, Yang K, Zhou L, Minhaowu, Wu Y, Zhu M, et al. MicroRNA-155 promotes autophagy to eliminate intracellular mycobacteria by targeting Rheb. *PloS Pathog* (2013) 9(10):e1003697. doi: 10.1371/journal.ppat.1003697
44. Etna MP, Sinigaglia A, Grassi A, Giacomini E, Romagnoli A, Pardini M, et al. *Mycobacterium tuberculosis*-induced miR-155 subverts autophagy by targeting ATG3 in human dendritic cells. *PloS Pathog* (2018) 14(1):e1006790. doi: 10.1371/journal.ppat.1006790
45. Liu F, Chen J, Wang P, Li H, Zhou Y, Liu H, et al. MicroRNA-27a controls the intracellular survival of *Mycobacterium tuberculosis* by regulating calcium-associated autophagy. *Nat Commun* (2018) 9(1):4295. doi: 10.1038/s41467-018-06836-4
46. Kim JK, Lee HM, Park KS, Shin DM, Kim TS, Kim YS, et al. MIR144* inhibits antimicrobial responses against *Mycobacterium tuberculosis* in human monocytes and macrophages by targeting the autophagy protein DRAM2. *Autophagy* (2017) 13(2):423–41. doi: 10.1080/15548627.2016.1241922
47. Ouimet M, Koster S, Sakowski E, Ramkhelawon B, van Solingen C, Oldebeken S, et al. *Mycobacterium tuberculosis* induces the miR-33 locus to reprogram autophagy and host lipid metabolism. *Nat Immunol* (2016) 17(6):677–86. doi: 10.1038/ni.3434
48. Guo L, Zhao J, Qu Y, Yin R, Gao Q, Ding S, et al. microRNA-20a Inhibits Autophagic Process by Targeting ATG7 and ATG16L1 and Favors Mycobacterial Survival in Macrophage Cells. *Front Cell Infect Microbiol* (2016) 6:134. doi: 10.3389/fcimb.2016.00134

Conflict of Interest: The authors declare that the research was conducted in the absence of any commercial or financial relationships that could be construed as a potential conflict of interest.

frontiers in Microbiology

REVIEW
published: 14 January 2021
doi: 10.3389/fmicb.2020.614313

Targeting Autophagy as a Strategy for Developing New Vaccines and Host-Directed Therapeutics Against Mycobacteria

*Emily J. Strong and Sunhee Lee**

Department of Microbiology and Immunology, University of Texas Medical Branch, Galveston, TX, United States

Mycobacterial disease is an immense burden worldwide. This disease group includes tuberculosis, leprosy (Hansen's disease), Buruli Ulcer, and non-tuberculous mycobacterial (NTM) disease. The burden of NTM disease, both pulmonary and ulcerative, is drastically escalating globally, especially in developed countries such as America and Australia. Mycobacteria's ability to inhibit or evade the host immune system has contributed significantly to its continued prevalence. Pre-clinical studies have highlighted promising candidates that enhance endogenous pathways and/or limit destructive host responses. Autophagy is a cell-autonomous host defense mechanism by which intracytoplasmic cargos can be delivered and then destroyed in lysosomes. Previous studies have reported that autophagy-activating agents, small molecules, and autophagy-activating vaccines may be beneficial in restricting intracellular mycobacterial infection, even with multidrug-resistant strains. This review will examine how mycobacteria evade autophagy and discusses how autophagy could be exploited to design novel TB treatment strategies, such as host-directed therapeutics and vaccines, against *Mycobacterium tuberculosis* and NTMs.

Keywords: autophagy, mycobacteria, host-directed therapies, non-tuberculous mycobacteria, host–microbe interactions, vaccines

OPEN ACCESS

Edited by:
Chinnaswamy Jagannath, Weill Cornell Medical College of Cornell University, United States

Reviewed by:
Roberta Olmo Pinheiro, Oswaldo Cruz Foundation, Brazil
Rosane M. B. Teles, University of California, Los Angeles, United States

***Correspondence:**
Sunhee Lee
sunhlee@utmb.edu

Specialty section:
This article was submitted to Microbial Immunology, a section of the journal Frontiers in Microbiology

Received: *05 October 2020*
Accepted: *21 December 2020*
Published: *14 January 2021*

Citation:
Strong EJ and Lee S (2021) Targeting Autophagy as a Strategy for Developing New Vaccines and Host-Directed Therapeutics Against Mycobacteria. Front. Microbiol. 11:614313. doi: 10.3389/fmicb.2020.614313

INTRODUCTION

While TB is a disease of significant global burden, the burden of non-tuberculosis mycobacteria (NTM) disease is higher than TB in many developed countries such as the United States and Australia (Prevots et al., 2010). NTMs are mycobacteria other than *Mycobacterium tuberculosis* (*Mtb*) and *Mycobacterium leprae* (the cause of leprosy/Hansen's Disease). Globally, the burden of NTM continues to increase substantially. Like many pathogenic diseases, drug-resistance has become a severe public health concern for mycobacterial infection. In 2018, there were approximately 500,000 new rifampicin-resistant TB cases, most of which also comprised multiple drug-resistant infections (World Health Organisation, 2020). In contrast, the NTM species display significant heterogeneity in their susceptibility to standard anti-TB drugs and thus the treatment for NTM diseases usually involves the use of macrolides and injectable aminoglycosides. Although well-established international guidelines are available, treatment of NTM disease is mostly empirical and not entirely successful. In general, the treatment duration is much longer for NTM diseases, compared to TB. Taken together, the considerable global burden of mycobacterial disease requires much needed further research and the development of new treatment and prevention strategies.

The development of TB disease occurs in only 10% of individuals exposed to the pathogen, which infers that competent host defense mechanisms exist to control the infection. In the last decade, autophagy has surfaced as an essential host immune defense mechanism against intracellular *Mtb* infection. Autophagy is a complex, essential, conserved cellular process allowing for the degradation of intracellular components, including proteins, organelles, and foreign bodies. Autophagy targeting by host-directed therapies to enhance treatment options against pathogenic viruses and bacteria has recently become a popular research topic. Similarly, autophagy has been proven not only as an effective antimicrobial mechanism for the clearance of *Mtb* and NTMs, but as a process preventing excessive inflammation to avoid adverse effects of infection on the host. Still, increasing evidence shows that in order to augment its intracellular survival, mycobacteria has evolved multiple strategies to prevent the optimal operation of host autophagic machinery.

This review will focus on autophagy during mycobacterial infection. However, it is worth noting that many intracellular pathogens are known to modulate autophagy to promote their survival. For example, *Legionella pneumophila* secrets bacterial effector that irreversibly inactivates Atg8 proteins unable to be reconjugated by the Atg7-Atg3 (Choy et al., 2012). Many other intracellular bacteria like *Shigella*, *Salmonella,* and *Mycobacteria* also secrete bacterial effectors that inhibit autophagy (Ogawa et al., 2005; D'Cruze et al., 2011; Popa et al., 2016; Saini et al., 2016; Jiao and Sun, 2019; Strong et al., 2020). A deeper understanding of the mechanisms by which these bacteria cause disease should foster better treatment options. Ongoing analysis is even more critical, given the rising infection rates of NTMs and rapidly growing mycobacteria (RGM), increased prevalence of drug-resistant TB, and TB/Diabetes and TB/HIV comorbidity. This review will cover the current understanding of the molecular mechanisms by which mycobacteria can modulate autophagy. Additionally, it will discuss the potential for these insights to be utilized and harnessed to develop host-directed therapies as treatment options against mycobacterial diseases.

AUTOPHAGY PATHWAY AS A GENERAL ANTIMICROBIAL DEFENSE

Macroautophagy is the most widely studied form of autophagy and is an evolutionarily conserved pathway controlling quality and quantity of eukaryotic organelles and the cytoplasmic biomass (Svenning and Johansen, 2013). Macroautophagy involves the formation of a double membrane phagosome, which fuses with a lysosome (Parzych and Klionsky, 2013). It is a constitutive cellular process that is induced under stress conditions such as nutrient starvation, which degrades cytoplasmic material into metabolites and degrades cytoplasmic foreign bodies (Svenning and Johansen, 2013). Macroautophagy can be selective, as it recognizes specific marked components by various receptor proteins such as p62 (SQSTM1) (Svenning and Johansen, 2013). The degradation of pathogens is called Xenophagy, whereby bacteria are engulfed by autophagosomes and degraded after fusion with lysosomes to form autolysosomes. This review will focus on Xenophagy, which will hereafter be referred to as "autophagy." The autophagy pathway is illustrated in **Figure 1A**, showing the minimal core components relevant for the discussion in this review.

The formation of the autophagosome and the fusion to a lysosome is broken down into five main steps (**Figure 1A**): (i) initiation, (ii) elongation, (iii) maturation, (iv) fusion, and (v) degradation. Autophagy initiation is regulated by the master regulator, the mammalian/mechanistic target of Rapamycin (mTOR). It is a negative regulator of autophagy, meaning its dephosphorylation is responsible for autophagy induction. Dephosphorylation of mTOR results in the translocation of the Unc-51 like autophagy activating kinase (Ulk1/2)-Autophagy related (Atg)13-FAK family-interacting protein (FIP200)-Atg101 complex to the endoplasmic reticulum (Itakura and Mizushima, 2010; Mizushima, 2010). The Class III phosphatidylinositol 3 kinase (PI3K) activates the VPS34-Beclin1-VPS15-Atg14 complex. The PI3K complex induces phosphatidylinositol-3-phosphate [PtdIns(3)P], which then recruits double FYVE-containing protein 1 (DFCP1) and WD-repeat domain phosphoinositide-interacting (WIPI) family proteins to initiate the omegasome formation (Axe et al., 2008; Matsunaga et al., 2009; Itakura and Mizushima, 2010; Polson et al., 2010). Elongation of the omegasome into the autophagosome is conducted by the Atg7–Atg10 complex and then conjugated to Atg12-Atg5-Atg16L on the omegasome membrane (Fujita et al., 2008). Atg4 cleaves LC3 into LC3-I, while the Atg7–Atg3 complex lipidates LC3-I into LC3-II by conjugating phosphatidyl-ethanolamine (PE). The completed autophagosome fuses with the lysosome to degrade the autophagosome cargo for subsequent metabolite recycling or antigen presentation (Knodler and Celli, 2011; Levine et al., 2011; Münz, 2016; Saini et al., 2016; Yu et al., 2018).

AUTOPHAGY AND TUBERCULOSIS

Autophagy Induction by *M. tuberculosis*

The global prevalence of mycobacterial diseases of all types has increased considerably. The most significant mycobacterial disease is tuberculosis (TB). In 2018, 1.4 million deaths were attributed to *Mtb* infection (World Health Organisation, 2020), meaning TB is one of the top 10 causes of death and the leading cause of worldwide death from a single infectious agent. One-quarter of the world's population is infected with *Mtb*. Approximately 5 to 10% of infections progress to the active disease at some point in their host lives. *Mtb* is a successful pathogen due to its capacity to evade the host immune systems and utilize phagocytes as a replication niche. The bacteria can significantly inhibit the phagolysosome's acidification and limit phagosome maturation, thereby forcing the infected cell to undergo programmed cell death (Russell et al., 2002). Several of the seminal observations regarding the antimicrobial role of autophagy have been made using *Mtb* (Gutierrez et al., 2004; Castillo et al., 2012) and such observations were followed by a gradual increase in studies on autophagy as a cell-autonomous,

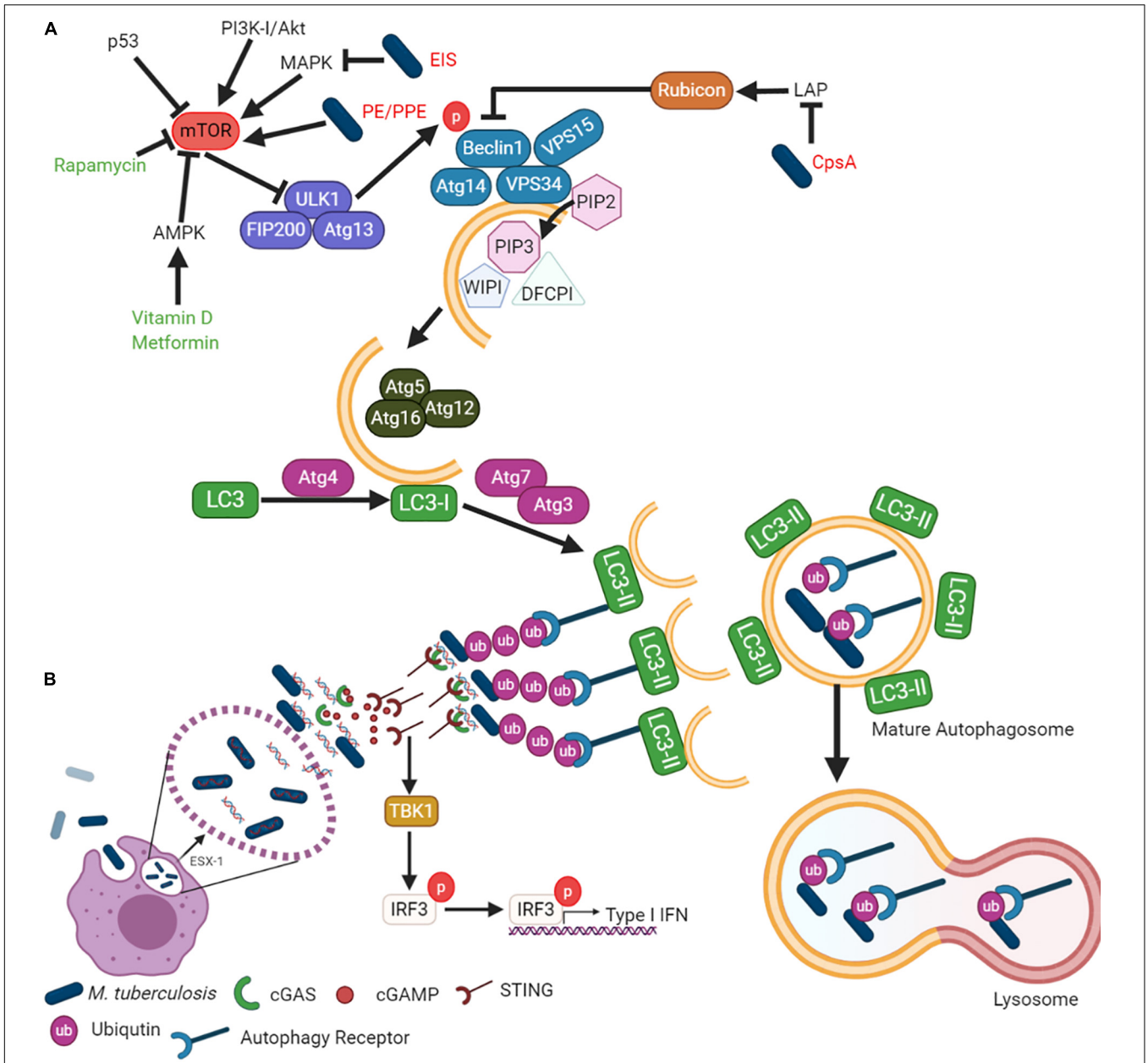

FIGURE 1 | *Mycobacterium tuberculosis* inhibits autophagy to enhance survival in host cells. **(A)** While autophagy can be explained in terms of its role in cell survival, the mechanism by which it is regulated is complicated and elaborate. The different steps of the autophagic pathway during mycobacterial infection are shown. **(B)** *Mtb*-autophagy interaction in macrophages. Following phagocytosis, *Mtb* resides in phagosome and blocks phagosome maturation. *Mtb* secretes Esx-1, promoting phagosome damages that trigger ubiquitination, recruitment of autophagic adaptors and mycobacterial capture via STING. The detailed molecular mechanisms of each steps and mycobacterial factors are discussed in the text.

pharmacologically, physiologically and immunologically inducible anti-mycobacterial process (Gutierrez et al., 2004; Seto et al., 2012; Watson et al., 2012; Sakowski et al., 2015). These studies revealed the colocalization of *Mtb* with autophagosomes and increased bacterial clearance during autophagy induction (Gutierrez et al., 2004; Seto et al., 2012; Watson et al., 2012; Sakowski et al., 2015). Most of these models have been explored in the context of Atg5 and its effect on autophagy. Examination of other important autophagy markers such as Ulk1 and Atg4b *in vivo* has uncovered that Atg5 may play a role independent of canonical autophagy in *Mtb* control (Kimmey et al., 2015).

Infection with mycobacteria induces significant levels of pro-inflammatory cytokines, known to be inducers of autophagy. However, little colocalization of *Mtb* and autophagosomes has been observed without non-mycobacterial stimulation of autophagy. An example of immunological induction of

mycobactericidal autophagy includes stimulation of infected macrophages with Th1 cytokines such as IFN-γ and TNF-α in a process that can be antagonized by Th2 cytokines including IL-4 and IL-13 (Harris et al., 2007; Ghadimi et al., 2010). Physiological induction of autophagy by IFN-γ generated significant autophagosome formation in mycobacteria-infected macrophages and dendritic cells. Although *Mtb* infection causes a robust IFN-γ response, the autophagy induction by virulent *Mtb* is limited, probably because mycobacteria inhibit IFN-γ mediated autophagy induction (Zullo and Lee, 2012a; Zullo et al., 2014). IFN-γ also plays a critical role in the nitric oxide (NO) response to *Mtb* infection. The deletion of IFN-γ significantly impedes NO production and leads to uncontrolled replication of bacilli *in vivo* (Cooper et al., 1993; Flynn et al., 1993). The inhibition of NO has previously been shown to induce autophagy substrates' clearance, highlighting the complex role of cytokine signaling in autophagy pathways (Sarkar et al., 2011). Virulent *Mtb* infection induces TNF-α, which is inactivated by the increased release of TNFR2 and results in inhibition of apoptosis (Balcewicz-Sablinska et al., 1998; Keane et al., 2000). This observation underscores the potential of virulent *Mtb* to inhibit autophagy by modulating cytokines' bioreactivity known to induce autophagy.

Manipulation of Autophagy Pathways by Mycobacterial Factors

Several bacterial effector proteins are known to modulate autophagy. Many of these effectors are secreted through the type I to type VII and type IX secretion systems (Jiao and Sun, 2019). Mycobacteria has numerous Type VII secretion systems (Esx1 – Esx5). *Mtb* ESX-1 is responsible for the puncture of the phagosome, allowing for mycobacterial escape (Conrad et al., 2017) (**Figure 1B**). *Mtb* cytosolic DNA is recognized by the cytosolic DNA sensor, cyclic GMP-AMP synthase (cGAS), resulting in the release of cyclic guanosine monophosphate (cGAMP). cGAMP is recognized by the stimulator of interferon genes (STING), leading to type I IFN release and the recruitment of autophagy receptors p62, NDP52, and optineurin (Watson et al., 2012, 2015). These receptors are recruited to the ubiquitinated pathogen, thereby allowing for specific targeting by the autophagosome. The receptors contain an LC3 interaction region (LIR) to bind the LC3 autophagy protein (Thurston et al., 2009; Zheng et al., 2009; Wild et al., 2011).

EspB is a part of the Esx1 secretory apparatus responsible for the secretion of early secretory antigenic target-6 (ESAT-6). Treatment of macrophages with EspB protein demonstrates downregulation of the IFN-γ receptor IFN-γR1, resulting in the inhibition of STAT-1 activation even in the presence of IFN-γ (Huang and Bao, 2016). EspB and ESAT-6 are not the only *Mtb* proteins linked to the inhibition of autophagy. The "enhanced intracellular survival" (*eis*) gene of *Mtb* can confer enhanced survival of *Mycobacterium smegmatis* in macrophages. However, it is not required for the persistence of *Mtb* in these cells (Wei et al., 2000; Shin et al., 2010). During *Mtb* infection, *eis* significantly inhibits the activation of JNK, which prevents the induction of non-canonical autophagy through Atg7. JNK activation also induced reactive oxygen species (ROS) generation and significantly increased type 2 macrophage cell death by *Mtb eis* deletion mutant (Shin et al., 2010). Eis was also found to substantially inhibit the production of TNF-α, IL-4, and IL-6, while simultaneously stimulating INF-γ and IL-10 secretion (Lella and Sharma, 2007; Samuel et al., 2007; Shin et al., 2010).

Mtb inhibits autophagy to protect against bacterial clearance and host cell death, which also impedes antigen presentation. The *Mtb* PE_PGRS47 protein inhibits autophagy and limits MHC class II antigen presentation (Saini et al., 2016). Several other *Mtb* PE/PPE proteins are also known to inhibit autophagy. For example, *Mtb* PE_PGRS41 (Deng et al., 2017), *Mycobacterium marinum* MMAR_0242 (Singh et al., 2016), and *Mtb* PE_PGRS29 (Chai et al., 2019) interact with autophagy machinery. *Mtb* also secrets a probable ligase (CpsA) to inhibit the non-canonical autophagy pathway designated as LC3-associated phagocytosis (LAP) and NADPH oxidase (Köster et al., 2017) (**Figure 1A**). In contrast to canonical autophagosomes, LAP does not result in double-membrane structures and instead promotes rapid phagosome maturation (Fazeli and Wehman, 2017). This cellular process limits the phagocytosed pathogen's ability to replicate by expediting phagosome maturation while regulating the IFN pathway and antigen presentation.

Additionally, studies have found that virulent *Mtb,* but not avirulent *Mtb,* can inhibit autophagy flux in macrophages and dendritic cells in an ESAT-6 and PhoP dependent manner (Chandra et al., 2015). Autophagy flux is an important cellular mechanism that degrades autophagosome cargo, which allows nutrient recycling or antigen presentation. Increased autophagic flux was found to improve bacterial clearance from macrophages and dendritic cells (Romagnoli et al., 2012; Chandra et al., 2015). The maturation of *Mtb*-containing autophagosomes into autolysosomes was inhibited by blocking recruitment of the late endosome marker Rab7 (Chandra et al., 2015). Inhibition of Rab5 conversion to Rab7 in endosomes is a well-established method in which mycobacteria inhibit lysosomal fusion (Via et al., 1997; Rink et al., 2005).

Mtb inhibits canonical and non-canonical autophagy by several means and it is apparent that the role of infection-induced autophagy is complicated. While overcoming autophagy inhibition by *Mtb* could lead to better treatment options, further consideration should be given to evidence suggesting that *Mtb* can inhibit autolysosome formation (Chandra et al., 2015). Additionally, there may be value in examining host-directed therapies targeting mTOR-independent autophagy pathways (Schiebler et al., 2015), since *Mtb* infection markedly activates mTOR. Exploring alternative autophagy-inducing pathways may lead to more efficacious drugs and may prove more useful in patients presenting with co-disease such as TB/Diabetes.

AUTOPHAGY AND NON-TUBERCULOSIS MYCOBACTERIA

NTM Disease

NTM is the broad term for diseases caused by over 170 mycobacteria. The most commonly isolated specie is the *Mycobacterium avium* Complex (MAC), accounting for 71.1%

of Australian cases and 31.3% of NTM cases in South America. *M. avium* is the most common species isolated in Europe, Asia, South America, and North America. At the same time, *M. intracellulare* is prevalent in South Africa and Australia (Johnson and Odell, 2014; Griffith, 2019; Gopalaswamy et al., 2020). *M. avium*, MAC, and *M. intracellulare* most commonly present as a pulmonary disease similar to TB. In 2013, a nearly six-fold increase in NTM cases were reported in America compared to the 1980s (Donohue and Wymer, 2016), with similar trends in the United Kingdom, Denmark, and Germany (Ratnatunga et al., 2020). Some studies have attributed this rise of NTM infections to a vaccination policy change from a blanket BCG vaccination to a limited vaccination only for specific groups (SAGE Working Group of BCG Vaccines and WHO Secretariat, 2017; Kontturi et al., 2018).

Other common NTMs include *Mycobacterium fortuitum*, *Mycobacterium kansasii*, *Mycobacterium abscessus*, *M. marinum*, and *Mycobacterium ulcerans*. NTMs are opportunistic environmental pathogens that are typically found in soil and water. Although NTM disease presentation is most commonly pulmonary, observation of lymphatic, skin/soft tissue and disseminated disease have been reported (Griffith et al., 2007; Bodle et al., 2008; Tortoli, 2009). Many species of mycobacteria can also cause ulcerative disease. Four main presentations of the mycobacterial ulcerative disease have been designated: (i) cutaneous *Mtb* infection, (ii) leprosy (the second most common mycobacterial disease; caused by *M. leprae* or *Mycobacterium lepromatosis*), (iii) Buruli Ulcer, the third most common mycobacterial disease (caused by *M. ulcerans*), and (iv) opportunistic infections caused by other non-tuberculosis mycobacteria such as *M. marinum*. Franco-Paredes et al. (2018) eloquently summarized the disease presentation of cutaneous mycobacterial infections in their 2018 review.

Besides *Mtb*, *M. leprae* and *M. ulcerans* account for the next highest mycobacterial disease burdens. Buruli Ulcer, caused by *M. ulcerans,* primarily occurs in the West and Central Africa, Asia, South America, the western Pacific, and Australasia (Simpson et al., 2019). Unlike the well-studied *Mtb* and *M. leprae*, the mode of transmission of *M. ulcerans* remains unknown (Röltgen and Pluschke, 2015). As with other mycobacteria, treatment of Buruli Ulcer is costly and takes a long time. Traditional antimycobacterial antibiotics are used for treatment, including rifampicin, streptomycin, clarithromycin, and moxifloxacin. However, wound interventions, such as lymphedema management and surgery, are commonly used to speed up healing (Yotsu et al., 2018; Converse et al., 2019; World Health Organisation, 2019). Though leprosy transmission remains on the decline with less than 200,000 cases in 2017 (World Health Organization, 2016), improved treatment options are a vital resource for continued disease decline (Fischer, 2017; Maymone et al., 2020; Scollard, 2020). Leprosy broadly presents two different clinical manifestations; paucibacillary tuberculoid, which is characterized by negative smears for acid-fast bacilli, and multibacillary lepromatous, which is characterized by positive smears for acid-fast bacilli (Nath, 2016).

Mycobacteria's unique cell wall and some species' ability to form biofilms, spread by aerosolization, slow growth, and intrinsic antibiotic resistance, also contribute to their ability to survive in unique and low nutrient environments (De Groote and Huitt, 2006). Their lipid-rich cell wall influences the bacteria's ability to modulate autophagy (Zullo and Lee, 2012a). The ability to form biofilms and survive in low nutrient environments indicates that these bacteria can form unique replication niches within the hosts' cells that traditional mycobacterial drugs cannot penetrate to be effective (Islam et al., 2012).

NTM and Autophagy

The induction of autophagy by mycobacteria is species-dependent. Although all mycobacteria elicit strong mTOR activation, most non-pathogenic mycobacteria simultaneously induce significant autophagy, unlike their pathogenic relatives (Zullo and Lee, 2012a). *M. smegmatis* is often utilized as a model organism to study pathogenic mycobacteria due to its short culture time and BSL2 classification (Deng et al., 2017). While a low concentration of mTOR-inhibiting drugs like Rapamycin and Torin are able to inhibit mTOR activation and induce autophagy during mycobacterial infection (Zullo et al., 2014), clearance of *M. smegmatis* requires up to 10 times higher quantity of those drugs than needed to inhibit mTOR activation. Interestingly, this killing was observed to be independent of LC3B or Atg5, indicating a non-canonical autophagy pathway is involved in the clearance of *M. smegmatis* from macrophages (Zullo et al., 2014). This interesting observation suggests that targeting a non-canonical autophagy pathway for mycobacterial treatment may be useful. It has previously been shown that treatment of *Mtb* infected macrophages with potent autophagy inducers such as *M. smegmatis* can clear bacteria (Singh et al., 2017).

The role of autophagy during NTM has not been studied extensively. However, evidence exists that genetic variants in the autophagy-related genes, nucleotide-binding oligomerization domain-containing 2 (NOD2), E3 ubiquitin-protein ligase parkin (PARK2), IRGM, and autophagy-related proteins 16-1 (ATG16L1), are associated with susceptibility to mycobacterial disease (Yang et al., 2014; Capela et al., 2016; Uaska Sartori Priscila et al., 2020). A single nucleotide polymorphism (SNP) in PARK2 correlates significantly with increased susceptibility to *M. ulcerans* infection, while an SNP in NOD2 is associated with increased disease progression. Conversely, an SNP in ATG16L1 protects against severe disease during *M. ulcerans* infection (Capela et al., 2016; Manry et al., 2020). Although not directly associated with autophagy, other SNPs in iNOS and IFN-γ have been associated with increased susceptibility to Buruli Ulcer, leprosy, and TB (Bibert et al., 2017).

The major virulence factor of *M. ulcerans* is mycolactone, a cytotoxic, immunosuppressive polyketide-derived macrolide. Mycolactone alone induces autophagy, although it impairs autophagy flux (Gama et al., 2014). The induction of autophagy is further evidenced by mycolactone's ability to inhibit mTOR, thereby resulting in the upregulation of apoptosis activating protein, Bim (Bieri et al., 2017). This pathway signals through the inactivation of Akt by an alternative mTOR pathway. As such, activation of mTOR could lead to inhibition of Bim and, subsequently, apoptosis, resulting in control of bacterial infection.

Two variants of *M. abscessus* and *M. fortuitum* are frequently observed: rough (R) and smooth (S) (Byrd and Lyons, 1999; Catherinot et al., 2007; Lee et al., 2016). It is widely accepted that the R variant is hypervirulent compared to its S counterpart. It is known that the loss of glycopeptidolipid (GPL) is the cause of the S-variant of *M. abscessus* in several animal models (Byrd and Lyons, 1999; Catherinot et al., 2007). A highly virulent clinical isolate of *M. abscessus*-R significantly inhibited autophagic flux than the S variant of *M. abscessus*. The R variant's intracellular survival is enhanced considerably by blocking the autophagosome-lysosome fusion in macrophages compared to the S variant (Kim et al., 2017c). These immunological effects of NTMs have been mostly studied from the perspective of respiratory illness and genome comparison studies focusing on traditional virulence factors for related opportunistic pathogens (N'Goma et al., 2015) indicates we have only a minimal understanding of their impact during ulcerative infection.

Whereas *M. abscessus* S utilizes phosphatidyl-*myoinositol* to mask TLR2 activation, *M. fortuitum* R does not induce the anti-inflammatory molecule TNFAIP3 (Lee et al., 2016). TNFAIP3 is an anti-apoptotic molecule that inhibits NF-κB and TNF-induced cell death (Lee et al., 2000). TNF- α and the TLR2 signaling pathway appear to play an essential role in *M. fortuitum* infection. Some lipids of RGMs have differential terminal modifications compared to those from pathogenic slow-growing mycobacteria. Specifically, lipoarabinomannan (LAM) in RGM is capped with phosphomyo-inositol (PI) caps compared to mannose (Man) caps in pathogenic mycobacteria. Purified PI-LAM induces significantly more apoptosis than purified Man-LAM in a TLR2 dependent manner (Bohsali et al., 2010). Similarly, PILAM caused significant autophagy induction, unlike ManLAM, which did not induce autophagy (Shui et al., 2011; Singh et al., 2019). Although terminal modifications of LAM appear to play a role in the modulation of apoptosis, total lipid from both pathogenic and non-pathogenic mycobacteria can induce autophagy (Zullo et al., 2014; Kim et al., 2017c; Mishra et al., 2019). Interestingly, while total lipids from *M. abscessus*-R induce a significant autophagy level, live *M. marinum* induces autophagy and simultaneously inhibits autophagy flux, which leads to increased intracellular survival (Lerena and Colombo, 2011; Kim et al., 2017c; Oliveira et al., 2020; Pohl et al., 2020).

It has been known for many years that autophagy is an efficient mechanism to clear *M. leprae* from macrophages (Evans and Levy, 1972). However, it has been recently described that autophagy may be a major modulating factor in leprosy disease presentation. In patients presenting with multibacillary leprosy, there is significantly less autophagic control in macrophages taken from patient lesions than patients presenting with paucibacillary tuberculoid leprosy (Silva et al., 2017a). This supports previous studies which found that the autophagy inhibiting cytokine IL-10 is predominant in multibacillary leprosy compared to high levels of IL-26, IFN-γ, and TNF-α, autophagy inducing cytokines, found during paucibacillary tuberculoid leprosy (Yamamura, 1992; Sieling and Modlin, 1994; Nath, 2016; Dang et al., 2019). Multibacillary leprosy patients who developed type 1 reaction (T1R) episodes demonstrated dysregulation of autophagy genes and significantly increased expression of the mTOR complex leading to overexpression of the NLRP3-inflammasome-IL-1B pathway. These data demonstrate that leprosy treatment with pro-autophagic drugs may improve treatment outcomes by reducing reversal reaction risk (de Mattos Barbosa et al., 2018).

The establishment of uncontrolled mycobacterial infection in an extracellular bacterial milieu or biofilm presents significant complications for treatment (Greendyke and Byrd, 2008). Many mycobacterial species causing ulcerative diseases are widely considered to have significantly reduced sensitivity to antibiotics and a natural ability to acquire antibiotic resistance, making it very hard to treat and leading to high failure rates (Moore and Frerichs, 1953; Jarlier and Nikaido, 1990; Sanguinetti et al., 2001; Nessar et al., 2012). Utilizing host-directed therapies, such as those inducing autophagy, to inhibit bacterial release from the cell and form biofilms or bacterial milieus may enhance the efficacy of currently available antibiotics.

HARNESSING AUTOPHAGY TO FIGHT MYCOBACTERIA

Targeting Autophagy to Treat a Mycobacterial Infection

Rapamycin has been the most frequently used autophagy-inducing drug for host-directed therapies. While Rapamycin appears to improve pathology during *Mtb* infection, there is evidence that it is directly antimycobacterial *in vitro* at the high concentration used for the reported studies. Rapamycin does not seem to have a direct effect on *M. smegmatis* or BCG for short periods. Still, it was found to significantly inhibit BCG, *M. kansasii, M. avium,* and multiple virulent *Mtb* strains over 7–8 days incubation (Greenstein et al., 2008; Zullo et al., 2014). This direct antimycobacterial activity is somewhat unsurprising as Rapamycin was initially discovered as a novel antifungal antibiotic (Singh et al., 1979). Rapamycin is not the only drug evaluated as a host-directed therapy for the treatment of tuberculosis. Some medications, such as azithromycin and metformin, have been found to decrease mycobacterial infections in patients with cystic fibrosis and diabetes due to their ability to increase the autophagic clearance of bacteria (Renna et al., 2011; Tseng, 2018). **Table 1** summarizes the drugs and compounds that have been tested for their ability to induce autophagy and treat mycobacterial diseases.

Of importance, the use of Rapamycin to treat infectious diseases is not practical due to its immunosuppressant actions. Gupta et al. (2014) have attempted to address this issue with the administration of Rapamycin by microparticles directly to the airway. Highlighting the delicate balance needed for host-directed therapies, the study found that the induction of autophagy in the lung macrophages was inverse to the dosing interval. *In vitro* and *in vivo* rapamycin microparticles induce autophagolysosomal formation in macrophages infected with *Mtb* in an mTOR-dependent manner (Gupta et al., 2014; Gupta et al., 2016). Rapamycin alone significantly improved pathology during *Mtb* infection in a mouse model but did

TABLE 1 | Summary of current experimental treatments inducing autophagy during *M. tuberculosis* infection.

Drug	Model	Mode	References
Small Molecule Enhancers of Rapamycin	*M. bovis* BCG infection of primary human macrophages	Induce autophagy independently of mTOR	Floto et al., 2007
Rifampicin	*Mtb* infection of human differentiated monocytes	Increased autolysosome formation, directly antimycobacterial	Genestet et al., 2018
Linezolid	*Mtb* infection of human differentiated monocytes	Increased autophagosomes production, directly antimycobacterial	Genestet et al., 2018
Bedaquiline	*Mtb* infection of human differentiated monocytes	Increased autophagosomes production, directly antimycobacterial	Genestet et al., 2018
Nitazoxanide	*Mtb* infection of human differentiated monocytes. *M. leprae* infection of mice	Increased autophagy by inhibition of NADPH quinone oxidoreductase 1 leading to mTOR inhibition by TSC2	Lam et al., 2012; Bailey et al., 2017
Baicalin	*Mtb* infection of mouse macrophages	Induce autophagy via the PI3K/Akt/mTOR pathway, inhibit NLRP3 inflammasome activation via the PI3K/Akt/NF-κB, reduction of proinflammatory cytokines	Lin et al., 2013; Zhang et al., 2017
Vitamin D	*Mtb*/HIV co-infection model of primary human macrophages	Cathelicidin dependent induction of autophagy	Liu et al., 2007; Martineau et al., 2007; Yuk et al., 2009; Jo, 2010; Campbell and Spector, 2012b
4-phenylbutyrate	*Mtb* infection of human monocytes	Induction of LL-37 promoting autophagy via P2RX7 receptor, increasing free Ca^{2+} and activation of AMPK and PtdIns3K pathway.	Rekha et al., 2015
Gefitinib	*Mtb* infection of murine bone marrow-derived macrophages	STAT3 dependent cytokine responses, increasing lysosomal trafficking	Stanley et al., 2014; Sogi et al., 2017
Carbamazepine	*Mtb* infection of human-derived macrophages or murine alveolar macrophages. *M. marinum* zebrafish model of infection. MDR *Mtb* infection of C57BL/6 mice	Induce autophagy by blocking myoinositol uptake, decreasing phosphatidylinositol, and activating AMP kinase in an mTOR independent manner.	Schiebler et al., 2015; Juárez et al., 2016
Valproic acid	*Mtb* infection of human-derived macrophages or murine alveolar macrophages	Increases colocalization of LC3 with *Mtb*	Schiebler et al., 2015; Juárez et al., 2016
Loperamide	*Mtb* infection of human-derived macrophages or murine alveolar macrophages	Increases colocalization of LC3 with *Mtb* and reduces TNF-α production	Juárez et al., 2016
Simvastatin	*Mtb* infection of C57BL/6 mice	Reduction of membrane cholesterol levels promotes phagosomal maturation and autophagy	Parihar et al., 2013
Metformin	*Mtb* infection of C57BL/6 mice	Induction of mitochondrial reactive oxygen species, AMPK activation, and autophagy induction	Singhal et al., 2014; Restrepo, 2016
Trehalose	*Mtb*/*M. avium*/*M. fortuitum* infection of human differentiated monocytes	Increase autophagy flux through activation of ptdIns3P by activation of PIKFYVE	Sarkar et al., 2007; Sharma et al., 2020
Mycobacterial PILAM	*Mtb* infection of murine macrophages	Induction of autophagy and pro-inflammatory cytokines, enhanced colocalization of *Mtb* with phagolysosomes	Shui et al., 2011; Singh et al., 2019
Nordi-hydroguaiaretic acid	Avirulent *Mtb* infection of human differentiated monocytes	Directly antimycobacterial, induce autophagosome formation and colocalization with *Mtb*	Guzmán-Beltrán et al., 2016
Lactoferricin peptides	*M. avium* infection of murine bone marrow macrophages	Increased autophagosome formation	Silva et al., 2017b

not clear bacteria. Co-administration of isoniazid and rifabutin with Rapamycin microparticles considerably improved bacterial clearance (Gupta et al., 2014, 2016). As the administration of microparticles with autophagy-inducing drugs may improve traditional antimycobacterial chemotherapies, an alternative strategy is utilizing microparticles that directly induce autophagy. Poly (lactic-co-glycolic acid) microparticles were found to be antimycobacterial in human macrophages. For example, NFκB activity was increased during microparticle treatment, and antimycobacterial effects were reversed by autophagy inhibitors (Lawlor et al., 2016).

An antiprotozoal drug, nitazoxanide, has been extensively tested to treat *Mtb* and NTMs alone and in conjunction with traditional antimycobacterial medicines. These conventional antibiotics were not found to inhibit autophagosome formation stimulated by nitazoxanide (Lam et al., 2012). Nitazoxanide has been previously explored as an autophagy agonist for treating multiple disease states such as Alzheimer's and cancer (Di Santo and Ehrisman, 2014; Li et al., 2020). It has also been examined as a potential treatment option against several mycobacteria including *M. leprae* (Bailey et al., 2017) and MAC (Rossignol, 1999). Nitazoxanide is metabolized into hydroxylamine by mycobacterial nitroreductase NfnB (Buchieri et al., 2017). Interestingly, nitazoxanide can kill replicating and non-replicating mycobacteria, emphasizing its potential role in combating latent mycobacterial infection (de Carvalho et al., 2009; Iacobino et al., 2019). Like Rapamycin and nitazoxanide, metformin also increases bacterial clearance during traditional anti-mycobacterial treatment, while inducing autophagy (Singhal et al., 2014; Lachmandas et al., 2019).

Two of the most promising experimental host-directed therapies against *M. tuberculosis* are Vitamin D3 and Metformin (Naicker et al., 2020). Metformin was shown to increase mitochondrial reactive oxygen species production, acting through AMPK, leading to control of drug-resistant *Mtb* and facilitation of phagolysosome fusion (Singhal et al., 2014; Yew et al., 2020). There also appears to be a correlation between metformin treatment for diabetes mellitus type II and delayed smear and culture conversion and reduced unfavorable outcomes (Singhal et al., 2014; Degner et al., 2017; Marupuru et al., 2017; Lee et al., 2018; Padmapriyadarsini et al., 2019). While metformin shows promise in preventing TB in type II diabetes patients, Vitamin D supplementation showed no improvement in TB treatment outcomes in patients with vitamin D sufficiency during drug sensitive *Mtb* infection. However, vitamin D deficiency is associated with an increased risk of *Mtb* infection (Ustianowski et al., 2005; Chun et al., 2011). Vitamin D supplementation did reduce the time to sputum culture conversion in patients with TaqI vitamin D receptor gene polymorphism, indicating that Vitamin D does play an important role in TB treatment outcomes. Vitamin D supplementation also improved the MDR-TB sputum culture conversion rate (Zhang et al., 2019). *In vitro* treatment with vitamin D during HIV and *Mtb* co-infection or *Mtb* infection alone concluded that autophagy induction was responsible for the better control of both HIV and *Mtb* in macrophages (Yuk et al., 2009; Fabri et al., 2011; Campbell and Spector, 2012a).

Many host pathways may constitute viable targets for host-directed therapies (HDTs). Apoptosis and autophagy have been the most explored HDT targets of *Mtb* and NTMs. Even though apoptosis may be a possible target, there is mounting evidence that NTMs can escape apoptotic bodies to ensure survival and disease progression (Early et al., 2011; Bento et al., 2020). Autophagy presents an exciting target as the induction of autophagy promotes bacterial clearance and antigen presentation (Castillo et al., 2012; Saini et al., 2016). The current recommended treatment for NTM infection is clarithromycin or azithromycin, ethambutol, and rifamycin (Griffith, 2018; Griffith, 2019; Daley et al., 2020; Gopalaswamy et al., 2020). Azithromycin was shown to inhibit autophagosome maturation resulting in an increased risk of *M. abscessus* infection (Renna et al., 2011; Torfs et al., 2019). It has also been found that many traditional anti-mycobacterials, though directly antimycobacterial, also have off-target effects that promote autophagy (Kim et al., 2012; Zullo and Lee, 2012b). Unfortunately, the development of new drugs targeting particular host pathways is often slow and expensive. One potential strategy to expedite this drug discovery is studying and assessing previous medications known to increase autophagy and their effect on mycobacteria (Williams et al., 2008; Sundaramurthy et al., 2013; Stanley et al., 2014; Kim et al., 2019). Potentially repurposed autophagy targeting host-directed therapies are summarized in **Table 2**. Many of these drugs are of interest because of the modulation of the host immune response. Accordingly, they should also be effective against a broad range of mycobacteria and other intracellular pathogens.

As a better understanding of the role of infection-induced autophagy transpires, more targeted host-directed therapy approaches can be developed and exploited. With C_4T_4 (a TLR4 agonist), autophagy was induced in guinea pigs infected with *Mtb* in a CLEC4E-dependent manner through MYD88 and PrdIns3K activation, leading to reduced mycobacterial burden (Pahari et al., 2020). Along with targeting cell receptors to activate autophagy, there is increasing evidence that many microRNAs (miRNAs) can be targeted to activate autophagy during mycobacterial infection (Wang et al., 2013; Kim et al., 2015, 2017a,b; Kumar et al., 2016; Etna et al., 2018; Liu et al., 2018; Li et al., 2019). These miRNAs modulate autophagy through different upstream pathways of mTOR. *Mtb* infection induces miRNA-144, which targets the DNA damage regulated autophagy modulator 2 (DRAM2), resulting in autophagy inhibition through AMPK (Kim et al., 2017b). Similar to targeting CLEC4E through TLR4 agonists, TLR2 and MYD88 are required to induce miRNA-125a during *Mtb* infection. *Mtb* induces expression of miR-125a in macrophages, which results in the inhibition of autophagy by targeting UV radiation resistance-associated gene (UVRAG) in the AMPK dependent manner (Kim et al., 2015).

Targeting Autophagy to Prevent Mycobacterial Infection

BCG is widely used as a vaccine against tuberculosis. BCG evades phagosome maturation, autophagy, MHC-II expression of antigen-presenting cells (APCs), and T-cell activation (Deretic et al., 1997; Singh et al., 2006; Münz, 2016; Saini et al., 2016;

TABLE 2 | Summary of repurposed autophagy targeting host-directed therapies against NTMs.

Drug	Model	Role in Autophagy	Reference
Azithromycin	*M. abscessus* infection of primary human macrophages and C57BL/6 mice	Blocks lysosomal acidification, impairing autophagosome degradation, directly antimycobacterial on susceptible strains	Renna et al., 2011
Carvacrol	Directly antimycobacterial against *M. abscessus*, *M. chelonae*, *M. fortuitum*, *M. mucogenicum*, *M. avium* sbsp paratuberculosis, and *M. smegmatis*	MEK inhibition of mTOR resulting in increased autophagy. Inhibition of autophagy during adipogenic differentiation.	Nowotarska et al., 2017; Potočnjak et al., 2018; Spalletta et al., 2018; Marini et al., 2019
Tetracycline	Directly antimycobacterial against *M. abscessus*, *M. chelonae*, and *M. fortuitum*	mTOR inhibition	Brüning et al., 2014; Kaushik et al., 2019; Shoen et al., 2019
Thioridazine	*In vitro* clearance of *M. avium* from Thp-1 macrophages, possible efflux pump inhibitor	Upregulation of AMPK activity leading to autophagy induction.	Rodrigues et al., 2008; Deshpande et al., 2016; Seervi et al., 2018; Chu et al., 2019
Mefloquine	Directly antimycobacterial against *M. avium* complex in culture. *In vivo* clearance in mice	Highly induced formation of autophagosomes in neuroblastoma cells	Bermudez et al., 1999, 2012; Shin et al., 2012
Clonidine/Verapamil/Minoxidil	Decreased disease progression in *in vitro*, fly, and zebrafish models of infection	Clearance of soluble huntingtin exon 1 during *M. leprae* infection by autophagy	Williams et al., 2008

Khan et al., 2019). Clinical isolates of *Mtb* that could not inhibit autophagy showed increased TB disease outcomes and the extent of disease (Li et al., 2016), strongly indicating that autophagy is a crucial host pathway for the control of TB. The ability to utilize this essential host pathway could prove a viable avenue for improving mycobacterial vaccines (Yuk and Jo, 2014; Flores-Valdez et al., 2018; Tao and Drexler, 2020). Notably, the yellow fever vaccine, YF-17D, one of the most successful vaccines, has been found to enhance autophagy-dependent antigen presentation. The mechanisms of the vaccine efficacy by YF-17D were not well understood until its role in autophagy modulation was deciphered (Ravindran et al., 2014).

Developing new vaccines or improving the BCG by harnessing autophagy is an area of interest and has garnered examination. BCG, like *Mtb*, expresses a wide array of bacterial effectors that modulate autophagy, but co-immunization of mice with BCG and rapamycin-treated dendritic cells enhanced Th1-mediated protection against *Mtb* infection (Jagannath et al., 2009). Similarly, it was demonstrated that a recombinant BCG expressing 85C5 (BCG^{85C5}) induced a robust MHC-II-dependent antigen presentation to $CD4^+$ T cells *in vitro*. The 85C5 peptide contains the TLR-2 activating C5 peptide from *Mtb* CFP-10 protein. The vaccine also elicited stronger Th1 cytokines from APCs of C57Bl/6 mice and enhanced MHC-II surface expression on macrophages by inhibiting the membrane associated RING-CH 1 (MARCH1) E3 ligase that degrades MHC-II. BCG^{85C5} infected APCs presented antigens in a MyD88 or a TLR-2 dependent manner (Khan et al., 2019). Additionally, activation of TLR3 or TLR4 by LPS cleared mycobacteria *in vitro* in an autophagy-dependent way (Xu et al., 2007, 2013).

BCG was genetically modified to improve its immunogenicity by replacing the urease C encoding gene with the listeriolysin encoding gene from *Listeria monocytogenes* (Nieuwenhuizen et al., 2017). Listeriolysin perturbates the phagosomal membrane at acidic pH and Urease C neutralize the phagosome harboring BCG. Deletion of *ureC* leads to rapid phagosome acidification and promotes phagolysosome fusion. Subsequently, BCGΔureC:hly elevates apoptosis and autophagy and accelerates release of mycobacterial antigens into the cytosol. The BCGΔ*ureC*:*hly* vaccine completed phase I and IIa clinical trials. Upon deleting the anti-apoptotic gene *nuoG* to enhance cross protection, BCGΔ*ureC*:*hly*Δ*nuoG* vaccine showed reduced *Mtb* burden in the lungs of mice leading to less pathology and, most importantly, enhanced immune responses. It was found that the *nuoG* deletion leads to significant induction of autophagy and an improved safety profile (Gengenbacher et al., 2016). *M. indicus pranii* is another potential immunotherapy and vaccine candidate under clinical trials (Gupta et al., 2012; Saqib et al., 2016; Sharma et al., 2017). Boosting BCG vaccination with *M. indicus pranii* resulted in improved protection in a murine model of *Mtb* infection. Increased IFN-γ, IL-12, and IL-17 were observed along with increased polyfunctional T cells (Saqib et al., 2016). This increased protection and immune response were subsequently due to increased autophagy induced by *M. indicus pranii*, potentially due to its PILAM (Singh et al., 2017, 2019).

While improving the BCG vaccine appears a viable short-term solution to improve vaccine efficacy against *Mtb*, the efforts

to develop new vaccines must be continued. BCG is a live attenuated vaccine, but it is not suitable for use in all cases. The development of other vaccine options, such as DNA vaccines or subunit vaccines, would significantly advance the vaccination strategy against *Mtb* and NTMs. A DNA vaccine encoding for the potent *Mtb* antigen 85B (Ag85B) significantly enhanced autophagy activation and vaccine efficacy when delivered with a plasmid encoding a kinase defective (mTOR-KD) (Meerak et al., 2013). This mTOR-KD DNA vaccine-elicited considerably higher Ag85B-specific antibodies, increased secretion of IFN-γ and IL-2 levels, and enhanced proliferation of $CD4^+$ T cells. Similar to this approach, it was found that an LC3-LpqH-Ag85B DNA vaccination reduced mycobacterial burden, increased IFN-γ and IL-2, and enhanced the Th1 immune response (Hu et al., 2014).

Adjuvating or boosting BCG with autophagy-inducing substrates has also been examined as a potential way to increase the efficacy of current vaccines. Curcumin-coated nanoparticles have been found to enhance autophagy, leading to increased Th1 and Th17 central memory T cells (Ahmad et al., 2019). Other studies have identified autophagy as having an essential role in forming and surviving memory T cells (Xu et al., 2014). Like curcumin nanoparticles, boosting BCG vaccine with nanofibers acting through the autophagy pathway improved BCG efficacy (Rudra et al., 2017; Chesson et al., 2018). While some DNA vaccines directly target autophagy, the development of an adjuvant system targeting autophagy may improve the efficacy of potential subunit vaccines. Utilizing the lactic acid bacteria (LAB) as an adjuvant for *Mtb* antigens showed improved IFN-γ and NO responses, polarizing a Th1 response and increasing autophagosome formation. Although LAB's protective efficacy was not tested, these improved immunological responses compared to *Mtb* antigen alone are promising (Ghadimi et al., 2010).

CONCLUSION

Autophagy has been established as an effective mechanism for the clearance of mycobacteria from the infected macrophages. Many studies have looked at the potential of autophagy-inducing drugs to improve current treatment regimens against mycobacteria. Due to the dramatic rise of antibiotic-resistant mycobacteria and the upsurge of NTMs that are intrinsically resistant to traditional antibiotics, host-directed therapies are even more relevant (Deretic, 2008; Kim et al., 2012; Zullo and Lee, 2012b; Kim et al., 2019; Bento et al., 2020).

While *Mtb* inhibits apoptosis for bacterial survival (Hinchey et al., 2007), NTMs utilize the hosts' cellular progression from apoptosis to secondary necrosis (Gao and Kwaik, 2000; Lee et al., 2011) or induce membrane perforation (similar to that observed during necrosis) to allow for bacterial escape and communication (Roux et al., 2016). Subsequent expression of bacterial factors that form an extracellular milieu or biofilm makes control by either phagocytic cells or administered antibiotics much more difficult. If host-directed therapies inhibiting apoptosis or inducing autophagy could be employed against these non-tuberculosis mycobacteria, infection control of the contained intracellular mycobacteria with traditional antibiotics may be far more successful. Additionally, it has been demonstrated that potent autophagy-inducing chemicals could increase mycobacterial clearance from macrophages, like seen during rapamycin treatment (Singh et al., 2017).

Autophagy-targeting host-directed therapies and vaccines for mycobacteria have numerous potential benefits. However, further understanding of the role of autophagy, its molecular mechanisms, and regulation during mycobacterial infection is required to develop persistent, viable, and safe host-directed therapies and vaccines. Additionally, examination of the crosstalk between autophagy and apoptosis during infection should significantly improve our understanding of the applicability of these host pathways as a viable target for treatment. Though host-directed therapies may play a vital role for intrinsically antibiotic-resistant NTMs and drug-resistant TB, they will need to be considered together with traditional anti-mycobacterial medicines, with the goal of shorter treatment times and improved outcomes.

AUTHOR CONTRIBUTIONS

ES and SL conceived the review. ES wrote the first draft of the manuscript. SL wrote sections of the manuscript and provided overall editing. All authors contributed to manuscript revision, read, and approved the submitted version.

FUNDING

This research was supported by the National Institute of Allergy and Infectious Diseases (R01 AI127711). The funders had no role in study design, data collection, interpretation, or the decision to submit the work for publication.

ACKNOWLEDGMENTS

Figure 1 was created with BioRender.com. The authors acknowledge and thank the kind contributions and discussion of Maria González Orozco and Jia Wang (University of Texas Medical Branch).

REFERENCES

Ahmad, S., Bhattacharya, D., Kar, S., Ranganathan, A., Van Kaer, L., and Das, G. (2019). Curcumin Nanoparticles Enhance *Mycobacterium bovis* BCG Vaccine Efficacy by Modulating Host Immune Responses. *Infect. Immun.* 87, e291–e219. doi: 10.1128/iai.00291-19

Axe, E. L., Walker, S. A., Manifava, M., Chandra, P., Roderick, H. L., Habermann, A., et al. (2008). Autophagosome formation from membrane compartments enriched in phosphatidylinositol 3-phosphate and dynamically connected to the endoplasmic reticulum. *J. Cell Biol.* 182, 685–701. doi: 10.1083/jcb.200803137

Bailey, M. A., Na, H., Duthie, M. S., Gillis, T. P., Lahiri, R., and Parish, T. (2017). Nitazoxanide is active against Mycobacterium

leprae. *PLoS One* 12:e0184107. doi: 10.1371/journal.pone.0184107

Balcewicz-Sablinska, M. K., Keane, J., Kornfeld, H., and Remold, H. G. (1998). Pathogenic *Mycobacterium tuberculosis* Evades Apoptosis of Host Macrophages by Release of TNF-R2, Resulting in Inactivation of TNF-α. *J. Immunol.* 161, 2636–2641.

Bento, C. M., Gomes, M. S., and Silva, T. (2020). Looking beyond Typical Treatments for Atypical Mycobacteria. *Antibiotics* 9:18.

Bermudez, L. E., Inderlied, C. B., Kolonoski, P., Chee, C. B., Aralar, P., Petrofsky, M., et al. (2012). Identification of (+)-Erythro-Mefloquine as an Active Enantiomer with Greater Efficacy than Mefloquine against *Mycobacterium avium* Infection in Mice. *Antimicrob. Agents Chemother.* 56, 4202–4206. doi: 10.1128/aac.00320-12

Bermudez, L. E., Kolonoski, P., Wu, M., Aralar, P. A., Inderlied, C. B., and Young, L. S. (1999). Mefloquine Is Active In Vitro and In Vivo against *Mycobacterium avium* Complex. *Antimicrob. Agents Chemother.* 43, 1870–1874. doi: 10.1128/aac.43.8.1870

Bibert, S., Bratschi, M. W., Aboagye, S. Y., Collinet, E., Scherr, N., Yeboah-Manu, D., et al. (2017). Susceptibility to *Mycobacterium ulcerans* Disease (Buruli ulcer) Is Associated with *IFNG* and *iNOS* Gene Polymorphisms. *Front. Microbiol.* 8:1903. doi: 10.3389/fmicb.2017.01903

Bieri, R., Scherr, N., Ruf, M.-T. S., Dangy, J.-P., Gersbach, P., Gehringer, M., et al. (2017). The Macrolide Toxin Mycolactone Promotes Bim-Dependent Apoptosis in Buruli Ulcer through Inhibition of mTOR. *Am. Chem. Soc. Chem. Biol.* 12, 1297–1307. doi: 10.1021/acschembio.7b00053

Bodle, E. E., Cunningham, J. A., Della-Latta, P., Schluger, N. W., and Saiman, L. (2008). Epidemiology of Nontuberculous Mycobacteria in Patients without HIV Infection. *Emerg. Infect. Dis.* 14, 390–396. doi: 10.321/eid1403.061143

Bohsali, A., Abdalla, H., Velmurugan, K., and Briken, V. (2010). The non-pathogenic mycobacteria *M. smegmatis* and *M. fortuitum* induce rapid host cell apoptosis via a caspase-3 and TNF dependent pathway. *BMC Microbiol.* 10:237. doi: 10.1186/1471-2180-10-237

Brüning, A., Brem, G. J., Vogel, M., and Mylonas, I. (2014). Tetracyclines cause cell stress-dependent ATF4 activation and mTOR inhibition. *Exp. Cell Res.* 320, 281–289. doi: 10.1016/j.yexcr.2013.11.012

Buchieri, M. V., Cimino, M., Rebollo-Ramirez, S., Beauvineau, C., Cascioferro, A., Favre-Rochex, S., et al. (2017). Nitazoxanide Analogs Require Nitroreduction for Antimicrobial Activity in Mycobacterium smegmatis. *J. Med. Chem.* 60, 7425–7433. doi: 10.1021/acs.jmedchem.7b00726

Byrd, T. F., and Lyons, C. R. (1999). Preliminary characterization of a Mycobacterium abscessus mutant in human and murine models of infection. *Infect. Immun.* 67, 4700–4707.

Campbell, G. R., and Spector, S. A. (2012a). Autophagy induction by vitamin D inhibits both Mycobacterium tuberculosis and human immunodeficiency virus type 1. *Autophagy* 8, 1523–1525. doi: 10.4161/auto.21154

Campbell, G. R., and Spector, S. A. (2012b). Vitamin D Inhibits Human Immunodeficiency Virus Type 1 and Mycobacterium tuberculosis Infection in Macrophages through the Induction of Autophagy. *PLoS Pathogens* 8:e1002689. doi: 10.1371/journal.ppat.1002689

Capela, C., Dossou, A. D., Silva-Gomes, R., Sopoh, G. E., Makoutode, M., Menino, J. F., et al. (2016). Genetic Variation in Autophagy-Related Genes Influences the Risk and Phenotype of Buruli Ulcer. *PLoS Neglec. Trop. Dis.* 10:4671. doi: 10.1371/journal.pntd.0004671

Castillo, E. F., Dekonenko, A., Arko-Mensah, J., Mandell, M. A., Dupont, N., Jiang, S., et al. (2012). Autophagy protects against active tuberculosis by suppressing bacterial burden and inflammation. *Proc. Natl. Acad. Sci. U S A* 109, E3168–E3176. doi: 10.1073/pnas.1210500109

Catherinot, E., Clarissou, J., Etienne, G., Ripoll, F., Emile, J.-F., Daffe, M., et al. (2007). Hypervirulence of a Rough Variant of the *Mycobacterium abscessus* Type Strain. *Infect. Immun.* 75, 1055–1058. doi: 10.1128/IAI.00835-06

Chai, Q., Wang, X., Qiang, L., Zhang, Y., Ge, P., Lu, Z., et al. (2019). A *Mycobacterium tuberculosis* surface protein recruits ubiquitin to trigger host xenophagy. *Nat. Commun.* 10:1973.

Chandra, P., Ghanwat, S., Matta, S. K., Yadav, S. S., Mehta, M., Siddiqui, Z., et al. (2015). *Mycobacterium tuberculosis* Inhibits RAB7 Recruitment to Selectively Modulate Autophagy Flux in Macrophages. *Sci. Rep.* 5:16320. doi: 10.1038/srep16320

Chesson, C. B., Huante, M., Nusbaum, R. J., Walker, A. G., Clover, T. M., Chinnaswamy, J., et al. (2018). Nanoscale Peptide Self-assemblies Boost BCG-primed Cellular Immunity Against Mycobacterium tuberculosis. *Sci. Rep.* 8:12519. doi: 10.1038/s41598-018-31089-y

Choy, A., Dancourt, J., Mugo, B., O'Connor, T. J., Isberg, R. R., Melia, T. J., et al. (2012). The *Legionella* Effector RavZ Inhibits Host Autophagy Through Irreversible Atg8 Deconjugation. *Science* 338, 1072–1076. doi: 10.1126/science.1227026

Chu, C.-W., Ko, H.-J., Chou, C.-H., Cheng, T.-S., Cheng, H.-W., Liang, Y.-H., et al. (2019). Thioridazine Enhances P62-Mediated Autophagy and Apoptosis Through Wnt/β-Catenin Signaling Pathway in Glioma Cells. *Int. J. Mole. Sci.* 20:473.

Chun, R. F., Adams, J. S., and Hewison, M. (2011). Immunomodulation by vitamin D: implications for TB. *Exp. Rev. Clin. Pharmacol.* 4, 583–591. doi: 10.1586/ecp.11.41

Conrad, W. H., Osman, M. M., Shanahan, J. K., Chu, F., Takaki, K. K., Cameron, J., et al. (2017). Mycobacterial ESX-1 secretion system mediates host cell lysis through bacterium contact-dependent gross membrane disruptions. *Proc. Natl. Acad. Sci.* 114, 1371–1376. doi: 10.1073/pnas.1620133114

Converse, P. J., Almeida, D. V., Tyagi, S., Xu, J., and Nuermberger, E. L. (2019). Shortening Buruli Ulcer Treatment with Combination Therapy Targeting the Respiratory Chain and Exploiting *Mycobacterium ulcerans* Gene Decay. *Antimicrob. Agents Chemother.* 63, e426–e419. doi: 10.1128/aac.00426-19

Cooper, A. M., Dalton, D. K., Stewart, T. A., Griffin, J. P., Russell, D. G., and Orme, I. M. (1993). Disseminated Tuberculosis in Interferon-γ Gene-disrupted Mice. *J. Exp. Med.* 178, 2243–2247. doi: 10/1084/jem.178.6.2243

Daley, C. L., Iaccarino, J. M., Lange, C., Cambau, E., Wallace, R. J. Jr., Andrejak, C., et al. (2020). Treatment of Nontuberculous Mycobacterial Pulmonary Disease: An Official ATS/ERS/ESCMID/IDSA Clinical Practice Guideline. *Clin. Infect. Dis.* 71, e1–e36. doi: 10.1093/cid/ciaa241

Dang, A. T., Teles, R. M. B., Weiss, D. I., Parvatiyar, K., Sarno, E. N., Ochoa, M. T., et al. (2019). IL-26 contributes to host defense against intracellular bacteria. *J. Clin. Invest.* 129, 1926–1939. doi: 10.1172/JCI99550

D'Cruze, T., Gong, L., Treerat, P., Ramm, G., Boyce, J. D., Prescott, M., et al. (2011). Role for the *Burkholderia pseudomallei* Type Three Secretion System Cluster 1 *bpscN* Gene in Virulence. *Infect. Immun.* 79, 3659–3664. doi: 10.1128/iai.01351-10

de Carvalho, L. P. S., Lin, G., Jiang, X., and Nathan, C. (2009). Nitazoxanide Kills Replicating and Nonreplicating Mycobacterium tuberculosis and Evades Resistance. *J. Med. Chem.* 52, 5789–5792. doi: 10.1021/jm9010719

De Groote, M. A., and Huitt, G. (2006). Infections Due to Rapidly Growing Mycobacteria. *Clin. Dis.* 42, 1756–1763. doi: 10.1086/504381

de Mattos Barbosa, M. G., de Andrade Silva, B. J., Assis, T. Q., da Silva, Prata, R. B., Ferreira, H., et al. (2018). Autophagy Impairment Is Associated With Increased Inflammasome Activation and Reversal Reaction Development in Multibacillary Leprosy. *Front. Immunol.* 9:1223. doi: 10.3389/fimmu.2018.01223

Degner, N. R., Wang, J.-Y., Golub, J. E., and Karakousis, P. C. (2017). Metformin Use Reverses the Increased Mortality Associated With Diabetes Mellitus During Tuberculosis Treatment. *Clin. Infect. Dis.* 66, 198–205. doi: 10.1093/cid/cix819

Deng, W., Long, Q., Zeng, J., Li, P., Yang, W., Chen, X., et al. (2017). *Mycobacterium tuberculosis* PE_PGRS41 Enhances the Intracellular Survival of M. smegmatis within Macrophages Via Blocking Innate Immunity and Inhibition of Host Defense. *Sci. Rep.* 7:46716. doi: 10.1038/srep46716

Deretic, V. (2008). Autophagy, an immunologic magic bullet: Mycobacterium tuberculosis phagosome maturation block and how to bypass it. *Future Microbiol.* 3, 517–524. doi: 10.2217/17460913.3.5.517

Deretic, V., Via, L. E., Fratti, R. A., and Deretic, D. (1997). Mycobacterial phagosome maturation, rab proteins, and intracellular trafficking. *Electrophoresis* 18, 2542–2547. doi: 10.1002/elps.1150181409

Deshpande, D., Srivastava, S., Musuka, S., and Gumbo, T. (2016). Thioridazine as Chemotherapy for *Mycobacterium avium* Complex Diseases. *Antimicrob. Agents Chemother.* 60, 4652–4658. doi: 10.1128/aac.02985-15

Di Santo, N., and Ehrisman, J. (2014). A functional perspective of nitazoxanide as a potential anticancer drug. *Mutation Res.* 768, 16–21. doi: 10.1016/j.mrfmmm.2014.05.005

Donohue, M. J., and Wymer, L. (2016). Increasing Prevalence Rate of Nontuberculous Mycobacteria Infections in Five States, 2008–2013. *Ann. Am. Thorac. Soc.* 13, 2143–2150. doi: 10.1513/AnnalsATS.201605-353OC

Early, J., Fischer, K., and Bermudez, L. E. (2011). Mycobacterium avium uses apoptotic macrophages as tools for spreading. *Microb. Pathogenesis* 50, 132–139. doi: 10.1016/j.micpath.2010.12.004

Etna, M. P., Sinigaglia, A., Grassi, A., Giacomini, E., Romagnoli, A., Pardini, M., et al. (2018). Mycobacterium tuberculosis-induced miR-155 subverts autophagy by targeting ATG3 in human dendritic cells. *PLoS Pathogens* 14:e1006790. doi: 10.1371/journal.ppat.1006790

Evans, M. J., and Levy, L. (1972). Ultrastructural Changes in Cells of the Mouse Footpad Infected with *Mycobacterium leprae*. *Infect. Immun.* 5, 238–247.

Fabri, M., Stenger, S., Shin, D.-M., Yuk, J.-M., Liu, P. T., Realegeno, S., et al. (2011). Vitamin D Is Required for IFN-γ–Mediated Antimicrobial Activity of Human Macrophages. *Sci. Trans. Med.* 3, ra102–ra104. doi: 10.1126/scitranslmed.3003045

Fazeli, G., and Wehman, A. M. (2017). Rab GTPases mature the LC3-associated midbody phagosome. *Commun. Integr. Biol.* 10, e1297349. doi: 10.1080/19420889.2017.1297349

Fischer, M. (2017). Leprosy – an overview of clinical features, diagnosis, and treatment. *JDDG* 15, 801–827. doi: 10.1111/ddg.13301

Flores-Valdez, M. A., Segura-Cerda, C. A., and Gaona-Bernal, J. (2018). Modulation of autophagy as a strategy for development of new vaccine candidates against tuberculosis. *Mole. Immunol.* 97, 16–19. doi: 10.1016/j.molimm.2018.03.006

Floto, R. A., Sarkar, S., Perlstein, E. O., Kampmann, B., Schreiber, S. L., and Rubinsztein, D. C. (2007). Small Molecule Enhancers of Rapamycin-Induced TOR Inhibition Promote Autophagy, Reduce Toxicity in Huntington's Disease Models and Enhance Killing of Mycobacteria by Macrophages. *Autophagy* 3, 620–622. doi: 10.4161/auto.4898

Flynn, J. L., Chan, J., Triebold, K. J., Dalton, D. K., Stewart, T. A., and Bloom, B. R. (1993). An Essential Role for Interferon-γ in Resistance to *Mycobacterium tuberculosis* Infection. *J. Exp. Med.* 178, 2249–2254. doi: 10.1084/jem.178.6.2249

Franco-Paredes, C., Marcos, L. A., Henao-Martínez, A. F., Rodríguez-Morales, A. J., Villamil-Gómez, W. E., Gotuzzo, E., et al. (2018). Cutaneous Mycobacterial Infections. *Clin. Microb. Rev.* 32, e69–e18. doi: 10.1128/CMR.00069-18s

Fujita, N., Itoh, T., Omori, H., Fukuda, M., Noda, T., and Yoshimori, T. (2008). The Atg16L Complex Specifies the Site of LC3 Lipidation for Membrane Biogenesis in Autophagy. *Mole. Biol. Cell* 19, 2092–2100. doi: 10.1091/mbc.e07-12-1257

Gama, J. B., Ohlmeier, S., Martins, T. G., Fraga, A. G., Sampaio-Marques, B. M., Carvalho, M. A., et al. (2014). Proteomic Analysis of the Action of the *Mycobacterium ulcerans* Toxin Mycolactone: Targeting Host Cells Cytoskeleton and Collagen. *PLoS Neglec. Trop. Dis.* 8:e3066. doi: 10.1371/journal.pntd.0003066

Gao, L.-Y., and Kwaik, Y. A. (2000). The modulation of host cell apoptosis by intracellular bacterial pathogens. *Trends Microbiol.* 8, 306–313. doi: 10.1016/S0966-842X(00)01784-4

Genestet, C., Bernard-Barret, F., Hodille, E., Ginevra, C., Ader, F., Goutelle, S., et al. (2018). Antituberculous drugs modulate bacterial phagolysosome avoidance and autophagy in Mycobacterium tuberculosis-infected macrophages. *Tuberculosis* 111, 67–70. doi: 10.1016/j.tube.2018.05.014

Gengenbacher, M., Nieuwenhuizen, N., Vogelzang, A., Liu, H., Kaiser, P., Schuerer, S., et al. (2016). Deletion of *nuoG* from the Vaccine Candidate *Mycobacterium bovis* BCG Δ*ureC*:: *hly* Improves Protection against Tuberculosis. *mBio* 7, e679–e616. doi: 10.1128/mBio.00679-16

Ghadimi, D., de Vrese, M., Heller, K. J., and Schrezenmeir, J. (2010). Lactic acid bacteria enhance autophagic ability of mononuclear phagocytes by increasing Th1 autophagy-promoting cytokine (IFN-γ) and nitric oxide (NO) levels and reducing Th2 autophagy-restraining cytokines (IL-4 and IL-13) in response to Mycobacterium tuberculosis antigen. *Int. Immunopharmacol.* 10, 694–706. doi: 10.1016/j.intimp.2010.03.014

Gopalaswamy, R., Shanmugam, S., Mondal, R., and Subbian, S. (2020). Of tuberculosis and non-tuberculous mycobacterial infections - a comparative analysis of epidemiology, diagnosis and treatment. *J.Biomed. Sci.* 27, 74–74. doi: 10.1186/s12929-020-00667-6

Greendyke, R., and Byrd, T. F. (2008). Differential Antibiotic Susceptibility of Mycobacterium abscessus Variants in Biofilms and Macrophages Compared to That of Planktonic Bacteria. *Antimicrob. Agents Chemother.* 52, 2019–2026. doi: 10.1128/AAC.00986-07

Greenstein, R. J., Su, L., Juste, R. A., and Brown, S. T. (2008). On the Action of Cyclosporine A, Rapamycin and Tacrolimus on M. avium Including Subspecies paratuberculosis. *PLoS One* 3:2496. doi: 10.1371/journal.pone.0002496

Griffith, D. E. (2018). Treatment of Mycobacterium avium Complex (MAC). *Semin. Respir. Crit. Care Med.* 39, 351–361. doi: 10.1055/s-0038-1660472

Griffith, D. E. (2019). "A comprehensive Approach to Diagnosis and Management," in *Nontuberculosis Mycobacterial Disease*, ed. D. E. Griffith (Berlin: Springer).

Griffith, D. E., Aksamit, T., Brown-Elliott, B. A., Catanzaro, A., Daley, C., Gordin, F., et al. (2007). An Official ATS/IDSA Statement: Diagnosis, Treatment, and Prevention of Nontuberculous Mycobacterial Diseases. *Am. J. Respir. Crit. Care Med.* 175, 367–416. doi: 10.1164.rccm.200604-571ST

Gupta, A., Ahmad, F. J., Ahmad, F., Gupta, U. D., Natarajan, M., Katoch, V., et al. (2012). Efficacy of Mycobacterium indicus pranii Immunotherapy as an Adjunct to Chemotherapy for Tuberculosis and Underlying Immune Responses in the Lung. *PLoS One* 7:e39215. doi: 10.1371/journal.pone.0039215

Gupta, A., Pant, G., Mitra, K., Madan, J., Chourasia, M. K., and Misra, A. (2014). Inhalable Particles Containing Rapamycin for Induction of Autophagy in Macrophages Infected with *Mycobacterium tuberculosis*. *Mole. Pharm.* 11, 1201–1207. doi: 10.1021/mp4006563

Gupta, A., Sharma, D., Meena, J., Pandya, S., Sachan, M., Kumar, S., et al. (2016). Preparation and Preclinical Evaluation of Inhalable Particles Containing Rapamycin and Anti-Tuberculosis Agents for Induction of Autophagy. *Pharm. Res.* 33, 1899–1912. doi: 10.1007/s11095-016-1926-0

Gutierrez, M. G., Master, S. S., Singh, S. B., Taylor, G. A., Colombo, M. I., and Deretic, V. (2004). Autophagy Is a Defense Mechanism Inhibiting BCG and *Mycobacterium tuberculosis* Survival in Infected Macrophages. *Cell* 119, 753–766. doi: 10.1016/j.cell.2004.11.038

Guzmán-Beltrán, S., Rubio-Badillo, M. Á, Juárez, E., Hernández-Sánchez, F., and Torres, M. (2016). Nordihydroguaiaretic acid (NDGA) and α-mangostin inhibit the growth of Mycobacterium tuberculosis by inducing autophagy. *Int. Immunopharm.* 31, 149–157. doi: 10.1016/j.intimp.2015.12.027

Harris, J., De Haro, S. A., Master, S. S., Keane, J., Roberts, E. A., Delgado, M., et al. (2007). T Helper 2 Cytokines Inhibit Autophagic Control of Intracellular Mycobacterium tuberculosis. *Immunity* 27, 505–517. doi: 10.1016/j.immuni.2007.07.022

Hinchey, J., Lee, S., Jeon, B. Y., Basaraba, R. J., Venkataswamy, M. M., Chen, B., et al. (2007). Enhanced priming of adaptive immunity by a proapoptotic mutant of Mycobacterium tuberculosis. *J. Clin. Invest.* 117, 2279–2288. doi: 10.1172/JCI31947

Hu, D., Wu, J., Zhang, R., Chen, L., Chen, Z., Wang, X., et al. (2014). Autophagy-targeted vaccine of LC3–LpqH DNA and its protective immunity in a murine model of tuberculosis. *Vaccine* 32, 2308–2314. doi: 10.1016/j.vaccine.2014.02.069

Huang, D., and Bao, L. (2016). *Mycobacterium tuberculosis* EspB protein suppresses interferon-γ-induced autophagy in murine macrophages. *J. Microbiol. Immunol. Infect.* 49, 859–865. doi: 10.1016/j.jmii.2014.11.008

Iacobino, A., Giannoni, F., Pardini, M., Piccaro, G., and Fattorini, L. (2019). The Combination Rifampin-Nitazoxanide, but Not Rifampin-Isoniazid-Pyrazinamide-Ethambutol, Kills Dormant *Mycobacterium tuberculosis* in Hypoxia at Neutral pH. *Antimicrob. Agents Chemother.* 63, e273–e219. doi: 10.1128/aac.00273-19

Islam, M. S., Richards, J. P., and Ojha, A. K. (2012). Targeting drug tolerance in mycobacteria: a perspective from mycobacterial biofilms. *Exp. Rev. Anti-infect. Ther.* 10, 1055–1066. doi: 10.1586/eri.12.88

Itakura, E., and Mizushima, N. (2010). Characterization of autophagosome formation site by a hierarchical analysis of mammalian Atg proteins. *Autophagy* 6, 764–776. doi: 10.4161/auto.6.6.12709

Jagannath, C., Lindsey, D. R., Dhandayuthapani, S., Xu, Y., Hunter, R. L., and Eissa, N. T. (2009). Autophagy enhances the efficacy of BCG vaccine by increasing peptide presentation in mouse dendritic cells. *Nat. Med.* 15, 267–276. doi: 10.1038/nm.1928

Jarlier, V., and Nikaido, H. (1990). Permeability barrier to hydrophilic solutes in Mycobacterium chelonei. *J. Bacteriol.* 172, 1418–1423. doi: 10.1128/jb.172.3.1418-1423.1990

Jiao, Y., and Sun, J. (2019). Bacterial Manipulation of Autophagic Responses in Infection and Inflammation. *Front. Immunol.* 10:2821–2821. doi: 10.3389/fimmu.2019.02821

Jo, E.-K. (2010). Innate immunity to mycobacteria: vitamin D and autophagy. *Cell. Microbiol.* 12, 1026–1035. doi: 10.1111/j.1462-5822.2010.01491.x

Johnson, M. M., and Odell, J. A. (2014). Nontuberculous mycobacterial pulmonary infections. *J. Thorac. Dis.* 6, 210–220. doi: 10.3978/j.issn.2072-1439.2013.12.24

Juárez, E., Carranza, C., Sánchez, G., González, M., Chávez, J., Sarabia, C., et al. (2016). Loperamide Restricts Intracellular Growth of Mycobacterium tuberculosis in Lung Macrophages. *Am. J. Respir. Cell Mole. Biol.* 55, 837–847. doi: 10.1165/rcmb.2015-0383OC

Kaushik, A., Ammerman, N. C., Martins, O., Parrish, N. M., and Nuermberger, E. L. (2019). In Vitro Activity of New Tetracycline Analogs Omadacycline and Eravacycline against Drug-Resistant Clinical Isolates of *Mycobacterium abscessus*. *Antimicrob. Agents Chemother.* 63, e470–e419. doi: 10.1128/aac.00470-19

Keane, J., Remold, H. G., and Kornfeld, H. (2000). Virulent *Mycobacterium tuberculosis* Strains Evade Apoptosis of Infected Alveolar Macrophages. *J. Immunol.* 164, 2016–2020. doi: 10.4049/jimmunol.164.4.2016

Khan, A., Bakhru, P., Saikolappan, S., Das, K., Soudani, E., Singh, C. R., et al. (2019). An autophagy-inducing and TLR-2 activating BCG vaccine induces a robust protection against tuberculosis in mice. *NPJ Vaccines* 4:34. doi: 10.1038/s41541-019-0122-8

Kim, J. K., Kim, T. S., Basu, J., and Jo, E.-K. (2017a). MicroRNA in innate immunity and autophagy during mycobacterial infection. *Cell. Microbiol.* 19:e12687. doi: 10.1111/cmi.12687

Kim, J. K., Lee, H.-M., Park, K.-S., Shin, D.-M., Kim, T. S., Kim, Y. S., et al. (2017b). MIR144* inhibits antimicrobial responses against Mycobacterium tuberculosis in human monocytes and macrophages by targeting the autophagy protein DRAM2. *Autophagy* 13, 423–441. doi: 10.1080/15548627.2016.1241922

Kim, J. K., Yuk, J.-M., Kim, S. Y., Kim, T. S., Jin, H. S., Yang, C.-S., et al. (2015). MicroRNA-125a Inhibits Autophagy Activation and Antimicrobial Responses during Mycobacterial Infection. *J. Immunol.* 194, 5355–5365. doi: 10.4049/jimmunol.1402557

Kim, J.-J., Lee, H.-M., Shin, D.-M., Kim, W., Yuk, J.-M., Jin, H. S., et al. (2012). Host Cell Autophagy Activated by Antibiotics Is Required for Their Effective Antimycobacterial Drug Action. *Cell Host Microbe* 11, 457–468. doi: 10.1016/j.chom.2012.03.008

Kim, S.-W., Subhadra, B., Whang, J., Back, Y. W., Bae, H. S., Kim, H.-J., et al. (2017c). Clinical *Mycobacterium abscessus* strain inhibits autophagy flux and promotes its growth in murine macrophages. *Pathogens Dis.* 75:107. doi: 10.1093/femspd/ftx107

Kim, Y. S., Silwal, P., Kim, S. Y., Yoshimori, T., and Jo, E.-K. (2019). Autophagy-activating strategies to promote innate defense against mycobacteria. *Exp. Mole. Med.* 51, 1–10. doi: 10.1038/s12276-019-0290-7

Kimmey, J. M., Huynh, J. P., Weiss, L. A., Park, S., Kambal, A., Debnath, J., et al. (2015). Unique role for ATG5 in PMN-mediated immunopathology during M. tuberculosis infection. *Nature* 528, 565–569. doi: 10.1038/nature16451

Knodler, L. A., and Celli, J. (2011). Eating the strangers within: host control of intracellular bacteria via xenophagy. *Cell. Microb.* 13, 1319–1327. doi: 10.1111/j.1462-5822.2011.01632.x

Kontturi, A., Soini, H., Ollgren, J., and Salo, E. (2018). Increase in Childhood Nontuberculous Mycobacterial Infections After Bacille Calmette-Guérin Coverage Drop: A Nationwide, Population-Based Retrospective Study, Finland, 1995-2016. *Clin. Infect. Dis.* 67, 1256–1261. doi: 10.1093/cid/ciy241

Köster, S., Upadhyay, S., Chandra, P., Papavinasasundaram, K., Yang, G., Hassan, A., et al. (2017). *Mycobacterium tuberculosis* is protected from NADPH oxidase and LC3-associated phagocytosis by the LCP protein CpsA. *Proc. Natl. Acad. Sci.* 114, E8711–E8720. doi: 10.1073/pnas.1707792114

Kumar, R., Sahu, S. K., Kumar, M., Jana, K., Gupta, P., Gupta, U. D., et al. (2016). MicroRNA 17-5p regulates autophagy in Mycobacterium tuberculosis-infected macrophages by targeting Mcl-1 and STAT3. *Cell. Microb.* 18, 679–691. doi: 10.1111/cmi.12540

Lachmandas, E., Eckold, C., Böhme, J., Koeken, V. A. C. M., Marzuki, M. B., Blok, B., et al. (2019). Metformin Alters Human Host Responses to Mycobacterium tuberculosis in Healthy Subjects. *J. Infect. Dis.* 220, 139–150. doi: 10.1093/infdis/jiz064

Lam, K. K. Y., Zheng, X., Forestieri, R., Balgi, A. D., Nodwell, M., Vollett, S., et al. (2012). Nitazoxanide Stimulates Autophagy and Inhibits mTORC1 Signaling and Intracellular Proliferation of Mycobacterium tuberculosis. *PLoS Pathogens* 8:e1002691. doi: 10.1371/journal.ppat.1002691

Lawlor, C., O'Connor, G., O'Leary, S., Gallagher, P. J., Cryan, S.-A., Keane, J., et al. (2016). Treatment of Mycobacterium tuberculosis-Infected Macrophages with Poly(Lactic-Co-Glycolic Acid) Microparticles Drives NFκB and Autophagy Dependent Bacillary Killing. *PLoS One* 11:e0149167. doi: 10.1371/journal.pone.0149167

Lee, E. G., Boone, D. L., Chai, S., Libby, S. L., Chien, M., Lodolce, J. P., et al. (2000). Failure to Regulate TNF-Induced NF-κB and Cell Death Responses in A20-Deficient Mice. *Science* 289, 2350–2354. doi: 10.1126/science.289.5488.2350

Lee, G. J., Lee, H.-M., Kim, T. S., Kim, J. K., Sohn, K. M., and Jo, E.-K. (2016). Mycobacterium fortuitum induces A20 expression that impairs macrophage inflammatory responses. *Pathog. Dis.* 74:015. doi: 10.1093/femspd/ftw015

Lee, J., Repasy, T., Papavinasasundaram, K., Sassetti, C., and Kornfeld, H. (2011). *Mycobacterium tuberculosis* Induces an Atypical Cell Death Mode to Escape from Infected Macrophages. *PLoS One* 6:18367. doi: 10.1371/journal.pone.0018367

Lee, Y.-J., Han, S. K., Park, J. H., Lee, J. K., Kim, D. K., Chung, H. S., et al. (2018). The effect of metformin on culture conversion in tuberculosis patients with diabetes mellitus. *Korean J. Int. Med.* 33, 933–940. doi: 10.3904/kjim.2017.249

Lella, R. K., and Sharma, C. (2007). Eis (Enhanced Intracellular Survival) Protein of *Mycobacterium tuberculosis* Disturbs the Cross Regulation of T-cells. *J. Biol. Chem.* 282, 18671–18675. doi: 10.1074/jbc.C600280200

Lerena, M. C., and Colombo, M. I. (2011). *Mycobacterium marinum* induces a marked LC3 recruitment to its containing phagosome that depends on a functional ESX-1 secretion system. *Cell. Microb.* 13, 814–835. doi: 10.1111/j.1462-5822.2011.01581.x

Levine, B., Mizushima, N., and Virgin, H. W. (2011). Autophagy in immunity and inflammation. *Nature* 469, 323–335. doi: 10.1038/nature09782

Li, F., Gao, B., Xu, W., Chen, L., and Xiong, S. (2016). The Defect in Autophagy Induction by Clinical Isolates of Mycobacterium Tuberculosis Is Correlated with Poor Tuberculosis Outcomes. *PLoS One* 11:e0147810. doi: 10.1371/journal.pone.0147810

Li, M., Cui, J., Niu, W., Huang, J., Feng, T., Sun, B., et al. (2019). Long non-coding PCED1B-AS1 regulates macrophage apoptosis and autophagy by sponging miR-155 in active tuberculosis. *Biochem. Biophy. Res. Commun.* 509, 803–809. doi: 10.1016/j.bbrc.2019.01.005

Li, X., Lu, J., Xu, Y., Wang, J., Qiu, X., Fan, L., et al. (2020). Discovery of nitazoxanide-based derivatives as autophagy activators for the treatment of Alzheimer's disease. *Acta Pharmaceutica Sinica B* 10, 646–666. doi: 10.1016/j.apsb.2019.07.006

Lin, C., Tsai, S.-C., Tseng, M. T., Peng, S.-F., Kuo, S.-C., Lin, M.-W., et al. (2013). AKT serine/threonine protein kinase modulates baicalin-triggered autophagy in human bladder cancer T24 cells. *Int. J. Oncol.* 42, 993–1000. doi: 10.3892/ijo.2013.1791

Liu, F., Chen, J., Wang, P., Li, H., Zhou, Y., Liu, H., et al. (2018). MicroRNA-27a controls the intracellular survival of Mycobacterium tuberculosis by regulating calcium-associated autophagy. *Nat. Commun.* 9:4295. doi: 10.1038/s41467-018-06836-4

Liu, P. T., Stenger, S., Tang, D. H., and Modlin, R. L. (2007). Cutting Edge: Vitamin D-Mediated Human Antimicrobial Activity against *Mycobacterium tuberculosis* Is Dependent on the Induction of Cathelicidin. *J. Immunol.* 179, 2060–2063. doi: 10.4049/jimmunol.179.4.2060

Manry, J., Vincent, Q. B., Johnson, C., Chrabieh, M., Lorenzo, L., Theodorou, I., et al. (2020). Genome-wide association study of Buruli ulcer in rural Benin highlights role of two LncRNAs and the autophagy pathway. *Sci. Rep.* 3:177. doi: 10.1038/s42003-020-0920-6

Marini, E., Di Giulio, M., Ginestra, G., Magi, G., Di Lodovico, S., Marino, A., et al. (2019). Efficacy of carvacrol against resistant rapidly growing mycobacteria in the planktonic and biofilm growth mode. *PLoS One* 14:e0219038. doi: 10.1371/journal.pone.0219038

Martineau, A. R., Wilkinson, K. A., Newton, S. M., Floto, R. A., Norman, A. W., Skolimowska, K., et al. (2007). IFN-γ- and TNF-Independent Vitamin D-Inducible Human Suppression of Mycobacteria: The Role of Cathelicidin LL-37. *J. Immunol.* 178, 7190–7198. doi: 10.4049/jimmunol.178.11.7190

Marupuru, S., Senapati, P., Pathadka, S., Miraj, S. S., Unnikrishnan, M. K., and Manu, M. K. (2017). Protective effect of metformin against tuberculosis infections in diabetic patients: an observational study of south Indian tertiary healthcare facility. *Brazilian J. Infect. Dis.* 21, 312–316.

Matsunaga, K., Saitoh, T., Tabata, K., Omori, H., Satoh, T., Kurotori, N., et al. (2009). Two Beclin 1-binding proteins, Atg14L and Rubicon, reciprocally regulate autophagy at different stages. *Nat. Cell Biol.* 11, 385–396. doi: 10.1038/ncb1846

Maymone, M. B. C., Venkatesh, S., Laughter, M., Abdat, R., Hugh, J., Dacso, M. M., et al. (2020). Leprosy: Treatment and management of complications. *J. Am. Acad. Dermatol.* 83, 17–30. doi: 10.1016/j.jaad.2019.10.138

Meerak, J., Wanichwecharungruang, S. P., and Palaga, T. (2013). Enhancement of immune response to a DNA vaccine against Mycobacterium tuberculosis Ag85B by incorporation of an autophagy inducing system. *Vaccine* 31, 784–790. doi: 10.1016/j.vaccine.2012.11.075

Mishra, M., Adhyapak, P., Dadhich, R., and Kapoor, S. (2019). Dynamic Remodeling of the Host Cell Membrane by Virulent Mycobacterial Sulfoglycolipid-1. *Sci. Rep.* 9:12844.

Mizushima, N. (2010). The role of the Atg1/ULK1 complex in autophagy regulation. *Curr. Opin. Cell Biol.* 22, 132–139. doi: 10.1016/j.ceb.2009.12.004

Moore, M., and Frerichs, J. B. (1953). An Unusual Acid-Fast Infection of the Knee with Subcutaneous, Abscess-Like Lesions of the Gluteal Region: Report of a Case with a Study of the Organism, *Mycobacterium abscessus,* n. sp. *J. Investig. Dermatol.* 20, 133–169. doi: 10.1038/jid.1953.18

Münz, C. (2016). Autophagy Beyond Intracellular MHC Class II Antigen Presentation. *Trends Immunol.* 37, 755–763. doi: 10.1016/j.it.2016.08.017

N'Goma, J. C. B., Le Moigne, V., Soismier, N., Laencina, L., Le Chevalier, F., Roux, A.-L., et al. (2015). *Mycobacterium abscessus* phospholipase C expression is induced during coculture within amoebae and enhances *M. abscessus* virulence in mice. *Infect. Immun.* 83, 780–791. doi: 10.1128/IAI.02032-14

Naicker, N., Sigal, A., and Naidoo, K. (2020). Metformin as Host-Directed Therapy for TB Treatment: Scoping Review. *Front. Microb.* 11:435–435. doi: 10.3389/fmicb.2020.00435

Nath, I. (2016). IMMUNOPATHOGENESIS OF LEPROSY: A MODEL FOR T CELL ANERGY. *EMJ Dermatol.* 4, 95–101.

Nessar, R., Cambau, E., Reyrat, J. M., Murray, A., and Gicquel, B. (2012). *Mycobacterium abscessus*: a new antibiotic nightmare. *J. Antimicrob. Chemother.* 67, 810–818. doi: 10.1093/jac/dkr578

Nieuwenhuizen, N. E., Kulkarni, P. S., Shaligram, U., Cotton, M. F., Rentshce, C. A., Eisele, B., et al. (2017). The Recombinant Bacille Calmette_Guerin Vaccine BPM1002: Ready for Clinical Efficacy Testing. *Front. Immunol.* 8:1147. doi: 10.3389/fimmu.2017.01147

Nowotarska, S. W., Nowotarski, K., Grant, I. R., Elliott, C. T., Friedman, M., and Situ, C. (2017). Mechanisms of Antimicrobial Action of Cinnamon and Oregano Oils, Cinnamaldehyde, Carvacrol, 2,5-Dihydroxybenzaldehyde, and 2-Hydroxy-5-Methoxybenzaldehyde against Mycobacterium avium subsp. paratuberculosis (Map). *Foods* 6:72.

Ogawa, M., Yoshimori, T., Suzuki, T., Sagara, H., Mizushima, N., and Sasakawa, C. (2005). Escape of Intracellular *Shigella* from Autophagy. *Science* 307, 727–731. doi: 10.1126/science.1106036

Oliveira, F. M., Marinho, F. V., Oliveira, S. C., Resende, D. P., Junqueira-Kipnis, A. P., and Kipnis, A. (2020). Mycobacterium abscessus subsp. massiliense expressing bacterioferritin have improved resistance to stressful conditions. *J. Appl. Microb.* 128, 1802–1813. doi: 10.1111/jam.14585

Padmapriyadarsini, C., Bhavani, P. K., Natrajan, M., Ponnuraja, C., Kumar, H., Gomathy, S. N., et al. (2019). Evaluation of metformin in combination with rifampicin containing antituberculosis therapy in patients with new, smear-positive pulmonary tuberculosis (METRIF): study protocol for a randomised clinical trial. *BMJ Open* 9:e024363. doi: 10.1136/bmjopen-2018-024363

Pahari, S., Negi, S., Aqdas, M., Arnett, E., Schlesinger, L. S., and Agrewala, J. N. (2020). Induction of autophagy through CLEC4E in combination with TLR4: an innovative strategy to restrict the survival of *Mycobacterium tuberculosis*. *Autophagy* 16, 1021–1043. doi: 10.1080/15548627.2019.1658436

Parihar, S. P., Guler, R., Khutlang, R., Lang, D. M., Hurdayal, R., Mhlanga, M. M., et al. (2013). Statin Therapy Reduces the Mycobacterium tuberculosis Burden in Human Macrophages and in Mice by Enhancing Autophagy and Phagosome Maturation. *J. Infect. Dis.* 209, 754–763. doi: 10.1093/infdis/jit550

Parzych, K. R., and Klionsky, D. J. (2013). An Overview of Autophagy: Morphology, Mechanism, and Regulation. *Antioxidants Redox Signal.* 20, 460–473. doi: 10.1089/ars.2013.5371

Pohl, K., Grimm, X. A., Caceres, S. M., Poch, K. R., Rysavy, N., Saavedra, M., et al. (2020). *Mycobacterium abscessus* clearance by neutrophils is independent of autophagy. *Infect. Immun.* 88, e24–e20. doi: 10.1128/IAI.00024-20

Polson, H. E. J., de Lartigue, J., Rigden, D. J., Reedijk, M., Urbé, S., Clague, M. J., et al. (2010). Mammalian Atg18 (WIPI2) localizes to omegasome-anchored phagophores and positively regulates LC3 lipidation. *Autophagy* 6, 506–522. doi: 10.4161/auto.6.4.11863

Popa, C., Li, L., Gil, S., Tatjer, L., Hashii, K., Tabuchi, M., et al. (2016). The effector AWR5 from the plant pathogen Ralstonia solanacearum is an inhibitor of the TOR signalling pathway. *Sci. Rep.* 6:27058. doi: 10.1038/srep27058

Potoènjak, I., Gobin, I., and Domitroviæ, R. (2018). Carvacrol induces cytotoxicity in human cervical cancer cells but causes cisplatin resistance: Involvement of MEK–ERK activation. *Phytother. Res.* 32, 1090–1097. doi: 10.1002/ptr.6048

Prevots, D. R., Shaw, P. A., Strickland, D., Jackson, L. A., Raebel, M. A., Blosky, M. A., et al. (2010). Nontuberculous Mycobacterial Lung Disease Prevalence at Four Integrated Health Care Delivery Systems. *Am. J. Respir. Crit. Care Med.* 182, 970–976. doi: 10.1164/rccm.201002-0310OC

Ratnatunga, C. N., Lutzky, V. P., Kupz, A., Doolan, D. L., Reid, D. W., Field, M., et al. (2020). The Rise of Non-Tuberculosis Mycobacterial Lung Disease. *Front. Immunol.* 11:303. doi: 10.3389/fimmu.2020.00303

Ravindran, R., Khan, N., Nakaya, H. I., Li, S., Loebbermann, J., Maddur, M. S., et al. (2014). Vaccine Activation of the Nutrient Sensor GCN2 in Dendritic Cells Enhances Antigen Presentation. *Science* 343, 313–317. doi: 10.1126/science.1246829

Rekha, R. S., Rao Muvva, S. S. V. J., Wan, M., Raqib, R., Bergman, P., Brighenti, S., et al. (2015). Phenylbutyrate induces LL-37-dependent autophagy and intracellular killing of Mycobacterium tuberculosis in human macrophages. *Autophagy* 11, 1688–1699. doi: 10.1080/15548627.2015.1075110

Renna, M., Schaffner, C., Brown, K., Shang, S., Henao Tamayo, M., Hegyi, K., et al. (2011). Azithromycin blocks autophagy and may predispose cystic fibrosis patients to mycobacterial infection. *J. Clin. Investig.* 1219, 2554–3563. doi: 10.1172/JCI46095

Restrepo, B. I. (2016). Metformin: Candidate host-directed therapy for tuberculosis in diabetes and non-diabetes patients. *Tuberculosis* 101, S69–S72. doi: 10.1016/j.tube.2016.09.008

Rink, J., Ghigo, E., Kalaidzidis, Y., and Zerial, M. (2005). Rab Conversion as a Mechanism of Progression from Early to Late Endosomes. *Cell* 122, 735–749. doi: 10.1016/j.cell.2005.06.043

Rodrigues, L., Wagner, D., Viveiros, M., Sampaio, D., Couto, I., Vavra, M., et al. (2008). Thioridazine and chlorpromazine inhibition of ethidium bromide efflux in *Mycobacterium avium* and *Mycobacterium smegmatis*. *J. Antimicrob. Chemother.* 61, 1076–1082. doi: 10.1093/jac/dkn070

Röltgen, K., and Pluschke, G. (2015). Epidemiology and disease burden of Buruli ulcer: a review. *Res. Rep. Trop. Med.* 6, 59–73. doi: 10.2147/RRTM.S62026

Romagnoli, A., Etna, M. P., Giacomini, E., Pardini, M., Remoli, M. E., Corazzari, M., et al. (2012). ESX-1 dependent impairment of autophagic flux by *Mycobacterium tuberculosis* in human dendritic cells. *Autophagy* 8, 1357–1370. doi: 10.4161/auto.20881

Rossignol, J.-F. (1999). Method For Treatment Of Opportunistic Infections With Pharmaceutical Compositions Of Tizoxanide And Nitazoxanide. *U S Patent Appl.* 5:590.

Roux, A.-L., Viljoen, A., Bah, A., Simeone, R., Bernut, A., Laencina, L., et al. (2016). The distinct fate of smooth and rough *Mycobacterium abscessus* variants inside macrophages. *Open Biol.* 6:160185. doi: 10.1098/rsob.160185

Rudra, J. S., Khan, A., Clover, T. M., Endsley, J. J., Zloza, A., Wang, J., et al. (2017). Supramolecular Peptide Nanofibers Engage Mechanisms of Autophagy in Antigen-Presenting Cells. *ACS Omega* 2, 9136–9143. doi: 10.1021/acsomega.7b00525

Russell, D. G., Mwandumba, H. C., and Rhoades, E. E. (2002). *Mycobacterium* and the coat of many lipids. *J. Cell Biol.* 158:200205034. doi: 10.1083/jcb.200205034

SAGE Working Group of BCG Vaccines, and WHO Secretariat (2017). *Report on BCG vaccine use for protection against mycobacterial infections including tuberculosis, leprosy, and other nontuberculous mycobacteria (NTM) infections*. Thousand Oaks,CA: SAGE.

Saini, N. K., Baena, A., Ng, T. W., Venkataswamy, M. M., Kennedy, S. C., Kunnath-Velayudhan, S., et al. (2016). Suppression of autophagy and antigen presentation by Mycobacterium tuberculosis PE_PGRS47. *Nat. Microb.* 1:16133. doi: 10.1038/nmicrobiol.2016.133

Sakowski, E. T., Koster, S., Portal Celhay, C., Park, H. S., Shrestha, E., Hetzenecker, S. E., et al. (2015). Ubiquilin 1 Promotes IFN-γ-Induced Xenophagy of Mycobacterium tuberculosis. *PLoS Pathogens* 11:e1005076. doi: 10.1371/journal.ppat.1005076

Samuel, L. P., Song, C.-H., Wei, J., Roberts, E. A., Dahl, J. L., and Barry, C. E. (2007). Expression, production and release of the Eis protein by *Mycobacterium tuberculosis* during infection of macrophages and its effect on cytokine secretion. *Microbiology* 153, 529–540. doi: 10.1099/mic.0.2006/002642-0

Sanguinetti, M., Ardito, F., Fiscarelli, E., La Sorda, M., D'Argenio, P., Ricciotti, G., et al. (2001). Fatal Pulmonary Infection Due to Multidrug-Resistant *Mycobacterium abscessus* in a Patient with Cystic Fibrosis. *J. Clin. Microb.* 39, 816–819. doi: 10.1128/JCM.39.2.816-819.2001

Saqib, M., Khatri, R., Singh, B., Gupta, A., Kumar, A., and Bhaskar, S. (2016). Mycobacterium indicus pranii as a booster vaccine enhances BCG induced immunity and confers higher protection in animal models of tuberculosis. *Tuberculosis* 101, 164–173. doi: 10.1016/j.tube.2016.10.002

Sarkar, S., Davies, J. E., Huang, Z., Tunnacliffe, A., and Rubinsztein, D. C. (2007). Trehalose, a Novel mTOR-independent Autophagy Enhancer, Accelerates the Clearance of Mutant Huntingtin and α-Synuclein. *J. Biol. Chem.* 282, 5641–5652. doi: 10.1074/jbc.M609532200

Sarkar, S., Korolchuk, V. I., Renna, M., Imarisio, S., Fleming, A., Williams, A., et al. (2011). Complex Inhibitory Effects of Nitric Oxide on Autophagy. *Mole. Cell* 43, 19–32. doi: 10.1016/j.molcel.2011.04.029

Schiebler, M., Brown, K., Hegyi, K., Newton, S. M., Renna, M., Hepburn, L., et al. (2015). Functional drug screening reveals anticonvulsants as enhancers of mTOR-independent autophagic killing of *Mycobacterium tuberculosis* through inositol depletion. *EMBO Mole. Med.* 7, 127–139. doi: 10.15252/emmm.201404137

Scollard, D. M. (2020). Leprosy treatment: Can we replace opinions with research? *PLoS Neglec. Trop. Dis.* 14:e0008636. doi: 10.1371/journal.pntd.0008636

Seervi, M., Rani, A., Sharma, A. K., and Santhosh Kumar, T. R. (2018). ROS mediated ER stress induces Bax-Bak dependent and independent apoptosis in response to Thioridazine. *Biomed. Pharmacother.* 106, 200–209. doi: 10.1016/j.biopha.2018.06.123

Seto, S., Tsujimura, K., and Koide, Y. (2012). Coronin-1a inhibits autophagosome formation around Mycobacterium tuberculosis-containing phagosomes and assists mycobacterial survival in macrophages. *Cell. Microb.* 14, 710–727. doi: 10.1111/j.1462-5822.2012.01754.x

Sharma, S. K., Katoch, K., Sarin, R., Balambal, R., Kumar Jain, N., Patel, N., et al. (2017). Efficacy and Safety of Mycobacterium indicus pranii as an adjunct therapy in Category II pulmonary tuberculosis in a randomized trial. *Sci. Rep.* 7:3354. doi: 10.1038/s41598-017-03514-1

Sharma, V., Makhdoomi, M., Singh, L., Kumar, P., Khan, N., Singh, S., et al. (2020). Trehalose limits opportunistic mycobacterial survival during HIV co-infection by reversing HIV-mediated autophagy block. *Autophagy* 2020, 1–20. doi: 10.1080/15548627.2020.1725374

Shin, D.-M., Jeon, B.-Y., Lee, H.-M., Jin, H. S., Yuk, J.-M., Song, C.-H., et al. (2010). *Mycobacterium tuberculosis* Eis Regulates Autophagy, Inflammation, and Cell Death through Redox-dependent Signaling. *PLoS Pathogens* 6:e1001230. doi: 10.1371/journal.ppat.1001230

Shin, J. H., Park, S. J., Jo, Y. K., Kim, E. S., Kang, H., Park, J. H., et al. (2012). Suppression of autophagy exacerbates Mefloquine-mediated cell death. *Neurosci. Lett.* 515, 162–167. doi: 10.1016/j.neulet.2012.03.040

Shoen, C., Benaroch, D., Sklaney, M., and Cynamon, M. (2019). *In Vitro* Activities of Omadacycline against Rapidly Growing Mycobacteria. *Antimicrob. Agents Chemother.* 63, e2522–e2518. doi: 10.1128/aac.02522-18

Shui, W., Petzold, C. J., Redding, A., Liu, J., Pitcher, A., Sheu, L., et al. (2011). Organelle Membrane Proteomics Reveals Differential Influence of Mycobacterial Lipoglycans on Macrophage Phagosome Maturation and Autophagosome Accumulation. *J. Prot. Res.* 10, 339–348. doi: 10.1021/pr100688h

Sieling, P. A., and Modlin, R. L. (1994). Cytokine Patterns at the Site of Mycobacterial Infection. *Immunobiology* 191, 378–387. doi: 10.1016/S0171-2985(11)80443-2

Silva, B. J. D. A., Barbosa, M. G. D. M., Andrade, P. R., Ferreira, H., Nery, J. A. D. C., Côrte-Real, S., et al. (2017a). Autophagy Is an Innate Mechanism Associated with Leprosy Polarization. *PLoS Pathogens* 13:e1006103. doi: 10.1371/journal.ppat.1006103

Silva, T., Moreira, A. C., Nazmi, K., Moniz, T., Vale, N., Rangel, M., et al. (2017b). Lactoferricin Peptides Increase Macrophages' Capacity To *Mycobacterium avium*. *mSphere* 2, e00301–e00317. doi: 10.1128/mSphere.00301-17

Simpson, H., Deribe, K., Tabah, E. N., Peters, A., Maman, I., Frimpong, M., et al. (2019). Mapping the global distribution of Buruli ulcer: a systematic review with evidence consensus. *Lancet. Glob. Health* 7, e912–e922. doi: 10.1016/S2214-109X(19)30171-8

Singh, B., Saqib, M., Chakraborty, A., and Bhaskar, S. (2019). Lipoarabinomannan from Mycobacterium indicus pranii shows immunostimulatory activity and induces autophagy in macrophages. *PLoS One* 14:224239. doi: 10.1371/journal.pone.0224239

Singh, B., Saqib, M., Gupta, A., Kumar, P., and Bhaskar, S. (2017). Autophagy induction by Mycobacterium indicus pranii promotes Mycobacterium tuberculosis clearance from RAW 264.7 macrophages. *PLoS One* 12:189606. doi: 10.1371/journal.pone.0189606

Singh, C. R., Moulton, R. A., Armitige, L. Y., Bidani, A., Snuggs, M., Dhandayuthapani, S., et al. (2006). Processing and Presentation of a Mycobacterial Antigen 85B Epitope by Murine Macrophages Is Dependent on the Phagosomal Acquisition of Vacuolar Proton ATPase and In Situ Activation of Cathepsin D. *J. Immunol.* 177, 3250–3259. doi: 10.4049/jimmunol.177.5.3250

Singh, K., Sun, S., and Vĕzina, C. (1979). Rapamycin (Ay-22, 989), A New Antifungal Antibiotic. *J. Antibiot.* 32:630. doi: 10.7164/antibiotics.32.630

Singh, V. K., Berry, L., Bernut, A., Singh, S., Carrère-Kremer, S., Viljoen, A., et al. (2016). A unique PE_PGRS protein inhibiting host cell cytosolic defenses and sustaining full virulence of *Mycobacterium marinum* in multiple hosts. *Cell. Microb.* 18, 1489–1507. doi: 10.1111/cmi.12606

Singhal, A., Jie, L., Kumar, P., Hong, G. S., Leow, M. K.-S., Paleja, B., et al. (2014). Metformin as adjunct antituberculosis therapy. *Sci. Trans. Med.* 6, ra159–ra263. doi: 10.1126/scitranslmed.3009885

Sogi, K. M., Lien, K. A., Johnson, J. R., Krogan, N. J., and Stanley, S. A. (2017). The Tyrosine Kinase Inhibitor Gefitinib Restricts Mycobacterium tuberculosis Growth through Increased Lysosomal Biogenesis and Modulation of Cytokine Signaling. *ACS Infect. Dis.* 3, 564–574. doi: 10.1021/acsinfecdis.7b00046

Spalletta, S., Flati, V., Toniato, E., Di Gregorio, J., Marino, A., Pierdomenico, L., et al. (2018). Carvacrol reduces adipogenic differentiation by modulating autophagy and ChREBP expression. *PLoS One* 13:e0206894. doi: 10.1371/journal.pone.0206894

Stanley, S. A., Barczak, A. K., Silvis, M. R., Luo, S. S., Sogi, K., Vokes, M., et al. (2014). Identification of Host-Targeted Small Molecules That Restrict Intracellular Mycobacterium tuberculosis Growth. *PLoS Pathogens* 10:e1003946. doi: 10.1371/journal.ppat.1003946

Strong, E. J., Jurcic Smith, K. L., Saini, N. K., Ng, T. W., Porcelli, S. A., and Lee, S. (2020). Identification of Autophagy-Inhibiting Factors of *Mycobacterium tuberculosis* by High-Throughput Loss-of-Function Screening. *Infect. Immun.* 88, e269–e220. doi: 10.1128/iai.00269-20

Sundaramurthy, V., Barsacchi, R., Samusik, N., Marsico, G., Gilleron, J., Kalaidzidis, I., et al. (2013). Integration of Chemical and RNAi Multiparametric Profiles Identifies Triggers of Intracellular Mycobacterial Killing. *Cell Host Microb.* 13, 129–142. doi: 10.1016/j.chom.2013.01.008

Svenning, S., and Johansen, T. (2013). Selective autophagy. *Essays Biochem.* 55, 79–92. doi: 10.1042/BSE0550079

Tao, S., and Drexler, I. (2020). Targeting Autophagy in Innate Immune Cells: Angel or Demon During Infection and Vaccination? *Front. Immunol.* 11:460. doi: 10.3389/fimmu.2020.00460

Thurston, T. L., Ryzhakov, G., Bloor, S., von Muhlinen, N., and Randow, F. (2009). The TBK1 adaptor and autophagy receptor NDP52 restricts the proliferation of ubiquitin-coated bacteria. *Nat. Immunol.* 10, 1215–1221. doi: 10.1038/ni.1800

Torfs, E., Piller, T., Cos, P., and Cappoen, D. (2019). Opportunities for Overcoming Mycobacterium tuberculosis Drug Resistance: Emerging Mycobacterial Targets and Host-Directed Therapy. *Int. J. Mole. Sci.* 20:2868.

Tortoli, E. (2009). Clinical manifestations of nontuberculous mycobacteria infections. *Clin. Microb. Infect.* 15, 906–910. doi: 10.1111/j.1469-0691.2009.03014.x

Tseng, C.-H. (2018). Metformin Decreases Risk of Tuberculosis Infection in Type 2 Diabetes Patients. *J. Clin. Med.* 7:264.

Uaska Sartori, Priscila, V., Penna, G. O., Bührer-Sékula, S., Pontes Maria, A. A., Gonçalves, H. S., et al. (2020). Human Genetic Susceptibility of Leprosy Recurrence. *Sci. Rep.* 10:1284. doi: 10.1038/s41598-020-58079-3

Ustianowski, A., Shaffer, R., Collin, S., Wilkinson, R. J., and Davidson, R. N. (2005). Prevalence and associations of vitamin D deficiency in foreign-born persons with tuberculosis in London. *J. Infect.* 50, 432–437. doi: 10.1016/j.jinf.2004.07.006

Via, L. E., Deretic, D., Ulmer, R. J., Hibler, N. S., Huber, L. A., and Deretic, V. (1997). Arrest of Mycobacterial Phagosome Maturation Is Caused by a Block in Vesicle Fusion between Stages Controlled by rab5 and rab7. *J. Biol. Chem.* 272, 13326–13331. doi: 10.1074/jbc.272.20.13326

Wang, J., Yang, K., Zhou, L., MinhaoWu, Wu, Y., Zhu, M., et al. (2013). MicroRNA-155 Promotes Autophagy to Eliminate Intracellular Mycobacteria by Targeting Rheb. *PLoS Pathogens* 9:e1003697. doi: 10.1371/journal.ppat.1003697

Watson, R. O., Manzanillo, P. S., and Cox, J. S. (2012). Extracellular M. tuberculosis DNA Targets Bacteria for Autophagy by Activating the Host DNA-Sensing Pathway. *Cell* 150, 803–816. doi: 10.1016/j.cell.2012.06.040

Watson, Robert, O., Bell, Samantha, L., MacDuff, Donna, A., et al. (2015). The Cytosolic Sensor cGAS Detects Mycobacterium tuberculosis DNA to Induce Type I Interferons and Activate Autophagy. *Cell Host Microb.* 17, 811–819. doi: 10.1016/j.chom.2015.05.004

Wei, J., Dahl, J. L., Moulder, J. W., Roberts, E. A., O'Gaora, P., Young, D. B., et al. (2000). Identification of a *Mycobacterium tuberculosis* Gene That Enhances Mycobacterial Survival in Macrophages. *J. Bacteriol.* 182, 377–384. doi: 10.1128/JB.182.2.377-384.2000

Wild, P., Farhan, H., McEwan, D. G., Wagner, S., Rogov, V. V., Brady, N. R., et al. (2011). Phosphorylation of the Autophagy Receptor Optineurin Restricts *Salmonella* Growth. *Science* 333, 228–233. doi: 10.1126/science.1205405

Williams, A., Sarkar, S., Cuddon, P., Ttofi, E. K., Saiki, S., Siddiqi, F. H., et al. (2008). Novel targets for Huntington's disease in an mTOR-independent autophagy pathway. *Nat. Chem. Biol.* 4, 295–305. doi: 10.1038/nchembio.79

World Health Organisation (2019). *Buruli ulcer (Mycobacterium ulcerans infection)* [Online]. Geneva: World Health Organisation.

World Health Organisation (2020). *Global tuberculosis report 2019*. Geneva: World Health Organisation.

World Health Organization (2016). Global leprosy update, 2015: time for action, accountability and inclusion. *Weekly Epidemiolog. Rec.* 91, 405–416.

Xu, X., Araki, K., Li, S., Han, J.-H., Ye, L., Tan, W. G., et al. (2014). Autophagy is essential for effector CD8+ T cell survival and memory formation. *Nat. Immunol.* 15, 1152–1161. doi: 10.1038/ni.3025

Xu, Y., Fattah, E. A., Liu, X.-D., Jagannath, C., and Eissa, N. T. (2013). Harnessing of TLR-mediated autophagy to combat mycobacteria in macrophages. *Tuberculosis* 93, S33–S37. doi: 10.1016/S1472-9792(13)70008-8

Xu, Y., Jagannath, C., Liu, X.-D., Sharafkhaneh, A., Kolodziejska, K. E., and Eissa, N. T. (2007). Toll-like Receptor 4 Is a Sensor for Autophagy Associated with Innate Immunity. *Immunity* 27, 135–144. doi: 10.1016/j.immuni.2007.05.022

Yamamura, M. (1992). Defining protective responses to pathogens: cytokine profiles in leprosy lesions. *Science* 255, 12–12. doi: 10.1126/science.1553522

Yang, D., Chen, J., Shi, C., Jing, Z., and Song, N. (2014). Autophagy gene polymorphism is associated with susceptibility to leprosy by affecting inflammatory cytokines. *Inflammation* 37, 593–598. doi: 10.1007/s10753-013-9773-1

Yew, W.-W., Chan, D. P., Chang, K.-C., and Zhang, Y. (2020). How does metformin act as a host-directed agent in tuberculosis associated with diabetes mellitus? *J. Thorac. Dis.* 12, 1124–1126. doi: 10.21037/jtd.2020.01.30

Yotsu, R. R., Richardson, M., and Ishii, N. (2018). Drugs for treating Buruli ulcer (*Mycobacterium ulcerans* disease). *Cochrane Database Syst. Rev.* 8:CD012118. doi: 10.1002/14651858.cd012118.pub2

Yu, L., Chen, Y., and Tooze, S. A. (2018). Autophagy pathway: Cellular and molecular mechanisms. *Autophagy* 14, 207–215. doi: 10.1080/15548627.2017.1378838

Yuk, J.-M., and Jo, E.-K. (2014). Host immune responses to mycobacterial antigens and their implications for the development of a vaccine to control tuberculosis. *cevr* 3, 155–167. doi: 10.7774/cevr.2014.3.2.155

Yuk, J.-M., Shin, D.-M., Lee, H.-M., Yang, C.-S., Jin, H. S., Kim, K.-K., et al. (2009). Vitamin D3 Induces Autophagy in Human Monocytes/Macrophages via Cathelicidin. *Cell Host Microb.* 6, 231–243. doi: 10.1016/j.chom.2009.08.004

Zhang, J., Chen, C., and Yang, J. (2019). Effectiveness of vitamin D supplementation on the outcome of pulmonary tuberculosis treatment in adults: a meta-analysis of randomized controlled trials. *Chin. Med. J.* 132, 2950–2959. doi: 10.1097/CM9.0000000000000554

Zhang, Q., Sun, J., Wang, Y., He, W., Wang, L., Zheng, Y., et al. (2017). Antimycobacterial and Anti-inflammatory Mechanisms of Baicalin via Induced Autophagy in Macrophages Infected with Mycobacterium tuberculosis. *Front. Microb.* 8:2142. doi: 10.3389/fmicb.2017.02142

Zheng, Y. T., Shahnazari, S., Brech, A., Lamark, T., Johansen, T., and Brumell, J. H. (2009). The Adaptor Protein p62/SQSTM1 Targets Invading Bacteria to the Autophagy Pathway. *J. Immunol.* 183, 5909–5916. doi: 10.4049/jimmunol.0900441

Zullo, A. J., and Lee, S. (2012a). Mycobacterial induction of autophagy varies by species and occurs independently of mammalian target of rapamycin inhibition. *J. Biol. Chem.* 287:32013. doi: 10.1074/jbc.M111.32013

Zullo, A. J., and Lee, S. (2012b). Old Antibiotics Target TB with a New Trick. *Cell Host Microb.* 11, 419–420. doi: 10.1016/j.chom.2012.05.002

Zullo, A. J., Jurcic Smith, K. L., and Lee, S. (2014). Mammalian target of Rapamycin inhibition and mycobacterial survival are uncoupled in murine macrophages. *BMC Biochem.* 15:4. doi: 10.1186/1471-2091-15-4

Conflict of Interest: The authors declare that the research was conducted in the absence of any commercial or financial relationships that could be construed as a potential conflict of interest.

frontiers in Immunology

ORIGINAL RESEARCH
published: 18 March 2021
doi: 10.3389/fimmu.2021.662987

PKCα Is Recruited to *Staphylococcus aureus*-Containing Phagosomes and Impairs Bacterial Replication by Inhibition of Autophagy

Maria Celeste Gauron[1,2], *Alexandra C. Newton*[2] *and María Isabel Colombo*[1]*

[1] *Laboratorio de Mecanismos Moleculares Implicados en el Tráfico Vesicular y la Autofagia-Instituto de Histología y Embriología (IHEM)- Universidad Nacional de Cuyo, CONICET- Facultad de Ciencias Médicas, Mendoza, Argentina,*
[2] *Department of Pharmacology, University of California San Diego, La Jolla, CA, United States*

Hijacking the autophagic machinery is a key mechanism through which invasive pathogens such as *Staphylococcus aureus* replicate in their host cells. We have previously demonstrated that the bacteria replicate in phagosomes labeled with the autophagic protein LC3, before escaping to the cytoplasm. Here, we show that the Ca^{2+}-dependent PKCα binds to *S. aureus*-containing phagosomes and that α-hemolysin, secreted by *S. aureus*, promotes this recruitment of PKCα to phagosomal membranes. Interestingly, the presence of PKCα prevents the association of the autophagic protein LC3. Live cell imaging experiments using the PKC activity reporter CKAR reveal that treatment of cells with *S. aureus* culture supernatants containing staphylococcal secreted factors transiently activates PKC. Functional studies reveal that overexpression of PKCα causes a marked inhibition of bacterial replication. Taken together, our data identify enhancing PKCα activity as a potential approach to inhibit *S. aureus* replication in mammalian cells.

Keywords: ***Staphylococcus aureus*, autophagy, xenophagy, Protein Kinase C, LC3**

OPEN ACCESS

Edited by:
Jere W. McBride, University of Texas Medical Branch at Galveston, United States

Reviewed by:
Marisa Mariel Fernandez, Institute of Studies on Humoral Immunity (IDEHU), Argentina
Eden Ramalho Ferreira, Federal University of São Paulo, Brazil

***Correspondence:**
María Isabel Colombo
mcolombo@fcm.uncu.edu.ar

Specialty section:
This article was submitted to Microbial Immunology, a section of the journal Frontiers in Immunology

Received: *02 February 2021*
Accepted: *03 March 2021*
Published: *18 March 2021*

Citation:
Gauron MC, Newton AC and Colombo MI (2021) PKCα Is Recruited to Staphylococcus aureus-Containing Phagosomes and Impairs Bacterial Replication by Inhibition of Autophagy. Front. Immunol. 12:662987. doi: 10.3389/fimmu.2021.662987

INTRODUCTION

Autophagy is a cellular degradative process that not only plays an essential role in cellular homeostasis, but also in clearing infection by certain pathogens, a process known as xenophagy. Specifically, xenophagy is a selective defense mechanism by which, once microorganisms are recognized by the cell, proteins known as autophagic adaptors/receptors recruit LC3 and components of the autophagic machinery toward them (1–4). Pathogens sequestered in the interior of autophagosomes are degraded by the fusion of these vacuoles with lysosomes. Many invasive bacterial pathogens, including species of *Salmonella, Shigella* and *Mycobacterium*, induce an autophagic response in host cells, which leads to the degradation of these pathogens or partial restriction of their intracellular growth (5–7). However, the generated autophagic response is occasionally unsuccessful, as some microorganisms are able to manipulate this pathway for their own benefit in order to survive and replicate in the host cells (8). A clear example of this behavior is *Staphylococcus aureus*, a major hospital- and community-acquired pathogen associated with significant mortality (9). Understanding the mechanism by which *S. aureus* evades xenophagy

has important therapeutic potential, particularly given the appearance of strains that manifest antibiotic resistance (10).

S. aureus exerts its effects both by the release of toxins and enzymes secreted by the bacterium, and by efficiently invading epithelial and endothelial cells (11–13). Once in the interior of the cells, *S. aureus* transits the phagosomal pathway, avoiding lysosomal degradation, to finally escape from phagosomes *via* a toxin-dependent mechanism to further replicate in the cytoplasm of the host cells (14, 15). It has been previously demonstrated that the *S. aureus*-containing phagosome is clearly marked by the autophagic protein LC3 (16). We have previously shown that, although *S. aureus* can localize into autophagosomes, their maturation is blocked and the fusion with lysosomes is inhibited, allowing bacterial replication inside this vacuole (16). Indeed, these *S. aureus*-containing compartments were also identified as autophagosomes by electron microscopy, due to their characteristic double membranes (17). Finally, *S. aureus* escapes from the autophagosomes and once in the cytoplasm, the bacterium induces apoptosis through a caspase-independent mechanism which allows the infection to spread (17).

S. aureus infection is accompanied by changes in the intracellular levels of second messengers. For example, it has been reported that when this pathogen invades cells, cAMP levels are decreased (18), leading to reduced activation of the protein Epac, in turn causing, higher levels of autophagy which are beneficial for the staphylococcal infection (19). On the other hand, it has also been reported that *S. aureus* invasion increases intracellular Ca^{2+} levels (20), suggesting that transducers of Ca^{2+} signals might also be involved in the regulation of *S. aureus*-induced autophagy.

A key transducer of Ca^{2+} signals is the subfamily of conventional isozymes of the Protein Kinase C (PKC) family of Ser/Thr kinases. PKC isozymes are involved in transduction of a wide range of extracellular signals that control important cellular functions, including the autophagic response (21). Conventional (PKCα, PKCβ and PKCγ) and novel (PKCδ, PKCε, PKCη and PKCθ) PKC family members are activated following receptor-mediated generation of diacylglycerol (DAG), which binds to their diacylglycerol-sensing C1 domains (22). Whereas novel PKC isozymes are activated by DAG alone, the conventional PKC isozymes have a lower affinity for DAG and require Ca^{2+}-dependent targeting to membranes *via* their Ca^{2+}-sensing C2 domain (22). It has been described that novel PKC isozymes participate both in xenophagy and in host cell responses against bacterial infection. For example, PKCε is implicated in innate immunity due to its role in the activation of macrophages in defense against *S. aureus* and *E. coli* infection (23). Also, it has been shown that both DAG and PKCδ have a role in the autophagy of *Salmonella typhimurium* (24). As for Ca^{2+}-regulated conventional PKCs, PKCα impairs intracellular replication of *Legionella pneumophila* in macrophages (25), in addition, PKCα has been shown to be important in phagosomal maturation of latex beads phagosomes (26). However, the role of conventional PKC isozymes in xenophagy remains to be elucidated.

In the present report we have determined that DAG is present in the membranes of phagosomes containing *S. aureus* and that a conventional PKC isozyme, PKCα, is able to associate with these compartments in an α-hemolysin dependent manner. We have determined that the presence of PKCα in the *S. aureus* phagosome depends on Ca^{2+} concentration but is independent of the presence of DAG on the phagosomal membranes. Interestingly, in those phagosomes labelled by PKCα, the recruitment of the autophagic protein LC3 was hampered, indicating that the association of both proteins with the phagosomal membrane was mutually exclusive. In addition, we have found that overexpression of PKCα impaired the efficient intracellular replication of the bacteria. In summary, we present evidence that PKCα modulates the autophagic response induced by *S. aureus* in epithelial cells.

MATERIALS AND METHODS

Materials

Cell culture media α-MEM was purchased from Gibco (Invitrogen, Argentina) and fetal bovine serum (FBS) (A15-101) was obtained from GE Healthcare Argentina S.A. Luria-Bertani (LB) broth and agar (Miller) were purchased from Merck (Merck S.A., Buenos Aires, Argentina). Chloramphenicol, gentamycin, U73122, 1-Butanol, Gö6976, PDBu (Phorbol 12,13-dibutirate) and *Staphylococcus aureus* α-hemolysin (H9395) were obtained from Sigma Aldrich. DNA markers Hoechst 33342 and Topro were from Molecular Probes (Buenos Aires, Argentina).

Cell Culture

Adherent epithelial CHO-K1 (Chinese Hamster Ovary) cells from ATCC were cultured in α-MEM supplemented with 10% of FBS, streptomycin (50μg/ml) and penicillin (50 U/ml).

Plasmids and Transfection

GFP-PKCα, GFP-PKCβII, GFP-PKCγ, and GFP-PKCη were provided by Dr. Yusuf Hannun (Medical University of South Carolina, USA), GFP-PKCδ and GFP-PKCε were a gift from Dr. Dominique Joubert (Universtités Montpellier, Francia). PKCδ-C1-GFP was kindly provided by Dr. Mauricio Terebiznik (University of Toronto, Canada). Cells were transfected with Lipofectamine 3000, Lipofectamine 2000 or JetPrime, following the manufacturer's instructions.

Bacteria Strains, Culture, and Infection

S. aureus wild type, wt (8325–4), the mutant deficient for α-hemolysin: Hla (–) (DU1090) or the mutant Hla (–) complemented with an α-hemolysin plasmid (DU1090/pDU1212): Hla (–)+pHla were used. All strains were kindly provided by Dr. Claudia Sola (CBICI-CONICET, Córdoba, Argentina) and built by Dr. Richard J. O'Callaghan. Bacterial strains were cultured overnight at 37°C in 10 ml of a LB broth with the proper antibiotics for strain selection: streptomycin for the selection of the plasmid DU1090 and chloramphenicol for

the selection of the plasmid pDU1212. For infection experiments, cells were resuspended in infection media (α-MEM supplemented with 10% FBS) to an OD=650 nm of 0.4 (~4x108 CFU) and diluted to a 10:1 multiplicity of infection (MOI). 1 hour post infection, the media was washed to eliminate extracellular bacteria and fresh infection media was added. Afterward, cells were incubated for an additional 3 hours at 37°C, washed with PBS, fixed with 4% paraformaldehyde, and processed for analysis by confocal microscopy.

Confocal Microscopy and Image Processing

Cells were analyzed with the microscope Olympus Confocal FV1000. The program FV10-ASW 3.0 was used for image acquisition and imaging configuration. The obtained images were processed by the deconvolution tool in ImageJ.

Real-Time Kinase Activity Monitoring

CHO-K1 cells co-transfected with mCherry-PKCα and CKAR2 (C Kinase Activity Reporter) were maintained in HBSS solution (ThermoFischer) during the experiment. 1 ml of LB broth was added to settle a baseline. After 5 minutes *S. aureus* culture supernatants were added and, after 10 minutes, 1 μM of the PKC inhibitor Gö6976 was added. To study the effect of α-hemolysin, 10 μg/ml or 30 μg/ml of pure protein was added to the cells, followed by 200 nM of the PKC activator PDBu and finally 1 μM Gö6976. Images were acquired using the microscope Zeiss Axiovert (CarlZeiss Microimaging, Inc.) with the digital camera MicroMax (Roper-Princeton Instruments) controlled by the software Metafluor (Universal Imaging, Corp.). FRET (Föster Resonance Energy Transfer) and CFP (Cyan Fluorescent Protein) were obtained every 25 seconds. YFP (Yellow Fluorescent Protein) and mCherry emissions were also obtained as transfection controls.

SDS-PAGE and Western Blot

CHO-K1 cells were treated as indicated and lysed with RIPA Buffer (150 mM NaCl, 1% Triton x-100, 50 mM Tris pH 7.5, 1% Sodium Deoxycholate, 0.1% SDS, 2 mM EDTA, 50 mM NaF). Bradford assays were performed to determine the protein concentration in the obtained samples. Samples were run in polyacrylamide gels and transferred to PVDF membranes (BioRad). Membranes were blocked during 30 minutes with a blocking solution (10% BSA, 0.05% Tween 20 in PBS) and washed twice with 0.05% Tween 20 in PBS. Afterward, they were incubated with specific antibodies diluted in 0.05% Tween 20 in PBS Tween: 1 μg/ml rabbit polyclonal anti-LC3 (Sigma-Aldrich), or 0.1 μg/ml rabbit monoclonal anti-actin (Developmental Studies Hybridoma Bank, University of Iowa, USA) overnight at 4°C. Membranes were incubated with secondary antibodies conjugated with peroxidase (Sigma-Aldrich). Detection of immunoreactive bands was performed by chemiluminescence in a FluorChem Q imaging system (Protein Simple).

Colony Forming Units (CFU) Assay

CHO-K1 cells were transfected with GFP empty vector (GFPv) or GFP-PKCα. Cells were subsequently infected for 2, 3 or 4 h with *S. aureus* wt. At 1 hour post infection (h.p.i.), cells were washed 3 times with 1X PBS, and incubated with gentamycin (100 μg/ml) for 30 minutes to eliminate all extracellular bacteria. After the infection period, cells were washed 3 times with 1X PBS, and once with HBSS. Afterward, cells were lysed with sterile distilled water for 10 minutes at room temperature. Cells were collected using a scraper, and lysates were diluted in 1X PBS, cultured in Brain Heart Infusion agar and incubated for 12 hours at 37°C. Colonies were counted in plates which showed between 50-100 visible colonies.

Statistical Analysis

All the data are shown as the mean ± standard error of the mean (SEM) and analyzed with GraphPad Prism version 5.01 (GraphPad Software Inc.) using the Student's t test. Figures shown are representative of ≥3 experiments.

RESULTS

Diacylglycerol Is Present in the *S. aureus*-Containing Phagosomes

Since DAG is required for activation of most members of the PKC family, we first asked whether the surface of the phagosomal membrane was conducive to PKC activation by assessing whether DAG was located in the *S. aureus* phagosomal membrane. CHO cells were transfected with the DAG sensor, PKCδ-C1-GFP, which consists of the C1 domain of PKCδ fused to green fluorescent protein (GFP). Cells were infected with *S. aureus* wild type (wt, labeled with Topro, shown in blue) and at 4 h.p.i. were fixed and processed for analysis by confocal microscopy. As depicted in **Figure 1**, DAG was clearly present in approximately 40% of the phagosomal membranes containing *S. aureus* (**Figures 1A, B** and **Supplementary Figure 1A**).

Because it has been shown that internalized *S. aureus* resides in autophagosomes (17), we next asked whether DAG was also present in these autophagosomal membranes. For this purpose, CHO cells were cotransfected with the DAG sensor and the autophagic protein LC3 tagged with red fluorescent protein (RFP-LC3). Following infection with *S. aureus* wt, examination by confocal microscopy revealed that approximately 40% of the *S. aureus*-containing autophagosomes, characterized by the presence of LC3 in their membranes, were also labelled with the DAG probe (**Figures 1C, D** and **Supplementary Figure 1B**). These results demonstrate that the second messenger DAG is part of the vacuolar membranes where *S. aureus* resides.

PKCα Is Recruited to the *S. aureus*-Containing Phagosome

We next assessed whether the DAG-dependent PKC isozymes (conventional and novel family members) associated with phagosomes harboring *S. aureus*. For this purpose, CHO cells were transfected with the conventional PKC isozymes GFP-PKCα, GFP-PKCβII or GFP-PKCγ (**Figure 2A**), or with the novel PKC isozymes GFP-PKCδ, GFP-PKCε or GFP-PKCη (**Figure 2B**). Cells were infected with *S. aureus* wt and, at

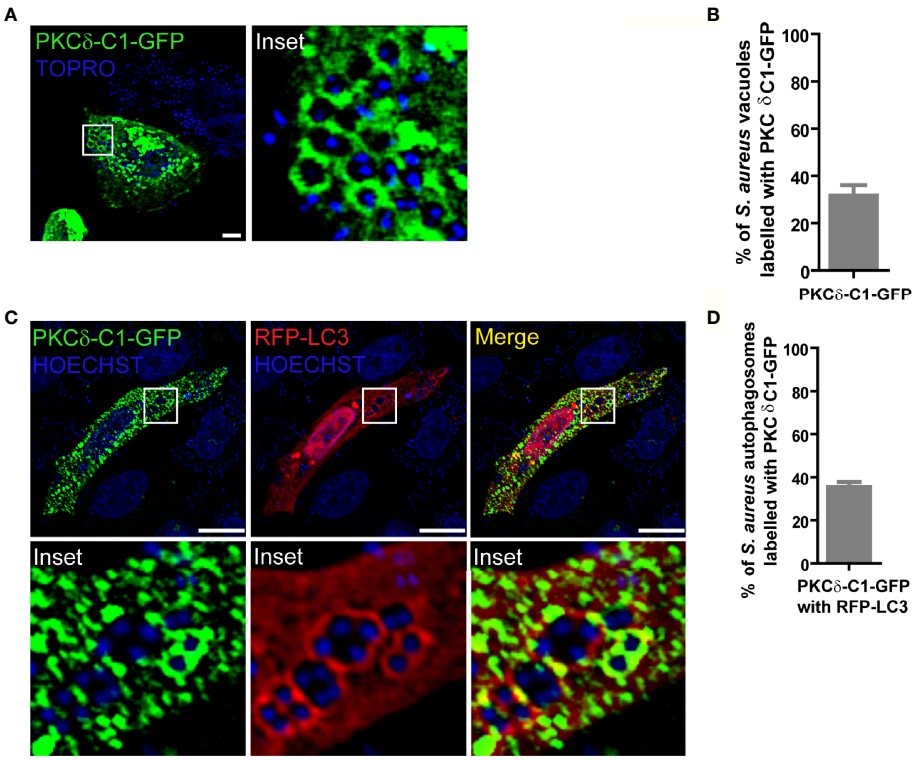

FIGURE 1 | DAG is present in the *S. aureus* phagosomal membranes. **(A)** Confocal microscopy images of CHO cells overexpressing PKCδ-C1-GFP. Cells were infected with *S. aureus* wt for 4 hours as indicated under Material and Methods. Bacteria were labelled with Topro (shown in blue). Images are representative of three independent experiments. Bar: 10 µm. **(B)** Quantification of *S. aureus* vacuoles labelled with PKCδ-C1-GFP. Data are the mean ± SEM of three independent experiments. **(C)** Confocal microscopy images of CHO cells overexpressing PKCδ-C1-GFP together with RFP-LC3 and infected with *S. aureus* wt for 4 hours. Bacteria were labelled with Hoechst (shown in blue). Bar: 10 µm. Images are representative of three independent experiments. **(D)** Quantification of *S. aureus* vacuoles labelled with PKCδ-C1-GFP and RFP-LC3. Data are the mean ± SEM of three independent experiments.

4 h.p.i., were analyzed by confocal microscopy. As shown in **Figure 2** (**Supplementary Figure 2A**), we observed that only the conventional isozyme PKCα was clearly recruited to the *S. aureus*-containing phagosomes. To confirm that the recruitment of the kinase was in fact to the phagosomal membranes containing *S. aureus*, GFP-PKCα was cotransfected with RFP-LAMP1, a late endosome marker, which has been proven to be present in the phagosomal membranes containing *S. aureus* (14). Cells were infected with *S. aureus* wt and at 4 h.p.i., confocal microscopy analysis showed that PKCα colocalized with LAMP1 at the membranes of phagosomes containing *S. aureus* (**Supplementary Figures 2B** and **2C**).

PKCα Recruitment to *S. aureus* Phagosomes Does Not Depend on DAG

To assess whether the DAG present in *S. aureus* phagosomal membranes was necessary to anchor PKCα to these compartments, we examined the effect of DAG synthesis inhibition on PKCα localization to the *S. aureus* phagosomal membranes. CHO cells were transfected with PKCδ-C1-GFP and subsequently treated with inhibitors of DAG synthesis. First, the enzyme phospholipase C (PLC) which generates DAG by the hydrolysis of PIP_2 (27) was inhibited using U73122. Treatment of *S. aureus* infected cells with the inhibitor U73122 had no significant effect on the amount of DAG present in the *S. aureus* phagosomal membranes (**Figures 3A, B**). Second, cells were treated with 1-butanol to inhibit phospholipase D (PLD). This enzyme catalyzes the hydrolysis of phosphatidylcholine to produce phosphatidic acid which is, in turn, converted into DAG by the action of the phosphatidic acid phosphatase (27). In contrast to the PLC inhibitor, treatment of *S. aureus*-infected cells with the PLD inhibitor caused a decrease in the amount of DAG present in phagosomal membranes (**Figures 3A, B**). These data revealed that PLD was the major pathway responsible for the production of DAG in the *S. aureus*-containing phagosomes.

Once we determined that the inhibition of PLD caused a marked decrease in the presence of DAG in the phagosomal membranes, we asked whether suppressing PLD activity altered the recruitment of PKCα. CHO cells were transiently transfected with GFP-PKCα, treated with either the PLC or PLD inhibitors, and infected with *S. aureus* wt. After 4 h.p.i., cells were fixed and analyzed by confocal microscopy. Surprisingly, as shown in **Figures 3C, D**, there was no change in the presence of the kinase at the *S. aureus*-containing phagosomes. Thus, we

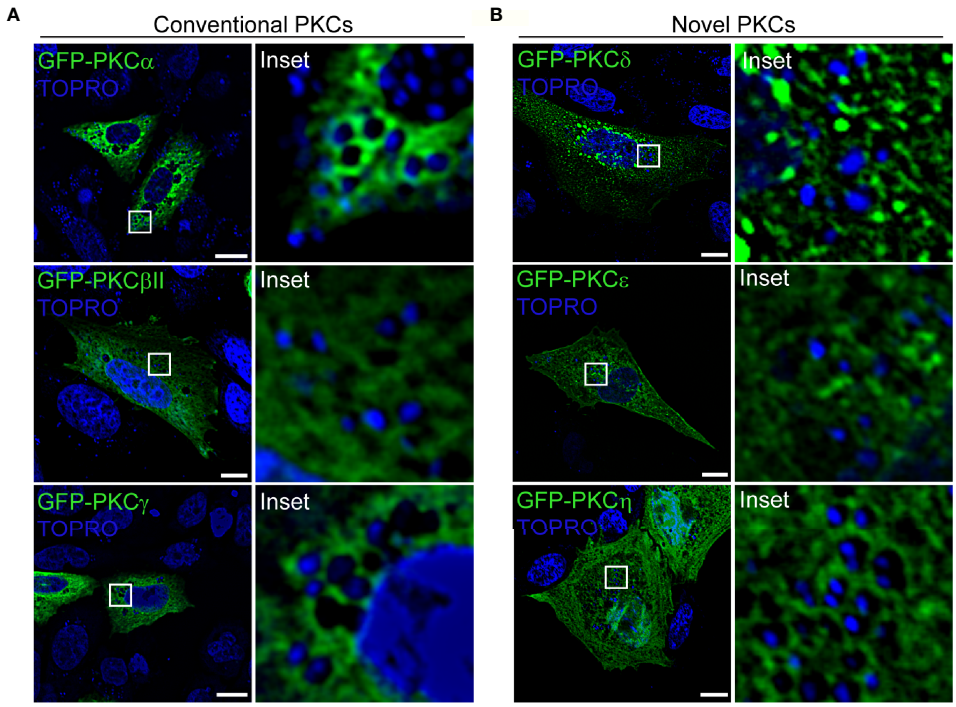

FIGURE 2 | PKCα is recruited to *S. aureus* phagosomes. **(A)** Confocal microscopy images of CHO cells overexpressing each of the three members of the conventional PKCs family: GFP-PKCα, GFP-PKCβII, GFP-PKCγ. Cells were infected with *S. aureus* wt for 4 hours. Bacteria were labelled with Topro (shown in blue). Bar: 10 µm. **(B)** Confocal microscopy images of CHO cells transfected with members of the novel PKC family: GFP-PKCδ, GFP-PKCε or GFP-PKCη. Cells were infected with *S. aureus* wt for 4 hours. Bacteria were labelled with Topro (shown in blue). Bar: 10 µm. Figures are representative of five independent experiments.

concluded that PKCα is recruited to the phagosomal membranes in a DAG-independent manner.

Because PKCα activity and membrane localization is Ca^{2+}-dependent, we next explored the dependence on Ca^{2+} in recruiting PKCα to *S. aureus*-containing phagosomes. CHO cells overexpressing GFP-PKCα were treated with the Ca^{2+} chelator BAPTA-AM. As we have previously described, *S. aureus* secretes cytotoxins that are able to generate pores in the plasma membrane allowing the entry of extracellular Ca^{2+} into the cellular cytosol, therefore, we assessed Ca^{2+} chelation in Krebs solution with or without Ca^{2+}. In both conditions, cells were infected with *S. aureus* wt and after 4 h.p.i. they were analyzed by confocal microscopy. As shown in **Figures 3E, F**, cells treated with BAPTA-AM in a medium without Ca^{2+} showed a significant decrease of PKCα recruitment to the phagosomal membranes, indicating that this second messenger is required for the translocation and binding of PKCα to the *S. aureus* phagosomes.

PKCα Recruitment Depends on *S. aureus* α-hemolysin

We next sought to determine whether the observed PKCα recruitment was dependent on *S. aureus* viability. For this purpose, bacteria were first inactivated by incubation at 95°C for 10 minutes, and subsequently internalized by CHO cells overexpressing GFP-PKCα. As shown in **Figures 4A, B**, PKCα was not recruited to heat-inactivated *S. aureus*, indicating that the recruitment of PKCα only occurs when the bacteria enclosed in the vacuoles are alive. Next, we addressed whether bacterial protein synthesis was required for PKCα recruitment. *S. aureus* wt was pre-incubated with the inhibitor of bacterial protein synthesis, chloramphenicol. CHO cells were transfected with GFP-PKCα and infected with these bacteria. PKCα was no longer recruited to *S. aureus* when its protein synthesis was prevented (**Figures 4A, B**), confirming that the synthesis of bacterial products was required for PKCα's association to the pathogen-containing phagosomes.

During staphylococcal infections, the bacteria produce a large amount of secreted virulence factors such as toxins and enzymes. One of the most important virulence factors secreted by *S. aureus* is α-hemolysin (Hla), a cytotoxin able to generate pores in cellular membranes (28). As we have previously demonstrated, this toxin is required for activation of the autophagic pathway during *S. aureus* cellular invasion (16). Having established that synthesis of bacterial proteins is necessary for the association of PKCα with pathogen-containing phagosomes (**Figures 4A, B**), we next addressed whether Hla was one of the bacterial secreted factors responsible for PKCα recruitment. CHO cells overexpressing GFP-PKCα were infected with *S. aureus* wt, the Hla deficient mutant strain *S. aureus* Hla (–), or the

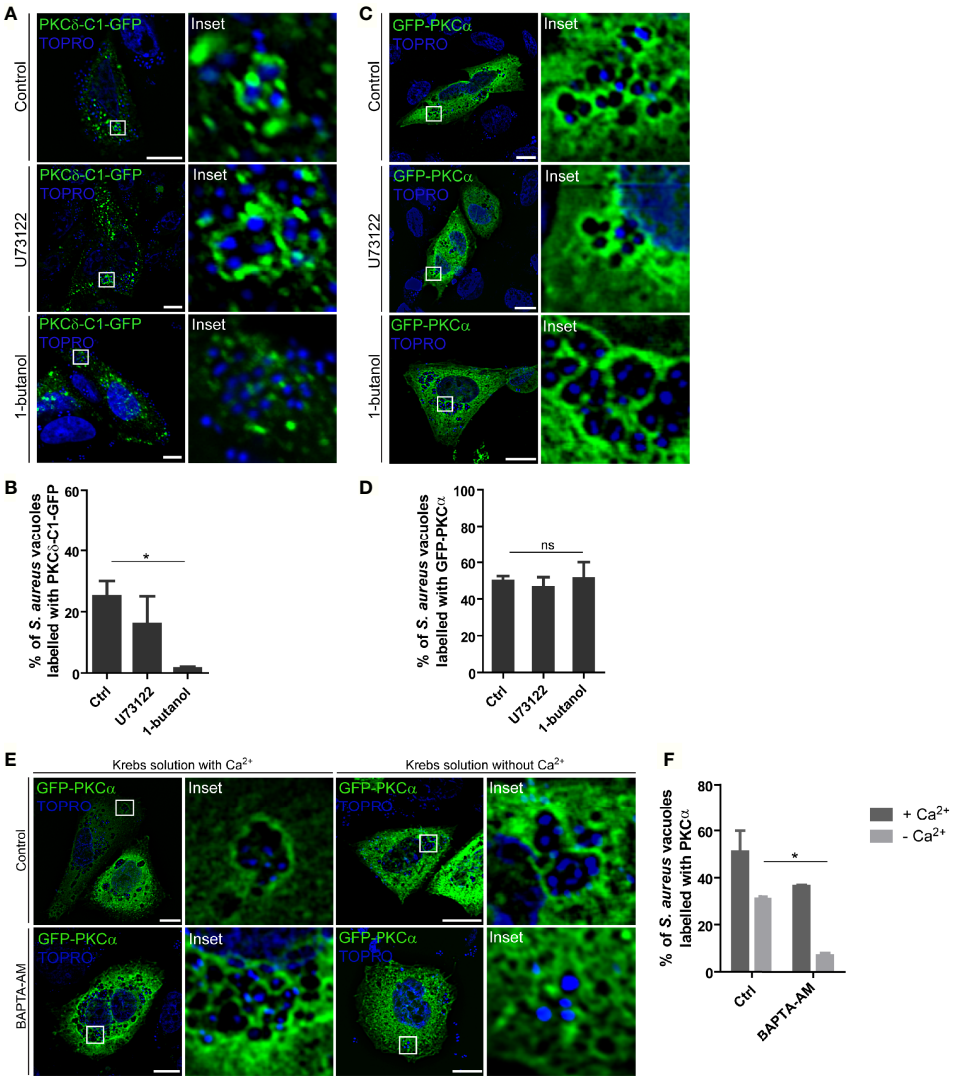

FIGURE 3 | PKCα recruitment to the *S. aureus* phagosomes is independent of DAG but depends on Ca^{2+}. **(A)** Confocal microscopy images of CHO cells overexpressing PKCδ-C1-GFP and treated with the PLC inhibitor, U73122 (1.5 μM), or the PLD inhibitor, 1-butanol (0.3% v/v), and infected for 4 hours with *S. aureus* wt. Bacteria were labelled with Topro (depicted in blue). Bar: 10μm. Images are representative of three independent experiments. **(B)** Quantification of *S. aureus* vacuoles decorated with PKCδ-C1-GFP. Data are the mean ± SEM of three independent experiments. *p ≤ 0.01. **(C)** Confocal microscopy images of CHO cells overexpressing GFP-PKCα and treated with the PLC inhibitor, U73122 (1.5 μM) and the PLD inhibitor, 1-butanol (0.3% v/v), and infected for 4 hours with *S. aureus* wt. Bacteria were labelled with Topro (shown in blue). Images are representative of three independent experiments. Bar: 10 μm. **(D)** Quantification of *S. aureus* vacuoles recruiting GFP-PKCα. Data are the mean ± SEM of three independent experiments. **(E)** Confocal microscopy images of CHO cells overexpressing GFP-PKCα treated with 10 μM BAPTA-AM in Krebs solution with (2.5 mM) or without Ca^{2+} and infected with *S. aureus* wt for 4 hours. Bacteria were labelled with Topro (shown in blue). Bar: 10 μm. Images are representative of three independent experiments. **(F)** Quantification of *S. aureus* vacuoles recruiting GFP-PKCα. Data are the mean ± SEM of three independent experiments. *p ≤ 0.05.

complemented mutant *S. aureus* Hla (–)+pHla, which overexpresses the toxin. The samples were processed and analyzed by confocal microscopy. As depicted in **Figures 4C** and **4D**, cells infected with the Hla-deficient mutant showed a marked decrease in the recruitment of PKCα to the bacterial phagosomes. PKCα association was restored to values similar to those observed upon *S. aureus* wt infection when the cells were infected with the complemented strain *S. aureus* Hla (–)+pHla. Taken together, these results indicate that the bacterial production of Hla was critical for the recruitment of PKCα to the phagosomes harboring *S. aureus*.

S. aureus Secreted Factors Activate PKCα

Having established that PKCα was recruited to *S. aureus*-containing phagosomes by a mechanism that depended on the

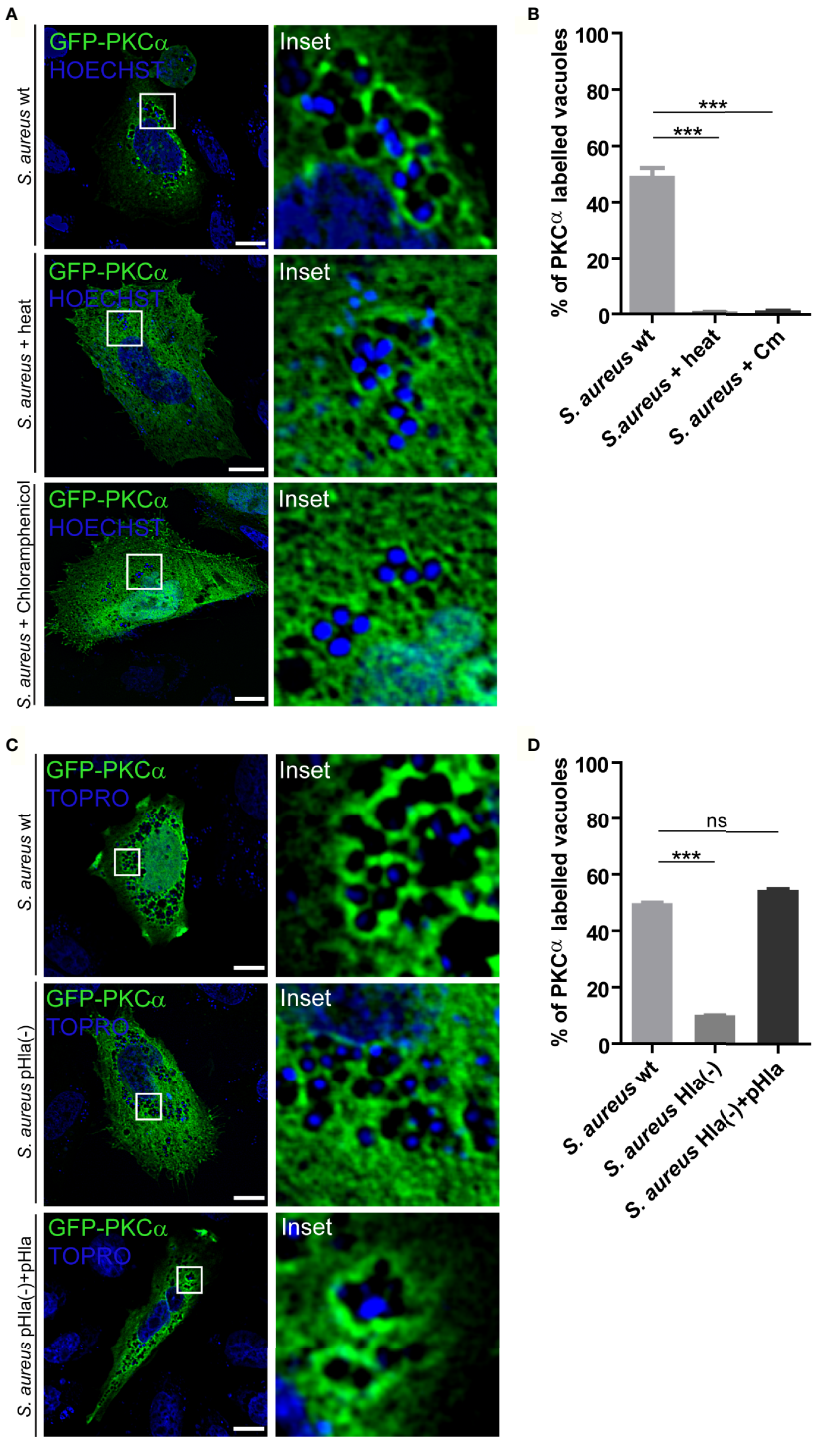

FIGURE 4 | PKCα recruitment to *S. aureus* phagosomes depends on α-hemolysin. **(A)** Confocal microscopy images of CHO cells overexpressing GFP-PKCα, and then infected for 4 hours with *S. aureus* wt, *S. aureus* wt killed by heat or *S. aureus* wt treated with chloramphenicol. Bacteria were labelled with Hoechst (shown in blue). Bar: 10 μm. Images are representative of four independent experiments. **(B)** Quantification of *S. aureus* vacuoles labelled with GFP-PKCα in cells infected with *S. aureus* wt, *S. aureus* wt heat killed or *S. aureus* wt inactivated by chloramphenicol treatment. Data are the mean ± SEM of four independent experiments. ***p ≤ 0.0001. **(C)** Confocal microscopy images of CHO cells overexpressing GFP-PKCα, and then infected with *S. aureus* wt, *S. aureus* Hla (–), mutant deficient of α-hemolysin or *S. aureus* Hla (–)+pHla, mutant complemented with the α-hemolysin for 4 hours. Bacteria were labelled with Topro (shown in blue). Images are representative of five independent experiments. Bar: 10 μm. **(D)** Quantification of *S. aureus* vacuoles labelled with GFP-PKCα in cells infected with *S. aureus* wt, *S. aureus* Hla (–) or *S. aureus* Hla (–)+pHla. Data are the mean ± SEM of five independent experiments. ***p ≤ 0.0001; ns, non significant.

secreted toxin α-hemolysin, we next examined whether bacterial factors were able to activate PKCα. To this end, we used a genetically encoded C Kinase Activity Reporter (CKAR2), which consists of a PKC specific substrate flanked by mCerulean and a yellow fluorescent protein (YFP) (29). Phosphorylation of the reporter by PKC results in a change in the fluorescence resonance energy transfer (FRET) that functions as a read out for activity of the kinase (30). CHO cells cotransfected with CKAR2 and mCherry-PKCα, were treated with *S. aureus* culture supernatants, in order to stimulate cells with those virulence factors secreted by the bacterium. Since the LB broth used to grow bacteria is yellow and interferes with the CFP emission, in all the experiments cells were first treated with LB broth to establish a new baseline and then stimulated with *S. aureus* culture supernatants. Following stimulation with *S. aureus* supernatant, cells were treated with the PKC inhibitor Gö6976, which inhibits conventional PKC isozymes (31). Treatment of cells with the culture supernatant of *S. aureus* wt (red line), but not LB broth alone (green line) resulted in a transient activation of PKC, as assessed by the increase in FRET ratio (**Figure 5A**). These data suggested that factors secreted by *S. aureus* activate PKCα.

We next addressed whether specifically α-hemolysin in the *S. aureus* supernatant was responsible for the observed PKCα activation. Cells overexpressing mCherry-PKCα and CKAR2 were treated with the supernatants from cultures of *S. aureus* wt, *S. aureus* Hla (–), or *S. aureus* Hla (–)+pHla. Whereas treatment of cells with *S. aureus* wt culture supernatant (red line) caused PKC activation, supernatant from the Hla-deficient mutant strain (violet line) did not cause activation of PKC (**Figure 5B**). As expected, activation was restored upon treatment of cells with the supernatant of the mutant complemented with the toxin, *S. aureus* Hla (–)+pHla (blue line) (**Figure 5B**). Indeed, the *S. aureus* Hla (–)+pHla's supernatant caused an even greater PKC activation peak than the one produced by the wild type strain. Thus, we concluded that the secreted α-hemolysin is necessary for PKCα activation.

Next, in order to determine whether the α-hemolysin itself was able to activate PKCα, CHO cells cotransfected with mCherry-PKCα and CKAR2 were stimulated with two different concentrations of purified toxin, 10 μg/ml and 30 μg/ml. Neither concentration induced activation of the kinase (**Figure 5C**). To confirm that the system was active, cells were stimulated with the phorbol ester PDBu, a PKC agonist, and the expected activation peak was observed. Thus, α-hemolysin was necessary, but not sufficient, for the activation of PKCα. These data suggest that the presence of other virulence factors secreted by the bacterium likely contribute to the activation of PKCα.

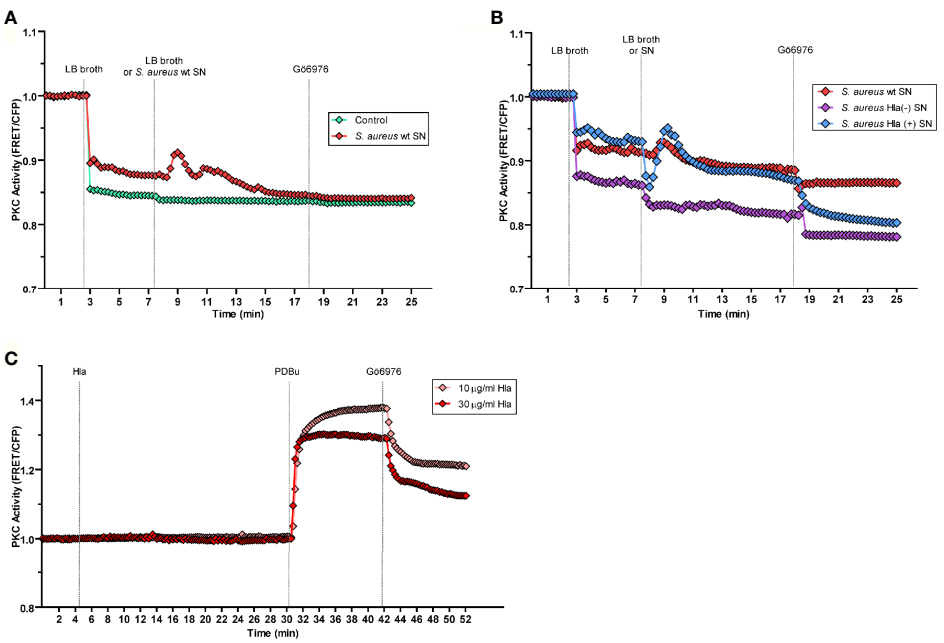

FIGURE 5 | PKCα is activated by the virulence factors secreted by *S. aureus*. By the use of a genetically encoded biosensor, the C kinase activity reporter (CKAR2), PKC activity was assessed as indicated in Material and Methods. **(A)** CHO cells co-expressing CKAR2 and mCherry-PKCα were treated with LB broth to set a baseline. After 5 minutes of stable baseline, they were treated with *S. aureus* wt culture supernatant (red line) and then treated with the PKC inhibitor Gö6976 (1 μM). The control condition (green line) corresponds to LB broth. **(B)** CHO cells co-expressing CKAR and mCherry-PKCα were treated with LB broth to settle a baseline, then, after 5 minutes they were treated with *S. aureus* wt (red line), *S. aureus* Hla (–) (blue line) or *S. aureus* Hla (–)+pHla (violet line) culture supernatants and then treated with the inhibitor Gö6976 (1 μM). **(C)** CHO cells co-overexpressing CKAR2 and mCherry-PKCα were treated with 10 μg/ml (pink line) or 30 μg/ml (red line) of α-hemolysin pure protein. After 25 minutes, cells were treated with the PKC agonist PDBu (200 nM) and 12 minutes afterward, the PKC inhibitor Gö6976 (1 μM) was added. Data are the mean of three independent experiments.

PKCα Inhibits the Autophagy Induced by *S. aureus* Invasion

After demonstrating that the conventional isozyme PKCα is recruited to the phagosomes where *S. aureus* resides during its invasion, and that the secreted factors produced by the bacterium activate the kinase, we next examined whether this enzyme regulates the autophagic response that is induced during infection. First, we analyzed whether PKCα presence in phagosomes affected the recruitment of the autophagic protein LC3 to the phagosomal membrane. Cells were cotransfected with RFP-LC3 and GFP-PKCα, or RFP-LC3 and GFP empty vector as a control, infected with *S. aureus* wt and, after 4 hours, cells were fixed and analyzed by confocal microscopy. Surprisingly, the overexpression of PKCα caused around 40% decrease in the recruitment of the autophagic protein LC3 to the phagosomal membranes (**Figures 6A, B**). We also observed that PKCα and LC3 did not colocalize at the phagosomal membranes, but rather they were mutually exclusive: phagosomes in which PKCα was present had no detectable LC3 and vice versa (**Figure 6C**).

We next examined whether PKCα modulated autophagy by assessing one of the earliest events in autophagy: processing of the autophagic protein LC3 from the cytoplasmic form LC3-I to the lipidated form LC3-II, which is able to bind to autophagosomal membranes. The conversion of LC3-I to LC3-II as detected by Western blot can be used to measure the activation of autophagy. CHO cells were treated in the following conditions: i) control cells; ii) infected with *S. aureus* wt for 4 hours; iii) transfected with mCherry-PKCα; iv) transfected with

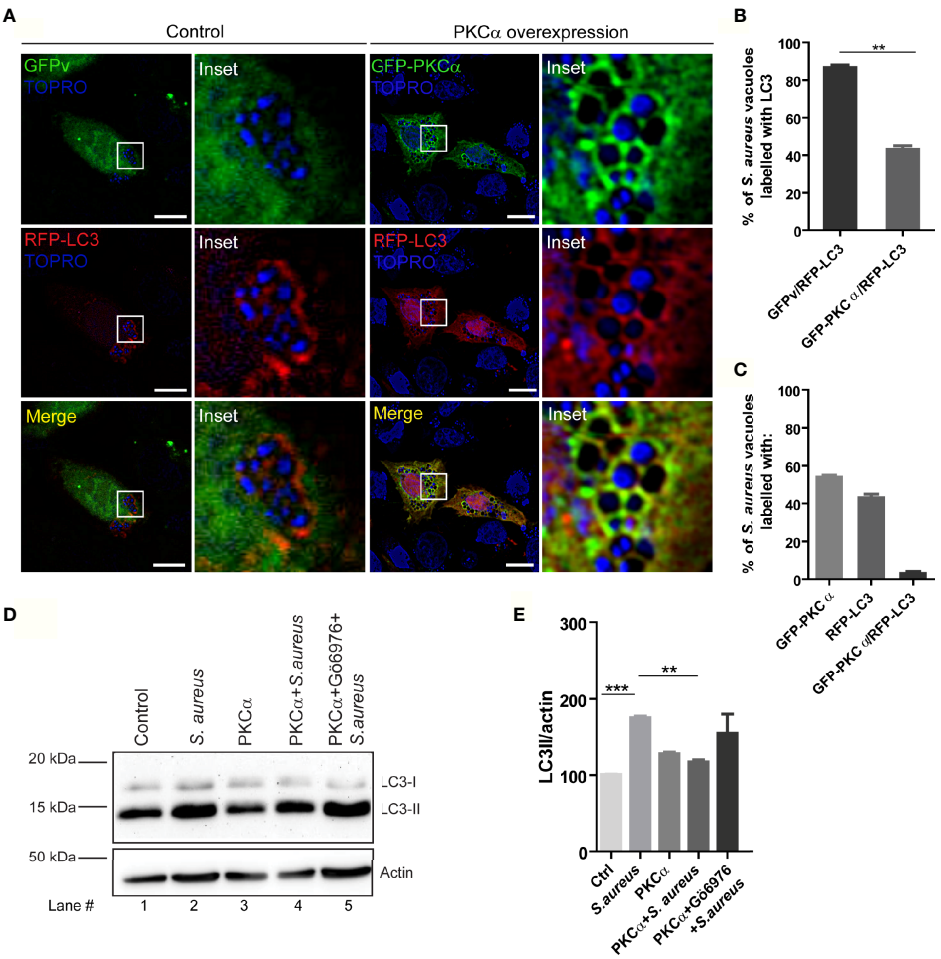

FIGURE 6 | PKCα inhibits autophagy induced by *S. aureus*. **(A)** Confocal microscopy images of CHO cells co-overexpressing GFP-PKCα or GFP empty vector (GFPv) and RFP-LC3 and infected for 4 hours with *S. aureus* wt. Bacteria were labelled with Topro, shown in blue. Bar: 10μm. Images are representative of five independent experiments. **(B)** Quantification of *S. aureus* vacuoles recruiting RFP-LC3. **p ≤ 0.001. **(C)** Quantification of *S. aureus* vacuoles recruiting GFP-PKCα, RFP-LC3 or both. Data are the mean ± SEM of five independent experiments. **(D)** Image of a Western blot analysis corresponding to a membrane incubated with specific antibodies against LC3 and actin (as a loading control), of cell lysates obtained from CHO cells subjected to the following conditions: lane 1, control; lane 2, infected with *S. aureus* wt for 4 hours; lane 3, transfected with mCherry-PKCα; lane 4, transfected with mCherry-PKCα and infected with *S. aureus* wt for 4 hours; line 5, transfected with mCherry-PKCα, treated with the PKC inhibitor Gö6976 (250 nM) and infected with *S. aureus* wt for 4 hours. The figure is representative of four independent experiments. **(E)** Quantification of the Western blot bands intensities with ImageJ. Data are the mean ± SEM of four independent experiments **p ≤ 0.001, ***p ≤ 0.0001.

mCherry-PKCα and infected with *S. aureus* wt; v) transfected with mCherry-PKCα, treated with the inhibitor Gö6976 and infected with *S. aureus* wt. Western blot analysis of cell lysates with a specific antibody for LC3 revealed that, as previously reported (19), LC3-II levels increased when the cells were infected with *S. aureus* wt (**Figures 6D, E**, lane 2). Interestingly, we found that when cells were transfected with PKCα and subsequently infected with *S. aureus*, LC3-II levels decreased significantly (**Figures 6D, E**, lane 4) compared to only infection and no kinase overexpression. Also, we observed that in cells treated with the inhibitor Gö6976 and infected with *S. aureus*, LC3-II levels were reestablished (**Figures 6D, E**, lane 5). Thus, PKCα overexpression results in reduced association of LC3 protein with phagosomes containing bacteria as assessed by confocal microscopy, and reduced LC3-II levels, as assessed by Western blot. Taken together, these results indicate that PKCα is able to inhibit the autophagic response induced during *S. aureus* infection.

PKCα Inhibits *S. aureus* Intracellular Replication

S. aureus is one of the pathogen microorganisms that modulates the autophagic pathway for its own benefit, utilizing the autophagosomes as a protective niche, where it actively replicates before escaping toward the cytoplasm (32). Given that PKCα inhibited the autophagic response induced by *S. aureus*, we reasoned that the ability of *S. aureus* to replicate in the interior of cells might be regulated by PKCα. To assess this, CHO cells were transfected with GFP-PKCα or GFP empty vector as a control, infected with *S. aureus* wt and lysed after 2, 3 or 4 hours. Samples were cultured in Brain Hearth Infusion Agar to allow quantification of bacterial colonies. As depicted in **Figure 7**, PKCα expression caused a significant decrease in the number of Colony Forming Units (CFU) compared to cells transfected with the empty vector. Therefore, we concluded that the overexpression of PKCα significantly impairs *S. aureus* intracellular replication.

DISCUSSION

S. aureus is a pathogen responsible for a broad range of diseases that vary from local controlled infections to life-threatening systemic infections. The understanding of staphylococcal infections has gained importance given the high antibiotic resistance that the bacterium has developed in recent years. It is crucial to find new ways of impairing the ability of this bacterium to replicate in the interior of cells in order to modulate the damage that it causes.

During bacterial infection, several mechanisms are triggered. It is a battle between the survival mechanisms of the bacteria and the countless signaling pathways that the cells activate in order to avoid bacterial replication and promote their removal from the host cell. Xenophagy is meant to be a degradation pathway that contributes to the elimination of foreign pathogens, but *S. aureus* utilizes the autophagosomes as a replicative niche (33). Here, we have unraveled one novel signaling pathway that can be used to prevent *S. aureus* from taking advantage of the autophagic pathway for its replication. In this study, we have demonstrated that the overexpression of PKCα during *S. aureus* infection causes the recruitment of this kinase to the phagosomal membranes, hampering the autophagic response induced by the invasion of the bacterium, most likely by phosphorylation of the autophagy protein LC3 (34). Moreover, we have shown that overexpression of PKCα generates an important decrease in the intracellular replication of *S. aureus* in epithelial cells.

Our proposed model suggests that during *S. aureus* infection, after internalization, the bacteria follow the previously described intracellular pathway, residing in a phagosome whose membrane

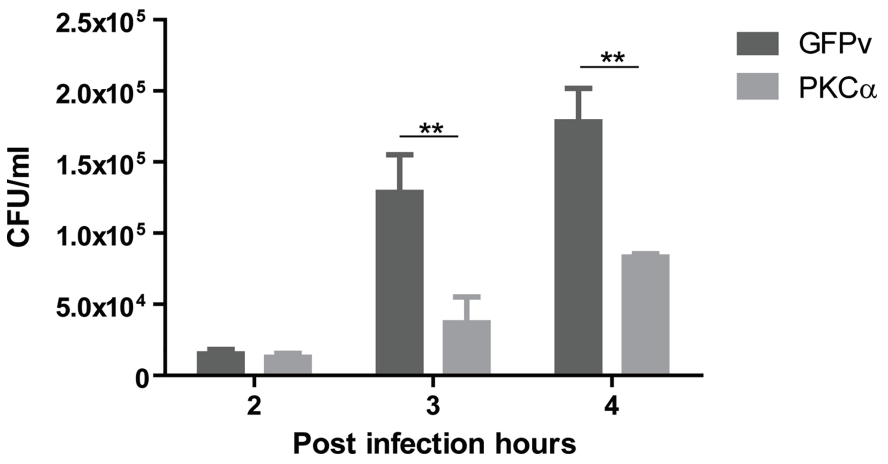

FIGURE 7 | PKCα decreases intracellular replication of *S. aureus*. Colony forming units (CFU) quantification (see Materials and Methods) of CHO cells overexpressing GFP-PKCα or GFPv and infected for 4 hours with *S. aureus* wt. Data are the mean ± SEM of three independent experiments. **p ≤ 0.001.

is disrupted by Hla causing the recruitment of the autophagic protein LC3. The bacteria use the double membrane autophagosomes to actively replicate and subsequently, escape toward the cytoplasm. However, when PKCα is overexpressed during *S. aureus* infection, the intracellular pathway that the bacteria transit is altered: the action of the bacterial Hla and other virulence factors secreted by *S. aureus* cause the activation of PKCα. Then, the kinase is recruited to the phagosomal membranes by action of the Hla. We hypothesize that PKCα phosphorylates LC3, preventing its association with the membranes of the compartments containing the bacteria, causing the inhibition of autophagy and in turn, inhibiting the intracellular replication of *S. aureus* (**Figure 8**).

The lipid DAG is an important second messenger involved in a wide range of signaling pathways. Jongstra-Bilen and collaborators showed an accumulation of DAG in the phagosomal membranes containing opsonized latex beads. A burst of DAG was observed during phagosomal formation by the action of Bruton's tyrosine kinase (Btk) (35). It has also been reported that the autophagosomes where *Salmonella typhimurium* resides present DAG in their membranes, which is required for the activation of antibacterial autophagy (36). Certain species of *Listeria* and *S. aureus* itself produce a phospholipase C enzyme that is able to generate DAG in the host cells (37). Indeed, *S. aureus* phospholipase C is considered an important virulence factor that contributes to lung injury during staphylococcal infections. In the present results, we have determined that DAG was present in 40% of phagosomes containing *S. aureus* (**Figure 1**), which were also labeled by the autophagic protein LC3 (i.e. autophagic compartments), a similar behavior as the one observed during *S. typhimurium* infection (36).

After screening the members of the PKC family that bind to DAG, we found that the conventional isozyme PKCα is recruited to the membranes of *S. aureus* containing-phagosomes (**Figure 2** and **Supplementary Figure 2**). It is known that PKCε is present in the phagosomal membranes of opsonized beads (38); it has also been observed that PKCα is recruited to phagosomes containing latex beads in murine macrophages, an interaction that is crucial for the maturation of those phagosomes (26). However, to the best of our knowledge, our findings report the presence of this kinase in the phagosomes containing live bacteria for the first time.

The activation of conventional PKC isozymes requires the binding of the two second messengers DAG and Ca^{2+} to the C1 and C2 domains respectively (39). When DAG synthesis was inhibited, we observed that despite the lack of DAG in the *S. aureus* phagosomal membranes, PKCα still associated with these membranes (**Figure 3**), suggesting that the binding of the kinase to these compartments is independent of DAG. This behavior has been reported in the past, and it has been shown that PKCα can also be bound to membranes by protein-protein interactions (40, 41). Further experiments would be necessary to identify possible PKCα recruitment molecules to the vacuole membranes harboring *S. aureus*. In contrast, we have demonstrated that Ca^{2+} was required for the recruitment of PKCα to the phagosomal membrane. Eichstaedt and collaborators provided evidence that *S. aureus* alpha toxin (Hla) leads to an increase in the intracellular Ca^{2+} levels in a dose- and time-dependent manner (20). We have also demonstrated that the recruitment of PKCα

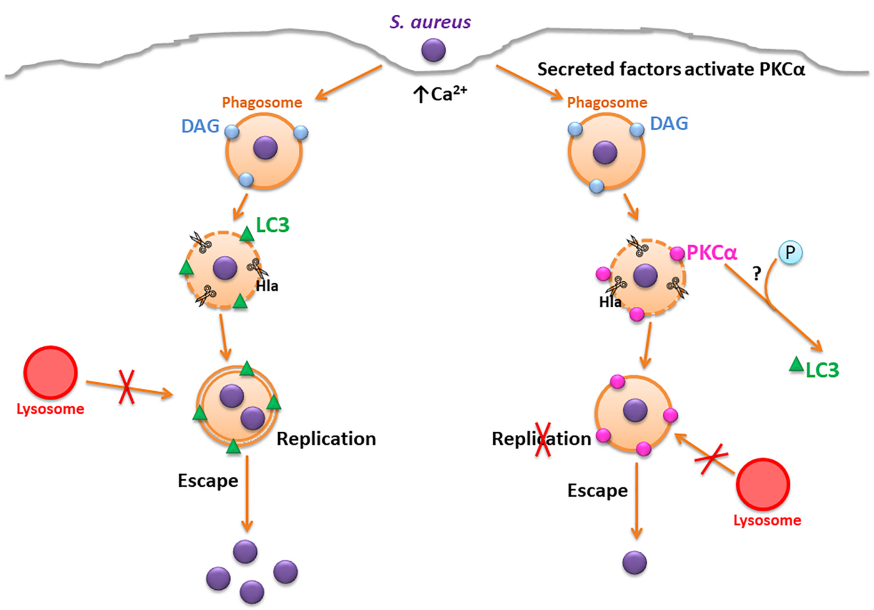

FIGURE 8 | Proposed model. On the left, the canonical *S. aureus* intracellular traffic is depicted, where Hla causes the disruption of the phagosomal membrane and the activation of autophagic response. *S. aureus* replicates in the interior of autophagosomes where it resides and finally, escapes to the cytoplasm. On the right, the overexpression of PKCα causes a disruption in the regular *S. aureus* traffic. Hla causes the recruitment of PKCα to the phagosomal membranes, which inhibits autophagy and impairs *S. aureus* intracellular replication.

to the phagosomes containing *S. aureus* is dependent on Hla, because in cells infected with the *S. aureus* mutant strain deficient for Hla, PKCα recruitment was lost (**Figure 4**). Taken together, it is likely that during *S. aureus* invasion, the pores made at the phagosomal membranes by the action of Hla, may cause a localized increase of Ca^{2+} concentration that promotes the association of this kinase to the phagosomes. In addition, we have established that the activation of PKCα needs the presence of Hla, although this toxin is not able to activate PKCα on its own, since other virulence factors produced and secreted by *S. aureus* seem to be required (**Figure 5**). The activation of PKC isozymes during bacterial infections has been described previously: *E. coli* activates PKCε during its invasion (23), *Listeria monocytogenes* activates PKC in order to be able to escape from phagosomes (42), and PKCδ is activated during *S. typhimurium* infection in order to activate the antibacterial autophagy (36). However, this is the first report showing that factors secreted by *S. aureus* activate PKCα.

Of note, we established that the overexpression of PKCα causes an inhibition in the autophagy induced by *S. aureus* (**Figure 6**). It has also been shown that PKCα has a role in the regulation of autophagy induced by other stimuli, for example, a pro-autophagy role has been assigned to PKCα in the autophagic response induced by palmitic acid (43). Additionally, it has been shown that PKCα can promote autophagy by mitochondrial disruption and ROS generation (44), but this is the first time that a role in the autophagy triggered by bacterial infection is given to PKCα. In the present report we have shown by confocal microscopy that the overexpression of PKCα during *S. aureus* infection caused a marked decrease in the recruitment of the autophagic protein LC3 to phagosomes containing the bacteria. We have also shown that PKCα negatively regulates the LC3-II levels by Western blot analysis when comparing cells infected with *S. aureus* with cells overexpressing the kinase and infected with the pathogen. Consistent with this, Jiang and collaborators have shown that PKC lead to inhibition of starvation-induced autophagy (34). It is likely that a similar mechanism is triggered during *S. aureus* infection, but further studies are needed to confirm this hypothesis.

We and others have previously demonstrated that transit of *S. aureus via* the autophagic pathway is beneficial for pathogen survival (16, 17, 32). The biological importance of all our findings is the fact that the overexpression of PKCα, through inhibition of autophagy, causes a marked hampering in the intracellular replication of *S. aureus* (**Figure 7**). It has been shown that PKCδ has a similar effect during *S. typhimurium* infection, causing the elimination of the bacterium, but in this case, the effect has been attributed to activation of autophagy (36). In this regard, it is important to note that autophagy is detrimental for *S. typhimurium*, but beneficial for *S. aureus*. Thus, both PKCs are important for bacterial degradation but by distinct mechanisms.

It has been shown that PKCα has an important role in controlling infections in macrophages, since the overexpression of a dominant negative mutant of PKCα caused enhanced survival of *Leishmania donovani* and further replication of *Legionella pneumophila* (25). All these findings point to a new important focus in the study of antibacterial mechanisms, where PKCs play an essential role in these processes and deserve further studies as therapeutic targets as an alternative to antibiotic treatments.

DATA AVAILABILITY STATEMENT

The original contributions presented in the study are included in the article/**Supplementary Material**. Further inquiries can be directed to the corresponding author.

AUTHOR CONTRIBUTIONS

MG: methodology and investigation. MG, AN, and MC: writing, review, and editing. MC and AN: funding acquisitions and resources. MC: supervision. All authors contributed to the article and approved the submitted version.

FUNDING

This work was supported by PICTs 2013-0305 and 2016-0443 from the ANPCYT and SIIIP 06/J470 (MC), NIH R35 GM122523 (AN). MG was supported by a CONICET (Consejo Nacional de Investigaciones Científicas y Técnicas de Argentina) Ph.D. Fellowship and in part by an IUBMB (International Union of Biochemistry and Molecular Biology) Wood-Whelan Fellowship.

ACKNOWLEDGMENTS

We thank Alejandra Medero, Rodrigo Militello and Jorge Ibanez, for valuable technical assistance. We also thank Dr. Gema Lordén Losada and Dr. Maya Kunkel for help and guidance with CKAR experiments.

SUPPLEMENTARY MATERIAL

The Supplementary Material for this article can be found online at: https://www.frontiersin.org/articles/10.3389/fimmu.2021.662987/full#supplementary-material

REFERENCES

1. Mostowy S. Autophagy and bacterial clearance: A not so clear picture. *Cell Microbiol* (2013) 15:395–402. doi: 10.1111/cmi.12063
2. Sorbara MT, Girardin SE. Emerging themes in bacterial autophagy. *Curr Opin Microbiol* (2015) 23:163–70. doi: 10.1016/j.mib.2014.11.020
3. Zheng YT, Shahnazari S, Brech A, Lamark T, Johansen T, Brumell JH. The Adaptor Protein p62/SQSTM1 Targets Invading Bacteria to the Autophagy Pathway. *J Immunol* (2009) 183:5909–16. doi: 10.4049/jimmunol.0900441

4. Thurston TLM, Wandel MP, von Muhlinen N, Foeglein A, Randow F. Galectin 8 targets damaged vesicles for autophagy to defend cells against bacterial invasion. *Nature* (2012) 482:414–8. doi: 10.1038/nature10744
5. Birmingham CL, Smith AC, Bakowski MA, Yoshimori T, Brumell JH. Autophagy controls Salmonella infection in response to damage to the Salmonella-containing vacuole. *J Biol Chem* (2006) 281:11374–83. doi: 10.1074/jbc.M509157200
6. Ogawa M, Sasakawa C. Shigella and autophagy. *Autophagy* (2006) 2:171–4. doi: 10.4161/auto.2829
7. Gutierrez MG, Master SS, Singh SB, Taylor GA, Colombo MI, Deretic V. Autophagy is a defense mechanism inhibiting BCG and Mycobacterium tuberculosis survival in infected macrophages. *Cell* (2004) 119:753–66. doi: 10.1016/j.cell.2004.11.038
8. Kwon DH, Song HK. A Structural View of Xenophagy, a Battle between Host and Microbes. *Mol Cells* (2018) 41:27–34. doi: 10.14348/molcells.2018.2274
9. Lowy FD. Staphylococcus aureus infections. *N Engl J Med* (1998) 339:520–32. doi: 10.1056/NEJM199808203390806
10. Taylor TA, Unakal CG. *Staphylococcus Aureus* (2018). Available at: http://www.ncbi.nlm.nih.gov/28722898 (Accessed November 14, 2018).
11. Kintarak S, Whawell SA, Speight PM, Packer S, Nair SP. Internalization of Staphylococcus aureus by Human Keratinocytes. *Infect Immun* (2004) 72:5668–75. doi: 10.1128/IAI.72.10.5668-5675.2004
12. Edwards AM, Potter U, Meenan NAG, Potts JR, Massey RC. Staphylococcus aureus Keratinocyte Invasion Is Dependent upon Multiple High-Affinity Fibronectin-Binding Repeats within FnBPA. *PLoS One* (2011) 6:e18899. doi: 10.1371/journal.pone.0018899
13. Mongodin E, Bajolet O, Cutrona J, Bonnet N, Dupuit F, Puchelle E, et al. Fibronectin-binding proteins of Staphylococcus aureus are involved in adherence to human airway epithelium(2002). (Accessed November 14, 2018).
14. Horn J, Stelzner K, Rudel T, Fraunholz M. Inside job: Staphylococcus aureus host-pathogen interactions. *Int J Med Microbiol* (2018) 308:607–24. doi: 10.1016/j.ijmm.2017.11.009
15. Grosz M, Kolter J, Paprotka K, Winkler AC, Schäfer D, Chatterjee SS, et al. Cytoplasmic replication of Staphylococcus aureus upon phagosomal escape triggered by phenol-soluble modulin α. *Cell Microbiol* (2014) 16:451–65. doi: 10.1111/cmi.12233
16. Mestre MB, Fader CM, Sola C, Colombo MI. Alpha-hemolysin is required for the activation of the autophagic pathway in *Staphylococcus aureus*-infected cells. *Autophagy* (2010) 6:110–25. doi: 10.4161/auto.6.1.10698
17. Schnaith A, Kashkar H, Leggio SA, Addicks K, Krönke M, Krut O. Staphylococcus aureus subvert autophagy for induction of caspase-independent host cell death. *J Biol Chem* (2007) 282:2695–706. doi: 10.1074/jbc.M609784200
18. Mestre MB, Colombo MI. Staphylococcus aureus promotes autophagy by decreasing intracellular cAMP levels. *Autophagy* (2012) 8:1865–7. doi: 10.4161/auto.22161
19. Mestre MB, Colombo MI. cAMP and EPAC are key players in the regulation of the signal transduction pathway involved in the α-hemolysin autophagic response. *PLoS Pathog* (2012) 8:e1002664. doi: 10.1371/journal.ppat.1002664
20. Eichstaedt S, Gäbler K, Below S, Müller C, Kohler C, Engelmann S, et al. Effects of Staphylococcus aureus-hemolysin A on calcium signalling in immortalized human airway epithelial cells. *Cell Calcium* (2009) 45:165–76. doi: 10.1016/j.ceca.2008.09.001
21. Wang T, Liu C, Jia L. The roles of PKCs in regulating autophagy. *J Cancer Res Clin Oncol* (2018) 144:2303–11. doi: 10.1007/s00432-018-2731-4
22. Newton AC. Protein kinase C: poised to signal. *Am J Physiol Endocrinol Metab* (2010) 298:E395–402. doi: 10.1152/ajpendo.00477.2009
23. Castrillo A, Pennington DJ, Otto F, Parker PJ, Owen MJ, Boscá L. Protein kinase Cepsilon is required for macrophage activation and defense against bacterial infection(2001). (Accessed September 19, 2017).
24. Shahnazari S, Namolovan A, Klionsky DJ, Brumell JH. A role for diacylglycerol in antibacterial autophagy. *Autophagy* (2011) 7:331–3. doi: 10.4161/auto.7.3.14045
25. St-Denis A, Caouras V, Gervais F, Descoteaux A. Role of protein kinase C-α in the control of infection by intracellular pathogens in macrophages. *J Immunol* (1999) 163:5505–11.
26. Ng Yan Hing JD, Desjardins M, Descoteaux A. Proteomic analysis reveals a role for protein kinase C-alpha in phagosome maturation. *Biochem Biophys Res Commun* (2004) 319:810–6. doi: 10.1016/j.bbrc.2004.05.054
27. Carrasco S, Mérida I. Diacylglycerol, when simplicity becomes complex. *Trends Biochem Sci* (2007) 32:27–36. doi: 10.1016/j.tibs.2006.11.004
28. Berube B, Wardenburg J. Staphylococcus aureus α-Toxin: Nearly a Century of Intrigue. *Toxins (Basel)* (2013) 5:1140–66. doi: 10.3390/toxins5061140
29. Ross BL, Tenner B, Markwardt ML, Zviman A, Shi G, Kerr JP, et al. Single-color, ratiometric biosensors for detecting signaling activities in live cells. *Elife* (2018) 7:e35458. doi: 10.7554/elife.35458
30. Violin JD, Zhang J, Tsien RY, Newton AC. A genetically encoded fluorescent reporter reveals oscillatory phosphorylation by protein kinase C. *J Cell Biol* (2003) 161:899–909. doi: 10.1083/jcb.200302125
31. Wu-Zhang AX, Newton AC. Protein kinase C pharmacology: Refining the toolbox. *Biochem J* (2013) 452:195–209. doi: 10.1042/BJ20130220
32. López de Armentia MM, Gauron MC, Colombo MI. Staphylococcus aureus Alpha-Toxin Induces the Formation of Dynamic Tubules Labeled with LC3 within Host Cells in a Rab7 and Rab1b-Dependent Manner. *Front Cell Infect Microbiol* (2017) 7:431. doi: 10.3389/fcimb.2017.00431
33. López de Armentia M, Amaya C, Colombo M. Rab GTPases and the Autophagy Pathway: Bacterial Targets for a Suitable Biogenesis and Trafficking of Their Own Vacuoles. *Cells* (2016) 5:11. doi: 10.3390/cells5010011
34. Jiang H, Cheng D, Liu W, Peng J, Feng J. Protein kinase C inhibits autophagy and phosphorylates LC3. *Biochem Biophys Res Commun* (2010) 395:471–6. doi: 10.1016/j.bbrc.2010.04.030
35. Jongstra-Bilen J, Puig Cano A, Hasija M, Xiao H, Smith CIE, Cybulsky MI. Dual Functions of Bruton's Tyrosine Kinase and Tec Kinase during Fcγ Receptor-Induced Signaling and Phagocytosis. *J Immunol* (2008) 181:288–98. doi: 10.4049/jimmunol.181.1.288
36. Shahnazari S, Yen WL, Birmingham CL, Shiu J, Namolovan A, Zheng YT, et al. A diacylglycerol-dependent signaling pathway contributes to regulation of antibacterial autophagy. *Cell Host Microbe* (2010) 8:137–46. doi: 10.1016/j.chom.2010.07.002
37. Daugherty S, Low MG. Cloning, expression, and mutagenesis of phosphatidylinositol-specific phospholipase C from Staphylococcus aureus: a potential staphylococcal virulence factor(1993). (Accessed September 19, 2017).
38. Larsen EC, Ueyama T, Brannock PM, Shirai Y, Saito N, Larsson C, et al. A role for PKC-epsilon in Fc gammaR-mediated phagocytosis by RAW 264.7 cells. *J Cell Biol* (2002) 159:939–44. doi: 10.1083/jcb.200205140
39. Antal CE, Newton AC. Tuning the signalling output of protein kinase C. *Biochem Soc Trans* (2014) 42:1477–83. doi: 10.1042/BST20140172
40. Mochly-Rosen D, Gordon AS. Anchoring proteins for protein kinase C: a means for isozyme selectivity(1998). (Accessed November 14, 2018).
41. Colón-González F, Kazanietz MG. C1 domains exposed: From diacylglycerol binding to protein-protein interactions. *Biochim Biophys Acta - Mol Cell Biol Lipids* (2006) 1761:827–37. doi: 10.1016/j.bbalip.2006.05.001
42. Poussin MA, Goldfine H. Involvement of Listeria monocytogenes Phosphatidylinositol-Specific Phospholipase C and Host Protein Kinase C in Permeabilization of the Macrophage Phagosome. *Infect Immun* (2005) 73:4410–3. doi: 10.1128/IAI.73.7.4410-4413.2005
43. Tan SH, Shui G, Zhou J, Li JJE, Bay BH, Wenk MR, et al. Induction of autophagy by palmitic acid via protein kinase C-mediated signaling pathway independent of mTOR (mammalian target of rapamycin). *J Biol Chem* (2012) 287:14364–76. doi: 10.1074/jbc.M111.294157
44. Silva RD, Manon S, Gonçalves J, Saraiva L, Côrte-Real M. Modulation of Bax mitochondrial insertion and induced cell death in yeast by mammalian protein kinase Cα. *Exp Cell Res* (2011) 317:781–90. doi: 10.1016/j.yexcr.2010.12.001

Conflict of Interest: The authors declare that the research was conducted in the absence of any commercial or financial relationships that could be construed as a potential conflict of interest.

frontiers in Immunology

REVIEW
published: 12 April 2021
doi: 10.3389/fimmu.2021.642771

Anaplasmataceae: Dichotomous Autophagic Interplay for Infection

LaNisha L. Patterson[1], *Caitlan D. Byerly*[1] *and Jere W. McBride*[1,2,3,4,5]*

[1] Department of Pathology, University of Texas Medical Branch, Galveston, TX, United States, [2] Department of Microbiology and Immunology, University of Texas Medical Branch, Galveston, TX, United States, [3] Center for Biodefense and Emerging Infectious Diseases, University of Texas Medical Branch, Galveston, TX, United States, [4] Sealy Institute for Vaccine Sciences, University of Texas Medical Branch, Galveston, TX, United States, [5] Institute for Human Infections and Immunity, University of Texas Medical Branch, Galveston, TX, United States

Autophagy is a vital conserved degradative process that maintains cellular homeostasis by recycling or eliminating dysfunctional cellular organelles and proteins. More recently, autophagy has become a well-recognized host defense mechanism against intracellular pathogens through a process known as xenophagy. On the host-microbe battlefield many intracellular bacterial pathogens have developed the ability to subvert xenophagy to establish infection. Obligately intracellular bacterial pathogens of the *Anaplasmataceae* family, including *Ehrlichia chaffeensis*, *Anaplasma phaogocytophilium* and *Orientia tsutsugamushi* have developed a dichotomous strategy to exploit the host autophagic pathway to obtain nutrients while escaping lysosomal destruction for intracellular survival within the host cell. In this review, the recent findings regarding how these master manipulators engage and inhibit autophagy for infection are explored. Future investigation to understand mechanisms used by *Anaplasmataceae* to exploit autophagy may advance novel antimicrobial therapies and provide new insights into how intracellular microbes exploit autophagy to survive.

Keywords: autophagy, xenophagy, *Anaplasmataceae*, *Ehrlichia*, *Anaplasma*, effector, autolysosome, phagolysosome

OPEN ACCESS

Edited by:
Gee W. Lau,
University of Illinois at Urbana-Champaign, United States

Reviewed by:
Daniel E. Voth,
University of Arkansas for Medical Sciences, United States
Eun-Kyeong Jo,
Chungnam National University, South Korea
Ivan Tattoli,
National Institute of Health (ISS), Italy

***Correspondence:**
Jere W. McBride
jemcbrid@utmb.edu

Specialty section:
This article was submitted to Microbial Immunology, a section of the journal Frontiers in Immunology

Received: *16 December 2020*
Accepted: *15 March 2021*
Published: *12 April 2021*

Citation:
Patterson LL, Byerly CD and McBride JW (2021) Anaplasmataceae: Dichotomous Autophagic Interplay for Infection. Front. Immunol. 12:642771. doi: 10.3389/fimmu.2021.642771

INTRODUCTION

Autophagy is a well characterized host defense mechanism in which invading microbes are tagged for degradation in a selective autophagic process known as xenophagy (1–7). Although xenophagy is a known host defense mechanism against invading microbes, various intracellular pathogens including obligately intracellular rickettsial pathogens in the family *Anaplasmataceae* can induce autophagy as a survival mechanism (2, 5–8). In contrast, evasion of the autophagic pathway is also a strategy utilized by intracellular pathogens for infection. Accumulating evidence provides insight regarding the dichotomous interplay that occurs between obligately intracellular bacteria and the autophagic pathway to promote infection.

In eukaryotic cells, autophagy is a highly conserved catabolic, lysosomal-dependent process that delivers long-lived proteins and damaged cytoplasmic components to the lysosome (9–12). At basal levels, autophagy plays an important role as a response to cellular stress and maintaining homeostasis through quality control of essential cellular components. Cellular homeostasis is maintained by degrading excessive, damaged, and/or aged proteins, peptides and organelles. Macroautophagy, the best described autophagy subtype, works to sequester damaged cytoplasmic

components in a double-membrane vesicle known as the autophagosome (13). Macroautophagy can be further categorized into nonselective autophagy which randomly engulfs cellular components within the cytoplasm into autophagosomes for degradation upon fusion with a lysosome, and selective autophagy which degrades a specific type of cargo tagged for degradation (14). Below, we will summarize the major steps of the autophagic process and the major autophagy protein groups that regulate each step of the autophagic process. Furthermore, we will discuss critical findings linking these proteins with *Anaplasmataceae*-induced autophagy.

The autophagic process can be divided into distinct stages, including autophagy induction, phagophore formation and elongation, cargo recognition, autophagosome maturation, lysosomal fusion and autophagosome degradation (13, 15). In coordination with these steps are several major signaling pathways and autophagy-related genes (ATGs). mTOR kinase is a major player in the regulation of the autophagic process (16, 17). Wnt and phosphoinositide 3-kinase (PI3K)/ATP dependent tyrosine kinase (Akt) signaling pathways regulate mTOR (18, 19). The Wnt pathway plays an essential role in inhibition of autophagy by regulating activation of the mTOR pathway. mTOR activation occurs downstream of PI3k/Akt signaling to inhibit autophagy (20, 21). Additionally, glycogen synthase kinase-3 (GSK3) inhibits the mTOR pathway by phosphorylating tuberous sclerosis complex 2 (TSC2) in a manner dependent on AMPK phosphorylation (22). Importantly, TSC2 is a Rheb GTPase-activating protein, a Ras family GTPase and an mTOR activator (23).

mTORC1 inhibition leads to autophagy induction due to activation of AMPK signaling (24). Upon decreased mTORC1 activity, the initiation of phagophore formation is stimulated by activation of the class III phosphatidylinositol 3-kinase (PtdIns3K) complex. The Ulk1 protein complex signals the formation of the PtdIns3K complex, which includes, Beclin-1 (Atg6/Vps30), Vps34 (vacuolar protein sorting 34), Vps15 (p150, a myristoylated serine/threonine kinase), Ambra-1 (Autophagy/Beclin-1 Regulator 1), and ATG14 (13, 25, 26). Together, the ULK1 protein complex and the PtdIns3K complex integrate nutrient status (ULK1) with autophagosome formation (PtdIns3K) (25).

Beclin-1, an orthologue of the Atg6/vacuolar protein sorting Vps30 protein in yeast, plays a central role in autophagy. Beclin-1 is important for localization of autophagic proteins to the PAS to regulate the lipid kinase Vps34 protein and promote formation of Beclin-1/Vps34/Vps15 core complexes (13, 26). The formation of the Beclin-1/Vps34/Vps15 complex marks the initiation of autophagy (27). The PtdIns3K complex, along with other Atg proteins, also recruits two ubiquitin-like conjugation systems, Atg12/Atg5/Atg16 and Atg8-phosphatidylethanolamine (PE), to the phagophore to recruit Atg8-PE machinery and regulate membrane elongation and expansion of the autophagosome (26, 28, 29).

Atg5/Atg12/Atg16 conjugation complex has been shown to lead to conjugation of microtubule-associated protein 1 light chain 3 (LC3), to the membrane of the autophagosome (29). This leads to the conjugation of LC3-I to phosphatidylethanolamine (PE) to form LC3-II. The p62/SQSTM1 (sequestosome 1) protein acts as a cargo receptor for ubiquitinated targets which are transported to the autophagosome for degradation (30, 31). Following phagophore expansion, the phagophore is completely sealed, forming the double membrane autophagosome containing all targeted components. Maturation of the autophagosome involves fusion with both early and late endosomes, which requires GTP bound small G protein Rab5, Rab7, and presenilin protein (32). The autophagosome fuses with the lysosome to form an autolysosome for degradation of engulfed components.

LC3-II and p62/SQSTM1 are also utilized as markers for autophagosome formation due to its degradation within the lysosome along with damaged and recycled components (33). Products, along with some of the autophagy cargo, are degraded by lysosomal hydrolases and recycled as amino acids supplements within the tricarboxylic acid cycle (TCA) cycle or as fatty acids, sugars, and proteins to increase energy for cell survival (9, 13).

Autophagy as an Intracellular Innate Defense Pathway

Although studies have demonstrated autophagy as a host defense mechanism against bacterial pathogens, many intracellular pathogens have evolved strategies to subvert autophagy for survival (34–36). Autophagy is considered a downstream effector mechanism that plays an integral role in both innate and adaptive immunity to various pathogens (9, 37). Xenophagy is a selective autophagy whereby intracellular pathogens are tagged by ubiquitin and subsequent targeting to autophagosomes for degradation in autolysosomes. Autophagy receptors such as p62/SQSTM1, nuclear domain 10 protein 52 (NDP52) and neighbor of BRCA1 gene 1 (NBR1) have been shown to bind ubiquitinated intracellular pathogens for autolysosome destruction and clearance (31). Autophagy plays an important role in both innate and adaptive immunity to various intracellular pathogens including *Mycobacterium tuberculosis*, *Streptococcus pyogenes*, *Listeria monocytogenes*, and *Salmonella enterica* (38–42).

This review presents the current knowledge regarding the dichotomous interplay between rickettsial pathogens in the family *Anaplasmataceae*, namely *Ehrlichia chaffeensis*, *Anaplasma phaogocytophilium* and *Orientia tsutsugamushi, and* the autophagic pathway during infection. These rickettsial pathogens utilize secreted effector proteins and host signaling pathways to hijack the autophagic pathway for survival.

ANAPLASMATACEAE: INTRACELLULAR PATHOGENS OF LIFE-THREATENING HUMAN INFECTIONS

Members of *Anaplasmataceae* are α-proteobacteria in the order of Rickettsiales that include genera *Anaplasma, Ehrlichia, Neorickettsia*, and *Orientia* (43–46). *Anaplasmataceae* family includes obligately intracellular bacteria that reside in membrane bound cytoplasmic vacuoles mainly within

phagocytic cells and are transmitted primarily by arthropod vectors that acquire the infection from persistently infected vertebrate hosts. These pathogens are master manipulators of the host cells (arthropod and mammalian) in which they infect. Successful intracellular infection occurs by hijacking conserved cellular signaling pathways, reprogramming host cell gene transcription, and by exploitation of other cellular processes to subvert host defense mechanisms including autophagy.

Anaplasmataceae members are best recognized for causing tick borne emerging life-threatening zoonotic diseases in the United States. Human monocytotropic ehrlichiosis (HME) and human granulocytic anaplasmosis (HGA) are group I NIAID tick-borne zoonoses caused by *E. chaffeensis* and *A. phagocytophilum*, respectively (47, 48). *E. chaffeensis* is maintained in nature by persistent infection of white-tailed deer, which is the primary mammalian reservoir. *E. chaffeensis* is transmitted by the lone star tick, *Amblyomma americanum*, which maintains the infection transstadially (1–3). *Anaplasma phagocytophilum* transstadially infects *Ixodes scapularis* ticks and other *Ixodes* spp. after acquiring the infection from infected small mammal reservoirs such as the white-footed mouse. In contrast, *O. tsutsugamushi* the etiologic agent of scrub typhus, a disease endemic to the Asian continent and present throughout Indonesia and northern Australia, is transmitted mainly by the bite of larva life stage-infected *Leptotrombidium* mites (49, 50). HME, HGA and scrub typhus have similar clinical presentations characterized by initial symptoms including fever, headache, myalgia, nausea, confusion, conjunctival injection (red eyes), and chills within the first two weeks following infection (1, 3, 15). Common laboratory abnormalities include thrombocytopenia, leukopenia, anemia, and elevated hepatic transaminases (2, 14, 16–18). Disease severity ranges from mild to life-threatening complications such as toxic shock-like syndrome, kidney failure, meningoencephalitis, and acute respiratory distress (1, 2, 4).

Members of the *Anaplasmataceae* family have small genomes but have evolved complex molecular strategies that enable them to create a permissive intracellular niche within professional phagocytes and other cells. Due to the obligately intracellular existence, *Anaplasmataceae* genomes have been shaped by a process known as reductive evolution resulting in loss of metabolic pathway genes that are no longer required for intracellular survival (51, 52). They replicate in membrane-bound cytoplasmic vacuoles within the host cell cytoplasm and undergo different developmental phases during infection. There are two well-defined ultrastructural forms, the dense-cored cell and reticulate cell, which have been identified by electron microscopy (53–56). The infectious dense-cored non replicating cell is small (0.4-0.6 μm), more electron dense, and has tightly coiled nucleoid DNA. In contrast, the reticulate cell is the replicative form and is larger (0.4-1.9 μm) with a dispersed nucleoid DNA. Dense-cored organisms interact with host cell receptors and enter the host cell by receptor-mediated endocytosis. After entry, dense-cored ehrlichiae transition into intermediate then full reticulate cell forms that replicate by binary fission, forming microcolonies known as morulae within host derived membrane-bound vacuoles. The ehrlichial replication cycle takes approximately 48 h, then the replicating reticulate cells transition into infectious dense-cored ehrlichiae which are released from the host cell by cell lysis or exocytosis to infect other cells (57, 58).

Secretion Systems and Effectors

As with some Gram-negative bacteria, *Anaplasmataceae* have well known secretion systems that secrete effector proteins into the host cell. Type I, II and IV secretion systems have been identified in *Anaplasmataceae*. Notably, the type III secretion system found in some obligately intracellular bacteria (i.e., chlamydiae), is absent (59–61). These macromolecular secretion nanomachines are distinctly different in secretion mechanisms and the secreted effectors. Several bacterial effectors are known to regulate selective autophagy through various mechanisms for survival (62–69). Below are listed some of the secreted effector proteins by members of *Anaplasmataceae* that play a significant role in the subversion of autophagy.

The T1SS is well characterized in many extracellular bacteria and is known to secrete a number repeat-containing pore-forming toxins known as the Repeats in Toxin Family (RTX) (70, 71). The T1SS is widespread in Gram-negative bacteria and transports substrates in a one-step process across two membranes without any periplasmic intermediate into the extracellular space (72–75). Several T1SS substrates have been identified that are secreted by members of *Anaplasmataceae*, including ankyrin repeat (AR) and tandem repeat effector proteins. There are currently four characterized T1SS tandem repeat protein (TRP) effectors that have been identified in *E. chaffeensis*-infected cells including TRP32, TRP47, TRP75 and TRP120 (60, 76–78). TRPs are nucleomodulins and TRP120 has also been shown to activate host cell signaling pathways (Notch and Wnt) to downregulate innate defense mechanisms (79–82). Several of the TRPs have been shown to play a role in inhibiting TFEB nuclear localization and autolysosome generation during *E. chaffeensis* infection by reprogramming signal transduction pathways, including the Wnt signaling pathway (21). *E. chaffeensis* Ank200 is a nucleomodulin secreted by the T1SS that binds adenine-rich *Alu* elements in host promoter and intron regions (83, 84). *O. tsutsugamushi* secrete T1SS AR family members that traffic to diverse subcellular localizations including the endoplasmic reticulum (61). The *O. tsutsugamushi* (Ikeda strain) genome encodes 38 Ank-containing ORFs, each of which display characteristics consistent with T1SS effectors (LDAVTSIF residues found in 37-63% in their final 60 amino acids, acidic pI values and very few cysteines) (85). *O. tsutsugamushi* Anks modulate NF-κβ to enhance infection; however, there is no evidence that *O. tsutsugamushi* T1SS substrates manipulate the autophagic pathway (86). Notably, *A. phagocytophilum* T1SS effectors have not been identified to date.

The T4SS is a well characterized ATP-dependent, double membrane-spanning multiprotein secretion nanomachine found in both Gram-negative and -positive bacteria (87–90). The archetypal Gram-negative T4SS is defined by the plant pathogen Agrobacterium tumefaciens VirB/D4 system (91). In Rickettsiales, a homologous but structurally different T4SS system is present with *vir* genes organized in three genome

locations (92). To date, there have been a total of six T4SS effector proteins identified between *E. chaffeensis* and *A. phagocytophilum;* however, functions for only five of these effectors have been reported (67, 93–97). *Anaplasma* translocated substrate 1 (Ats-1) and ankyrin repeat domain-containing protein A (AnkA) have been functionally characterized. Ats-1 is an orthologue of the *E. chaffeensis* T4SS effector protein, Etf-1. Both Ats-1 and Etf-1 play roles in subverting apoptosis and host autophagy for intracellular survival (66, 67, 94, 98). Etf-2 delays endosomal maturation to avoid routing *E. chaffeensis* to phagolysosomes (95). Another *E. chaffeensis* effector, ECH0825, is highly upregulated during early stages of infection during exponential growth in THP-1 human monocytic leukemia cells and has been shown to translocate to mitochondria where it inhibits reactive oxygen species production and host cell apoptosis by upregulating MnSOD, an essential mitochondrial antioxidant enzyme (93).

PATHOGEN-HOST INTERACTIONS

E. chaffeensis

Utilizing TRP and other effectors, *E. chaffeensis* avoids host immune defenses of the mononuclear phagocyte making it a remarkable model organism for examining novel host-pathogen interactions involved in cellular reprogramming. *E. chaffeensis* TRP effectors are secreted by the T1SS and translocate the vacuole membrane by an unknown mechanism to access the host cell. During infection, TRPs interact with a multitude of host proteins and elicit strong protective antibody responses to molecularly defined linear epitopes (99–102). TRPs are nucleomodulins that translocate to the host cell nucleus through a noncanonical NLS-independent mechanism (79–81). In addition, TRP120 has other defined functional roles during infection, and thus, is considered a moonlighting protein. These roles include promoting ehrlichial entry (103, 104), activation of host signaling pathways through ligand mimicry (99, 105), nucleomodulin activity (106–108), and as a HECT E3 ubiquitin ligase that targets host substrates for degradation (106, 107, 109, 110). The ability of *E. chaffeensis* to interface with the host cell is known to involve post-translation modifications including sumolyation (104), ubiquitination (109) and others (104). *E. chaffeensis* appears to exploit host cell machinery to acquire post translational modifications (PTMs) in some instances, but ehrlichial encoded ubiquitin ligases such as TRP120 are involved in creating PTMs that play a role in host-pathogen interplay (109). *E. chaffeensis* gene knockout studies have shown that TRP120 is essential for *E. chaffeensis* survival *in vivo* which can be attributed to the many defined functions of TRP120 and highlights the major role TRP120 plays in infection and survival (58).

A. phagocytophilum

A. phagocytophilum utilizes an array of bacterial proteins for adherence, invasion, and survival within the host cell. Infection is known to depend on numerous type IV secreted effector proteins, transmembrane proteins, surface proteins, and *A. phagocytophilum*-occupied vacuole membrane (AVM) proteins. These proteins include major surface protein 4 (MSP4), nucleomodulin AnkA, adhesin protein Asp14, and heat shock protein 70 (HSP70). The nucleomodulin AnkA binds host DNA and protein complexes within the nucleus of neutrophils to alter gene transcription (111). Ats-1 plays a role in preventing apoptosis by stabilizing mitochondria through the disruption of Bax-induced apoptosis to promote *A. phagocytophilum* infection (94).

PTMs are also involved in pathogen-host interactions. Effector protein APH0032 decorates the AVM interface and is a sumoylated by co-opting host SUMO machinery during infection. Similarly, *A. phagocytophilum* protein A (AmpA) is a critical effector protein that is also sumoylated to promote infection. AmpA localizes to the AVM throughout infection colocalizing with SUMO 2/3 and SUMO1 as the infection progresses (112). The nucleomodulin AnkA binds host DNA and protein complexes within the nucleus of neutrophils to alter gene transcription (111).

O. tsutsugamushi

O. tsutsugamushi encodes multiple T1SS ankyrin-repeat-containing effector proteins (Anks), known to interact with host cells and largely target the endoplasmic reticulum (113). Notably, Ank9 was the first effector shown to function during infection whereby a unique Ank9 motif mimics the GRIP domain of the host golgins, supporting *O. tsutsugamushi* localization to the host Golgi. Ank9 binds host protein COPB2 to hijack the endoplasmic reticulum *via* retrograde trafficking from the Golgi. Following its translocation, Ank9 activates the transcription factor 4-dependent unfolded protein response to support *O. tsutsugamushi* infection (114). Studies have revealed *O. tsutsugamushi* nucleomodulins Ank1 and Ank6 abrogate NF-kB-activated transcription utilizing exportin-1 independent mechanisms to decrease TNFα-induced p65 nuclear levels (86).

ANAPLASMATACEAE-MEDIATED EXPLOITATION OF CONSERVED HOST CELL SIGNALING PATHWAYS

Conserved signaling pathways Wnt and Notch which play an important role in regulating innate host defenses, including phagocytosis, autophagy, and toll-like receptor (TLR) expression are exploited by *E. chaffeensis* for intracellular survival (20, 115–117). The Wnt/β-catenin signaling pathway regulates both basal and stress-induced autophagy (20). β-catenin suppresses autophagosome formation and directly suppresses p62/SQSTM1 through T-cell factor 4 (TCF4), one of the transcriptional factors in the Wnt signaling pathway (20). Autophagy has also been shown to inhibit Notch signaling though modulation of the PTEN-PI3K/Akt/mTOR pathway (115). Inhibition of Wnt and Notch signaling dramatically reduces *E. chaffeensis* infection demonstrating the importance of the conserved cell signaling pathways for persistent infection

and survival (105, 118). Notably, *E. chaffeensis* hijacks the canonical and non-canonical Wnt signaling pathways *via* effector proteins to promote infection (58). In addition, nucleomodulins TRP32, TRP47, and TRP120 bind DNA motifs within the promoter regions of Wnt target genes and may modulate Wnt gene transcription (118). Furthermore, yeast-two-hybrid (Y2H) analysis has identified protein-protein interactions between *E. chaffeensis* effector proteins (TRP32 and TRP120) and host proteins involved in Wnt signaling and transcriptional regulation of Wnt genes (99, 101). Of those identified, were interactions with Wnt signaling negative regulators (CEP164, KLHL12, ILF3 and LMO2) and positive regulators (PPP3R1 and VPS29) (99, 101).

TRP120 interaction with the host cell facilitates entry and this appears to occur *via* activation of non-canonical Wnt signaling resulting in Ca^{2+} signaling and triggering uptake through phagocytosis (118). Wnt signaling has been shown to enhance infection as RNA silencing of Wnt signaling components, including β-catenin, NFAT, CK1, and CAMKII significantly reduces *E. chaffeensis* infection, indicating that Wnt signaling is required to maintain infection (118). RNA silencing of the ubiquitously expressed Fzd5 and Fzd9 Wnt receptors, as well as the Wnt co-receptor LRP6 also results in reduced infection, indicating a possible role of the receptors for *E. chaffeensis* entry into the host. More specifically, RNA silencing of Fzd5 or its ligand Wnt5a results in a highly significant reduction of infection, suggesting the necessity of Wnt5a-Fzd5 signaling for *E. chaffeensis* entry and survival.

The Notch signaling pathway is an evolutionarily conserved pathway with critical roles in cellular homeostasis, cell proliferation and differentiation; however, Notch activation has also been shown to have significant roles in MHC class II expansion, B and T cell development, and regulation of innate immune mechanisms such as autophagy and apoptosis (119). Recently, Notch activation by *E. chaffeensis* was shown to downregulate TLR2/4 expression (105). Interestingly, TRP120 was identified as a Notch ligand mimic resulting in Notch activation as shown by nuclear translocation of the Notch intracellular domain (NICD), a hallmark for Notch activation. TRP120 is also a HECT E3 ubiquitin ligase that ubiquitinates Notch negative regulator FBW7 for proteasomal degradation resulting in increased oncoproteins levels including induced myeloid leukemia cell differentiation protein (MCL1) and NICD (107). Collectively, the data demonstrate that exploitation of conserved signaling pathways, such as Wnt and Notch is a major strategy involved in ehrlichial survival and possibly other members of the *Anaplasmataceae* family by modulating autophagy and other innate host defense mechanism.

ANAPLASMATACEAE EFFECTOR-INDUCED AUTOPHAGY FOR NUTRIENT ACQUISITION

Anaplasmataceae are auxotrophic with a limited capacity to synthesize required nutrients for survival, and thus, obtain essential nutrients from the host cell. Both *A. phagocytophilum* and *E. chaffeensis* survive by replicating within a host cell-derived membrane bound vacuole. Autophagosomes are induced by *E. chaffeensis* and *A. phagocytophilum* secreted T4SS effector proteins, Etf-1 and Ats-1, respectively (67, 94) (**Figures 1** and **2**). Etf-1 and Ats-1 are secreted into the host cell cytoplasm where they nucleate autophagosome formation. This effector-induced autophagosome formation is independent of mTOR activity. Ultimately, the effector generated autophagosomes fuse with the pathogen occupied vacuoles to deliver host-derived components. Ats-1 and Etf-1 induce autophagy in a class III PtdIns3K-dependent manner and localize to inclusions with autophagosomal markers. *A. phagocytophilum* inclusions colocalize with early autophagosomal markers Beclin 1 and Vps34-Atg14 and are enveloped by double-lipid bilayer membranes (**Figure 1**) (94). Furthermore, Ats-1 directly binds to Beclin 1 and induces autophagosome formation in an ATG14 dependent manner (53); however, no interaction appears to occur with Ats-1 and UVRAG, an autophagy protein that regulates autophagosome maturation.

Studies have shown that *E. chaffeensis* autophagosome nucleation is dependent on Rab5-GTP and Rab5-regulated trafficking for the biogenesis of *E. chaffeensis* vacuoles (**Figure 2**) (89). Etf-1 is known to bind Rab5, Beclin 1 and phosphatidylinositol 3-kinase (PI3KC3) to induce Rab5-regulated autophagy. Furthermore, *E. chaffeensis* ATG5 and Etf-1 were shown to localize to the membrane of inclusions and are essential for infection (54). Importantly, Etf-1 activates class III PtdIns3K, localizes with ATG5 and LC3, and interacts with RAB5-GTP, PI3CK and Beclin 1 to form a multimeric complex that fuses with *E. chaffeensis* inclusions. Collectively, these findings show that Etf-1 facilitates induction of RAB5-GTP autophagy through PI3CK and Beclin 1 recruitment, as well as class III PtdIns3K and ATG5 localization to *E. chaffeensis* inclusions. Importantly, *Ehrlichia*-containing vacuoles contain the late endosomal marker RAB7, as shown by mass spectrometry and confocal microscopy, but do not fuse with lysosomes (**Figure 2**) (120, 121).

O. tsutsugamshi induces autophagy during infection but actively escapes from autophagic destruction in dendritic cells (122). *O. tsutsugamshi* significantly increased endogenous LC3-II protein levels in phagocytic and nonphagocytic cells during early infection, however no significant colocalization of the bacteria and LC3-postive autophagosomes occurs (122, 123). Autophagy induction does not affect growth of *O. tsutsugamshi* as demonstrated by 3MA or rapamycin (autophagy inducer) treatment or use of atg3-knockout mouse embryonic fibroblasts ($Atg3^{-/-}$ MEFs) (123). Therefore, unlike *E. chaffeensis* and *A. phagocytophilum, O. tsutsugamshi* induces autophagy; however, evades autophagosomal degradation by actively escaping from host autophagosomes. Currently, the mechanism of evasion is unknown, but is predicted to be mediated by bacterial gene expression or bacterial effector proteins.

While some pathogens hijack the autophagic pathway to replicate intracellularly, pathogens of the *Anaplasmataceae*

family exploit autophagy and specific ATG proteins to acquire nutrients. However, exactly how pathogens of the *Anaplasmataceae* family manipulate autophagy proteins for exploitation is still unknown. Ats-1 and Etf-1 are orthologous proteins that may subvert autophagy through a similar sequence to exploit specific autophagy proteins important for nutrient acquisition (124). Additionally, some bacteria escape host autophagy through inhibition of autophagy induction. For example, *S. Typhimurium* inhibits autophagy initiation through regulation of the AMPK-dependent activation pathway of mTOR, while *M. tuberculosis* inhibits autophagy induction by disruption of JNK-ROS (reactive oxygen species) signaling pathway to avoid destruction (34, 36). In comparison, both *A. phagocytophilum* and *E. chaffeensis*, induce autophagy independent of mTOR to acquire nutrients and remodel their vacuoles. This mechanism is regulated by T4SS effector proteins regulating key host autophagy proteins involved in the initiation step of autophagy.

ANAPLASMATACEAE PREVENT ENDOSOMAL MATURATION TO AVOID LYSOSOMAL FUSION

E. chaffeensis occupied vacuoles have features of early endosomes including RAB5, transferrin receptor (TFRC), early endosome antigen 1 (EEA1), annexins I, II, IV and VI, clathrin heavy chain and α-adaptin (67, 121, 125). *A. phagocytophilum* selectively recruits Rab GTPases to avoid endosomal maturation and subsequent destruction by lysosomes (**Figure 1**) (126). *A. phagocytophilum* selectively recruits Rab GTPases that are primarily associated with recycling endosomes, including Rab4a, Rab10, Rab11A, Rab14, Rab22A and Rab35. Rab1 which mediates endoplasmic reticulum to Golgi apparatus trafficking, is also recruited to the *A. phagocytophilum* vacuoles (ApV). Selectivity of Rab GTPases is shown to be dependent on *A. phagocytophilum* protein synthesis, allowing the ApV to disguise itself as a host recycling endosome. Importantly, the ApV does not mature along the endocytic pathway or resemble early endosomes due to the lack of endosomal markers including RAB5, transferrin receptor (TFRC), early endosome antigen 1 (EEA1), annexins I, II, IV and VI, clathrin heavy chain and α-adaptin (127). Additionally, *A. phagocytophilum* inclusions are not acidic and do not acquire the late endosomal markers, including myeloperoxidase, CD63, LAMP-1 and V-type H+ ATPase. Therefore, *A. phagocytophilum* hijacks Rab GTPases and host cell membrane traffic pathways to disguise the ApV as a recycling endosome to avoid endosomal maturation and subsequent lysosomal fusion.

Etf-2, another T4SS *E. chaffeensis* secreted protein effector, localizes to *E. chaffeensis* vacuoles, binds to RAB5-GTP and delays endosome maturation (**Figure 2**) (21). Etf-2 contains a Tre2-Bub2-Cdc16 (TBC) domain lacking Rab-GTPase activity, as well as an Arg and a Gln finger motif required for Etf-2 localization to the endosomal membrane, resulting in delayed maturation of phagosomes to phagolysosomes. EtpE is an *E. chaffeensis* outer membrane protein that functions as an invasion to mediate host cell entry. The C-terminal fragment of EtpE (EtpE-C) appears to be primarily responsible for *E. chaffeensis* binding and entry. The phagocytosis of EtpE-C-coated latex beads in Etf-2-GFP transfected cells was significantly reduced in comparison to GFP-transfected control cells. RAB5, but not RAB7, was shown to localize to a significant amount of EtpE-C-coated latex bead containing phagosomes for a prolonged period, and no late endosomes and phagolysosomes were detected in Etf-2-GFP transfected cells, indicating delayed endosomal maturation. Etf-2 also prevents RABGAP5 localization to endosomes (95). Therefore, Etf-2 participates in blocking endosomal maturation and fusion with lysosomes to promote ehrlichial infection. Other pathogens have been shown to selectively block maturation of autophagosomes through various mechanisms, including avoidance of RAB7 recruitment (69, 128–131). Importantly, studies have indicated that Rab7 is essential for autophagosome maturation in general (132). Selective modulation of RAB5 function by *E. chaffeensis* Etf-2 leading to alterations in the autophagosome explains the selectivity in autophagosome maturation. In comparison, how the ApV recruits and hijacks specific Rab-GTPases is still unknown. Identification of *A. phagocytophilum* effector proteins that interact with Rab-GTPases associated with the ApV is critical.

Preventing lysosomal fusion is a common strategy that underlies pathogen survival. *A. phagocytophilum and E. chaffeensis* vacuoles fuse with autophagosomes to form intermediate organelles. *E. chaffeensis* intermediate organelles have been described as amphisomes (**Figures 1** and **2**) (21, 98). Autophagosome markers Beclin 1 and LC3/GABARAP were found to colocalize with ehrlichial vacuoles indicating the fusion between autophagosomes and inclusions. Curiously, differences in LC3II localization to *E. chaffeensis* vacuoles have been reported. Rikihisa et al. reported no LC3II localization to ehrlichial vacuoles in RF/6A cells; however, others have detected ehrlichial vacuole localization with LC3/GABARAP in both THP-1 and RF/6A *E. chaffeensis*-infected cells (95). Moreover, significant increases in LC3II levels were observed during infection and consistent with those reported for *A. phagocytophilum*. Notably, colocalization of the *A. phagocytophilum* and *E. chaffeensis* inclusions with lysosomal markers, including LAMP-1 and LAMP-2 were not detected. Increased p62/SQSTM1 levels were also detected in *E. chaffeensis*-infected cells in comparison to control cells, as another indication of inhibited lysosomal fusion. Collectively, *Anaplasmataceae* pathogens induce autophagy for nutrient acquisition but inhibit lysosomal maturation through selective recruitment and avoidance of specific Rab GTPases.

EHRLICHIA-EXPLOITATION OF WNT SIGNALING TO INHIBIT AUTOLYSOSOME GENERATION AND AUTOPHAGIC DESTRUCTION

Wnt and PI3k/Akt pathways are important for ehrlichial survival, and regulation of autophagy by Wnt signaling has

been documented. *E. chaffeensis* utilizes TRP effectors to exploit both the Wnt and PI3k/AKT pathways to activate mTOR signaling and regulate TFEB nuclear translocation to inhibit lysosomal biogenesis and autolysosomal fusion with the pathogen occupied vacuole. *E. chaffeensis* activates the PI3k/Akt pathway, a regulator of mTOR (**Figure 2**) (21). PI3K/Akt phosphorylates various proteins involved in regulation of cellular processes such as proliferation, apoptosis, and autophagy (133). Phosphorylated PI3K and Akt levels increase in *E. chaffeensis* infected cells, while phosphatase and tensin homolog (PTEN), a PI3K/Akt pathway inhibitor, levels decrease (21). The role of mTOR signaling in ehrlichial infection was also confirmed by siRNA knockdown of Rheb, a GTPase that activates mTOR. siRNA knockdown of both Rheb and phospho-p70 S6 kinase decreased *E. chaffeensis* infection (21). Thus, the mTOR activity is required for *E. chaffeensis* survival.

The Wnt signaling also regulates the PI3K/Akt pathway. GSK3-β is as a common protein and mediates crosstalk between PI3K/Akt and Wnt signaling pathways. More specifically, GSK3-β regulates mTOR by induction of Tuberous Sclerosis 2 Protein (TSC2) through phosphorylation and is also a negative regulator of Wnt/β-catenin (22, 134–136). Increased levels of GSK3-β were detected in -infected cells. These effects were abrogated with treatment of a Wnt-Dvl inhibitor (21). Additionally, inhibition of Akt and induction of GSK3 resulted in a significant decrease in infected cells at early and late infection intervals. Increased levels of phospho-GSK3-β were shown to be stimulated by T1SS effectors TRP120 and TRP32 (21). Therefore, TRP effectors activate the

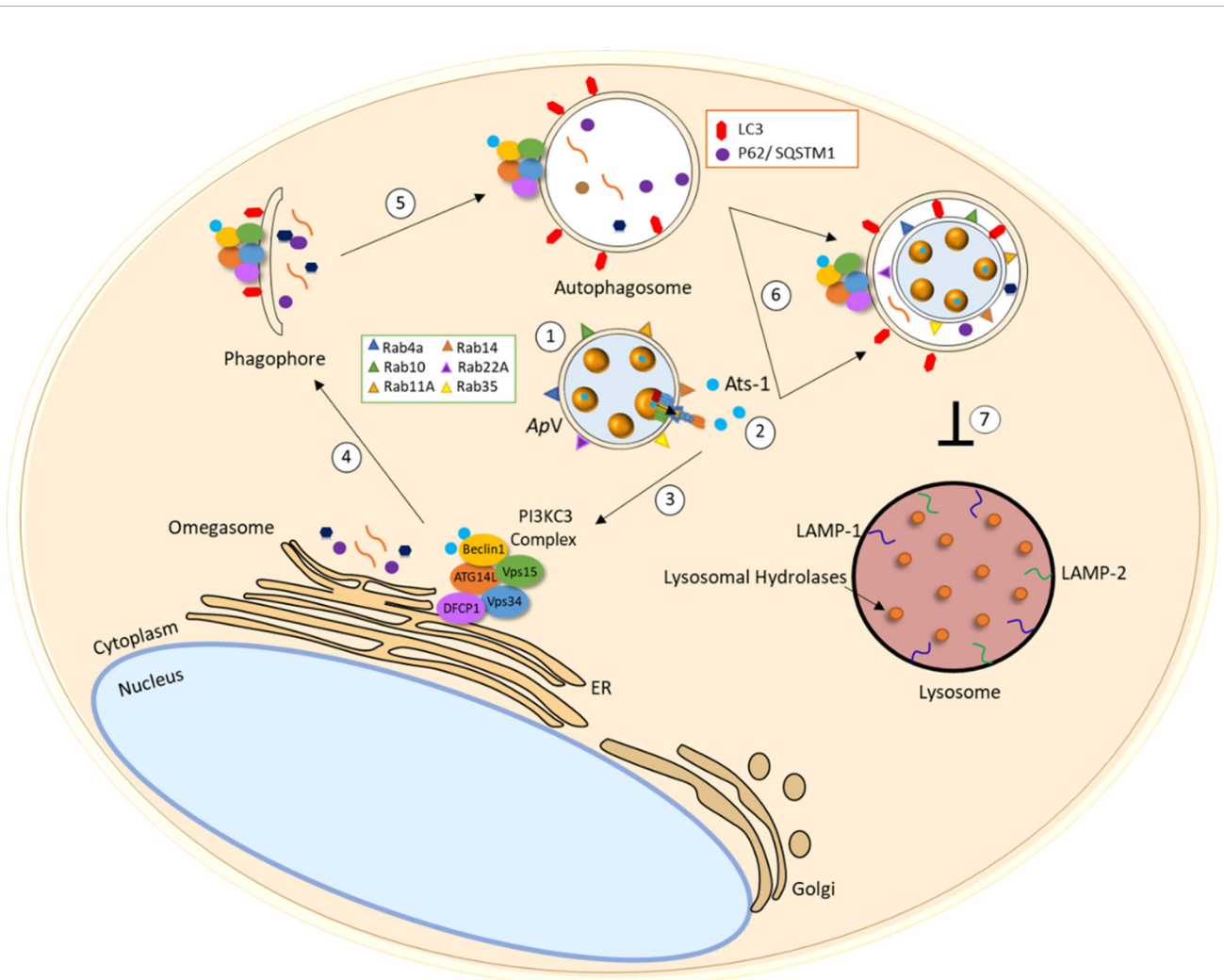

FIGURE 1 | *A. phagocytophilum* interplay with the autophagic pathway. (1) *A. phagocytophilum* selectively recruits Rab GTPases Rab4A, Rab10, Rab11A, Rab14, Rab22A, Rab35 which regulate endocytic recycling and Rab1 which regulates vesicular protein transport from the endoplasmic reticulum (ER) to the Golgi compartment. (2) T4SS effector Ats-1 is translocated from the ApV into the host cell cytoplasm and (3) directly interacts with autophagsome initiation complex (Atg14-Beclin 1-Vps34) to initiate omegasome formation in the ER. (4) Isolation membrane elongates and (5) double-membrane autophagosome decorated with LC3 form. (6) Autophagosomes are recruited to the ApV that fuse to release autophagic body content. (7) *A. phagocytopilum* blocks lysosomal fusion potentially by preventing endosomal maturation and/or through other unknown mechanisms.

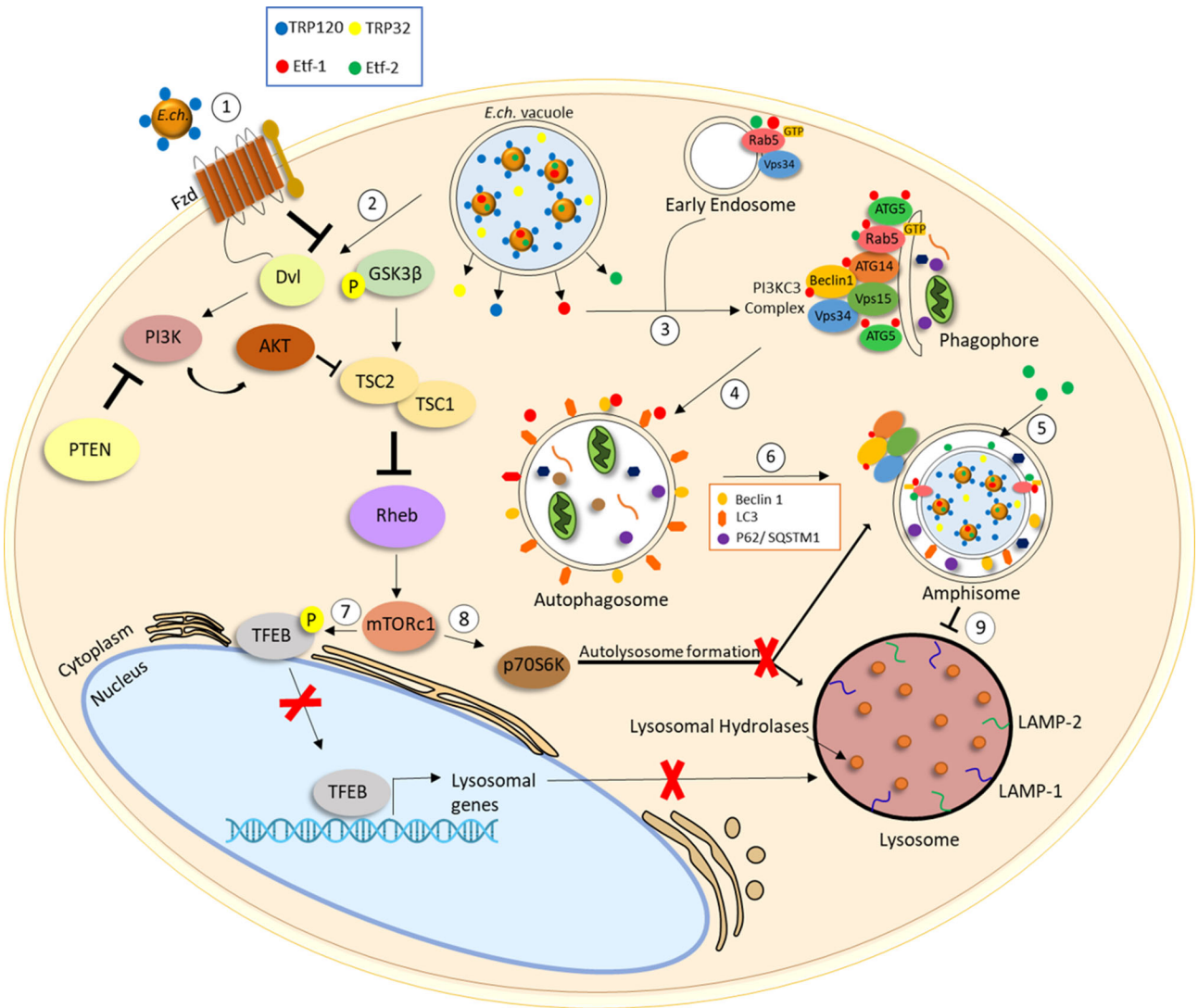

FIGURE 2 | *E. chaffeensis* interplay with the autophagic pathway. (1) *E. chaffeensis* dense-cored cells express effectors important for Wnt signaling including T1SS effectors TRP120 and TRP32. *E. chaffeensis* stimulates phagocytosis for entry through interaction between TRP120 and the Fzd receptor/co-receptor complex. (2) *E. chaffeensis*-mediated Wnt-PI3K/Akt signaling stimulates increased levels of phospho-GSK3-β reducing TSC2 and increasing Rheb activity leading to mTOR activation. (3) *E. chaffeensis* T4SS effector Etf-1 is secreted into the host cell cytoplasm and interacts with Beclin1, PI3CK complex and Rab5-GTP to stimulate phagophore formation. (4) ATG5 and LC3 engage to induce autophagosome formation in a class III PtdIns3K-dependent manner. (5) *E. chaffeensis* T4SS effector Etf-2 localizes to *E. chaffeensis* vacuole membrane and binds to RAB5-GTP to delay endosome maturation. (6) Autophagosomes displaying Beclin1, LC3II and p62/SQSTM1 fuse with *E. chaffeensis* inclusions to form amphisomes. (7) mTOR activation leads to TFEB phosphorylation and inhibition of TFEB nuclear translocation. Inhibition of TFEB nuclear translocation prevents transcription of genes involved in lysosomal biogenesis and (8) increased phospho-p70 S6 kinase activity inhibits autolysosome formation.

PI3K/Akt pathway and inhibit GSK3 activity by phosphorylation. Decreased levels of TSC2 were also shown in *E. chaffeensis*-infected cells. Collectively, these findings demonstrate activation of the PI3K/Akt pathway, phosphorylation and inactivation of GSK3 and inhibition of TSC2 during *E. chaffeensis* infection.

Phosphorylation and inactivation of GSK3, as well as inhibition of TSC2, results in activation of mTORC1 and subsequent phosphorylation and inhibition of TFEB nuclear translocation. TFEB is a transcription factor that coordinates expression of lysosomal hydrolases, membrane proteins and genes involved in autophagy signaling (**Figure 2**). TFEB was demonstrated to remain localized in the cytoplasm during *E. chaffeensis* infection and was confirmed to be mediated by *E. chaffeensis* Wnt activation. These finding support the conclusion that *E. chaffeensis* exploits Wnt-PI3K-/mTOR signaling in part to regulate mTOR signaling and TFEB nuclear localization to inhibit autolysosomal generation and promote ehrlichial survival.

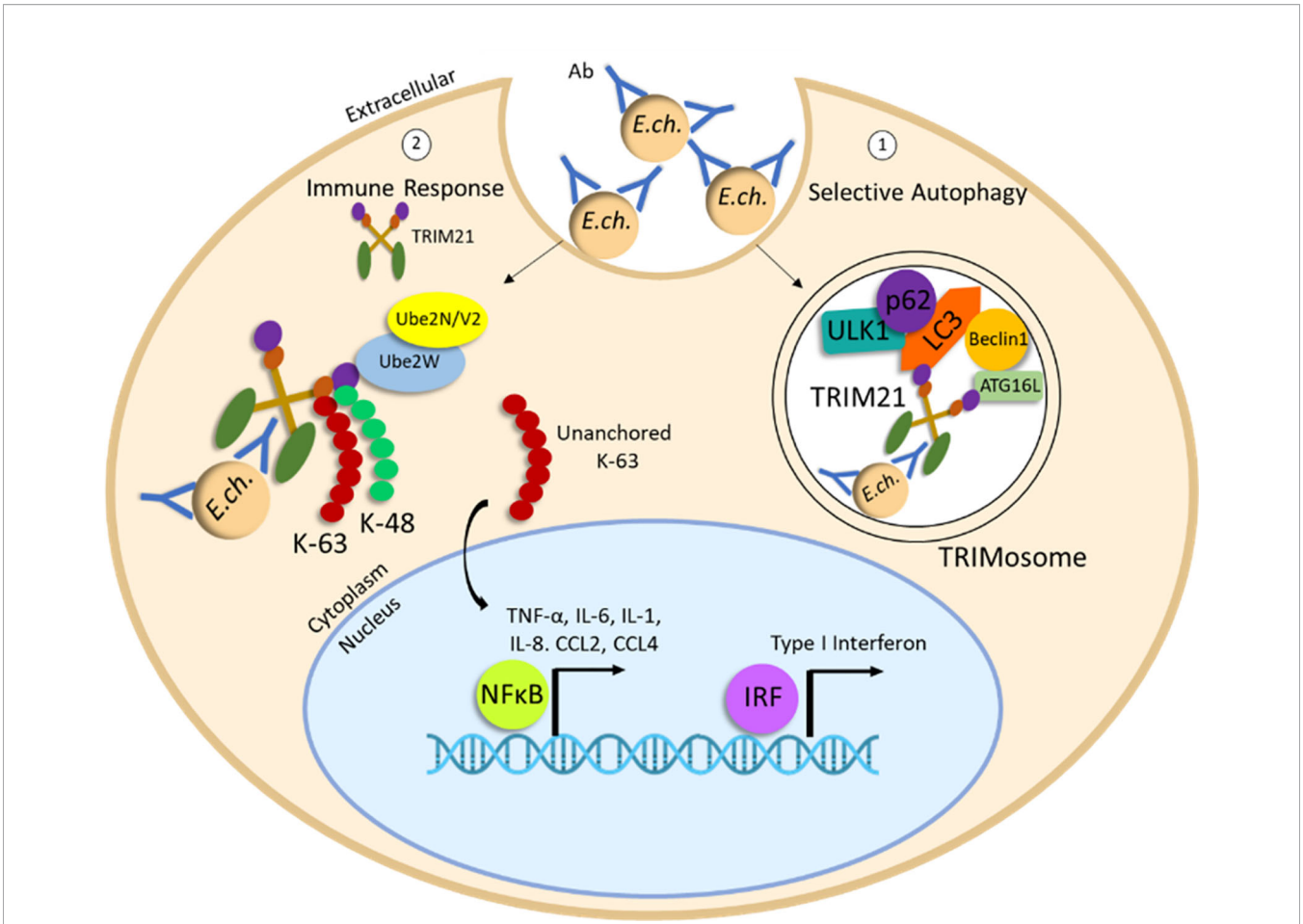

FIGURE 3 | Degradation of *E. chaffeensis* by antibody-TRIM21-mediated selective autophagy. Ehrlichiae opsonized with *E. chaffeensis*-OMP-1 specific antibody are internalized by unknown uptake mechanism. Intracellular antibody-opsonized ehrlichiae are recognized by cytosolic Fc receptor TRIM21. (1) Induction of TRIMosome formation and selective autophagy occurs through recruitment of autophagy regulators, ULK1, Beclin 1, ATG16L and autophagy effectors LC3/GABARAP and p62/SQSTM1. (2) *E. chaffeensis*-Ab/TRIM21 complex stimulates rapid immune signaling and a proinflammatory response through accumulation of K48 and K63 polyUb chains and activation and nuclear translocation of NF-κB and IRF.

Various studies have demonstrated the inhibition of autolysosome generation and autophagic destruction. *M. tuberculosis* inhibits Rab7 recruitment on Mtb-containing autophagosomes, while other pathogens neutralize lysosomal pH (69, 131, 137). This is the first study to elucidate the mechanism of *E. chaffeensis* inhibition of lysosomal fusion and, ultimately, destruction in the autolysosome. *E. chaffeensis* modulating conserved signal transduction pathways, including Wnt and Notch, to inhibit autolysosome generation may be applicable to other *Anaplasmataceae* bacterial pathogens.

EHRLICHIA SELECTIVE AUTOPHAGIC DESTRUCTION MEDIATED BY ANTIBODY-TRIM21 COMPLEX

Antibody-mediated immunity to *E. chaffeensis* is well documented involving the classical antibody Fc receptor-dependent mechanism (**Figure 3**). However, intracellular antibody opsonized *E. chaffeensis* complexes engage TRIM21, an intracellular Fc receptor (138). Antibody opsonized ehrlichiae-TRIM21 complexes recruit autophagy regulators, ULK1, Beclin 1 and autophagy effectors LC3/GABARAP and p62/SQSTM1 resulting in proinflammatory responses and localized selective autophagic degradation of the ehrlichiae-antibody complexes. These findings demonstrate the importance of autophagy engagement of adaptive immune mechanisms and provide the first example of autophagic elimination of an intracellular pathogen by a TRIM21-mediated mechanism.

CONCLUSIONS AND FUTURE DIRECTIONS

Obligately intracellular pathogens of the *Anaplasmataceae* family have evolved highly sophisticated strategies to circumvent host immune response during infection. Autophagy is a cellular process targeted by microbial pathogens to promote infection.

Mechanisms used by *Anaplasmataceae* for dichotomous engagement and subversion of autophagy for intracellular survival provides insight into the interplay that exists between the autophagic pathway and intracellular pathogens. Common amongst members of *Anaplasmataceae* are effector-mediated initiation of autophagy and the ability to hijack autophagy (ATG) proteins responsible for initiation and activation of the autophagic process. In contrast, effector interference with endosomal maturation contributes to pathogen survival. The ability to inhibit lysosomal destruction is a common theme demonstrated by *Anaplasmataceae*. This mechanism involves activation of cellular pathways such as Wnt and altering the pathogen vacuole to prevent lysosomal biogenesis and autolysosome generation. Studies to understand how *Anaplasmataceae* exploit the autophagic process may provide new insight; however, it is still unclear how intracellular pathogens out-compete the host for autophagy by-products and how autophagy by-products are obtained by *Anaplasmataceae* pathogens. It is also important to note that autophagy is an anti-inflammatory process, and it is therefore possible that Anaplasmataceae bacterial pathogens may strive to inhibit inflammation through activation of the autophagic pathway. Furthermore, very few details on the specific mechanisms that enable *A. phagocytophilum* and *O. tsutsugamshi* escape destruction by autophagy have been elucidated and need further investigation. Understanding mechanisms involved in autophagy induction and inhibition will inevitably help define how intracellular microbes exploit autophagy and could lead to novel antimicrobial therapeutic approaches.

DATA AVAILABILITY STATEMENT

The original contributions presented in the study are included in the article/supplementary material. Further inquiries can be directed to the corresponding author.

AUTHOR CONTRIBUTIONS

LP and JM conceptualized the work. LP gathered information and contributed all sections. CB contributed to sections pertaining to *O. tsutsugamushi* and exploitation of Wnt signaling. LP performed artwork. All authors contributed to the article and approved the submitted version.

FUNDING

This work was supported by the National Institutes of Health grants AI149136, AI137779, and AI123610 awarded to JM, NIH 1F31AI152424-01 fellowship to LP, and T32AI007526-20 biodefense training fellowship to CB.

REFERENCES

1. Huang J, Brumell JH. Bacteria-autophagy interplay: a battle for survival. *Nat Rev Microbiol* (2014) 12(2):101–14. doi: 10.1038/nrmicro3160
2. Ravenhill BJ, Boyle KB, von Muhlinen N, Ellison CJ, Masson GR, Randow F, et al. The Cargo Receptor NDP52 Initiates Selective Autophagy by Recruiting the ULK Complex to Cytosol-Invading Bacteria. *Mol Cell* (2019) 74(2):320–29.e6. doi: 10.1016/j.molcel.2019.01.041
3. Thurston TL, Wandel MP, von Muhlinen N, Foeglein A, Randow F. Galectin 8 targets damaged vesicles for autophagy to defend cells against bacterial invasion. *Nature* (2012) 482(7385):414–8. doi: 10.1038/nature10744
4. Xu Y, Jagannath C, Liu XD, Sharafkhaneh A, Kolodziejska KE, Eissa NT. Toll-like receptor 4 is a sensor for autophagy associated with innate immunity. *Immunity* (2007) 27(1):135–44. doi: 10.1016/j.immuni.2007.05.022
5. Yuk JM, Yoshimori T, Jo EK. Autophagy and bacterial infectious diseases. *Exp Mol Med* (2012) 44(2):99–108. doi: 10.3858/emm.2012.44.2.032
6. Gomes, Ligia C, Dikic I. Autophagy in Antimicrobial Immunity. *Mol Cell* (2014) 54(2):224–33. doi: 10.1016/j.molcel.2014.03.009
7. Mao K, Klionsky DJ. Xenophagy: A battlefield between host and microbe, and a possible avenue for cancer treatment. *Autophagy* (2017) 13(2):223–4. doi: 10.1080/15548627.2016.1267075
8. Mitchell G, Isberg RR. Innate Immunity to Intracellular Pathogens: Balancing Microbial Elimination and Inflammation. *Cell Host Microbe* (2017) 22(2):166–75. doi: 10.1016/j.chom.2017.07.005
9. Klionsky DJ, Cuervo AM, Dunn WAJr, Levine B, van der Klei I, Seglen PO. How shall I eat thee? *Autophagy* (2007) 3(5):413–6. doi: 10.4161/auto.4377
10. Levine B, Kroemer G. Biological Functions of Autophagy Genes: A Disease Perspective. *Cell* (2019) 176(1-2):11–42. doi: 10.1016/j.cell.2018.09.048
11. Mizushima N. Autophagy: process and function. *Genes Dev* (2007) 21 (22):2861–73. doi: 10.1101/gad.1599207
12. Mizushima N. A brief history of autophagy from cell biology to physiology and disease. *Nat Cell Biol* (2018) 20(5):521–7. doi: 10.1038/s41556-018-0092-5
13. Nakatogawa H. Mechanisms governing autophagosome biogenesis. *Nat Rev Mol Cell Biol* (2020) 21(8):439–58. doi: 10.1038/s41580-020-0241-0
14. Wen X, Klionsky DJ. An overview of macroautophagy in yeast. *J Mol Biol* (2016) 428(9 Pt A):1681–99. doi: 10.1016/j.jmb.2016.02.021
15. Guo H, Yang Y, Feng M, Liu B, Ren X, Zhou H. Autophagy modulation in bladder cancer development and treatment (Review). *Oncol Rep* (2019) 42 (5):1647–55. doi: 10.3892/or.2019.7286
16. Yuan HX, Russell RC, Guan KL. Regulation of PIK3C3/VPS34 complexes by MTOR in nutrient stress-induced autophagy. *Autophagy* (2013) 9(12):1983–95. doi: 10.4161/auto.26058
17. Ma X, Zhang S, He L, Rong Y, Brier LW, Sun Q, et al. MTORC1-mediated NRBF2 phosphorylation functions as a switch for the class III PtdIns3K and autophagy. *Autophagy* (2017) 13(3):592–607. doi: 10.1080/15548627.2016.1269988
18. Manning BD, Cantley LC. AKT/PKB signaling: navigating downstream. *Cell* (2007) 129(7):1261–74. doi: 10.1016/j.cell.2007.06.009
19. Ma T, Tzavaras N, Tsokas P, Landau EM, Blitzer RD. Synaptic stimulation of mTOR is mediated by Wnt signaling and regulation of glycogen synthetase kinase-3. *J Neurosci* (2011) 31(48):17537–46. doi: 10.1523/JNEUROSCI.4761-11.2011
20. Petherick KJ, Williams AC, Lane JD, Ordóñez-Morán P, Huelsken J, Collard TJ, et al. Autolysosomal beta-catenin degradation regulates Wnt-autophagy-p62 crosstalk. *EMBO J* (2013) 32(13):1903–16. doi: 10.1038/emboj.2013.123
21. Lina TT, Luo T, Velayutham TS, Das S, McBride JW. *Ehrlichia* activation of Wnt-PI3K-mTOR signaling inhibits autolysosome generation and autophagic destruction by the mononuclear phagocyte. *Infect Immun* (2017) 85(12). doi: 10.1128/IAI.00690-17
22. Inoki K, Ouyang H, Zhu T, Lindvall C, Wang Y, Zhang X, et al. TSC2 integrates Wnt and energy signals via a coordinated phosphorylation by AMPK and GSK3 to regulate cell growth. *Cell* (2006) 126(5):955–68. doi: 10.1016/j.cell.2006.06.055
23. Zhang H, Cicchetti G, Onda H, Koon HB, Asrican K, Bajraszewski N, et al. Loss of Tsc1/Tsc2 activates mTOR and disrupts PI3K-Akt signaling through

downregulation of PDGFR. *J Clin Invest* (2003) 112(8):1223–33. doi: 10.1172/JCI200317222
24. Lee JW, Park S, Takahashi Y, Wang HG. The association of AMPK with ULK1 regulates autophagy. *PLoS One* (2010) 5(11):e15394. doi: 10.1371/journal.pone.0015394
25. Sica V, Galluzzi L, Bravo-San Pedro JM, Izzo V, Maiuri MC, Kroemer G. Organelle-Specific Initiation of Autophagy. *Mol Cell* (2015) 59(4):522–39. doi: 10.1016/j.molcel.2015.07.021
26. Mizushima N, Yoshimori T, Ohsumi Y. The role of Atg proteins in autophagosome formation. *Annu Rev Cell Dev Biol* (2011) 27:107–32. doi: 10.1146/annurev-cellbio-092910-154005
27. Kang R, Zeh HJ, Lotze MT, Tang D. The Beclin 1 network regulates autophagy and apoptosis. *Cell Death Differ* (2011) 18(4):571–80. doi: 10.1038/cdd.2010.191
28. He C, Klionsky DJ. Regulation mechanisms and signaling pathways of autophagy. *Annu Rev Genet* (2009) 43:67–93. doi: 10.1146/annurev-genet-102808-114910
29. Harada K, Kotani T, Kirisako H, Sakoh-Nakatogawa M, Oikawa Y, Kimura Y, et al. Two distinct mechanisms target the autophagy-related E3 complex to the pre-autophagosomal structure. *Elife* (2019) 8. doi: 10.7554/eLife.43088
30. Pankiv S, Clausen TH, Lamark T, Brech A, Bruun JA, Outzen H, et al. p62/SQSTM1 binds directly to Atg8/LC3 to facilitate degradation of ubiquitinated protein aggregates by autophagy. *J Biol Chem* (2007) 282 (33):24131–45. doi: 10.1074/jbc.M702824200
31. Tsuchiya M, Ogawa H, Koujin T, Mori C, Osakada H, Kobayashi S. p62/SQSTM1 promotes rapid ubiquitin conjugation to target proteins after endosome rupture during xenophagy. *FEBS Open Bio* (2018) 8(3):470–80. doi: 10.1002/2211-5463.12385
32. Berg TO, Fengsrud M, Strømhaug PE, Berg T, Seglen PO. Isolation and characterization of rat liver amphisomes. Evidence for fusion of autophagosomes with both early and late endosomes. *J Biol Chem* (1998) 273(34):21883–92. doi: 10.1074/jbc.273.34.21883
33. Glick D, Barth S, Macleod KF. Autophagy: cellular and molecular mechanisms. *J Pathol* (2010) 221(1):3–12. doi: 10.1002/path.2697
34. Ganesan R, Hos NJ, Gutierrez S, Fischer J, Stepek JM, Daglidu E, et al. *Salmonella Typhimurium* disrupts Sirt1/AMPK checkpoint control of mTOR to impair autophagy. *PLoS Pathog* (2017) 13(2):e1006227. doi: 10.1371/journal.ppat.1006227
35. Dong N, Zhu Y, Lu Q, Hu L, Zheng Y, Shao F. Structurally distinct bacterial TBC-like GAPs link Arf GTPase to Rab1 inactivation to counteract host defenses. *Cell* (2012) 150(5):1029–41. doi: 10.1016/j.cell.2012.06.050
36. Shin DM, Jeon BY, Lee HM, Jin HS, Yuk JM, Song CH, et al. *Mycobacterium tuberculosis* eis regulates autophagy, inflammation, and cell death through redox-dependent signaling. *PLoS Pathog* (2010) 6(12):e1001230. doi: 10.1371/journal.ppat.1001230
37. Shahnazari S, Brumell JH. Mechanisms and consequences of bacterial targeting by the autophagy pathway. *Curr Opin Microbiol* (2011) 14 (1):68–75. doi: 10.1016/j.mib.2010.11.001
38. Deretic V, Delgado M, Vergne I, Master S, De Haro S, Ponpuak M. Autophagy in immunity against *Mycobacterium tuberculosis*: a model system to dissect immunological roles of autophagy. *Curr Top Microbiol Immunol* (2009) 335:169–88. doi: 10.1007/978-3-642-00302-8_8
39. Kimmey JM, Huynh JP, Weiss LA, Park S, Kambal A, Debnath J, et al. Unique role for ATG5 in neutrophil-mediated immunopathology during *M. tuberculosis* infection. *Nature* (2015) 528(7583):565–9. doi: 10.1038/nature16451
40. Nakagawa I, Amano A, Mizushima N, Yamamoto A, Yamaguchi H, Kamimoto T, et al. Autophagy defends cells against invading group *A Streptococcus*. *Science* (2004) 306(5698):1037–40. doi: 10.1126/science.1103966
41. Birmingham CL, Canadien V, Gouin E, Troy EB, Yoshimori T, Cossart P, et al. *Listeria monocytogenes* evades killing by autophagy during colonization of host cells. *Autophagy* (2007) 3(5):442–51. doi: 10.4161/auto.4450
42. Wu S, Shen Y, Zhang S, Xiao Y, Shi S. *Salmonella* Interacts With Autophagy to Offense or Defense. *Front Microbiol* (2020) 11:721. doi: 10.3389/fmicb.2020.00721
43. Min CK, Yang JS, Kim S, Choi MS, Kim IS, Cho NH. Genome-based construction of the metabolic pathways of *Orientia tsutsugamushi* and comparative analysis within the Rickettsiales order. *Comp Funct Genomics* (2008) 2008:623145. doi: 10.1155/2008/623145
44. Dumler JS, Barbet AF, Bekker CP, Dasch GA, Palmer GH, Ray SC, et al. Reorganization of genera in the families *Rickettsiaceae* and *Anaplasmataceae* in the order *Rickettsiales*: unification of some species of *Ehrlichia* with *Anaplasma*, *Cowdria* with *Ehrlichia* and *Ehrlichia* with *Neorickettsia*, descriptions of six new species combinations and designation of *Ehrlichia* equi and 'HGE agent' as subjective synonyms of *Ehrlichia phagocytophila*. *Int J Syst Evol Microbiol* (2001) 51(Pt 6):2145–65. doi: 10.1099/00207713-51-6-2145
45. Pruneau L, Lebrigand K, Mari B, Lefrançois T, Meyer DF, Vachiery N. Understanding *Anaplasmataceae* pathogenesis using "Omics" approaches. *Front Cell Infect Microbiol* (2014) 4:86. doi: 10.3389/fcimb.2014.00086
46. McBride JW, Walker DH. Molecular and cellular pathobiology of *Ehrlichia* infection: targets for new therapeutics and immunomodulation strategies. *Expert Rev Mol Med* (2011) 13:e3. doi: 10.1017/S1462399410001730
47. Anderson BE, Sumner JW, Dawson JE, Tzianabos T, Greene CR, Olson JG, et al. Detection of the etiologic agent of human ehrlichiosis by polymerase chain reaction. *J Clin Microbiol* (1992) 30(4):775–80. doi: 10.1128/JCM.30.4.775-780.1992
48. Chen SM, Dumler JS, Bakken JS, Wlaker DH. Identification of a granulocytotropic *Ehrlichia* species as the etiologic agent of human disease. *J Clin Microbiol* (1994) 32(3):589–95. doi: 10.1128/JCM.32.3.589-595.1994
49. Paris DH, Shelite TR, Day NP, Walker DH. Unresolved problems related to scrub typhus: a seriously neglected life-threatening disease. *Am J Trop Med Hyg* (2013) 89(2):301–7. doi: 10.4269/ajtmh.13-0064
50. Valbuena G, Walker DH. Approaches to vaccines against *Orientia tsutsugamushi*. *Front Cell Infect Microbiol* (2012) 2:170. doi: 10.3389/fcimb.2012.00170
51. Dunning Hotopp JC, Lin M, Madupu R, Crabtree J, Angiuoli SV, Eisen JA, et al. Comparative genomics of emerging human ehrlichiosis agents. *PLoS Genet* (2006) 2(2):e21. doi: 10.1371/journal.pgen.0020021
52. Andersson SG, Kurland CG. Reductive evolution of resident genomes. *Trends Microbiol* (1998) 6(7):263–8. doi: 10.1016/S0966-842X(98)01312-2
53. Munderloh UG, Jauron SD, Fingerle V, Leitritz L, Hayes SF, Hautman JM, et al. Invasion and intracellular development of the human granulocytic ehrlichiosis agent in tick cell culture. *J Clin Microbiol* (1999) 37(8):2518–24. doi: 10.1128/JCM.37.8.2518-2524.1999
54. Popov VL, Han VC, Chen SM, Dumler JS, Feng HM, Andreadis TG, et al. Ultrastructural differentiation of the genogroups in the genus *Ehrlichia*. *J. Med. Microbiol* (1998) 47(3):235–51. doi: 10.1099/00222615-47-3-235
55. Troese MJ. *Anaplasma phagocytophilum* dense-cored organisms mediate cellular adherence through recognition of human P-selectin glycoprotein ligand 1. *Infect Immun* (2009) 77(9):4018–27. doi: 10.1128/IAI.00527-09
56. Frutos R, Viari A, Vachiery N, Boyer F, Martinez D. *Ehrlichia ruminantium*: genomic and evolutionary features. *Trends Parasitol* (2007) 23(9):414–9. doi: 10.1016/j.pt.2007.07.007
57. Paddock CD, Childs JE. *Ehrlichia chaffeensis*: a prototypical emerging pathogen. *Clin Microbiol Rev* (2003) 16(1):37–64. doi: doi: 10.1128/cmr.16.1.37-64.2003
58. Lina TT, Farris T, Luo T, Mitra S, Zhu B, McBride JW. Hacker within! *Ehrlichia chaffeensis* effector driven phagocyte reprogramming strategy. *Front Cell Infect Microbiol* (2016) 6:58. doi: doi: 10.3389/fcimb.2016.00058
59. Al-Khedery B, Lundgren AM, Stuen S, Granquist EG, Munderloh UG, Nelson CM, et al. Structure of the type IV secretion system in different strains of *Anaplasma phagocytophilum*. *BMC Genomics* (2012) 13(1):678. doi: 10.1186/1471-2164-13-678
60. Wakeel A, den Dulk-Ras A, Hooykaas PJ, McBride JW. *Ehrlichia chaffeensis* tandem repeat proteins and Ank200 are type 1 secretion system substrates related to the repeats-in-toxin exoprotein family. *Front Cell Infect Microbiol* (2011) 1:22. doi: doi: 10.3389/fcimb.2011.00022
61. VieBrock L, Evans SM, Beyer AR, Larson CL, Beare PA, Ge H, et al. *Orientia tsutsugamushi* ankyrin repeat-containing protein family members are Type 1 secretion system substrates that traffic to the host cell endoplasmic reticulum. *Front Cell Infect Microbiol* (2014) 4:186. doi: 10.3389/fcimb.2014.00186
62. Choy A, Dancourt J, Mugo B, O'Connor TJ, Isberg RR, Melia TJ. The *Legionella* effector RavZ inhibits host autophagy through irreversible Atg8

deconjugation. *Science* (2012) 338(6110):1072–6. doi: 10.1126/science.1227026
63. Itakura E, Kishi-Itakura C, Mizushima N. The hairpin-type tail-anchored SNARE syntaxin 17 targets to autophagosomes for fusion with endosomes/lysosomes. *Cell* (2012) 151(6):1256–69. doi: 10.1016/j.cell.2012.11.001
64. Matsushima N, Yoshida H, Kumaki Y, Kamiya M, Tanaka T, et al. Flexible structures and ligand interactions of tandem repeats consisting of proline, glycine, asparagine, serine, and/or threonine rich oligopeptides in proteins. *Curr Protein Pept Sci* (2008) 9(6):591–610. doi: 10.2174/138920308786733886
65. Li R, Tan S, Yu M, Jundt MC, Zhang S, Wu M. Annexin A2 Regulates Autophagy in *Pseudomonas aeruginosa* Infection through the Akt1-mTOR-ULK1/2 Signaling Pathway. *J Immunol* (2015) 195(8):3901–11. doi: 10.4049/jimmunol.1500967
66. Niu H, Rikihisa Y. Ats-1: a novel bacterial molecule that links autophagy to bacterial nutrition. *Autophagy* (2013) 9(5):787–8. doi: 10.4161/auto.23693
67. Lin M, Liu H, Xiong Q, Niu H, Cheng Z, Yamamoto A. *Ehrlichia* secretes Etf-1 to induce autophagy and capture nutrients for its growth through RAB5 and class III phosphatidylinositol 3-kinase. *Autophagy* (2016) 12(11):2145–66. doi: 10.1080/15548627.2016.1217369
68. Yoshikawa Y, Ogawa M, Hain T, Yoshida M, Fukumatsu M, Kim M, et al. *Listeria monocytogenes* ActA-mediated escape from autophagic recognition. *Nat Cell Biol* (2009) 11(10):1233–40. doi: 10.1038/ncb1967
69. Chandra P, Ghanwat S, Matta SK, Yadav SS, Mehta M, Siddiqui Z, et al. *Mycobacterium tuberculosis* Inhibits RAB7 Recruitment to Selectively Modulate Autophagy Flux in Macrophages. *Sci Rep* (2015) 5:16320. doi: 10.1038/srep16320
70. Bumba L, Masin J, Macek P, Wald T, Motlova L, Bibova I, et al. Calcium-Driven Folding of RTX Domain beta-Rolls Ratchets Translocation of RTX Proteins through Type I Secretion Ducts. *Mol Cell* (2016) 62(1):47–62. doi: 10.1016/j.molcel.2016.03.018
71. Thomas S, Holland IB, Schmitt L. The Type 1 secretion pathway - The hemolysin system and beyond. *Biochim Biophys Acta* (2013) 1843(8):1629–41. doi: 10.1016/j.bbamcr.2013.09.017
72. Green ER, Mecsas J. Bacterial Secretion Systems: An Overview. *Microbiol Spectr* (2016) 4(1). doi:10.1128/microbiolspec.VMBF-0012-2015
73. Spitz O, Erenburg IN, Beer T, Kanonenberg K, Holland IB, Schmitt L. Type I Secretion Systems-One Mechanism for All? *Microbiol Spectr* (2019) 7(2). doi: 10.1128/microbiolspec.PSIB-0003-2018
74. Holland IB, Schmitt L, Young J. Type 1 protein secretion in bacteria, the ABC-transporter dependent pathway (review). *Mol Membr Biol* (2005) 22(1-2):29–39. doi:10.1080/09687860500042013
75. Delepelaire P. Type I secretion in gram-negative bacteria. *Biochim Biophys Acta* (2004) 1694(1-3):149–61. doi:10.1016/j.bbamcr.2004.05.001
76. Luo T, Zhang X, Wakeel A, Popov VL, McBride JW. A variable-length PCR target protein of *Ehrlichia chaffeensis* contains major species-specific antibody epitopes in acidic serine-rich tandem repeats. *Infect Immun* (2008) 76(4):1572–80. doi: 10.1128/IAI.01466-07
77. Luo T, Zhang X, McBride JW. Major species-specific antibody epitopes of the *Ehrlichia chaffeensis* p120 and E. canis p140 orthologs in surface-exposed tandem repeat regions. *Clin Vaccine Immunol* (2009) 16(7):982–90. doi: 10.1128/CVI.00048-09
78. Luo T, Zhang X, Nicholson WL, Zhu B, McBride JW, et al. Molecular characterization of antibody epitopes of *Ehrlichia chaffeensis* ankyrin protein 200 and tandem repeat protein 47 and evaluation of synthetic immunodeterminants for serodiagnosis of human monocytotropic ehrlichiosis. *Clin Vaccine Immunol* (2010) 17(1):87–97. doi: 10.1128/CVI.00331-09
79. Klema VJ, Sepuru KM, Füllbrunn N, Farris TR, Dunphy PS, McBride JW, et al. *Ehrlichia chaffeensis* TRP120 nucleomodulin binds DNA with disordered tandem repeat domain. *PLoS One* (2018) 13(4):e0194891. doi: 10.1371/journal.pone.0194891
80. Farris TR, Dunphy PS, Zhu B, Kibler CE, McBride JW. *Ehrlichia chaffeensis* TRP32 is a nucleomodulin that directly regulates expression of host genes governing differentiation and proliferation. *Infect Immun* (2016) 84(11):3182–94. doi: 10.1128/IAI.00657-16
81. Kibler CE, Milligan SL, Farris TR, Zhu B, Mitra S, McBride JW. *Ehrlichia chaffeensis* TRP47 enters the nucleus via a MYND-binding domain-dependent mechanism and predominantly binds enhancers of host genes associated with signal transduction, cytoskeletal organization, and immune response. *PLoS One* (2018) 13(11):e0205983. doi: 10.1371/journal.pone.0205983
82. Dunphy PS, Luo T, McBride JW. *Ehrlichia* moonlighting effectors and interkingdom interactions with the mononuclear phagocyte. *Microbes Infect* (2013) 15(14-15):1005–16. doi: 10.1016/j.micinf.2013.09.011
83. Wakeel A, Zhang X, McBride JW. Mass spectrometric analysis of *Ehrlichia chaffeensis* tandem repeat proteins reveals evidence of phosphorylation and absence of glycosylation. *PLoS One* (2010) 5(3):e9552. doi: 10.1371/journal.pone.0009552
84. Zhu B, Nethery KA, Kuriakose JA, Wakeel A, Zhang X, McBride JW. Nuclear translocated *Ehrlichia chaffeensis* ankyrin protein interacts with a specific adenine-rich motif of host promoter and intronic Alu elements. *Infect Immun* (2009) 77(10):4243–55. doi: 10.1128/IAI.00376-09
85. Beyer AR, VieBrock L, Rodino KG, Miller DP, Tegels BK, Marconi RT, Carlyon JA. *Orientia tsutsugamushi* Strain Ikeda Ankyrin Repeat-Containing Proteins Recruit SCF1 Ubiquitin Ligase Machinery via Poxvirus-Like F-Box Motifs. *J Bacteriol* (2015) 197(19):3097–109. doi: 10.1128/JB.00276-15
86. Evans SM, Rodino KG, Adcox HE, Carlyon JA. *Orientia tsutsugamushi* uses two Ank effectors to modulate NF-kappaB p65 nuclear transport and inhibit NF-kappaB transcriptional activation. *PLoS Pathog* (2018) 14(5):e1007023. doi: 10.1371/journal.ppat.1007023
87. Fronzes R, Christie PJ, Waksman G. The structural biology of type IV secretion systems. *Nat Rev Microbiol* (2009) 7(10):703–14. doi: 10.1038/nrmicro2218
88. Berge C, Waksman G, Terradot L. Structural and Molecular Biology of Type IV Secretion Systems. *Curr Top Microbiol Immunol* (2017) 413:31–60. doi: 10.1007/978-3-319-75241-9_2
89. Chandran Darbari V, Waksman G. Structural Biology of Bacterial Type IV Secretion Systems. *Annu Rev Biochem* (2015) 84:603–29. doi: 10.1146/annurev-biochem-062911-102821
90. Fronzes R, Schäfer E, Wang L, Saibil HR, Orlova EV, Waksman G. Structure of a type IV secretion system core complex. *Science* (2009) 323(5911):266–8. doi: 10.1126/science.1166101
91. Bundock P, Meaney RS, Hamadache S, Janakirama P, Edgell DR, Karas BJ. Trans-kingdom T-DNA transfer from *Agrobacterium tumefaciens* to *Saccharomyces cerevisiae*. *EMBO J* (1995) 14(13):3206–14. doi: 10.1002/j.1460-2075.1995.tb07323.x
92. Gillespie JJ, Ammerman NC, Dreher-Lesnick SM, Rahman MS, Worley MJ, Setubal JC, et al. An anomalous type IV secretion system in *Rickettsia* is evolutionarily conserved. *PLoS One* (2009) 4(3):e4833. doi: 10.1371/journal.pone.0004833
93. Liu H, Bao W, Lin M, Niu H, Rikihisa Y. *Ehrlichia* type IV secretion effector ECH0825 is translocated to mitochondria and curbs ROS and apoptosis by upregulating host MnSOD. *Cell Microbiol* (2012) 14(7):1037–50. doi: 10.1111/j.1462-5822.2012.01775.x
94. Niu H, Kozjak-Pavlovic V, Rudel T, Rikihisa Y. *Anaplasma phagocytophilum* Ats-1 is imported into host cell mitochondria and interferes with apoptosis induction. *PLoS Pathog* (2010) 6(2):e1000774. doi: 10.1371/journal.ppat.1000774
95. Yan Q, Lin M, Huang W, Teymournejad O, Johnson JM, Hays FA, et al. *Ehrlichia* type IV secretion system effector Etf-2 binds to active RAB5 and delays endosome maturation. *Proc Natl Acad Sci U S A* (2018) 115(38):E8977–86. doi: 10.1073/pnas.1806904115
96. Caturegli P, Asanovich KM, Walls JJ, Bakken JS, Madigan JE, Popov VL, Dumler JS. ankA: an *Ehrlichia phagocytophila* group gene encoding a cytoplasmic protein antigen with ankyrin repeats. *Infect Immun* (2000) 68(9):5277–83. doi: 10.1128/iai.68.9.5277-5283.2000
97. Sinclair SH, Garcia-Garcia JC, Dumler JS. Bioinformatic and mass spectrometry identification of *Anaplasma phagocytophilum* proteins translocated into host cell nuclei. *Front Microbiol* (2015) 6:55. doi: 10.3389/fmicb.2015.00055
98. Rikihisa Y. Subversion of RAB5-regulated autophagy by the intracellular pathogen *Ehrlichia chaffeensis*. *Small GTPases* (2017) p:1–7. doi: 10.1080/21541248.2017.1332506
99. Luo T, Kuriakose JA, Zhu B, Wakeel A, McBride JW. *Ehrlichia chaffeensis* TRP120 interacts with a diverse array of eukaryotic proteins involved in

transcription, signaling, and cytoskeleton organization. *Infect Immun* (2011) 79(11):4382–91. doi: 10.1128/IAI.05608-11

100. Wakeel A, Kuriakose JA, McBride JW. An *Ehrlichia chaffeensis* tandem repeat protein interacts with multiple host targets involved in cell signaling, transcriptional regulation, and vesicle trafficking. *Infect Immun* (2009) 77 (5):1734–45.
101. Luo T, McBride JW. *Ehrlichia chaffeensis* TRP32 interacts with host cell targets that influence intracellular survival. *Infect Immun* (2012) 80(7):2297–306. doi: 10.1128/IAI.00154-12
102. Luo T, Mitra S, McBride JW. *Ehrlichia chaffeensis* TRP75 Interacts with host cell targets involved in homeostasis, cytoskeleton organization, and apoptosis regulation to promote infection. *mSphere* (2018) 3(2):e00147–18. doi: 10.1128/mSphere.00147-18
103. Popov VL, Yu X, Walker DH. The 120 kDa outer membrane protein of *Ehrlichia chaffeensis*: preferential expression on dense-core cells and gene expression in Escherichia coli associated with attachment and entry. *Microb Pathog* (2000) 28(2):71–80. doi: 10.1006/mpat.1999.0327
104. Dunphy PS, Luo T, McBride JW. *Ehrlichia chaffeensis* exploits host SUMOylation pathways to mediate effector-host interactions and promote intracellular survival. *Infect Immun* (2014) 82(10):4154–68. doi: 10.1128/IAI.01984-14
105. Lina TT, Dunphy PS, Luo T, McBride JW. *Ehrlichia chaffeensis* TRP120 activates canonical Notch signaling to downregulate TLR2/4 expression and promote intracellular survival. *MBio* (2016) 7(4). doi: 10.1128/mBio.00672-16
106. Mitra S, Dunphy PS, Das S, Zhu B, Luo T, McBride JW. *Ehrlichia chaffeensis* TRP120 effector targets and recruits host polycomb group proteins for degradation to promote intracellular infection. *Infect Immun* (2018) 86(4). doi: 10.1128/IAI.00845-17
107. Wang JY, Zhu B, Patterson LL, Rogan MR, Kibler CE, McBride JW. *Ehrlichia chaffeensis* TRP120-mediated ubiquitination and proteasomal degradation of tumor suppressor FBW7 increases oncoprotein stability and promotes infection. *PLoS Pathog* (2020) 16(4):e1008541. doi: 10.1371/journal.ppat.1008541
108. Zhu B, Kuriakose JA, Luo T, Ballesteros E, Gupta S, Fofanov Y, McBride JW. *Ehrlichia chaffeensis* TRP120 binds a G+C-rich motif in host cell DNA and exhibits eukaryotic transcriptional activator function. *Infect Immun* (2011) 79(11):4370–81. doi: 10.1128/IAI.05422-11
109. Zhu B, Das S, Mitra S, Farris TR, McBride JW. *Ehrlichia chaffeensis* TRP120 moonlights as a HECT E3 ligase involved in self and host ubiquitination to influence protein interactions and stability for intracellular survival. *Infect Immun* (2017). doi: 10.1128/IAI.00290-17
110. Zhu B, Farris TR, Milligan SL, Chen H, Zhu R, Hong A, et al. Rapid identification of ubiquitination and sumoylation target sites by microfluidic peptide array. *Biochem Biophysical Res Comm* (2015) 5:430–8. doi: 10.1016/j.bbrep.2016.02.003
111. Park J, Kim KJ, Choi KS, Grab DJ, Dumler JS. *Anaplasma phagocytophilum* AnkA binds to granulocyte DNA and nuclear proteins. *Cell Microbiol* (2004) 6(8):743–51. doi: 10.1111/j.1462-5822.2004.00400.x
112. Beyer AR, Truchan HK, May LJ, Walker NJ, Borjesson DL, Carlyon JA. The *Anaplasma phagocytophilum* effector AmpA hijacks host cell SUMOylation. *Cell Microbiol* (2015) 17(4):504–19. doi: 10.1111/cmi.12380
113. Wongsantichon J, Jaiyen Y, Dittrich S, Salje J. *Orientia tsutsugamushi*. *Trends Microbiol* (2020) 28(9):780–1. doi: 10.1016/j.tim.2020.02.014
114. Beyer AR, Rodino KG, VieBrock L, Green RS, Tegels BK, Oliver LD Jr, et al. *Orientia tsutsugamushi* Ank9 is a multifunctional effector that utilizes a novel GRIP-like Golgi localization domain for Golgi-to-endoplasmic reticulum trafficking and interacts with host COPB2. *Cell Microbiol* (2017) 19(7). doi: 10.1111/cmi.12727
115. Song BQ, Chi Y, Li X, Du WJ, Han ZB, Tian JJ, et al. Inhibition of Notch Signaling Promotes the Adipogenic Differentiation of Mesenchymal Stem Cells Through Autophagy Activation and PTEN-PI3K/AKT/mTOR Pathway. *Cell Physiol Biochem* (2015) 36(5):1991–2002. doi: 10.1159/000430167
116. Hu X, Chung AY, Wu I, Foldi J, Chen J, Ji JD, et al. Integrated regulation of Toll-like receptor responses by Notch and interferon-gamma pathways. *Immunity* (2008) 29(5):691–703. doi: 10.1016/j.immuni.2008.08.016
117. Maiti G, Naskar D, Sen M. The Wingless homolog Wnt5a stimulates phagocytosis but not bacterial killing. *Proc Natl Acad Sci U S A* (2012) 109 (41):16600–5. doi: 10.1073/pnas.1207789109
118. Luo T, Dunphy PS, Lina TT, McBride. *Ehrlichia chaffeensis* exploits canonical and noncanonical host Wnt signaling pathways to stimulate phagocytosis and promote intracellular survival. *Infect Immun* (2015) 84 (3):686–700. doi: 10.1128/IAI.01289-15
119. Palaga T, Ratanabunyong S, Pattarakankul T, Sangphech N, Wongchana W, Hadae Y, Kueanjinda P. Notch signaling regulates expression of Mcl-1 and apoptosis in PPD-treated macrophages. *Cell Mol Immunol* (2013) 10(5):444–52. doi: 10.1038/cmi.2013.22
120. Cheng Y, Liu Y, Wu B, Zhang JZ, Gu J, Liao YL, et al. Proteomic analysis of the *Ehrlichia chaffeensis* phagosome in cultured DH82 cells. *PLoS One* (2014) 9(2):e88461. doi: 10.1371/journal.pone.0088461
121. Rikihisa Y. Molecular Pathogenesis of *Ehrlichia chaffeensis* Infection. *Annu Rev Microbiol* (2015) 69:283–304. doi: 10.1146/annurev-micro-091014-104411
122. Choi JH, Cheong TC, Ha NY, Ko Y, Cho CH, Jeon JH, et al. *Orientia tsutsugamushi* subverts dendritic cell functions by escaping from autophagy and impairing their migration. *PLoS Negl Trop Dis* (2013) 7(1):e1981. doi: 10.1371/journal.pntd.0001981
123. Ko Y, Choi JH, Ha NY, Kim IS, Cho NH, Choi MS. Active escape of *Orientia tsutsugamushi* from cellular autophagy. *Infect Immun* (2013) 81(2):552–9. doi: 10.1128/IAI.00861-12
124. Rikihisa Y. Role and function of the Type IV secretion system in *Anaplasma* and *Ehrlichia* species. *Curr Top Microbiol Immunol* (2017) 413:297–321. doi: 10.1007/978-3-319-75241-9_12
125. Barnewall RE, Rikihisa Y, Lee EH. *Ehrlichia chaffeensis* inclusions are early endosomes which selectively accumulate transferrin receptor. *Infect Immun* (1997) 65(4):1455–61. doi: 10.1128/IAI.65.4.1455-1461.1997
126. Huang B, Hubber A, McDonough JA, Roy CR, Scidmore MA, Carlyon JA. The *Anaplasma phagocytophilum*-occupied vacuole selectively recruits Rab-GTPases that are predominantly associated with recycling endosomes. *Cell Microbiol* (2010) 12(9):1292–307. doi: 10.1111/j.1462-5822.2010.01468.x
127. Mott J, Barnewall RE, Rikihisa Y. Human granulocytic ehrlichiosis agent and *Ehrlichia chaffeensis* reside in different cytoplasmic compartments in HL-60 cells. *Infect Immun* (1999) 67(3):1368–78. doi: 10.1128/IAI.67.3.1368-1378.1999
128. Seto S, Matsumoto S, Tsujimura K, Koide Y. Differential recruitment of CD63 and Rab7-interacting-lysosomal-protein to phagosomes containing *Mycobacterium tuberculosis* in macrophages. *Microbiol Immunol* (2010) 54 (3):170–4. doi: 10.1111/j.1348-0421.2010.00199.x
129. Kumar R, Sahu SK, Kumar M, Jana K, Gupta P, Gupta UD, et al. MicroRNA 17-5p regulates autophagy in *Mycobacterium tuberculosis*-infected macrophages by targeting Mcl-1 and STAT3. *Cell Microbiol* (2016) 18 (5):679–91. doi: 10.1111/cmi.12540
130. Yasir M, Pachikara ND, Bao X, Pan Z, Fan H. Regulation of chlamydial infection by host autophagy and vacuolar ATPase-bearing organelles. *Infect Immun* (2011) 79(10):4019–28. doi: 10.1128/IAI.05308-11
131. Pujol C, Klein KA, Romanov GA, Palmer LE, Cirota C, Zhao Z, Bliska JB. *Yersinia pestis* can reside in autophagosomes and avoid xenophagy in murine macrophages by preventing vacuole acidification. *Infect Immun* (2009) 77 (6):2251–61. doi: 10.1128/IAI.00068-09
132. Jager S, Bucci C, Tanida I, Ueno T, Kominami E, Saftig P, Eskelinen EL. Role for Rab7 in maturation of late autophagic vacuoles. *J Cell Sci* (2004) 117(Pt 20):4837–48. doi: 10.1242/jcs.01370
133. Yu JS, Cui W. Proliferation, survival and metabolism: the role of PI3K/AKT/mTOR signalling in pluripotency and cell fate determination. *Development* (2016) 143(17):3050–60. doi: 10.1242/dev.137075
134. Zhang HH, Lipovsky AI, Dibble CC, Sahin M, Manning BD. S6K1 regulates GSK3 under conditions of mTOR-dependent feedback inhibition of Akt. *Mol Cell* (2006) 24(2):185–97. doi: 10.1016/j.molcel.2006.09.019
135. Vigneron F, Dos Santos P, Lemoine S, Bonnet M, Tariosse L, Couffinhal T, Duplaà C, Jaspard-Vinassa B. GSK-3beta at the crossroads in the signalling of heart preconditioning: implication of mTOR and Wnt pathways. *Cardiovasc Res* (2011) 90(1):49–56. doi: 10.1093/cvr/cvr002

136. Inoki K, Li Y, Zhu T, Wu J, Guan KL. TSC2 is phosphorylated and inhibited by Akt and suppresses mTOR signalling. *Nat Cell Biol* (2002) 4 (9):648–57. doi: 10.1038/ncb839
137. Miao Y, Li G, Zhang X, Xu H, Abraham SN. A TRP Channel Senses Lysosome Neutralization by Pathogens to Trigger Their Expulsion. *Cell* (2015) 161(6):1306–19. doi: 10.1016/j.cell.2015.05.009
138. Velayutham TS, Kumar S, Zhang X, Kose N, Walker DH, Winslow G, Crowe JE Jr, McBride JW. *Ehrlichia chaffeensis* Outer Membrane Protein 1-Specific Human Antibody-Mediated Immunity Is Defined by Intracellular TRIM21-Dependent Innate Immune Activation and Extracellular Neutralization. *Infect Immun* (2019) 87(12). doi: 10.1128/IAI.00383-19

Conflict of Interest: The authors declare that the research was conducted in the absence of any commercial or financial relationships that could be construed as a potential conflict of interest.

frontiers in Immunology

ORIGINAL RESEARCH
published: 12 April 2021
doi: 10.3389/fimmu.2021.638469

Subversion of Host Innate Immunity by *Rickettsia australis via* a Modified Autophagic Response in Macrophages

Jeremy Bechelli[1,2], *Claire S. Rumfield*[1,3], *David H. Walker*[1,4], *Steven Widen*[5], *Kamil Khanipov*[6] *and Rong Fang*[1,4]*

[1] Department of Pathology, University of Texas Medical Branch at Galveston, Galveston, TX, United States, [2] Department of Biological Sciences, Sam Houston State University, Huntsville, TX, United States, [3] Laboratory of Tumor Immunology and Biology, National Cancer Institute, National Institutes of Health, Bethesda, MD, United States, [4] Center for Biodefense and Emerging Infectious Diseases, University of Texas Medical Branch, Galveston, TX, United States, [5] Department of Biochemistry & Molecular Biology, University of Texas Medical Branch at Galveston, Galveston, TX, United States, [6] Department of Pharmacology and Toxicology, University of Texas Medical Branch at Galveston, Galveston, TX, United States

OPEN ACCESS

Edited by:
Isabelle Vergne,
UMR5089 Institut de Pharmacologie et de Biologie Structurale (IPBS), France

Reviewed by:
Dan-Li Xie,
Wenzhou Medical University, China
Chinnaswamy Jagannath,
Weill Cornell Medical College of Cornell University, United States
Oliver Voss,
University of Maryland, Baltimore, United States

***Correspondence:**
Rong Fang
rofang@utmb.edu

Specialty section:
This article was submitted to Microbial Immunology, a section of the journal Frontiers in Immunology

Received: 06 December 2020
Accepted: 11 March 2021
Published: 12 April 2021

Citation:
Bechelli J, Rumfield CS, Walker DH, Widen S, Khanipov K and Fang R (2021) Subversion of Host Innate Immunity by Rickettsia australis via a Modified Autophagic Response in Macrophages. Front. Immunol. 12:638469. doi: 10.3389/fimmu.2021.638469

We recently reported that the *in vitro* and *in vivo* survivals of *Rickettsia australis* are *Atg5*-dependent, in association with an inhibited level of anti-rickettsial cytokine, IL-1β. In the present study, we sought to investigate how *R. australis* interacts with host innate immunity *via* an *Atg5*-dependent autophagic response. We found that the serum levels of IFN-γ and G-CSF in *R. australis*-infected *Atg5*$^{flox/flox}$Lyz-*Cre* mice were significantly less compared to *Atg5*$^{flox/flox}$ mice, accompanied by significantly lower rickettsial loads in tissues with inflammatory cellular infiltrations including neutrophils. *R. australis* infection differentially regulated a significant number of genes in bone marrow-derived macrophages (BMMs) in an *Atg5*-depdent fashion as determined by RNA sequencing and Ingenuity Pathway Analysis, including genes in the molecular networks of IL-1 family cytokines and PI3K-Akt-mTOR. The secretion levels of inflammatory cytokines, such as IL-1α, IL-18, TNF-α, and IL-6, by *R. australis*-infected *Atg5*$^{flox/flox}$Lyz-*Cre* BMMs were significantly greater compared to infected *Atg5*$^{flox/flox}$ BMMs. Interestingly, *R. australis* significantly increased the levels of phosphorylated mTOR and P70S6K at a time when the autophagic response is induced. Rapamycin treatment nearly abolished the phosphorylated mTOR and P70S6K but did not promote significant autophagic flux during *R. australis* infection. These results highlight that *R. australis* modulates an *Atg5*-dependent autophagic response, which is not sensitive to regulation by mTORC1 signaling in macrophages. Overall, we demonstrate that *R. australis* counteracts host innate immunity including IL-1β-dependent inflammatory response to support the bacterial survival *via* an mTORC1-resistant autophagic response in macrophages.

Keywords: *Rickettsia*, mTOR signaling, autophagy, macrophages, innate immunity

INTRODUCTION

Rickettsiae are Gram-negative, obligately intracellular bacteria transmitted to humans by arthropod vectors. Highly virulent rickettsial species, such as *Rickettsia rickettsii*, can cause life-threatening disease with fatality as high as 40% (1). Clinically, rickettsial illnesses often present with fever, headache, and petechial rash. Although microvascular endothelial cells are the primary target of rickettsial infection (2), rickettsiae effectively invade macrophages and other types of cells, such as dendritic cells and hepatocytes. We, and others, have recently demonstrated that *Rickettsia* invades and survives in human macrophages, while macrophages play an important role in the pathogenesis of rickettsioses (3–9). However, it remains poorly understood how virulent rickettsiae utilize macrophages to develop a systemic infection in mammalian hosts.

Autophagy is an intracellular, bulk degradation process in which a portion of a cytoplasmic component of the cell is engulfed in double-membrane structures known as autophagosomes and is subsequently degraded upon fusion with lysosomes (10, 11). *Atg5* (autophagy-related gene 5) is essential for autophagic vesicle formation as part of the ATG12-ATG5-ATG16 complex (12). A number of studies have employed *Atg5*-conditional knockout mice to investigate the interactions of autophagy with pathogenic microbes (13–15). *Atg5*$^{flox/flox}$ Lyz-*Cre* mice were generated by breeding *Atg5* $^{flox/flox}$ mice to mice expressing the *Cre* recombinase from the endogenous lysozyme M locus (14), leading to an autophagy deficit mainly in macrophages resulting from deletion of the ATG5 gene. The mechanistic (formerly "mammalian") target of rapamycin (mTOR) is an atypical serine-threonine protein kinase that plays a critical role in maintaining a balance between cellular anabolism and catabolism (16). The mTOR affects several aspects of cellular functions, including metabolism, aging, growth, apoptosis, and autophagy (17). It forms two complexes, mTOR complex 1 (mTORC1) and mTOR complex 2 (mTORC2), with distinct composition and function (18). Toll-like receptor activation, cytokines, and low concentrations of amino acids will activate mTORC1 signaling leading to the phosphorylation of p70S6 kinase (p70S6K), mTOR and S6 kinase, which are established markers of mTORC1 activation (19–22). The mTORC1 is a master regulator of autophagy, since inhibition of mTORC1 was required to initiate the autophagy process (16, 23). Increasing evidence shows that mTORC1 has been implicated in the regulation of fusion of autophagosome to lysosome and the termination of autophagic flux (16).

Although autophagy has been considered a cornerstone of intracellular surveillance and host defense, intracellular bacteria and viruses are known to subvert or modify autophagy to facilitate their infection course (24–26). Recently, we have demonstrated that *R. australis* accumulates and co-localizes with LC3 (+) autophagosomes in macrophages, but not accompanied by a significantly reduced level of SQSTM1/p62 (4). In addition, pharmacological inhibition of mTOR signaling promotes the survival of *R. australis* in macrophages (4). Thus, *R. australis* induces a modified autophagic response, instead of autophagic flux. Using *Atg5* $^{flox/flox}$ Lyz-*Cre* and *Atg5* $^{flox/flox}$ mice, our recent studies clearly demonstrated that: 1) *R. australis* supports its infection in macrophages by inhibiting anti-rickettsial effect mediated by IL-1β *via Atg5*-dependent autophagic response; 2) *Atg5*-dependent autophagic response in macrophages facilitates the systemic infection of *R. australis* in association with suppressed serum levels of IL-1β (4). Notably, it is unknown how *R. australis* subverts the elements of the host innate immune system to support rickettsial infection *via* a modified autophagic response. Thus, we determined whether inflammatory and anti-inflammatory cytokines other than IL-1β were regulated by *Atg5*-dependent autophagic response *via* utilizing *Atg5* $^{flox/flox}$ and *Atg5* $^{flox/flox}$ Lyz-*Cre* mice. In addition, we investigated the interactions of *R. australis* with mTOR and its effect on the autophagic response in macrophages. Our studies demonstrate that *R. australis* induces a modified autophagic response while activating mTORC1 signaling in macrophages. Our findings suggest that *R. australis* subverts host innate immunity to support rickettsial infection in association with *Atg5*-dependent regulation of G-CSF and IFN-γ, in addition to IL-1β.

MATERIALS AND METHODS

Rickettsiae and Mice

Rickettsia australis (Cutlack strain) was cultivated in Vero cells and purified by either Renografin density gradient centrifugation or using a Renografin "cushion" as previously described (27–29) for use in *in vitro* infections. The concentration of rickettsiae propagated in cell culture was determined by plaque assay after purification as described previously (28). Rickettsial stocks were stored at -80°C until use. All the experiments described in this study were conducted in a certified biosafety level 3 (BSL3) laboratory at UTMB. Wild type (WT) B6 mice were purchased from The Jackson Laboratory (catalog number 000664). *Atg5* $^{flox/flox}$ Lyz-*Cre* (autophagy deficient), and *Atg5* $^{flox/flox}$ (control) mice were kindly provided by Dr. Noboru Mizushima at the University of Tokyo and Dr. Herbert Virgin IV at Washington University School of Medicine in St. Louis (14, 15, 30). For *in vivo* experiments, mice were maintained and handled in a certified animal biosafety level-3 (ABSL3) facility at UTMB and inoculated intravenously (i.v.) through the tail vein with *R. australis* at the doses indicated. *R. australis* used in animal studies was grown in embryonated chicken egg yolk sac culture as described previously (31). Animals were monitored daily for signs of illness and sacrificed at indicated times. *In vivo* experiments were performed according to the Guide for the Care and Use of Laboratory Animals guidelines and approved by the Institutional Animal Care and Use Committee at UTMB.

Generation of Bone Marrow-Derived Macrophages

Primary bone marrow-derived macrophages (BMMs) were generated from 6-8 week old female WT B6 mice, *Atg5* $^{flox/flox}$ mice and *Atg5* $^{flox/flox}$ Lyz-*Cre* mice as previously described (4, 14, 15, 30, 32). Briefly, femurs and tibias were dissected, bone marrow was flushed using sterile medium, and cells were cultivated in

low-endotoxin DMEM containing 10% (v/v) fetal bovine serum (FBS; Hyclone, Utah, SV30160) supplemented with either 20% supernatant from L929 cell culture or recombinant M-CSF (PeproTech, NJ, 315-02) at 37 °C in 5% CO_2. Cells were harvested on day 6 and characterized by flow cytometric analysis by staining with anti-F4/80 and CD11b antibodies. Cultures were used when approximately 90% of these cells stained positive for F4/80 and CD11b. BMMs were plated at a density of 1×10^6 cells/well in 24-well plates in RPMI 1640 containing 10% FBS, and experiments were initiated within 24 hrs.

Macrophage *In Vitro* Infections

Primary mouse BMMs were infected with *R. australis* at a multiplicity of infection (MOI) of 5. In order to synchronize the internalization of bacteria, rickettsiae were centrifuged onto the cells at 560 × g for 5 min and incubated at 37°C in 5% CO_2. Cells were collected and washed for further experiments at indicated times for each experiment, and uninfected cells served as the negative control.

Immunoblotting of Molecules Involved in Autophagy and mTOR Signaling

To assess the conversion of LC3-I to the lipidated LC3-II form, cells were lysed with RIPA lysis buffer (EMD Millipore, MA, 20-188) containing protease and phosphatase inhibitors (Roche, IN). Cell lysates were centrifuged to obtain soluble proteins, separated by SDS-PAGE, transferred to polyvinylidene difluoride (PVDF) membranes and probed with polyclonal antibodies against LC3B (Cell Signaling Technology, MA, 4108). Bands were visualized using appropriate secondary antibodies and enhanced chemiluminescence (ECL) detection reagents (Thermo Scientific, Pierce, IL, 32106). Beta-actin was used to determine equal loading of the gel and was detected with mouse monoclonal antibody (mAb, Sigma, MO, A1978). Blotting against SQSTMI was performed using antibodies directed against SQSTM1 (Cell Signaling Technology, MA, 5114). Antibodies directed against phospho-mTOR (Ser2448) (D9C2) XP® rabbit mAb and phospho-p70 S6 Kinase (Thr389) (1A5) mouse mAb (Cell Signaling Technology, MA) were used for the analysis of the mTOR signaling pathway according to the manufacturer's instructions. Densitometric analysis was quantitatively measured using Image J (33).

Immunofluorescence Microscopy

For immunofluorescence detection of LC3 puncta in *R. australis*-infected BMMs, cells were first seeded on glass coverslips in 12-well plates one day before infection as described previously (4). At 1 h post-infection (p.i.), cells were washed with PBS, fixed with 4% paraformaldehyde in PBS for 20 min, permeabilized with 0.5% Triton-X in PBS for 20 min and blocked with 3% BSA in PBS for 30 min. Samples were incubated with rabbit monoclonal antibody against LC3B (Cell Signaling Technology, #3868) followed by appropriate secondary antibody. Nuclei were stained with DAPI in ProLong® Gold Antifade Mountant (Life Technology, NY, P-36931). Coverslips were sealed with nail polish, and visualized by confocal microscopy with a 20 × lens (Olympus Fluoview 1000) using FV10-ASW software (Olympus, PA).

The levels of LC3 in cells were quantified as previously described (34). In brief, using Image J, an outline was drawn around each cell and circularity, area, mean fluorescence measured along with several adjacent background readings. The total corrected cellular fluorescence (TCCF) = integrated density – (area of selected cell × mean fluorescence of background readings) was calculated. This TCCF was then equalized against the mean TCCF of neighboring interphase cells in the same field of view, with results presented as fold increase over interphase levels. Box plots and statistical analysis (2-sided unpaired Student t tests) were performed using GraphPad Prism 5.

Pharmacological Inhibition of mTORC1 Signaling

Rapamycin, the pharmacologic gold standard for inhibiting mTOR, which acts by associating with FK-506 binding protein 12, was used to selectively inhibit mTORC1 (35). To inhibit mTORC1 signaling, cells were treated with 50 ng/mL of rapamycin (Sigma-Aldrich, St. Louis MO) for 4 hours prior to infection with rickettsiae. The cell number was counted, morphology observed by microscopy, and cell viability determined with the trypan blue dye exclusion method (36). The inhibitory effect of rapamycin on mTOR was examined by immunoblotting with antibodies against phospho-mTOR (Ser2448) (D9C2) XP® rabbit mAb and phospho-p70 S6 Kinase (Thr389) (1A5) mouse mAb (Cell Signaling Technology, MA).

Measurement of Cytokines by ELISA

Supernatants from *Rickettsia*-infected cells and uninfected controls were filter-sterilized and stored as aliquots at - 80°C. The concentration of IL-18 present in the supernatant of *R. australis*-infected BMMs was measured by ELISA using the Mouse IL-18 ELISA Kit (MBL International Corporation), following the manufacturer's instructions. The detection limit for the ELISA cytokine concentrations was 25 pg/mL for IL-18. Samples were assayed in duplicate and are presented as the average of two independent experiments. Absorbance values were obtained using a VersaMax ELISA microplate reader (Molecular Devices, Sunnyvale, CA), and the concentrations were calculated from values obtained within the linear range of the standard curve.

Bio-plex Assay for Cytokine Analysis

Cell culture supernatants and mouse sera were processed according to the manufacturer's instructions and then analyzed using a Bio-plex 200 system (Bio-Rad, Hercules, CA). Briefly, the samples were filter sterilized and subsequently centrifuged for 10 minutes at 450 × g at 4°C to remove debris. The resulting supernatants were collected and aliquoted into 96-well plates and processed for analysis on the Bio-plex system. The cytokines were coupled to cytokine-specific multi-plex beads (Bio-Rad) in the Bio-Plex mouse cytokine immunoassay following the manufacturer's instructions. The pre-designed assay kit measured the concentrations of cytokines/chemokines including interleukin (IL)-1α, IL-6, IL-10, IFN-γ, granulocyte colony-stimulating factor (G-CSF), and tumor necrosis factor (TNF)-α.

Next-Generation Sequencing (NGS) and Pathway Analysis

RNA-seq analysis (next-generation sequencing) was performed on *R. australis*-infected BMMs of *Atg5* $^{flox/flox}$ mice and *Atg5* $^{flox/flox}$ Lyz-*Cre* mice at 24 h p.i. as described previously (37). Briefly, 1 μg of total RNA from uninfected and infected BMMs was poly A+ selected and fragmented using divalent cations and heat (94°C, 8 min). Illumina TruSeq v2 sample preparation kits (Illumina Inc., San Diego, CA) were used for the RNA-Seq library construction. NGS was performed at the NGS core facility, Sealy Center for Molecular Medicine, the University of Texas Medical Branch (UTMB). Sample libraries were sequenced by the Illumina HiSeq 1500 using a 2 × 50 base paired-end run protocol, with TruSeq v3 sequencing-by-synthesis chemistry. Reads were aligned to the mouse GRCm38 reference genome using the STAR alignment program, version 2.5.3a, with the recommended ENCODE options. GFOLD V1.1.4 was used to calculate the fold change differences between treatments. GFOLD generalizes the fold change by considering the posterior distribution of log fold change to overcome the problem of no replicate samples. Heatmap and hierarchical cluster analysis were generated to demonstrate the expression patterns of the top 100 genes differentially expressed. The dataset was filtered for a Log2 (fold change) ≥ 2.5 or ≤ -2.5 and then uploaded to Ingenuity Pathway Analysis (IPA) software (Ingenuity Systems, Redwood City, CA) for further analysis of the *Atg5*-dependent regulation of transcriptome profile of mouse macrophages during *R. australis* infection.

Histopathological Analyses

Formalin-fixed, hematoxylin and eosin (H&E)-stained tissue sections from infected and uninfected *Atg5* $^{flox/flox}$ and *Atg5* $^{flox/flox}$ Lyz-*Cre* mice were evaluated by a pathologist *via* both low-magnification and high-magnification microscopy. Images were taken using an Olympus BX41 photomicroscope (Olympus America, Inc., Center Valley, PA) or using a Revolution Microscope and an iPad Pro® tablet (Echo Laboratory, San Diego, CA). The histopathology slides were read by a board-certified Pathologist who has extensive experience with pathological analysis of rickettsial infections.

Statistical Analysis

The one-way analysis of variance (ANOVA) with Bonferroni's procedure was used for comparisons of multiple experimental groups, and a Student t-test or Welch's t-test was used for two-group comparisons depending on whether the variance between two groups was significantly different. The statistical analyses were performed using GraphPad Prism software version 5.01. p values of 0.05 or less were the threshold for statistical significance.

RESULTS

R. australis Subverts Host Innate Immunity in Association With an *Atg5*-Dependent Autophagic Response

We have previously reported that a type 1 immune cytokine profile is closely associated with the host protective immunity against rickettsial diseases (38, 39). MyD88-dependent cytokines, including IFN-γ, IL-6, IL-12, and IL-1β, are the early signatures of a protective host innate immune response against *R. australis* (38). Inhibiting systemic production of IL-1β by *Atg5*-dependent autophagic response in macrophages contributes to the enhanced *R. australis* infection *in vivo*, as evidenced by our previous published studies employing *Atg5* $^{flox/flox}$ Lyz-*Cre* and *Atg5* $^{flox/flox}$ mice (4). The important question in this study is whether other components in host innate immunity, in addition to IL-1β, were subverted by *R. australis* to support rickettsial infection *in vivo* in an *Atg5*-dependent mechanism. To answer this question, we determined the association of the *Atg5*-dependent autophagic response with four pro-inflammatory cytokines, IL-1α, TNF-α,IFN-γ and G-CSF, and one anti-inflammatory cytokine, IL-10, in host innate immunity against *R. australis*. First, no significant difference in cytokine levels was identified in uninfected *Atg5* $^{flox/flox}$ Lyz-*Cre* and *Atg5* $^{flox/flox}$ mice (**Figure 1**). On day 4 p.i., a time point in host innate immunity at which serum levels of IL-1β and *R. australis* load in tissues were determined in our previous studies, the systemic production levels of IL-1α, TNF-α, and IL-10 in *R. australis*-infected *Atg5* $^{flox/flox}$ Lyz-*Cre* mice were not significantly different from those in infected *Atg5* $^{flox/flox}$ mice (**Figure 1**). Surprisingly, serum levels of IFN-γ and G-CSF in *Atg5* $^{flox/flox}$ Lyz-*Cre* animals were significantly reduced in association with a previously documented lower *R. australis* load in tissues (4), compared to *Atg5* $^{flox/flox}$ animals (**Figure 1**). Therefore, our results suggest that *R. australis* modulates *Atg5*-dependent regulation of G-CSF and IFN-γ, in addition to IL-1β, in host innate immunity to support rickettsial infection *in vivo*.

Inflammatory Cellular Accumulation Upon Infection With *R. australis* in Tissue of *Atg5* $^{flox/flox}$ Mice Is Quantitatively and Qualitatively Different Compared to *Atg5* $^{flox/flox}$ Lyz-*Cre* Mice

Histologic analysis of the H&E-stained liver and lung sections of infected animals showed inflammatory cell infiltrations and lesions in both *R. australis*-infected *Atg5* $^{flox/flox}$ and infected *Atg5* $^{flox/flox}$ Lyz-*Cre* mice on day 4 p.i. compared to uninfected controls (**Figure 2**). Livers of infected *Atg5* $^{flox/flox}$ Lyz-*Cre* mice showed numerous perivascular foci of inflammatory infiltration either around the central vein and portal triad or in the lobules (**Figure 2A**). Compared to *Atg5* $^{flox/flox}$ mice, deficiency in *Atg5* in macrophages resulted in thrombosis and infarction in the liver (**Figure 2B**). In the liver of infected *Atg5* $^{flox/flox}$ Lyz-*Cre* mice, inflammatory foci were randomly distributed throughout the tissue. These cellular infiltrations consisted of mainly macrophages, but also lymphocytes and neutrophils (**Figures 2C, D**). Furthermore, *R. australis*-infected *Atg5* $^{flox/flox}$ Lyz-*Cre* mice showed interstitial pneumonia in the lungs (**Figures 2E, F**).

Evaluation of histopathological changes in livers of infected *Atg5* $^{flox/flox}$ mice showed cellular infiltration in widely distributed foci consisting of macrophages, but fewer or no neutrophils compared to *Atg5* $^{flox/flox}$ Lyz-*Cre* mice (**Figures 2G–J**). The lungs

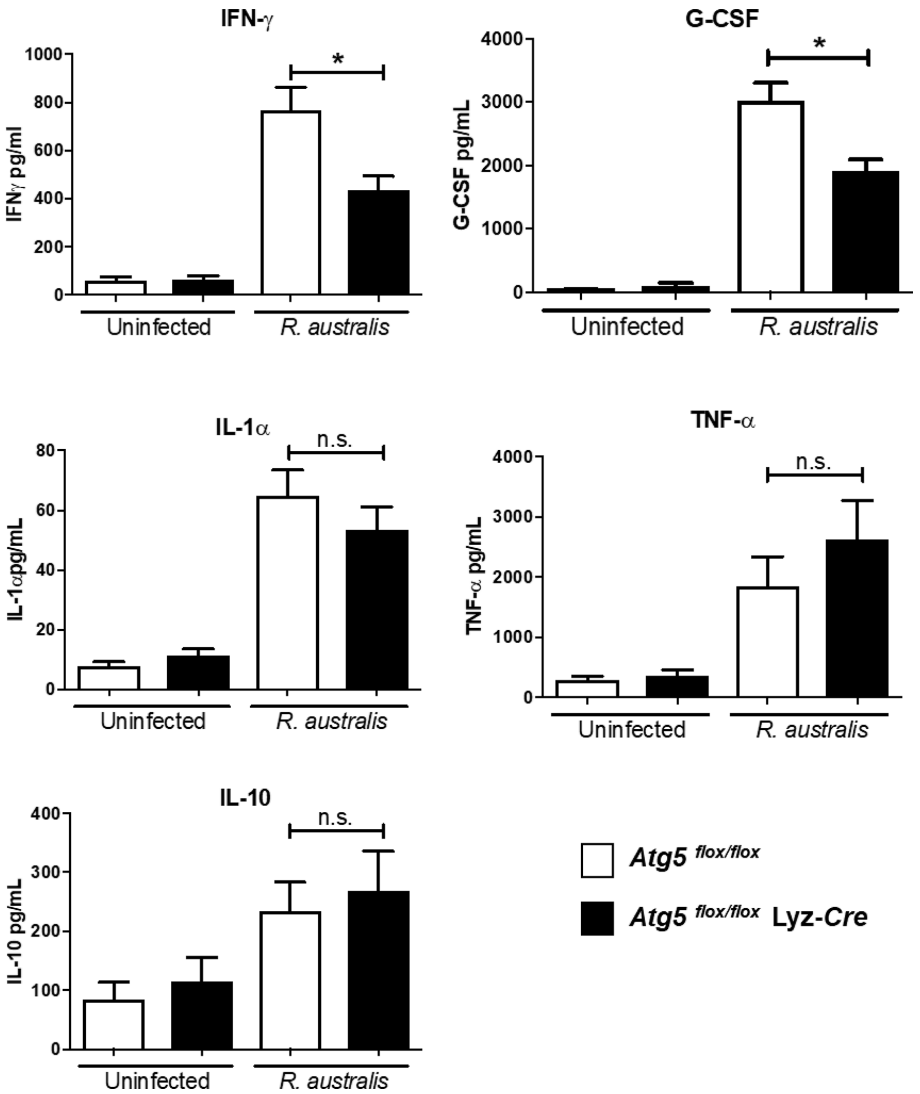

FIGURE 1 | (previous Figure 6). *R. australis* subverts host innate immunity against rickettsioses *via Atg5*-dependent autophagic response. *Atg5* $^{flox/flox}$ Lyz-*Cre* and *Atg5* $^{flox/flox}$ mice were infected with *R. australis* i.v. at a dose of 3×10^5 PFU per mouse. On day 4 p.i., mice were euthanized, and serum was collected. Systemic production levels of cytokines/chemokines including IFN-γ, G-CSF, TNF-α, IL-1α, and IL-10 in mouse serum were determined by Bioplex assay. Results are means ± SE of data from three independent experiments containing 4-6 mice per group. *p<0.05; n.s., not statistically significant.

of *R. australis*-infected *Atg5* $^{flox/flox}$ mice also showed interstitial pneumonia (**Figures 2K, L**). Interestingly, the frequency of pathological lesions was significantly reduced in livers of infected *Atg5* $^{flox/flox}$ Lyz-*Cre* mice compared to *Atg5* $^{flox/flox}$ mice (**Figure 2M**). In contrast, the inflammatory lesions in the livers of infected *Atg5* $^{flox/flox}$ Lyz-*Cre* mice were significantly greater in size compared to infected *Atg5* $^{flox/flox}$ mice (**Figure 2N**). Considering the greater *R. australis* load in tissues of *Atg5* $^{flox/flox}$ mice vs *Atg5* $^{flox/flox}$ Lyz-*Cre* mice, these results suggest that *R. australis* subverts host innate immunity *via Atg5* to support their infection in association with histopathological changes featured by increased frequency and reduced size of cellular infiltrations consisting of few or no neutrophils.

Atg5-Dependent Gene Regulation by *R. australis* Infection in Macrophages

No prior studies have examined the *Atg5*-dependent regulation of host gene expression by *Rickettsia* in macrophages. We performed four comparisons in this study, including infected *Atg5* (+) vs uninfected *Atg5* (+), infected *Atg5* (-) vs infected *Atg5* (+), infected *Atg5* (-) vs infected *Atg5* (+), and uninfected *Atg5* (-) vs uninfected *Atg5* (+). As shown in **Figure 3**, *Atg5* (-) refers to *Atg5* $^{flox/flox}$ Lyz-*Cre* while *Atg5* (+) refers to *Atg5* $^{flox/flox}$. First, a list of the top 100 differentially expressed genes in each comparison was used to generate a heat map (**Figure 3A**). Approximately half of these 100 genes were upregulated in infected macrophages in all four comparisons, notably

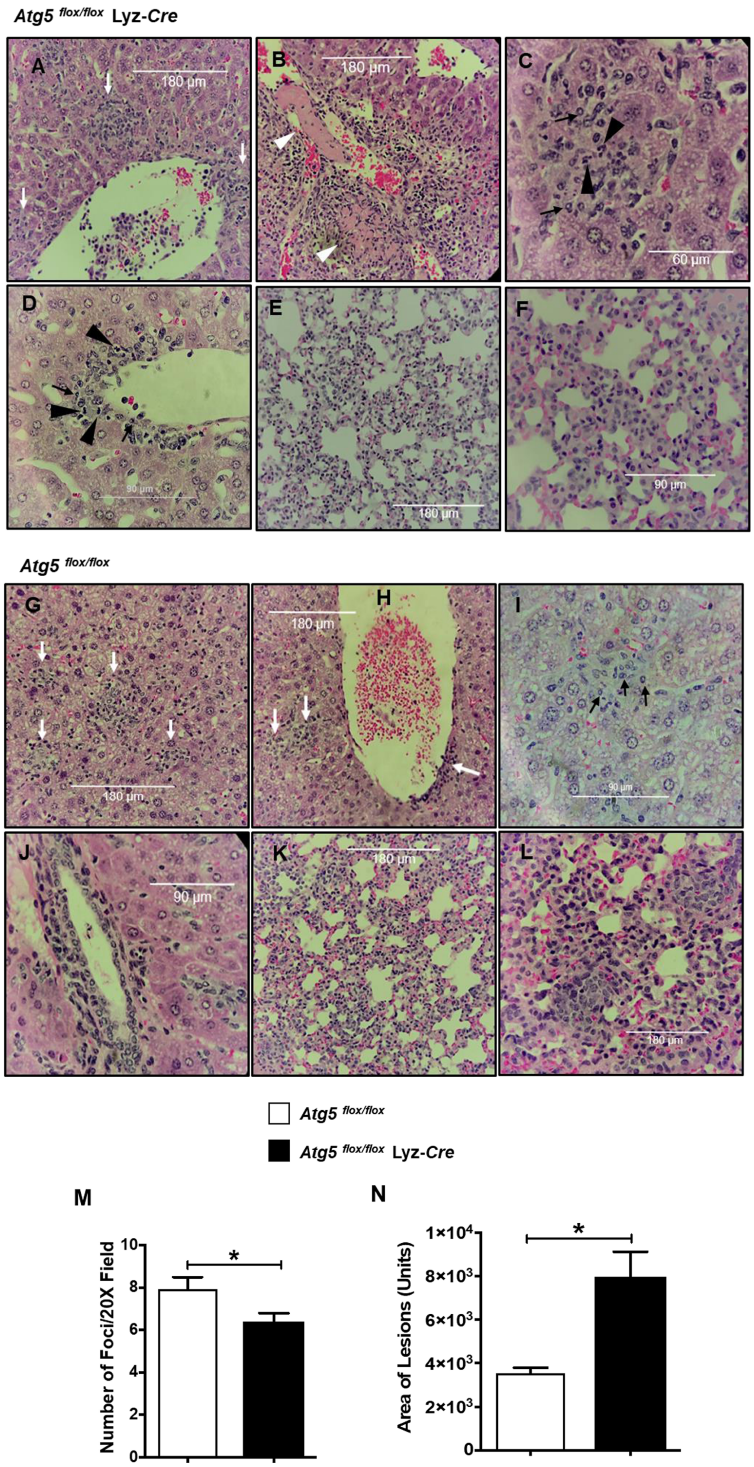

FIGURE 2 | (previous Figure 7). Inflammatory cellular accumulation upon infection with *R. australis* in tissues of *Atg5* $^{flox/flox}$ mice and *Atg5* $^{flox/flox}$ Lyz-*Cre* mice. Mice were infected i.v. with *R. australis* (3×10^5 PFU per mouse). On day 4 p.i., mice were sacrificed, and tissues were isolated and analyzed. Histological analysis of livers and lungs from infected *Atg5* $^{flox/flox}$ Lyz-*Cre* mice **(A–F)** and *Atg5* $^{flox/flox}$ mice **(G–L)**. Foci of inflammatory infiltration are indicated by white arrows. Thrombus or necrotic cells related to thrombosis is shown as white arrowheads **(B)**. Polymorphonuclear neutrophils (PMNs) (black arrowheads) and macrophages (black arrows) are shown in livers. Furthermore, the size **(M)** and frequency **(N)** of inflammatory lesions in livers were analyzed using ImageJ (magnification, ×20). Images were taken using an Olympus BX41 photomicroscope (Olympus America, Inc., Center Valley, PA) or using a Revolution Microscope and an iPad Pro® tablet (Echo Laboratory, San Diego, CA). *p<0.05.

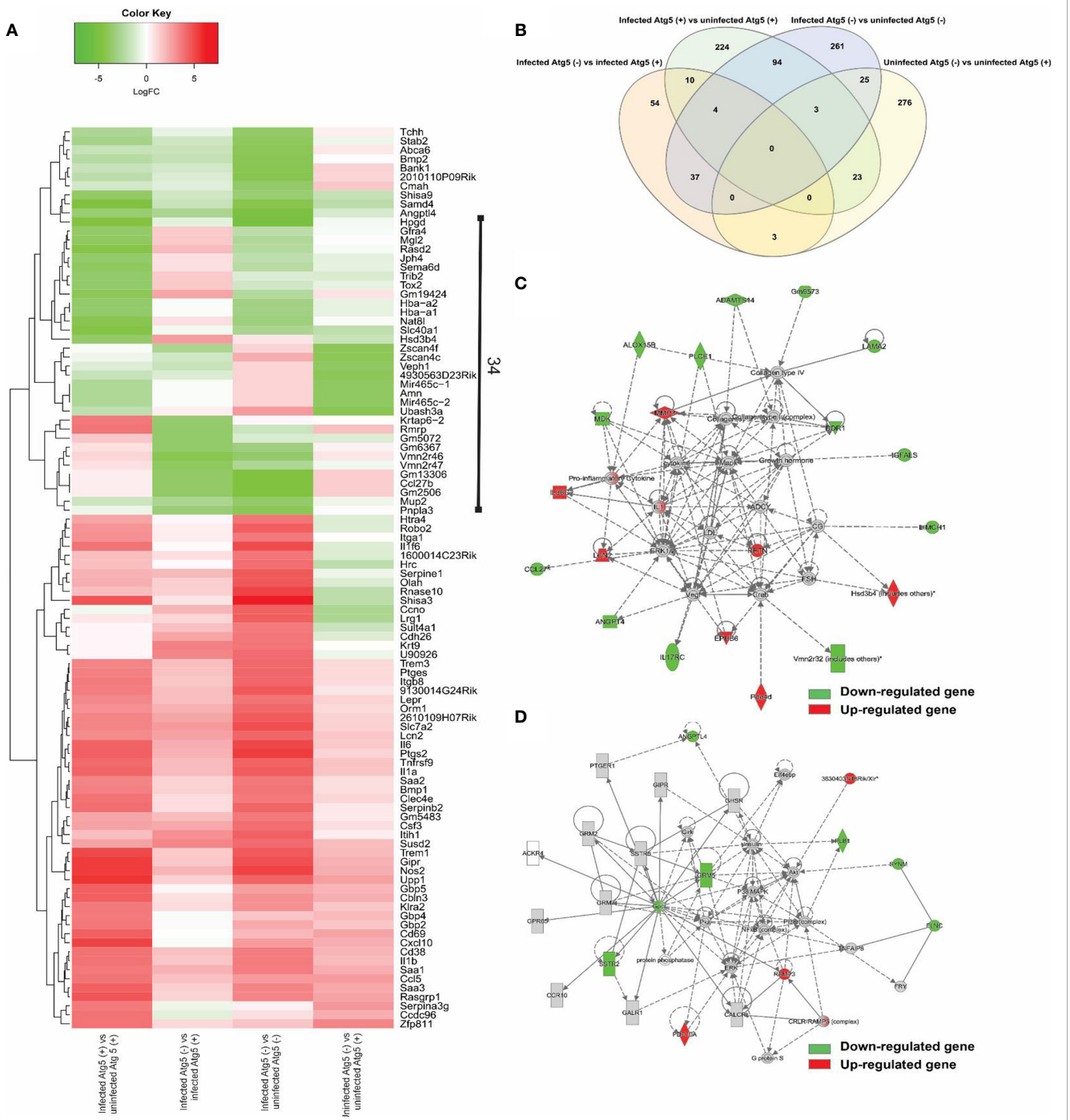

FIGURE 3 | (previous Figure 3). Comparative transcriptional analysis of *R. australis*-infected *Atg5* $^{flox/flox}$ Lyz-*Cre* and *Atg5* $^{flox/flox}$ BMMs. BMMs were isolated from *Atg5* $^{flox/flox}$ Lyz-*Cre* and *Atg5* $^{flox/flox}$ *mice*, and then infected with *R. australis* at an MOI of 5. At 24 h p.i., cells were collected and total RNA was extracted. RNA-seq analysis was performed as described in *Materials and Methods*. *Atg5* (+), *Atg5* $^{flox/flox;}$ *Atg5* (-), *Atg5* $^{flox/flox}$ Lyz-*Cre*. **(A)**, Heatmap and hierarchical clustering of the top 100 genes differentially regulated by *Atg5* during *R. australis* infection in mouse macrophages. The expression levels of genes are indicated by the color bar above the heatmap. Red color indicates the increased expression whereas green color indicates the decreased expression in four comparisons. **(B)**, Venn diagram showing overlap of significantly modulated genes for each of the four comparisons. **(C, D)**, IPA molecular networks analysis of differentially expressed genes in IL-1 family cytokines signaling and PI3K-Akt-mTOR signaling in *R. australis*-infected *Atg5* $^{flox/flox}$ Lyz-*Cre* BMMs vs *R. australis*-infected *Atg5* $^{flox/flox}$ BMMs. Red, up-regulated; green, down-regulated.

pro-inflammatory cytokines (IL-1 family of cytokines and TNF-alpha) and chemokines (CCL5 and CXCL10), that may be of particular interest for the purpose of our studies. Moreover, 34 genes were differentially expressed in each comparison, suggesting that the expression levels of these genes are closely associated with *Atg5*-dependent autophagy and/or *R. australis* infection (**Figure 3A**). We generated a Venn diagram showing the overlap of significantly modulated genes among four comparisons InteractiVenn (**Figure 3B**). No gene was shared among the four comparisons. The majority of modulated genes were unique to either infected *Atg5* (-) vs uninfected *Atg5* (-), infected *Atg5* (+) vs uninfected *Atg5* (+), or uninfected *Atg5* (-) vs uninfected *Atg5* (+).

The focus of the present study is on the subversion of the host response in macrophages by *R. australis* observed in an *Atg5*-competent vs. *Atg5*-compromised mice. The networks generated by IPA analysis illustrate the interrelationships between genes and the temporal changes in gene modulation. Two molecular networks, in which IL-1 family cytokines (**Figure 3C**) and PI3K-Akt-mTOR (**Figure 3D**) were central hub molecules, were identified by IPA. The first network (**Figure 3C**) consists of 22 genes differentially expressed in infected *Atg5* (-) and infected *Atg5* (+) BMMs. In IL-1 family cytokine signaling, nine and thirteen genes were up- and down-regulated, respectively, by *R. australis* infection in *Atg5*-deficient macrophages compared to *Atg5*-competent macrophages. Thus, *Atg5* specifically down-regulated nine genes during *R. australis* infection, including IL-1, IL-36G, lipocalin-2 (LCN2), resistin (RETN), NADPH-dependent 3-keto-steroid reductase (Hsd3b4), matrix metallopeptidase 3 (MMP3), and ephrin type-B receptor 6 (EPHB6), some of which have been shown to contribute to host innate immunity against infections (40). Therefore, *Atg5* benefits *R. australis* infection in macrophages, at least in part in association with inhibiting the members of IL-1 family cytokines in the host innate immune system. In **Figure 3D**, the hub molecules are PI3K, Akt, insulin, and eukaryotic initiation factor 4E-binding protein 1 (Eif4ebp) (41). When mTORC1 is active, it phosphorylates (activates) p70S6 kinase (S6K) and the eIF4e binding protein (42). Thus, the PI3K-Akt-mTOR signaling pathway was regulated by *R. australis* infection. Compared to infected *Atg5* $^{flox/flox}$ BMMs, 4 genes including RAMP3 and PDE10A were upregulated while 7 genes including ANGPTL4 and Gpcr were downregulated in infected *Atg5* $^{flox/flox}$ Lyz-*Cre* BMMs by *R. australis* infection (**Figure 3D**). These results suggest that the enhanced *R. australis* infection in *Atg5*-competent macrophages is associated with the alterations of the key cellular signaling pathway, PI3K-Akt- mTOR.

R. australis Suppresses the Production of Inflammatory Cytokines by Infected Macrophages *via* a Modified *Atg5*-Dependent Autophagic Response

Our recently published studies have shown that *R. australis* induces a modified *Atg5*-dependent autophagic response to benefit its replication through inhibiting the secretion of rickettsicidal IL-1β, although IL-1β-independent mechanisms also contribute to this process (4). To explore IL-1β-independent factors involved in supporting *R. australis* infection in macrophages, we measured the secretion levels of five cytokines in *R. australis*-infected *Atg5* $^{flox/flox}$ Lyz-*Cre* BMMs and *Atg5* $^{flox/flox}$ BMMs at 24 h p.i. Uninfected BMMs of *Atg5*-conditional knockout mice did not produce any significant levels of the examined cytokines (**Figure 4**). The deficiency of *Atg5*-dependent autophagy did not change the levels of either IFN-γ or G-CSF secreted by infected macrophages (**Figure 4**). Interestingly, *R. australis*-infected *Atg5* $^{flox/flox}$ Lyz-*Cre* BMMs produced significantly greater levels of IL-6, IL-1α, and TNF-α compared to infected *Atg5* $^{flox/flox}$ BMMs (**Figure 4**). The enhanced production of IL-6, IL-1α and TNF-α was associated with reduced *R. australis* infection in *Atg5*-deficient macrophages (4). These results suggest that *R. australis* exploits the *Atg5*-dependent autophagic response to inhibit the production of IL-6, IL-1α, and TNF-α in macrophages to support their infection.

IL-18 is an important member of the IL-1 family of cytokines (43–45). To determine the effect of autophagy on production of IL-18 by *R. australis*-infected macrophages, we employed BMMs from both *Atg5*- and *Atg16l1*-conditional knockout mice. *R. australis* infection resulted in significantly greater production levels of IL-18 in *Atg5* $^{flox/flox}$ Lyz-*Cre* BMMs compared to *Atg5* $^{flox/flox}$ BMMs (**Figure 5A**). Furthermore, the secretion levels of IL-18 by *R. australis*-infected *Atg16l1* $^{flox/flox}$ BMMs were significantly less than those by infected *Atg16l1* $^{flox/flox}$ Lyz-*Cre* BMMs (**Figure 5B**). We had demonstrated that deletion of *Atg16l1* significantly reduces the concentrations of *R. australis* (4). Thus, the reduced IL-18 production by *Atg16l1* $^{flox/flox}$ BMMs was associated with a greater rickettsial load in these BMMs compared to *Atg16l1* $^{flox/flox}$ Lyz-*Cre* BMMs. These results clearly revealed that *R. australis* suppressed the production of IL-18 in an autophagy-dependent manner, consistent with the results of *Atg5*-dependent regulation of IL-1 family cytokines at the transcriptional level by this bacterium, as shown in **Figure 3C**.

R. australis Induces Activation of mTORC1 Signaling

As described above (**Figure 3D**), *R. australis* differentially regulated the genes in the PI3K-Akt-mTOR signaling pathway in macrophages *via* an *Atg5*-dependent mechanism. Since inhibition of mTORC1 by rapamycin treatment promotes *R. australis* infection (4), mTORC1 activation is likely important to regulate the cellular environment during rickettsial infection. This was the impetus to study whether *R. australis* infection has an impact on mTORC1 signaling and if mTORC1 signaling regulates autophagy induction. To address these questions, we infected B6 BMMs with *R. australis* and determined the phosphorylation of mTOR and P70S6 kinase as a read-out for mTORC1 activity. Surprisingly, *R. australis* infection induced direct phosphorylation of mTOR on serine 2448 and phosphorylation of P70S6 kinase (threonine 389) in B6 BMMs compared to uninfected controls at as early as 1 h p.i. when autophagic response is induced by these bacteria (**Figure 6A**) (4). Densitometry analysis from three independent experiments showed that the expression levels of phosphorylated mTOR

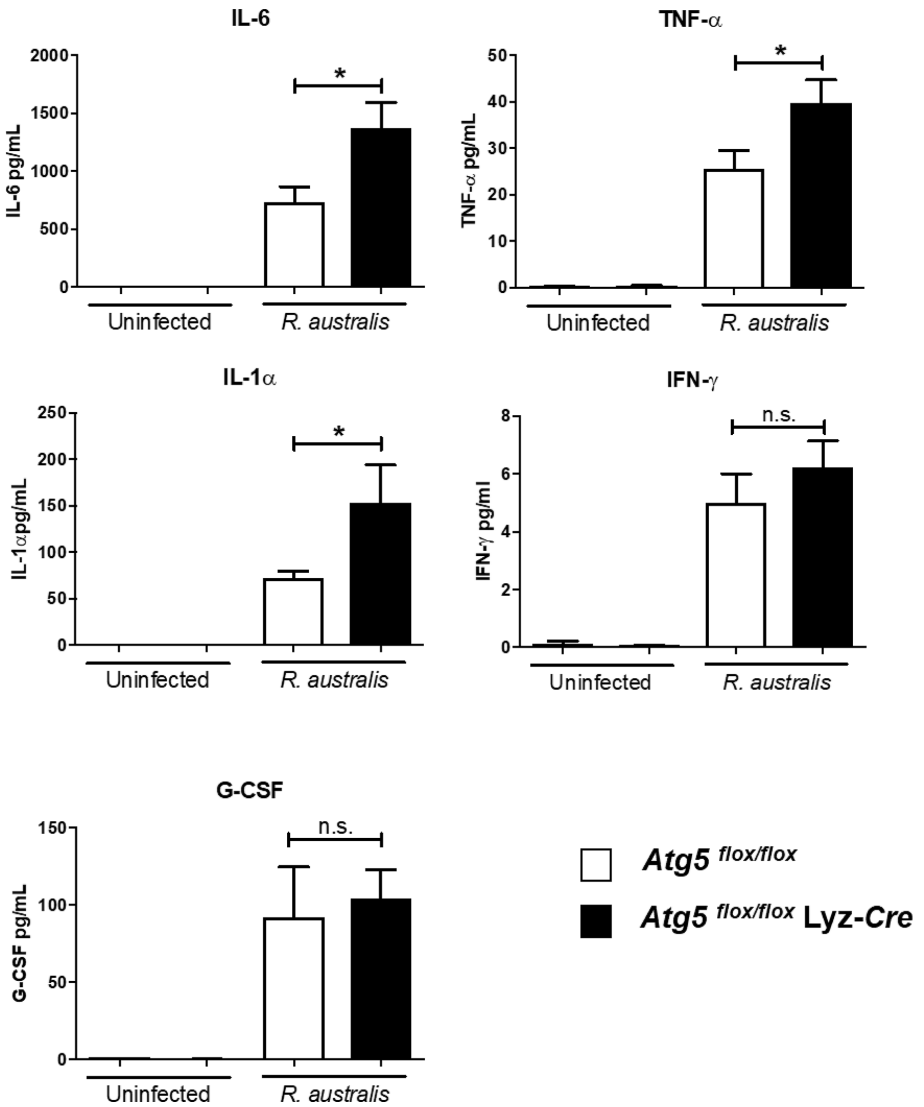

FIGURE 4 | (previous Figure 4). *R. australis* counteracts the production of pro-inflammatory cytokines by infected macrophages *via Atg5*-dependent autophagy. BMMs were isolated from *Atg5* $^{flox/flox}$ Lyz-*Cre* and *Atg5* $^{flox/flox}$ mice, and they were infected with *R. australis* at an MOI of 5. At 24 h p.i., supernatant was harvested. Production levels of cytokines including IL-6, TNF-α, IL-1α, IFN-γ and G-CSF in the supernatant were assessed by Bioplex assay. Results are means ± SE of data from three independent experiments. *$p<0.05$; n.s., not statistically significant.

and P70S6 in *R. australis*-infected macrophages were significantly greater than in uninfected macrophages (**Figures 6B, C**). These results suggest that infection with *R. australis* leads to both direct and indirect activation of mTORC1 in infected macrophages (4). To confirm that the increase in phosphorylated mTOR and P70S6 kinase represents the activation of mTORC1 signaling, B6 BMM macrophages were pre-treated with rapamycin prior to infection. Blockage of mTORC1 signaling by treatment with rapamycin for less than 6 h nearly abolished the increase in both phosphorylated mTOR and P70S6 (**Figure 6**). Thus, these results demonstrated that *R. australis* infection activated mTORC1 signaling in mouse macrophages, which can be effectively eliminated by treatment with rapamycin.

R. australis Induces Autophagic Response While Activating mTORC1 Signaling

Our previous studies have reported that *R. australis* induces ATG5 (+) LC3 (+) autophagosomes with less likely degradative autophagy in macrophages at 1 h p.i (4). As shown in **Figure 6**, *R. australis* activated mTORC1 at the same time when *Atg5*-dependent autophagic response was induced in the same type of cells. This is interesting to us because mTOR-dependent autophagy would have decreased phosphorylation of mTOR. To this end, we stimulated B6 BMMs with rapamycin in the context of *R. australis* infection and analyzed autophagy induction by examining the levels of LC3-II, SQSTM1 and the conversion of soluble LC3-I to lipid bound LC3-II. At 1 h p.i.,

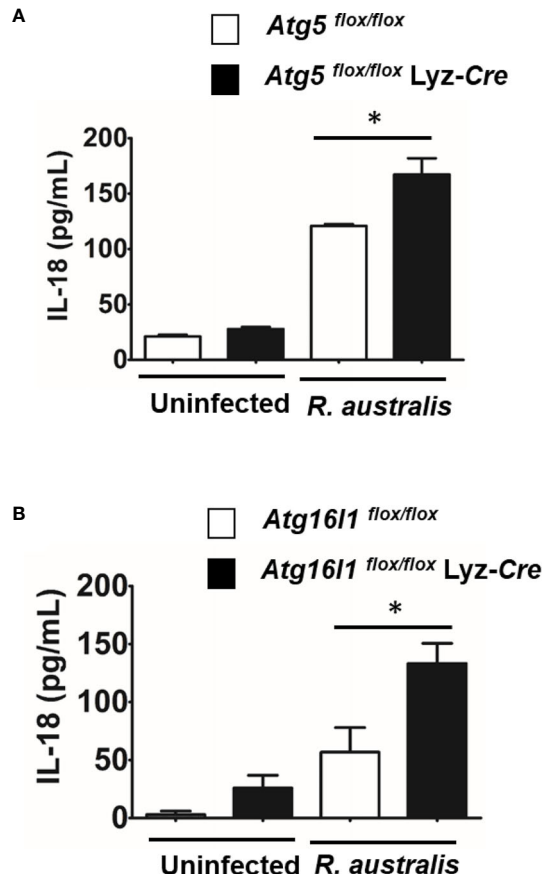

FIGURE 5 | (previous Figure 5). *R. australis* suppressed the production of IL-18 by infected macrophages *via Atg5*-dependent autophagy. BMMs were isolated from *Atg5* $^{flox/flox}$ Lyz-*Cre* and *Atg5* $^{flox/flox}$ mice, and *Atg16l1* $^{flox/flox}$ Lyz-*Cre* and *Atg16l1* $^{flox/flox}$ mice. Macrophages were infected with *R. australis* at an MOI of 5. At 24 h p.i., supernatant was harvested. Concentrations of IL-18 in the supernatant of infected *Atg5* $^{flox/flox}$ Lyz-*Cre* BMMs and *Atg5* $^{flox/flox}$ BMMs **(A)**, and infected *Atg16l1* $^{flox/flox}$ Lyz-*Cre* BMMs and *Atg16l1* $^{flox/flox}$ BMMs **(B)** were assessed by ELISA. Results are means ± SE of data from two independent experiments. *$p < 0.05$.

consistent with our previous report, *R. australis* alone induced significantly increased levels of LC3-II compared to uninfected controls without a significantly reduced level of SQSTM1/p62, indicating a modified autophagic response (**Figures 7A, B**). In contrast, rapamycin treatment slightly increased levels of LC3-II/LC3-I and slightly reduced levels of SQSTM1/p62 in *R. australis*-infected macrophages at 1 h p.i. (**Figures 7A, B**). However, these changes were not statistically significant (**Figure 7B**). At 3 h p.i., we did not find any significant change in expression levels of LC3-II, LC3-II/LC3-I conversion, or SQSTM1/p62 in *R. australis*-infected macrophages treated with rapamycin compared to controls (**Figures 7A, B**). Since *R. australis* is known to modify autophagy into an *Atg5*-dependent autophagic response (4), we decided to determine the quantity of LC3 (+) autophagosomes by immunofluorescence confocal microscopy. Indeed, at 1 h p.i., LC3 puncta staining was significantly increased in *R. australis*-infected BMMs treated with rapamycin compared to macrophages infected with rickettsiae alone (**Figures 7C, D**). However, *R. australis*-infected macrophages with rapamycin treatment did not show significantly increased LC3-II fluorescence intensities compared to rapamycin-treated uninfected cells. In other words, we did not observe synergistic or additive effects by *R. australis* infection in rapamycin-treated macrophages at 1 h p.i. (**Figures 7C, D**). Thus, inhibition of mTORC1 most likely enhanced the accumulation of autophagosomes in *R. australis*-infected macrophages. These data suggest that *R. australis* induces a modified mTORC1-independent autophagic response in macrophages.

DISCUSSION

Our recent report on interactions of autophagy with *R. australis* paved the way for the present study (4). Autophagy is a fundamental cellular homeostasis program that degrades surplus cellular contents in cytoplasm to provide sources of energy (46). Increasing evidence has demonstrated various mechanisms by which host autophagy interacts with invading microbial pathogens. However, the interplay of autophagy with the host inflammatory response to infectious agents *in vivo* and the subsequent pathological changes in tissues are not well understood. Studies revealing such roles of autophagy are likely to provide insightful information toward understanding the pathogenesis of these infectious diseases and the potential development of novel therapeutics targeting autophagy. In this regard, our studies demonstrated several novel findings. *R. australis*, a member in the transitional group of the *Rickettsia* genus, was revealed to activate mTORC1 signaling in primary mouse macrophages. Moreover, mTORC1 control of autophagy was dysregulated during *R. australis* infection at least at 1 h p.i. (**Figure 8**). Our studies also demonstrated that deficiency of *Atg5* enhanced the host control of *R. australis in vivo* accompanied by numerous infiltrations of inflammatory cells in tissues, including neutrophils. *R. australis* infection significantly regulated mammalian host genes and subverted host innate inflammatory responses to support the infection by modifying *Atg5*-dependent autophagy.

The mTOR signaling pathway is widely expressed in tissues and cells of mammalian hosts, and functions as an evolutionarily conserved sensor of environmental and endogenous stress (47). The mTOR is a down-stream effector of PI3K-Akt signaling pathway and mediates nutrient-dependent intracellular signaling related to cell growth, proliferation, and differentiation (16, 48). Hepatitis C virus (HCV) activates mTOR *via* the viral nonstructural protein 5A (NS5A) to enhance cell survival by blocking apoptosis (49). Human cytomegalovirus (HCMV) induces mTOR activation and maintains this activation throughout infection (50). Zullo and Lee reported that several *Mycobacterium* species activate mTOR signaling and induce autophagy; however, they show that the induction of autophagy in macrophages is mTOR-independent (51). Rapamycin has been reported to mainly inhibit mTORC1, particularly within 24 hour of stimulation (52, 53). In the present study, treatment with

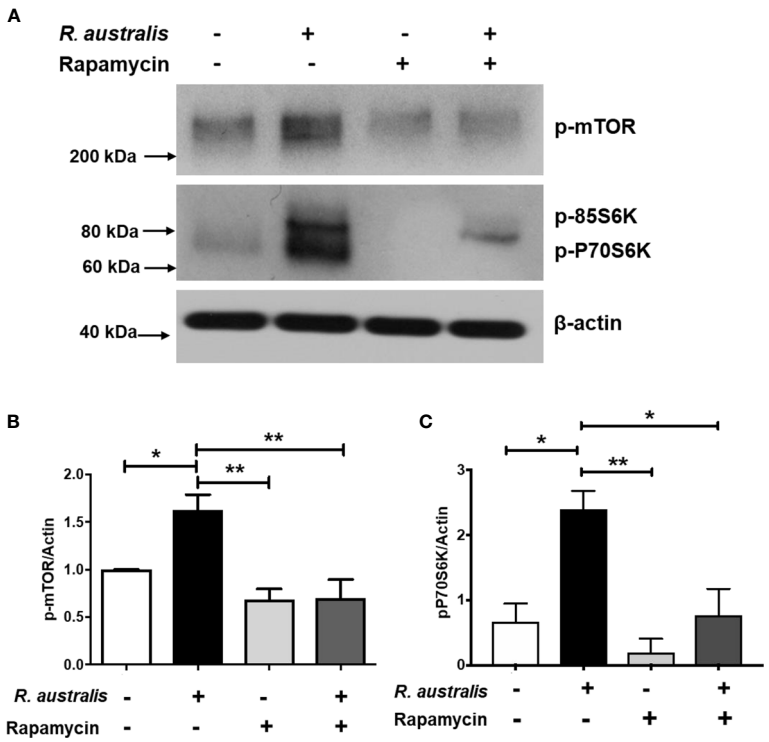

FIGURE 6 | (previous Figure 1). *R. australis* activates mTORC1 in mouse macrophages. BMMs of WT B6 mice were isolated and infected with *R. australis* at an MOI of 5. To inhibit mTORC1 signaling, cells were treated with 50 ng/mL of rapamycin for 4 hours prior to infection with *R. australis*. At 1 h p.i., cells were collected, and cell lysates were immunoblotted with antibodies directed against phosphorylated mTOR, phosphorylated p70S6K, and β-actin **(A)**. The activation of phosphorylated mTOR **(B)** and phosphorylated p70S6K **(C)** was analyzed by densitometry using β-actin as a normalization control with three independent replicates. $^{*}p < 0.05$; $^{**}p < 0.01$.

rapamycin for 5 hours nearly abolished the increase in phosphorylated mTOR and P70S6 in *R. australis*-infected macrophages (**Figures 6** and **7**), suggesting activation of mTORC1 signaling by rickettsiae. Although the results in **Figures 6** and **7** provided both direct and indirect evidence that *R. australis* activates mTORC1 signaling, this conclusion can even be further supported by the unaltered total expression levels of mTOR and P70S6 in these infected macrophages. We are currently performing such experiments in our laboratory. Furthermore, it remains unknown whether *R. australis* activates mTORC2 signaling or not. It is not surprising to us that *R. australis* dysregulated the control of autophagy by mTORC1 in macrophages at 1 h p.i. based on two findings previously reported (4, 54). First, *R. australis* does not induce a canonical autophagy pathway characterized by increased LC3-II and reduced p62 (4). Instead, *R. australis* manipulates an *Atg5*-dependent autophagic response in order to facilitate their infection (**Figure 8**). Secondly, given the recent discovery that *R. typhi* activates both Class I and III PI3Ks (54), it is interesting to speculate that *R. australis* activates class III PI3K complex to further trigger the activation of mTORC1 (**Figure 8**). Increasing evidence indicates that mTORC1 also directly regulates the subsequent steps of the autophagy process, including the nucleation, autophagosome elongation, autophagosome maturation and termination (16). It is, therefore, worthwhile to investigate whether and how mTORC1 is involved in regulating the accumulation of autophagosomes and maturation of autophagosome into autolysosome during *R. australis* infection. Furthermore, previous studies have demonstrated that inhibition of apoptosis is essential for endothelial cell survival during *R. rickettsii* infection. *R. rickettsii* even protects host endothelial cells from staurosporine-induced cell death (55, 56). We also reported that *R. australis* does not induce cell death in infected mouse BMMs (5). Activation of mTOR is known to promote cell survival (57). Thus, it is an attractive hypothesis that the activation of mTOR, including mTORC1 and/or mTORC2 signaling, in cells infected with rickettsiae may serve as a mechanism for promoting cell survival.

Autophagy has been shown to negatively regulate host inflammatory cytokines, particularly the IL-1 family of cytokines. *R. australis* inhibits IL-1β secretion in infected BMMs *in vitro* and in sera by modulating *Atg5*-dependent autophagy (4). *In vitro* neutralization of IL-1β by specific antibodies abolishes the enhanced *R. australis* infection by an *Atg5*-dependent autophagic response in macrophages (4). *R. australis* has been reported to induce significant levels of IL-18, another member in IL-1 family cytokines, by B6 BMMs (5). The differences in production levels of IL-18 by BMMs of *Atg5*- and *Atg16l1*-conditional knockout mice (**Figure 5**) from

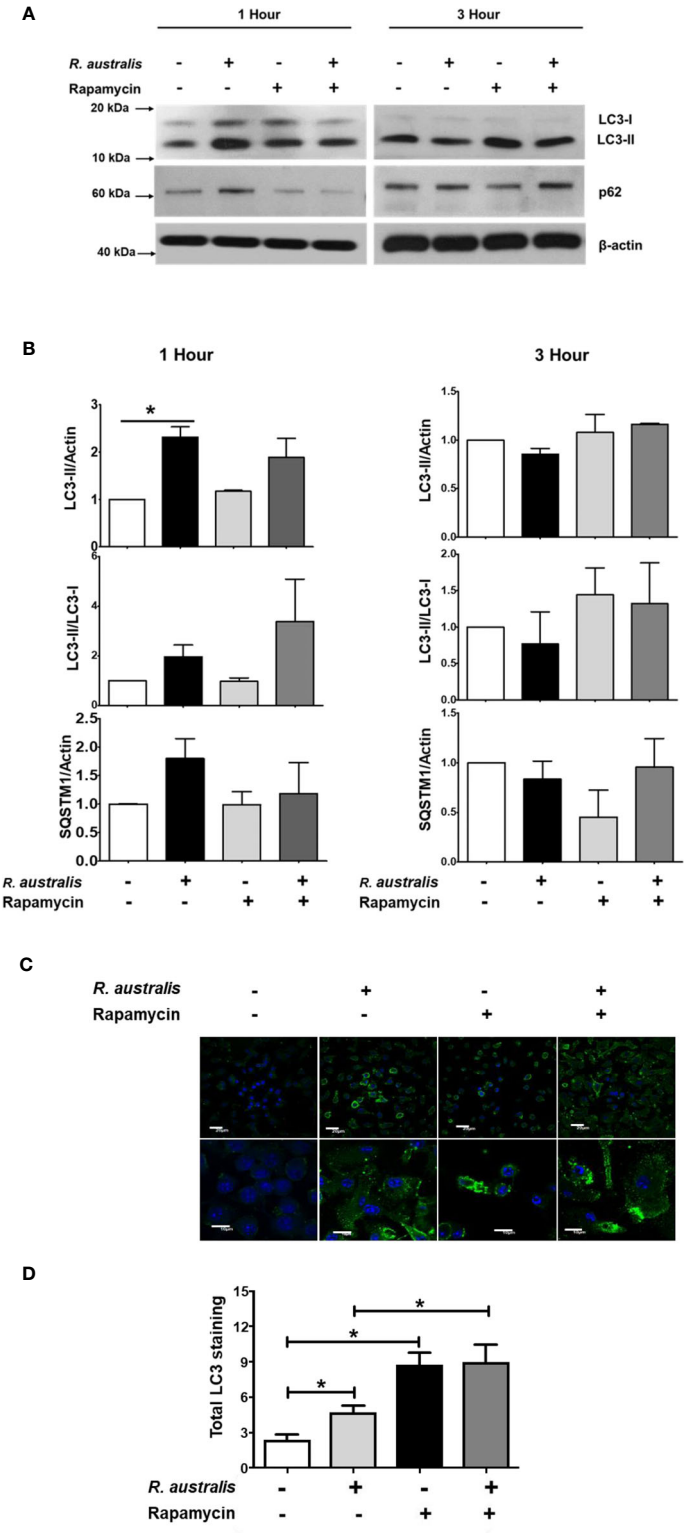

FIGURE 7 | Continued

FIGURE 7 | (previous Figure 2). Interactions of mTORC1 and autophagy with *R. australis* in macrophages. BMMs of WT B6 mice were isolated and infected with *R. australis* at an MOI of 5. To inhibit mTORC1 signaling, cells were treated with 50 ng/mL of rapamycin for 4 hours prior to infection with *R. australis*. Cells were collected at 1 h and 3 h p.i., and cell lysates were immunoblotted with antibodies directed against LC3-II, p62 and β-actin **(A)**. **(B)**, The ratios of LC3-II/Actin, LC3-II/LC3-I, and SQSTM1/Actin in uninfected and infected BMMs with or without rapamycin treatment at 1 h and 3 h p.i. were analyzed by densitometry. **(C)**, Representative confocal immunofluorescence microscopic images of uninfected and infected BMMs with or without rapamycin treatment at 1 h p.i. at a magnification of 20x. Green, LC3 puncta; blue, nuclei (DAPI). Bar = 20 μm in the upper and 10 μm in the bottom row, respectively. **(D)**, Total LC3 staining was quantified using Image J software. Microscopy data represent two to three independent experiments. Data shown are mean ± SE. Group comparison was not labeled if not statistically significant. *$p < 0.05$.

those by B6 BMMs could result from the variabilities in mouse genetic background. Interestingly, IL-1, IL-2, IL-6, TNF-α, IFN-γ, and TGF-β are known to induce autophagy while IL-4, IL-10 and IL-13 inhibit autophagy (58). Our present study demonstrated autophagy-dependent regulation of IL-1α, IL-6, IL-18, and TNF-α in murine macrophages infected with *R. australis in vitro* (**Figures 4** and **5**). These inflammatory cytokines upregulated by *Atg5*-dependent autophagy may contribute to reduced rickettsial loads in tissues of *R. australis*-infected *Atg5*-deficient macrophages (4). However, *R. australis* primarily targets microvascular endothelial cells *in vivo* while macrophages are the initial target cells at the cutaneous entry site of rickettsiae (3, 59, 60). It is not surprising to see a difference in cytokine profiles in *R. australis*-infected BMMs and sera of *R. australis*-infected *Atg5*-conditional knockout mice. For example, macrophages are not a major producer of IFN- γ, and our *in vitro* data confirm this conclusion (**Figure 4**). In contrast, in *Rickettsia*-infected mice, NK and T cells are both the major cells secreting IFN-γ (28, 31, 38, 39). Although an effective Th1-type cytokine response is critical for controlling rickettsial infection as demonstrated by us and other groups (28, 31, 38, 39, 61–63), the serum of *R. australis*-infected *Atg5*$^{flox/flox}$ Lyz-*Cre*

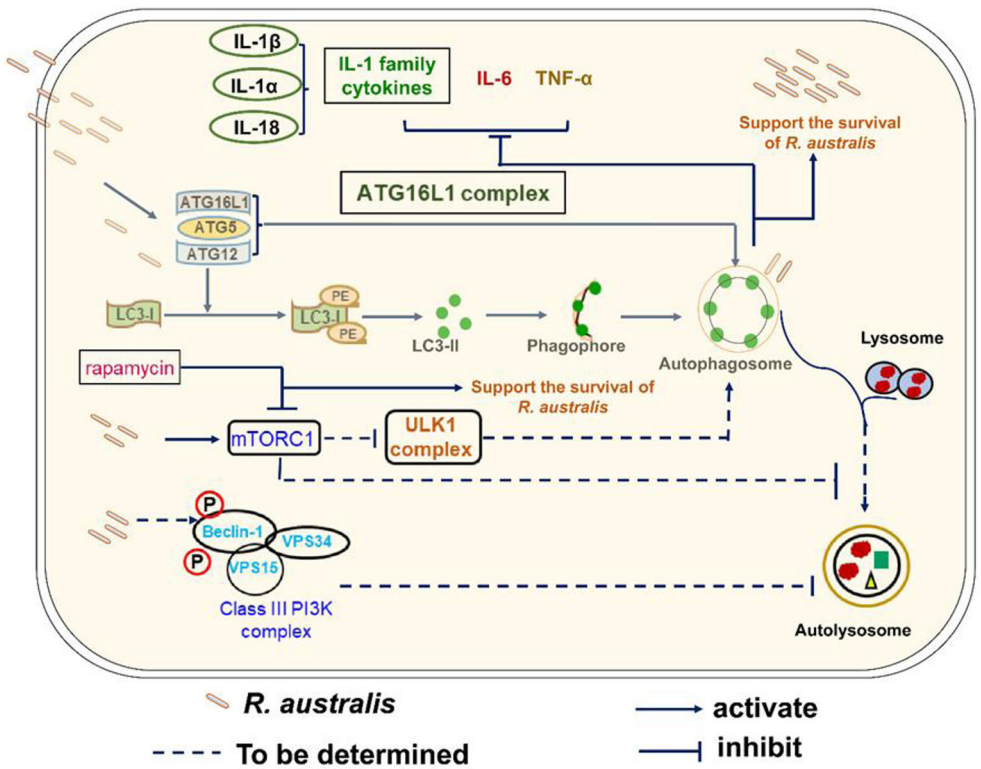

FIGURE 8 | Schematic diagram of interactions of *Atg5*-dependent autophagy and mTORC1 with *R. australis* in macrophages. This schematic diagram depicts the molecular mechanisms involved in the modulation of autophagy and activation of mTORC1 by *R. australis* in order to benefit bacterial infection. *R. australis* activates the ATG5-ATG12-ATG16L1 complex leading to accumulation of LC3 (+) autophagosomes. *Atg5* (+) LC3 (+) autophagosomes induced by *R. australis* in macrophages inhibit production levels of IL-1 family cytokines including IL-1β, IL-1α and IL-18 as well as other inflammatory cytokines such as IL-6 and TNF-α, the effects of which favor rickettsial infection. *R. australis* activates mTORC1 signaling at 1 h p.i. in macrophages when the *Atg5*-dependent autophagic response is induced. Thus, *R. australis*-induced autophagic response is resistant to regulation by mTORC1 signaling. It would be interesting to explore whether *R. australis*-induced autophagosomes can fuse with lysosome and mature into autolysosomes, and how ULK and class III PI3K complex are involved in this process in the future. Solid lines represent pathways demonstrated in our current and previous studies, while dashed lines refer to the mechanisms hypothesized but not tested.

mice had significantly lower levels of IFN-γ, with lower bacterial loads in tissues, compared to *Atg5* $^{flox/flox}$ mice (**Figure 6**) (4). The lower level of IFN-γ in the serum of *Atg5* $^{flox/flox}$ Lyz-*Cre* mice compared to *Atg5* $^{flox/flox}$ animals may result from reduced rickettsial loads in the tissues. Another explanation is that the enhanced systemic production of IFN-γ in *Atg5* $^{flox/flox}$ mice may result from robust activation of NK and T cells by autophagy-competent macrophages in host innate immunity. Overall, *R. australis* ultimately subverted the host innate inflammatory response, which favored its own infection *in vivo*.

The histopathological data of *R. australis*-infected *Atg5*-conditional knockout mice showed that *Atg5* $^{flox/flox}$ Lyz-*Cre* mice had significantly fewer pathological foci with larger size in liver compared to *Atg5* $^{flox/flox}$ mice (**Figure 2**). We hypothesize that the pathological changes in infected *Atg5* $^{flox/flox}$ Lyz-*Cre* mice represent effective host control of pathogenic *Rickettsia* in infected tissues resulting from recruiting a number of potent innate immune cells. In contrast, the pathological changes in *R. australis*-infected *Atg5* $^{flox/flox}$ mice represent paralysis or subversion of innate host immunity, as manifested by the greater frequency of foci but a limited area of cellular infiltration. Our *in vivo* pathology results strongly suggest that *Atg5*-deficiency promotes an inflammatory response consisting of a considerable frequency of neutrophils. IL-1β is a major stimulator of leukocyte recruitment through its ability to up-regulate adhesion to endothelial cells (64, 65). *R. australis* infection induces significantly greater levels of IL-1β in the serum of infected *Atg5* $^{flox/flox}$ Lyz-*Cre* mice vs *Atg5* $^{flox/flox}$ mice (4). The accumulation of neutrophils in the inflammatory foci in liver of infected *Atg5* $^{flox/flox}$ Lyz-*Cre* mice was possibly associated with the greater production levels of IL-1β compared to infected *Atg5* $^{flox/flox}$ mice.

This study revealed that *R. australis* induced *Atg5*-dependent autophagic response while activating mTORC1 signaling in macrophages. Additionally, our data demonstrated that *R. australis* modulated *Atg5*-dependent autophagy to inhibit inflammatory cytokines at both transcriptional and post-transcriptional levels in macrophages, including IL-6, IL-1α, TNF-α, and IL-18. In conclusion, the *R. australis*-modified autophagic response in macrophages supports the *in vivo* infection through subversion of host innate immunity against rickettsiae.

DATA AVAILABILITY STATEMENT

The data has been uploaded to the GEO, with accession number GSE171160.

ETHICS STATEMENT

The animal study was reviewed and approved by the Institutional Animal Care and Use Committee at UTMB.

AUTHOR CONTRIBUTIONS

JB and CR performed the experiments. JB and RF wrote the manuscript. JB, CR, and RF designed the experiments and collected data. DW performed the histopathological analysis as a board-certified pathologist, analyzed the data, and revised the manuscript. SW performed the RNA-Seq and data analysis. KK analyzed the RNA-Seq results by IPA analysis and generated **Figure 3**. All authors contributed to the article and approved the submitted version.

FUNDING

This work was supported by grant AI133359 to RF from the National Institute of Allergy and Infectious Diseases. JB was supported by the National Institutes of Health T32 Training Grant (AI060549) at the University of Texas Medical Branch.

ACKNOWLEDGMENTS

We thank Dr. Seungmin Hwang at the University of Chicago for kindly providing bone marrows of *Atg16l1* $^{flox/flox}$ Lyz-*Cre* and *Atg16l1* $^{flox/flox}$ mice.

REFERENCES

1. Straily A, Drexler N, Cruz-Loustaunau D, Paddock CD, Alvarez-Hernandez G. Notes from the Field: Community-based prevention of Rocky Mountain spotted fever - Sonora, Mexico, 2016. *MMWR Morb Mortal Wkly Rep* (2016) 65(46):1302–3. doi: 10.15585/mmwr.mm6546a6
2. Sahni SK, Rydkina E. Progress in the functional analysis of rickettsial genes through directed mutagenesis of *Rickettsia prowazekii* phospholipase D. *Future Microbiol* (2009) 4(10):1249–53. doi: 10.2217/fmb.09.99
3. Rumfield C, Hyseni I, McBride JW, Walker DH, Fang R. Activation of ASC inflammasome driven by Toll-like receptor 4 contributes to host immunity against rickettsial Infection. *Infect Immun* (2020) 88(4):e00886–19. doi: 10.1128/IAI.00886-19
4. Bechelli J, Vergara L, Smalley C, Buzhdygan TP, Bender S, Zhang W, et al. *Atg5* supports *Rickettsia australis* infection in macrophages *in vitro* and *in vivo*. *Infect Immun* (2018) 87(1):e00651–18. doi: 10.1128/IAI.00651-18
5. Smalley C, Bechelli J, Rockx-Brouwer D, Saito T, Azar SR, Ismail N, et al. *Rickettsia australis* activates inflammasome in human and murine macrophages. *PloS One* (2016) 11(6):e0157231. doi: 10.1371/journal.pone.0157231
6. Curto P, Simões I, Riley SP, Martinez JJ. Differences in intracellular fate of two spotted fever group *Rickettsia* in macrophage-like cells. *Front Cell Infect Microbiol* (2016) 6:80. doi: 10.3389/fcimb.2016.00080
7. Curto P, Riley SP, Simões I, Martinez JJ. Macrophages infected by a pathogen and a non-pathogen spotted fever group *Rickettsia* reveal differential reprogramming signatures early in infection. *Front Cell Infect Microbiol* (2019) 9:97. doi: 10.3389/fcimb.2019.00097
8. Radulovic S, Price PW, Beier MS, Gaywee J, Macaluso JA, Azad A. *Rickettsia*-macrophage interactions: host cell responses to *Rickettsia akari* and *Rickettsia typhi*. *Infect Immun* (2002) 70(5):2576–82. doi: 10.1128/iai.70.5.2576-2582.2002
9. Banajee KH, Embers ME, Langohr IM, Doyle LA, Hasenkampf NR, Macaluso KR. Correction: *Amblyomma maculatum* feeding augments *Rickettsia parkeri* infection in a rhesus Macaque model: a pilot study. *PloS One* (2015) 10(8):

e0137598. doi: 10.1371/journal.pone.0137598. Erratum for: PLoS One (2015) 10(8):e0135175.
10. Mizushima N, Noda T, Yoshimori T, Tanaka Y, Ishii T, George MD, et al. A protein conjugation system essential for autophagy. *Nature* (1998) 395 (6700):395–8. doi: 10.1038/26506
11. Levine B, Klionsky DJ. Development by self-digestion: molecular mechanisms and biological functions of autophagy. *Dev Cell* (2004) 6(4):463–77. doi: 10.1016/s1534-5807(04)00099-1
12. Li W, Zhang L. Regulation of ATG and autophagy initiation. *Adv Exp Med Biol* (2019) 1206:41–65. doi: 10.1007/978-981-15-0602-4_2
13. Kuma A, Hatano M, Matsui M, Yamamoto A, Nakaya H, Yoshimori T, et al. The role of autophagy during the early neonatal starvation period. *Nature* (2004) 432:1032–6. doi: 10.1038/nature03029
14. Hara T, Nakamura K, Matsui M, Yamamoto A, Nakahara Y, Suzuki-Migishima R, et al. Suppression of basal autophagy in neural cells causes neurodegenerative disease in mice. *Nature* (2006) 441:885–89. doi: 10.1038/nature04724
15. Zhao Z, Thackray LB, Miller BC, Lynn TM, Becker MM, Ward E, et al. Coronavirus replication does not require the autophagy gene ATG5. *Autophagy* (2007) 3:581–5. doi: 10.4161/auto.4782
16. Dossou AS, Basu A. The Emerging Roles of mTORC1 in Macromanaging Autophagy. *Cancers (Basel)* (2019) 11(10):1422. doi: 10.3390/cancers11101422
17. Weichhart T, Säemann MD. The multiple facets of mTOR in immunity. *Trends Immunol* (2009) 30(5):218–26. doi: 10.1016/j.it.2009.02.002
18. Jhanwar-Uniyal M, Amin AG, Cooper JB, Das K, Schmidt MH, Murali R. Discrete signaling mechanisms of mTORC1 and mTORC2: Connected yet apart in cellular and molecular aspects. *Adv Biol Regul* (2017) 64:39–48. doi: 10.1016/j.jbior.2016.12.001
19. Hong S, Mannan AM, Inoki K. Evaluation of the nutrient-sensing mTOR pathway. *Methods Mol Biol* (2012) 821:29–44. doi: 10.1007/978-1-61779-430-8_3
20. Gelsomino F, Bertolini F, Luppi G, Spallanzani A, Pettorelli E, Reggiani Bonetti L, et al. Cascinu S. A Dose-finding and Biomarker Evaluation Phase Ib Study of Everolimus in Association With 5-Fluorouracil and Pelvic Radiotherapy as Neoadjuvant Treatment of Locally Advanced Rectal Cancer (E-LARC Study). *Clin Colorectal Cancer* (2017) 16(4):410–15.e1. doi: 10.1016/j.clcc.2017.03.011
21. Zhang F, Hu X, Gu Y, Bian H, Xu Z, Wang Q, et al. URI knockdown induces autophagic flux in gastric cancer cells. *Am J Cancer Res* (2018) 8(10):2140–9. Available at: www.ajcr.us/ISSN:2156-6976/ajcr0078088.
22. Li SH, Lin WC, Huang TL, Chen CH, Chiu TJ, Fang FM, et al. Significance of mammalian target of rapamycin in patients with locally advanced stage IV head and neck squamous cell carcinoma receiving induction chemotherapy with docetaxel, cisplatin, and fluorouracil. *Head Neck* (2016) 38 Suppl 1:E844–52. doi: 10.1002/hed.24111
23. Katholnig K, Linke M, Pham H, Hengstschläger M, Weichhart T. Immune responses of macrophages and dendritic cells regulated by mTOR signalling. *Biochem Soc Trans* (2013) 41(4):927–33. doi: 10.1042/BST20130032
24. Deretic V, Levine B. Autophagy, immunity, and microbial adaptations. *Cell Host Microbe* (2009) 5(6):527–49. doi: 10.1016/j.chom.2009.05.016
25. Choi Y, Bowman JW, Jung JU. Autophagy during viral infection - a double-edged sword. *Nat Rev Microbiol* (2018) 16(6):341–54. doi: 10.1038/s41579-018-0003-6
26. Paulus GL, Xavier RJ. Autophagy and checkpoints for intracellular pathogen defense. *Curr Opin Gastroenterol* (2015) 31(1):14–23. doi: 10.1097/MOG.0000000000000134
27. Hanson BA, Wisseman CL Jr, Waddell A, Silverman DJ. Some characteristics of heavy and light bands of *Rickettsia prowazekii* on Renografin gradients. *Infect Immun* (1981) 34(2):596–604. doi: 10.1128/IAI.34.2.596-604.1981
28. Fang R, Ismail N, Shelite T, Walker DH. CD4+ CD25+ Foxp3- T-regulatory cells produce both gamma interferon and interleukin-10 during acute severe murine spotted fever rickettsiosis. *Infect Immun* (2009) 77(9):3838–49. doi: 10.1128/IAI.00349-09
29. Ammerman NC, Beier-Sexton M, Azad AF. Laboratory maintenance of Rickettsia rickettsii. *Curr Protoc Microbiol* (2008) 11(1):3A.5.1–5.21. doi: 10.1002/9780471729259.mc03a05s11
30. Zhao Z, Fux B, Goodwin M, Dunay IR, Strong D, Miller BC, et al. Autophagosome-independent essential function for the autophagy protein *Atg5* in cellular immunity to intracellular pathogens. *Cell Host Microbe* (2008) 4(5):458–69. doi: 10.1016/j.chom.2008.10.003
31. Fang R, Ismail N, Walker DH. Contribution of NK cells to the innate phase of host protection against an intracellular bacterium targeting systemic endothelium. *Am J Pathol* (2012) 181(1):185–95. doi: 10.1016/j.ajpath.2012.03.020
32. Zhang X, Goncalves R, Mosser DM. The isolation and characterization of murine macrophages. *Curr Protoc Immunol* (2008) 83(1):14.1.1–1.14. doi: 10.1002/0471142735.im1401s83
33. Schneider CA, Rasband WS, Eliceiri KW. NIH Image to ImageJ: 25 years of image analysis. *Nat Methods* (2012) 9(7):671–5. doi: 10.1038/nmeth.2089
34. McCloy RA, Rogers S, Caldon CE, Lorca T, Castro A, Burgess A. Partial inhibition of Cdk1 in G 2 phase overrides the SAC and decouples mitotic events. *Cell Cycle* (2014) 13(9):1400–12. doi: 10.4161/cc.28401
35. Yu K, Toral-Barza L. Biochemical and pharmacological inhibition of mTOR by rapamycin and an ATP-competitive mTOR inhibitor. *Methods Mol Biol* (2012) 821:15–28. doi: 10.1007/978-1-61779-430-8_2
36. Altman SA, Randers L, Rao G. Comparison of trypan blue dye exclusion and fluorometric assays for mammalian cell viability determinations. *Biotechnol Prog* (1993) 9(6):671–4. doi: 10.1021/bp00024a017
37. Thangamani S, Hermance ME, Santos RI, Slovak M, Heinze D, Widen SG, et al. Transcriptional immunoprofiling at the tick-virus-host interface during early stages of tick-borne encephalitis virus transmission. *Front Cell Infect Microbiol* (2017) 7:494. doi: 10.3389/fcimb.2017.00494
38. Bechelli J, Smalley C, Zhao X, Judy B, Valdes P, Walker DH, et al. MyD88 mediates instructive signaling in dendritic cells and protective inflammatory response during rickettsial infection. *Infect Immun* (2016) 84(4):883–93. doi: 10.1128/IAI.01361-15
39. Fang R, Ismail N, Soong L, Popov VL, Whitworth T, Bouyer DH, et al. Differential interaction of dendritic cells with *Rickettsia conorii*: impact on host susceptibility to murine spotted fever rickettsiosis. *Infect Immun* (2007) 75(6):3112–23. doi: 10.1128/IAI.00007-07
40. Chan YR, Liu JS, Pociask DA, Zheng M, Mietzner TA, Berger T, et al. Lipocalin 2 is required for pulmonary host defense against Klebsiella infection. *J Immunol* (2009) 182(8):4947–56. doi: 10.4049/jimmunol.0803282
41. Jossé L, Xie J, Proud CG, Smales CM. mTORC1 signalling and eIF4E/4E-BP1 translation initiation factor stoichiometry influence recombinant protein productivity from GS-CHOK1 cells. *Biochem J* (2016) 473(24):4651–64. doi: 10.1042/BCJ20160845
42. Buchkovich NJ, Yu Y, Zampieri CA, Alwine JC. The TORrid affairs of viruses: effects of mammalian DNA viruses on the PI3K-Akt-mTOR signalling pathway. *Nat Rev Microbiol* (2008) 6(4):266–75. doi: 10.1038/nrmicro1855
43. Dinarello CA. The IL-1 family of cytokines and receptors in rheumatic diseases. *Nat Rev Rheumatol* (2019) 15(10):612–32. doi: 10.1038/s41584-019-0277-8
44. Ghose P, Ali AQ, Fang R, Forbes D, Ballard B, Ismail N. The interaction between IL-18 and IL-18 receptor limits the magnitude of protective immunity and enhances pathogenic responses following infection with intracellular bacteria. *J Immunol* (2011) 187(3):1333–46. doi: 10.4049/jimmunol.1100092
45. Arend WP, Palmer G, Gabay C. IL-1, IL-18, and IL-33 families of cytokines. *Immunol Rev* (2008) 223:20–38. doi: 10.1111/j.1600-065X.2008.00624.x
46. Chun Y, Kim J. Autophagy: An essential degradation program for cellular homeostasis and life. *Cells* (2018) 7(12):278. doi: 10.3390/cells7120278
47. Cipponi A, Goode DL, Bedo J, McCabe MJ, Pajic M, Croucher DR, et al. MTOR signaling orchestrates stress-induced mutagenesis, facilitating adaptive evolution in cancer. *Science* (2020) 368(6495):1127–31. doi: 10.1126/science.aau8768
48. Cao GD, Xu XY, Zhang JW, Chen B, Xiong MM. Phosphorylated Mammalian Target of Rapamycin p-mTOR Is a Favorable Prognostic Factor than mTOR in Gastric Cancer. *PloS One* (2016) 11(12):e0168085. doi: 10.1371/journal.pone.0168085
49. Peng L, Liang D, Tong W, Li J, Yuan Z. Hepatitis C virus NS5A activates the mammalian target of rapamycin (mTOR) pathway, contributing to cell survival by disrupting the interaction between FK506-binding protein 38 (FKBP38) and mTOR. *J Biol Chem* (2010) 285(27):20870–81. doi: 10.1074/jbc.M110.112045

50. Kudchodkar SB, Yu Y, Maguire TG, Alwine JC. Human cytomegalovirus infection induces rapamycin-insensitive phosphorylation of downstream effectors of mTOR kinase. *J Virol* (2004) 78(20):11030–9. doi: 10.1128/JVI.78.20.11030-11039.2004
51. Zullo AJ, Lee S. Mycobacterial induction of autophagy varies by species and occurs independently of mammalian target of rapamycin inhibition. *J Biol Chem* (2012) 287(16):12668–78. doi: 10.1074/jbc.M111.320135
52. Sarbassov DD, Ali SM, Sengupta S, Sheen JH, Hsu PP, Bagley AF, et al. Prolonged rapamycin treatment inhibits mTORC2 assembly and Akt/PKB. *Mol Cell* (2006) 22(2):159–68. doi: 10.1016/j.molcel.2006.03.029
53. Lamming DW, Ye L, Katajisto P, Goncalves MD, Saitoh M, Stevens DM, et al. Rapamycin-induced insulin resistance is mediated by mTORC2 loss and uncoupled from longevity. *Science* (2012) 335(6076):1638–43. doi: 10.1126/science.1215135
54. Voss OH, Gillespie JJ, Lehman SS, Rennoll SA, Beier-Sexton M, Rahman MS, et al. Risk1, a Phosphatidylinositol 3-Kinase Effector, Promotes *Rickettsia typhi* Intracellular Survival. *mBio* (2020) 11(3):e00820–20. doi: 10.1128/mBio.00820-20
55. Clifton DR, Goss RA, Sahni SK, van Antwerp D, Baggs RB, Marder VJ, et al. NF-kappa B-dependent inhibition of apoptosis is essential for host cellsurvival during *Rickettsia rickettsii* infection. *Proc Natl Acad Sci USA* (1998) 95 (8):4646–51. doi: 10.1073/pnas.95.8.4646
56. Bechelli JR, Rydkina E, Colonne PM, Sahni SK. Rickettsia rickettsii infection protects human microvascular endothelial cells against staurosporine-induced apoptosis by a cIAP(2)-independent mechanism. *J Infect Dis* (2009) 199 (9):1389–98. doi: 10.1086/597805
57. Covarrubias AJ, Aksoylar HI, Horng T. Control of macrophage metabolism and activation by mTOR and Akt signaling. *Semin Immunol* (2015) 27 (4):286–96. doi: 10.1016/j.smim.2015.08.001
58. Harris J. Autophagy and cytokines. *Cytokine* (2011) 56(2):140–4. doi: 10.1016/j.cyto.2011.08.022
59. Cragun WC, Bartlett BL, Ellis MW, Hoover AZ, Tyring SK, Mendoza N, et al. The expanding spectrum of eschar-associated rickettsioses in the United States. *Arch Dermatol* (2010) 146:641–8. doi: 10.1001/archdermatol.2010.48
60. Walker DH, Hudnall SD, Szaniawski WK, Feng HM. Monoclonal antibody-based immunohistochemical diagnosis of rickettsialpox: the macrophage is the principal target. *Mod Pathol* (1999) 12:529–33.
61. Mansueto P, Vitale G, Cascio A, Seidita A, Pepe I, Carroccio A, et al. New insight into immunity and immunopathology of Rickettsial diseases. *Clin Dev Immunol* (2012) 2012:967852. doi: 10.1155/2012/967852
62. Li H, Jerrells TR, Spitalny GL, Walker DH. Gamma interferon as a crucial host defense against *Rickettsia conorii in vivo*. *Infect Immun* (1987) 55(5):1252–5. doi: 10.1128/IAI.55.5.1252-1255.1987
63. Feng HM, Popov VL, Walker DH. Depletion of gamma interferon and tumor necrosis factor alpha in mice with *Rickettsia conorii*-infected endothelium: impairment of rickettsicidal nitric oxide production resulting in fatal, overwhelming rickettsial disease. *Infect Immun* (1994) 62(5):1952–60. doi: 10.1128/IAI.62.5.1952-1960.1994
64. Prince LR, Allen L, Jones EC, Hellewell PG, Dower SK, Whyte MK, et al. The role of interleukin-1beta in direct and toll-like receptor 4-mediated neutrophil activation and survival. *Am J Pathol* (2004) 165(5):1819–26. doi: 10.1016/s0002-9440(10)63437-2
65. Furie MB, McHugh DD. Migration of neutrophils across endothelial monolayers is stimulated by treatment of the monolayers with interleukin-1 or tumor necrosis factor-alpha. *J Immunol* (1989) 143(10):3309–17.

Conflict of Interest: The authors declare that the research was conducted in the absence of any commercial or financial relationships that could be construed as a potential conflict of interest.

frontiers in Immunology

ORIGINAL RESEARCH
published: 16 April 2021
doi: 10.3389/fimmu.2021.649475

Genome-Wide Gene Expression Analysis of Mtb-Infected DC Highlights the Rapamycin-Driven Modulation of Regulatory Cytokines *via* the mTOR/GSK-3β Axis

Marilena P. Etna[1], Martina Severa[1], Valerio Licursi[2], Manuela Pardini[1], Melania Cruciani[1], Fabiana Rizzo[1], Elena Giacomini[1], Gianfranco Macchia[3], Orazio Palumbo[4], Raffaella Stallone[4], Massimo Carella[4], Mark Livingstone[5], Rodolfo Negri[2], Sandra Pellegrini[5] and Eliana M. Coccia[1]**

[1] Department of Infectious Diseases, Istituto Superiore di Sanità, Rome, Italy, [2] Department of Biology and Biotechnology, Sapienza University, Rome, Italy, [3] Proteomics Core Facility, Istituto Superiore di Sanità, Rome, Italy, [4] Division of Medical Genetics, Fondazione IRCCS-Casa Sollievo della Sofferenza, San Giovanni Rotondo, Italy, [5] Cytokine Signaling Unit, Inserm, Institut Pasteur, Paris, France

OPEN ACCESS

Edited by:
Jere W. McBride,
University of Texas Medical Branch at Galveston, United States

Reviewed by:
Carlos Arterio Sorgi,
University of São Paulo Ribeirão Preto, Brazil
Stefan Oehlers,
Royal Prince Alfred Hospital, Australia

***Correspondence:**
Marilena P. Etna
marilenapaola.etna@iss.it
Eliana M. Coccia
eliana.coccia@iss.it

Specialty section:
This article was submitted to Microbial Immunology, a section of the journal Frontiers in Immunology

Received: 04 January 2021
Accepted: 10 March 2021
Published: 16 April 2021

Citation:
Etna MP, Severa M, Licursi V, Pardini M, Cruciani M, Rizzo F, Giacomini E, Macchia G, Palumbo O, Stallone R, Carella M, Livingstone M, Negri R, Pellegrini S and Coccia EM (2021) Genome-Wide Gene Expression Analysis of Mtb-Infected DC Highlights the Rapamycin-Driven Modulation of Regulatory Cytokines via the mTOR/GSK-3β Axis. Front. Immunol. 12:649475. doi: 10.3389/fimmu.2021.649475

In human primary dendritic cells (DC) rapamycin—an autophagy inducer and protein synthesis inhibitor—overcomes the autophagy block induced by *Mycobacterium tuberculosis* (Mtb) and promotes a Th1 response *via* IL-12 secretion. Here, the immunostimulatory activity of rapamycin in Mtb-infected DC was further investigated by analyzing both transcriptome and translatome gene profiles. Hundreds of differentially expressed genes (DEGs) were identified by transcriptome and translatome analyses of Mtb-infected DC, and some of these genes were found further modulated by rapamycin. The majority of transcriptome-associated DEGs overlapped with those present in the translatome, suggesting that transcriptionally stimulated mRNAs are also actively translated. *In silico* analysis of DEGs revealed significant changes in intracellular cascades related to cytokine production, cytokine-induced signaling and immune response to pathogens. In particular, rapamycin treatment of Mtb-infected DC caused an enrichment of IFN-β, IFN-λ and IFN-stimulated gene transcripts in the polysome-associated RNA fraction. In addition, rapamycin led to an increase of IL-12, IL-23, IL-1β, IL-6, and TNF-α but to a reduction of IL-10. Interestingly, upon silencing or pharmacological inhibition of GSK-3β, the rapamycin-driven modulation of the pro- and anti-inflammatory cytokine balance was lost, indicating that, in Mtb-infected DC, GSK-3β acts as molecular switch for the regulation of the cytokine milieu. In conclusion, our study sheds light on the molecular mechanism by which autophagy induction contributes to DC activation during Mtb infection and points to rapamycin and GSK-3β modulators as promising compounds for host-directed therapy in the control of Mtb infection.

Keywords: host-directed therapy, *Mycobacterium tuberculosis*, tuberculosis, rapalogs, IFN, autophagy, transcriptome, translatome

INTRODUCTION

As reported by World Health Organization, millions of people in the world continue to fall ill each year with tuberculosis (TB), one of the top killer infectious disease caused by *Mycobacterium tuberculosis* (Mtb) (1). The reasons behind Mtb capacity to maintain this sad primacy must be sought in the different strategies employed by this pathogen to survive inside the host, ranging from the establishment of a latent infection to several mechanisms for evading the immune response (2). In this context, the host innate immune system and its plethora of defense mechanisms critically influence the fate of the infection (2). Among innate immune cells, macrophages and dendritic cells (DC) are early infected by Mtb and, in turn, these cells orchestrate the immune response against the pathogen. In particular, DC, as professional antigen presenting cells (APC), undergo phenotypic modifications and produce a panel of pro-inflammatory and regulatory cytokines which tune the immune response by acting on different cell populations, including naïve T cells (3). A critical prerequisite for DC activation is the sensing of Mtb-associated molecular structures by pattern recognition receptors whose stimulation leads to a range of cellular events that contribute to host mycobacterial control. However, during its co-evolution with the host, Mtb has evolved numerous evasion mechanisms to hijack innate immune response, such as cytosolic escape, block of phagosome maturation, apoptosis, inflammasome activation/modulation as well as autophagy inhibition (4). In particular, the relevance of autophagy in the anti-mycobacterial response is well documented. Indeed, it was shown that, in order to promote its own survival, virulent Mtb impairs phagosome maturation by altering the acidic, hydrolytic environment of the intracellular compartment (5), it compromises the autophagy-mediated antigen-processing capacity of macrophages and DC (6, 7) and blocks autophagosome formation and maturation (2, 8, 9). Interestingly, in the last decade many authors have investigated the effect of autophagy modulators to improve anti-mycobacterial host cell functions and proposed their use as potential therapeutic treatment. Since autophagy is regulated by several intracellular pathways and some of them converge on the master regulatory kinase mammalian target of rapamycin (mTOR), autophagy-targeting strategies can either inhibit mTOR or can be mTOR-independent (10). In this context, we previously showed that the block of autophagy caused by Mtb in human DC is overcome by rapamycin, an autophagy inducer and mTOR inhibitor. Moreover, treatment with rapamycin leads also to increased expression of interferon-β (IFN-β) and increased production of the pro-Th1 cytokine, interleukin 12 (IL-12) (9).

In the current study, we investigated the molecular mechanisms underlying rapamycin-mediated immune-stimulatory action, by studying both transcriptome and translatome gene profiles of DC infected with Mtb in presence or absence of rapamycin. We found that, during Mtb infection, the drug can act as a selective inducer of protein translation, by promoting the association of type I and type III IFN mRNAs to polysomes and by preventing the inhibition of the constitutively active glycogen synthase kinase 3 beta (GSK-3β) through which rapamycin impinges on the balance of secreted pro- and anti-inflammatory cytokines.

MATERIALS AND METHODS

Ethics Statement

Istituto Superiore di Sanità Review Board approved the present research project (CE/13/387). No informed consent was given since the data were analyzed anonymously. Peripheral blood mononuclear cells were isolated from freshly collected buffy coats obtained from healthy voluntary blood donors (Blood Bank of University "La Sapienza", Rome, Italy).

DC Preparation and Cell Culture

DC were prepared as previously described (11). Briefly, DC were generated by culturing $CD14^+$ monocytes with 50 ng/ml GM-CSF and 1000 U/ml IL-4 (R&D Systems, Minneapolis, MN, USA) for 5 days at $0.5x10^6$ cells/ml in RPMI 1640 (Lonza, Basel, Switzerland), supplemented with 2 mM L-glutamine and 15% Fetal Bovine Serum (FBS) (Lonza). At day 5 the cells were tested for their differentiation status by evaluating CD1a expression (>90% $CD1a^+$) and lack of CD14 (>95% $CD14^-$). Before infection, the medium was replaced with RPMI without antibiotics and supplemented with 2 mM L-glutamine and 15% FBS. Cytokine deprivation did not affect DC survival rate, which was >90%.

Antibodies (Abs) and Other Reagents

For immunoblotting analysis, rabbit anti-phospho-p70S6K (S371), rabbit anti-phospho- p70S6K (T389), rabbit anti-GSK-3β, rabbit anti-phospho-GSK-3β (S9), rabbit anti-phospho-GS (S641), rabbit-anti-p38, rabbit-anti-phospho-p44/42 (T202/Y204), rabbit anti-phospho-p38 (T180/Y182) (Cell Signaling, Danvers, MA, USA), mouse anti-actin (Sigma-Aldrich, St. Louis, MO, USA), and horseradish peroxidase-conjugate secondary anti-mouse and anti-rabbit Abs (Santa Cruz Biotechnology) were used. Rapamycin (0.2 μM, Sigma-Aldrich) or Torin 1 (0.5 μM Tocris, Bristol, UK) were added to DC culture 4 h after Mtb-infection for studying mammalian target of rapamycin complex 1 (mTORC1) and mTOR inhibition respectively. For the selective inhibition of GSK-3β and p70S6K1 respectively, SB216763 (5 μM, Sigma-Aldrich) and PF4708671 (0.1 μM, Sigma-Aldrich) were used to treat DC 30 min before infection and rapamycin treatment. To evaluate rapamycin bystander effect, DC were treated for 30 min before infection and rapamycin treatment with SB203580 (10 μM, Sigma-Aldrich) or SB202129 (10 μM, Sigma-Aldrich) to inhibit p38 or with PD980509 (0.1 μM, Sigma-Aldrich) to block p44/42.

Bacterial Strain Description and Preparation

Mtb H37Rv (ATCC 27294; American Type Culture Collection) was grown as previously described (8). Logarithmically growing cultures were centrifuged at 800 rpm for 10 min to eliminate clumped mycobacteria and then washed three times in RPMI

1640. Mycobacteria were re-suspended in RPMI 1640 containing 10% FBS and then stored at - 80°C. Bacterial frozen vials were thawed and bacterial viability was determined by counting the number of colony forming units. All bacterium preparations were tested for endotoxin contamination (<1 Endotoxin Unit/ml) by the Limulus lysate assay (Lonza). DC cultures were then infected with a multiplicity of infection (MOI) of 1 bacterium/cell as previously described (8).

Total RNA Extraction, Quantification, and Quality Assessment

Total RNA was isolated from $10x10^6$ infected or not infected DC, treated or not with rapamycin using Trizol (Invitrogen, Thermo Fisher Scientific) and by following manufacturer's recommendations. RNA was quantified using a Nanodrop 2000 spectrophotometer (Thermo Fisher Scientific, Waltham, MA, USA) and quality assessed with an established cut-off of 1.8 for both the 260/280 and 260/270 absorbance ratios. RNA integrity was instead inspected by bioanalyzer analysis (Agilent Technologies, Santa Clara, CA, USA) considering a cut-off of 1.8 for 28S/18S ratio.

Isolation of Polysome-Associated RNA

For RNA fraction isolation, 10×10^6 cells for untreated DC (CTRL), DC treated for 12 h with rapamycin (0.2 μM) and DC infected for 16 h with Mtb (MOI 1) and treated or not with rapamycin (12 h, 0.2 μM) were used. Polysome-associated RNA were prepared as previously described (8). Briefly, each gradient was fractionated in BSL3 facility by hand collection from the top of the gradient into 2 samples, light phase (low polysome occupancy) and heavy phase (high polysome occupancy). The hand collection method was previously tested to parallel with fraction collection using a fractionator coupled with an UV optical reader (A 254nm). The obtained fractions were immediately mixed with an equal volume of Trizol (Invitrogen, Thermo Fisher Scientific) for later RNA isolation following Trizol manufacturing instructions.

Microarray Analysis

Gene expression profiling was performed using the GeneChip® Human Transcriptome Array 2.0 (Thermo Fisher Scientific, Waltham, MA, USA) including more than 6.0 million distinct probes covering both coding and non-coding genes built on transcript mappings from hg19 human reference sequence (GRCh37). A total of 400,000 full length transcripts were combined from available public data sources: RefSeq NCBI, UCSC Genes, Vega, GENCODE, Ensembl, Mammalian Gene Collection. Additional long non-coding content was combined from the UCSC genome browser, noncode.org, Broad Human Body Map. Probes are distributed across the full length of the gene including specific probes (>339.000 probe sets) covering splice junction, providing a complete and accurate picture of overall gene expression with the additional ability for transcript isoform analysis.

For each sample enrolled for the study, 100 ng of total RNA were processed according to the GeneChip Whole Transcript Sense Target Labeling Assay following the manufacturer's instructions (Thermo Fisher Scientific, Waltham, MA, USA). Briefly, a random priming method was used to generate cDNA from all RNA transcripts present in a sample. The random primers incorporate a T7 promoter sequence, which is subsequently used in an *in vitro* transcription to produce antisense cRNA fragments. Single stranded cDNA complementary to the cRNA is then produced, in the sense orientation, where a modified dUTP is incorporated instead of dTTP. The modified dUTP is subsequently recognized by the enzymes Uracil-DNA glycosylase and human apurinic/apyrimidinic endonuclease 1 which will cut the DNA, resulting in fragmentation of the cDNA. Each DNA fragment is end-labelled with biotin using terminal deoxynucleotidyltransferase before being hybridized to the arrays for 16 h at 45°C in a GeneChip Hybridization Oven 640. Following hybridization and post hybridization washes each array were scanned using the GeneChip Scanner 3000 7G to generate the raw data (.CEL file). The QC steps of the experiment were performed using Expression Console v1.4 (Thermo Fisher Scientific, Waltham, MA, USA) software.

CEL files were first processed with the Affymetrix collection of command line programs Analysis Power Tools (APT, v1.16.0) using the *apt-probeset-summarize* command in order to estimate the intensity at gene level with the *RMA-sketch* normalization. In this step background corrected raw data were Log2-transformed and quantile-normalized following the Robust Multichip Average (RMA) procedure as described in Irizarry et al. (12). For gene annotation the file "HTA-2_0.na34.hg19.transcript" (obtained from Affymetrix) was used. R v3.1.2 (www.r-project.org) environment and Bioconductor (www.bioconductor.org) packages were used for the following preprocessing and statistical analysis. PCA was performed with the native R function *prcomp* on RMA-normalized data and the first two principal components were plotted with *ggplot2* package functions. Hierarchical clustering of sample Euclidean distances was performed with *hclust* and *dist* native R functions and the resulting heatmap was plotted with *gplots* package *heatmap.2* function. Finally, *tRanslatome* package pipeline was used to find out the probe sets that showed significant (FDR < 0.01) differential expression between experimental conditions and to perform the Gene Ontology (GO) Database (13) enrichment analysis, internally using the *limma* - Linear Models for Microarray Data - (14) and *topGO* methods, respectively. The GO and pathway enrichment analysis were obtained using *clusterProfiler* (15) package with annotation of KEGG (16) and Reactome (17) databases.

Microarray data accompanying this paper are available through NCBI Gene Expression Omnibus (GEO) repository, under accession number GSE163531.

Quantitative Real-Time PCR and Digital PCR

For the analysis of IL12p40 and IL-10 mRNA levels, total RNA was reverse transcribed as previously described (11) and then analyzed using the appropriate TaqMan assay (Applied

Biosystems) and TaqMan Universal Master Mix II (Applied Biosystems) according to the manufacturer's instructions. Transcripts expression were normalized to the GAPDH level by using the equation $2^{-\Delta Ct}$; the values are mean ± SEM of triplicate determinations.

The validation of translatome data was conducted by Digital PCR on total and heavy phase-associated RNA that was reverse transcribed as previously described (8). In particular, experiments were carried out to test the mRNA copy number of *IFNA1*, *IFNB1*, *IFNL1* and some IFN stimulated genes (ISGs). Among ISGs we tested CXCL9, CXCL11, two chemokines involved in T cell recruitment; IFN induced with helicase C domain 1 (IFIH1, alias MDA5) - an RNA sensing molecule recently proposed as innate restriction factor for Mtb growth (18), IFN induced protein with tetratricopeptide repeats (IFIT3) - the bridging adapter of TANK binding kinase 1 (TBK1)/ mitochondrial antiviral signaling protein (MAVS) implicated in TBK1 activation and IFN regulatory factor 3 (IRF3) phosphorylation (19) - and IRF7 - a transcription factor stimulated by the autocrine action of IFN-β induced in STING/ IRF3-dependent manner (20). Digital PCR experiments were carried out on the BioMark HD System (Fluidigm, San Francisco, CA, USA) by loading cDNA samples into Fluidigm's 37K Digital Array microfluidic chip as previously described (8). Briefly, Fluidigm's 37K Digital Array consists of 48 panels, each of which is further partitioned into 770 reaction chambers. The reaction for each panel was set up with the specific TaqMan assay probe and with TaqMan Universal Master Mix II (Applied Biosystems) into a final volume of 5 µl. For each sample, six serial dilutions were loaded in triplicate reactions and the chip was then thermocycled and imaged on Fluidigm's BioMark HD real-time PCR system. Positive chambers that originally contained 1 or more molecules has been counted by the Digital PCR analysis software (Fluidigm) and only templates that yielded 150–360 amplified molecules per panel were chosen for technical replication in order to obtain absolute quantification of target RNA copy number.

DC Transfection and Gene Silencing by siRNA

Predesigned siRNA oligonucleotide for GSK-3β (iGSK-3β) was obtained from Ambion (Thermo Fisher Scientific). A negative-control siRNA oligonucleotide [neg ctrl (Ambion, Thermo Fisher Scientific)] was used to address the specificity of the observed effect to the specific GSK-3β sequence. SiRNA transfection efficiency was determined as previously described (8). For each condition, $4x10^5$ DC were plated in a 12-well plate. Lipoplexes were prepared in Opti-MEM serum-free medium (Invitrogen, Thermo Fisher Scientific) at 1:1 ratio. Briefly, siRNA plus fluorescent oligonucleotide and 10 µl of Lipofectamine (1 mg/mL) were diluted separately in 250 µl of Opti-MEM medium.

The Lipofectamine solution was added to the siRNA solution and placed for 5 min at room temperature and then added to DC. Four hours (h) after incubation, medium was replaced with fresh Opti-MEM medium supplemented with 15% FCS and 2 mM L-glutamine for at least 8 h. After the indicated time, cells were infected with Mtb and, where required, treated with rapamycin. After the indicated time, DC were harvested to recover culture supernatants and to isolate RNA. Transfection effect on DC viability, maturation and activation was evaluated as previously described (8).

Immunoblotting Analysis

Total protein extracts were prepared from $1x10^6$ infected or not infected DC, treated or not with rapamycin by using the CelLytic cell lysis reagent (Sigma-Aldrich) supplemented with protease and phosphatase inhibitor cocktails and by following manufacturer's recommendations.

For P-p70S6K S371, P-p70S6K T389, total GSK-3β, P-GSK-3β S9, P-GS S641, P-p44/42 T202/Y204, total p38 and P-p38 Y180/Y182 determination 25 µg of total protein extract were separated on 10% NuPAGE Bis-Tris gel (Invitrogen, Thermo Fisher Scientific) and electroblotted onto nitrocellulose membranes (GE Healthcare, Pittsburgh, PA, USA). Blots were incubated with primary Abs in 5% nonfat dry milk in TBS plus 0.1% Tween20 (Sigma-Aldrich) overnight at 4°C. Detection was achieved using horseradish peroxidase-conjugate anti-rabbit or anti-mouse or anti-goat (Santa Cruz) secondary Abs and visualized with Clarity Western ECL Substrate (Bio-Rad, Segrate, Italy). The quantifications of P-p70S6K S371, P-p70S6K T389, total GSK-3β, P-GSK-3β S9, P-GS S641, P-p44/42 T202/Y204, total p38 and P-p38 Y180/Y182 were performed by calculating their ratio compared to the actin level by using ImageLab software (Bio-Rad) and then calculating the ratio among infected/treated vs uninfected conditions.

Cytokine Determination

Supernatants of DC cultures were harvested 24 h after infection, filtered (0.2 µm) and stored at −80°C. The production of IL-1β, TNF-α, IL-6, IL-12, and IL-10 was measured by human Inflammatory Cytokine bead array kit (BD Bioscience). IL-23 release was instead assayed by ELISA (R&D Systems).

Statistical Analysis

Statistical analysis was performed using One-way Repeated-Measures ANOVA. In case of significant ANOVA, the pairwise comparisons were carried out by the use of the post-hoc Tukey's test, in order to test the significance of the difference between two stimulation effects. In all the cases above, a p value < 0.05 was considered statistically significant: "*" refers to the p-value ≥ 0.01 and < 0.05; "**" refers to the p-value is ≥ 0.001 and < 0.01; "***" the p-value is <0.001. Data analysis was carried out using native functions of R language version 4.0.3.

RESULTS

Profiling of Human Primary DC Infected With Mtb and Treated With Rapamycin

We have previously shown that in human primary DC the autophagy inducer rapamycin overcomes the block exerted by Mtb on autophagosome/lysosome fusion, and enhances IL-12 secretion driving a protective Th1 response (9). Here, to further investigate how rapamycin, known to inhibit translation by

blocking mTORC1, impacts on the immunoregulatory properties of Mtb-infected DC, a comparative analysis of global transcriptome and translatome profiles was conducted (**Supplementary Figure 1**).

Total and polysome-associated (heavy) RNA samples were prepared from uninfected DC or DC infected for 16 h with live H37Rv Mtb alone or in combination with rapamycin. Principal component analysis and sample correlation/clustering study of our gene expression profiles clearly showed a distinct pattern of total and heavy RNA samples and of Mtb-infected *vs* uninfected DC for the four analyzed donors (**Figure 1**). In particular, the MA-plots displaying the logged intensity ratio (M) *vs* the mean logged intensities (A) of mRNAs whose profiles were significantly modulated in treated and/or infected DC *vs* uninfected cells (adjusted p-value [FDR] < 0.01 and at least 1.5-log2 fold change), revealed 228 and 404 differentially expressed genes (DEGs) in transcriptome and translatome of Mtb-infected DC, respectively. No difference was observed in uninfected cells treated with rapamycin *vs* control cells. When rapamycin was added to Mtb-infected DC, DEGs increased to 378 in the transcriptome and 729 in the translatome (**Supplementary Figure 2**). Interestingly, the majority of genes identified in the transcriptome were found in the list of translatome-modulated genes, suggesting that host mRNAs induced by Mtb alone or in combination with rapamycin are efficiently loaded on polysomes, where actively translated mRNAs reside.

Functional GO annotation study and pathway enrichment analysis were performed on the transcriptome- or translatome-associated DEGs and revealed biological processes and signaling cascades associated to Mtb infection and rapamycin treatment (**Figures 2**, **3**). In particular, in the transcriptomes of both Mtb-infected DC and Mtb-infected DC treated with rapamycin there was an enrichment in GO terms related to *cytokine production*, *cytokine signaling* and *innate immune response* (**Figure 2A**). In the GO enrichment profile of the translatome, in addition to *innate immune response*, biological processes linked to *type I interferon (IFN) signaling* and *defense response to other organisms* were found (**Figure 2B**).

Pathway enrichment analysis was performed with both Reactome and KEGG databases and, in line with GO study results, the modulation of signaling cascades related to *antigen processing and presentation*, *TLR receptors signaling*, *cytosolic nucleic acid sensors* and *cytokine-cytokine receptors* was highlighted at transcriptome level for Mtb-infected DC in a rapamycin-independent manner (**Figure 3**). However, while the transcriptome profile of Mtb-infected DC was enriched for the *TRIF-mediated TLR signaling pathway*, mostly involved in CREB-binding protein (CBP)/p300 nuclear translocation for anti-inflammatory cytokine production, the profile of infected DC treated with rapamycin pointed to the *TRAF6-mediated NF-kB activation*, notably involved in the transcription of regulatory and pro-inflammatory cytokines. Interestingly, the analysis of signaling cascades enriched in the translatome of Mtb-infected DC and more pronounced in the presence of rapamycin, revealed modulation of *IFN signaling* and *antiviral mechanism*

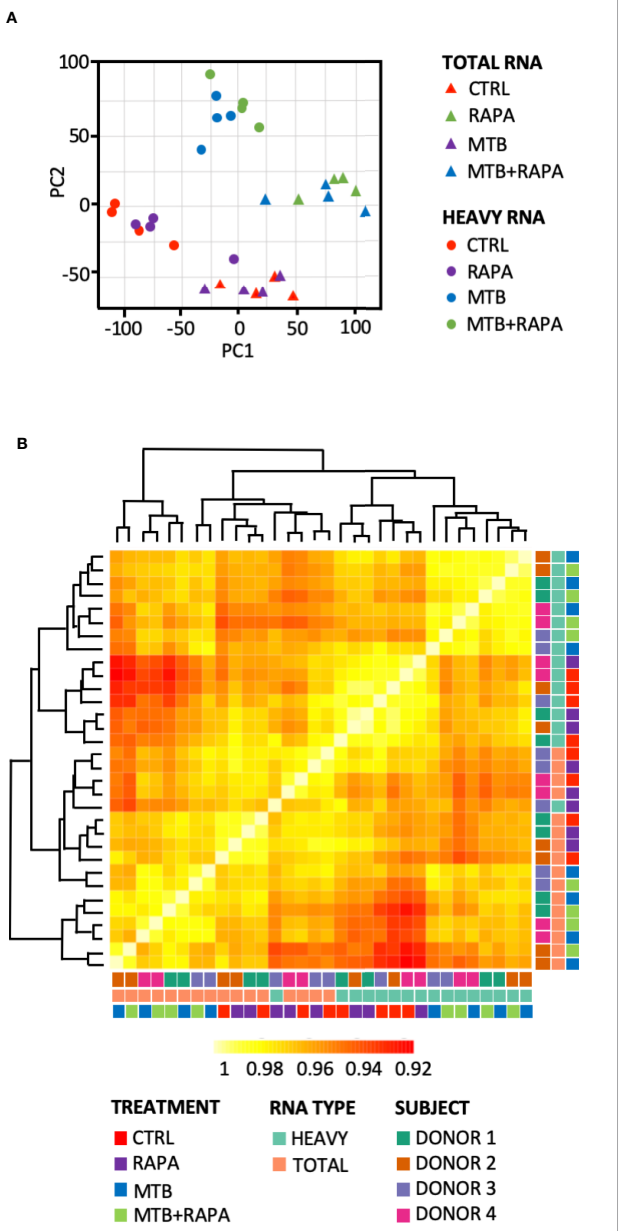

FIGURE 1 | Analysis of transcriptome and translatome of human DC infected with Mtb and treated with rapamycin. DC isolated from 4 healthy donors were left unstimulated (CTRL), treated with rapamycin (RAPA) or infected with Mtb alone (MTB) or in presence of rapamycin added 4 h post infection (MTB+RAPA). Cells were harvested 16 h post infection for total and polysome-associated RNA isolation and microarray analysis. **(A)** Principal component analysis of gene expression profile of samples. Triangles indicate total RNA samples (TOTAL), circles refer to RNA fraction associated with polysome chains (HEAVY). **(B)** Heatmap showing hierarchical clustering of sample correlation. The dendrogram clusters together the significantly regulated treatment conditions with most similar expression profiles among the 4 donors. Correlation is represented by a color code according to the legend where yellow indicates higher correlation. A color code was used to distinguish among treatment conditions (CTRL, RAPA; MTB, MTB+RAPA), RNA type (TOTAL vs HEAVY) and DC culture prepared from different subjects (D1, D2, D3, D4).

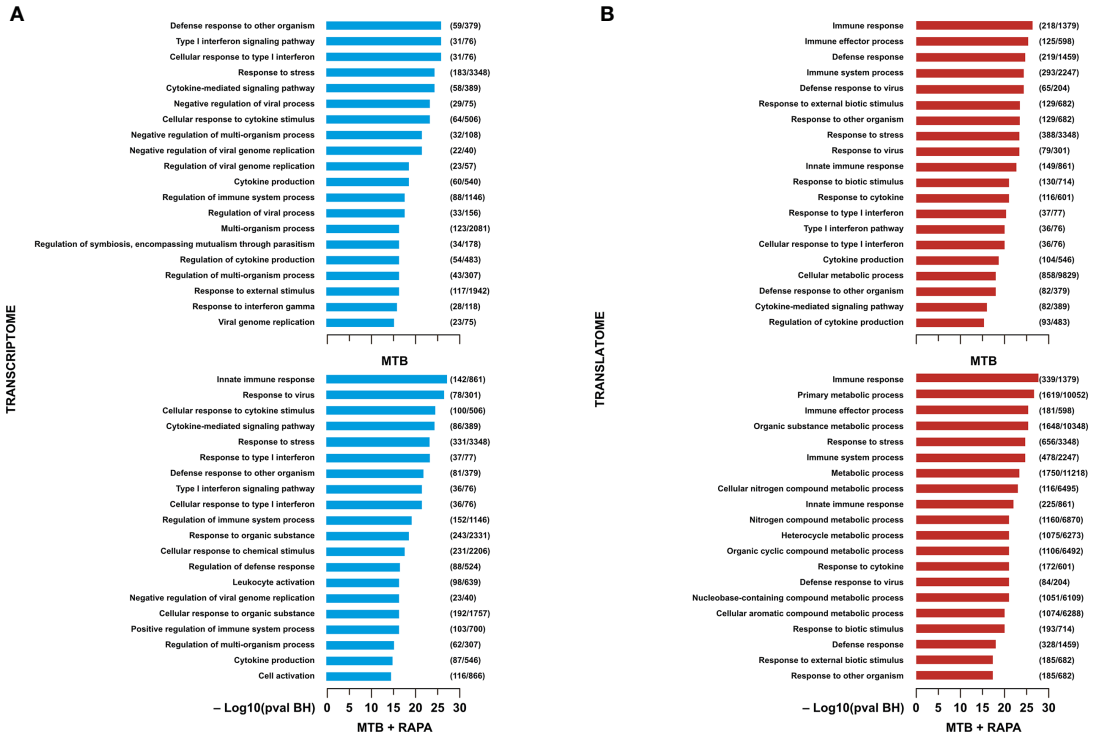

FIGURE 2 | Gene ontology analysis of genes regulated/modulated in transcriptome and in translatome of human DC infected with Mtb alone or in presence of rapamycin. Top 20 gene ontology (GO) terms within the biological process (BP) branch emerged from the list of genes found de-regulated (log2 FC > 1.5; FDR < 0.01) in transcriptome **(A)** (blue panels) and translatome **(B)** (red panels) of human DC infected with Mtb (MTB) and treated with rapamycin (MTB+RAPA). Relevant BP have been graphed by using the formula -$\log_{10}$ of their Benjamini-Hochberg false discovery rate adjusted p-values. The numbers next to BP name, represent the total number of genes that may be significantly involved in the corresponding biological processes. The graph displays the classification term enrichment status and term hierarchy.

by IFN-stimulated genes. The addition of rapamycin to infected DC impacted, as expected, on different metabolic pathways, and on *JAK/STAT signaling* at both transcriptome and translatome levels.

Rapamycin Promotes the Association of type I and III IFNs and ISG mRNAs With Polysomes

In silico analysis of translatome-associated DEGs indicated that rapamycin up-regulated anti-microbial factors. Among the top genes up-regulated in the translatome of Mtb-infected DC alone or in presence of rapamycin, type I and III IFNs and several ISGs encoding for chemokines, transcription factors, innate immune receptors and antimicrobial guanylate binding proteins were found. All the above proteins are involved in host protection against microbial injuries (**Table 1**).

Considering that the majority of translatome DEGs were also modulated at the transcriptome level (**Table 2**), to identify mRNAs influenced by rapamycin at the translational level, we determined by quantitative digital PCR the copy number of relevant top genes in total RNA and polysome-associated RNA fraction (heavy) (**Figure 4**). We found higher levels of *IFNB1* and *IFNL1* mRNA copies associated to polysomes in Mtb-infected DC in presence of rapamycin, in accordance with the microarray data (**Figures 3A** and **4A**). Some discrepancies with microarray data were instead observed in the number of *IFNA1, CXCL9* and *CXCL11* mRNA copies detected in the polysome heavy fraction that were reduced upon rapamycin treatment of Mtb-infected DC (**Figures 4A, B**). Yet, rapamycin weakly and not significantly reduced the level of CXCL9 and CXCL11 (**Figure 4B** and **Supplementary Figure 3**).

Among the ISGs whose expression was promoted by rapamycin during Mtb infection, *IFIH1*, *IFIT3* and *IRF7* were validated by digital PCR (**Figure 4C**). As expected, the levels of *IFIH1*, *IFIT3* and *IRF7* mRNAs were induced by Mtb and further enhanced by rapamycin in polysome-associated RNA fraction only.

The Mtb-Driven Pro-Inflammatory/ Regulatory DC Phenotype Is Enhanced by Rapamycin

From the *in silico* analysis of transcriptome data, *IL-12B* (also known as *IL12p40*), *IL-23A* (also known as *IL23p19*), *IL-1A*, *IL-1B*, *IL-8*, *IRAK2*, *RIPK2* and *MAP3K8* were the top genes induced by Mtb and further stimulated by rapamycin. In addition, *USP18* - a key negative regulator of type I IFN

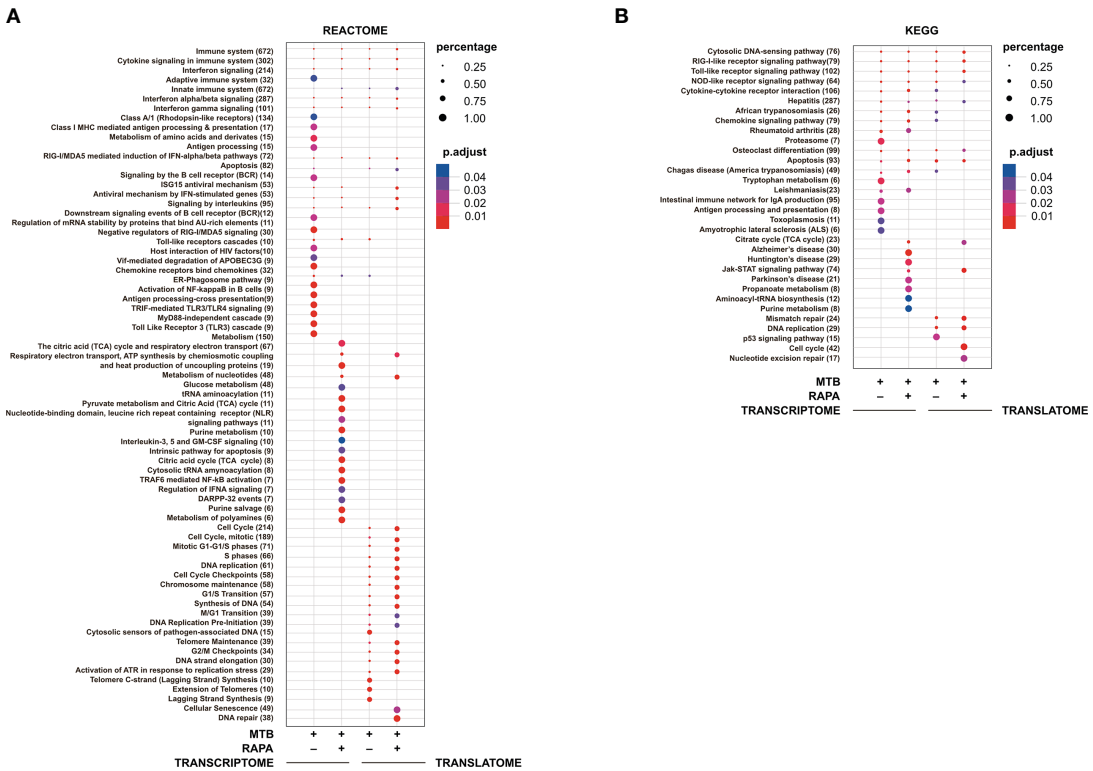

FIGURE 3 | Pathway enrichment analysis of genes modulated in transcriptome and in translatome of human DC infected with Mtb alone or in presence of rapamycin. Pathway enrichment analysis performed using Reactome **(A)** and KEGG **(B)** databases on the list of genes found de-regulated (log2 FC > 1.5; FDR < 0.01) in transcriptome and translatome of human DC infected with Mtb and treated with rapamycin. Dot size is correlated with the ratio between the total number of differentially expressed genes and the number of genes that belong to a pathway. Dots are colored according to the Benjamini-Hochberg false discovery rate adjusted *p*-values (p adjust) from blue (higher *p*-value) to red (lower *p*-value).

signaling (21) - was found among genes transcriptionally down-regulated by rapamycin in Mtb-infected DC (**Table 2**). Validation by qRT-PCR was obtained for *USP18* and for *IL12p40* and *IL23p19* (encoding the IL-23 subunits) (**Figure 5A**).

Consistent with the gene expression results, the release of IL-1β and IL-23 was robustly increased when rapamycin was added to Mtb-infected DC (**Figure 5B**). Similarly, TNF-α and IL-6 mRNAs were up-regulated upon Mtb infection and further enhanced by rapamycin. Yet, rapamycin significantly promoted TNF-α release, while IL-6 production was not significantly regulated. As expected (9), the expression of *IL12p35* subunit and the secretion of IL-12 doubled following rapamycin addition to infected cells (**Figures 5C, D**). To better define the involvement of mTOR in cytokine regulation during Mtb infection, Torin1, an inhibitor of both mTORC1 and mTORC2, was used. The secretion of IL-12 was not significantly altered when Torin1 was added to infected cells (**Figure 6A**). Interestingly, the Mtb-induced expression of the anti-inflammatory cytokine IL-10 was reduced by rapamycin and enhanced by Torin1 (**Figures 5C, D** and **Figure 6B**). All together these data indicate that Mtb mainly impinges on the balance of pro- and anti-inflammatory cytokines *via* mTORC1 signaling.

GSK-3β Behaves as Molecular Switch of Rapamycin-Driven Cytokine Expression During Mtb Infection

Next, we performed a kinetic study to monitor the activation status of the 70 kDa ribosomal S6 kinase 1 (p70S6K), a Ser/Thr kinase and critical effector of the mTOR and the phosphoinositide-3 kinase (PI3K) signaling cascades (**Figure 7**), whose activation requires a multi-site phosphorylation (22, 23). We measured the level of phosphorylation at S371 and T389. While the level of phosphorylation at S371 was only slightly modulated by Mtb, a two-fold induction in p70S6K-T389 phosphorylation was observed at 4 h post-infection and lasted at least 24 h (**Figure 7A**). The time-dependent reduction of p70S6K-T389 phosphorylation in control cells was likely due to deprivation of GM-CSF (24) before the infection.

These data prompted us to investigate whether the fine modulation of pro- and anti-inflammatory cytokine levels in our experimental model involved GSK-3β, a constitutively active Ser/Thr kinase, which, when phosphorylated at the inhibitory S9 site by p70S6K, undergoes proteasomal degradation (25–27). To address this hypothesis, GSK-3β phosphorylation status was

TABLE 1 | List of top genes de-regulated at the translatome level in human DC after Mtb infection and rapamycin treatment.

GENES UP-REGULATED BY RAPAMYCIN IN MTB-INFECTED DC AT TRANSLATOME LEVEL					
Gene ID	**Gene Name**	**Translatome log2 FC**		**Transcriptome log2 FC**	
		MTB	**MTB+RAPA**	**MTB**	**MTB+RAPA**
NM_005409	**CXCL11**	6.28	7.54	5.61	5.40
NM_052941	**GBP4**	5.31	6.14	4.76	5.06
NM_0011300	**CCL20**	4.69	5.73	3.64	4.77
NM_001838	**CCR7**	4.20	5.31	3.38	4.02
NM_001547	**IFIT2**	4.91	5.28	4.57	4.44
NM_002416	**CXCL9**	4.32	5.04	3.73	3.75
NM_001031	**IFIT3**	4.47	4.72	4.33	4.11
NM_001134	**GBP5**	3.51	4.31	3.48	4.19
NM_002981	**CCL1**	2.60	4.29		4.20
NM_022168	**IFIH1**	3.63	4.24	3.60	3.59
NM_000856	**GUCY1A3**		2.97		1.71
NM_004120	**GBP2**	2.05	2.86	1.81	2.55
NM_002176	**IFNB1**	1.78	2.75		1.84
NM_172140	**IFNL1**	1.59	2.35	1.50	1.65
NM_000857	**GUCY1B3**		2.04		
NM_004031	**IRF7**		1.69		
NM_024013	**IFNA1**		1.53		
GENES DOWN-REGULATED BY RAPAMYCIN IN MTB-INFECTED DC AT TRANSLATOME LEVEL					
Gene ID	**Gene Name**	**Translatome log2 FC**		**Transcriptome log2 FC**	
		MTB	**MTB+RAPA**	**MTB**	**MTB+RAPA**
NM_003246	**THBS1**	3.67	2.94	3.02	2.95
NM_0011357	**TP53INP1**	-2.23	-1.50		
NM_001005	**TRIM37**		-1.62		
NM_003544	**HIST1H4B**		-1.94		
NM_006068	**TLR6**	-2.39	-2.86	-1.50	
NM_001237	**CCNA2**		-3.26		
NM_003537	**HIST1H3B**		-4.09		

List of top genes showing a statistically significant modulation at translatome level in Mtb-infected DC in presence or absence of rapamycin, with respect to uninfected DC.
FC, fold change; MTB, Mtb-infected DC; MTB+RAPA, Mtb-infected DC treated with rapamycin; CXCL11, C-X-C motif chemokine 11; GBP4, Guanylate Binding protein 4; CCL20, Chemokine (C-C motif) ligand 20; CCR7, C-C Chemokine receptor type 7; IFIT2, Interferon Induced Protein With Tetratricopeptide Repeats 2; CXCL9, C-X-C Motif Chemokine Ligand 9; IFIT3, Interferon Induced Protein With Tetratricopeptide Repeats 3; GBP4, Guanylate Binding protein 5; CCL1, Chemokine (C-C motif) ligand 1; IFIH1, Interferon Induced With Helicase C Domain 1; GUCY1A3, Guanylate cyclase soluble subunit alpha-3; GBP2, Guanylate Binding protein 2; IFNB1, Interferon beta; IFNL1, Interferon lambda 1; GUCY1B3, Guanylate cyclase soluble subunit beta-3; IRF7, Interferon regulatory factor 7; IFNA1, Interferon alfa 1; THBS1, Thrombospondin 1; TP53INP1, Tumor Protein P53 Inducible Nuclear Protein 1; TRIM37, Tripartite Motif Containing 37; HIST1H4B, H4 Clustered Histone 2; TLR6, Toll-like receptor 6; CCNA2, Cyclin A2; HIST1H3B, H3 Clustered Histone 2.

investigated. A gradual increase in the phosphorylation level at S9 site was revealed indicating that, in DC, GSK-3β is rapidly and persistently turned off upon Mtb infection (**Figure 7A**). Interestingly, phosphorylation of p70S6K at T389 was lowered by the addition of rapamycin in both control and Mtb-infected DC at 16 and 24 h, with a more pronounced effect in infected cells at the latter time point (**Figure 7B**). Similarly, GSK-3β phosphorylation at S9 site was abrogated by rapamycin, which in turn promoted also the phosphorylation of glycogen synthase (GS), one of the canonical substrates of GSK-3β. All together, these results indicate that rapamycin prevents the inhibition of GSK-3β.

Next, we studied whether the activation of the mitogen-activated protein kinases (MAPK) p44/42 and p38 - well-known regulators of the pro- and anti-inflammatory cytokines during Mtb infection (11, 28, 29) - was influenced by rapamycin in Mtb-infected DC. A kinetic analysis was performed to monitor the phosphorylation/activation status of these proteins (**Supplementary Figure 4**). An increase in p38 phosphorylation at T180/Y182 was observed as early as 4 h post-infection, while p44/42 activation was unchanged. Rapamycin weakly increased p38 phosphorylation in both control and Mtb-infected DC (**Supplementary Figures 4A, B**).

The rapamycin effect on the p70S6K/GSK-3β axis was further investigated by analyzing the release of the pro-inflammatory/regulatory cytokines in the presence of a GSK-3β chemical inhibitor, SB216763. In this experimental setting, rapamycin lost its impact on cytokine secretion. In contrast, the inhibition of p70S6K by PF4708671 cooperated with rapamycin in enhancing pro-inflammatory cytokine expression in Mtb-infected DC (**Figure 8A** and **Supplementary Figure 5A**).

The inhibition of p38 signaling by SB203580 or SB202129 also mitigated the production of IL-12 and IL-10 induced by Mtb alone or in presence of rapamycin. On the other hand, p44/42 inhibition by PD980509 did not affect IL-12 production, but it reduced IL-10 secretion by Mtb-infected DC irrespective of the presence of rapamycin (**Supplementary Figure 4C**).

TABLE 2 | List of top genes de-regulated at the transcriptome level in human DC after Mtb infection and rapamycin treatment.

GENES UP-REGULATED BY RAPAMYCIN IN MTB-INFECTED DC AT TRANSCRIPTOME LEVEL					
Gene ID	**Gene Name**	**Transcriptome log2FC**		**Traslatome log2 FC**	
		MTB	**MTB+RAPA**	**MTB**	**MTB+RAPA**
NM_002187	**IL12B**	3.78	5.17	4.56	5.82
NM_0011300	**CCL20**	3.64	4.77	4.69	5.73
NM_000417	**IL2RA**	3.79	4.50	4.24	4.88
NM_002981	**CCL1**		4.20	2.60	4.29
NM_000584	**IL8**	3.37	4.07	3.78	4.53
NM_000575	**IL1A**		4.03	3.63	3.95
NM_001838	**CCR7**	3.38	4.02	4.20	5.31
NM_016584	**IL23A**	1.46	3.82	1.94	4.28
NM_001570	**IRAK2**	2.40	3.09	2.81	3.42
NM_003821	**RIPK2**	2.31	3.03	2.18	2.94
NM_001165	**BIRC3**	2.31	2.95	2.47	3.27
NM_021127	**PMAIP1**	1.99	2.64	2.16	3.06
NM_000576	**IL1B**		2.53		2.39
NM_002176	**IFNB1**		1.84	1.78	2.75
NM_001244	**MAP3K8**		1.82	2.60	1.93
NM_0011273	**CFLAR**		1.64		1.66
NM_138723	**BCL2L14**		1.65		2.03
GENES DOWN-REGULATED BY RAPAMYCIN IN MTB-INFECTED DC AT TRANSCRIPTOME LEVEL					
Gene ID	**Gene Name**	**Transcriptome log2 FC**		**Translatome log2 FC**	
		MTB	**MTB+RAPA**	**MTB**	**MTB+RAPA**
NM_001565	**CXCL10**	7.71	6.92	7.44	7.70
NM_005623	**CCL8**	5.19	4.57	4.38	3.96
NM_001548	**IFIT1**	4.65	3.92	4.24	4.14
NM_017414	**USP18**	4.32	3.82	4.40	4.44
ENST000004	**USP41**	3.74	3.32	3.87	3.89
NM_001080	**LILRB1**	1.50		1.77	
NM_006877	**GMPR**	3.65	3.04	3.50	3.59
NM_0011396	**ATF5**	1.70		1.54	
NM_002168	**IDH2**		-1.58		-1.64
NM_003839	**TNFRSF11A**		-1.74		-1.40
NM_000962	**PTGS1**	-1.57	-2.09	-1.53	-2.17
NM_0011280	**PAK1**		-2.09	-1.95	-2.87
NM_004536	**NAIP**		-2.16	-2.05	-3.52

List of top genes showing a statistically significant modulation at transcriptome level in Mtb-infected DC in presence or absence of rapamycin, with respect to uninfected DC. FC, fold change; MTB, Mtb-infected DC; MTB+RAPA, Mtb-infected DC treated with rapamycin; IL12B, Interleukin 12B; CCL20, Chemokine (C-C motif) ligand 20; IL2RA, Interleukin 2 Receptor Subunit Alpha; CCL1, C-C Motif Chemokine Ligand 1; IL8, Interleukin 8; IL1A, Interleukin 1 Alpha; CCR7; C-C Motif Chemokine Receptor 7; IL23A, Interleukin 23A; IRAK2, Interleukin 1 Receptor Associated Kinase 2; RIPK2, Receptor Interacting Serine/Threonine Kinase 2; BIRC3, Baculoviral IAP Repeat Containing 3; PMAIP1, PMA-Induced Protein 1; IL1B, Interleukin 1B; IFNB1, Interferon beta; MAP3K8, Mitogen-Activated Protein Kinase 8; CFLAR, CASP8 And FADD Like Apoptosis Regulator; BCL2L14, BCL2 Like 14; CXCL10, C-X-C Motif Chemokine Ligand 11; CCL8, C-C Motif Chemokine Ligand 8; IFIT1, Interferon Induced Protein With Tetratricopeptide Repeats 1; USP18, Ubiquitin Specific Peptidase 18; USP41, Ubiquitin Specific Peptidase 41; LILRB1, Leukocyte Immunoglobulin Like Receptor B1; GMPR, Guanosine Monophosphate Reductase; ATF5, Activating Transcription Factor 5; IDH2, Isocitrate Dehydrogenase (NADP(+)) 2; TNFRSF11A, TNF Receptor Superfamily Member 11A; PTGS1, Prostaglandin-Endoperoxide Synthase 1; PAK1, P21 (RAC1) Activated Kinase 1; NAIP, NLR Family Apoptosis Inhibitory Protein.

The involvement of GSK-3β in the rapamycin effect on cytokine expression was further analyzed by silencing GSK-3β in Mtb-infected DC with a specific siRNA (iGSK-3β) (**Figure 8B** and **Supplementary Figure 5B**). DC were also transfected with a non-specific siRNA as negative control (neg ctrl). Upon GSK-3β silencing, the levels of IL-12, IL-23, IL1β, TNF-α and IL-6 were not further enhanced by rapamycin, while the level of IL-10 was increased. As observed for the chemical inhibition (**Supplementary Figure 5A**), GSK-3β silencing impacted also on *IL-12* and *IL-10* mRNA levels (**Supplementary Figure 5B**). Taken together, these results support the view that in Mtb-infected DC rapamycin modulates pro- and anti-inflammatory cytokine production through the regulation of mTOR/GSK-3β axis.

DISCUSSION

For several decades major efforts in TB treatment have focused on the development of antibiotics targeting Mtb. The current regimens for drug-susceptible TB requires the administration of a cocktail of antibiotics for at least 6 months, thus making the cure complicated to administer, lengthy, hepatotoxic and not well tolerated by the patients. These drawbacks lead to poor adherence to the cure, low success rates and, consequently, high risk of development of drug-resistant TB (2, 30). Indeed, recently, the burden of TB disease has been exacerbated by the emergence of rifampicin-resistant, multidrug-resistant and extensively-drug resistant Mtb strains whose treatment requires

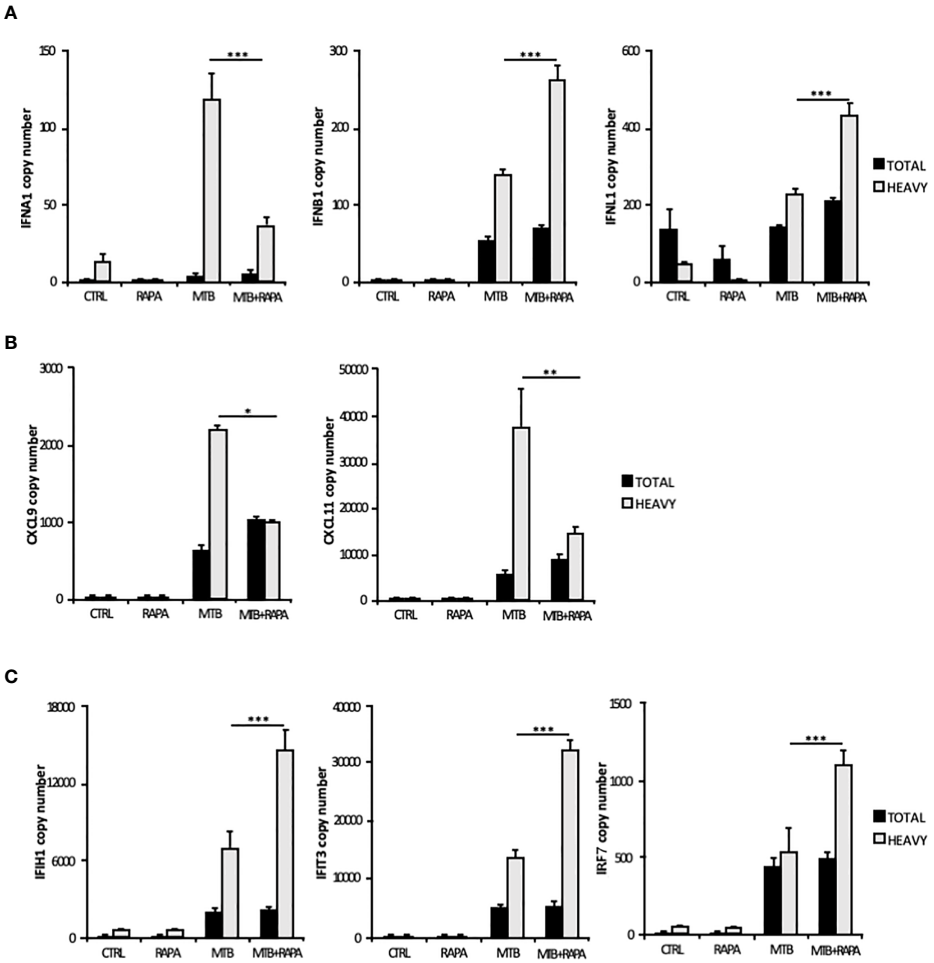

FIGURE 4 | Validation of translatome data on IFNs and IFN-induced gene expression. Total RNA (Total) and high occupancy (Heavy) polysome-associated mRNAs were extracted from untreated DC (CTRL), DC stimulated with rapamycin for 12 h (RAPA) or DC infected for 16 h with Mtb alone (MTB) or in combination with rapamycin (MTB+RAPA, added 4 h after infection). **(A)** *IFNA1*, *IFNB1* and *IFNL1*, **(B)** *CXCL9* and *CXCL11*, **(C)** *IFIH1*, *IFIT3* and *IRF7* copy numbers were determined by digital PCR. Data are represented as the mean copy number per sample ± standard error of 4 experiments performed with RNAs derived from a set of experiments independent than those used in transcriptome/translatome studies and that yielded similar results. Significance was calculated by analysis of variance (ANOVA) followed by multiple comparison performed with Tukey's test as specified in *Materials and Methods* section.

the administration of second-line drugs for at least 9 months and even up to 20 months (1). In this scenario, the host-directed therapies (HDT) have garnered international interest, moving from the concept that the modulation of host defense contributes to the control and resolution of the infection, overcoming the problem of acquired resistance to pathogen-directed therapies (31). Moreover, HDT can control the antimicrobial resistance by either boosting host-cellular responses or activating innate and adaptive immunity and, thus, immunological memory against the pathogens (32). Therefore, the development of HDT is particularly useful for diseases like TB, where the host immune response can successfully limit infection in the majority of latently infected individuals. In this context, there is growing evidence that HDT, such as those based on autophagy enhancement, could be successfully employed as therapeutics for Mtb treatment (10).

Among autophagy inducers, rapamycin and its analogs (rapalogs) have been shown to possess interesting immunoregulatory properties and their use is of interest to the field (33). However, the precise molecular mechanism by which rapamycin exerts its function has not been fully elucidated. In line with evidences demonstrating a multi-level regulation of immune cell activity, including RNA transcription and stability as well as translation (34, 35), the transcriptome and the translatome profiles were obtained to study in depth the effect of rapamycin in human primary DC infected with Mtb. Our data show for the first time that rapamycin selectively tunes cytokine production in Mtb-infected DC by two mechanisms: i) promoting the association of type I and III IFN mRNAs to polysome chains and, in turn, their translation; ii) preventing the inhibition of GSK-3β to tune pro- and anti-inflammatory cytokine production. In this scenario, mTOR plays a central

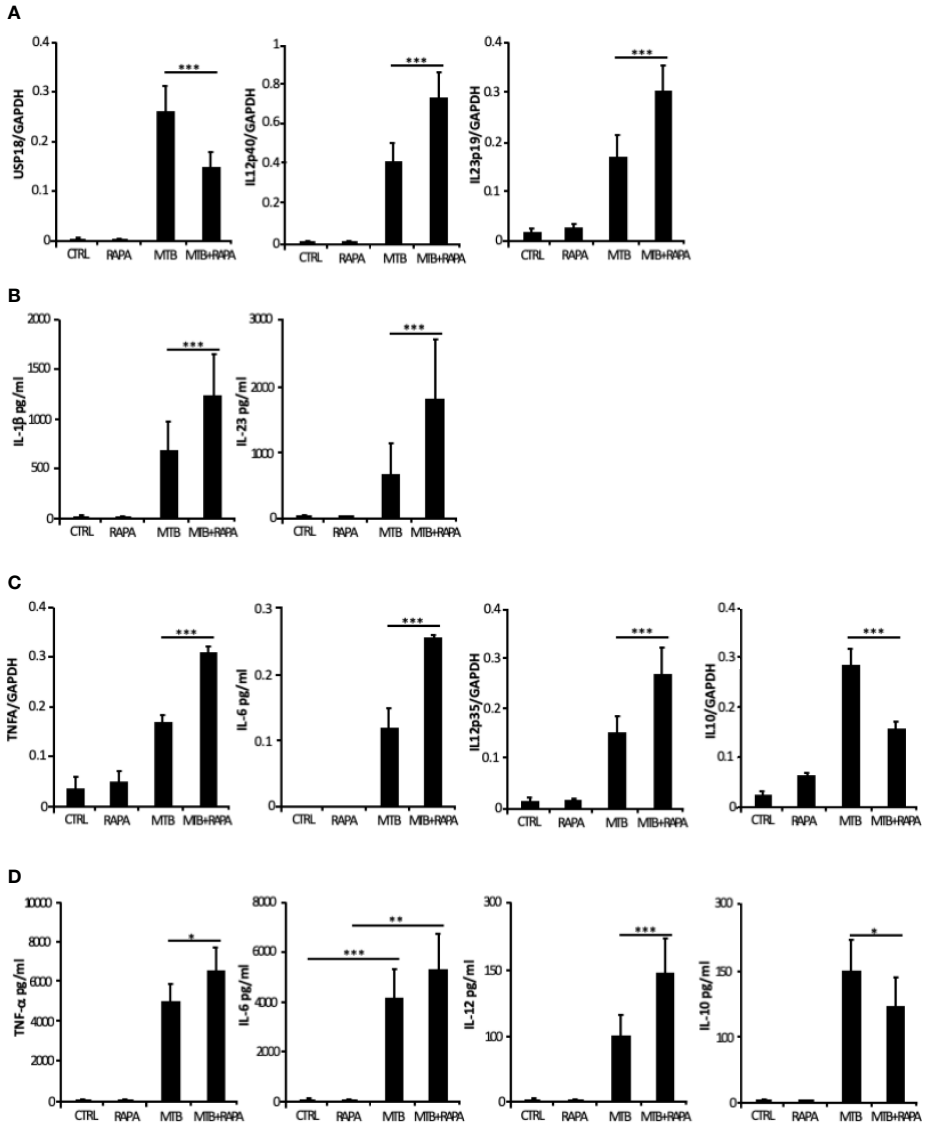

FIGURE 5 | Validation of transcriptome data on cytokine expression and production. Total RNA was extracted from untreated DC (CTRL), DC stimulated for 12 h with rapamycin (RAPA) or infected for 16 h with Mtb alone (MTB) or in combination with rapamycin added 4 h post infection (MTB+RAPA). For protein determination in culture supernatants, DC were left untreated (CTRL) or stimulated for 20 h with rapamycin (RAPA) or infected for 24 h with Mtb alone (MTB) or in combination with rapamycin added 4 h post infection (MTB+RAPA). **(A)** *USP18, IL12p40*, and *IL23p19* levels were evaluated by quantitative real time PCR. Data are represented as the mean copy number per sample ± standard error of 4 experiments performed with RNAs derived from a set of experiments independent than those used in transcriptome/translatome studies and that yielded similar results. **(B)** IL-1β production was evaluated by Inflammatory Cytokine bead array kit, while IL-23 release was measured by ELISA. The results represent mean values ± standard error of 8 independent experiments. **(C)** *TNFA*, *IL6*, *IL12p35*, and *IL10* levels were analyzed as described in **(A)**. **(D)** The secretion of TNF-α, IL-6, IL-12, and IL-10 was quantified by using Inflammatory Cytokine bead array kit. The results represent mean values ± standard error of 8 independent experiments. Significance was calculated by analysis of variance (ANOVA) followed by multiple comparison performed with Tukey's test as specified in *Materials and Methods* section.

role in the transcriptional and translational regulation of immune cell function (34, 35). Indeed, mTOR regulates p70S6K1 phosphorylation, which in turn blocks the activity of the eukaryotic translation initiation factor 4E-binding protein 1 (4E-BP1) and promotes mRNA translation. Yet, the contribution of mTOR to phagocytic cell functions during Mtb infection is poorly defined (36, 37). Our translatome analysis of Mtb-infected DC identified, among the rapamycin-induced mRNAs efficiently loaded on polysome, *IFNB1* and *IFNL1*, as well as three ISG - *IFIH1*, *IFIT3* and *IRF7* - whose role in Mtb infection was recently described (18, 20, 38).

Interestingly, in addition to activating host DNA sensors, like cyclic GMP-AMP synthase and stimulator of IFN genes (39, 40), Mtb RNA may trigger also through RNA sensing molecules (18, 20, 41, 42). Moreover, few studies reported that Mtb RNA is present in endosome-derived membrane vesicles, is released into

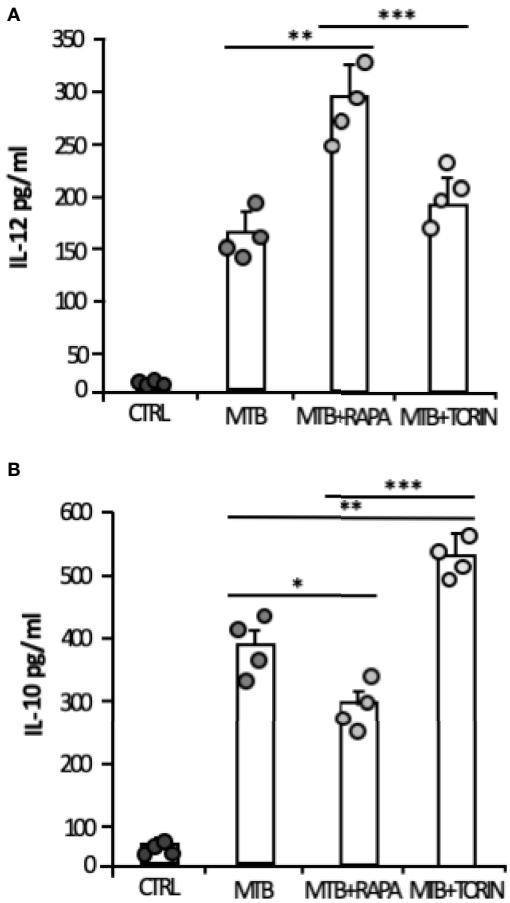

FIGURE 6 | Effect of mTORC1 or mTORC1/mTORC2 inhibition on IL-12 and IL-10 cytokine production in Mtb-infected DC. DC were left untreated (CTRL) or stimulated for 20 h with rapamycin (RAPA) or infected for 24 h with Mtb (MTB) and treated or not with rapamycin (MTB+RAPA, added 4 h post infection) or with Torin1 (MTB+TORIN, added 4 h after infection). Secreted IL-12 **(A)** and IL-10 **(B)** were quantified by using Inflammatory Cytokine bead array kit. The results represent mean values ± standard error of 4 independent experiments. Circles represents values obtained, for the specified cytokine, from each single donor/experiment. Significance was calculated by analysis of variance (ANOVA) followed by multiple comparison performed with Tukey's test as specified in *Materials and Methods* section.

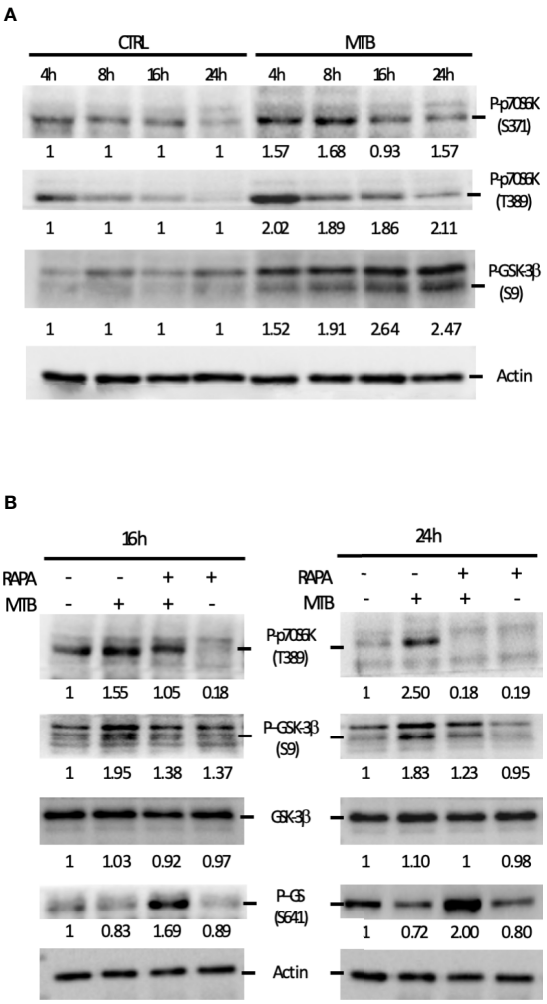

FIGURE 7 | Analysis of the signaling cascades modulated by Mtb alone or in combination with rapamycin and leading to cytokine production. **(A)** DC were left untreated (CTRL) or infected with Mtb (MTB) in kinetic. Activation of p70S6K and GSK-3β was investigated by western blotting on whole cell extracts. Quantification of the phospho-p70S6K (S371 and T389) and phospho-GSK-3β (S9) bands is shown below each immunoblot. **(B)** The impact of rapamycin on p70S6K and GSK-3β was investigated at the indicated time points in DC left unstimulated (CTRL) or infected with Mtb alone (MTB) or in presence of rapamycin added 4 h after infection (MTB+RAPA). Quantification of phospho-p70S6K (S371 and T389), total GSK-3β, phospho-GSK-3β (S9) and phospho-GS (S641) is shown below each immunoblot. Actin levels were analyzed to verify protein content. A representative experiment out of 3 experiments that yielded similar results is shown.

macrophage cytosol by means of SecA and ESX-1 secretion systems and stimulates IFN-β production through of retinoic acid-inducible gene (RIG-I), IFIH1, MAVS, protein kinase R (PKR) and IRF7 signaling cascades (18, 20). In this context, we found that the level of *USP18* - encoding a factor limiting long-lasting IFN response (21, 43) - was reduced by rapamycin in Mtb-infected DC, further suggesting a link between IFN signaling activation and mTOR inhibition. Collectively, the enhanced polysome loading of the above mentioned ISGs, combined with the reduced expression of *USP18*, suggested that mTORC1 inhibition by rapamycin promotes an IFN signature in Mtb-infected DC. Thus, in addition to the well-known effect of PI3K-mTOR pathway on IFN signature (44, 45), our data suggest a detrimental mTORC1 effect on ISG induction, and likely a beneficial mTORC2 activity as shown in previous studies (46, 47).

The unexpected role of mTOR in the control of cytokine production in human DC infected with Mtb was further analyzed through a global transcriptome. This study showed that rapamycin likely promotes transcription of a panel of pro-inflammatory/regulatory cytokines including IL-23, TNF-α, IL-

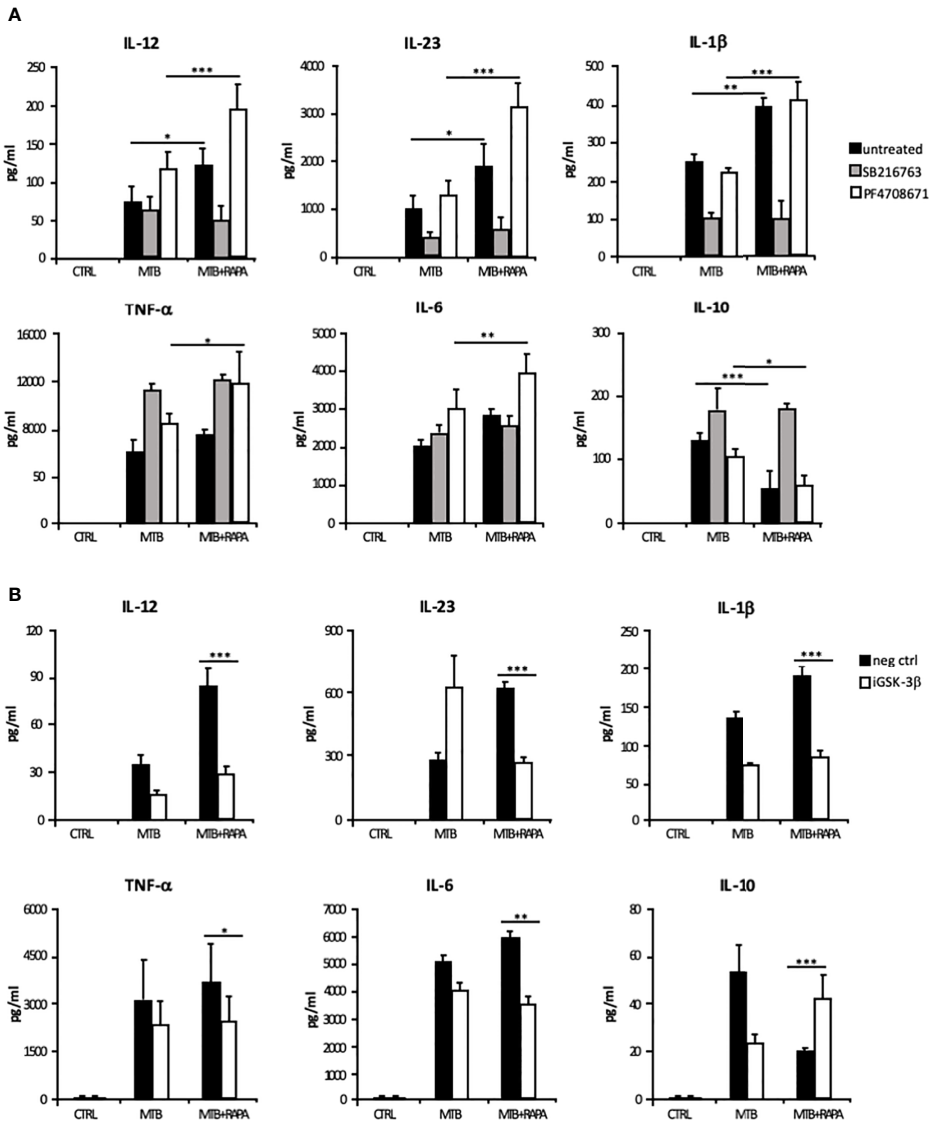

FIGURE 8 | Characterization of GSK-3β and p70S6K involvement in Mtb-mediated cytokine production during rapamycin treatment of human DC. **(A)** DC were left unstimulated (CTRL) or infected for 24 h with Mtb alone (MTB) or in combination with rapamycin added 4 h post infection (MTB+RAPA), with or without the GSK-3β (SB216763) or the p70S6K (PF4708671) inhibitors. IL-12, IL-1β, TNF-α, IL-6 and IL-10 production was evaluated by Inflammatory Cytokine bead array kit, while IL-23 release was measured by ELISA. **(B)** DC were transfected with 100 nM of siRNA specific for GSK-3β (iGSK-3β) or with a control siRNA (neg ctrl) for 8 h and then left unstimulated (CTRL) or infected for 24 h with Mtb alone or in combination with rapamycin. Cytokine amount was determined as in **(A)**. The results represent mean values ± standard error of 4 independent experiments. Significance was calculated by analysis of variance (ANOVA) followed by multiple comparison performed with Tukey's test as specified in *Materials and Methods* section.

1β and IL-6 in addition to IL-12 and inhibits the expression of the anti-inflammatory IL-10. These findings mirror previous data on rapamycin-driven $CD4^+$ T-cell activation and differentiation *via* IL-12/IL10 release from LPS-stimulated DC (48). Our data were validated by measuring the level of secreted cytokines. In addition to the PI3K/mTOR pathway, it has been shown that the constitutively active kinase GSK-3β contributes to the balance of pro- and anti-inflammatory cytokines in LPS- or *Listeria monocytogenes*-stimulated APC (25, 37, 49, 50). In particular, the mTOR-dependent inhibition of GSK-3β favors nuclear translocation of CREB and in turn its binding to the coactivator of transcription CBP, while it reduces the amount of NF-kB p65 associated with CBP, thus impacting on the balance of pro- and anti-inflammatory cytokines (25, 26). In line with these evidences, our results indicate that: i) Mtb inactivates GSK-3β by acting on mTOR/p70S6K; ii) rapamycin overturns this block by suppressing the inhibitory phosphorylation of GSK-3β; iii) in Mtb-infected DC, rapamycin promotes the release of pro-

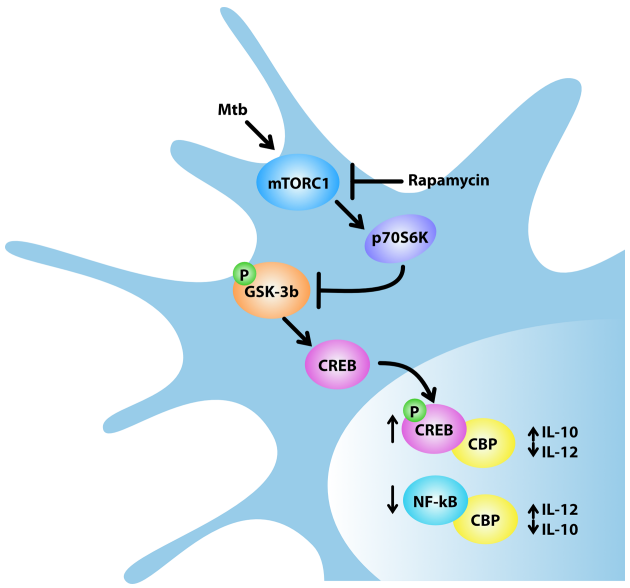

FIGURE 9 | Model for rapamycin-triggered cytokine regulation during Mtb infection. Mtb infection of human DC activates mTORC1/p70S6K axis that phosphorylates and, in turn, inhibits the multifunctional protein kinase GSK-3β. The mTORC1/p70S6K-mediated suppression of GSK-3β favors the nuclear translocation of CREB and in turn its binding to the coactivator of transcription CBP, while it reduces the amount of NF-kB p65 associated with CBP. In Mtb-infected DC, rapamycin, by blocking mTORC1, prevents GSK-3β inhibition thus impinging on IL-12/IL-10 expression and production.

inflammatory/regulatory cytokines while it reduces the secretion of IL-10 (**Figure 9**). The key function of GSK-3β was confirmed by lower levels of secreted IL-12, IL-23 and IL-1β and higher level of IL-10 following silencing or pharmacological inhibition of GSK-3β in Mtb-infected DC.

Given the relevance of the IL-12/IL-23 axis in driving the differentiation of $CD4^+$ T-cells towards a protective Th1 phenotype (9, 51–53), our data suggest that GSK-3β may be a potential target for the development of novel HDT to fight Mtb infection. This possibility is relevant also in light of the rapamycin-driven reduction of IL-10, a cytokine detrimental in TB, acting on the stability of TB granuloma, on Mtb persistence into the host,and promoting Mtb evasion from the autophagic machinery (54–56). Consistent with these observations, the use of inhalable particles containing rapamycin in combination with anti-TB drugs may contribute to lung tissue regeneration and, at the same time, to Mtb killing (57). Accordingly, the combined analysis of DC transcriptome and translatome corroborates the exploitation of molecules, such as rapamycin or GSK-3β modulators, as novel HDT to treat TB. Finally, these findings might be relevant for other respiratory infections, including those caused by coronaviruses, where the aerosol delivery of molecules tuning autophagy and mTOR/GSK-3β axis might exert a therapeutic effect.

DATA AVAILABILITY STATEMENT

The data sets presented in this study can be found in online repositories. The names of the repository/repositories and accession number(s) can be found in the article/supplementary material.

AUTHOR CONTRIBUTIONS

ME participated in experimental design, performed experiments, analyzed data, and prepared the manuscript. MS and VL performed experiments and analyzed data. MP, MCr, FR, EG, GM, OP, and RS performed experiments. ML discussed the data. MCa and RN contributed to data interpretation. SP contributed to data interpretation and manuscript writing. EC participated in experimental design, data analysis, and manuscript writing. All authors contributed to the article and approved the submitted version.

FUNDING

This work was supported by grant RF-2010-235199 (to EC) from Italian Ministry of Health and grant FILAS-RU-2014-1036 (to EC) from Lazio Region. The funders had no role in study design, data collection and analysis, decision to publish, or preparation of the manuscript.

SUPPLEMENTARY MATERIAL

The Supplementary Material for this article can be found online at: https://www.frontiersin.org/articles/10.3389/fimmu.2021.649475/full#supplementary-material

REFERENCES

1. WHO. *Global Tuberculosis Report 2020*. (2020). Available at: https://apps.who.int/iris/bitstream/handle/10665/336069/9789240013131-eng.pdf.
2. Chai Q, Wang L, Liu CH, Ge B. New insights into the evasion of host innate immunity by Mycobacterium tuberculosis. *Cell Mol Immunol* (2020) 17 (9):901–13. doi: 10.1038/s41423-020-0502-z
3. Pulendran B. The varieties of immunological experience: of pathogens, stress, and dendritic cells. *Annu Rev Immunol* (2015) 33:563–606. doi: 10.1146/annurev-immunol-020711-075049
4. Liu CH, Liu H, Ge B. Innate immunity in tuberculosis: host defense vs pathogen evasion. *Cell Mol Immunol* (2017) 14(12):963–75. doi: 10.1038/cmi.2017.88
5. Simeone R, Bobard A, Lippmann J, Bitter W, Majlessi L, Brosch R, et al. Phagosomal rupture by Mycobacterium tuberculosis results in toxicity and host cell death. *PLoS Pathog* (2012) 8(2):e1002507. doi: 10.1371/journal.ppat.1002507
6. Ramachandra L, Noss E, Boom WH, Harding CV. Processing of Mycobacterium tuberculosis antigen 85B involves intraphagosomal formation of peptide-major histocompatibility complex II complexes and is

inhibited by live bacilli that decrease phagosome maturation. *J Exp Med* (2001) 194(10):1421–32. doi: 10.1084/jem.194.10.1421
7. Saini NK, Baena A, Ng TW, Venkataswamy MM, Kennedy SC, Kunnath-Velayudhan S, et al. Suppression of autophagy and antigen presentation by Mycobacterium tuberculosis PE_PGRS47. *Nat Microbiol* (2016) 1(9):16133. doi: 10.1038/nmicrobiol.2016.133
8. Etna MP, Sinigaglia A, Grassi A, Giacomini E, Romagnoli A, Pardini M, et al. Mycobacterium tuberculosis-induced miR-155 subverts autophagy by targeting ATG3 in human dendritic cells. *PLoS Pathog* (2018) 14(1): e1006790. doi: 10.1371/journal.ppat.1006790
9. Romagnoli A, Etna MP, Giacomini E, Pardini M, Remoli ME, Corazzari M, et al. ESX-1 dependent impairment of autophagic flux by Mycobacterium tuberculosis in human dendritic cells. *Autophagy* (2012) 8(9):1357–70. doi: 10.4161/auto.20881
10. Cerni S, Shafer D, To K, Venketaraman V. Investigating the Role of Everolimus in mTOR Inhibition and Autophagy Promotion as a Potential Host-Directed Therapeutic Target in Mycobacterium tuberculosis Infection. *J Clin Med* (2019) 8(2):232. doi: 10.3390/jcm8020232
11. Etna MP, Giacomini E, Pardini M, Severa M, Bottai D, Cruciani M, et al. Impact of Mycobacterium tuberculosis RD1-locus on human primary dendritic cell immune functions. *Sci Rep* (2015) 5:17078. doi: 10.1038/srep17078
12. Irizarry RA, Bolstad BM, Collin F, Cope LM, Hobbs B, Speed TP. Summaries of Affymetrix GeneChip probe level data. *Nucleic Acids Res* (2003) 31(4):e15. doi: 10.1093/nar/gng015
13. Ashburner M, Ball CA, Blake JA, Botstein D, Butler H, Cherry JM, et al. Gene ontology: tool for the unification of biology. The Gene Ontology Consortium. *Nat Genet* (2000) 25(1):25–9. doi: 10.1038/75556
14. Ritchie ME, Phipson B, Wu D, Hu Y, Law CW, Shi W, et al. limma powers differential expression analyses for RNA-sequencing and microarray studies. *Nucleic Acids Res* (2015) 43(7):e47. doi: 10.1093/nar/gkv007
15. Yu G, Wang LG, Han Y, He QY. clusterProfiler: an R package for comparing biological themes among gene clusters. *OMICS* (2012) 16(5):284–7. doi: 10.1089/omi.2011.0118
16. Kanehisa M, Goto S. KEGG: kyoto encyclopedia of genes and genomes. *Nucleic Acids Res* (2000) 28(1):27–30. doi: 10.1093/nar/28.1.27
17. Croft D, Mundo AF, Haw R, Milacic M, Weiser J, Wu G, et al. The Reactome pathway knowledgebase. *Nucleic Acids Res* (2014) 42(Database issue):D472–7. doi: 10.1093/nar/gkt1102
18. Ranjbar S, Haridas V, Nambu A, Jasenosky LD, Sadhukhan S, Ebert TS, et al. Cytoplasmic RNA Sensor Pathways and Nitazoxanide Broadly Inhibit Intracellular Mycobacterium tuberculosis Growth. *iScience* (2019) 22:299–313. doi: 10.1016/j.isci.2019.11.001
19. Liu XY, Chen W, Wei B, Shan YF, Wang C. IFN-induced TPR protein IFIT3 potentiates antiviral signaling by bridging MAVS and TBK1. *J Immunol* (2011) 187(5):2559–68. doi: 10.4049/jimmunol.1100963
20. Cheng Y, Schorey JS. Mycobacterium tuberculosis-induced IFN-beta production requires cytosolic DNA and RNA sensing pathways. *J Exp Med* (2018) 215(11):2919–35. doi: 10.1084/jem.20180508
21. Francois-Newton V, Magno de Freitas Almeida G, Payelle-Brogard B, Monneron D, Pichard-Garcia L, Piehler J, et al. USP18-based negative feedback control is induced by type I and type III interferons and specifically inactivates interferon alpha response. *PLoS One* (2011) 6(7):e22200. doi: 10.1371/journal.pone.0022200
22. Weng QP, Kozlowski M, Belham C, Zhang A, Comb MJ, Avruch J. Regulation of the p70 S6 kinase by phosphorylation in vivo. Analysis using site-specific anti-phosphopeptide antibodies. *J Biol Chem* (1998) 273(26):16621–9. doi: 10.1074/jbc.273.26.16621
23. Shin S, Wolgamott L, Yu Y, Blenis J, Yoon SO. Glycogen synthase kinase (GSK)-3 promotes p70 ribosomal protein S6 kinase (p70S6K) activity and cell proliferation. *Proc Natl Acad Sci U S A* (2011) 108(47):E1204–13. doi: 10.1073/pnas.1110195108
24. Lehman JA, Calvo V, Gomez-Cambronero J. Mechanism of ribosomal p70S6 kinase activation by granulocyte macrophage colony-stimulating factor in neutrophils: cooperation of a MEK-related, THR421/SER424 kinase and a rapamycin-sensitive, m-TOR-related THR389 kinase. *J Biol Chem* (2003) 278 (30):28130–8. doi: 10.1074/jbc.M300376200
25. Wang H, Brown J, Gu Z, Garcia CA, Liang R, Alard P, et al. Convergence of the mammalian target of rapamycin complex 1- and glycogen synthase kinase 3-beta-signaling pathways regulates the innate inflammatory response. *J Immunol* (2011) 186(9):5217–26. doi: 10.4049/jimmunol.1002513
26. Martin M, Rehani K, Jope RS, Michalek SM. Toll-like receptor-mediated cytokine production is differentially regulated by glycogen synthase kinase 3. *Nat Immunol* (2005) 6(8):777–84. doi: 10.1038/ni1221
27. Yang D, Li S, Duan X, Ren J, Liang S, Yakoumatos L, et al. TLR4 induced Wnt3a-Dvl3 restrains the intensity of inflammation and protects against endotoxin-driven organ failure through GSK3beta/beta-catenin signaling. *Mol Immunol* (2020) 118:153–64. doi: 10.1016/j.molimm.2019.12.013
28. Gagliardi MC, Teloni R, Giannoni F, Mariotti S, Remoli ME, Sargentini V, et al. Mycobacteria exploit p38 signaling to affect CD1 expression and lipid antigen presentation by human dendritic cells. *Infect Immun* (2009) 77 (11):4947–52. doi: 10.1128/IAI.00607-09
29. Surewicz K, Aung H, Kanost RA, Jones L, Hejal R, Toossi Z. The differential interaction of p38 MAP kinase and tumor necrosis factor-alpha in human alveolar macrophages and monocytes induced by Mycobacterium tuberculois. *Cell Immunol* (2004) 228(1):34–41. doi: 10.1016/j.cellimm.2004.03.007
30. Tiberi SdP N, Walzl G, Vjecha MJ, Rao M, Ntoumi F, Mfinanga S, et al. Tuberculosis: progress and advances in development of new drugs, treatment regimens, and host-directed therapies. *Lancet Infect Dis* (2018) 18(7):E183–98. doi: 10.1016/S1473-3099(18)30110-5
31. Gygli SM, Borrell S, Trauner A, Gagneux S. Antimicrobial resistance in Mycobacterium tuberculosis: mechanistic and evolutionary perspectives. *FEMS Microbiol Rev* (2017) 41(3):354–73. doi: 10.1093/femsre/fux011
32. Baindara P. Host-directed therapies to combat tuberculosis and associated non-communicable diseases. *Microb Pathog* (2019) 130:156–68. doi: 10.1016/j.micpath.2019.03.003
33. Jones RG, Pearce EJ. MenTORing Immunity: mTOR Signaling in the Development and Function of Tissue-Resident Immune Cells. *Immunity* (2017) 46(5):730–42. doi: 10.1016/j.immuni.2017.04.028
34. Snyder JP, Amiel E. Regulation of Dendritic Cell Immune Function and Metabolism by Cellular Nutrient Sensor Mammalian Target of Rapamycin (mTOR). *Front Immunol* (2018) 9:3145. doi: 10.3389/fimmu.2018.03145
35. Piccirillo CA, Bjur E, Topisirovic I, Sonenberg N, Larsson O. Translational control of immune responses: from transcripts to translatomes. *Nat Immunol* (2014) 15(6):503–11. doi: 10.1038/ni.2891
36. Paik S, Jo EK. An Interplay Between Autophagy and Immunometabolism for Host Defense Against Mycobacterial Infection. *Front Immunol* (2020) 11:603951. doi: 10.3389/fimmu.2020.603951
37. Weichhart T, Costantino G, Poglitsch M, Rosner M, Zeyda M, Stuhlmeier KM, et al. The TSC-mTOR signaling pathway regulates the innate inflammatory response. *Immunity* (2008) 29(4):565–77. doi: 10.1016/j.immuni.2008.08.012
38. Hare NJ, Chan B, Chan E, Kaufman KL, Britton WJ, Saunders BM. Microparticles released from Mycobacterium tuberculosis-infected human macrophages contain increased levels of the type I interferon inducible proteins including ISG15. *Proteomics* (2015) 15(17):3020–9. doi: 10.1002/pmic.201400610
39. Watson RO, Bell SL, MacDuff DA, Kimmey JM, Diner EJ, Olivas J, et al. The Cytosolic Sensor cGAS Detects Mycobacterium tuberculosis DNA to Induce Type I Interferons and Activate Autophagy. *Cell Host Microbe* (2015) 17 (6):811–9. doi: 10.1016/j.chom.2015.05.004
40. Collins AC, Cai H, Li T, Franco LH, Li XD, Nair VR, et al. Cyclic GMP-AMP Synthase Is an Innate Immune DNA Sensor for Mycobacterium tuberculosis. *Cell Host Microbe* (2015) 17(6):820–8. doi: 10.1016/j.chom.2015.05.005
41. Choudhary E, Bullen CK, Goel R, Singh AK, Praharaj M, Thakur P, et al. Relative and Quantitative Phosphoproteome Analysis of Macrophages in Response to Infection by Virulent and Avirulent Mycobacteria Reveals a Distinct Role of the Cytosolic RNA Sensor RIG-I in Mycobacterium tuberculosis Pathogenesis. *J Proteome Res* (2020) 19(6):2316–36. doi: 10.1021/acs.jproteome.9b00895
42. Burkert S, Schumann RR. RNA Sensing of Mycobacterium tuberculosis and Its Impact on TB Vaccination Strategies. *Vaccines (Basel)* (2020) 8(1):67. doi: 10.3390/vaccines8010067
43. Francois-Newton V, Livingstone M, Payelle-Brogard B, Uze G, Pellegrini S. USP18 establishes the transcriptional and anti-proliferative interferon alpha/beta differential. *Biochem J* (2012) 446(3):509–16. doi: 10.1042/BJ20120541
44. Livingstone M, Sikstrom K, Robert PA, Uze G, Larsson O, Pellegrini S. Assessment of mTOR-Dependent Translational Regulation of Interferon Stimulated Genes. *PLoS One* (2015) 10(7):e0133482. doi: 10.1371/journal.pone.0133482

45. Joshi S, Kaur S, Kroczynska B, Platanias LC. Mechanisms of mRNA translation of interferon stimulated genes;. *Cytokine* (2010) 52(1-2):123–7. doi: 10.1016/j.cyto.2010.03.019
46. Kaur S, Kroczynska B, Sharma B, Sassano A, Arslan AD, Majchrzak-Kita B, et al. Critical roles for Rictor/Sin1 complexes in interferon-dependent gene transcription and generation of antiproliferative responses. *J Biol Chem* (2014) 289(10):6581–91. doi: 10.1074/jbc.M113.537852
47. Kaur S, Sassano A, Majchrzak-Kita B, Baker DP, Su B, Fish EN, et al. Regulatory effects of mTORC2 complexes in type I IFN signaling and in the generation of IFN responses. *Proc Natl Acad Sci U S A* (2012) 109(20):7723–8. doi: 10.1073/pnas.1118122109
48. Turnquist HR, Cardinal J, Macedo C, Rosborough BR, Sumpter TL, Geller DA, et al. mTOR and GSK-3 shape the CD4+ T-cell stimulatory and differentiation capacity of myeloid DCs after exposure to LPS. *Blood* (2010) 115(23):4758–69. doi: 10.1182/blood-2009-10-251488
49. Rodionova E, Conzelmann M, Maraskovsky E, Hess M, Kirsch M, Giese T, et al. GSK-3 mediates differentiation and activation of proinflammatory dendritic cells. *Blood* (2007) 109(4):1584–92. doi: 10.1182/blood-2006-06-028951
50. Park DW, Kim JS, Chin BR, Baek SH. Resveratrol inhibits inflammation induced by heat-killed Listeria monocytogenes. *J Med Food* (2012) 15(9):788–94. doi: 10.1089/jmf.2012.2194
51. Etna MP, Giacomini E, Severa M, Coccia EM. Pro- and anti-inflammatory cytokines in tuberculosis: a two-edged sword in TB pathogenesis. *Semin Immunol* (2014) 26(6):543–51. doi: 10.1016/j.smim.2014.09.011
52. Abebe F. Synergy between Th1 and Th2 responses during Mycobacterium tuberculosis infection: A review of current understanding. *Int Rev Immunol* (2019) 38(4):172–9. doi: 10.1080/08830185.2019.1632842
53. Lyadova IV, Panteleev AV. Th1 and Th17 Cells in Tuberculosis: Protection, Pathology, and Biomarkers. *Mediators Inflamm* (2015) 2015:854507. doi: 10.1155/2015/854507
54. O'Leary S, O'Sullivan MP, Keane J. IL-10 blocks phagosome maturation in mycobacterium tuberculosis-infected human macrophages. *Am J Respir Cell Mol Biol* (2011) 45(1):172–80. doi: 10.1165/rcmb.2010-0319OC
55. Duan L, Yi M, Chen J, Li S, Chen W. Mycobacterium tuberculosis EIS gene inhibits macrophage autophagy through up-regulation of IL-10 by increasing the acetylation of histone H3. *Biochem Biophys Res Commun* (2016) 473 (4):1229–34. doi: 10.1016/j.bbrc.2016.04.045
56. Upadhyay R, Sanchez-Hidalgo A, Wilusz CJ, Lenaerts AJ, Arab J, Yeh J, et al. Host Directed Therapy for Chronic Tuberculosis via Intrapulmonary Delivery of Aerosolized Peptide Inhibitors Targeting the IL-10-STAT3 Pathway. *Sci Rep* (2018) 8(1):16610. doi: 10.1038/s41598-018-35023-0
57. Gupta A, Sharma D, Meena J, Pandya S, Sachan M, Kumar S, et al. Preparation and Preclinical Evaluation of Inhalable Particles Containing Rapamycin and Anti-Tuberculosis Agents for Induction of Autophagy. *Pharm Res* (2016) 33(8):1899–912. doi: 10.1007/s11095-016-1926-0

Conflict of Interest: The authors declare that the research was conducted in the absence of any commercial or financial relationships that could be construed as a potential conflict of interest.

frontiers in Immunology

REVIEW
published: 31 May 2021
doi: 10.3389/fimmu.2021.667664

Autophagy in *Tenebrio molitor* Immunity: Conserved Antimicrobial Functions in Insect Defenses

Yong Hun Jo[1], *Jung Hee Lee*[1], *Bharat Bhusan Patnaik*[2], *Maryam Keshavarz*[3], *Yong Seok Lee*[4] *and Yeon Soo Han*[1]*

[1] Department of Applied Biology, Institute of Environmentally-Friendly Agriculture (IEFA), College of Agriculture and Life Sciences, Chonnam National University, Gwangju, South Korea, [2] P. G. Department of Biosciences and Biotechnology, Fakir Mohan University, Balasore, India, [3] Department of Evolutionary Biology, Institute for Biology–Zoology, Free University of Berlin, Berlin, Germany, [4] Department of Biology, College of Natural Sciences, Soonchunhyang University, Asan City, South Korea

The yellow mealworm beetle (*Tenebrio molitor*) has been exploited as an experimental model to unravel the intricacies of cellular and humoral immunity against pathogenic infections. Studies on this insect model have provided valuable insights into the phenotypic plasticity of immune defenses against parasites and pathogens. It has thus been possible to characterize the hemocoelic defenses of *T. molitor* that rely on the recognition of non-self-components of pathogens by pattern recognition receptors (PRRs). The subsequent signaling cascade activating pathways such as the NF-κB controlled by Toll and IMD pathways lead to the synthesis of antimicrobial peptides (AMPs), onset of hemocyte-driven phagocytosis, and activation of the prophenoloxidase cascade regulating the process of melanization. Nevertheless, the activation of autophagy-mediated defenses of *T. molitor* against the facultative intracellular gram-positive bacterium *Listeria monocytogenes* provides clear evidence of the existence of a cross-talk between autophagy and the IMD pathway. Moreover, the identification of several autophagy-related genes (*Atgs*) in *T. molitor* transcriptome and expressed sequence tag (EST) databases has contributed to the understanding of the autophagy-signaling cascade triggered by *L. monocytogenes* challenge. Providing further evidence of the cross-talk hypothesis, *TmRelish* has been shown to be required not only for regulating the synthesis of AMPs through the PGRP-LE/IMD pathway activation but also for the expression of *Atgs* in *T. molitor* larvae following *L. monocytogenes* challenge. Notably, *L. monocytogenes* can stimulate the *T. molitor* innate immune system by producing molecules recognized by the multifunctional PRR (*Tm*PGRP-LE), which stimulates intracellular activation of the IMD pathway and autophagy. Considering the conservation of autophagy components involved in combating intracellular pathogens, it will be interesting to extrapolate a dynamic cross-talk model of immune activation. This review summarizes the most significant findings on the regulation of autophagy in *T. molitor* during *L. monocytogenes* infection and on the role of the innate immunity machinery, including the NF-κB pathway, in the control of pathogenic load.

Keywords: *Tenebrio molitor*, Listeria monocytogenes, autophagy, NF-kappaB, innate immunity

OPEN ACCESS

Edited by:
Jere W. McBride, University of Texas Medical Branch at Galveston, United States

Reviewed by:
Fengliang Jin, South China Agricultural University, China
Chaozheng Li, Sun Yat-Sen University, China

***Correspondence:**
Yeon Soo Han
hanys@jnu.ac.kr

Specialty section:
This article was submitted to Microbial Immunology, a section of the journal Frontiers in Immunology

Received: *14 February 2021*
Accepted: *13 May 2021*
Published: *31 May 2021*

Citation:
Jo YH, Lee JH, Patnaik BB, Keshavarz M, Lee YS and Han YS (2021) Autophagy in Tenebrio molitor Immunity: Conserved Antimicrobial Functions in Insect Defenses. Front. Immunol. 12:667664. doi: 10.3389/fimmu.2021.667664

INTRODUCTION

Autophagy is well-known as a conserved cellular mechanism by which the cell degrades unnecessary and/or dysfunctional cellular components through the action of lysosomes. It maintains homeostasis during cellular stress and pathogen or infective organism invasion. For instance, under nutrient starvation, oxidative stress, and intracellular pathogen invasion, the autophagic machinery is activated in order to detoxify cells and maintain a surveillance of cellular components for intensified cell function (1, 2). Further, in coordination with apoptosis regulator Bcl-2, the autophagy protein Beclin-2 inhibits apoptosis in normal physiological and pathological conditions (3).

There are three known forms of autophagy, namely microautophagy, macroautophagy and chaperone-mediated autophagy (CMA). Although all the autophagy forms culminate in the lysosomal degradation of cellular cargo including viruses intracellularly they are distinguished from one another on the basis of the pathway by which the cargo is delivered to the lumen of the autolysosome (4). Microautophagy is initiated by a direct and random invagination of a membrane around a portion of the cytoplasm that subsequently differentiates into an autophagic tube to enclose portions of the cytosol (5). The much well-studied and conserved macroautophagy mechanism in eukaryotes requires the formation of a double-membrane vesicular structure called the autophagosome (6). In this process, targeted cellular components are isolated from the rest of the cellular cytosolic components within the newly developing autophagosome. Subsequently, the autophagosome fuses with the lysosome to form the autolysosome in which the enclosed cellular components are degraded and/or recycled (**Figure 1**). In yeast, the autophagosome formation is mediated by the hierarchical recruitment of autophagy-related (Atg) proteins to the phagophore assembly site or preautophagosomal structure (PAS). In contrast, PAS-like structure have not been identified in mammals, wherein multiple cellular organelles serve as origins for the assembly of the phagophore (7, 8). Consequent upon the recruitment of Atg proteins, the phagophore gets extended to form an autophagosome. Upon maturity, the autophagosome are transported along the endocytic pathway before fusing with the lysosomes to form autophagolysosome. Subsequently, the cellular cargos are degraded by the hydrolytic enzymes of lysosomes and degradation products are released back to the cytoplasm for cell use (9). Viruses such as the Severe acute respiratory syndrome coronavirus 2 (SARS-CoV-2) escape the macroautophagy regulatory cascade as the viral protein ORF3a block the fusion of the autophagosome to the lysosome, thus evading eventual degradation (10). With the exception of SARS-CoV-2, the autophagy regulatory cascade involving *Atg* genes have been found to be receptive to vesicular stomatitis virus (VSV), Rift Valley fever virus (RVFV) or Zika virus infection in *Drosophila* model (11, 12). In contrast, the dengue virus (DENV-2) titers in mosquito *Aedes aegypti* Aag2 cells were not affected in *Atg* silenced individuals suggesting diverse autophagic response in insects (13). In CMA, all proteins containing the penta-peptide motif 'KFERQ' in their amino acid sequences are selectively recognized by a specialized cytosolic chaperone known as the heat shock cognate protein of 70 kDa (HSC70) (14). The resulting complex is targeted to the lysosomal membrane where it binds to a receptor called lysosome-

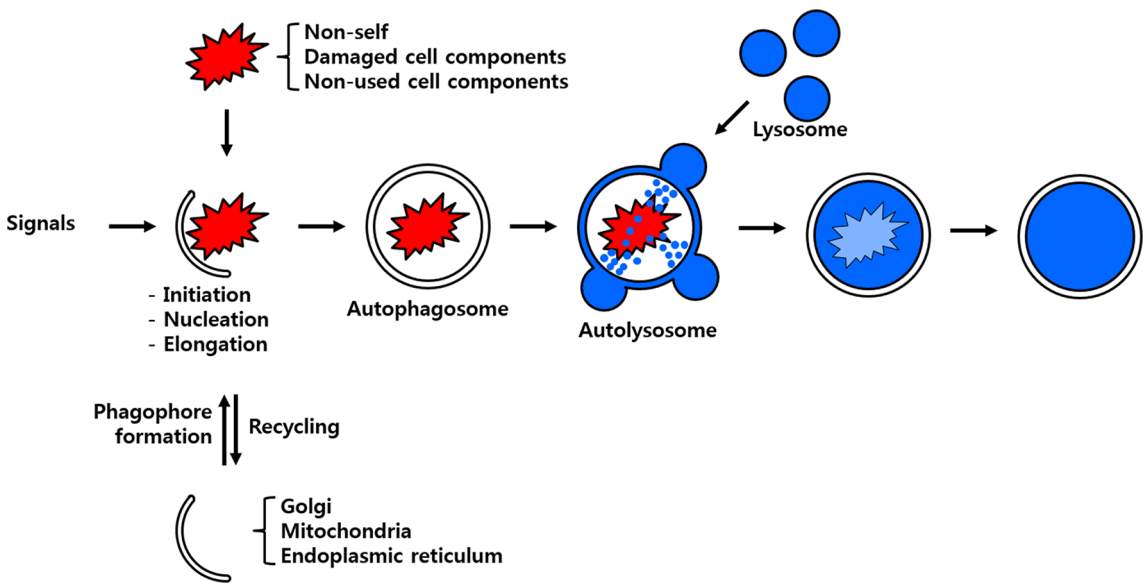

FIGURE 1 | Scheme of the process of autophagy. Non-self-entities such as pathogenic bacteria and unused or damaged cell components are enclosed by membrane particles believed to stem from the Golgi apparatus, mitochondria and/or endoplasmic reticulum. The developing autophagosome fuses with the lysosome to deliver its cargo to hydrolytic enzymes for eventual degradation and/or recycling.

associated membrane protein type 2A (LAMP-2A) (5). The presence of a luminal form of HSC70 (lys-HSC70) is required for the complete translocation of the chaperone-associated target protein complex into the lysosomal lumen for its eventual degradation.

In this review, we focused on the regulatory autophagy signaling cascade (illustrating macroautophagy) in the yellow mealworm, *Tenebrio molitor* and its putative role in the host during *Listeria monocytogenes* infection. Further, a cross-talk mechanism of autophagy process and the NF-κB pathway in *T. molitor* in response to invasion of infective microorganisms have been suggested.

MECHANISM AND REGULATION OF AUTOPHAGY

Macroautophagy (here-after referred to as autophagy) is a highly regulated process that can be conveniently divided into three major steps: autophagy induction (or initiation), vesicle nucleation, and vesicle expansion (or elongation) and completion.

Autophagy Induction and Formation of the Initiation Complex

The induction of autophagy is triggered by a variety of stress cues that include, but are not limited to, nutrient deprivation, hypoxia, endoplasmic reticulum (ER) stress, and oxidative stress (15). In most cases, these stimuli trigger autophagy induction through activation of the nutrient energy sensor AMP-activated protein kinase (AMPK) or inhibition of the negative regulator of autophagy target of rapamycin (TOR) (15). Among the several pathways mediating the transmission of autophagic signals, the TOR-dependent autophagic pathway is relatively well-characterized. The detailed description of TOR-dependent autophagic pathway is discussed in **Figure 2**.

In eukaryotes, autophagy induction is achieved through Atg1 [insect homolog of unc-51 like autophagy activating kinase 1 (ULK1)] complex formation, following inactivation of its upstream negative regulator TOR (**Figure 2**). However, there are significant differences in the composition and function of the core components of the Atg1 complex among yeast, mammals, and insects (16). In yeast, for example, Atg1 interacts with at least eight other Atg proteins and TOR regulates the formation of Atg1-Atg13-Atg17 complex (17). Conversely, humans and *Drosophila* do not possess clear orthologs of Atg17 or its interacting proteins Atg29 and Atg31 (16, 18, 19). Instead, the mammalian Atg1 ortholog ULK1 forms a complex with Atg13 and two additional proteins Atg101 and the focal adhesion kinase family-interacting protein of 200 kDa (FIP200), both of which are required for autophagosome formation. Furthermore, while TOR-mediated phosphorylation of Atg13 must be suppressed to allow Atg13 to interact with and activate Atg1 in yeast, the mammalian and *Drosophila* orthologs of Atg13 are associated with ULK1. Moreover, in *Drosophila*, Atg13 becomes hyper-phosphorylated upon autophagy induction (20). In addition, overexpression of *Drosophila* Atg1 has been shown to induce autophagy; whereas overexpression of ULK1 inhibits autophagy (21, 22). The proposed explanations for this difference include the influence of additional regulatory proteins and the existence of feedback regulation between Atg1 and TOR (16, 17).

Vesicle Nucleation

Vesicle nucleation starts with the recruitment of yeast Atg proteins, or their equivalents in higher animals, to the PAS. The mechanism regulating this process is not yet clear, but the activation of the class III phosphatidylinositol 3-kinase (PI3K) complex is indispensable (20). In fact, following autophagy induction by the activated Atg1/ULK1 complex, a structure enriched in phosphatidylinositol-3-phosphate [PI3P, also known as PtdIns (3)P] appears at the site of autophagosome formation (16).

PI3P is synthesized by enzymes of the PI3K family, which phosphorylate the 39-hydroxyl group on the inositol ring of phosphoinositides (23). Three classes of PI3K enzymes are known: class I enzymes are composed of p100 catalytic subunits and p85 adaptors: class II enzymes are large (> 200 kDa) and characterized by a C2 domain at the C-terminus; finally, class III enzymes are homologous to the vacuolar protein sorting 34 (Vps34), the only PI3K characterized in yeast (23). In yeast, Vps34 can form complexes with other autophagic components such as Atg6, Atg14, and Vps15. The mammalian orthologs of such proteins have been named Vps34, Beclin-1, Atg14, and p150, respectively (24).

In higher animals, complexes formed by class I PI3Ks are considered negative regulators of autophagy. For example, the activation of class I PI3Ks by the insulin receptor leads to phosphorylation of plasma membrane lipids, which in turn recruit and activate Akt/protein kinase B (PKB), a downstream negative regulator of autophagy (25). In contrast, complexes formed by class III PI3Ks are divided into several types depending on the proteins that interact with the core components, namely Atg6 or Beclin, Vps34 and Vps15 (20). Proteins such as UV-resistance associated gene (UVRAG), activating molecule in Beclin-1-regulated autophagy (AMBRA1), Atg14L, and Bax-interacting factor-1 (Bif-1) are known to positively regulate autophagy when interacting with the core complex proteins. Conversely, other proteins interacting with class III PI3Ks such as run domain Beclin-1- interacting and cysteine-rich containing protein (Rubicon), Cln-2, and Bcl-x_L are negative regulators of autophagy (16, 24, 26, 27).

Although PI3P production is essential for autophagosome formation, its exact role in phagophore formation is yet to be deciphered. It has been proposed that PI3P production is involved in altering the composition of the ER-derived lipid bilayer to create a phagophore or simply in the recruitment of PI3P-binding proteins that are required for the synthesis of the phagophore (28). For instance, the autophagy proteins Atg18 and Atg21 are known to be recruited by PI3P to the developing phagophore. Moreover, in yeast, Atg18 can form a complex with Atg2, which localizes to the PAS depending on the PI3P-binding ability of Atg18 (29).

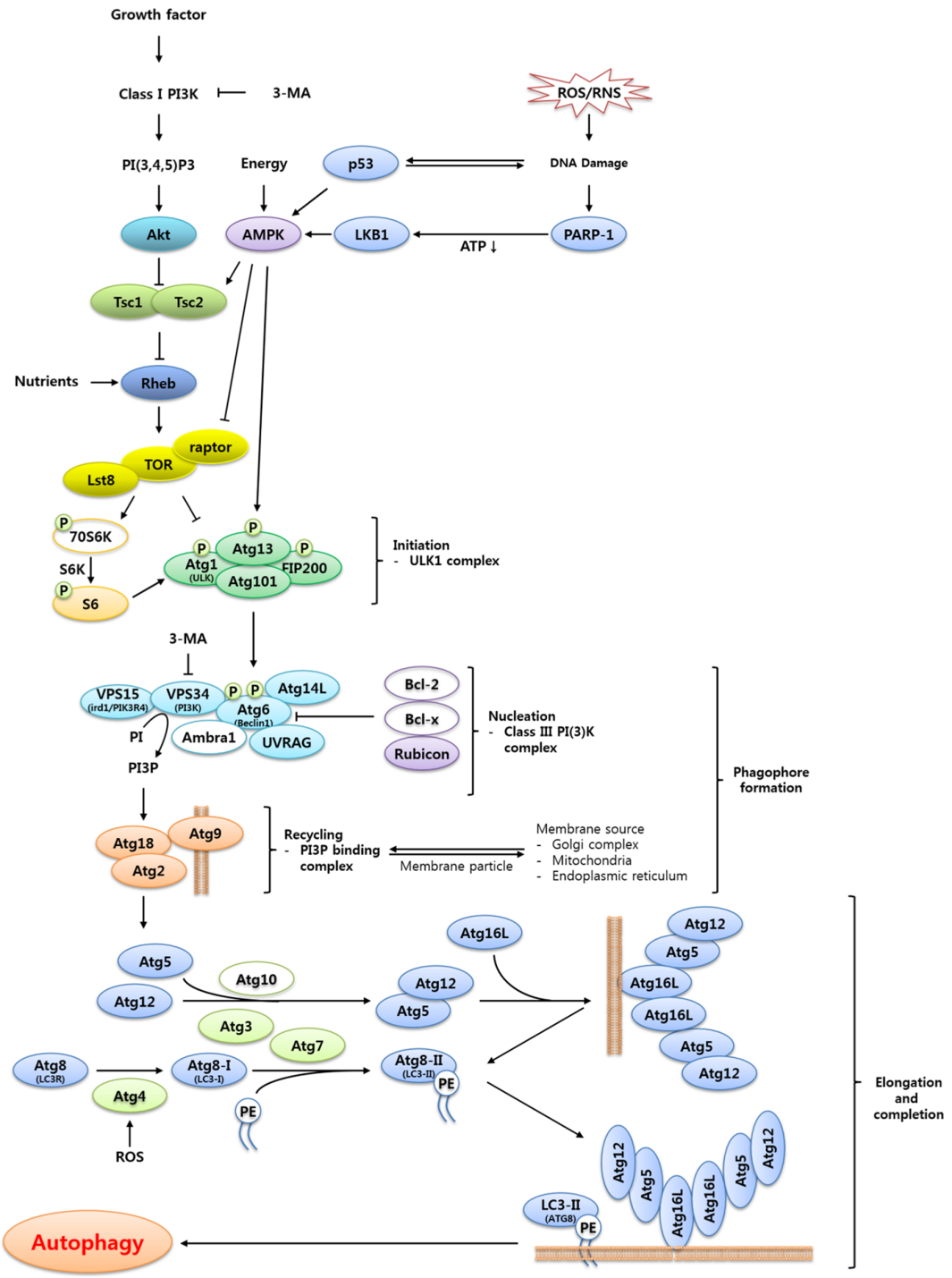

FIGURE 2 | Proposed signaling cascade triggering TOR-regulated autophagy in *T. molitor*. Most of the autophagy-related genes included in the scheme were identified in the *T. molitor* RNA-Seq and EST databases. Growth factors such as the insulin receptor and nutrient-rich conditions negatively regulate autophagy, while reactive oxygen/nitrogen species (ROS/RNS), DNA damage and a low cellular energy status (that is, a high AMP/ATP ratio) induce autophagy. Upon generation of autophagy signals by the appropriate stimuli, an initiation complex comprising Atg1, Atg13, Atg101 and Fip200 is formed. Subsequently, the nucleation complex consists of the Vps15-Vps34-Atg6-Atg14-UVRAG complex, alternatively named Class III PI (3)K complex. In addition, the Atg2-Atg18 complex supports the delivery of the membrane particles from the Golgi, mitochondria or endoplasmic reticulum. Vesicle elongation is carried out by two ubiquitin-like complexes: the Atg5-Atg12: Atg16 complex, generated through the E1- and E2-like enzymatic activity of Atg7 and Atg10, respectively; and the Atg8-PE complex, generated by the proteolytic activity of Atg4 before transfer of Atg8 to the E1- and E2-like enzymes Atg7 and Atg3, respectively. Open circles show either non-Atg components (3-MA, PI3P, Class I PI3K, PI(3,4,5)P3 and PE) or autophagy related genes (70S6K, Bcl-2, Bcl-x, Ambra1 and Atg10) unidentified in *T. molitor*.

The appearance of a developing phagophore is crucial for the completion of the vesicle nucleation step. However, the exact source of the developing phagophore is unknown. Nevertheless, two proposed models have received considerable scientific support. The first model suggests that the phagophore is synthesized by a *de novo* mechanism and expands through the addition of lipids from other sources, transported to the site by Atg9 (30). The second model suggests that the initial cradle for the formation of the phagophore is derived from a subdomain of the ER and later expands between the ER domains to which it is physically linked (31, 32). However, there is an increasing body of literature that implicates several other intracellular organelles, including the Golgi apparatus, endosomes, mitochondria and the plasma membrane as sources of initial building material for the phagophore (16, 33–35). The mechanism for determining the site of phagophore formation within the cytosol of higher eukaryotes is also not well understood. In yeast, the PAS functions as an organizing center for autophagosome formation because most of the Atg proteins necessary for the formation of the developing phagophore are usually recruited to the PAS (16). It is not clear, however, if an equivalent of the PAS does exists in higher eukaryotes.

Vesicle Expansion and Completion

In the canonical autophagy machinery, vesicle expansion and completion involve at least eight Atg proteins. These proteins are grouped into two major sets according to their functional participation in ubiquitin-like conjugation reactions. In particular, Atg5-Atg12/Atg16 complex requires Atg7 and Atg10 as E1- and E2-like enzymes, respectively. Similarly, Atg8-[known as microtubule-associated protein 1 light chain 3 (LC3) in mammals]-phosphatidylethanolamine (PE) complex requires the proteolytic activity of Atg4 together with the E1- and E2-like enzymatic activity of Atg7 and Atg3, respectively. The *Drosophila* genome contains two orthologs of the yeast *Atg*8, denoted as *Atg8a* and *Atg8b*. Similarly, the human genome includes four orthologs with high sequence identity to the yeast *Atg4*.

The regulation of vesicle expansion and completion is mediated by the activity of two highly conserved ubiquitin-like protein complexes, namely Atg5-Atg12/Atg16 complex and Atg8-PE complex. In the Atg5-Atg12/Atg16 complex, Atg12 is a ubiquitin-like protein containing a C-terminal glycine residue. Atg12 is first activated by the E1-like enzyme Atg7, which transfers it to the E2-like enzyme Atg10. In turn, Atg10 catalyzes the covalent binding of the C-terminal glycine residue of Atg12 to a lysine residue of Atg5 (36). The Atg12-Atg5 complex then associates non-covalently with Atg16; such interaction is required for the localization of the Atg12-Atg5 complex to the PAS (37, 38).

The formation of the Atg8-PE complex is accomplished through the conjugation of the ubiquitin-like protein Atg8 to the head-group of a membrane PE lipid molecule. Atg8 is normally synthesized with a C-terminal arginine residue masking the penultimate C-terminal glycine residue. Due to the proteolytic activity of Atg4, such arginine is removed, thus exposing the glycine residue to the activity of the ubiquitin-like enzyme. The cleaved Atg8 is then transferred to Atg7, which in turn transfers Atg8 to Atg3, an E2-like enzyme. Next, Atg3 transfers Atg8 to a membrane PE. The resulting Atg8-PE complex is thought to mediate membrane tethering, thereby assisting the expansion of the isolation membrane through the promotion of vesicle carrier fusion (39). In particular, the inhibition of the Atg8 conjugation system in mammalian cells has been shown to lead to failure of isolation -membrane closure into a complete autophagosome (38), suggesting that Atg8 is responsible for the late step of autophagosome formation.

Based on the above-mentioned findings, it is noted that the hierarchical functioning of several Atg proteins are crucial towards regulation of autophagic machinery in eukaryotes. In addition to the extensively studied yeast autophagy model, considerable work on autophagy has been carried out in mammalian and *Drosophila* model systems (16). The autophagy pathway induced by various pathogens (Mycobacteria and virus) and PAMPs (PGN, LPS and ssRNA) has been nicely illustrated in humans (**Figure 3**) (40, 41). However, autophagy research in the beetle, *T. molitor* is still in its infancy. Therefore, an attempt has been made to review the identification and characterization of Atg protein orthologs in *T. molitor* and the role during host-pathogen interactions.

CONSERVATION OF THE AUTOPHAGY SYSTEM IN *T. MOLITOR*

The sequences of the *Atg* genes of *Drosophila* were used as query against unpublished RNA sequencing (RNA-Seq) and expressed sequence tag (EST) sequence databases of *T. molitor* to identify *Atg* genes in *T. molitor* (42). After confirmation of search results *via* local-TBLASTN analysis, the candidate *T. molitor Atg* genes were grouped based on their functional location along the autophagy signaling pathway. The genes were thus placed within the categories "upstream signaling", "initiation of autophagy", "vesicle nucleation", and "vesicle expansion and completion".

Upstream Genes Regulating Autophagy Induction in *T. molitor*

A total of 13 genes putatively involved in the regulation of autophagy induction upstream of/or in conjunction with TOR, a central cell growth regulator that integrates signals from growth factors and nutrient dynamics (43), were identified in *T. molitor*. These candidate genes are presented along with their orthologs in humans, yeast (*Saccharomyces cerevisiae* S288c) and *Drosophila* in **Table 1**. Except for liver kinase B1 (*Lkb1*) and *p53*, which were only detected in the *T. molitor* EST database, the rest other genes were identified in both the *T. molitor* RNA-Seq and EST databases. Notably, TOR is present in two copies (*TOR1* and *TOR2*) in the genome of yeast, whereas only one copy of this gene has been characterized in humans, *Drosophila*, and *T. molitor*. Furthermore, putative orthologs of all other genes of *Drosophila* and humans belonging to the category, "upstream regulatory genes" were identified in *T. molitor*. However, homologs of genes such as *p53*, poly-(ADP-ribose) polymerase (*Parp*), Tuberose sclerosis 1 (*Tsc1*) and *Tsc2* have not been characterized in yeast, despite having been identified from humans and *T. molitor*.

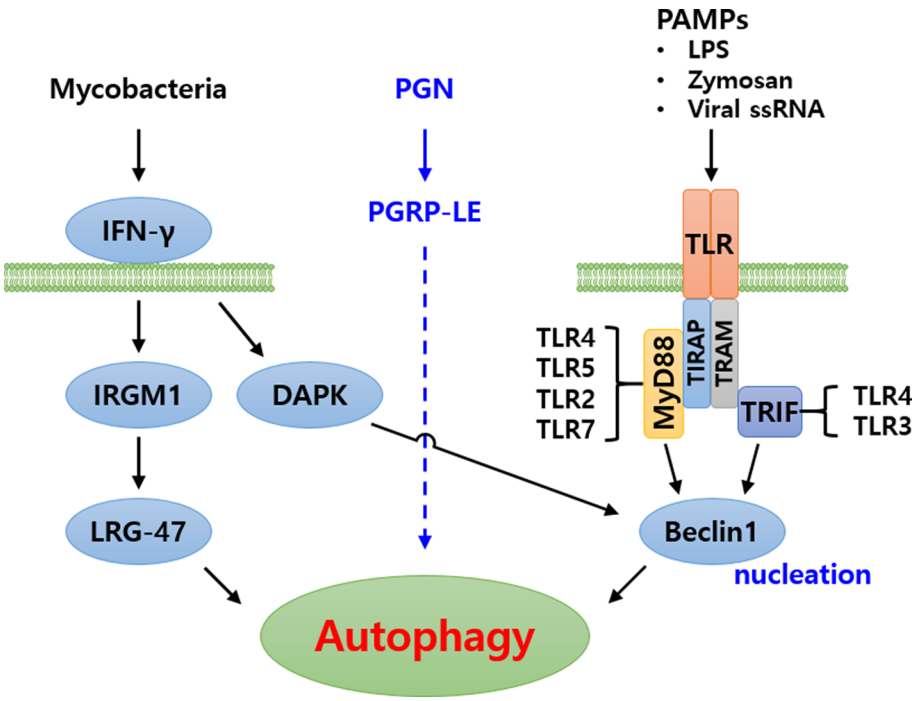

FIGURE 3 | Schematic representation of autophagy signaling cascade induced by pathogenic bacteria in humans. Three major signaling cascades have been identified. In the first, Mycobacteria are recognized by IFN-γ, subsequently inducing autophagy. In the second, bacterial peptidoglycans (PGN) are recognized by PGRP-LE and induce autophagy. The signaling cascade is yet to be identified. In the third cascade, Pathogen associated molecular patterns (PAMPs) are recognized by Toll-like receptor forming Toll-MyD88-TIRAP complex or Toll-TRIF-TRAM complex, intracellularly. These complexes subsequently signal to Beclin1 (Atg6) for induction of autophagy.

Genes Involved in Autophagy Initiation in *T. molitor*

The composition of the autophagy initiation complex varies among eukaryotes although two of its components, the yeast Atg1 and Atg13, have orthologs conserved in both insects and mammals. A total of four genes putatively required for the formation of the initiation complex in higher eukaryotes, namely *Atg1*, *Atg13*, *Atg101* and *FIP200*, were identified by screening the *T. molitor* RNA-Seq database (**Table 2**). Orthologs of all these candidate genes were also found in representative higher eukaryotes such as *Drosophila* and humans.

Two additional genes required for the formation of the initiation complex in yeast, *Atg29 and Atg31* (16) were not characterized in higher eukaryotes including *T. molitor*. Similarly, *Atg17*, whose protein product is required for the formation of the initiation complex in yeast, is not known to have clear orthologs in higher eukaryotes. However, a non-orthologous functionally equivalent gene, *FIP200*, existing in both *Drosophila* and humans was also identified in *T. molitor*.

Genes Involved in Vesicle Nucleation in *T. molitor*

In yeast, vesicle nucleation during autophagy is achieved through the regulatory activity of a complex consisting of Vps34 and three other proteins: Vps15, Vps30/Atg6 and Atg14. The mammalian orthologs of these proteins have been identified and named Vps34, p150, Beclin-1 and Atg14 (24). Orthologs of these proteins have also been identified in the RNA-Seq database of *T. molitor*. Putative orthologs of UVRAG and Rubicon, which is part of a Beclin-1-Vps34-containing autophagy complex in mammals (44), have also been identified in *T. molitor*. Furthermore, orthologs of the PI3P–binding protein Atg18 and its interaction partner Atg2, required for autophagosome formation in yeast, *Drosophila* and humans, were also identified in *T. molitor* (**Table 3**). Additionally, we also identified *T. molitor* Atg9, a multi-spanning membrane protein supporting the supply of lipid bilayers required for the formation of the autophagosome in yeast and mammalian systems (45, 46). Notably, the *AMBRA1*, *Bcl-2* and *Bcl-x* regulatory genes were not identified in the *T. molitor* RNA-Seq database. These three genes have also not been identified in the genome of yeast (**Table 3**).

Genes Involved in Vesicle Expansion and Completion in *T. molitor*

As detailed earlier, two ubiquitin-like protein complexes (the Atg5-Atg12/Atg16 and Atg8-PE complexes) and four important enzymes, namely the proteolytic enzyme Atg4, the E1-like enzyme Atg7, and the E2-like enzymes Atg3 and Atg10, are required for vesicle expansion and completion. The eight

TABLE 1 | Up-stream autophagy signaling genes in *T. molitor*.

Generic name	*Homo sapiens*			*Saccharomyces cerevisiae* S288c			*Drosophila melanogaster*			*Tenebrio molitor*		
	Specific name	Accession No.	Amino acid length	Specific name	Accession No.	Amino acid length	Specific name	Accession No.	AminoAcid length	Specificname	Amino acid Lengths (Tm/Tc)*	Source
Akt1	*Akt1*	AAL55732.1	480	–	–	–	*Akt1*	NP_732114.1	530	*Akt1*	515(F)**/ 510	EST, RNA-Seq
AMP-activated protein kinase (*AMPK*)	*AMPK*	AAB32732.1	552	AMPK gamma	P12904.1	322	*SNF1A*	NP_477313.1	582	*AMPK*	526(F)**/526	EST, RNA-Seq
liver kinase B1 (*LKB1*)	*LKB1*	AAB05809.1	433	–	–	–	*LKB1*	NP_650302.1	567	*LKB1*	458(F)**/443	EST
Lethal with Sec Thirteen 8 (*Lst8*)	*Lst8*	AAO73410.1	260	Lst8	NP_014392.3	303	*Lst8*	NP_572572.1	313	*Lst8*	309(F)**/309	RNA-Seq
P53	*p53*	BAC16799.1	393	–	–	–	*p53*	NP_001247252.1	318	*p53*	375(F)**/350	EST
Poly-(ADP-ribose) polymerase (*Parp*)	*Parp1*	NP_001609.2	1,014	–	–	–	*Parp*	NP_001104452.1	994	*Parp*	983(P)**/991	RNA-Seq
Regulatory-associated protein of mTOR (Raptor)	*Raptor*	AAM09075.1	1,335	Mitochondrial DNA polymerase-encoding 1 (Mip1p)	NP_014975.2	1,254	*Raptor*	NP_572294.2	1,621	*Raptor*	1,273(F)**/1,264	RNA-Seq
Ras homolog enriched in brain (*Rheb*)	*Rheb*	NP_005605.1	184	Rheb1p	NP_009956.2	209	*Rheb*	NP_730950.2	182	*Rheb*	182(F)**/182	EST, RNA-Seq
Ribosomal Protein S6 (*RpS6*)	*S6*	NP_001001.2	249	–	–	–	*RpS6*	NP_511073.1	248	*RpS6*	248(F)**/248	EST, RNA-Seq
Ribosomal protein S6 kinase (*S6k*)	*S6K*	NP_003152.1	525	ribosomal 40S subunit protein S6B	DAA07295.1	236	*S6k* (CG10539)	NP_523941.2	490	*S6K*	746(F)**/738	RNA-Seq
Target of rapamycin (TOR)	*mTOR*	NP_004949.1	2,549	Tor1p Tor2p	NP_012600.1 NP_012719.2	2,470 2,474	*TOR*	NP_001260427.1	2,471	*TOR*	2,397(F)**/2,400	RNA-Seq
Tuberous sclerosis 1 (*TSC1*)	hamartin	NP_001155898.1	1,163	–	–	–	*Tsc1*	NP_477415.1	1,100	*TSC1*	1,056(F)**/1,047	RNA-Seq
Tuberous sclerosis 2 (*TSC2*)	*TSC2*	AAI50301.1	1,784	–	–	–	gigas	NP_524177.1	1,847	*TSC2*	1,735(F)**/1,722	RNA-Seq

**Amino acid lengths have been predicted based on the length of T. molitor (Tm) and T. castaneum genes (Tc) genes.*

***(F) and (P) indicate full-length open reading frame (ORF) cDNA sequences, respectively.*

Genes putatively involved in the generation and processing of the signals that eventually activate the master regulator TOR. Most of them were identified in the T. molitor RNA-Seq database (but only a few in the EST database) using the Drosophila orthologs as a reference. A comparison of the identified genes with their homologs in the unicellular eukaryote S. cerevisiae and the multicellular human (H. sapiens) is given. Blank boxes indicate that no homologs of the respective genes, especially those of S. cerevisiae, were found.

TABLE 2 | Autophagy-related genes involved in autophagy initiation in *T. molitor*.

Generic name	*Homo sapiens*			*Saccharomyces cerevisiae* S288c			*Drosophila melanogaster*			*Tenebrio molitor*		
	Specific name	Accession No.	Amino Acid length	Specific name	Accession No.	Amino Acid length	Specific name	Accession No.	Amino Acid length	Specific name	Amino Acid Lengths (Tm/Tc)*	Source
Autophagy-specific gene 1 (*Atg1*)	unc-51 like autophagy activating kinase 1 (*ULK1*)	NP_003556.1	1,050	*Atg1p*	NP_011335.1	897	*Atg1*	NP_001163433.1	855	*Atg1*	792(F)**/779	RNA-Seq
Autophagy-specific gene 13 (*Atg13*)	*Atg13*	NP_001192048.1	550	*Atg13p*	NP_015511.1	738	*Atg13*	NP_649796.1	523	*Atg13*	391(F)**/399	RNA-Seq
Autophagy-specific gene 29 (*Atg29*)	–	–	–	*Atg29p*	NP_015159.1	213	-	–	–	-	–	–
Autophagy-specific gene 31 (*Atg31*)	–	–	–	*Atg31p*	NP_010305.1	196	–	–	–	-	–	–
Autophagy-specific gene 101 (*Atg101*)	*Atg101*	NP_068753.2	218	-	–	–	CG7053	NP_573326.1	218	*Atg101*	220(F)**/220	RNA-Seq
FAK family-interacting protein of 200 kDa (*Fip200*)	RB1-inducible coiled-coil 1 (*RB1CC1*)	NP_055596.3	1,594	*Atg17p*	NP_013527.3	417	CG1347	NP_649573.2	1357	*Fip200*	1,387 (F)**/1,382	RNA-Seq

*Amino acid lengths have been predicted based on the length of T. molitor (Tm) and T. castaneum genes (Tc) genes.

**(F) and (P) indicate full-length ORF cDNA sequences and partial ORF cDNA sequences, respectively.

Genes involved in the formation of the autophagy initiation complex. Following activation of TOR in response to up-stream autophagic signals, a signaling cascade is activated by the relief of TOR-dependent suppression, culminating in the formation of the initiation complex. The genes involved in the assembly of the initiation complex are Atg1 and Atg13, together with Atg17, Atg29, and Atg31 in yeast or Atg101 and Fip200 in higher eukaryotes, including T. molitor.

corresponding genes were highly conserved in all experimental species, from yeast to humans. Of note, four isotypes of *Atg4* genes and two isotypes of the *Atg8* have been identified in humans and *Drosophila*, respectively. Putative orthologs of the autophagy genes involved in vesicle expansion and completion were identified in the *T. molitor* RNA-Seq and EST databases, except for the gene encoding Atg10, acting as an E2-like enzyme for the assembly of the Atg5-Atg12/Atg16 complex (**Table 4**).

AUTOPHAGIC SIGNATURES OF *T. MOLITOR* IN RESPONSE TO THE INTRACELLULAR BACTERIUM, *LISTERIA MONOCYTOGENES*

T. molitor has been exploited as an experimental model for host-pathogen interaction studies, especially those to unravel the intricacies of the insect innate immunity. In the last decade, owing to the availability of whole genome, transcriptome, and EST sequences, researchers in the field were able to explore the intricacies of cellular and humoral immunity against pathogenic infections in this model insect. In particular, elegant biochemical, molecular, and *in silico* studies allowed to identify the components of the *T. molitor* Toll and IMD signaling cascades and to propose their role in insect immunity (47, 48). The conserved role of both extracellular and intracellular pathwaypathway components have been elucidated through protein induction, gene expression and RNA interference (RNAi)-based gene silencing studies (49–51).

Most significantly, valuable insights into humoral immunity were obtained through the study of the synthesis of antimicrobial peptides (AMPs), hemocyte-driven phagocytosis, and the prophenoloxidase cascade regulating the process of melanization (52). In the context of autophagic control of *T. molitor* defenses, the RNA-Seq and EST databases have contributed to unravel the mysteries of the autophagy-signaling cascade upon *L. monocytogenes* challenge. Further, in some recent studies, the existence of a cross-talk between autophagy and the NF-κB-controlled IMD pathway upon *L. monocytogenes* challenge in *T. molitor* has been advocated (53); this could help extrapolate general mechanism describing the regulation of host immune strategies

TABLE 3 | Autophagy-related genes involved in vesicle nucleation in *T. molitor*.

Generic name	*Homo sapiens*			*Saccharomyces cerevisiae* S288c			*Drosophila melanogaster*			*Tenebrio molitor*		
	Specific name	Accession No.	Amino acid length	Specific name	Accession No.	Amino acid length	Specific name	Accession No.	Amino acid length	Specific name	Amino acid lengths (Tm/Tc)*	Source
Activating molecule in Beclin1-regulated autophagy (*AMBRA1*)	*AMBRA1*	ABI74670.1	1,269	–	–	–	–	–	–	–	–	–
Autophagy-specific gene 2 (*Atg2*)	*Atg2a* *Atg2b*	NP_055919.2 NP_060506.5	1,938 2,078	*Atg2p*	NP_014157.1	1,592	*Atg2*	NP_647748.1	1906	*Atg2*	1,945(P)***/ 2,040	RNA-Seq
Autophagy-specific gene 6 (*Atg6*)	Bcl-2 interacting coiled-coil protein (*Beclin1*)	AAD27650.1	450	*Vps30p*	NP_015205.1	557	*Atg6*	NP_651209.1	422	*Atg6*	386(F)***/ 396	RNA-Seq
Autophagy-specific gene 9 (*Atg9*)	*Atg9a* *Atg9b*	NP_001070666.1 NP_775952.4	839 924	*Atg9p*	NP_010132.1	997	*Atg9*	NP_001261023.1	852	*Atg9*	718(F)***/ 662	RNA-Seq
Autophagy-specific gene 14 (*Atg14*)	*Atg14*	NP_055739.2	492	*Atg14p*	NP_009686.1	344	*CG11877*	NP_651669.1	503	*Atg14*	472(F)***/ 478(Bt)**	RNA-Seq
Autophagy-specific gene 18 (*Atg18*)	WD repeat domain, Phosphoinositide interacting 1 (*WIPI1*)	NP_060453.3	446	*Atg18p*	NP_444297.1	500	*Atg18*	NP_648184.1	377	*Atg18*	406(F)***/ 409	RNA-Seq
B-cell leukemia/ lymphoma-2-alpha protein (*Bcl-2*)	*Bcl-2*	ABX60202.1	239	–	–	–	*Debcl*	NP_788278.1	300	–	–	–
Bcl-x	*Bcl-x*	AAB17354.1	227	–	–	–	–	–	–	–	–	–
Run domain Beclin-1-interacting and cystein-rich containing protein (Rubicon)	*KIAA0226*	NP_001139114.1	927	–	–	–	–	–	–	*Rubicon*	880(F)***/ 884	EST
UV-resistance associated gene (*Uvrag*)	*UVRAG*	BAA90829.1	699	–	–	–	*Uvrag*	NP_609632.1	696	*UVRAG*	729(F)***/ 716	RNA-Seq
Phosphoinositide 3-kinase regulatory subunit 4 (*PIK3R4*)	*PIK3R4*	NP_055417.1	1,358	Vacuolar protein sorting 15 (*VPS15p*)	NP_009655.2	1,454	Immune response Deficient 1 (*ird1*)	NP_649868.1	1342	*VPS15*	1,337(F)***/ 1,330	RNA-Seq
Phosphotidyl-inositol 3 kinase (*PI3K*)	*PIK3C3*	NP_002638.2	887	Vacuolar protein sorting 34 (*VPS34p*)	NP_013341.1	875	Phosphatidyl-inositol 3 kinase 59F (*Pi3K59F*)	NP_477133.1	949	*VPS34*	1,700(P)***/ 2,070	RNA-Seq

**Amino acid lengths have been predicted based on the length of T. molitor (Tm) and T. castaneum genes (Tc) genes.*

***Bt; Amino acid lengths based on Bombus terrestris gene.*

****(F) and (P) indicate full-length ORF cDNA sequences and partial ORF cDNA sequences*

This step involves the recruitment of Atg proteins to the phagophore assembly site (PAS) in yeast or its equivalents in higher animals. Various Atg proteins taking part in this process were identified in the RNA-Seq database.

TABLE 4 | Autophagy related genes involved in elongation and completion in *T. molitor*.

Generic name	*Homo sapiens*			*Saccharomyces cerevisiae* S288c			*Drosophila melanogaster*			*Tenebrio molitor*		
	Specific Name	Accession No.	Amino acid length	Specific name	Accession No.	Amino acid length	Specific name	Accession No.	Amino acid length	Specific name	Amino acid lengths (Tm/Tc)*	Source
Autophagy-specific gene 3 (*Atg3*)	*Atg3*	NP_071933.2	314	*Atg3p*	NP_014404.3	310	*Aut1*	NP_649059.1	330	*Atg3*	320(F)***/ 316	EST, RNA-Seq
Autophagy-specific gene 4 (*Atg4*)	*Atg4a* *Atg4b* *Atg4c* *Atg4d*	AAH61696.1 EAW71278.1 EAX06579.1 AAH68992.1	398 415 458 474	*Atg4p*	NP_014176.2	494	*Atg4*	NP_608563.1	411	*Atg4*	369(F)***/ 366	RNA-Seq
Autophagy-specific gene 5 (*Atg5*)	*Atg5*	AGC52703.1	275	*Atg5p*	NP_015176.1	294	*Atg5*	NP_572390.1	269	*Atg5*	263(F)***/ 263	RNA-Seq
Autophagy-specific gene 7 (*Atg7*)	*Atg7*	NP_006386.1	703	*Atg7p*	NP_012041.1	630	*Atg7*	NP_611350.1	684	*Atg7*	623(F)***/ 621	RNA-Seq
Autophagy-specific gene 8 (*Atg8*)	microtubule-associated protein 1 light chain 3 alpha (*MAP1LC3A*)	NP_852610.1	125	*Atg8p*	NP_009475.1	117	*Atg8a* *Atg8b*	NP_727447.1 NP_650649.1	121 120	*Atg8*	120(F)***/ 120	RNA-Seq
Autophagy-specific gene 10 (*Atg10*)	*ATG10*	NP_001124500.1	220	*Atg10p*	NP_013058.1	167	*CG12821*	NP_001097216.1	212	-	–	–
Autophagy-specific gene 12 (*Atg12*)	*Atg12*	ACD74941.1	187	*Atg12p*	NP_009776.1	186	*Atg12*	NP_648551.3	111	*Atg12*	129(F)***/ 124	RNA-Seq
Autophagy-specific gene 16 (*Atg16*)	*Atg16*	NP_110430.5	607	*Atg16p*	NP_013882.1	150	*CG31033*	NP_733313.2	604	*Atg16*	544(F)***/ 552(Bt)**	EST, RNA-Seq

**Amino acid lengths have been predicted based on the length of T. molitor (Tm) and T. castaneum (Tc) genes.*

***Bt; amino acid lengths predicted based on the lengths of Bombus terrestris (Bt) gene.*

****(F) and (P) indicate full-length ORF cDNA sequences and partial ORF cDNA sequences, respectively.*

against pathogenic microorganisms. In the next paragraphs, we review the components of the conserved autophagy signaling cascade in *T. molitor* and show that they are functionally required to counteract the pathogenicity of *L. monocytogenes*. We not only lay emphasis on the role of *Atgs* in beetle immunity, with special reference to autophagy-based clearance of *Listeria* in the *T. molitor* model, but also delineate reasonable hypotheses on the extent of the cross-talk between autophagy and the IMD pathway.

In separate studies, we have functionally characterized TOR (54), the HORMA-domain-containing protein Atg13 (55), Atg6 (Beclin-1 in humans) (56), Atg3/Atg5 (42), and Atg8 [microtubule-associated protein 1 light chain 3 alpha (MAPILC3A) in humans] (57) in the *T. molitor* model. The corresponding genes have been listed together with other *T. molitor Atgs* in **Table 5** and have been categorized, due to their conserved functions, as upstream autophagy signaling genes (*TmTOR*), autophagy-related genes involved in autophagy initiation (*TmAtg13*), autophagy-related genes for vesicle nucleation (*TmAtg6*), and autophagy-related genes for elongation and completion of autophagosome formation (*TmAtg3, TmAtg5*, and *TmAtg8*). Specifically, the autophagy machinery of *T. molitor* has been functionally dissected in the process of *L. monocytogenes* clearance or suppression by the host. Notably, *L. monocytogenes*, a facultative gram-positive bacterium, has been used for the study of host-pathogen interactions in both vertebrates and invertebrates (58).

In *Drosophila*, the autophagy machinery is stimulated after recognition of *L. monocytogenes* invasion by PGRP-LE, whereas transcription factors downstream of the NF-κB pathway (Relish, Dif, and Dorsal) and Atg5 are not required for PGRP-LE-dependent suppression of *L. monocytogenes* growth (59). Similar to the *Drosophila* model, the requirement of *Tm*PGRP-LE for defense of *T. molitor* against *L. monocytogenes* infection was established using a gene silencing assay (60). In fact,

TABLE 5 | Summary of the autophagic signatures functionally characterized in *T. molitor* implicated in autophagy-mediated clearance of the gram-positive bacterium *L. monocytogenes*.

Autophagy genes	Autophagy functional category	Nucleotide and protein features			Role in autophagy in relation to *L. monocytogenes* infection	Reference
		Nucleotide length (ORF)	Protein length	Domain analysis		
Atg3	Elongation and completion of autophagosome formation	963 bp	320 aa	N-terminal domain, catalytic (autophagy-related protein 3) domain and C-terminal domain	Putative role in mediating autophagy-based clearance of *Listeria* in the *T. molitor* model	(42)
Atg5	Elongation and completion of autophagosome formation	792 bp	263 aa	Autophagy-related protein 5 domain	Putative role in mediating autophagy-based clearance of *Listeria* in the *T. molitor* model	(42)
Atg13	Initiation (ULK1 complex)	1,176 bp	391 aa	N-terminal Atg13 domain with a HORMA (Hop1, Rev7 and Mad2 fold)	Not studied	(55)
Atg8 (Atg8-II/PE complex)	Elongation and completion of autophagosome formation	363 bp	120 aa	Microtubule-associated proteins 1a/1b light chain B-related domain	Putative role in autophagy-based clearance of *Listeria* in *T. molitor*	(57)
Target of rapamycin (*TOR*)	Upstream signaling genes	7,197 bp	2,398 aa	Huntington domain, EF3A, ATM, TOR (HEAT) repeat, and focal adhesion kinase targeting (FAT), rapamycin binding, phosphatidylinositol 3-/4-kinase, and FRAP, ATM and TRRAP C-terminal (FATC) domains	Negative correlation with autolysosome formation after bacterial challenge	(54)
Atg6	Nucleation (class III PI(3)K complex)	1,161 bp	386 aa	Atg6 domain	Putative role in autophagy-based clearance of *Listeria* in *T. molitor*	(56)

**A cross-talk mechanism between the IMD and autophagy pathways is established as TmRelish, a transcription factor of the IMD pathway is implicated not only in the regulation of AMP genes but also in the induction of autophagy genes in response to L. monocytogenes challenge. In fact, TmAtg1 was downregulated both in hemocytes and fat body upon TmRelish knockdown*

knockdown of *TmPGRP-LE* followed by *L. monocytogenes* challenge led to a marked reduction in the survival of *T. molitor* larvae, thereby clearly indicating that *Tm*PGRP-LE is a fundamental component of the pathogen recognition system, which could modulate the downstream NF-κB signaling cascade or the autophagic machinery to eliminate or suppress the pathogenicity of microorganisms.

Although it is logical to assume that the *L. monocytogenes*-induced autophagy is independent of the IMD pathway in *Drosophila*, the existence of a cross-talk between autophagy and the IMD pathway seems more of a reasonable hypothesis. In this regard, we have observed that knocking down *TmRelish*, encoding a transcription factor downstream of the PGRP-LE/IMD pathway, could directly or indirectly influence the expression of AMP and *Atg* genes after *L. monocytogenes* challenge in the fat body and hemocytes of *T. molitor* larvae (**Figure 4**). Ultimately, *L. monocytogenes* infection led to reduced survival of *TmRelish*-knockdown *T. molitor* larvae. While assessing the expression of *Atg* genes, it was found that the mRNA levels of *TmAtg1* were significantly decreased in the fat body and hemocytes of *T. molitor* larvae after *L. monocytogenes* infection (53). Atg1/ULK-1 is related to autophagy initiation, and its increased expression level is necessary to initiate an appropriate autophagic response in *Drosophila* and *Bombyx mori* (22, 61). Furthermore, the formation of the Atg1/Atg13 complex leads to the nucleation of the autophagosome membrane, thereby possibly promoting autophagy. Although *Drosophila* Atg13 has been reported to enhance both the pro-autophagic activity of Atg1 and the inhibition of TOR signaling, the role of Atg13 in the molecular mechanisms underlying autophagy initiation in other insects has been studied to a lesser extent. For instance in *Bombyx mori*, Atg13 (*BmAtg13*) knockdown and overexpression have been implicated in autophagy inhibition (62). In fact, overexpression of *BmAtg13* gene promotes the replication and proliferation of *B. mori* nucleopolyhedrovirus (*Bm*NPV) and silencing results in suppression of *Bm*NPV replication (63). *TmAtg13* is implicated in the survival of the host to both *Escherichia coli* and *Staphylococcus aureus* infection, since *TmAtg13*-silenced larvae exhibited reduced survival under microorganism challenge (55).

Atg8/MAP1LC3A is a ubiquitin-like protein controlling the expansion of the phagophore during autophagosome formation. Moreover, it is a reliable marker of autophagosome formation, and its expression during autophagy has been studied in various insect species. In *Galleria mellonella*, increased activity of Atg8 in parallel to autophagosome formation has been associated with the perivisceral fat body remodeling (64). The Atg8/LC3 positive hemocytes in *G. mellonella* 24 and 48 hours post-infection with entomopathogenic fungus, *Conidiobolus coronatus* also relate to autophagosome formation and autophagy (65). Further, in the hematophagous insect *Rhodnius prolixus*, silencing of *Atg8* transcripts led to disrupted lipophagy (sequestration of lipid droplets and degradation of triacylglycerol generating free fatty-acids for β-oxidation) (66). In *Drosophila*, elevation of Atg8-II

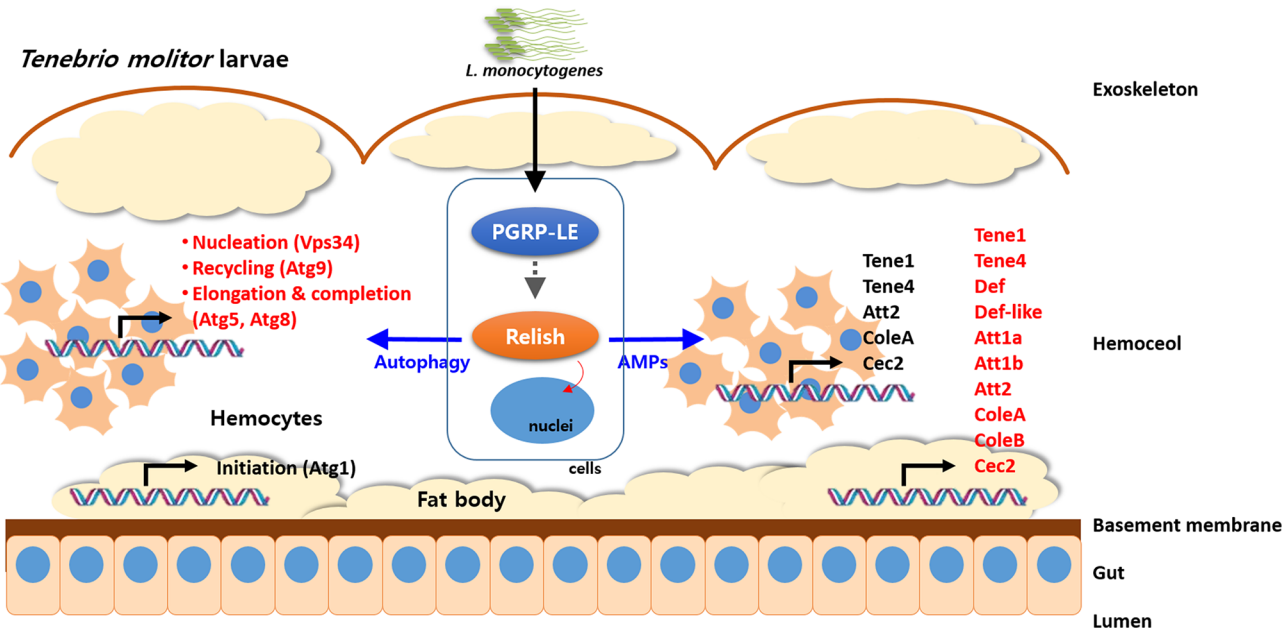

FIGURE 4 | Schematic illustration depicting cross-talk of autophagy process and NF-κB (Relish) pathway in response to pathogens in *T. molitor*. The intracellular Gram-positive bacterium, *Listeria monocytogenes* is recognized by PGRP-LE and the signaling cascade activates the NF-κB transcription factor, Relish. Subsequently, Relish regulates activation of autophagy by direct or indirect stimulation of nucleation step in hemocytes and AMP production in fat body. In addition, the Atg genes related to the nucleation (*TmVPS34*), recycling (*TmAtg9*), and elongation and recycling (*TmAtg5* and *TmAtg8*) were significantly regulated by silencing of *TmRelish* in hemocytes.

level and accumulation of Atg8 in the autophagic punctae have been demonstrated after infection with VSV, RVFV or Zika virus as evidenced through silencing experiments (67, 68). In *Laodelphax striatellus*, Atg8 facilitates Rice stripe virus (RSV) infection in an autophagy-independent manner (69). The higher mortality rates in *Aedes albopictus* mosquitoes after blood-feeding of microorganisms and not systemic challenge in *Atg8*-silenced hosts suggest modulation of autophagy in gut immunity (70). The role of the Atg8 homolog of *T. molitor* (*Tm*Atg8) in mediating autophagy-based clearance of *L. monocytogenes* has been demonstrated through dsRNA-induced gene silencing and recombinant protein expression analysis. Furthermore, the expression levels of *TmAtg8* in hemocytes were also found to be markedly reduced after *L. monocytogenes* infection. In contrast, the increasing expression level of autophagy genes with time in *L. monocytogenes*-infected larvae injected with *dsEGFP* (negative control for RNAi) suggested autophagic control of *L. monocytogenes* clearance (57). Another member of the Atg8 family, the microtubule-associated proteins 1A/1B light chain 3C-like protein (*Tm*Lc3), exhibiting low amino acid identity (34%) to *Tm*Atg8 has been characterized in *T. molitor*; however, its exact role in autophagy-based immunity is yet to be deciphered. Moreover, *Tm*Atg8 protein expression failed to be induced in hemocytes of *TmAtg5*- knockdown larvae, suggesting a coordinated functional role of elongation and completion of autophagosome assembly for the clearance of *L. monocytogenes* in the host. Consistently, RNAi-mediated loss of function of *TmAtg5* led to impaired formation of the Atg12-Atg5-Atg16 complex, which facilitates the lipidation of Atg8, that is, the conversion of Atg8-I to Atg8-II, to form the Atg8-PE complex. Further, the lack of induction of the autophagy marker *Tm*Atg8-II in the fat body tissues of *T. molitor* following *L. monocytogenes* infection is interesting and warrants detailed studies for understanding the mechanism of preferential establishment of autophagy in certain tissues following *L. monocytogenes* challenge. Certainly, the increase in Atg8 (Atg8-II) signals overtime after exposure to *L. monocytogenes* infection is indicative of an increasing autophagic control in the host. The involvement of Atg8 in *Leishmania* parasite survival while infecting macrophages *in vitro* suggests regulatory control of autophagy by autophagosome formation (71).

In another study, the requirement of *Tm*Atg3 and *Tm*Atg5 for the autophagic control of *Listeria* infection was thoroughly investigated. RNAi-mediated silencing of *TmAtg3* and *TmAtg5* led to an increased susceptibility of *T. molitor* larvae to *L. monocytogenes* infection, further confirming the requirement of Atg3 and Atg5 for Atg8 lipidation, formation of the Atg8-PE complex, and subsequent activation of autophagic clearance of microorganisms (42). While *Tm*Atg3 is an E2 ubiquitin-like enzyme responsible for covalent binding of PE to the C-terminus of Atg8, Atg5 is part of the Atg12-Atg5-Atg16 complex, which regulates the formation of the Atg8-PE complex. Downregulation of *Atg8* transcript also downregulating *Atg3* expression in insects is suggestive of an interconnection between the two genes (72).

*Tm*Atg6 (Beclin-1 in mammals), involved in the vesicle nucleation step of the autophagy pathway, has also been found to be required to protect *T. molitor* larvae against *L. monocytogenes* challenge (56). Although Atg6 is a multifunctional protein involved in sorting of vacuolar contents, pollen germination, and tumor suppression, its role in autophagy is highly conserved. In the autophagic pathway, Atg6 forms a complex with Vps34, Vps15, UVRAG, and Vps38 to generate the phagophore. Hence, Atg6 supports autophagy-mediated immune responses against *L. monocytogenes*.

SUMMARY STATEMENT

Genes involved in the canonical TOR-regulated autophagy pathway, which were reviewed here, can be conveniently divided into categories depending on their presumed location along the pathway. Upstream regulatory genes in the *T. molitor* autophagy pathway include the master- regulator *TOR* and at least seven genes, namely, *Akt1*, *Lkb1*, *p53*, *Parp*, *RpS6*, *Tsc1*, and *Tsc2*, that appear to be absent in the yeast genome are conserved in higher eukaryotes such as *Drosophila* and humans. Most of these genes have been reported to be active regulators of autophagy induction and tumor suppressors in model organisms. Similarly, the gene sets required for the formation of the autophagy initiation complex (Atg1 kinase complex) after successful induction vary between yeast and higher eukaryotes. For instance, the absence of Atg17 and its interacting proteins Atg29 and Atg31 in higher eukaryotes including *T. molitor* highlights the discrepancy in the identity of the core components of the autophagy initiation complex. Indeed, in higher eukaryotes Atg17 seems to have been mechanistically replaced by a non-homologous functional equivalent, Fip200 (73). Adding to this complexity, the protein Atg101, absent in yeast interacts with both Atg1 and Fip200 to form the Atg1-kinase complex in higher eukaryotes.

The variation in the composition and function of the core autophagy machinery between yeast and higher eukaryotes discussed above highlights the fact that, although genetic screening in *S. cerevisiae* laid the foundation for the molecular understanding of autophagy, fundamental differences in active components and processes exist between yeast and higher eukaryotes. Indeed, the autophagy core machinery of higher eukaryotes has been extensively modified, partly to satisfy the fundamental need to account for the greater genetic diversity and complexity of higher eukaryotes with respect to those of unicellular eukaryotes. Such difference is substantiated by the presence of multiple isoforms of certain *Atg* genes, including *Atg4*, *Atg8*, *Atg2*, and *Atg9* in higher eukaryotes, although no evidence of this rare phenomenon in *S. cerevisiae* was found in *T. molitor* (74).

FUTURE PERSPECTIVES

The early discovery of Atg8 lipidation in the 1990s prompted researchers to focus on the mechanisms and functional roles of autophagy-related proteins; in addition, recent studies have raised considerable interest in a wide range of research directions to dissect the autophagy pathway. Current findings on the autophagy pathway in insect model systems derived from various fields such as developmental biology, immunology, epidemiology, and molecular biology, have improved our understanding of the fundamental framework of the autophagy process. In particular, the *T. molitor Atg* genes have been largely identified, and the functional roles of these signaling components have been demonstrated through gene silencing studies. However, many unanswered questions on the importance of autophagy in metamorphosis and starvation of *T. molitor*, as well as the role of the interaction between Atg proteins and membrane lipids remains to be answered. Importantly, recent studies in *T. molitor* and *Drosophila* have revealed the regulation of *Atg* genes through NF-κB factors, suggesting a possible connection between different pathways of immune response, including the IMD pathway and autophagy. In *Drosophila*, while the activation of autophagy by the plasma membrane receptor Toll-7 is independent of NF-κB response during VSV infection, the autophagic response to Zika virus infection is NF-κB-dependent (67, 68, 75). Despite the significance of altered *NF-κB* expression at the transcriptional level, the levels of the corresponding protein level seems to be critical in *T. molitor*. Further, it would be interesting to note the levels of conservation in the transcription factors inhibiting autophagy induction such as Hox-family of proteins in *Drosophila* and the zinc finger with a SCAN and KRAB domain 3 (ZKSCAN3) in humans. With transcriptome signatures of pathogenic responses in the host readily available in the research domain, a high-throughput unraveling of Atg genes and its regulatory roles in autophagy would become a reality. In fact, the transcriptome of *An. aquasalis* midgut epithelium is implicated to trigger an autophagic response to *Plasmodium vivax* invasion (76). In conclusion, the fascinating results obtained from previous studies on *T. molitor* autophagy has established promising future directions for newcomers and experts in this field of research.

AUTHOR CONTRIBUTIONS

YJ and YH: Design manuscript concepts. YJ and JL: wrote the draft manuscript. YJ, BP, MK, and YH: Wrote the manuscript. YH and YL: revised the manuscript. All authors contributed to the article and approved the submitted version.

FUNDING

This research was supported by Korea Institute of Planning and Evaluation for Technology in Food, Agriculture, Forestry and Fisheries (IPET) through Export Promotion Technology Development Program (Grant no. 617077-5), funded by Ministry of Agriculture, Food, and Rural Affairs (MAFRA).

REFERENCES

1. Lee J, Giordano S, Zhang J. Autophagy, Mitochondria and Oxidative Stress: Cross-Talk and Redox Signaling. *Biochem J* (2012) 441(2):523–40. doi: 10.1042/BJ20111451
2. Fouillet A, Levet C, Virgone A, Robin M, Dourlen P, Reiusset J, et al. ER Stress Inhibites Neuronal Death by Promoting Autophagy. *Autophagy* (2012) 8 (6):915–26. doi: 10.4161/auto.19716
3. Decuypere J, Parys JB, Bultynck G. Regulation of the Autophagic bcl-2/beclin 1 Interaction. *Cells* (2012) 1(3):284–312. doi: 10.3390/cells1030284
4. Peracchio C, Alabiso O, Valente G, Isidoro C. Involvement of Autophagy in Ovarian Cancer: A Working Hypothesis. *J Ovarian Res* (2012) 5(1):22. doi: 10.1186/1757-2215-5-22
5. Li WW, Li J, Bao JK. Microautophagy: Lesser-Known Self-Eating. *Cell Mol Life Sci* (2012) 69(7):1125–36. doi: 10.1007/s00018-011-0865-5
6. Feng Y, He D, Yao Z, Klionsky DJ. The Machinery of Macroautophagy. *Cell Res* (2014) 24(1):24–41. doi: 10.1038/cr.2013.168
7. Ohashi Y, Munro S. Membrane Delivery to the Yeast Autophagosome From the Golgi-endosomal System. *Mol Biol Cell* (2010) 21(22):3998–4008. doi: 10.1091/mbc.e10-05-0457
8. Abounit K, Scarabelli TM, McCauley RB. Autophagy in Mammalian Cells. *World J Biol Chem* (2012) 3(1):1–6. doi: 10.4331/wjbc.v3.i1.1
9. Polson HEJ, de Lartigue J, Rigden DJ, Reedijk M, Urbe S, Clague MJ, et al. Mammalian Atg18 (WIPI2) Localizes to Omegasome-Anchored Phagophores and Positively Regulated LC3lipidation. *Autophagy* (2012) 6 (4):506–22. doi: 10.4161/auto.6.4.11863
10. Zhang Y, Sun H, Pei R, Mao B, Zhao Z, Li H, et al. The SARS-CoV2 Protein ORF3a Inhibits Fusion of Autophagosomes With Lysosomes. *Cell Discovery* (2021) 7(1):31. doi: 10.1038/s41421-021-00268-z
11. Shelly S, Lukinova N, Bambina S, Berman A, Cherry S. Autophagy is an Essential Component of *Drosophila* Immunity Against Vesicular Stomatitis Virus. *Immunity* (2009) 30(4):588–98. doi: 10.1016/j.immuni.2009.02.009
12. Echavarria-Consuegra L, Smit JM, Reggiori F. Role of Autophagy During the Replication and Pathogenesis of Common Mosquito-Borne Flavi- and Alphaviruses. *Open Biol* (2019) 9:190009. doi: 10.1098/rsob.190009
13. Brackney DE, Correa MA, Cozens DW. The Impact of Autophagy on Arbovirus Infection of Mosquito Cells. *PloS Neg Trop Dis* (2020) 14(5): e0007754. doi: 10.1371/journal.pntd.0007754
14. Kaushik S, Bandyopadhyay U, Sridhar S, Kiffin R, Martinez-Vicente M, Kon M, et al. Chaperone-Mediated Autophagy At a Glance. *J Cell Sci* (2011) 124(Pt 4):495–9. doi: 10.1242/jcs.073874
15. Levine B, Abrams J. P53: The Janus of Autophagy? *Nat Cell Biol* (2008) 10 (6):637–9. doi: 10.1038/ncb0608-637
16. Zirin J, Perrimon N. *Drosophila* as a Model System to Study Autophagy. *Semin Immunopathol* (2010) 32(4):363–72. doi: 10.1007/s00281-010-0223-y
17. Mizushima N. The Role of the Atg1/ULK1 Complex in Autophagy Regulation. *Curr Opin Cell Biol* (2010) 22(2):132–9. doi: 10.1016/j.ceb.2009.12.004
18. Kawamata T, Kamada Y, Suzuki K, Kuboshima N, Akimatsu H, Ota S, et al. Characterization of a Novel Autophagy-Specific Gene, ATG29. *Biochem Biophys Res Commun* (2005) 338(4):1884–9. doi: 10.1016/j.bbrc.2005.10.163
19. Kawamata T, Kamada Y, Kabeya Y, Sekito T, Ohsumi Y. Organization of the Pre-Autophagosomal Structure Responsible for Autophagosome Formation. *Mol Biol Cell* (2008) 19(5):2039–50. doi: 10.1091/mbc.E07-10-1048
20. Chen Y, Klionsky DJ. The Regulation of Autophagy - Unanswered Questions. *J Cell Sci* (2011) 124(Pt 2):161–70. doi: 10.1242/jcs.064576
21. Chan EY, Kir S, Tooze SA. siRNA Screening of the Kinome Identifies ULK1 as a Multidomain Modulator of Autophagy. *J Biol Chem* (2007) 282(35):25464–74. doi: 10.1074/jbc.M703663200
22. Scott RC, Juhasz G, Neufeld TP. Direct Induction of Autophagy by Atg1 Inhibits Cell Growth and Induces Apoptotic Cell Death. *Curr Biol* (2007) 17 (1):1–11. doi: 10.1016/j.cub.2006.10.053
23. Petiot A, Ogier-Denis E, Blommaart EF, Meijer AJ, Codogno P. Distinct Classes of Phosphatidylinositol 3'-Kinases are Involved in Signaling Pathways That Control Macroautophagy in HT-29 Cells. *J Biol Chem* (2000) 275 (2):992–8. doi: 10.1074/jbc.275.2.992
24. Itakura E, Kishi C, Inoue K, Mizushima N. Beclin 1 Forms Two Distinct Phosphatidylinositol 3-Kinase Complexes With Mammalian Atg14 and UVRAG. *Mol Biol Cell* (2008) 19(12):5360–72. doi: 10.1091/mbc.E08-01-0080
25. Baehrecke EH. Autophagy: Dual Roles in Life and Death? *Nat Rev Mol Cell Biol* (2005) 6(6):505–10. doi: 10.1038/nrm1666
26. Liang C, Feng P, Ku B, Dotan I, Canaani D, Oh BH, et al. Autophagic and Tumour Suppressor Activity of a Novel Beclin1-binding Protein UVRAG. *Nat Cell Biol* (2006) 8(7):688–99. doi: 10.1038/ncb1426
27. Matsunaga K, Saitoh T, Tabata K, Omori H, Satoh T, Kurotori N, et al. Two Beclin 1-Binding Proteins, Atg14L and Rubicon, Reciprocally Regulate Autophagy At Different Stages. *Nat Cell Biol* (2009) 11(4):385–96. doi: 10.1038/ncb1846
28. Tooze SA, Yoshimori T. The Origin of the Autophagosomal Membrane. *Nat Cell Biol* (2010) 12(9):831–5. doi: 10.1038/ncb0910-831
29. Obara K, Sekito T, Niimi K, Ohsumi Y. The Atg18-Atg2 Complex is Recruited to Autophagic Membranes Via Phosphatidylinositol 3-Phosphate and Exerts an Essential Function. *J Biol Chem* (2008) 283(35):23972–80. doi: 10.1074/jbc.M803180200
30. Kovacs AL, Palfia Z, Rez G, Vellai T, Kovacs J. Sequestration Revisited: Integrating Traditional Electron Microscopy, *De Novo* Assembly and New Results. *Autophagy* (2007) 3(6):655–62. doi: 10.4161/auto.4590
31. Hayashi-Nishino M, Fujita N, Noda T, Yamaguchi A, Yoshimori T, Yamamoto A. A Subdomain of the Endoplasmic Reticulum Forms a Cradle for Autophagosome Formation. *Nat Cell Biol* (2009) 11(12):1433–7. doi: 10.1038/ncb1991
32. Yla-Anttila P, Vihinen H, Jokitalo E, Eskelinen EL. 3D Tomography Reveals Connections Between the Phagophore and Endoplasmic Reticulum. *Autophagy* (2009) 5(8):1180–5. doi: 10.4161/auto.5.8.10274
33. Geng J, Nair U, Yasumura-Yorimitsu K, Klionsky DJ. Post-Golgi Sec Proteins are Required for Autophagy in *Saccharomyces cerevisiae*. *Mol Biol Cell* (2010) 21(13):2257–69. doi: 10.1091/mbc.E09-11-0969
34. Hailey DW, Rambold AS, Satpute-Krishnan P, Mitra K, Sougrat R, Kim PK, et al. Mitochondria Supply Membranes for Autophagosome Biogenesis During Starvation. *Cell* (2010) 141(4):656–67. doi: 10.1016/j.cell.2010.04.009
35. Lynch-Day MA, Bhandari D, Menon S, Huang J, Cai H, Bartholomew CR, et al. Trs85 Directs a Ypt1 Gef, TRAPPIII, to the Phagophore to Promote Autophagy. *Proc Natl Acad Sci U.S.A.* (2010) 107(17):7811–6. doi: 10.1073/pnas.1000063107
36. Mizushima N, Noda T, Ohsumi Y. Apg16p is Required for the Function of the Apg12p-Apg5p Conjugate in the Yeast Autophagy Pathway. *EMBO J* (1999) 18(14):3888–96. doi: 10.1093/emboj/18.14.3888
37. Suzuki K, Kirisako T, Kamada Y, Mizushima N, Noda T, Ohsumi Y. The Pre-Autophagosomal Structure Organized by Concerted Functions of APG Genes is Essential for Autophagosome Formation. *EMBO J* (2001) 20(21):5971–81. doi: 10.1093/emboj/20.21.5971
38. Fujita N, Itoh T, Omori H, Fukuda M, Noda T, Yoshimori T. The Atg16L Complex Specifies the Site of LC3 Lipidation for Membrane Biogenesis in Autophagy. *Mol Biol Cell* (2008) 19(5):2092–100. doi: 10.1091/mbc.E07-12-1257
39. Nakatogawa H, Ichimura Y, Ohsumi Y. Atg8, a Ubiquitin-Like Protein Required for Autophagosome Formation, Mediates Membrane Tethering and Hemifusion. *Cell* (2007) 130(1):165–78. doi: 10.1016/j.cell.2007.05.021
40. Shi CS, Kehrl JH. MyD88 and Trif Target Beclin 1 to Trigger Autophagy in Macrophages. *J Biol Chem* (2008) 283(48):33175–82. doi: 10.1074/jbc.M804478200
41. He C, Klionsky DJ. Regulation Mechanisms and Signaling Pathways of Autophagy. *Annu Rev Genet* (2009) 43:67–93. doi: 10.1146/annurev-genet-102808-114910
42. Tindwa H, Jo YH, Patnaik BB, Noh MY, Kim DH, Kim I, et al. Depletion of Autophagy-Related Genes ATG3 and ATG5 in *Tenebrio molitor* Leads to Decreased Survivability Against an Intracellular Pathogen, *Listeria monocytogenes*. *Arch Insect Biochem Physiol* (2015b) 88(1):85–99. doi: 10.1002/arch.21212
43. Kim J, Kundu M, Viollet B, Guan KL. AMPK and mTOR Regulate Autophagy Through Direct Phosphorylation of Ulk1. *Nat Cell Biol* (2011) 13(2):132–41. doi: 10.1038/ncb2152
44. Yang CS, Lee JS, Rodgers M, Min CK, Lee JY, Kim HJ, et al. Autophagy Protein Rubicon Mediates Phagocytic NADPH Oxidase Activation in Response to Microbial Infection or TLR Stimulation. *Cell Host Microbe* (2012) 11(3):264–76. doi: 10.1016/j.chom.2012.01.018
45. Orsi A, Razi M, Dooley HC, Robinson D, Weston AE, Collinson LM, et al. Dynamic and Transient Interactions of Atg9 With Autophagosomes, But Not

Membrane Integration, are Required for Autophagy. *Mol Biol Cell* (2012) 23 (10):1860–73. doi: 10.1091/mbc.E11-09-0746
46. Yamamoto H, Kakuta S, Watanabe TM, Kitamura A, Sekito T, Kondo-Kakuta C, et al. Atg9 Vesicles are an Important Membrane Source During Early Steps of Autophagosome Formation. *J Cell Biol* (2012) 198(2):219–33. doi: 10.1083/jcb.201202061
47. Jo YH, Patnaik BB, Hwang J, Park KB, Ko HJ, Kim CE, et al. Regulation of the Expression of Nine Antimicrobial Peptide Genes by TmIMD Confers Resistance Against Gram-negative Bacteria. *Sci Rep* (2019) 9(1):10138. doi: 10.1038/s41598-019-46222-8
48. Park S, Jo YH, Park KB, Ko HJ, Kim CE, Bae YM, et al. Tmtoll-7 Plays a Crucial Role in Innate Immune Responses Against Gram-Negative Bacteria by Regulating 5 AMP Genes in *Tenebrio molitor*. *Front Immunol* (2019) 10:310. doi: 10.3389/fimmu.2019.00310
49. Patnaik BB, Patnaik HH, Seo GW, Jo YH, Lee YS, Lee BL, et al. Gene Structure, cDNA Characterization and RNAi-based Functional Analysis of a Myeloid Differentiation Factor 88 Homolog in *Tenebrio molitor* Larvae Exposed to *Staphylococcus aureus* Infection. *Dev Comp Immunol* (2014) 46 (2):208–21. doi: 10.1016/j.dci.2014.04.009
50. Jo YH, Kim YJ, Park KB, Seong JH, Kim SG, Park S, et al. TmCactin Plays an Important Role in Gram-negative and -Positive Bacterial Infection by Regulating Expression of 7 AMP Genes in *Tenebrio molitor*. *Sci Rep* (2017) 7:46459. doi: 10.1038/srep46459
51. Keshavarz M, Jo YH, Park KB, Ko HJ, Edosa TT, Lee YS, et al. TmDorX2 Positively Regulates Antimicrobial Peptides in *Tenebrio molitor* Gut, Fat Body, and Hemocytes in Response to Bacterial and Fungal Infection. *Sci Rep* (2019) 9(1):16878. doi: 10.1038/s41598-019-53497-4
52. Vigneron A, Jehan C, Rigaud T, Moret Y. Immune Defenses of a Beneficial Pest: The Mealworm Beetle, *Tenebrio molitor*. *Front Physiol* (2019) 10:138. doi: 10.3389/fphys.2019.00138
53. Keshavarz M, Jo YH, Edosa TT, Han YS. Two Roles for the *Tenebrio Molitor* Relish in the Regulation of Antimicrobial Peptides and Autophagy-Related Genes in Response to *Listeria monocytogenes*. *Insects* (2020) 11(3):188. doi: 10.3390/insects11030188
54. Jo YH, Lee JH, Tindwa H, Patnaik HH, Seong JH, Kim SG, et al. Molecular Characterization and Expression Analysis of Target of Rapamycin (TmTOR) in Coleopteran Insect *Tenebrio molitor*. *Entomol Res* (2016) 46(2):139–47. doi: 10.1111/1748-5967.12163
55. Lee JH, Jo YH, Patnaik BB, Park KB, Tindwa H, Seo GW, et al. Cloning, Expression Analysis, and RNA Interference Study of a HORMA Domain Containing Autophagy-Related Gene 13 (ATG13) From the Coleopteran Beetle, *Tenebrio molitor*. *Front Physiol* (2015) 6:180. doi: 10.3389/fphys.2015.00180
56. Edosa TT, Jo YH, Keshavarz M, Park KB, Cho JH, Bae YM, et al. Tmatg6 Plays an Important Role in Anti-Microbial Defense Against *Listeria monocytogenes* in the Mealworm, *Tenebrio molitor Int J Mol Sci* (2020) 21(4):1232. doi: 10.3390/ijms21041232
57. Tindwa H, Jo YH, Patnaik BB, Lee YS, Kang SS, Han YS. Molecular Cloning and Characterization of Autophagy-Related Gene TmATG8 in *Listeria*-invaded Hemocytes of *Tenebrio molitor*. *Dev Comp Immunol* (2015a) 51 (1):88–98. doi: 10.1016/j.dci.2015.02.017
58. Pizarro-Cerda J. Pascale Cossart: *Listeria monocytogenes*, Host-Pathogen Interactions & Beyond. *Cell Microbiol* (2020) 22(4):e13165. doi: 10.1111/cmi.13165
59. Yano T, Mita S, Ohmori H, Oshima Y, Fujimoto Y, Ueda R, et al. Autophagic Control of *Listeria* Through Intracellular Innate Immune Recognition in *Drosophila*. *Nat Immunol* (2008) 9(8):908–16. doi: 10.1038/ni.1634
60. Tindwa H, Patnaik BB, Kim DH, Mun S, Jo YH, Lee BL, et al. Cloning, Characterization and Effect of TmPGRP-LE Gene Silencing on Survival of *Tenebrio molitor* Against *Listeria monocytogenes* Infection. *Int J Mol Sci* (2013) 14(11):22462–82. doi: 10.3390/ijms141122462
61. Casati B, Terova G, Cattaneo AG, Rimoldi S, Franzetti E, de Eguileor M, et al. Molecular Cloning, Characterization and Expression Analysis of ATG1 in the Silkworm, *Bombyx mori*. *Gene* (2012) 511(2):326–37. doi: 10.1016/j.gene.2012.09.086
62. Li Z, Lyu Z, Ye Q, Cheng J, Wang C, Lin T. Cloning, Expression Analysis, 20-Hydroxyecdysone Induction, and RNA Interference Study of Autophagy-related Gene 8 From *Heortia vitessoides* Moore. *Insects* (2020) 11(4):245. doi: 10.3390/insects11040245
63. Xiao Q, Wang L, Zhou XL, Zhu Y, Dong ZQ, Chen P, et al. BmAtg13 Promotes the Replication and Proliferation of *Bombyx mori* Nucleopolyhedrovirus. *Pestic Biochem Physiol* (2019) 157:143–51. doi: 10.1016/j.pestbp.2019.03.016
64. Tinartis EP, Goncu E, Koc K. Apoptotic and Autophagic Characteristics of Perivisceral Fat Body Remodeling of the Greater Wax Moth *Galleria mellonella* and Effects of Juvenile Hormone Analog, Fenoxycarb, on These Processes. *Insect Biochem Physiol* (2021) 107:e21780. doi: 10.1002/arch.21780
65. Kazek M, Kaczmarek A, Wronska AK, Bogus MI. *Conidiobolus coronatus* Induces Oxidative Stress and Autophagy Response in *Galleria mellonella* Larvae. *PloS One* (2020) 15(2):e0228407. doi: 10.1371/journal.pone.0228407
66. Santos-Araujo S, Bomfim L, Araripe LO, Bruno R, Ramos I, Gondim KC. Silencing of ATG6 and ATG8 Promotes Increased Levels of Triacylglycerol (TAG) in the Fat Body During Prolonged Starvation Periods in the Chagas Disease Vector *Rhodnius prolixus*. *Insect Biochem Mol Biol* (2020) 127:103484. doi: 10.1016/j.ibmb.2020.103484
67. Moy RH, Gold B, Molleston JM, Schad V, Yanger K, Salzano M-V, et al. Antiviral Autophagy Restricts Rift Valley Fever Virus Infection and is Conserved From Flies to Mammals. *Immunity* (2014) 40(1):51–65. doi: 10.1016/j.immuni.2013.10.020
68. Liu X-M, Yamasaki A, Du X-M, Coffmann VC, Ohsumi Y, Nakatogawa H, et al. Lipidation-Independent Vacoular Functions of Atg8 Rely on its Noncanonical Interaction With a Vacoule Membrane Protein. *eLife* (2018) 7:e41237. doi: 10.7554/eLife.41237
69. Yu YL, Zhang MT, Huo Y, Tang JL, Liu Q, Chen XY, et al. *Laodelphax striatellus* Atg8 Facilitates Rice Stripe Virus Infection in an Autophagy-Independent Manner. *Insect Sci* (2021) 28(2):315–29. doi: 10.1111/1744-7917.12771
70. Kim CE, Park KB, Ko HJ, Keshavarz M, Bae YM, Kim B, et al. *Aedes albopictus* Autophagy-Related Gene 8 (AaAtg8) is Required to Confer Anti-Bacterial Gut Immunity. *Int J Mol Sci* (2020) 21(8):2944. doi: 10.3390/ijms21082944
71. Giri S, Shaha C. *Leishmania Donovani* Parasite Requires Atg8 Protein for Infectivity and Survival Under Stress. *Cell Death Dis* (2019) 10(11):808. doi: 10.1038/s41419-019-2038-7
72. Li S, Xu J, Xu X, Ma W, Tian L, Li K. Functional Identification of *Bombyx mori* Atg13 in Autophagy. *Insect Biochem Physiol* (2020) 105(1):e21718. doi: 10.1002/arch.21718
73. Nagy P, Karpati M, Varga A, Pircs K, Venkei Z, Takats S, et al. Atg17/FIP200 Localizes to Perilysosomal Ref(2)P Aggregates and Promotes Autophagy by Activation of Atg1 in *Drosophila*. *Autophagy* (2014) 10(3):453–67. doi: 10.4161/auto.27442
74. Alers S, Loffler AS, Wesselborg S, Stork B. The Incredible Ulks. *Cell Commun Signal* (2012) 10(1):7. doi: 10.1186/1478-811X-10-7
75. Nakamoto M, Moy RH, Xu J, Bambina S, Yasunaga A, Shelly SS, et al. Virus Recognition by Toll-7 Activates Antiviral Autophagy in *Drosophila*. *Immunity* (2012) 36(4):658–67. doi: 10.1016/j.immuni.2012.03.003
76. Santana RAG, Oliveira MC, Cabral I, Silva Junior RCA, de Sousa DRT, Ferreira L, et al. *Anopheles aquasalis* Transcriptome Reveals Autophagic Responses to *Plasmodium vivax* Midgut Invasion. *Parasit Vectors* (2019) 12 (1):261. doi: 10.1186/s13071-019-3506-8

Conflict of Interest: The authors declare that the research was conducted in the absence of any commercial or financial relationships that could be construed as a potential conflict of interest.

frontiers in Immunology

ORIGINAL RESEARCH
published: 14 July 2021
doi: 10.3389/fimmu.2021.639019

Salmonella spvC Gene Inhibits Autophagy of Host Cells and Suppresses NLRP3 as Well as NLRC4

Liting Zhou[‡], Yuanyuan Li[‡], Song Gao[†], Haibo Yuan, Lingli Zuo[†], Chaoyi Wu, Rui Huang and Shuyan Wu[*]

Department of Medical Microbiology, School of Biology and Basic Medical Science, Medical College of Soochow University, Suzhou, China

Salmonella spvC gene, encoding a phosphothreonine lyase on host mitogen-activated protein kinases, facilitates systemic infection of *Salmonella* while the precise mechanisms remain elusive. Autophagy and pyroptosis dependent on the activation of inflammasomes, as parts of innate immune response, contribute to host defense against *Salmonella* infection. Recently, we reported that *spvC* could inhibit pyroptosis. To explore the effect of *spvC* on autophagy and the relationship between its function in pyroptosis and autophagy, infection models of macrophages J774A.1 and epithelial HeLa cells co-cultured with *Salmonella* Typhimurium wild type, *spvC* deletion, site-directed mutant which lacks phosphothreonine lyase activity, or complemented strain were established. The levels of LC3 turnover and Beclin 1 of J774A.1 cells were determined by western blot. Confocal laser scanning microscopy was used to visualize the autophagic flux after being transfected with mRFP-GFP-LC3 plasmid in HeLa cells. Results showed that SpvC inhibited autophagosome formation through its phosphothreonine lyase activity. Additionally, analysis of nucleotide-binding oligomerization domain, leucine-rich repeat and pyrin domain-containing 3 (NLRP3) and NLR with CARD domain-containing 4 (NLRC4) in J774A.1 cells indicated that *spvC* decreased the protein levels of NLRP3 and NLRC4, which were significantly changed by autophagy inhibitor Bafilomycin A1. Together, our observations reveal a novel mechanism of *spvC* in *Salmonella* pathogenesis and host inflammatory response *via* inhibiting autophagy and NLRP3 as well as NLRC4. These pathways and their subversion by diverse pathogen virulence determinants are expected to throw light on the design of anti-infective agents.

Keywords: *Salmonella*, *spvC*, autophagy, NLRP3, NLRC4

OPEN ACCESS

Edited by:
Isabelle Vergne, UMR5089 Institut de Pharmacologie et de Biologie Structurale (IPBS), France

Reviewed by:
Jere W. McBride, University of Texas Medical Branch at Galveston, United States
Shourong Shi, Poultry Institute, Chinese Academy of Agricultural Sciences, China
Michiel Van Der Vaart, Leiden University, Netherlands

***Correspondence:**
Shuyan Wu
wushuyan@suda.edu.cn

***Present address:**
Song Gao, Department of Central Laboratory, Liaocheng People's Hospital, Liaocheng, China
Lingli Zuo, Medical Research Center, The People's Hospital of Suzhou New District, Suzhou, China

These authors have contributed equally to this work

Specialty section:
This article was submitted to Microbial Immunology, a section of the journal Frontiers in Immunology

Received: *08 December 2020*
Accepted: *28 June 2021*
Published: *14 July 2021*

Citation:
Zhou L, Li Y, Gao S, Yuan H, Zuo L, Wu C, Huang R and Wu S (2021) Salmonella spvC Gene Inhibits Autophagy of Host Cells and Suppresses NLRP3 as Well as NLRC4. Front. Immunol. 12:639019. doi: 10.3389/fimmu.2021.639019

INTRODUCTION

Salmonella is a facultative intracellular pathogen that causes a serious threat to global public health. Centers for Disease Control and Prevention estimates approximately 1.35 million infections, 26,500 hospitalizations, and 420 deaths caused by *Salmonella* in the United States every year (1). Among 2600 *Salmonella enterica* serovars, *Salmonella enterica* serovar typhimurium (*S.* Typhimurium) is

one of the most common isolates causing infection with a broad range of hosts (2). Therefore, it will be clinically important to develop new strategies to control *S.* Typhimurium infection. In particular, pathogenesis of *S.* Typhimurium requires the action of multiple virulence factors. SpvB and SpvC, virulence factors encoded within the *Salmonella* plasmid virulence (*spv*) operon, are responsible for pathogenicity of *S.* Typhimurium (3). Previously we reported a novel contribution of *spvB* to *Salmonella* pathogenesis through interfering with intracellular iron homeostasis (4). *spvC*, another essential factor of *Salmonella* virulence determinant encoding phosphothreonine lyase, suppresses intestinal inflammation and aggravates systemic dissemination through mitogen-activated protein kinase (MAPK) signaling pathway (5, 6). However, the underlying mechanisms have been only partly illuminated.

Intracellular pathogens invade mammalian host cells in membrane bound vesicles called phagosomes. Of note, autophagy is a process whereby a double-membrane structure (autophagosome) engulfs unnecessary invading pathogens and delivers them to the lysosome for degradation. But the pathogens have developed several survival mechanisms to prevent this degradation event (7). *S.* Typhimurium, including its effectors, has evolved to block host signaling cascades or even create favorable conditions for self-replication and survival by virtue of autophagy through specific mechanisms, so as to resist the host defense (8, 9). It has been reported that *spvC* is responsible for the anti-inflammatory effect of *S.* Typhimurium to facilitate bacterial dissemination, and the host can eliminate intracellular bacteria by autophagy, which can inhibit the further spread of bacteria. In light of this, we hypothesize that autophagy is also involved in *spvC*-mediated infection while the precise mechanism remains obscure.

Innate immune recognition is initiated by pattern-recognition receptors (PRRs), of which nucleotide-binding domain and leucine-rich repeat receptors (NLRs) function in the recognition of danger signals introduced into the host cell cytosol. Nucleotide-binding oligomerization domain, leucine-rich repeat and pyrin domain-containing 3 (NLRP3) responds to a diverse range of stimuli, including pathogens, microbial toxins, etc. NLRP3 plays a pivotal role in regulating live-or-die cell-fate decisions (10, 11). Inhibition of the NLRP3 inflammasome using MCC950 enhances host protection against *B. cereus*-induced infection (12). Besides, NLR with CARD domain-containing 4 (NLRC4) in epithelium is sufficient to protect against *S.* Typhimurium invasion (13). Assembly of the NLRP3 and NLRC4 inflammasomes leads to caspase 1-dependent/independent release of the pro-inflammatory cytokines IL-1β and IL-18, as well as to gasdermin D-mediated pyroptosis (14, 15). NLRP3 recruited by NLRC4 had been considered distinct inflammasome scaffolds in response to *S.* Typhimurium infection (16). Moreover, NLRP3 could be activated by flagellin under conditions of suboptimal NAIP/NLRC4 activation in *S.* Typhimurium infected macrophages (17). Our recent research revealed that *spvC* inhibits NLRP3 and NLRC4-associated pyroptosis against *S.* Typhimurium (18). Reports showed autophagy machinery constitutes a key cellular monitoring system that prevents excessive NLRP3 inflammasome activation (19, 20). However, more thorough investigation is required to shed light on the fundamental mechanisms underlying autophagy regulated NLRP3 and NLRC4 mediated by *spvC*.

Herein, both macrophages J774A.1 and epithelial HeLa cells were co-cultured with *S.* Typhimurium wild type, *spvC* deletion, site-directed mutant which lacks phosphothreonine lyase activity or complemented strain. We report a novel contribution of *spvC* to *S.* Typhimurium pathogenesis through the inhibition of host autophagy *via* its phosphothreonine lyase activity which affects the protein level of NLRP3 and NLRC4.

MATERIALS AND METHODS

Bacterial Strains and Culture Conditions

S. Typhimurium wild type strain (STM-WT) was kindly supplied by Professor Qian Yang (Nanjing Agricultural University, Nanjing, China). STM-WT, *spvC* deletion mutant (STM-*ΔspvC*), *spvC* site-directed mutant (STM-*ΔspvC*/p*spvC* K136A) which lacks phosphothreonine lyase activity and *spvC* complemented strain (STM-*ΔspvC*/p*spvC*) were grown to log phase at 37°C in Luria Bertani (LB, Hangwei, China) broth overnight. STM-*ΔspvC*/p*spvC* K136A and STM-*ΔspvC*/p*spvC* were cultured in the media with 100 μg/ml ampicillin (Sigma, USA).

Construction of Mutant Strains

STM-*ΔspvC* was constructed with λRed recombination system basically as previously described (21) and the corresponding plasmids were gifts from Professor Daoguo Zhou (Purdue University, West Lafayette, USA). STM-*ΔspvC*/p*spvC* K136A mutation was constructed by overlap PCR. STM-*ΔspvC*/p*spvC* K136A and STM-*ΔspvC*/p*spvC* was complemented with STM-*ΔspvC* using pBAD/gIII expression system (22). *spvC* deletion mutant, site-directed mutant and complemented strain were identified by PCR and sequencing.

Cell Culture

J774A.1 cells were purchased from the Procell Life Science & Technology Co.,Ltd. HeLa cells were acquired from National Collection of Authenticated Cell Cultures. Cells were routinely cultured in complete medium that Dulbecco's modified Eagle medium (HyClone Laboratories, Logan, UT, USA) supplemented with 10% (v/v) fetal bovine serum (Biological Industries, Kibbutz Beit-Haemek, Israel) and in a humidified incubator containing 5% CO_2 at 37°C.

Bacterial Infection

J774A.1 cells (1×10^6/well) and HeLa cells (5×10^5/well) were seeded in 12-well plates. On the day of infection, *S.* Typhimurium were diluted 1:100 with LB broth to subculture for 3 h. Both STM-*ΔspvC*/p*spvC* K136A and STM-*ΔspvC*/p*spvC* were supplemented with 0.2% L-arabinose (Sigma, USA). Bacteria were then washed three times in PBS. The optical

density of bacteria was determined by spectrophotometry at 600 nm with viable plate counts before infection. The bacterial suspension was subsequently added to cultured cells at the multiplicity of infection (MOI) described in the figure legends. Fresh medium containing amikacin (100 μg/ml, Sigma, Burlington, MA, USA) was added to kill the extracellular bacteria at 1 hour post infection (hpi). Afterwards, infected cells were washed and subsequently cultured in fresh medium containing amikacin (10 μg/ml) to limit extracellular replication of bacteria. PD0325901 (50 nM, Selleck, USA) functioned as an ERK inhibitor was added to the complete medium mentioned in *Cell Culture* section 24 h before infection. Cells were pretreated with Bafilomycin A1 (100 nM, Sigma, USA) 2 h before infection to inhibit autophagosome-lysosome fusion. At different time points following infection, cells were processed in the following ways.

Western Blot Analysis

Proteins were extracted using RIPA buffer containing protease inhibitors and phosphatase inhibitors (Beyotime, China). Samples were homogenized on ice, centrifuged for supernatant at 12,000 g for 15 min at 4°C and heated to 100°C for 5 min. Protein extracts resuspended in sample loading buffer were separated by electrophoresis through 12% polyacrylamide gels and transferred to PVDF membranes (Millipore, USA). After blocking with 5% non-fat milk (Sangon Biotech Shanghai Co., Ltd., China), membranes were incubated with primary antibodies anti-LC3 (4108S, CST, USA; 1: 1,000 dilution), anti-Beclin 1 (3738, CST, USA; 1: 1,000 dilution), anti-NLRP3 (15101S, CST, USA; 1: 1,000 dilution), anti-NLRC4 (ab201792, abcam, UK; 1: 1,000 dilution), anti-GAPDH (BA2913, Boster, China; 1: 1,000 dilution), anti-Tubulin (AF1216, Beyotime, China; 1: 1,000 dilution) and anti-Histone H3 (ab194681, abcam, UK; 1: 1,000 dilution) overnight at 4°C. Membranes were then washed and incubated with the horseradish peroxidase (HRP)-labeled goat anti-rabbit IgG (A0208, Beyotime, China; 1: 3,000 dilution) for 1 h at room temperature. Proteins were visualized using ECL luminescence reagent (Meilunbio, China). The gray-scale values of the bands were determined by Image J launcher broken symmetry software program (National Institutes of Health, Bethesda, MD, USA).

Confocal Laser Scanning Microscopy

For immunofluorescence microscopy, HeLa cells transfected with mRFP-GFP-LC3 plasmid were used to establish the infection model. HeLa cells were collected at 2 hpi, bacteria and cell nucleus were labeled by Hoechst (33258, Beyotime, China; 1: 10,000 dilution). The samples were imaged under a confocal laser scanning microscopy (Fluoview FV1000, Olympus, Japan). GFP-LC3 and mRFP-LC3 punctate dots were counted in more than 100 cells and measured by Image J software program for quantification.

Statistical Analysis

Statistical significance was determined by ANOVA for three or more groups. $P < 0.05$ was considered to be statistically significant.

RESULTS

spvC Suppresses Autophagy and Increases Intracellular Survival of *Salmonella* Typhimurium in Macrophages at the Early Stage of Infection

Our previous study revealed that *Salmonella* plasmid virulence gene *spvB* impair autophagic flux in infected macrophages for pathogen clearance (23). To determine the role of *spvC* on host cell autophagy, J774A.1 cells were collected to detect the expression of Microtubule associated protein light chain 3 (LC3) by western blot after being co-cultured with STM-WT, STM-Δ*spvC* or STM-Δ*spvC*/p*spvC* at 2 hpi, 8 hpi, 16 hpi and 24 hpi (**Figure 1A**). We found an increasing evidence of LC3-II in the early stage of infection (2 hpi and 8 hpi) compared with that in the late stage of infection (16 hpi and 24 hpi). At 2 hpi, higher level of LC3-II was found in STM-Δ*spvC* infected J774A.1 cells than those in STM-WT or STM-Δ*spvC*/p*spvC* infected cells. We next focused on the early stage of infection, and data confirmed that much more LC3-II and Beclin 1 were assessed in macrophages infected with STM-Δ*spvC* than in those infected with *S.* Typhimurium carrying *spvC* (**Figure 1B**). These data suggest that *spvC* suppresses autophagy in macrophages at the early stage of infection.

Autophagy is a cellular mechanism involving the degradation of cellular components or intracellular microbes through lysosomal machinery. We next examined the effect of the *Salmonella spvC* gene on intracellular bacterial loads. In agreement with our previous studies *in vivo* (18), macrophages J774A.1 infected with STM-Δ*spvC* showed significantly lower bacterial burden than those infected with STM-WT or STM-Δ*spvC*/p*spvC* since 2 hpi *in vitro* (**Figure 1C**). The aforementioned results suggest s*pvC* restricts elimination of pathogens in host cells which may be related to its contribution to autophagy, while the underlying mechanism remains elusive.

spvC Inhibits the Formation of Autophagosomes in Host Cells During *Salmonella* Typhimurium Infection

LC3-II, as the marker of autophagosomes, associates with both the outer and inner membranes of the autophagosomes. The increased protein level of LC3-II in **Figures 1A, B** indicates that *spvC* disturbs the number of autophagosomes in *S.* Typhimurium infected macrophages. Since autophagy is a dynamic process, the raised number of autophagosomes in STM-Δ*spvC* infected cells may represent either the increased formation of autophagosomes and/or the inhibition in autophagosomal maturation. Of interest, treatment of *S.* Typhimurium-infected macrophages with Bafilomycin A1, which blocks autophagosome-lysosome fusion, led to the accumulation of autophagosomes in all groups, but the magnitude of the increase was significantly lower in the STM-Δ*spvC* infected group than STM-WT or STM-Δ*spvC*/p*spvC* infected groups (**Figure 2A**). These data suggest that *spvC* negatively regulates autophagic activity and intervenes in the formation of autophagosomes in host cells. Furthermore,

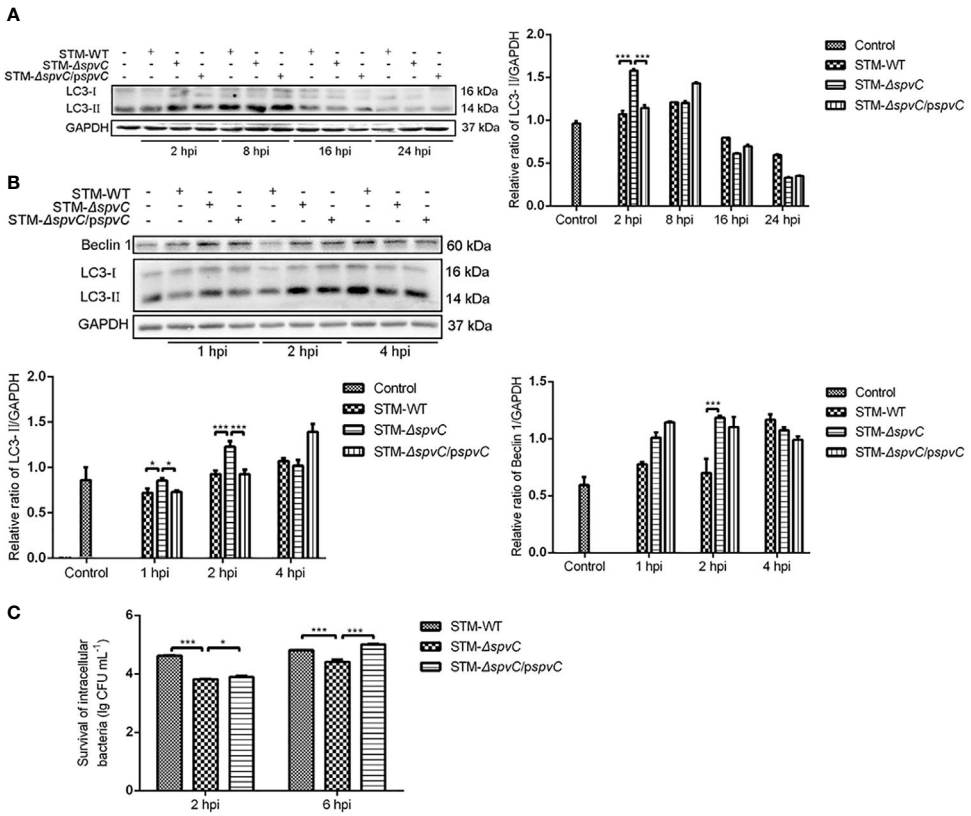

FIGURE 1 | *SpvC* suppresses autophagy and increases intracellular survival of *Salmonella* Typhimurium in macrophages at the early stage of infection. **(A, B)** J774A.1 cells were infected with STM-WT, STM-*ΔspvC* or STM-*ΔspvC*/p*spvC* at an MOI of 10. Cell lysates were analysed by western blot with specific antibodies to LC3 and the control GAPDH at 2 hpi, 8 hpi, 16 hpi and 24 hpi **(A)**, to Beclin 1, LC3 and the control GAPDH at 1 hpi, 2 hpi and 4 hpi **(B)**. **(C)** Intracellular bacterial loads of J774A. 1 cells were assayed by colony forming units counting. Data were compared by ANOVA. Values are expressed as the means ± S.D., n = 3. Statistically significant differences are indicated. ***$P < 0.001$; *$P < 0.05$.

autophagic flux was morphologically monitored by mRFP-GFP-LC3. Autophagosomes and autolysosomes are labeled with yellow (RFP and GFP merged) and red (RFP only) puncta, respectively, since RFP exhibits more stable fluorescence in acidic compartments while GFP signal quenches for the low pH inside the lysosome (24). HeLa cells transfected with mRFP-GFP-LC3 were infected with different *S.* Typhimurium strains. More yellow LC3 puncta were visualized in STM-*ΔspvC* infected cells than those in STM-*ΔspvC* or STM-*ΔspvC*/p*spvC* infected cells at 2 hpi (**Figures 2B, C**). These results demonstrate that *spvC* inhibits autophagy by suppressing the formation of autophagosomes.

spvC Phosphothreonine Lyase Activity Is Critical for Inhibiting Autophagy in *Salmonella* Typhimurium Infection

Previous literature reported that SpvC is a *Salmonella* effector with phosphothreonine lyase activity on host MAPK (6). To investigate whether the enzymatic activity of SpvC is involved in its effect on autophagy, J774A.1 cells were co-cultured with STM-WT, STM-*ΔspvC*, site-directed mutant STM-*ΔspvC*/p*spvC* K136A which lacks phosphothreonine lyase activity and STM-*ΔspvC*/p*spvC*, respectively. As expected, both STM-*ΔspvC* and STM-*ΔspvC*/p*spvC* K136A gave rise to elevated levels of LC3-II in their infected macrophages compared with *S.* Typhimurium carrying *spvC* (**Figure 3A**). Concomitantly, levels of Beclin 1 were in line with the changing trend of LC3-II (**Figure 3B**). These results reveal that SpvC suppresses autophagy in macrophages through its phosphothreonine lyase activity.

ERK is an essential component in MAPK signaling pathway. To further elucidate the relationship between the effect of SpvC on autophagy and its phosphothreonine lyase activity on MAPK, HeLa cells were pretreated with ERK inhibitor PD0325901 before co-cultured with STM-WT, STM-*ΔspvC* or STM-*ΔspvC*/p*spvC*. In line with the results obtained in **Figure 1B**, significantly more LC3-II and Beclin 1 were determined in HeLa cells infected with STM-*ΔspvC* than those in cells infected with *S.* Typhimurium carrying *spvC* at 2 hpi. The conversion from LC3-I to LC3-II also correlates well with the number of autophagosomes (24). PD0325901 only decreased the expression of LC3-II and Beclin 1 in STM-*ΔspvC* infected cells rather than those infected with STM-WT or STM-*ΔspvC*/p*spvC*. Additionally, there was no

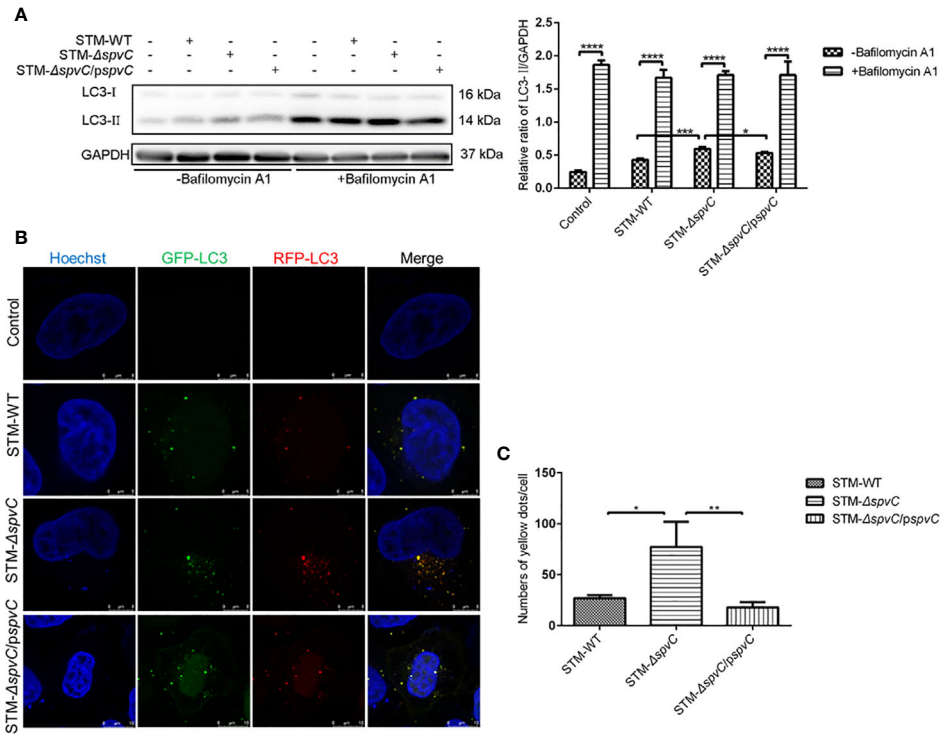

FIGURE 2 | *SpvC* inhibits the formation of autophagosomes in host cells during *Salmonella* Typhimurium infection. **(A)** J774A.1 cells were infected with STM-WT, STM-*ΔspvC* or STM-*ΔspvC*/*pspvC* at an MOI of 10 after being pretreated with Bafilomycin A1. Cell lysates were analysed by western blot with specific antibodies to LC3 and the control GAPDH at 2 hpi. n = 3. **(B, C)** HeLa cells stability expressing mRFP-GFP-LC3 were used to establish an infection model. **(B)** LC3 puncta were visualized at 2 hpi by CLSM. Cell nucleus were labeled by Hoechst. **(C)** Punctate LC3 dots were measured by Image J. Number of punctate dots was enumerated in at least 100 cells. Scale bar, 5 μm. Data were compared by ANOVA. Values are expressed as the means ± S.D. and statistically significant differences are indicated. $^{*}P < 0.05$; $^{**}P < 0.01$; $^{***}P < 0.001$; $^{****}P < 0.0001$.

significant difference of the expression of LC3-II and Beclin 1 among STM-WT, STM-*ΔspvC* or STM-*ΔspvC*/p*spvC* infected cells after PD0325901 treatment, which indicates that ablation of ERK signaling pathway virtually eliminates the inhibition of *spvC* on autophagy (**Figure 3C**). Collectively, these data indicate that phosphothreonine lyase activity of SpvC is required to inhibit the formation of autophagosomes.

spvC Down-Regulates NLRP3 and NLRC4 in an Autophagy Related Manner

Previous studies have reported that SpvC exerts as an anti-inflammatory effector in systemic infection of *Salmonella* (5). Our earlier research has showed that *spvC* inhibits pyroptosis of host cells and it could also modulate NLRP3 and NLRC4-associated inflammatory response against *S.* Typhimurium. Of note, various literatures suggest that autophagy, a cellular waste removal and rejuvenation process, serves a crucial role as a macrophage-intrinsic negative regulator of NLRP3 inflammasome (25). In order to explore whether the autophagic response contributed to the effect of *spvC* on NLRP3 and NLRC4, we first co-cultured macrophages J774A.1 with STM-WT, STM-*ΔspvC*, or STM-*ΔspvC*/p*spvC* to investigate the dynamic function of *spvC* on NLRP3 and NLRC4. Western blot analysis showed the increasing evidence of NLRP3 and NLRC4 at 8 hpi due to the absence of *spvC* (**Figures 4A, B**), which suggests that *spvC* down-regulates NLRP3 and NLRC4.

Next, we generated the infection model pretreated with Bafilomycin A1. As previously mentioned, western blot analysis exhibited that in the absence of Bafilomycin A1, the levels of NLRP3 and NLRC4 in cells infected with STM-*ΔspvC* were significantly higher than that in cells infected with *Salmonella* carrying *spvC*. After Bafilomycin A1 treatment to inhibit autophagosome-lysosome fusion, the levels of NLRP3 and NLRC4 significantly changed though differences among three groups were still observed (**Figures 4C, D**). The results indicate that the effect of *spvC* on NLRP3 and NLRC4 is closely related to autophagy, but other factors are also involved in this process.

DISCUSSION

S. Typhimurium is not only a leading cause of human morbidity and mortality worldwide, but also a model pathogen for investigating the mechanisms of host-bacterium interactions (26). It is well known that macrophages, the professional

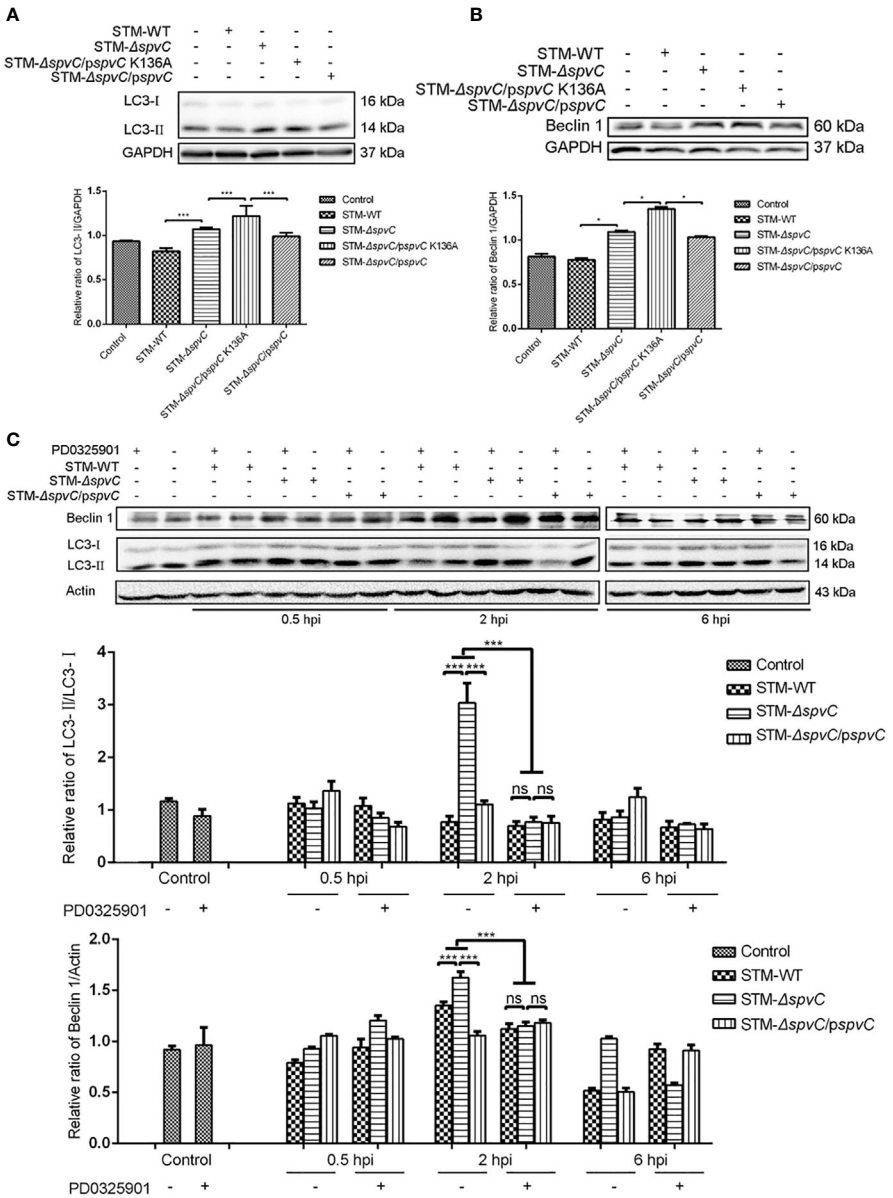

FIGURE 3 | SpvC phosphothreonine lyase activity is critical for inhibiting autophagy in *Salmonella* Typhimurium infection. **(A, B)** J774A.1 cells were infected with STM-WT, STM-*ΔspvC*, STM-*ΔspvC*/p*spvC* or STM-*ΔspvC*/p*spvC* K136A at an MOI of 10 for 2 h. Cell lysates were analysed by western blot with specific antibodies to LC3 **(A)**, Beclin 1 **(B)** and the control GAPDH. **(C)** HeLa cells were infected with STM-WT, STM-*ΔspvC* or STM-*ΔspvC*/p*spvC* at an MOI of 100 after being pretreated with PD0325901. Cell lysates were analysed by western blot with specific antibodies to LC3, Beclin 1 and the control Actin at 0.5 hpi, 2 hpi and 6 hpi. Data were compared by ANOVA. Values are expressed as the means ± S.D., n = 3. Statistically significant differences are indicated. ***$P < 0.001$; *$P < 0.01$; ns, not significant.

phagocytes in host innate immune system, play a pivotal role in the clearance of *S.* Typhimurium. Autophagy is an important component of the innate immune system in host anti-bacterial defense, which is known to target a population of *Salmonella* for degradation and restrict *Salmonella* replication (27, 28). Beclin 1 interacts with several cofactors (*e.g.*, Atg14L, HMGB1, IP3R and PINK) to promote the formation of Beclin 1-Vps34-Vps15 core complexes, thereby inducing autophagy (9). LC3, a mammalian homolog of yeast Atg8, is known to serve as a widely used marker for autophagosomes. To assess a possible correlation between autophagy and *spvC*, we extended these studies by monitoring the time course of autophagy in macrophages during 24 h. Data showed that *spvC* restrains autophagy at the early stage of infection (2 hpi). Concomitantly, much more bacteria were counted in macrophages infected with *S.* Typhimurium carrying *spvC* at 2 hpi and 6 hpi, suggesting that *spvC* gene restricts elimination of pathogens in host cells which may related to autophagy.

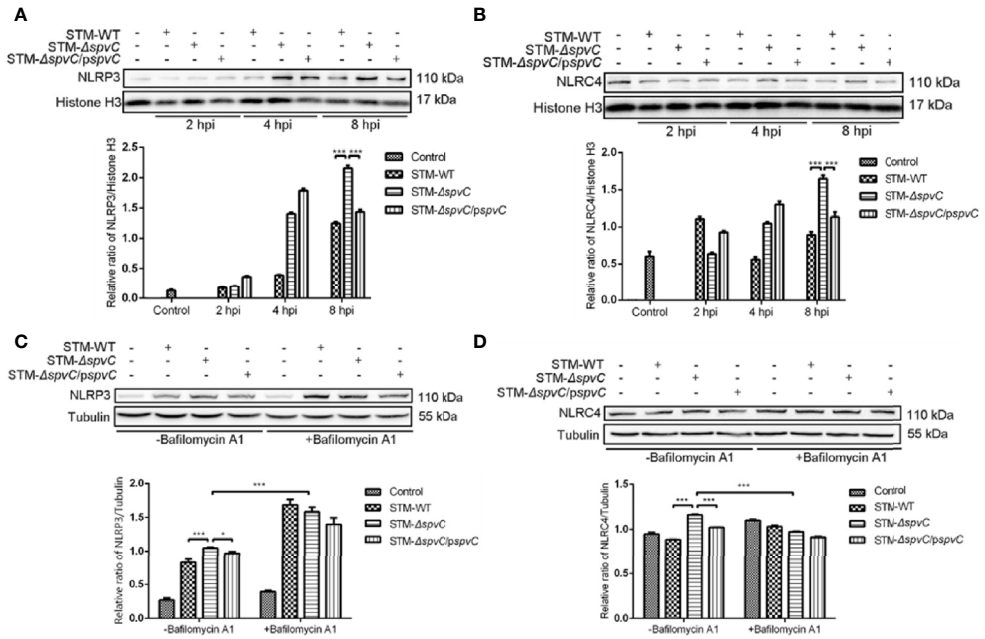

FIGURE 4 | *spvC* down-regulates NLRP3 and NLRC4 in an autophagy related manner. **(A, B)** J774A.1 cells were infected with STM-WT, STM-*ΔspvC* and STM-*ΔspvC*/p*spvC* at an MOI of 10. Cell lysates were analysed by western blot with specific antibodies to NLRP3 **(A)**, NLRC4 **(B)** and the control Histone H3 at 2 hpi, 4 hpi and 8 hpi. **(C, D)** J774A.1 cells were infected with STM-WT, STM-*ΔspvC* and STM-*ΔspvC*/p*spvC* at an MOI of 10 at 8 hpi after being pretreated with Bafilomycin A1. Cell lysates were analysed by western blot with specific antibodies to NLRP3 **(C)**, NLRC4 **(D)** and the control Tubulin. Data were compared by ANOVA. Values are expressed as the means ± S.D., n = 3. Statistically significant differences are indicated. ***$P < 0.001$; *$P < 0.01$.

However, some pathogens have evolved complex escape mechanisms of autophagy. We have previously shown that *spvB* blocks initial stage of autophagy and enhanced intracellular bacterial survival (29). In this study, we pretreated the infection model with Bafilomycin A1 which inhibits autophagosome-lysosome fusion, and results showed that *spvC* blocks the formation of autophagosomes. It is now appreciated that the devoured *Salmonell*a can survive after internalization into professional phagocytes (*e.g.* macrophages and neutrophils) and nonprofessional cells (*e.g.* epithelial cells) (30). Consistent with this, morphologically tracked autophagosomes (yellow puncta) and autolysosomes (red puncta) with mRFP-GFP-LC3 tandem construct indicates that *S.* Typhimurium harboring *spvC* inhibits the formation of autophagosomes.

As mentioned above, SpvC is a phosphothreonine lyase which exerts anti-inflammatory effects by inactivating dual-phosphorylated MAPK through beta elimination (31). A site-directed mutant STM-*ΔspvC*/p*ΔspvC* K136A which lacks phosphothreonine lyase activity was constructed. We found that the enzymatic activity of SpvC contributes to down-regulation of autophagy in macrophages. To date, study showed that *S.* Typhimurium *spvC* alleviated phospho-ERK1/2 expression in the villus epithelial cells and lamina propria of caeca, but no significant difference in phospho-p38 or phospho-JNK levels in the caeca infected with all strains (5). Based on this, HeLa cells were pretreated with ERK inhibitor PD0325901 before co-cultured with *S.* Typhimurium. We demonstrated that *spvC* affects the formation of autophagosomes in an ERK dependent manner. Besides we have proved that *spvC* inactivates phospho-ERK1/2, phospho-JNK and phospho-p38, leading to the interference of NLRP3 and NLRC4 in *S.* Typhimurium infected macrophages J774A.1 (18). Given all this, whether JNK and p38 are involved in *spvC* suppressed autophagy remains to be fully elucidated.

Several studies employing diverse bacterial species have highlighted the tactical interplay between autophagy and NLRP3 or NLRC4 inflammasomes. Therefore, macrophages J774A.1, applied in inflammation related research, were used to firstly valid that *spvC* down-regulates NLRP3 and NLRC4 at 8 hpi. Activation of NLRP3 inflammasome involves in damage to the mitochondria and the increased production of reactive oxygen species (ROS) (32). Autophagy plays a role in the removal of misfolded proteins, and the clearance of damaged mitochondria and ROS (33). Notably, we demonstrated that alleviated autophagosome formation is closely related to the effect of *spvC* on NLRP3. On the other hand, type ι interferon-dependent host response performs a negative feedback that represses expression of NLRC4 during *Salmonella* infection (34). Besides, we have reported that *Salmonella spv* locus could affect type ι interferon response *via* inhibiting autophagy in macrophages (35). Thus, we speculate that *spvC*-inhibited autophagy may be related to NLRC4. Indeed, experimental evidence reveals that the inhibition of autophagosome formation by *spvC* interferes with the level of NLRC4. Furthermore, MAPK can transmit signals from the cell

membrane to the nucleus, which may provide the first signal for transcription of inflammasomes (36). This pathway is independent on the effect of autophagy on NLRP3 and NLRC4. Hence, repression of NLRP3 and NLRC4 by *spvC* contributes to the alleviation of pyroptosis, subsequently promotes bacterial dissemination in mice (18). Therefore, the role of NLRP3 and NLRC4 regulated by *spvC* to drive cell fate decisions between autophagy and pytoptosis in *Salmonella* infection deserves further investigation.

Taken together, we identify a novel contribution of the *spvC* gene to the pathogenesis of *Salmonella via* impairing the formation of autophagosome, thereby interfering with protein levels of NLRP3 and NLRC4. These findings have important implications for understanding the intricate evolutionary adaptations that shape host-pathogen cross-talk.

DATA AVAILABILITY STATEMENT

The original contributions presented in the study are included in the article/supplementary material. Further inquiries can be directed to the corresponding author.

ETHICS STATEMENT

This study was approved by Soochow University Institutional Review Board.

AUTHOR CONTRIBUTIONS

LTZ, YL, and SW designed the research and wrote the manuscript. LTZ, YL, SG, HY, LLZ, and CW performed the research and conducted the data analysis. YL, RH, and SW supervised the project and edited the manuscript. All authors contributed to the article and approved the submitted version.

FUNDING

The research leading to these results has received funding from the Natural Science Foundation of China (No. 31970132, No. 81971899), the Suzhou Municipal Science and Technology Foundation (SYS2019031), and the Priority Academic Program Development of Jiangsu Higher Education Institutions (PAPD).

REFERENCES

1. Hurley D, Hoffmann M, Muruvanda T, Allard MW, Brown EW, Martins M, et al. Atypical *Salmonella Enterica* Serovars in Murine and Human Macrophage Infection Models. *Infect Immun* (2020) 88(4):e00353-19. doi: 10.1128/IAI.00353-19
2. Kharroubi S, Nasser NA, El-Harakeh MD, Sulaiman AA, Kassem II. First Nation-Wide Analysis of Food Safety and Acceptability Data in Lebanon. *Foods* (2020) 9(11):1717. doi: 10.3390/foods9111717
3. Käppeli R, Kaiser P, Stecher B, Hardt W-D. Roles of *spvB* and *spvC* in *S.* Typhimurium Colitis Via the Alternative Pathway. *Int J Med Microbiol* (2011) 301(2):117–24. doi: 10.1016/j.ijmm.2010.08.017
4. Yang SD, Deng QF, Sun LQ, Dong KD, Li YY, Wu SY, et al. *Salmonella* Effector SpvB Interferes With Intracellular Iron Homeostasis *via* Regulation of Transcription Factor Nrf2. *FASEB J* (2019) 33(12):13450–64. doi: 10.1096/fj.201900883RR
5. Haneda T, Ishii Y, Shimizu H, Ohshima K, Iida N, Danbara H, et al. *Salmonella* Type III Effector SpvC, a Phosphothreonine Lyase, Contributes to Reduction in Inflammatory Response During Intestinal Phase of Infection. *Cell Microbiol* (2012) 14(4):485–99. doi: 10.1111/j.1462-5822.2011.01733.x
6. Mazurkiewicz P, Thomas J, Thompson JA, Liu M, Arbibe L, Sansonetti P, et al. SpvC Is a *Salmonella* Effector With Phosphothreonine Lyase Activity on Host Mitogen-Activated Protein Kinases. *Mol Microbiol* (2008) 67(6):1371–83. doi: 10.1111/j.1365-2958.2008.06134.x
7. Ammanathan V, Mishra P, Chavalmane AK, Muthusamy S, Jadhav V, Siddamadappa C, et al. Restriction of Intracellular *Salmonella* Replication by Restoring TFEB-Mediated Xenophagy. *Autophagy* (2019) 16(9):1584–97. doi: 10.1080/15548627.2019.1689770
8. Kang JW, Yan J, Ranjan K, Zhang X, Turner JR, Abraham C. Myeloid Cell Expression of LACC1 Is Required for Bacterial Clearance and Control of Intestinal Inflammation. *Gastroenterology* (2020) 159(3):1051–67. doi: 10.1053/j.gastro.2020.07.024
9. Jiao Y, Zhang YG, Lin ZJ, Lu R, Xia YL, Meng C, et al. *Salmonella* Enteritidis Effector AvrA Suppresses Autophagy by Reducing Beclin-1 Protein. *Front Immunol* (2020) 11:686. doi: 10.3389/fimmu.2020.00686
10. Samir P, Kesavardhana S, Patmore DM, Gingras S, Malireddi RKS, Karki R, et al. DDX3X Acts as a Live-Or-Die Checkpoint in Stressed Cells by Regulating NLRP3 Inflammasome. *Nature* (2019) 573(7775):590–4. doi: 10.1038/s41586-019-1551-2
11. Xue Y, Enosi Tuipulotu D, Tan WH, Kay C, Man SM. Emerging Activators and Regulators Of Inflammasomes and Pyroptosis. *Trends Immunol* (2019) 40 (11):1035–52. doi: 10.1016/j.it.2019.09.005
12. Jiang H, Gong T, Zhou RB. The Strategies of Targeting the NLRP3 Inflammasome to Treat Inflammatory Diseases. *Adv Immunol* (2020) 145:55–93. doi: 10.1016/bs.ai.2019.11.003
13. Fattinger SA, Geiser P, Samperio Ventayol P, Di Martino ML, Furter M, Felmy B, et al. Epithelium-Autonomous Naip/Nlrc4 Prevents TNF-Driven Inflammatory Destruction of the Gut Epithelial Barrier in *Salmonella*-Infected Mice. *Mucosal Immunol* (2021) 14(3):615–29. doi: 10.1038/s41385-021-00381-y
14. Kay C, Wang R, Kirkby M, Man SM. Molecular Mechanisms Activating the NAIP-NLRC4 Inflammasome: Implications in Infectious Disease, Autoinflammation, and Cancer. *Immunol Rev* (2020) 297(1):67–82. doi: 10.1111/imr.12906
15. Swanson KV, Deng M, Ting JP. The NLRP3 Inflammasome: Molecular Activation and Regulation to Therapeutics. *Nat Rev Immunol* (2019) 19 (8):477–89. doi: 10.1038/s41577-019-0165-0
16. Qu Y, Misaghi S, Newton K, Maltzman A, Izrael-Tomasevic A, Arnott D, et al. NLRP3 Recruitment by Nlrc4 During *Salmonella* Infection. *J Exp Med* (2016) 213(6):877–85. doi: 10.1084/jem.20132234
17. Gram AM, Wright JA, Pickering RJ, Lam NL, Booty LM, Webster SJ, et al. *Salmonella* Flagellin Activates NAIP/NLRC4 and Canonical NLRP3 Inflammasomes in Human Macrophages. *J Immunol* (2021) 206(3):631–40. doi: 10.4049/jimmunol.2000382
18. Zuo LL, Zhou LT, Wu CY, Wang YL, Li YY, Huang R, et al. Salmonella spvC Gene Iinhibits Pyroptosis and Intestinal Inflammation to Aggravate Systemic Infection in Mice. *Front Microbiol* (2020) 11:562491. doi: 10.3389/fmicb.2020.562491
19. Zhou RB, Yazdi AS, Menu P, Tschopp J. A Role for Mitochondria in NLRP3 Inflammasome Activation. *Nature* (2011) 469(7329):221–5. doi: 10.1038/nature09663
20. Crother TR, Porritt RA, Dagvadorj J, Tumurkhuu G, Slepenkin AV, Peterson EM, et al. Autophagy Limits Inflammasome During *Chlamydia Pneumoniae* Infection. *Front Immunol* (2019) 10:754. doi: 10.3389/fimmu.2019.00754
21. Song J, Dong HQ, Ma C, Zhao BY, Shang GD. Construction and Functional Characterization of an Integrative Form Lambda Red Recombineering *Escherichia Coli* Strain. *FEMS Microbiol Lett* (2010) 309(2):178–83. doi: 10.1111/j.1574-6968.2010.02036.x

22. Szeliova D, Krahulec J, Safranek M, Liskova V, Turna J. Modulation of Heterologous Expression From P_{bad} Promoter in *Escherichia Coli* Production Strains. *J Biotechnol* (2016) 236:1–9. doi: 10.1016/j.jbiotec.2016.08.004
23. Chu YY, Yang YR, Li Y, Ye Y, Yan J, Wang T, et al. A *Salmonella Enterica* Conjugative Plasmid Impairs Autophagic Flux in Infected Macrophages. *Microbes Infect* (2014) 16(7):553–61. doi: 10.1016/j.micinf.2014.05.001
24. Mizushima N, Yoshimori T, Levine B. Methods in Mammalian Autophagy Research. *Cell* (2010) 140(3):313–26. doi: 10.1016/j.cell.2010.01.028
25. Zhong ZY, Elsa S, Michael K. Autophagy, NLRP3 Inflammasome and Auto-Inflammatory/Immune Diseases. *Clin Exp Rheumatol* (2016) 34(4 Suppl 19): 12–6.
26. Keestra-Gounder AM, Tsolis RM, Baumler AJ. Now You See Me, Now You Don't: The Interaction of *Salmonella* With Innate Immune Receptors. *Nat Rev Microbiol* (2015) 13(4):206–16. doi: 10.1038/nrmicro3428
27. Wu S, Shen YR, Zhang S, Xiao YQ, Shi SR. *Salmonella* Interacts With Autophagy to Offense or Defense. *Front Microbiol* (2020) 11:721. doi: 10.3389/fmicb.2020.00721
28. Xu Y, Zhou P, Cheng S, Lu QH, Nowak K, Hopp AK, et al. A Bacterial Effector Reveals the V-Atpase-Atg16l1 Axis That Initiates Xenophagy. *Cell* (2019) 178 (3):552–66.e20. doi: 10.1016/j.cell.2019.06.007
29. Chu YY, Gao S, Wang T, Yan J, Xu GM, Li YY, et al. A Novel Contribution of *spvB* to Pathogenesis of *Salmonella* Typhimurium by Inhibiting Autophagy in Host Cells. *Oncotarget* (2016) 7(7):8295–309. doi: 10.18632/oncotarget.6989
30. Boada-Romero E, Martinez J, Heckmann BL, Green DR. The Clearance of Dead Cells by Efferocytosis. *Nat Rev Mol Cell Biol* (2020) 21(7):398–414. doi: 10.1038/s41580-020-0232-1
31. Li HT, Xu H, Zhou Y, Zhang J, Long CZ, Li SQ, et al. The Phosphothreonine Lyase Activity of a Bacterial Type III Effector Family. *Science* (2007) 315 (5814):1000–3. doi: 10.1126/science.1138960
32. Zhong ZY, Liang S, Sanchez-Lopez E, He F, Shalapour S, Lin XJ, et al. New Mitochondrial DNA Synthesis Enables NLRP3 Inflammasome Activation. *Nature* (2018) 560(7717):198–203. doi: 10.1038/s41586-018-0372-z
33. Wu AG, Zhou XG, Qiao G, Yu L, Tang Y, Yan L, et al. Targeting Microglial Autophagic Degradation in Nlrp3 Inflammasome-Mediated Neurodegenerative Diseases. *Ageing Res Rev* (2020) 65:101202. doi: 10.1016/j.arr.2020.101202
34. Akhade AS, Atif SM, Lakshmi BS, Dikshit N, Hughes KT, Qadri A, et al. Type 1 Interferon-Dependent Repression of NLRC4 and Ipla2 Licenses Down-Regulation Of *Salmonella* Flagellin Inside Macrophages. *Proc Natl Acad Sci USA* (2020) 117(47):29811–22. doi: 10.1073/pnas.2002747117
35. Wang LD, Li YL, Liu YH, Zuo LL, Li YY, Wu SY, et al. *Salmonella Spv* Locus Affects Type I Interferon Response and the Chemotaxis of Neutrophils *via* Suppressing Autophagy. *Fish Shellfish Immunol* (2019) 87:721–9. doi: 10.1016/j.fsi.2019.02.009
36. Zhao WM, Ma L, Cai C, Gong XH. Caffeine Inhibits NLRP3 Inflammasome Activation by Suppressing MAPK/NF-κb and A2aR Signaling in LPS-Induced THP-1 Macrophages. *Int J Biol Sci* (2019) 15(8):1571–81. doi: 10.7150/ijbs.34211

Conflict of Interest: The authors declare that the research was conducted in the absence of any commercial or financial relationships that could be construed as a potential conflict of interest.

Advantages of publishing in Frontiers

OPEN ACCESS
Articles are free to read for greatest visibility and readership

FAST PUBLICATION
Around 90 days from submission to decision

HIGH QUALITY PEER-REVIEW
Rigorous, collaborative, and constructive peer-review

TRANSPARENT PEER-REVIEW
Editors and reviewers acknowledged by name on published articles

Frontiers
Avenue du Tribunal-Fédéral 34
1005 Lausanne | Switzerland

Visit us: www.frontiersin.org
Contact us: frontiersin.org/about/contact

REPRODUCIBILITY OF RESEARCH
Support open data and methods to enhance research reproducibility

DIGITAL PUBLISHING
Articles designed for optimal readership across devices

FOLLOW US
@frontiersin

IMPACT METRICS
Advanced article metrics track visibility across digital media

EXTENSIVE PROMOTION
Marketing and promotion of impactful research

LOOP RESEARCH NETWORK
Our network increases your article's readership